Edited by Sabu Thomas, Kuruvilla Joseph,
S. K. Malhotra, Koichi Goda, M. S. Sreekala

WILEY-VCH

Polymer Composites

Volume 3: Biocomposites

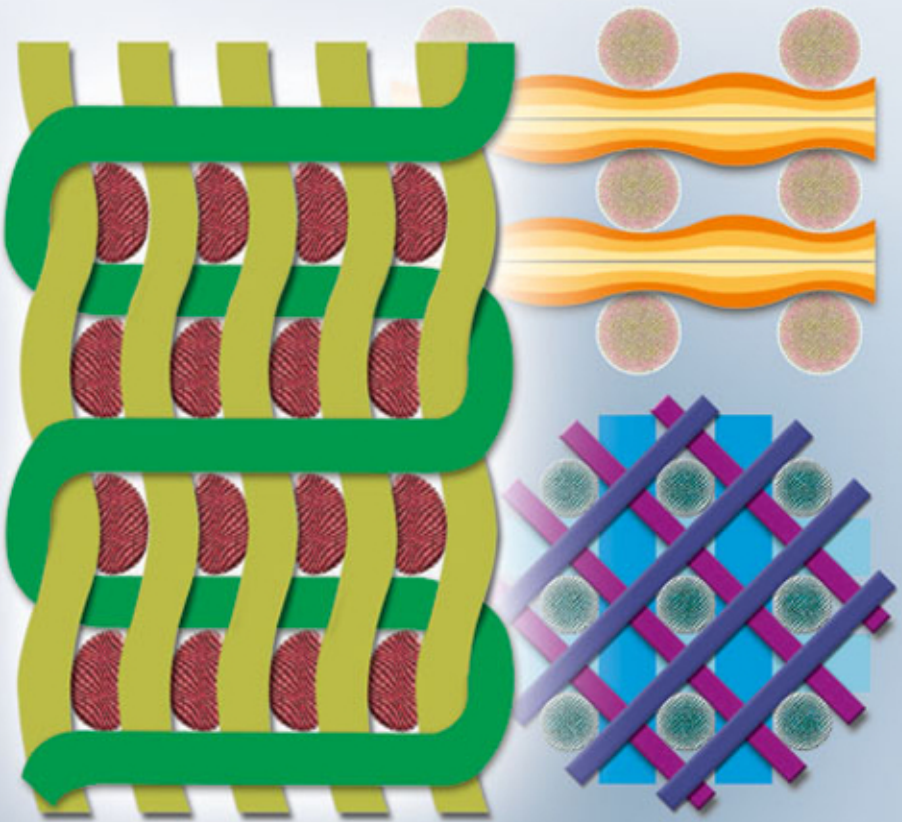

Edited by
Sabu Thomas, Kuruvilla Joseph,
Sant Kumar Malhotra, Koichi Goda, and
Meyyarappallil Sadasivan Sreekala

Polymer Composites

Related Titles

Thomas, S., Joseph, K., Malhotra, S. K., Goda, K., Sreekala, M. S. (eds.)

Polymer Composites

Series: Polymer Composites

Volume 1
2012
ISBN: 978-3-527-32624-2

Volume 2
2013
ISBN: 978-3-527-32979-3

3 Volume Set
2014
ISBN: 978-3-527-32985-4

Thomas, S., Durand, D., Chassenieux, C., Jyotishkumar, P. (eds.)

Handbook of Biopolymer-Based Materials

From Blends and Composites to Gels and Complex Networks

2 Volumes
2013
ISBN: 978-3-527-32884-0

Decher, G., Schlenoff, J. (eds.)

Multilayer Thin Films

Sequential Assembly of Nanocomposite Materials
Second, completely revised and enlarged edition

2012
ISBN: 978-3-527-31648-9

Mittal, V. (ed.)

Optimization of Polymer Nanocomposite Properties

2010
ISBN: 978-3-527-32521-4

Mittal, V. (ed.)

In-situ Synthesis of Polymer Nanocomposites

Series: Polymer Nano-, Micro- and Macrocomposites (Volume 2)

2011
ISBN: 978-3-527-32879-6

Mittal, V. (ed.)

Characterization Techniques for Polymer Nanocomposites

Series: Polymer Nano-, Micro- and Macrocomposites (Volume 3)

2012
ISBN: 978-3-527-33148-2

Mittal, V. (ed.)

Modeling and Prediction of Polymer Nanocomposite Properties

Series: Polymer Nano-, Micro- and Macrocomposites (Volume 4)

2013
ISBN: 978-3-527-33150-5

Lendlein, A., Sisson, A. (eds.)

Handbook of Biodegradable Polymers

Synthesis, Characterization and Applications

2011
Hardcover
ISBN: 978-3-527-32441-5

Edited by Sabu Thomas, Kuruvilla Joseph, S. K. Malhotra, Koichi Goda, M. S. Sreekala

Polymer Composites

Volume 3

WILEY-VCH Verlag GmbH & Co. KGaA

Editors

Sabu Thomas
Mahatma Gandhi University
School of Chemical Sciences
Priyadarshini Hills P.O.
School of Chemical Sciences
Kottayam 686 560
Kerala
India

Kuruvilla Joseph
Indian Institute of Space Science and Technology
ISRO P. O.
Veli, Thiruvananthapuram 695 022
Kerala
India

Dr. S. K. Malhotra
Flat-YA, Kings Mead
Srinagar Colony
South Mada Street 14/3
Srinagar Colony
Saidapet, Chennai 600 015
India

Prof. Koichi Goda
Faculty of Engineering
Yamaguchi University
Tokiwadai 2-16-1
Yamaguchi University
755-8611 Ube, Yamaguchi
Japan

Dr. M. S. Sreekala
Department of Chemistry
Sree Sankara College
Kalady 683 574
Kerala
India

Library of Congress Card No.:
applied for

British Library Cataloguing-in-Publication Data
A catalogue record for this book is available from the British Library.

Bibliographic information published by the Deutsche Nationalbibliothek
The Deutsche Nationalbibliothek lists this publication in the Deutsche Nationalbibliografie; detailed bibliographic data are available on the Internet at <http://dnb.d-nb.de>.

Print ISBN: 978-3-527-32980-9
ePDF ISBN: 978-3-527-67425-1
ePub ISBN: 978-3-527-67424-4
mobi ISBN: 978-3-527-67423-7
oBook ISBN: 978-3-527-67422-0

Cover Design Adam-Design, Weinheim, Germany
Typesetting Laserwords Private Limited, Chennai, India
Printing and Binding betz-druck GmbH, Darmstadt

Printed on acid-free paper

Contents

The Editors

Sabu Thomas is a Professor of Polymer Science and Engineering at Mahatma Gandhi University (India). He is a Fellow of the Royal Society of Chemistry and a Fellow of the New York Academy of Sciences. Thomas has published over 430 papers in peer reviewed journals on polymer composites, membrane separation, polymer blend and alloy, and polymer recycling research and has edited 17 books. He has supervised 60 doctoral students.

Kuruvilla Joseph is a Professor of Chemistry at Indian Institute of Space Science and Technology (India). He has held a number of visiting research fellowships and has published over 50 papers on polymer composites and blends.

S. K. Malhotra is Chief Design Engineer and Head of the Composites Technology Centre at the Indian Institute of Technology, Madras. He has published over 100 journal and proceedings papers on polymer and alumina–zirconia composites.

Koichi Goda is a Professor of Mechanical Engineering at Yamaguchi University. His major scientific fields of interest are reliability and engineering analysis of composite materials and development and evaluation of environmentally friendly and other advanced composite materials.

M. S. Sreekala is an Assistant Professor of Chemistry at Post Graduate Department of Chemistry, SreeSankara College, Kalady (India). She has published over 40 papers on polymer composites (including biodegradable and green composites) in peer reviewed journals and has held a number of Scientific Positions and Research Fellowships including those from the Humboldt Foundation, Germany, and Japan Society for Promotion of Science, Japan.

List of Contributors

Kurungattu Arjunan Nair Ajith Kumar
Mahatma Gandhi University
Department of Chemistry
Sree Sankara College
Mattoor, Kalady 683 574
Kerala
India

Preetha Balakrishnan
Mahatma Gandhi University
Department of Chemistry
Sree Sankara College
Mattoor, Kalady 683 574
Kerala
India

Dongwan Cho
Kumoh National Institute of Technology
Department of Polymer Science and Engineering
Polymer/Bio-Composites Research Lab
61 Daehak-ro
Gumi, Gyeongbuk 730-701
Republic of Korea

Taek-Jun Chung
Seoul National University
Laboratory of Adhesion and Bio-Composites
1 Daehak-ro, Gwanak-gu
Seoul 151-921
Republic of Korea

Lawrence T. Drzal
Michigan State University
Composite Materials and Structures Center
428 S. Shaw Lane, 2100
Engineering Building
East Lansing, MI 48824
USA

Alain Dufresne
Grenoble INP-Pagora
Laboratoire Génie des Procédés Papetiers (LGP2)
461 rue de la Papeterie
CS 10065
38402 Saint-Martin d'Hères cedex
France

Raju Francis
Mahatma Gandhi University
School of Chemical Sciences
Priyadarshini Hills
Kottayam 686 560
Kerala
India

Toru Fujii
Doshisha University
Department of Mechanical Engineering and Systems
Kyoutanabe-city
Kyoto 610-0394
Japan

Koichi Goda
Yamaguchi University
Department of Mechanical Engineering
2-16-1 Tokiwadai
Ube 755-8611, Yamaguchi
Japan

Preetha Gopalakrishnan
LGP2, CNRS, UMR 5518
Grenoble INP
Rue de la Papeterie
BP-65
38402 St. Martin d'Hères Cedex
France

Geethy P. Gopalan
Mahatma Gandhi University
School of Chemical Sciences
Priyadarshini Hills
Kottayam 686 560
Kerala
India

Hirokazu Ito
Yamaha Livingtec Corporation
Business Planning Division
1370, Nishiyama-cho, Nishi-ku
Hamamatu 432-8001
Japan

Kuruvilla Joseph
Indian Institute of Space Science and Technology
ISRO P.O.
Veli, Thiruvananthapuram
695 022
Kerala
India

Balbir Singh Kaith
Dr. B. R. Ambedkar National Institute of Technology (Deemed University)
Department of Chemistry
Jalandhar 144 011
Punjab
India

Susheel Kalia
Bahra University
Department of Chemistry
Waknaghat (Shimla Hills)
173 234, District Solan (H.P.)
India

Inderjeet Kaur
H.P. University
Department of Chemistry
Shimla 171 005, (H.P.)
India

Hyun-Joong Kim
Seoul National University
Laboratory of Adhesion and Bio-Composites
1 Daehak-ro, Gwanak-gu
Seoul 151-921
Republic of Korea

and

Seoul National University
Research Institute for Agriculture and Life Sciences
1 Daehak-ro, Gwanak-gu
Seoul 151-921
Republic of Korea

Masatoshi Kubouchi
Tokyo Institute of Technology
Graduate School of Science and Engineering
Department of Chemical Engineering
2-12-1, S4-5, O-okayama, Meguro-ku
Tokyo 152-8552
Japan

Hyeok-Jin Kwon
Seoul National University
Laboratory of Adhesion and Bio-Composites
1 Daehak-ro, Gwanak-gu
Seoul 151-921
Republic of Korea

Louis Laberge Lebel
Bombardier Aerospace
1800 Marcel Laurin
Saint-Laurent, Québec
H4R 1K2
Canada

Hyun-Ji Lee
Seoul National University
Laboratory of Adhesion and Bio-Composites
1 Daehak-ro, Gwanak-gu
Seoul 151-921
Republic of Korea

Sant Kumar Malhotra
Flat-YA, Kings Mead Srinagar Colony
14/3, South Mada Street
Saidapet
Chennai 600 015
India

Luiz H.C. Mattoso
Laboratório Nacional de Nanotecnologia para o Agronegócio (LNNA)
Embrapa Instrumentação Agropecuária (CNPDIA)
Rua XV de Novembro
1452 Centro
13.560-970 São Carlos, SP
Brazil

Eliton S. Medeiros
Universidade Federal da Paraíba (UFPB)
Departamento de Engenharia de Materiais (DEMAT)
Cidade Universitária
58.051-900 João Pessoa, PB
Brazil

Dionysis E. Mouzakis
Higher Technological Educational Institute of Thessaly
Department of Mechanical Engineering
Larissas-Trikalon Highway
41110 Thessaly
Greece

Ajalesh Balachandran Nair
Cochin University of Science and Technology
Department of Polymer Science and Rubber Technology
Kochi 682 022
Kerala
India

Asami Nakai
Gifu University
Dept. of Mechanical and Systems Engineering
Gifu City, 501-1193
Japan

Rie Nakamura
Nihon University
Department of Mechanical Engineering
1 Nakakawahara Tamura
Koriyama, 963-8642, Fukushima
Japan

Anil N. Netravali
Cornell University
Department of Fiber Science and Apparel Designs
Fiber Science Program
201 MVR Hall
Ithaca, NY 14853
USA

Takashi Nishino
Kobe University
Department of Chemical Science and Engineering
Graduate School of Engineering
Rokko, Nada-ku, Kobe 657-8501
Japan

James Njuguna
Cranfield University
Department of Sustainable Systems
Bedfordshire MK43 0AL
UK

Kazuya Okubo
Doshisha University
Department of Mechanical Engineering and Systems
Kyoutanabe-city
Kyoto 610-0394
Japan

William J. Orts
United States Department of Agriculture (USDA)
Western Regional Research Center (WRRC)
Bioproduct Chemistry and Engineering (BCE)
800 Buchanan Street
Albany, CA 94710
USA

Jean Marc Saiter
Jubail Industrial College
Department of Chemical and Process Engineering Technology
Al-Jubail, 31961
Kingdom of Saudi Arabia

and

Université de Rouen
Laboratoire Polymères Biopolymères et Membranes
Institut des Matériaux Rouen
FRE 3101, équipe LECAP
BP 12
76801 Saint Etienne du Rouvray
France

Amélia S.F. Santos
Universidade Federal do Rio Grande do Norte (UFRN)
Departamento de Engenharia de Materiais (DEMAT)
Avenida Salgado Filho
3000 – Lagoa Nova
59078-970 Natal, RN
Brazil

Soumya Sasikumar
Mahatma Gandhi University
School of Chemical Sciences
Priyadarshini Hills
Kottayam 686 560
Kerala
India

Yoshinobu Shimamura
Shizuoka University
Department of Mechanical Engineering
3-5-1 Johoku
Naka-ku, Hamamatsu
Shizuoka 432-8561
Japan

Palanisamy Sivasubramanian
Mahatma Gandhi University
Department of Mechanical Engineering
Saint GITS College of Engineering
Pathamuttom, Kottayam 686 532
Kerala
India

Meyyarappallil Sadasivan Sreekala
Mahatma Gandhi University
Department of Chemistry
Sree Sankara College
Mattoor
Kalady 683 574
Kerala
India

Parambath Madhom Sreekumar
Jubail Industrial College
Department of Chemical and Process Engineering Technology
Al-Jubail, 31961
Kingdom of Saudi Arabia

Tatsuya Tanaka
Doshisha University
Department of Mechanical and Systems Engineering
1-3 Tatara Miyakodani
Kyotanabe City 610-0394
Japan

Sabu Thomas
Mahatma Gandhi University
School of Chemical Sciences
Priyadarshini Hills
Kottayam 686 560
Kerala
India

Terence P. Tumolva
University of the Philippines-Diliman
Department of Chemical Engineering
Quezon City 1101
Philippines

William Tai Yin Tze
University of Minnesota
Department of Bioproducts and Biosystems Engineering
2004 Folwell Avenue
Saint Paul, MN 55108
USA

1
Advances in Polymer Composites: Biocomposites – State of the Art, New Challenges, and Opportunities

Koichi Goda, Meyyarappallil Sadasivan Sreekala, Sant Kumar Malhotra, Kuruvilla Joseph, and Sabu Thomas

1.1
Introduction

Environmental compatibility of polymer composites has become an important characteristic as the need to reduce environmental hazards is increasing worldwide. Many incidents taking place around the world are enough to bring us around to this point of view. A catastrophic earthquake and *tsunami* devastated the Pacific coast of north-eastern Japan on 11 March 2011. The earthquake, which was the most powerful earthquake ever measured in Japan, was of magnitude 9.0 on the Richter scale. About 19 000 were dead and missing. Three prefectures in the Tohoku (north-eastern) region of Japan, Miyagi, Iwate, and Fukushima, were most severely damaged. Reconstruction is yet to take place in many of the affected cities and towns. The area around the Fukushima Daiichi Nuclear Power Plant was evacuated owing to radioactive contamination. It is said that complete restoration will take more than 30 years, because the influence of the Chernobyl nuclear power plant disaster, which happened more than 25 years ago, continues to be felt. In Fukushima prefecture, many residents are still forced to lead lives as long-term refugees, and the residents in certain areas outside the refuge zone continue to live under threat of radiation that is much higher than is normal. The damage caused by radioactivity has also been considerable: it has already affected the soil of schoolyards, tapwater, grass, agricultural products, marine products, and so on, in large areas within the Fukushima prefecture. It is not clear how much of this damage is due to sea pollution and how long its effects will last in the future.

Against such a background, a planned conversion to renewable natural power sources as recommended by the energy policy, depending on nuclear power generation, attracts attention. For instance, it has been decided to abolish nuclear power generation systems in Germany; they propose to convert from 16% of total energy generation from the natural power sources at present to 35% by 2020 and to 80% by 2050 [1]. In the report ''The Green New Deal'' published in 2009 [2], promotion of use and development of alternative and renewable energy, improvement in energy efficiency, greenhouse gas reduction, and so on, have also been proposed. Today,

Polymer Composite: Volume 3, First Edition.
Edited by Sabu Thomas, Kuruvilla Joseph, S. K. Malhotra, Koichi Goda and M. S. Sreekala.

technologies for various natural power sources, such as solar power, hydraulic power, woody biomass, and wind force power generation, are already in practical use. The authors believe that many people in the world desire realization of a sustainable society that uses such renewable energy power generation technologies.

To realize a sustainable society, various supplies around our life also need to be made from renewable materials. Biomass-derived materials are one of the most sustainable materials, which can also be used as industrial materials. On the other hand, most engineering plastic products are petroleum-derived products. As is well-known, the use of fossil resources causes difficulties in recycling and induces the problem of waste plastic and petroleum products, of which the incineration also causes an increase in carbon dioxide linking to global warming. In addition, fossil resources are an exhaustible resource. To maintain a sustainable society, we are of the opinion that biomass resources may be suitably exploited socially/ecologically as much as possible, by their replacing fossil resources. Since the arrival of such a society will result in a carbon-neutral system, this would also greatly contribute to global environmental protection. It is said that biodegradable plastics, for example, polylactic acid (*PLA*) and polyhydroxyalkanoic acid (*PHA*), are among the leading biomass-derived materials, which are finally decomposed by microorganisms into water and carbon dioxide. Therefore, there are only a few impacts on natural environment compared with those of conventional petroleum-derived plastics. Such biomass-derived materials are expected to be more widely applicable for the commodities used by us on a daily basis, for industrial products, and so on.

The main drawbacks of biodegradable resins are low strength and stiffness, and therefore, it is not appropriate to apply resins directly for structural components. Plastics are often reinforced with inorganic fibers such as glass or carbon, as described in Volume I of this series. Carbon fiber-reinforced plastic matrix composites (*CFRP*), in particular, have been recently used for primary structural components in airplanes and automobiles as well as sport goods and construction materials, because of their excellent mechanical properties. Biodegradable resin may also be reinforced with such fibers, similarly to the conventional petroleum-derived plastics. However, let us recall here how we should construct a sustainable society. If the final products do not really require high strength and durability, do we need to use strong artificial fiber-reinforced composites? Cellulosic materials, namely, plant-based natural fibers such as flax, hemp, bamboo, and wood, have low densities, are biodegradable, and inexpensive, and they have relatively high stiffness and less wear/abrasion to material partners. If such cellulosic materials are used as reinforcements of biomass-derived plastics, this material would be a quite suitable for building a sustainable society. We call such a biomass-based composite material a *biocomposite*. This idea of using natural fibers had already been adopted in the experimentally developed automotive body in 1940s by Henry Ford [3]. Fifty years later, Mercedes-Benz applied composites produced from natural fibers and polypropylene to their car interior parts in the 1990s. Although the matrix used in the cars was petroleum-derived thermoplastic resin, this business should be evaluated as an advanced measure in terms of practical and large-scale production. The use of natural fiber-reinforced composites using biomass-based biodegradable

resin began in the 2000s. Toyota Motors first applied these composites to their spare tire covers in 2003, the constituents of which were kenaf fibers and PLA resin [4]. NEC and UNITIKA collaborated to develop a biocomposite of the same system, applicable for the body of mobile phones in 2005 [5]. Today, novel biocomposites are further being developed in research institutes and industries.

Technological innovation, which replaces all petroleum-based materials by biomass-based ones would be the task imposed on scientists and engineers of the twenty-first century, because it is anticipated that fossil resources will disappear in the near future. We consider that this innovation also includes the improvement and development of biomass-based fibers and resins, of which the mechanical properties are comparable to those of artificial fibers and petroleum-based resins, respectively. In this sense, the study of biocomposites must not end with just their being ''environmental-friendly,'' but must be advanced in the future in the quest toward establishing a sustainable society.

1.2
Development of Biocomposite Engineering

Biocomposites (the title of Volume III), are often interpreted as either biomass-based or biomedical materials. The former have a wider meaning than the latter, because they are available for various industrial purposes. A biomass-based composite consists of biomass and/or biomass-derived substance. On the other hand, a biomedical composite is a specified material because it is limited merely to biomedical use. In this use, the constituents are not necessarily biomass-based or biodegradable, but should be biocompatible. In the present volume, as stated earlier, by biocomposites, we mean biomass-based composites.

In this volume, the application of biocomposites is premised on structural use rather than functional one. From this point of view, we need to know exactly the mechanical properties, such as tensile strength and Young's modulus, of natural fibers and wood flours, similarly to the case of artificial reinforcing materials such as carbon and glass fibers. Tensile properties of natural fibers such as cotton, flax, wool, and silk have been examined in detail in the field of textile engineering. According to the book titled ''Physical Properties of Textile Fibers'' [6] published in 1962, the strength of fibers is mainly evaluated as maximum load divided by fiber specimen weight, denoted by the tenacity (g tex^{-1}) or the specific strength (g $denier^{-1}$). In textile engineering, a continuous filament called a *spun yarn* is a basic configuration [7]. Spun yarns are produced by spinning short fibers using a spinning machine or wheel, because most natural fibers are finite in length. Some of the spun yarns are further processed into twisted or blended yarns. To evaluate the various and complicated configurations, the concept of normalization by ''load per weight'' may be convenient to understand. The relation between the basic structure of spun yarns and their mechanical properties had already been clarified in the 1970s. The field of such study, called *yarn mechanics*, was extended to regenerated and chemical fibers, as well as natural fibers [8]. In the 1980s,

natural fibers began to attract attention as a sustainable material, in addition to textile use, which is deeply related to the solution of environmental and energy problems. India, especially, played a pioneering role regarding production and application of several materials containing jute fibers, as shown in many papers [9–13] and review articles [14, 15]. During this period, jute fiber composites using thermosetting resins had been the main targets of research; thus the idea of hybrid composites with glass fibers was proposed [9, 16, 17]. Application of plant-based natural fibers into cement concrete had also been reported by several Indian institutes [18, 19].

Meanwhile, the project known as *Poverty and Environment Amazonia* (*POEMA*) in Brazil, established by Daimler-Chrysler, also started in 1981 [20]. This organization contracted with the residents of the Amazon valley, and encouraged them to apply natural resources such as coconut fibers to car interior parts. In the 1980s, however, the natural fiber composites were not biodegradable, because the resins applied were petroleum based. In the 1990s, a new type of fibrous composites was reported, in which the reinforcement and matrix of the composites were both biodegradable; the constituents were respectively natural fibers and polyvinyl alcohol (*PVA*) [21]. Netravali *et al*. [22] also developed in 1998 the composite system of natural fibers and biomass-derived resin, and these were termed as *fully green composites*. Since then, green composites have been recognized as one of the representative biodegradable materials reinforced with natural fibers. Various production methods and properties of green composites have been studied, and they are applied for several industries, as mentioned above. In the studies of green composites, most of researchers treat the tensile strength of natural fibers as ''load per cross-sectional area.'' To estimate the exact strength, even the morphology of the fiber cross-section has often been investigated, because it is quite complicated and different from the circular cross-section seen in many artificial fibers [23–28]. In relation to such mechanics or strength estimation, several researchers have further extended it to the numerical [29–31] or stochastic [24, 32] viewpoint. Not only such academic points of view of natural fibers but also the mechanics of composites reinforced with textile yarns such as spun or twisted yarn is on the rise [33, 34] (see, also Chapter 10.1).

The study on the above-mentioned natural fiber strength is one example concerning the progress of biocomposite engineering, in which natural fibers are evaluated as a structural material. Meanwhile, studies on the improvement of interface between wood fibers/flour (*WF/F*) and polymeric resin have also been progressing, of which the material is known by the name of *wood–plastic composite*s (*WPC*s) [35] (see, also Chapter 5.2). This material is an in-between field that needs knowledge of both polymer chemistry and wood science. We also consider that WPC is in a category of biocomposites. The compatibility between WF/F and polymeric resin is quite poor, which leads to nonuniform dispersion of WF/F and low mechanical properties. The relation between wood and plastic is similar to that between oil and water – they do not mix so easily. Thermoplastic resins often used as a matrix material are hydrophobic, while WF/F is hydrophilic. These two contrary properties result in poor interfacial strength. As in the development of the

silane-coupling agent linking glass fibers to polymeric resin, studies on the effect of various chemical treatments on the interfacial strength, such as cross-liking and acetylation of cellulose, grafting, use of coupling agent, have been conducted since the 1970s. It has been reported in many papers [36–38] (see Chapter 5.2) that, for example, WPC is improved in strength and impact properties by addition of a compatibilizer such as maleic anhydride-*grafted*-polypropylene (*MAPP*). WPCs were first introduced into the decking market in the early 1990s, in which 50% wood flours and 50% low density polyethylene (LDPE) were combined. Today, the WPC industry has grown into one of the greatest in the various fields of biocomposites. Although surface treatments on inorganic filler or reinforcement have been developed in conventional composite engineering, the above polar and nonpolar interface improving technology, a common subject to natural fibers, has also been creating biocomposite engineering (see, Chapter 4). In the 2000s, such chemical treatment in the WPC production process has been extended to achieve compatibility with biodegradable resins such as PLA [39]. This research progress quite matches the idea of as-mentioned fully green composites. WPC is further progressing through a technology fibrillating WF/F into the nanoscale [40].

As in the above, hitherto unknown issues inherent in biocomposites are being solved and meanwhile the appropriate evaluation methods are also being built up. We believe that development of various researches and technologies, such as the following would lead to an unwavering future for biocomposite engineering:

- Structure–property relationships in biopolymers (Chapter 2)
- Basic and applied researches of cellulose (Chapter 3)
- Interface improvement technology (Chapter 4)
- Production technology for thermoplastic–resin matrix biocomposites (Chapter 5)
- Production technology for thermoset–resin matrix biocomposites (Chapter 6)
- Biofiber reinforcement in thermoplastics (Chapter 7)
- Biofiber reinforcement in natural rubber (Chapter 8)
- Cellulose containing effect for improvement of interfacial strength (Chapter 9)
- Yarn optimization for natural fiber composites (Chapter 10)
- Bionanocomposites (Chapter 11)
- Fully biodegradable green composites (Chapter 12)
- Applications and future scope of natural fiber composites (Chapter 13)
- Biomedical applications of polymer composites (Chapter 14)
- Environmental effects, biodegradability, and life cycle analysis of biocomposites (Chapter 15).

1.3 Classification of Biocomposites

In this section, we try to clarify where biocomposites are positioned among the whole composite materials. In the previous section, the importance of green composite studies was described, and related to the biocomposite-engineering field. The combination of natural fibers and biomass-derived biodegradable resin is

common to both biocomposites and green composites. What is the difference between biocomposites and green composites? PLA containing hydroxyapatite, a representative bioabsorbable biomedical composite, is expected to be applied widely as a bone-connecting material. Hydroxyapatite is a mineral-derived natural resource, but it is neither biodegradable nor biomass-based. Therefore, this composite cannot be denoted as a fully green composite, though it is partially biodegradable and biomass-based. Meanwhile, carbon fiber had originally been made from a biomass, as represented in a carbonized bamboo fiber filament developed by Thomas Edison. Although most of them are made from petroleum-derived acrylic fibers in the present technology, even now, some carbon fibers are made from pulp-originated rayon fibers. When we apply such a carbonized bamboo fiber to reinforcement, this may be called a *fully biomass-based composite* by combining it with biomass-derived resin even if the resin used is nonbiodegradable. Wood ceramics [41] is also a carbonized composite material composed of wood flour and phenolic resin, which is produced by sintering its precursor at high temperatures under inert atmosphere. (The precursor of ceramics is often called *green body*.) This material is expected to be applied to electromagnetism shields, tribological components, and heat-resistant and corrosion-resistant materials, because of their excellent properties. Wood ceramics is not green, but the great part of this material is biomass-based. Such carbonized biomass materials also attract attention from the viewpoint of carbon fixation technology, called *biochar*. It seems from the aforementioned that biocomposites can be defined as a biomass-based composite occupying a larger category than green composites.

On the other hand, we must not forget that ''green'' often means ''environment-friendly'' as well as biodegradable. Many unnecessary textiles and discarded composite products are often treated as industrial waste, but we understand that these are recyclable. For example, when waste uniform clothes composed of polyester and wool fibers are combined with PVA, they can be used as an agricultural material [42]. Growth of plants is promoted more effectively through this application. In this case, this could be termed *green* composite material. Discarded glass fiber-reinforced plastic (GFRP) or CFRP products are decomposed thermally and/or chemically, and can be used as a recycle glass or carbon fiber [43, 44]. If such fibers are used again as reinforcement of composites, then we could also call these *green* composites. Green chemistry means chemical technology aiming at lower environmental impact, in which one of the purposes is to improve life cycle efficiency for petroleum-based plastics. Another purpose is furthermore directed to refining of bioethanol from biomass resources and even polyolefin materials production using this ethanol. Composites made from such improved petroleum-based plastics or biopolyolefins may also be called *green* composites, despite the fact that they are not biodegradable. Thus, we should know that green composites are not necessarily a subset of biocomposites, but consist of the intersection of biocomposites and a disjoint part.

From such a point of view, we have classified biocomposites and green composites, as shown in Figure 1.1. This classification is based on the various matrix and

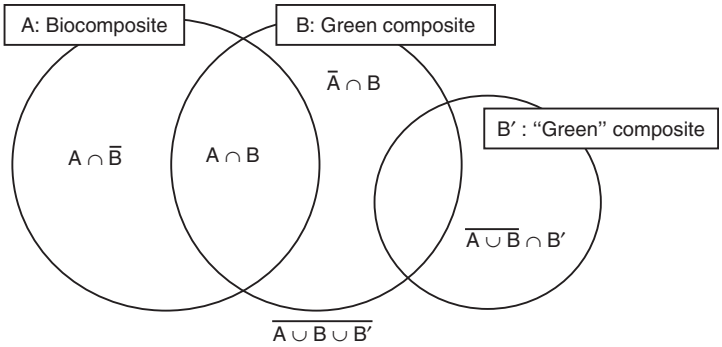

Figure 1.1 Classification of biocomposites and green composites.

Table 1.1 Various matrix materials and reinforcements (filler included).

(a) Matrix

	Biomass derived	**Petroleum derived**
Biodegradability	(Group BM1) PLA, PHA	(Group PM1) PCL, PVA
Nonbiodegradability	(Group BM2) cellulose ester, bioethylene, biopolypropylene	(Group PM2) ethylene, polypropylene

(b) Reinforcement or filler

	Biomass derived (including inorganic)	**Petroleum derived or inorganic**
Biodegradability	(Group BF1) natural fibers, wood flour, spider silk	(Group PF1) fibers made from PM1
Nonbiodegradability	(Group BF2) rayon-based carbon, carbonized wood flour, carbonized cellulose	(Group PF2) chemical fibers, glass, PAN-based carbon, hydroxyl-apatite, nanoclay, and crashed shell

PCL, poly(ε-caprolactone); PAN, polyacrylonitrile.

reinforcement (or filler) properties as shown in Table 1.1a,b, and the meaning of green is defined as biodegradability.

$A \cap B$ is the intersection of biocomposites and green composites. In this category, the materials of matrix and/or reinforcement consist of a biomass-based and biodegradable substances. The group combinations are given as BM1/BF1, BM1/PF1, PM1/BF1, BM1/BF2, BM1/PF2, PM1/BF2, BM2/BF1, BM2/PF1, and PM2/BF1. The first combination, i.e., BM1/BF1, leads to a fully biomass-based and biodegradable composite material.

$A \cap \overline{B}$ is the intersection of biocomposites and nongreen composites. In this category, the materials of matrix and reinforcement consist of a biomass-based and

nonbiodegradable substance. In addition, in case the material of either matrix or reinforcement satisfies this substance, its counterpart must not be biomass-based or biodegradable. The group combinations are given as BM2/BF2, BM2/PF2, and PM2/BF2.

$\overline{A} \cap B$ is the intersection of nonbiocomposites and green composites. In this category, the materials of matrix and/or reinforcement consist of a petroleum-derived (or inorganic) and biodegradable substance. However, the materials of matrix and reinforcement must not be petroleum derived (or inorganic) and nonbiodegradable. The group combinations are given as PM1/PF1, PM1/PF2, and PM2/PF1.

$\overline{A \cup B}$ is the compliment of biocomposites or green composites. In this category, the materials of matrix and reinforcement are both petroleum derived (or inorganic) and nonbiodegradable. The group combination is given as PM2/PF2. However, in case the material of reinforcement consists of recycled textiles or fibers or that of the matrix consists of recycled resin, it can be called a *green* composite. If the matrix material is an excellent life cycle resin in conformity with the concept of green chemistry, this material is also accepted as ''green'' composite even if it is petroleum derived and nondegradable. This category is presented as $\overline{A \cup B} \cap B'$.

Meanwhile, biocomposite research needs many tasks to identify. Identification and effective utilization of renewable resource materials are needed for biocomposite preparation. Finding out effective and economic processing methods is necessary for the separation of starting biomaterials into their pure forms for the production of biocomposites. Performance of the biocomposites is dependent on the inherent properties of the matrix and reinforcement and their interface characteristics. We can tailor the properties of the biocomposites by optimizing processing parameters and by employing suitable physical or chemical modifications to improve the interface. Identifying the thrust areas for the application of biocomposites and manufacture of prototypes and fabrication of useful products has an important role in biocomposite research. The biocomposites will play a major role in replacing nonbiodegradable synthetic materials in the near future.

References

1. Law for the Priority of Renewable Energies (Renewable-Energy-Law) – EEG, *http://www.gesetze-im-internet.de/bundesrecht/eeg_2009/gesamt.pdf* (accessed 1 April 2013).
2. UNEP Global Green New Deal, *http://www.unep.org/pdf/G20_policy_brief_Final.pdf* (accessed 1 April 2013).
3. Popular Mechanics Magazine (Dec. 1941), Vol. 76, No. 6.
4. Inoh, T., Industrial products of plant origin material – effective use of plant origin plastics for recycling society, *J. Jpn. Soc. Mech. Eng.*, **109**, 51–52 (2006) (in Japanese).
5. Iji M., Serizawa, S. and Inoue, K., Development of polylactic acid with kenaf and its application to electronic products, *Seikei-Kakou (J. JSPP)*, **15**, 602–604 (2003) (in Japanese).
6. Morton, W.E. and Hearle, J.W.S., *Physical Properties of Textile Fibers*, (1962) The Textile Institute & Butterworths, Manchester and London.
7. Hearle, J.W.S., Grosberg, P. and Backer, S., *Structural Mechanics of Fibers, Yarns*

and Fabrics, Vol. I (1969) John Wiley & Sons, Inc., New York.
8. Hearle, J.W.S. and Konopasek, M., On united approaches to twisted yarn mechanics, *Appl. Polym. Symp.*, **27** 253–273 (1975).
9. Shah, A. N. and Lakkad, S. C., Mechanical properties of jute-reinforced plastics, *Fibre Sci. Technol.*, **15**, 41–46 (1981).
10. Mukherjea, R.N., Pal, S.K., Sanyal, S.K., Studies on jute fiber composites with polyesteramide polyols as interfacial agent, *J. Appl. Polym. Sci.*, **28**, 3029–3040 (1983).
11. Pal, P.K., Jute reinforced plastics: a low cost composite material, *Plast. Rubber Process. Appl.*, **4**, 215–219 (1984).
12. Sanadi, A.R., Prasad, S.V., Rohatgi, P.K., Natural fibers and agro-wastes as fillers and reinforcements in polymer composites, *J. Sci. Ind. Res.*, **44**, 437–442 (1985).
13. Prashant, K., Mechanical behavior of jute fibers and their composites, *Indian J. Technol.*, **24**, 29–32 (1986).
14. Chand, N., Tiwary, R.K., Rohatgi, P.K., Bibliography resource structure properties of natural cellulosic fibres – an annotated bibliography, *Mater. Sci.*, **23**, 381–387 (1988).
15. Mohanty, A.K. and Misra, M., Studies on jute composites – a literature review, *Polym. Plast. Technol. Eng.*, **4**, 729–792 (1995).
16. Mohan, R., Kishore, A., Shridhar, M.K., and Rao, R.M.V.G.K., Compressive strength of jute-glass hybrid fibre composites, *J. Mater. Sci. Lett.*, **2**, 99–102 (1983).
17. Varma, I.K., Anantha Krishnan, S.R. and Krishnamoorthy, S., Composites of glass/modified jute fabric and unsaturated polyester resin, *Composites*, **20**, 383–388 (1989).
18. Parameswaran, V.S., Krishnamoorthy, T.S. and Balasubramanian, K., Current research and applications of fiber reinforced concrete composites in India, *Transp. Res. Rec.*, **1226**, 1–6 (1989).
19. Sethunarayanan, R., Chockalingam, S., Ramanathan, R, Natural fiber reinforced concrete, *Transp. Res. Rec.*, **1226**, 57–60 (1989).
20. Tomari, M. and Harago, Y., *Amazon no Hatake de Toreru Mercedes-Benz* (1997) Tsukiji-Shokan, Tokyo (in Japanese).
21. Herrmann, A.S., Nickel, J. and Riedel, U., Construction materials based upon biologically renewable resources, *Polym. Degrad. Stab.*, **59**, 251–261 (1998).
22. Luo, S. and Netravali, A.N., Interfacial and mechanical properties of environment-friendly 'green' composites made from pineapple fibers and poly (hydroxybutyrate-co-valerate) resin, *J. Mater. Sci.*, **34**, 3709–3719 (1999).
23. Suzuki, K., Kimpara, I., Saito, H. and Funami, K., Cross-sectional area measurement and monofilament strength test of kenaf bast fibers, *J. Soc. Mater. Sci. Jpn.*, **54**, 887–894 (2005) (in Japanese).
24. Tanabe, K., Matsuo, T., Gomes, A., Goda, K. and Ohgi, J., Strength evaluation of curaua fibers with variation in cross-sectional area, *J. Soc. Mater. Sci. Jpn.*, **57**, 454–460 (2008) (in Japanese).
25. Silva, F. A., Chawla, N., Filho, R. D. T., Tensile behavior of high performance natural (sisal) fibers, *Compos. Sci. Technol.*, **68**, 3438–3443 (2008).
26. (a) Virk, A.S., Hall, W. and Summerscales, J., Multiple data set (MDS) weak-link scaling analysis of jute fibres, *Composites Part A*, **40**, 1764–1771 (2009); (b) Virk, A. S., Hall, W. and Summerscales, J., Tensile properties of jute fibres, *Mater. Sci. Technol.*, **25**, 1289–1295 (2009).
27. Xu, X.W. and Jayaraman, K., An image-processing system for the measurement of the dimensions of natural fiber cross-section, *J. Comput. Appl. Technol.*, **34** (2), 115–121 (2009).
28. Goda, K., Current status and future prospects of biocomposites II: strength evaluation of plant-based natural fibers for green composites, *J. Soc. Mater. Sci. Jpn.*, **59** (12), 977–983 (2010) (in Japanese).
29. Gassan, J., Chate, A. and Bledzki, A.K., Calculation of elastic properties of natural fibers, *J. Mater. Sci.*, **36**, 3715–3720 (2001).
30. Baley, C., Analysis of the flax fibres tensile behaviour and analysis of the tensile

stiffness increase, *Composites Part A* **33** 939–948 (2002).
31. Xu, P. and Liu, H., Models of microfibril elastic modulus parallel to the cell axis, *Wood Sci. Technol.*, **38**, 363–374 (2004).
32. Andersons, J., Porike, E. and Sparnins, E., The effect of mechanical defects on the strength distribution of elementary flax fibres, *Compos. Sci. Technol.*, **69**, 2152–2157 (2009).
33. Shioya, M., Itoh, T., Kunugi, T. and Takaku, A., Variation of longitudinal modulus with twist for yarns composed of high modulus fibers, *Text. Res. J.*, **71** (10), 928–936 (2001).
34. Yoshida, K., Kurose, T., Nakamura, R., Noda, J., and Goda, K., Effect of yarn structure on mechanical properties of natural fiber twisted yarns and green composites reinforced with the twisted yarn, *J. Soc. Mater. Sci. Jpn.*, **61** (2), 111–118 (2012) (in Japanese).
35. Ashori, A., Wood–plastic composites as promising green-composites for automotive industries! (Review Paper) *Bioresour. Technol.*, **99**, 4661–4667 (2008).
36. Felix, J.M. and Gatenholm, P., Nature of adhesion in composites of modified cellulose fibers and polypropylene, *J. Appl. Polym. Sci.*, **42**, 609–620 (1991).
37. Kazayawoko, M., Balatinecz, J. and Matuana, L.M., Surface modification and adhesion mechanisms in woodfiber-polypropylene composites, *J. Mater. Sci.*, **34**, 6189–6199 (1999).
38. La Mantia, F.P. and Morreale, M., Green composites: a brief review, *Composites Part A*, **42**, 579–588 (2011).
39. Takatani, M. and Okamoto, T., Wood/plastic composite of high filler content, *Mol. Cryst. Liq. Cryst.*, **483**, 326–338 (2008).
40. Abe, K., Iwamoto, S. and Yano, H., Obtaining cellulose nanofibers with a uniform width of 15 nm from wood, *Biomacromolecules*, **8**, 3276–3278 (2007).
41. Okabe, T., *et al.*, *Wood Ceramics*, (1996) Uchida Rokakuho, Tokyo (in Japanese).
42. Sekkuden, M., Yamamura, T., Okazawa, T., Sano, T., Tanaka, K., Goda, K., Ogawa, K., and Okabe, T. (2012) Eco-friendly utilization of uniform cloths waste – composites with PVA and anti-fungal biomass oil. Proceedings of the 10th International Conference on Ecomaterials (ICEM-10), pp. 203–206.
43. Shima, H., Takahashi, H., and Mizuguchi, J., Recovery of glass fibers from fiber reinforced plastics, *Mater. Trans.*, **52**, 1327–1329 (2011).
44. Liu, Y., Liu, J., Jiang, Z. and Tang, T., Chemical recycling of carbon fibre reinforced epoxy resin composites in subcritical water: synergistic effect of phenol and KOH on the decomposition efficiency, *Polym. Degrad. Stab.*, **97** (3), 214–220 (2012).

2
Synthesis, Structure, and Properties of Biopolymers (Natural and Synthetic)

Raju Francis, Soumya Sasikumar, and Geethy P. Gopalan

2.1
Introduction

Natural biodegradable polymers are, in general, called *biopolymers* and they have broad applications in various fields of the economy. They are large macromolecules composed of single or many repeating monomer units. These polymers are of very high molecular weight and monomer composition influences their material characteristics. Polysaccharides such as starch and cellulose signify the most characteristic family of these natural polymers. Other natural polymers such as proteins can also be used to produce biodegradable materials [1–8]. However, the synthetic applications of polynucleotides are limited owing to the fact that the field is still in the growing stage. Starch, fibers, and so on are the most common biopolymers and they can be incorporated into a variety of biological materials. Each biopolymer has its own material-specific properties, for example, toughness, crystallinity, barrier properties such as oxygen permeability. The packaging industry has special significance because more than 60% of the synthetic polymer products are used in this industry, according to a US statistics (Figure 2.1). Figure 2.1 also shows that the maximum postconsumer waste is produced by the packaging industry, according to the data prepared in the year 2000. Here, more than 90% of the material corresponds to nonbiodegradable thermoplastics. But recently, there have been a large number of reports on the use of biodegradable polymers in the packaging industry [9]. The barrier properties are relevant to the choice of biopolymers for the packaging of particular products. Bioplastics have very promising prospects for use in packaging in-flight catering products, for packaging dairy products, and in pesticide soil pins. The predominant mechanism in the case of biodegradable materials, which makes them capable of undergoing decomposition into carbon dioxide, water, inorganic compounds, methane, or biomass, is the enzymatic action of microorganisms. This biodegradation can be measured by reported procedures and thereby establish the natural processes of disposal [9].

Over the last decade, depletion in the petroleum reserves has resulted in the emergence of biodegradable polymers as a possible alternative to traditional plastics [9]. In addition, increased production of these plastics has proven to be a severe

Polymer Composite: Volume 3, First Edition.
Edited by Sabu Thomas, Kuruvilla Joseph, S. K. Malhotra, Koichi Goda and M. S. Sreekala.

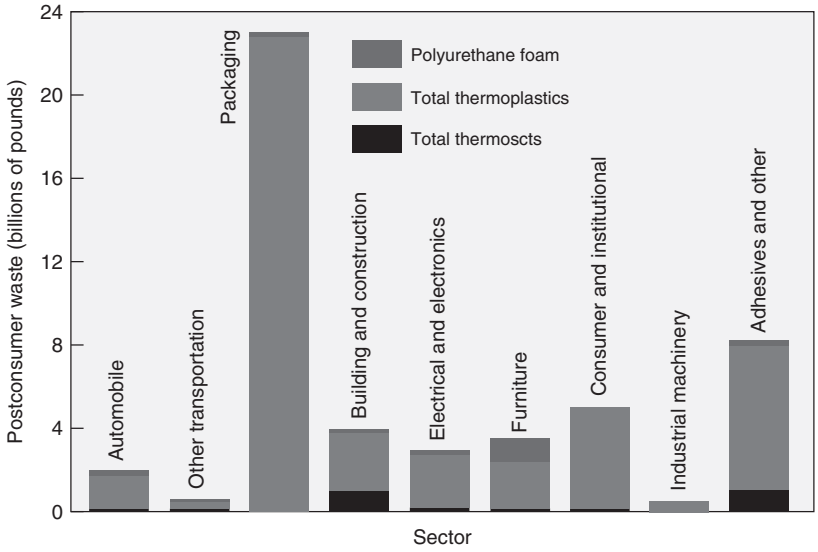

Figure 2.1 A projection of postconsumer plastic waste is shown for different sectors in the year 2000.

threat to the environment. Plastic disposal is a major concern because plastics are nonbiodegradable in nature. Hence, biodegradable polymers are considered to be a potential solution because of their biocompatibility, making them suitable for various applications [10]. Natural polymers or agro-polymers are renewable sources that are formed in nature during the growth cycles of all organisms. The use of biorenewable resources for the production of biopolymers has gained a huge amount of interest over the past decade because of their low cost and ready availability [11].

The interest toward biopolymers is mainly due to their biodegradability. Nonbiodegradable polymers have raised questions on sustainability of the environment from all walks of life. Biodegradability is sometimes initiated by nonbiological degradation such as photodegradation, oxidation by atmospheric oxygen, and hydrolysis. Biological degradation takes place through the actions of enzymes or by-products (such as peroxides and acids) secreted by microorganisms (bacteria, fungi, and yeast) [12–14]. Hydrolyzable or oxidizable groups are present along the main chain in most of the natural biodegradable polymers and synthetic biodegradable polymers [15].

Biopolymers are most commonly used for the following purposes:

1) Packaging (wraps, food containers, nets, foams)
2) Plastic bags for collection and composting of food waste and as carrier bags
3) Catering products (plates, cutlery, cups straws, etc.)
4) Agriculture (plant pots, mulch films, nursery films, etc.)
5) Hygiene products (wound healing pads, diapers, etc.)
6) Medical and dental implants (artificial teeth, sutures, etc.).

2.2
Classification

Biopolymers are polymers that are environmentally benign. They contain monomeric units that are covalently bonded to form larger structures. There are two main classes of biopolymers:

1) Natural biopolymers
2) Synthetic biopolymers.

Figure 2.2 presents the general classification of biopolymers. Natural biopolymers are further divided into various types of proteins, polysaccharides, and nucleic acids. On the other hand, a general classification is not possible for synthetic biopolymers. However, they can be classified in a broad sense according to the method of preparation. For instance, biopolymers synthesized by condensation and addition polymerization reaction are listed separately.

2.3
Natural Biopolymers

Natural polymer materials serve as fundamental templates for the existence of life on earth. All of them have specific functions and structural identity. They are broadly divided into proteins, polysaccharides, and nucleic acids. Among the three basic natural biopolymers, the type, units, and function can be given broadly as follows (Table 2.1) [16].

Here, it is interesting to note that one amino acid on combining with itself or with another amino acid gives only one type of compound called a *dipeptide*.

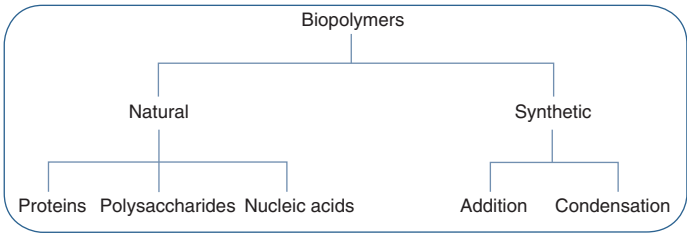

Figure 2.2 General classification of biopolymers.

Table 2.1 The type, units, and function of the three basic natural biopolymers.

Type	Unit (monomer)	Function
Oligopeptide	Amino acid	Builds/destroys
Oligosaccharide	Sugar	Gatekeepers
Oligonucleotide	Nucleic acid	Gives orders

Similarly, the combination of two nucleotides will give a dinucleotide. In contrast to this, the combination of two sugar molecules will give large number of variants of oligosaccharides – approximately 20. This clearly indicates that there are structurally different molecules of polysaccharides, whereas such variations are limited in the case of proteins and polynucleotides. Hence it is important to see that the bulk of the biopolymers for commercial exploitation come from polysaccharides.

2.3.1 Proteins

The basic structural units in proteins are amino acids connected via peptide bonds that are nothing but amide linkages. All the 20 natural amino acids are called *oligopeptides* and *polypeptides* according to the size of the peptide. Among them, glycine is the only amino acid that is not optically active. The basic amino acid sequence represents the primary structure and the secondary structure is represented by the helical or β-pleated structures formed by hydrogen bonds. The tertiary structure of a protein is represented by the formation of disulfidic linkages or other intramolecular bonds that represent the three-dimensional structure of a protein. Finally, the quaternary structure is formed by the specific joining of more than one protein molecule. The primary functions of living systems in terms of skeleton, growth, and regulation are controlled by the protein molecules. Biologically, proteins are synthesized by the command obtained from the deoxyribonucleic acid (DNA). Depending on the codon present, each protein molecule is synthesized for a particular function. The synthesis is carried out on ribonucleic acid (RNA) by attaching specific amino acids through peptide linkages one by one, when the required polypeptide is formed. The various steps involved in protein synthesis, namely, initiation, elongation, and termination are depicted in Figure 2.3. These steps are very similar to the steps in a polymerization reaction except for the fact that protein synthesis occurs in a physiological environment. The structure of a protein has a great influence on its function. Hence, understanding the structure of proteins is of supreme importance. The most modern techniques such as X-ray crystallography and other microscopic techniques are employed to develop the structure of proteins. The α-helix and β-pleated sheets are represented along with the random arrangement. The given picture shows the crystal structure of a protein considerably simplified to represent only the overall shape and groves present in it (Figure 2.4). Here, the straight ribbonlike portion represents a β-pleated sheet and the helical ribbon represents the α-helix. In a protein, these are generally crystalline regions and the loose bonds are amorphous.

Proteins and other amino acid-derived polymers have been a favored biomaterial for sutures, scaffolds for tissue engineering, drug delivery vehicles, and hemostatic agents, as they serve as a major component of natural tissues. For instance, silk was studied for various biomedical applications decades ago [17, 18]. Furthermore, protein-based biomaterials are known to undergo naturally controlled degradation processes.

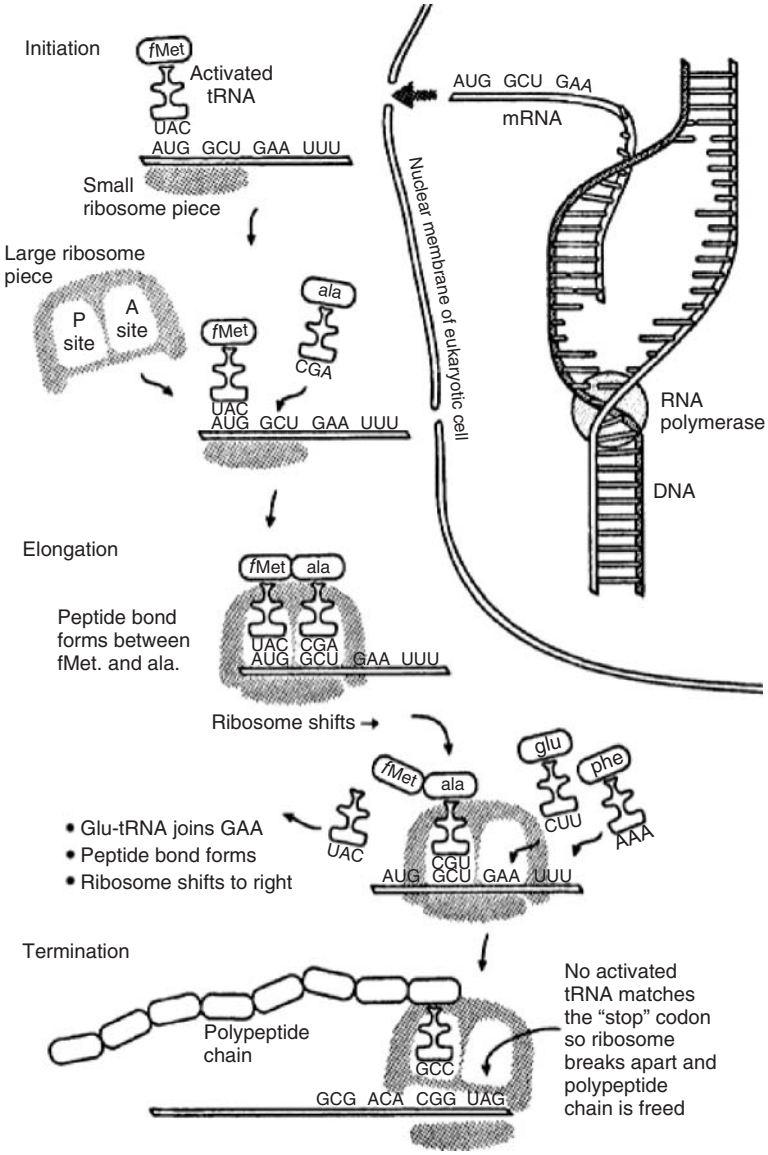

Figure 2.3 Cartoon showing protein synthesis in a cell.

2.3.1.1 **Collagen**

Collagen is a major structural protein that provides structure to all animal bodies, shielding and supporting the softer tissues and connecting them with the skeleton. The tendons and vast, resilient sheets that support the skin and internal organs are strengthened by the molecular strands formed by collagen. Bones and teeth are composed of collagen combined with mineral crystals, mainly hydroxyapatites

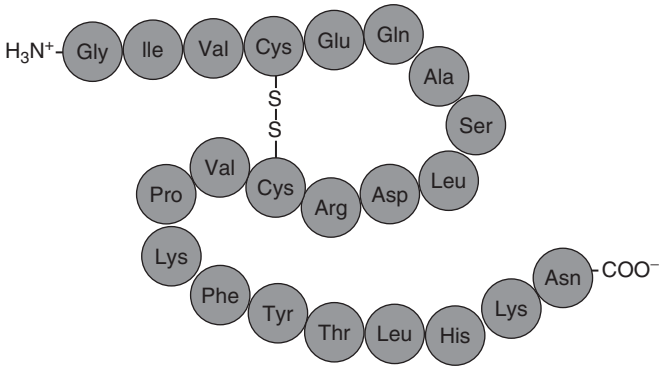

Figure 2.4 Simplified skeletal structure of a protein.

(HAPs). Collagen is a rod-type polymer nearly 300 nm long with a molecular weight of 300 000 Da and each chain contains 1000 amino acids. Collagen may be processed into a variety of formats, including sheet, sponge, and gel and can be cross-linked with chemicals or put through physical treatments to make it stronger or alter its degradation rate [19–22]. There are more than 22 different types of collagen in the human body. The most common types of collagen are Types I–IV and Type I collagen is the single most abundant protein present in mammals. Type I collagen is composed of three polypeptide subunits with similar amino acid compositions. Each polypeptide is made up of about 1050 amino acids, containing approximately 33% glycine, 25% proline, and 25% hydroxyproline with a relative abundance of lysine [23]. These collagen types can be found as part of fibrillar structures that form an essential part of tissue architecture and integrity [24–29]. The ability to form fibers with extra strength and stability through its self-aggregation and cross-linking is the major reason for the usefulness of collagen in

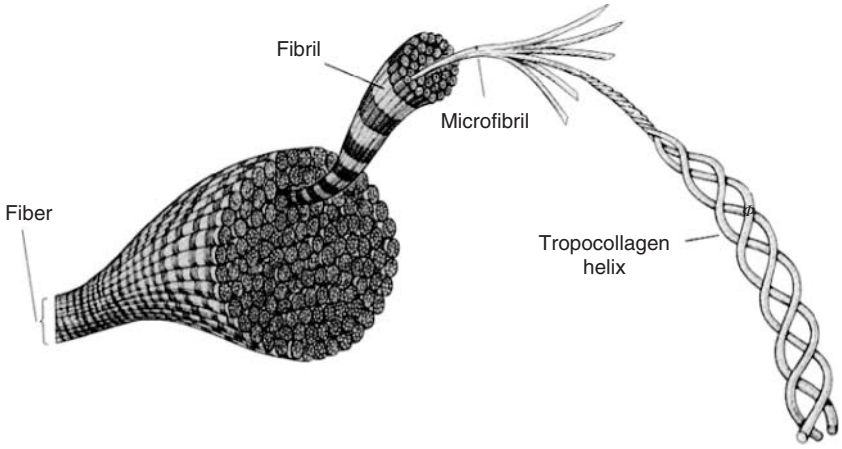

Figure 2.5 Cartoon structure of collagen showing the packing.

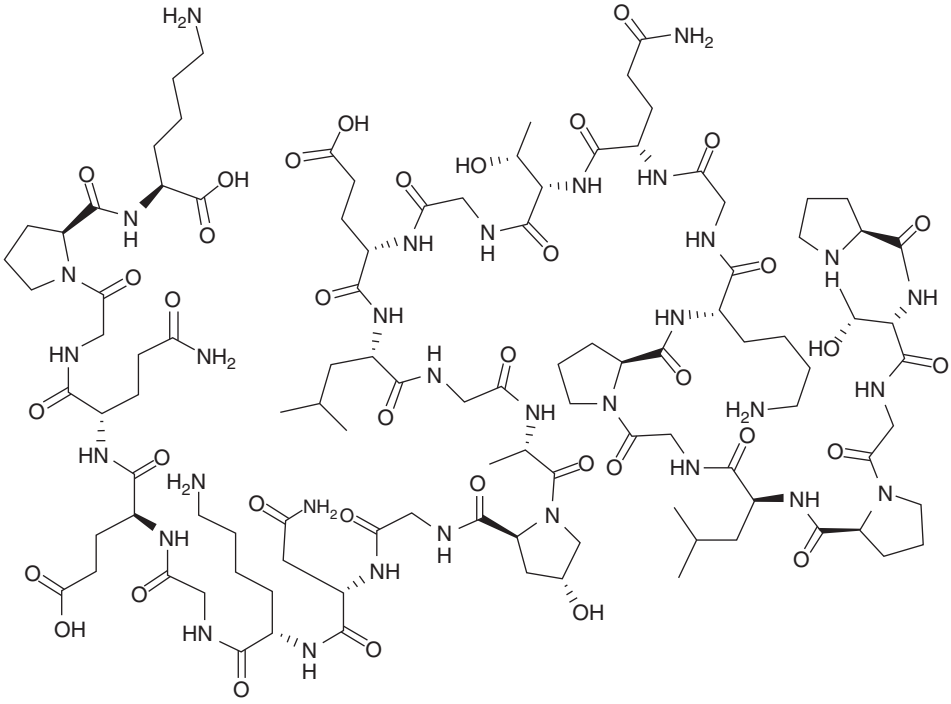

Figure 2.6 Collagen Type II fragment showing the amino acid sequences.

biomedical applications. It has been comprehensively investigated for the localized delivery of low molecular weight drugs including antibiotics [30]. Figure 2.5 shows the cartoon of collagen fibers joined in the nanoscale to form a macrostructure. Collagen is built up of single strands that form triple helices, which then further assemble into bundles and fibers [31]. A more representative structure of collagen with the amino acid sequences is presented in Figure 2.6.

Collagen has been extensively used for the regeneration of tissues, predominantly for the repair of soft tissues. It favors cell adhesion and provides cellular recognition for regulating cell attachment and function. Collagen undergoes enzymatic degradation in the body by means of enzymes, such as collagenases and metalloproteinases, to yield the corresponding amino acids [30]. This enzymatically degradable biopolymer shows unique physicochemical, mechanical, and biological properties in various applications. It can be processed in sheets, fleeces, injectable viscous solutions, dispersions, tubes, sponges, foams, and nanofibrous powders. The degradation rate can be modified by various treatments. Novel spongy collagen matrix containing oxidized cellulose has been recently introduced in US and European markets for treating exuding diabetic and ulcer wounds [32, 33]. Degradable collagen sponges have been broadly studied as scaffold material for accelerated tissue reproduction, owing to their excellent biocompatibility and porous structure. The composite of collagen, HAP, and TCP (tricalcium phosphate) is used as a

biodegradable synthetic in bone graft replacement. It has wide applications as scaffold for musculoskeletal and nervous tissue engineering. Bovine or porcine skin or bovine or equine Achilles tendons are the major sources of collagen currently used for biomedical applications. One major disadvantage of these collagen-based biomaterials, which is a limiting factor for the extensive clinical application, is their mild immunogenicity imparted by the composition of the terminal region and the antigenic sites in the central helix [26]. Collagen shows variable physical, chemical, and degradation properties and is difficult to handle owing to the risk of infection [27]. Oral drug molecules, for instance, proteins coated with collagen, have already been marketed.

2.3.1.2 **Elastin**

Elastin contains glycine, proline, and alanine as the main amino acids and it is an extracellular matrix (ECM) protein, which is major component of skin, blood vessels, such as the aorta, and lung tissues in mammals. Elastin is a highly cross-linked insoluble polymer composed of a number of covalently bonded tropoelastin molecules. Elastin has specific cross-linkages – desmosine and isodesmosine, which account for the formation of a three-dimensional network with 60–70 amino acids between two cross-linking points [34, 35]. Multifunctional cross-linking agents that are also amino acids are presented in it. The cross-linking agents commonly found in elastin are shown in Figure 2.7. The tropoelastin molecules are produced intracellularly by smooth muscle cells and fibroblasts and they are cross-linked extracellularly to form a secondary structure with β-turns [36]. The tropoelastin is composed of numerous repeating sequences of the pentapeptide VPGVG, hexapeptide APGVGV, nonapeptide VPGFGVGAG, and the tetrapeptide VPGG. Among these, the pentapeptide VPGVG recurs up to 50 times in a single molecule [36]. Elastin has been evaluated as biological coating for synthetic vascular grafts owing to its minimal interaction with platelets [37].

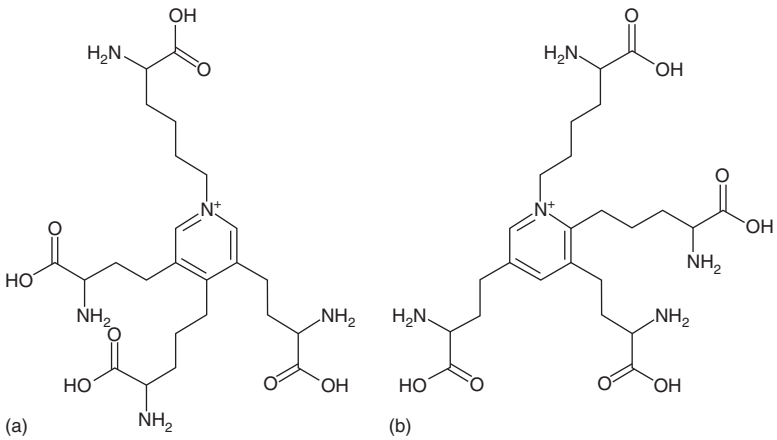

Figure 2.7 Cross-linking agents in elastin: the amino acids desmosine (a) and isodesmosine (b).

Although it is extremely difficult to blend elastin with synthetic polymers, it forms an excellent basis for biomaterials, such as dermal substitute, arterial prosthesis, hydrogels, and for scaffolds [38–42].

2.3.1.3 **Albumin**

Albumin has a high content of cystine and charged amino acids, such as aspartic and glutamic acids, lysine and arginine, and a low content of tryptophan and methionine [43], and it is the most abundant water-soluble protein in human blood plasma, accounting for almost 50% of total plasma mass. It has a molecular weight of 66 kDa. A portion of human serum albumin is shown in Figure 2.8. Albumin can be easily processed into various shapes and forms such as membranes, microspheres, nanofibers, and nanospheres owing to its solubility and the presence of functional groups along the polymer chain. The basic function of albumin is to carry hydrophobic fatty acid molecules through the bloodstream and maintain blood pH. Preproalbumins are synthesized in the liver and undergo further processing before getting released into the circulatory system. Owing to its excellent blood compatibility, albumin has been extensively investigated as a carrier vehicle for intravenous drug/gene delivery [44]. Albumin-based surgical adhesives have also been approved by the US Federal Drug Administration (FDA) for reapproximating the layers of large vessels, such as femoral and carotid arteries and aorta, and are composed of bovine serum albumin, glutaraldehyde, and gelatin. Albumin is also used as coating in cardiovascular devices [45].

2.3.1.4 **Fibrin**

Fibrin, a biopolymer similar to collagen, is involved in the natural blood-clotting process. Fibrinogen, which is a 360 kDa protein, composed of three pairs of polypeptide chains is the source of fibrin. The structure of fibrin can be divided into three major sections consisting of a central domain composed of fibrinopeptide E with two pairs of fibrinopeptide A and B molecules and two terminal domains of fibrinopeptide D. Spontaneous fibrillogenesis is the formation of a linear fibril by

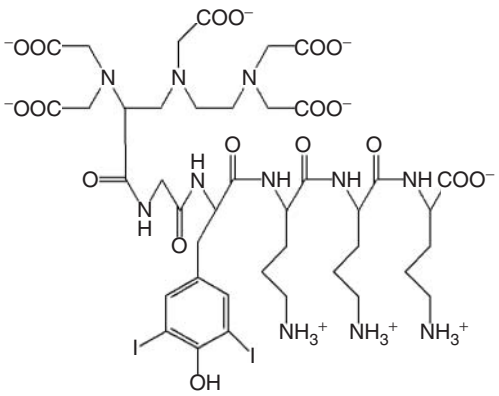

Figure 2.8 A portion of human serum albumin.

the cleavage of fibrinopeptide A and B in the presence of enzyme thrombin, which undergoes lateral association to form fibers of varying diameters ranging from 10 to 200 nm, according to the changes in environmental conditions. These fibrin clots, once formed, can undergo degradation called *fibrinolysis* in the body, initiated by a complex cascade of enzymes present in the human body [46].

Owing to the excellent biocompatibility, biodegradability, injectability, and the presence of several ECM proteins, such as fibronectin (FN), that favorably affect cell adhesion and proliferation, fibrin has broad applications as a biomaterial. One of the first products developed from fibrin was a fibrin sealant. Worldwide, various fibrin sealant products are being used clinically for hemostasis and tissue-sealing applications in various surgical procedures. Owing to its injectability and biodegradability, fibrin has also been investigated as a carrier vehicle for bioactive molecules. It has been found that proteins interact differently with fibrin clots, with certain growth factors demonstrating a strong interaction with fibrin matrices [47].

2.3.1.5 **Fibronectin**

FN is a very large glycosylated protein of about 450–550 kDa. It forms a main constituent of ECM around and beneath many cells containing a complex structural organization made of two chains connected at their carboxyl termini by a pair of disulfide bonds. Each subunit is composed of three types of repeating modules, called *FNI*, *FNII*, and *FNIII* (12, 2, and 15 copies, respectively). The modules are linearly connected by short chains of variable flexibility. Characterization methods such as X-ray crystallography and NMR spectroscopy were used to elucidate the structure of some individual modules or short fragments. The structure of these modules is found as being mainly β-sheet, and the three types of modules are considered globular [48].

FN is largely responsible for the functional properties of ECM, including cell adhesion, migration, and proliferation [49, 50]. It has broad applications in cellular research into proliferation, development, differentiation, and morphology. Precoating of plastic, glass, and microcarrier beads aids cell attachment, particularly of that cell which is deficient in cell surface FN. The proteolytic digests of FN are mitogenic for fibroblasts that will bind to commonly used cell-culture surfaces. The various cell-connecting domains of FN are given in Figure 2.9. It can increase plating efficiency of fastidious cells and cloning efficiency. Variation in plating efficiency found in different serum batches can be minimized by using FN [19].

2.3.1.6 **Zein**

Zein is an alcohol-soluble protein contained in the endosperm tissue of Zeamais and occurs as a by-product of corn processing. It is a natural film-forming polymer and is inherently resistant to water and grease penetration. Although zein has been empirically used as an edible coating for foods and pharmaceuticals for many decades, it has not attracted significant attention as a potential alternative for film-forming agents in drug formulations such as derivatives of cellulose or polyacrylates [51] (Figure 2.10). It might serve as an inexpensive and most efficient substitute for the fast-disintegrating synthetic and semisynthetic film coatings

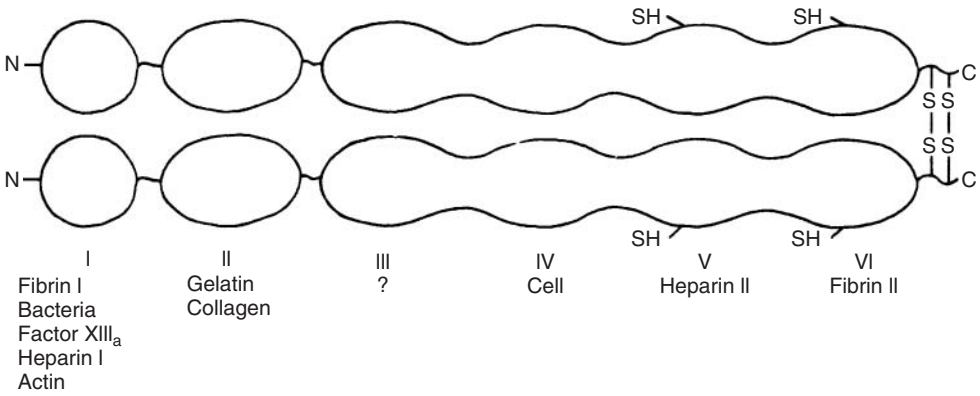

Figure 2.9 Functional domains of fibronectin.

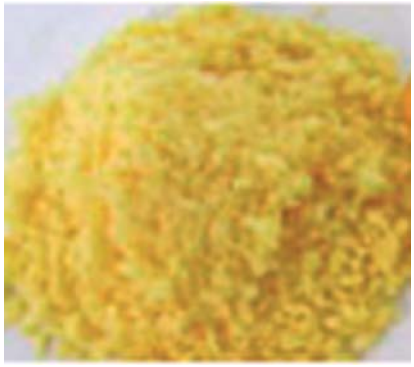

Figure 2.10 Zein powder.

currently used for the formulation of substrates that allow extrusion coating [52]. Biodegradable plastics or thermoplastic can be made from zein. It is nonallergenic, which allows its use in food products.

2.3.1.7 **Gluten**

Gluten, a fully biodegradable, nontoxic, protein composite found in foods processed from wheat and related grain species, including barley and rye (a type of wheat), is a storage endosperm protein, which is used today as a wheat protein marker. Gluten is a direct gene product, having a complex genetic determination and is a big natural biopolymer. The two basic structural characteristics of gluten are its evolutionary conservatism and, at the same time, its relatively high degree of polymorphism [53]. It is readily obtainable in high quantity and at low cost.

Wheat gluten is a combination of a *gliadin* and a *glutelin* (Figure 2.11). Gliadins, the glycoproteins containing only intramolecular disulfide links are mainly present in wheat and several other cereals within the grass genus. These glycoproteins are slightly soluble in ethanol. They have low molecular weight and a low level of aminoacids with charged side groups. Glutelins have a three-dimensional structure

Figure 2.11 Structure of gluten, a hybrid of gliadin and glutenin.

and are soluble in dilute acids and bases. Because of their complicated structure, their molecular weight is at least 10 times higher than that of gliadins. Wheat gluten materials have the fastest degradation rates.

Excellent films can be formed with wheat gluten. While preparing wheat gluten films, a plasticizer must be used to decrease the brittleness of the films [54]; there are reports on the effects of glycerol, water, and sorbitol on the glass-transition temperature of wheat gluten [55]. Glycerol and sorbitol have high molecular weights and low evaporation rates and this reduces their plasticizing effect to less than that of water. When gluten is plasticized with glycerol, a malleable phase [56, 57] resembling a structured viscoelastic solid with pseudoplastic behavior is obtained. As cross-linking reactions occur at temperatures higher than 60 °C, the temperature range of the use of wheat gluten is limited [54].

2.3.1.8 **Gelatin**

Gelatin, which is obtained by the partial hydrolysis of collagen inside animals' skin and bones, is a transparent, colorless, brittle (when dry), flavorless, solid, water-soluble protein compound containing 19 amino acids and a mixture of peptides and proteins. Since collagen is the main fibrous protein constituent in bones, cartilages, and skins, the source, age of the animal, and type of collagen, are all important factors influencing the properties of gelatins [58]. A general repeat unit found in gelatin is presented in Figure 2.12. In water, gelatin forms a highly viscous solution that sets to a gel on cooling. The chemical composition of gelatin resembles that of collagen. Gelatin has the ability to form a homogeneous gel for concentrations in the range of approximately 1–50% and below this range there are insufficient molecules to support an infinite three-dimensional gel network [59–61].

The mechanical and barrier properties of the gelatin films are influenced by the physical and chemical characteristics of gelatin, especially the amino acid

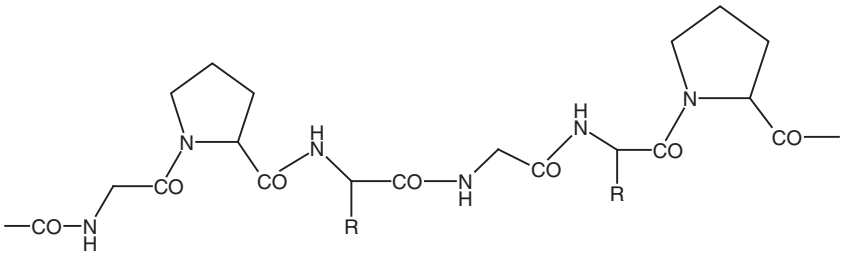

Figure 2.12 A general repeat unit found in gelatin.

composition and the molecular weight distribution. The physical properties of gelatin films can be improved by combining gelatin with other biopolymers such as oils and fatty acids, soy protein, or certain polysaccharides [62]. Mechanical and water vapor barrier properties of gelatin films are also influenced by the plasticizers used [63]. Gelatin can also be modified by means of grafting [64].

Gelatin is mainly used in cosmetic industry, photography, for decorating food items, and it has broad applications in the biomedical field as coatings and for microencapsulating various drugs [65]; these applications are based mainly on its gel-forming and viscoelastic properties. Gelatin has excellent applications in the food industry as emulsifiers, foaming agents, fining agents, colloid stabilizers, biodegradable packaging materials, and microencapsulating agents [66].

2.3.1.9 **Soy Protein**

Soy protein, a protein isolated from soybean (Figure 2.13), is a widely used food ingredient owing to its emulsification and texturizing properties. It is generally considered as the storage protein held in discrete particles called *protein bodies*. Soy protein can aid in preventing heart problems and therefore, of late, its popularity has increased at a fast rate. Depending on the method of production, the different categories of soy proteins are soy protein isolate, soy protein concentrate, and textured soy protein (TSP). Soy protein isolate contains about 90% protein and is the most refined form of soy protein. Soy protein concentrate is basically soybean without the water-soluble carbohydrates, containing about 70% protein [67]. TSP is made from soy protein concentrate by giving it some texture. The major proteins stored in soybean are globulins [68]. Because of their hydrophilic nature, soy protein films do not have good mechanical and barrier properties as do most protein films, and they are used to produce flexible and edible films.

Soy protein has been regarded as a practical substitute to the petroleum polymers in the manufacture of plastics, adhesives, and packaging materials [69] Water sensitivity and poor mechanical performance, which limit the applications of soy

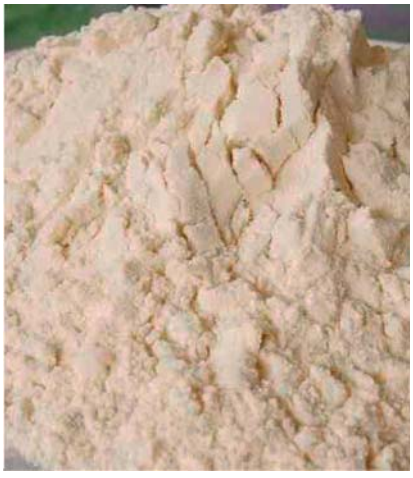

Figure 2.13 Soy powder.

protein materials [70], could be resolved, for example, by blending with polyurethane (PU) [71], gelatin [72], natural rubber [73], cellulose derivates [74], chitosan [75, 76], lipid [77], and beeswax [78], filling with nanoparticles [79], or by chemical modification [80].

2.3.1.10 **Whey Protein**

Caseins and whey are the two major sources of protein in milk (Figure 2.14). After processing occurs, the whey remains in an aqueous environment, while caseins are the proteins responsible for making curds. Whey protein is a mixture of globular proteins isolated from whey. Whey was considered a cure-all used to heal ailments ranging from gastrointestinal complaints to joint and ligament problems. Whey is a popular dietary protein supplement supposed to provide immune modulation, antimicrobial activity, improved body composition and muscle strength, and to prevent cardiovascular disease and osteoporosis. The components of whey include β-lactoglobulin, immunoglobulins, lactoperoxidase enzymes, α-lactalbumin, bovine serum albumin, lactoferrin, glycomacropeptides, lactose, and minerals [81]. Whey proteins have all the essential amino acids and in higher concentrations when compared to various vegetable protein sources such as soy, corn, and wheat gluten. It has strong antioxidant activity, by contributing cysteine-rich proteins that help in the synthesis of glutathione (GSH), a powerful intracellular antioxidant [81] containing glycine, cysteine, and glutamate.

2.3.1.11 **Casein**

Caseins are a family of phosphoproteins (α_{s1}, α_{s2}, β, κ) synthesized in the mammary gland in response to lactogenic hormones and other stimuli. It is secreted as large colloidal aggregates termed *micelles*, which account for many of the unique physical properties of milk and is a widely studied food protein [82]. An optical photograph of casein powder is shown in Figure 2.15. These proteins are commonly found in mamallian milk – cow's milk contains 80%, while human milk contains between 20% and 45% [83]. It is a major component of cheese, and is used as a food additive and as binder for safety matches [84]. It is a food source that supplies carbohydrates, amino acids, and two inorganic elements, calcium and phosphorus [85]. Caseins have been used as the model to study mammary development and regulation [86] and they forms the largest protein component in most milks of industrial significance [87]. They are composed of two discrete fractions – one

Figure 2.14 Whey protein powder.

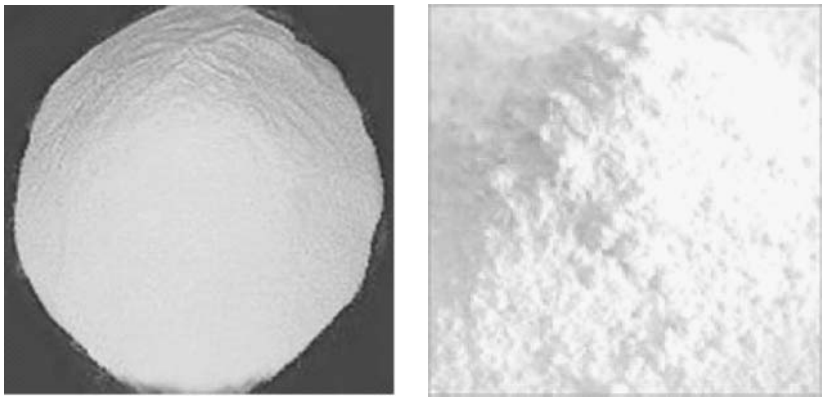

Figure 2.15 Optical photograph of Casein powder. (a) Edible acid casein powder and (b) technical acid casein.

that is precipitated in the presence of calcium, the calcium-sensitive caseins, and the other that is responsible for stabilizing the former against precipitation, the calcium-insensitive caseins [88]. The α-caseins, which are calcium-sensitive caseins, are characterized by their greater solubility in the presence of calcium. The α_{s1}- and α_{s2}-like families are classified on the basis of their amino acid sequence properties [89–91]. α_{s1}-Casein is the major protein fraction of bovine milk and is a highly phosphorylated protein. The bovine α_{s1}-casein exists as one major and one minor form containing 8 and 9 bound phosphate groups per molecule, respectively [92]. The amino acid sequence has been determined directly or inferred from DNA sequencing of the genes for the α_{s1}-caseins of a number of other eutherian species [93–98]. The α_{s2}-like caseins represent a more dissimilar group than the α_{s1}-caseins and they have been identified from a number of eutherian species – these include ruminant α_{s2}, rat γ, mouse γ and o, guinea pig casein A, and rabbit α_{s2a} and α_{s2b} caseins. The difference between α_{s1}- and α_{s2}-like caseins is based on their amino acid sequencing properties [90, 99–107]. Similar to the α_{s1}-caseins, the α_{s2}-like caseins are highly phosphorylated peptides. Bovine milk contains four differentially phosphorylated isoforms containing 10–13 phosphate groups per molecule [92, 102]. The β-casein family includes at least seven eutherian, and two marsupials, proteins for which the amino acid and nucleotide sequence is known [90, 108–118]. Bovine β-casein exists in one fully phosphorylated form containing 5 phosphate per molecule of protein. In the milk of other species (human, goat, and possum) β-casein has multiple phosphorylation states [119–122].

κ-Casein is the only eutherian casein that has conclusively been shown to contain carbohydrate moieties and it differs from the calcium-sensitive caseins in a number of respects. It is the only casein that is soluble in the presence of calcium ions and has a much smaller phosphate component than any of the other caseins. The phosphorylation sites are limited to the C-terminal region of the molecule and are present as single sites rather than the clusters found in the calcium-sensitive

caseins. The single peptide of κ-casein is 21 residues in length compared to 15 in calcium-sensitive caseins and these features have led to the conclusion that κ-casein is not related to the calcium-sensitive caseins [123–125].

2.3.1.11.1 Uses of Casein

Casein is one of the comprehensively studied natural proteins and technologically developed for various other applications [126].

1) *Paint*

Casein paints were very popular in early 1960s until the introduction of acrylic paint. It is a fast-drying, water-soluble medium used by artists and has been used since ancient Egyptian times as a form of tempera paint.

2) *Glue*

Casein-based glues were well liked for woodworking, including for aircraft, as late as the de Havilland Mosquito [127].

3) *Cheesemaking*

Cheese contains proteins and fat from milk, usually produced by coagulation of casein in which the milk is acidified and then rennet, containing a proteolytic enzyme, is added for coagulation. Then the solids are separated and made into final form [128].

Casein is not coagulated by heat. During the process of clotting, milk-clotting proteases operate on the soluble portion of the caseins, κ-casein, thus forming an unstable micellar state that results in clot formation. Casein is sometimes called *paracasein*, when coagulated with chymosin. Chymosins, an aspartic protease that specifically hydrolyzes the peptide bond in Phe_{105}–Met_{106} of κ-casein, are considered to be the most capable protease for the cheese-making industry [129]. On the other hand, British terminology uses the terms *caseinogen* for the uncoagulated protein and *casein* for the coagulated protein. Casein exists in milk as a salt of calcium.

4) *Plastics and fiber*

Some of the earliest plastics were based on casein and fiber can be made from extruded casein. In particular, galalith was well known for use in buttons. Lanital, a fabric made from casein fiber products, was very popular in Italy during the 1930s.

5) *Protein supplements*

The casein molecule has a striking property of forming a gel or clot in the stomach and this makes it very efficient in nutrient supply. The clot is able to give a constant, slow release of amino acids into the blood stream, sometimes lasting for several hours [130]. This provides better nitrogen retention and use by the body [131]. Plasma immunoreactive insulin-like growth factor-1 (IGF-1) concentration in rats given a casein diet was higher than that in rats given a soya-bean-protein or protein-free diet [132]. Body builders use casein to maintain an anabolic state because it digests very slowly [133].

6) *Medical and dental uses*

Tooth remineralization products contain casein-derived compounds that stabilize amorphous calcium phosphate (ACP) and release the ACP onto tooth surfaces, where it can facilitate remineralization [134, 135].

2.3.2 Polysaccharides

Polysaccharides are macromolecules formed from many monosaccharide units joined together by glycosidic linkages and they have unique biological functions ranging from cell signaling to immune recognition [23].

Many polysaccharides contain branched structures and are chemically modified by the addition of other molecules. Their monomeric or repeat units are often made up of more than one sugar molecule and, consequently, can be quite complex. They form protective capsules of some of the most virulent microorganisms, capsules that, nevertheless, carry information that activate mammalian defenses: the immune, interferon, and properdin systems [9, 136]. They are found as key portions of the exoskeletons of insects and arthropods and cell walls of plants and microbes and perform as reserve foodstuffs and important components of intercellular, mucous secretions, synovial and ocular fluids, and blood serum in many organisms. **Food Applications** compiles recent data on the food applications of marine polysaccharides from such various sources as fishery products, microorganisms, seaweeds, microalgae, and corals [137, 138]. One of the applications of this biopolymer relates to a method for protecting against diseases induced by *Streptococcus pneumoniae* infections, which comprises mucosal administration of a *S. pneumoniae* capsular polysaccharide to a patient in need.

2.3.2.1 Cellulose

Natural cellulose, a polysaccharide, is a linear natural polymer of β-(1 → 4)-D-glucopyranose possessing abundant surface hydroxyl groups that form abundant inter- and intramolecular hydrogen bonds (Figure 2.16). The polymer chains accumulate into elementary fibrils (diameter 1.5–3.5 nm), and bundle to microfibrils (nanofibers, diameter tens to hundreds of nanometers), further form randomly interconnected hierarchical networks of microfibrillar fibers (microfibers, diameter in the micrometer scale or larger), resulting in the familiar bulk cellulose

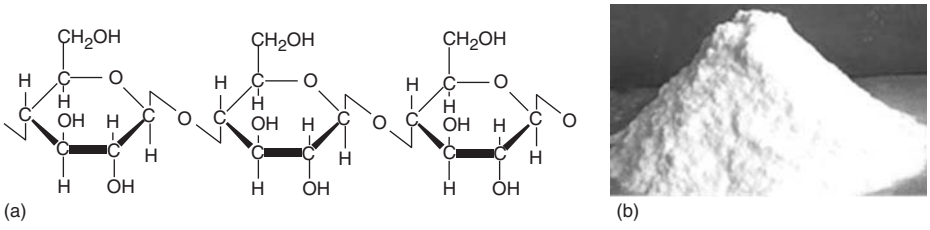

Figure 2.16 (a) Structure of cellulose and (b) cellulose powder.

Figure 2.17 Biodegradable cellulose tapes.

substances such as wood and cotton, and, moreover, in paper-based products after artificial processing. The wide hydrogen bond network forms a defined hierarchical order of supramolecular organization as well as the partially crystalline fiber domains, which contribute to the characteristic properties of cellulose substances such as hydrophilicity, strong mechanical properties, high flexibilities, and significant adsorption and swelling behaviors [139]. These low-cost, widely available, and easy-to-process hierarchical structured natural cellulose substances are good platforms for the design and preparation of advanced materials, either as scaffold, template, or precursor (Figure 2.17). Plasma treatment of cellulose sheets to etch amorphous domains of the fibers led to the increase of surface roughness and made the surfaces hydrophobic [140, 141]. Cellulose nanofibers were reported to aid the patterned growth of guest matters such as single-crystalline selenium [142] and polyelectrolyte complexes [143].

Biodegradation of cellulose progresses by enzymatic oxidation, with peroxidase secreted by fungi; it can also be degraded by bacteria. As for starch, the degradation products are nontoxic [144]. Cellulose should be transformed to become processable because of its insolubility and infusibility. Important derivatives of cellulose are produced by the reaction of one or more of the hydroxyl groups present in the repeating unit. Esters, ethers, and acetals are the main derivatives of cellulose. Cellulose esters are modified polysaccharides and various degrees of substitution can be obtained. Their mechanical properties and their biodegradation decrease when the degree of substitution increases [145, 146]. Cellulose acetate (CA) is one of the most important cellulose derivatives and the tensile strength of CA films is comparable to that of polystyrene. CA can be obtained from agricultural by-products [147].

A recent invention is directed to an aqueous ophthalmic solution comprising an effective amount of ketorolac, consisting of carboxymethyl cellulose, which promotes epithelial wound healing in a patient's cornea [148]. The degree of polymerization and the length of the polymer chain affect the properties of the cellulose polymers [149].

2.3.2.2 **Starch**

Starch, a well-known hydrocolloid biopolymer is a low cost polysaccharide, plentifully available and is one of the cheapest biodegradable polymers. It is produced by agricultural plants in the form of hydrophilic granules. Starch is mainly extracted from potatoes, wheat, corn, and rice. It is composed of amylose (poly-α-1,4-D-glucopyranoside), a linear and crystalline polymer, and amylopectin (poly-α-1,4-D-glucopyranoside and α-1,6-D-glucopyranoside), a branched and amorphous polymer. The relative amounts and molar masses of amylose and amylopectin vary

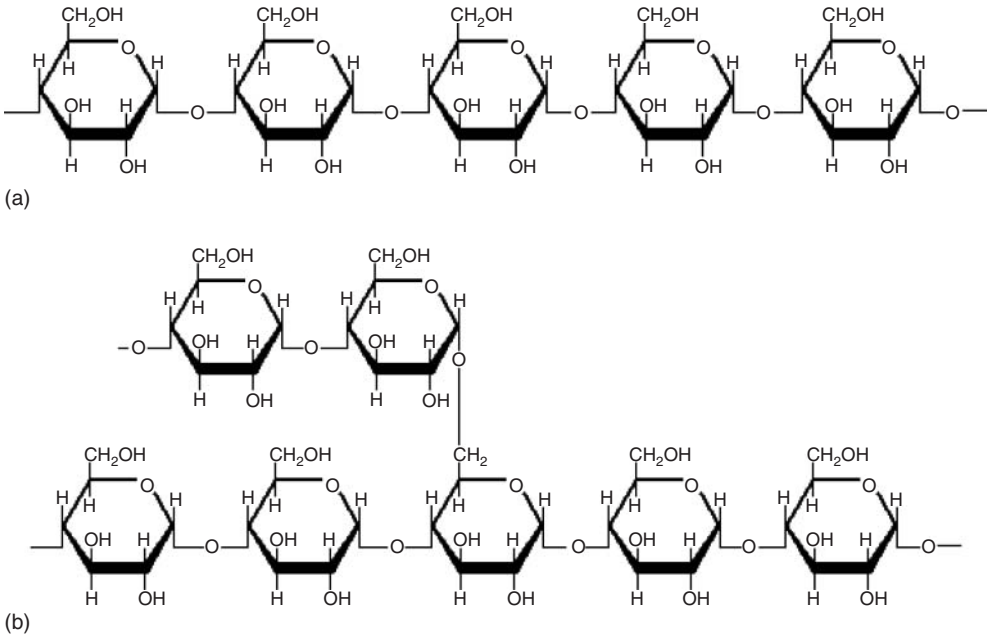

Figure 2.18 (a) Structure of amylose. (b) Structure of amylopectin.

with the starch source, yielding materials of diverse mechanical properties and biodegradability [150, 151] (Figure 2.18a,b). The amylose content has a positive effect on the elongation and strength of starch. Biodegradation of starch is achieved via hydrolysis at the acetal link by enzymes [152, 153]. The α-1,4 link is attacked by amylases, while glucosidases attack the α-1,6 link. The degradation products are nontoxic. Thermoplastic starch or plasticized starch offers an interesting alternative for synthetic polymers in specific applications and is used, for example, in starch-based composites. Significant research has been done in developing a new class of fully biodegradable "green" composites called *biocomposites* [154]. They consist of biodegradable plastics with reinforcements of biodegradable natural fibers.

The major crops used for starch production include corn, potatoes, and rice. In all of these plants, starch is produced as granules and these granules vary in size and somewhat in composition from plant to plant. Because of increasing prices and decreasing availability of conventional film-forming resins, starch has been widely used as a raw material in film production. Starch films are thus attractive materials for food packaging, owing to their low permeability. Starch is also useful for making agricultural mulch films because it degrades into harmless products when placed in contact with soil microorganisms [155].

A current invention relates to a starch adhesive mixed with zeolite powder to give appropriate absorption function for corrugated cardboards, and a method for making the adhesive [156].

2.3.2.3 **Chitosan**

Chitosan is a relatively nontoxic, inexpensive polysaccharide possessing reactive amino groups and has a wide commercial importance due to its wound-healing properties (Figure 2.19). It is a naturally derived random copolymer of β-(1-4)-linked D-glucosamine and *N*-acetyl-D-glucosamine units. It is commercially obtained in various grades from shrimp or crab shell chitin (*N*-acetylglucosamine polymer) by alkaline deacetylation (Figure 2.20). It was reported that chitosan simulated the migration of polymorphonuclear (PMN) as well as mononuclear cells and accelerated re-epithelization and normal skin regeneration. It confers substantial antibacterial activity against a broad spectrum of bacteria. Chitosan film is also a suitable candidate in healing diabetic foot ulcers, which are common in patients with diabetic mellitus. The patients having diabetis mellitus are known to be at high risk of developing chronic dermal ulcers in presence of long-term complications of the disease arising from peripheral neuropathy or mechanical changes in the foot architecture, which finally lead to limb loss if proper treatment is delayed [157, 158].

Chitosan has broad applications in the biomedical field for burn treatment, wound healing, paper production, photographic products, textile finishes, cements, heavy metal chelating agents, coatings, and waste removal and is used as a hemostatic agent. It has antioxidant properties. Because of their porous structure, gel forming properties, biocompatibility, antibacterial activity, biodegradability, ease of chemical modification, and high affinity to *in vivo* macromolecules, chitosan and its derivatives are used for tissue-engineering applications. Various types of

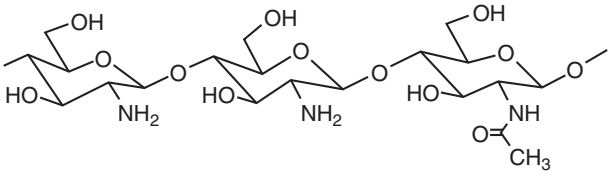

Figure 2.19 Structure of chitosan.

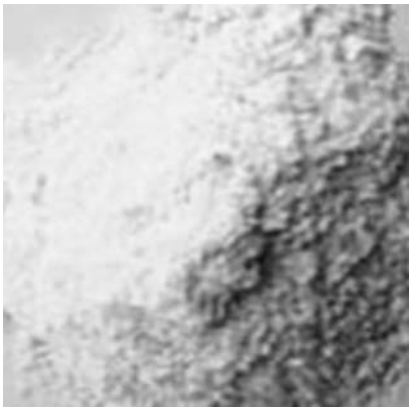

Figure 2.20 Chitosan powder.

chitosan derivatives have been used in skin, liver, nerve, bone cartilage, and blood vessels. Chitosan can be used in biosensors and electrochemistry [159].

Chitosan-based products are suitable for the delivery of chemotherapeutics such as antibiotics, anesthetics, antiparasitics, painkillers, and growth promotants to mucosal epithelium for absorption for local or systemic activity [160]. Chitosan promotes wound healing on its own and produces less scarring [161–163]. Chitosan seems to improve vascularization and the supply of chito-oligomers at the lesion site, which have been implicated in better collagen fibril incorporation into the ECM [164, 165]. Chitosan-based systems are used for the delivery of anti-inflammatory drugs, antibiotics, proteins/peptides, growth factors, as well as in gene therapy, besides having bioimaging applications.

2.3.2.4 **Chitin**

Chitin is the most abundant biopolymer in nature after cellulose. When the degree of deacetylation of chitin reaches about 50%, it becomes soluble in aqueous acidic media and is called *chitosans*. It is present in the cell walls of fungi and is the fundamental substance in the exoskeletons of crustaceans, spiders, and insects (Figure 2.21).

The structure of chitin is identical to that of cellulose, apart from the replacement of the OH group on the C-2 carbon of each of the glucose units with an $-NHCOCH_3$

(a) (b)

Figure 2.21 Chitin – the fundamental substance in the exoskeletons of shrimps, crabs, and many organisms.

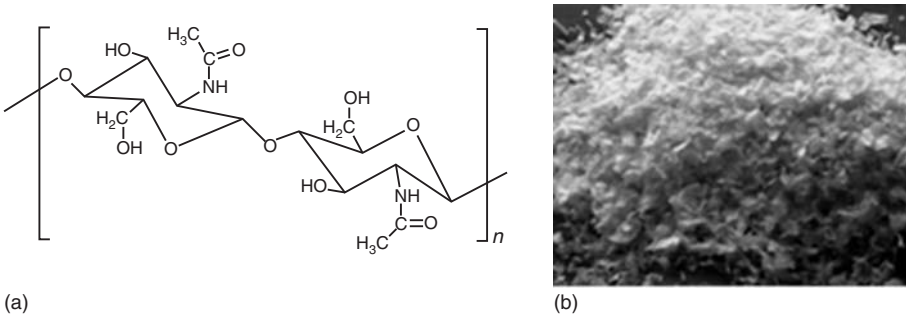

(a) (b)

Figure 2.22 Structure of (a) chitin and (b) chitin powder.

group [166, 167] (Figure 2.22), and the principal source is shellfish waste. Chitin waste finds commercial applications in the manufacture of edible plastic food wrap and in the cleaning up of industrial wastewater.

Chitin is not only abundant as biomass resources but also as specialty biopolymers for preparing advanced functional materials. Since it is insoluble in common solvents, there are serious difficulties in modification reactions to prepare well-defined derivatives of chitin [168].

2.3.2.5 **Hyaluronic Acid (HA)**

Hyaluronic acid (also called *hyaluronan*, *hyaluronate*, or *HA*), an anionic nonsulfated member of the glycosaminoglycan family, is a linear polysaccharide consisting of alternating units of *N*-acetyl-D-glucosamine and glucuronic acid (GlcA), being found in virtually every tissue of invertebrates [169, 170] (Figure 2.23). HA has broad applications as injectable soft-tissue fillers [171] as it acts as a substitute for collagen-based materials. It has the capability to promote angiogenesis, to modulate wound-site inflammation by acting as a free radical scavenger, and to be recognized by receptors on a variety of cells associated with tissue repair [172]. HA can be used in irregular-shaped defects and implanted with minimal invasion. Viscous HA solutions are clinically used to improve join mobility in osteoarthritis patients and as a synovial fluid substitute to relieve pain [173]. HA is water soluble and forms highly viscous solutions with unique viscoelastic properties; it can form three-dimensional structures in solution with extensive intramolecular hydrogen bonding.

2.3.2.6 **Alginic Acid**

Alginic acid, also called *algin* or *alginate*, is an anionic polysaccharide containing linear chains of 1,4′-linked β-D-mannuronic acid and α-L-guluronic acid (Figure 2.24) distributed widely in the cell walls of brown algae, where it forms a viscous gum through binding water. It absorbs water quickly in extracted form and is capable of absorbing 200–300 times its own weight in water. The color of alginic acid ranges from white to yellowish-brown and it is available in granular, filamentous, or powdered forms. It is a biocompatible, biodegradable, nontoxic, and low cost polymer and shows many interesting properties, such as ion-exchangeability, wound healing, and absorption of metal ions. Therefore, this natural product has many applications in the food and pharmaceutical industries, such as in the manufacture of tissue engineering material, surgical tape, and artificial skin [174].

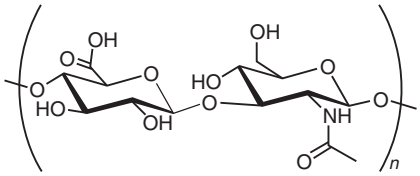

Figure 2.23 Structure physical appearance of hyaluronic acid.

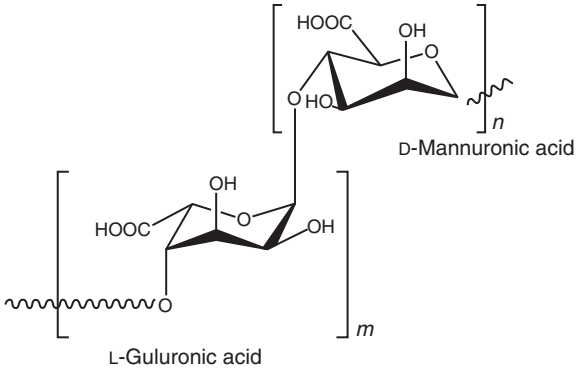

(a)

(b)

Figure 2.24 (a) Structure and (b) physical appearance of alginic acid.

Alginic acid is used in biomedical applications owing to its high functionality. Alginic acid, because of its high acid content, undergoes spontaneous and mild gelling in the presence of divalent cations, such as calcium ions. This mild gelling property allows the encapsulation of various molecules or even cells within alginate gels with minimal negative impact [175]. Alginate has been extensively investigated as a drug delivery device wherein the rate of drug release can be varied by varying the drug–polymer interaction as well as by chemically immobilizing the drug to the polymer backbone using the reactive carboxylate groups. The encapsulation of proteins and bioactive factors within ionically cross-linked alginate gels are known to greatly improve their efficiency and targetability and as a result, extensive investigation has been undertaken to develop protein delivery systems based on alginate gels [176].

2.3.2.7 **Pectin**

Pectin is a linear polysaccharide of α-linked anhydrogalacturonic acid with a certain degree of methyl esterification of carboxyl groups (degree of esterification), depending on the polysaccharide quality and source (Figure 2.25) [177]. Pectin can undergo gelation by thermal, acidic, or cationic treatment and the resulting gel nanostructure is considerably influenced by the choice of the pectin source as well as the gelation mechanism [178]. The degree of esterification and the distribution of methoxyl-esters of each pectin type determine the main interactions taking place between the polymer chains (hydrogen bonding, hydrophobic and ionic

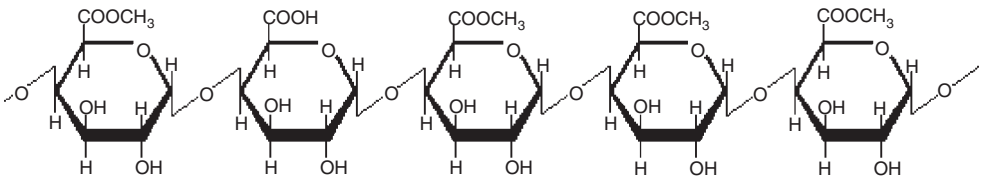

Figure 2.25 Structure of pectin.

interactions) and the extent of chain alignment (junction zones) [179]. Thermal treatment (heating) promotes the dissolution of pectin in water and, upon cooling below setting temperature; gelation takes place by hydrogen bonding between free carboxyl groups on the pectin molecules and also between the hydroxyl groups of neighboring molecules [180]. Acidic gelation promotes the hydrolysis of the methyl esters inducing a pectin structure mainly composed of galacturonic acid [181]. Pectin is the key component of citrus processing by-products with useful properties in many applications [182, 183].

2.3.3 Polysaccharides from Marine Sources

2.3.3.1 Agar

Agar (AG), a gelatinous product from the red algae class (Rhodophyceae), is a heterogeneous complex mixture of related polysaccharides processing the same backbone chain structure. The main components of the chain are D-galactopyranose and 3,6-anhydro-L-galactopyranose, which alternate through α-(1,4) and β-(1,3) linkages (Figure 2.26) [184]. Substitutions can be made in this disaccharide by sulfate esters and methoxyl, and they may also contain pyruvic acid residues [185]. AG is insoluble in cold water, whereas it is soluble in hot water [186]. It has been regarded as a potential candidate for future use in biodegradable plastics [184] because of its biodegradability and renewability as well as enormous gelling power [187].

2.3.3.2 Agarose

Agarose is a linear and neutral polymer derived from red algae (Solieriaceae family, namely, Rhodophyta) and seaweeds, which find abundant speciality high-added-value applications in food industry, cosmetic formulations, and pharmaceuticals. Its molar mass is about 120 000. The composition of agarose is agarobiose-repeating disaccharide units with alternating 1,3-linked-β-D-galactopyranose and 1,4-linked-3,6-anhydro-α-L-galactopyranose (Figure 2.27). Agarose is a polysaccharide generated from seaweed that forms a gel at room temperature. The characteristics of agarose gels depend on the concentration of agarose, weight-average molar mass, and solvent and molar mass distribution [188].

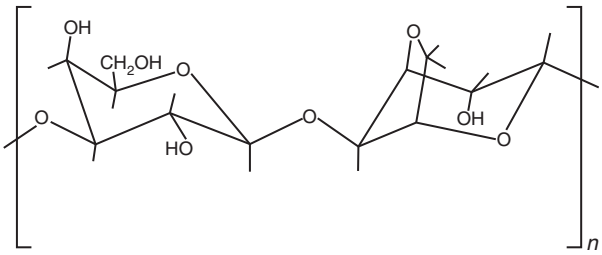

Figure 2.26 Structure of agar.

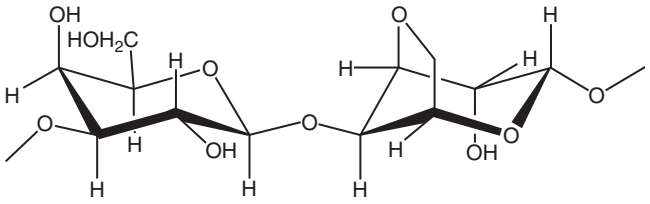

Figure 2.27 Structure of agarose.

2.3.3.3 Alginic Acid/Alginate

Alginate, which is derived from brown algae, carries carboxyl groups capable of forming complexes with metal cations [189]. The most well-known and commercially important constituent of the brown algae is polyuronide alginic acid. This is composed of a linear copolymer of mannuronic acid and guluronic acid, the relative amounts of which vary greatly between alginic acids from different species of algae [190]. Alginic acids from different sources vary in the arrangement of the uronic acids within the molecule so that alginic acid may be considered as a copolymer consisting of homopolymeric blocks of mannuronic acid and of guluronic acid together with blocks with an alternating sequence (Figure 2.28) [191].

Owing to its ability to form gels by ion-exchange reaction with multivalent metal ions, alginate can be used as a metal adsorbent. Depending on the source, it exists as randomly arranged homogeneous blocks (MM and GG) and heterogeneous blocks (GM) along the polymer chains. It contains three different functional groups: –COO– (carboxylate), –C–O–C– (ether) and –OH (alcohol) [192–199]. In the presence of divalent cations (exclusive of Mg^{2+}), alginate has been well known to form ionotropic hydrogels that act as cross-linkers between the functional groups of alginate monomers [200–204].

Alginate is nontoxic, noncarcinogenic, biocompatible, and sterilizable and offers a cheap processing technique. Alginic acid and its sodium/calcium salts have promising applications in food, cosmetics, and drug industries and are used for drug delivery, tissue engineering, and so on. Alginate wound dressing has recently

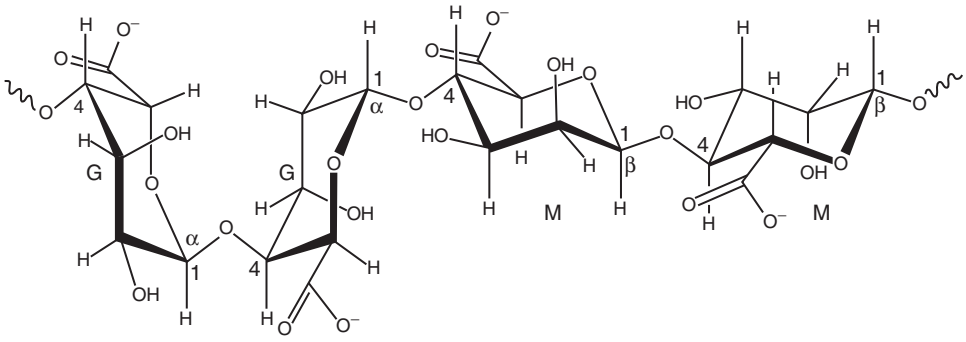

Figure 2.28 Structure of alginate.

been introduced for heavy exudation wounds as occlusive dressing by pharmacy industries [205].

2.3.3.4 **Carrageenan**

The major source of carrageenans is sulfated linear polysaccharides extracted from certain red seaweed of the Rhodophyceae class. In the food industry, it is used as thickening agent, gelling agent, and, more recently, as excipient in pills and tablets [206] (Scheme 2.1). Different types of carrageenan are used in cooking and baking. Since natural carrageenans are mixtures of different sulfated polysaccharides, their composition differs from batch to batch. Carrageenan from particular seaweed species and geographic district differ considerably in their structure and rheological properties of solutions and gels. Therefore, the quantitative analysis of carrageenan batches is of greatest importance for industry to deliver a standard product and to develop new applications based on their unique intrinsic properties. In dairy industry, the main application of kappa carrageenan is to form strong gels.

Eucheuma cottonii is the major source of kappa carrageenan, which is mainly produced in the Philippines and Indonesia. The yield and physical properties of carrageenan such as gel strength, gelling and melting temperature, as well as chemical properties, determine its value to the industry. Carrageenan is usually extracted from the seaweeds with alkali at elevated temperature [207]. Alkaline treatment, which is the most important and well-known method of extraction of carrageenan, is used to commercially enhance gelation behavior [207, 208]. The reason for its good stabilization properties is that both the sulfate group and the three hydroxy groups are expected to interact with the mineral surface. In addition, its tendency to gel after binding creates a stable protection layer that adds a number of other advantageous characteristics. It has valuable applications in the food and pharmaceutical industries owing to its low toxic nature [209] (Figure 2.29).

2.3.3.5 **Cutan**

Cutan is a waxy polymer found along with the two polymers (including cutin) commonly found in the protective covering (cuticle) of the plant leaves. Cutan is a hydrocarbon polymer and is believed to be an acid- and base-hydrolysis-resistant biopolymer [210–212]. However, the structural composition and synthesis of cutan are not yet fully understood. The hydrophobic nature of the cuticle is enhanced by cutan, affording a physiological adaptation for survival under drought conditions [213]. It is a highly cross-linked biopolymer [214–216] consisting of a network of saturated and unsaturated polymethylenic long chains (up to C33) with free carboxylic functionalities [211–213, 217, 218]. Tegelaar *et al.* [217] suggested that cutan is composed of polysaccharide moieties that are covalently attached to polymethylenic units. McKinney *et al.* [216] proposed a cutan model having a backbone of aromatic rings with hydroxyl groups that form ester linkages with fatty acids of varying chain lengths. Deshmukh *et al.* [214] suggested that cutan contains a higher degree of carboxylic and hydroxy functionalities, which form ester linkages with long-chain primary and secondary alcohols. Cutan mainly consists of a higher

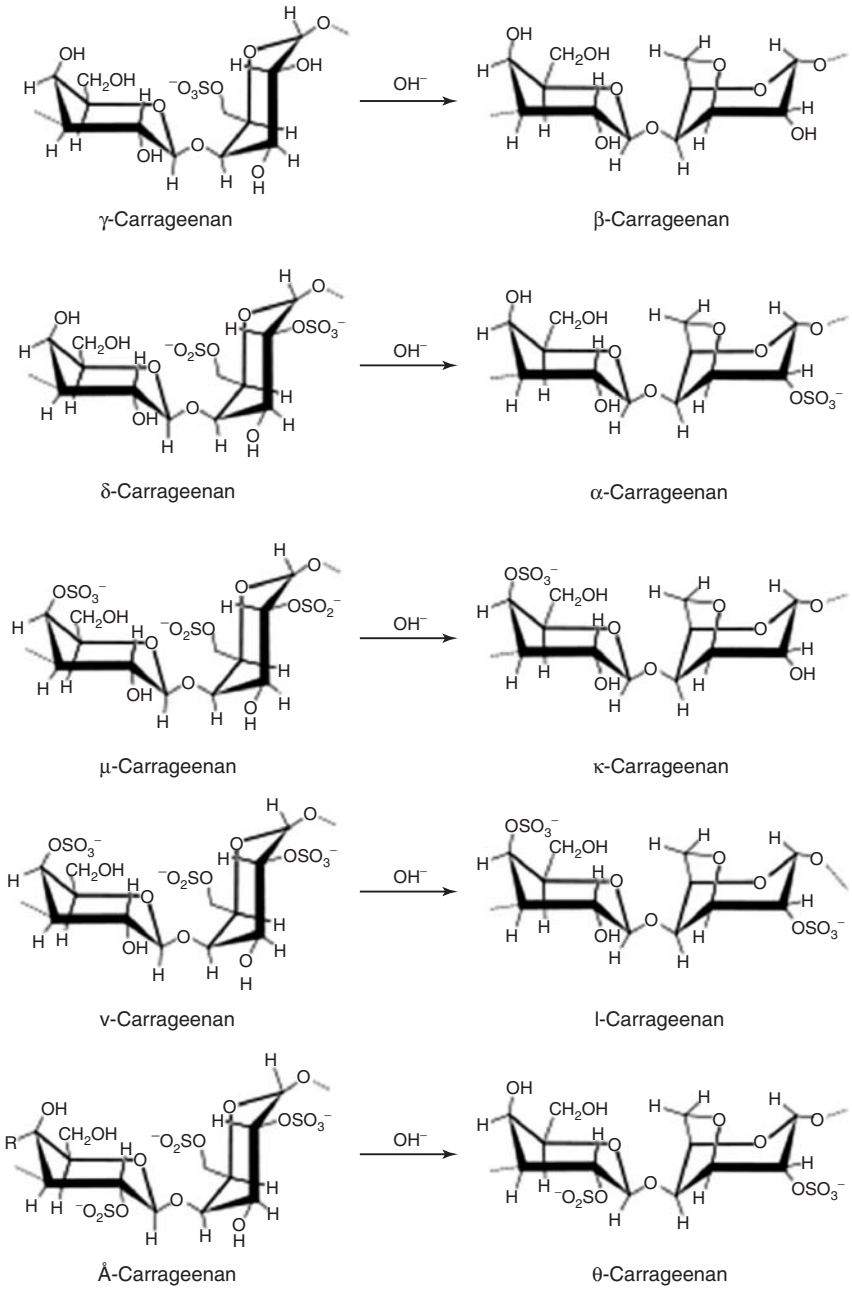

Scheme 2.1 The structure of several varieties of carrageenan.

Figure 2.29 Physical appearance of carrageenan.

level of rigid paraffinic moieties and is less attractive as sorbent because of its less polar nature [219, 220].

2.3.3.6 **Cutin**

Cuticular membranes or cuticles of higher plants are chemically heterogeneous in nature, basically consisting of a wax fraction soluble in common organic solvents, and an insoluble cuticular matrix, which forms the framework of the cuticle. This cuticular matrix is cutin, a high-molecular-weight polyester composed of various interesterified C16 and C18 hydroxy and hydroxy–epoxy fatty acids. It is derived from the common cellular fatty acids such as palmitic and oleic acids (Figure 2.30) [221].

Cutin is a support biopolyester involved in waterproofing the leaves and fruits of higher plants, regulating the flow of nutrients among various plant cells and organs, and minimizing the deleterious impact of pathogens. Cutin, which is the major constituent (between 40% and 80% of weight) of cuticle, can be depolymerized by cleavage of the ester bonds by alkaline hydrolysis, transesterification, and

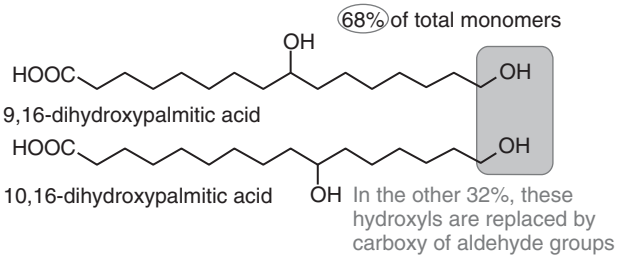

Figure 2.30 Structure of monomers of cutin, a cross-linked polyester found in the cuticle of plant leaves.

other methods [222, 223]. These chemical methods yield monomers and/or their derivatives, depending on the reagent used.

The major components of the C16 cutins are 9- or 10,16-dihydroxyhexadecanoic acid, and 16-hydroxyhexadecanoic acid. 16-Hydroxy-10-oxo-C16 acid and 16-oxo-9 or 10-hydroxy C16 acid are monomers in only some cases. The major components of the C18 family of monomers are 18-hydroxy-9,10-epoxyoctadecanoic acid and 9,10,18-trihydroxyoctadecanoic acid, together with their monounsaturated homologs. Omega hydroxyacids and their derivatives are the main components of cutin, which are interlinked via ester bonds, forming a polyester polymer of indeterminate size [211].

2.3.4 Low Molecular Weight Biopolymers

2.3.4.1 Guar Gum

Guar gum, obtained from the endosperm of the guar plant, has abundant industrial applications (Figure 2.31) [224]. This natural hydrophilic polysaccharide is one of the excellent representatives of the new generation of plant gums. Its source is an annual pod-bearing, drought-resistant plant, called *guar*, or cluster bean belonging to the family Leguminosae. The height of the guar plant is about 0.6 m, and it resembles the soybean plant. It is used as a ''water sealer'' in oil well drilling or in protecting explosives from getting wet. Stability over virtually the entire usable pH range is the one of the characteristics. Guar gum may be identified among others by its perfect solubility in cold water, resulting in a viscous sol that gives a gel-like complex with Fehling and borax solutions. In industries; guar gum is used in massive proportions. It is further used – apart from being used as a dispersant and suspending agent – for sizing and coating in the paper industry. It also serves as a pigment dispersing aid, and, above all, as a thickening agent for color printing pastes in the textile industry. The ceramic industry also uses sizeable quantities of guar gum as a binder, thickener, and fixing agent for enamels, porcelain, and so

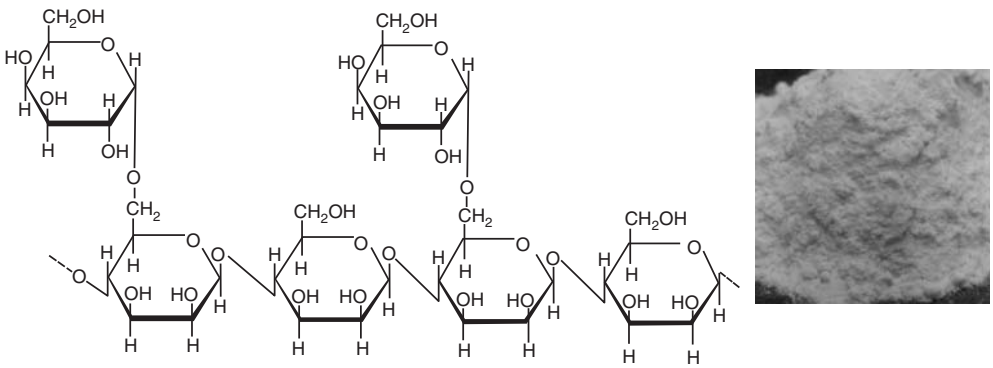

Figure 2.31 (a) Structure and (b) physical appearance of guar gum.

on. In the food industry, it is widely used in salad dressings, ice creams, lollipops, and sherbets, in bakery products and confections, meats and sausages, cheese spreads, and many other applications. Dry guar gum is used as a disintegrant and, in solution, as a binder in compressed tablet manufacture in the pharmaceutical industry [225]. It is also used in liquid dietetic preparations as a low calorie thickener to improve their mouth feel, body, and pour characteristics. Guar gum solutions are compatible and mix well with most detergent systems (shampoos, cleansers, etc.) giving them "body" and abolishing or minimizing their harsh after feel. Guar gum is also used as a thickener in hair-coloring products [226].

2.3.4.2 **Rosin**

Rosin is a natural nonvolatile resinous mass having excellent biocompatibility and biodegradation features [227]. It is derived from *Pinus palustris* Miller, and other species such as *Pinus linnae*. It primarily contains resin tricyclic diterpene carboxylic acids (abietic and pimaric) and small quantities of nonacidic components (Figure 2.32). Traditional applications of rosin and its derivatives including those such as paper sizing agents, adhesives, printing inks, and chewing gum have declined owing to escalating production and labor costs. However, rosin remains an attractive renewable source of chemicals useful for polymer synthesis and in the formulation of different pharmaceutical preparations [228].

Rosin biomaterial has film-forming ability, utilized in the development of film-based drug delivery systems and dosage forms. Sustained release of the drug has been achieved with rosin-coated pellets prepared using diclofenac sodium as a model drug. Therefore, rosins can be used in the development of transdermal drug delivery systems.

In tablet formulation, it finds use as a matrix-forming polymer. Rosin has been pharmaceutically evaluated for its encapsulating properties [229]. The biodegradable property of rosin makes it possible to implant them into the body without the need of subsequent removal by the surgical operation. Drugs formulated with these polymers can be released in a controlled manner, by which the drug concentration in the target site is maintained within the therapeutic range. Biodegradation

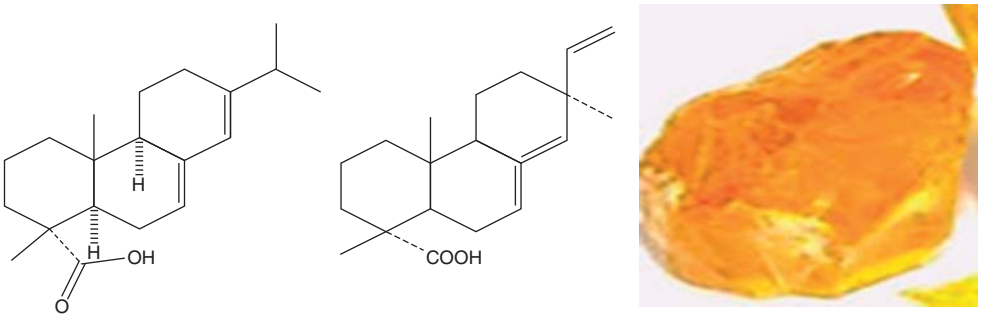

Figure 2.32 Abietic acid and pimaric acid found in rosin and the physical appearance.

kinetics of the polymers [230–232] and physicochemical properties of the polymers and drugs [232–234] influence the drug release rate from biodegradable polymers.

The main applications of rosin and its derivatives are in paints, varnishes, cosmetics, printing inks, and chewing gums. Spherical microcapsules can be synthesized from it by a method that is based on phase separation using solvent evaporation.

2.3.4.3 **Chondroitin Sulfate**

Chondroitin sulfate (CS) is the most abundant glycosaminoglycan found in the proteoglycans of articular cartilage [10], consisting of a repeating unit formed by *N*-acetyl galactosamine (GalNAc) and GlcA modified by sulfation, where the position of sulfation varies with the type of CS. It is a major component of aggrecan. CS hydrogels have been extensively investigated for wound-dressing applications (Figure 2.33) [235]. CS plays an important role in regulating the expression of the chondrocyte phenotype; it has been extensively studied as a scaffolding material for cartilage tissue engineering [236] as CS can stimulate the metabolic response of cartilage tissue and has antiinflammatory properties [237].

CS possesses outstanding biocharacteristics, including the binding and modulation of certain growth factors. Chemical cross-linking of CS is required for *in vitro* or *in vivo* hydrogel application, as natural CS is readily water soluble.

2.3.4.4 **Gum Copal**

Gum copal (GC) is a pale yellow, transparent, crystalline, natural resinous material with softening point range of 79–82 °C (Figure 2.34). Its major source is plant *Bursera bipinnata*. The glass-transition temperature is 38.79 °C. It is used as a raw material for varnish because it produces glossy films with good weather-protection properties [238]. It has been used in varnishes as a pigment binder [239]. It has been extensively used as emulsifier and stabilizer for the production of color, paints, printing inks, aromatic emulsions, and meat preservatives [240]. GC was used as medicine for several different ailments such as in treatment of burns, headache,

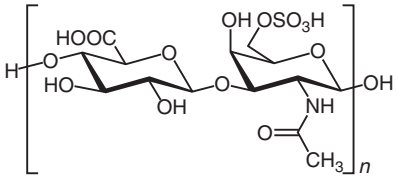

Figure 2.33 Basic structure of chondroitin sulfate.

Figure 2.34 Physical appearance of gum copal.

Figure 2.35 Physical appearance of gum damar.

nosebleed, fever, and stomach ache, in the preparation of dental products, and as a remedy for loose teeth and dysentery [241].

2.3.4.5 **Gum Damar**

Gum damar (GD) is a whitish to yellowish natural gum (Figure 2.35) containing about 40% alpha-resin (resin that dissolves in alcohol), 22% beta-resin, 23% dammarol acid, and 2.5% water [242]. It is obtained from the plant *Shorea wiesneri* (family Dipterocarpaceae). It has wide range of applications in pharmaceutical and dental industries for its strong binding properties and can be used for water-resistant coating [243]. It has been mainly used for the production of color, inks, paints, and aromatic emulsions in food and cosmetic industries owing to its emulsifying and stabilizing properties. It is also used in the manufacture of wood, varnishes, paper, lacquers, polishes, and additives for beverages [244]. Sal damar has been widely utilized as an indigenous system of medicine [245].

2.3.5
Microbial Synthesized Biopolymers

2.3.5.1 **Pullulan**

Pullulan, a linear α-D-glucan built of maltotriose subunits, that is, α-(1 → 4)Glup-α-(1 → 4)Glup-α-(1 → 6)Glup-, connected by (1 → 6)-α-D-glucosidic linkages, is synthesized by the yeastlike fungus *Aureobasidium pullulans* (Figure 2.36) [246].

It is a water-soluble, random coil glucan that serves as a paradigm for the behavior of aqueous polysaccharides [247–249]. This biodegradable polymer has extensive applications in food and pharmaceutical industry [250].

It exhibits distinctive physical properties, such as adhesive ability, the capacity to form fibers, and the capacity to form thin and biodegradable film, which is transparent and highly impermeable to oxygen [251]. Other applications of pullulan include blood plasma substitutes, food and cosmetic additives, adhesive additives, flocculants, resins, and environmental remediation agents [246, 252, 253].

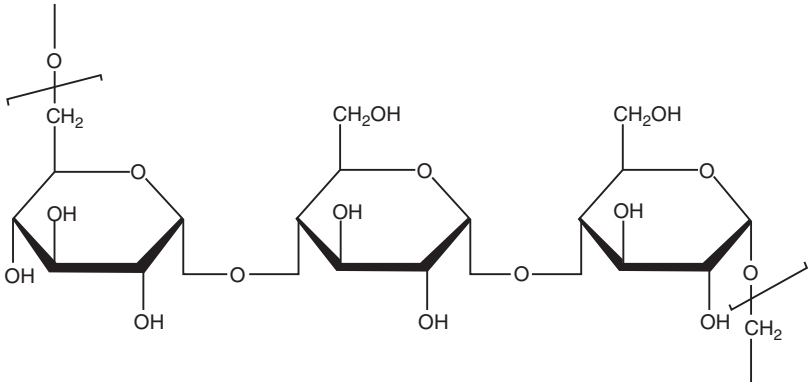

Figure 2.36 Basic structure of pullulan.

Pullulan can be used as a partial replacement for starch in pastas or baked goods. Pullulan is not a readily assimilable carbon source for bacteria, molds, and fungi responsible for spoilage of food and it improves the shelflife of the food. It is also superior to starch in water retention, thus retarding the spoilage of food by drying out. The films and fibers made of pullulan are colorless, tasteless, odorless, transparent, and flexible with excellent mechanical properties. These properties provide pullulan with high possibility to form hydrogels with good absorbent capacity and excellent mechanical strength [254–257].

Pullulan films are used for coating or packaging material of dried foods, including nuts, noodles, confectioneries, vegetables, and meats [258]. Pullulan derivatives are promising as nontoxic conjugates for vaccines [259, 260].

Pullulan is used as paper-coating adhesives. Pullulan paper is high in strength and folding resistance and tougher than a wood pulp paper. It is highly hydrophilic in nature and therefore favors ink receptivity, hence making it suitable for printing and writing [261, 262]. Pullulan is used in paints to improve its properties [263]. The other applications of pullulan and its derivatives are in photographic, lithographic, and electronic fields [246, 250, 264–268].

2.3.5.2 **Dextran**

Dextran is a nontoxic water-soluble polysaccharide consisting mainly of α-1,6 linked D-glucopyranose residues with a low percentage of α-1,2, α-1,3, and α-1,4-linked side chains (Figure 2.37) [269]. It is mainly used as a blood plasma substitute [270]. The chemical structure of dextran includes α-(1 → 6) linkages that can vary from 97% to 50% of total glucosidic bonds [271, 272]. Dextran has wide applications in novel drug delivery systems as a polymeric carrier.

Dextran is a biocompatible polymer used for the preparation of hydrogels. Dextran hydrogels can be obtained by several different approaches and they have received increased attention due to the variety of their biotechnological and biomedical applications. Dextran hydrogels have been frequently considered as a potential matrix system for colon-specific delivery and/or controlled release (CR) of bioactive

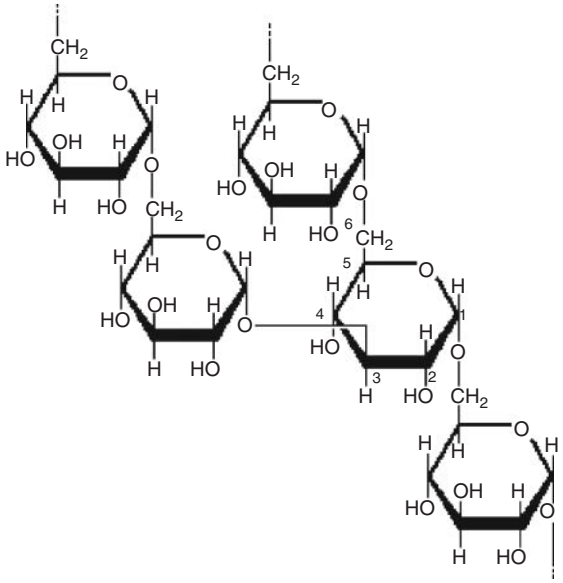

Figure 2.37 Structure of dextran.

agents due to their low tissue toxicity and high enzymatic degradability at desired sites [273].

2.3.5.3 **Curdlan**

Curdlan is a microbial polysaccharide that occurs naturally as a linear (triple-helix) polysaccharide composed of 1,3-β-linked D-glucose units, produced by a strain of *Alcaligenes faecalis* (Figure 2.38). It is a neutral, bacterial polysaccharide without branched chains. It is insoluble in water and alcohol but soluble in alkaline solution and dimethyl sulfoxide (DMSO) [274–276]. It occurs as a tasteless powder, stable in dry state. It was reported as a support matrix for enzyme immobilization, through activation with epichlorohydrin that can be covalently linked to the available amino, hydroxyl, and sulfhydryl enzyme groups [277]. It has the specific character to form an irreversible gel by heating of a water suspension [278]. Its water-insoluble nature helps to improve a material's water barrier capability, and its solubility in

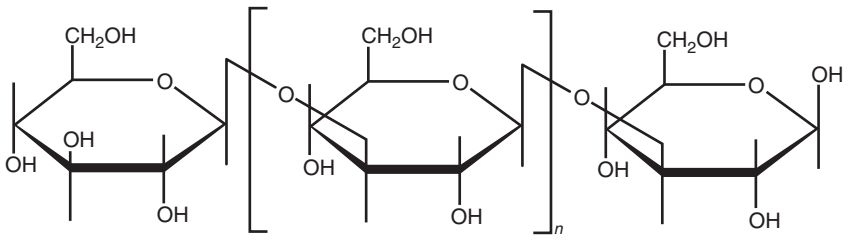

Figure 2.38 Structure of curdlan.

alkaline aqueous solutions (pH > 12) is due to its ability to undergo conformational changes. Curdlan has potentially inhibitory effects against HIV virus infections and blood anticoagulant activity, as well as low toxicity *in vitro* and *in vivo*. This polysaccharide has been actively investigated as a drug delivery carrier owing to its gelation property, which varies according to temperature and pH, and its anti-HIV and antitumor activities [279].

2.3.5.4 **Xanthan**

Xanthan gum is an extracellular heteropolysaccharide having excellent rheological properties. It is obtained by the aerobic fermentation of *Xanthomonas campestris* [280] (Figure 2.39). It has wide applications in the food industry as a thickening, suspending, and stabilizing agent [281].

This acidic polymer, which is made up of pentasaccharide subunits, forms a cellulose backbone with trisaccharide side chains composed of mannose (β1,4) GlcA (β1,2) mannose attached to alternate glucose residues in the backbone by α-1,3 linkages. The molecular weight of xanthan gum is approximately 2 million but it can go to as high as 13–50 million [282].

It has many uses in the paper mill and textile industry where it is used as a thickener, stabilizing the suspensions and emulsions [283] and also in enhanced oil recovery. It has numerous applications in the food industry because of its solubility in hot or cold water, high viscosity at low concentrations, and little variation in viscosity with changes in temperature, and stability in acid systems. It is used in the food industry as a thickener, stabilizer, gelling agent, and suspending agent; as a flocculation agent in food; as creams, artificial juices, sauces for salads, meat,

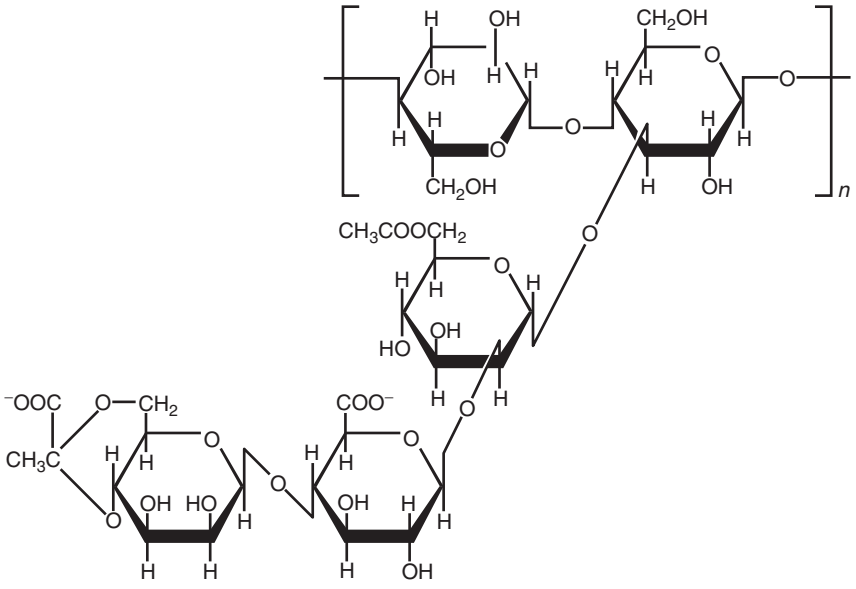

Figure 2.39 Structure of xanthan.

chicken, or fish, as well as for syrups and coverings for ice creams and desserts. It also shows excellent suspending properties owing to a high yield value and also an ability to provide good freeze–thaw stability [284, 285].

It has been used to improve the flow-ability in fungicides, herbicides, and insecticides formulations by uniformly suspending the solid component [286]. It is used in pharmaceutical, cosmetics, paint, textile, and agricultural products (in suspensions, as an agent for stabilizing herbicides, pesticides, fertilizers, and fungicides) [287–290]. It still presents compatibility with most of the colloids used in foods, including the starch, fact that turns its ideal for the preparation of breads and other products for breadmaking [291, 292].

2.3.5.5 Bacterial Cellulose

Bacterial cellulose (BC) is the most abundant biopolymer in nature. It is a homopolymer of β-(1,4) glucose and can be produced by some bacterial strains, for example, acetic acid bacteria, and it is a major component of higher plants [293]. This extracellular biomaterial finds applications in, cosmetics, advanced acoustic diaphragms, biomedicine papermaking, and food and textile industries because of its attractive properties, such as high purity (free of lignin and hemicellulose), high crystallinity, high degree of polymerization, nanostructured network, high wet tensile strength, and good biocompatibility, polyfunctionality, and hydrophilicity [294–297]. It is used in speaker diaphragms, artificial blood vessels, face masks, wound dressings, severe body burns, treatment for skin injuries, chronic ulcers, and skin grafts [296], and also as a viscous substance and temporary skin substitute [295, 298]. BC is also used in drug delivery systems [299], as an immobilization medium for enzymes [300], and also as a conductive material for various applications [301–303].

It has ribbon shape with diameter ranging from 8 to 50 nm, which is about a 1000 times smaller than that of common plant fibers (10–600 μm) [304]. The fibril is composed of a bundle of much finer microfibrils 2–4 nm in diameter [305, 306].

2.3.6 Natural Poly(Amino Acids)

Natural poly(amino acids) are biodegradable ionic polymers that differ from proteins in certain aspects. Natural poly(amino acids), such as cyanophycin, poly(ε-lysine) (ε-PL), and poly-γ-glutamic acid are mainly composed of one type of amino acid. These molecules exhibit polydispersity and in addition to α-amide linkages, they exhibit other types of amide linkages that involve β- and γ-carboxylic groups as well as ε-amino groups. Poly(amino acids), an important kind of biocompatible and biodegradable synthetic polymers, have been studied for biomedical applications in many fields [82]. Their insolubility or pH-dependent solubility and lack of functional groups limits their practical applications.

There are several differences between the proteins and the poly(amino acids): (i) protein is composed of a variety of amino acids, whereas a poly(amino acid) consists of only one type of amino acid, at least in the backbone. (ii) Protein is

biosynthesized under the direction of DNA, which means that protein synthesis is in a template-dependent mode, including complex ribosome transcription and translation mechanism. Because the biosynthesis of poly(amino acids) is catalyzed by some simple enzymes, the inhibitors of translation such as chloramphenicol do not affect their biosynthesis. The enzymes catalyzing the biosynthesis of poly(amino acids) are grouped under the carbon–amino binding enzymes. (iii) Proteins exhibit exact length, whereas poly(amino acids) show remarkable dispersal in molecular weight. (iv) While amide linkages in proteins are only formed between α-amino and γ-carboxylic groups (α-amide linkages), amide bonds in poly(amino acids) involve other side-chain functions (i.e., β- and γ-carboxylic and ε-amino groups).

1) *Polyglutamic Acid*

γ-PGA, a kind of water-soluble and biodegradable natural biopolymer, is made of D- and L-glutamic acid units linked by amide linkages between α-amino and γ-carboxylic acid groups (Figure 2.40) [307]. γ-PGA and its derivatives have high water solubility and biodegradability and that makes them potential substitutes for hydrogels and thermoplastic polymers, traditionally synthesized from petroleum. All γ-PGA-producing strains can also metabolize γ-PGA as a carbon resource as well as a nitrogen resource. γ-PGA has many applications in different fields and can be used as a drug carrier in medicine to increase drug solubility and decrease their side-effects [308]. It can also be used as biological adhesive in sealing air leakage from the lungs. γ-PGA has high affinity with water and heavy metal ions and because of this property, it finds applications in cosmetics as a moisture container [309] and as an absorbing material in wastewater treatment.

2) *Cyanophycin*

Cyanophycin granule polypeptide (CGP) is a microbial poly(amino acid) synthesized and sequestered as inclusion bodies by cyanobacteria [310] and other microorganisms [311]. CGP is composed of a poly(aspartic acid) (poly(Asp)) backbone chain with arginine (Arg) residues attached as pendant groups (Figure 2.41) [311].

CGP seems to be a compound whose distribution is limited to cyanobacteria [312]. No ultrastructural evidence exists so far for the occurrence of similar inclusions in other organisms, and as such it is not possible to identify material with the typical characteristics of cyanophycin from other sources. The granules made of cyanophycin vary in size and shape [313, 314] and occur in all cyanobacterial groups: unicellular and filamentous, nitrogen-fixing, and non-nitrogen-fixing. Cyanophycin

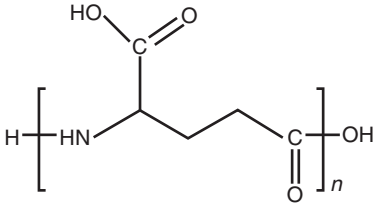

Figure 2.40 Structure of polyglutamic acid.

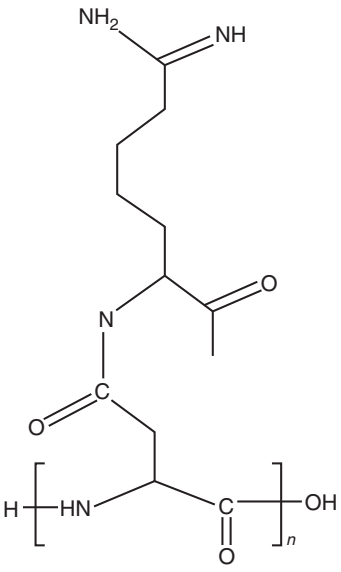

Figure 2.41 Structure of cyanophycin.

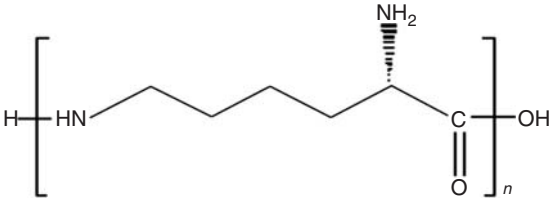

Figure 2.42 Structure of poly(ε-lysine).

has high solubility, high viscosity, and biodegradability. The applications are similar to those of γ-PGA including medicine, cosmetics, environment protection, and agriculture [315].

3) *Poly(ε-lysine)*

ε-PL is a homo-poly(amino acid) characterized by the peptide bond between the carboxyl and ε-amino groups of L-lysine (Figure 2.42). The compound is a homo-poly(amino acid) consisting of L-lysine. The length of ε-PL produced by the strain is about 25 L-lysine monomers [316, 317]. ε-PL is capable of antibiotic activity and is mainly used in the food industry. ε-PL is proven a safe food additive and causes no toxicity in reproduction, neurological and immunological functions, embryonic and fetal development, and growth of offspring, and development of embryos or foetuses for two generations. Because ε-PL is harmless to human and biodegradable besides possessing water-binding capability, ε-PL has also been used for the synthesis of hydrogel by cross-linking of ε-PL and polysaccharides [318].

2.3.6.1 Jute

Jute, a stiff and strong natural fiber is the aggregate of the single cells consisting of cellulose cemented by lignin and hemicellulose, which gives tenacity and flexibility to the fiber, making the fiber quite coarse, so it is hard to make high quality textiles [319, 320]. The dark color, harshness, and branching patterns depend on lignin. Owing to the poor elongation and high flexural rigidity, the spinnability of the fiber is greatly reduced [321]. Jute fibers are the world's second most common natural cellulosic fiber [322]. Jute fiber is extracted by degumming the jute plant stem using biological, chemical, or biochemical methods, and is composed mainly of cellulose, hemicellulose, and lignin [323–325].

2.3.6.2 Coir

Coir is an abundant, versatile, renewable, cheap, and biodegradable lignocellulosic fiber, which is used for making a wide variety of products [326]. Coir also has applications as filler or reinforcement in different composite materials [327–330].

It is a fibrous material. Coir is found between the hard, internal shell, and the outer coat of a coconut. Other uses of brown coir (made from ripe coconut) are in upholstery padding, sacking, and horticulture. White coir, harvested from unripe coconuts, is used for making finer brushes, string, rope, and fishing nets.

Erosion control blankets are used on slopes and disturbed soils where mulch must be anchored and other methods such as crimping or tackifying are neither feasible nor adequate. They are used on steep slopes, generally steeper than 3 : 1, and slopes where erosion hazard is high; their use is especially appropriate for critical slopes adjacent to sensitive areas, such as streams and wetlands, and disturbed soil areas, where planting is likely to be slow in providing adequate protective cover.

2.3.6.3 Yarn

Yarn is a long continuous length of interlocked fiber, suitable for use in sewing, crocheting, production of textiles, knitting, weaving, embroidery, and rope making. Thread is a variety of yarn intended for sewing by hand or machine.

2.3.6.4 Silk

Silks are generally defined as protein polymers that are spun into fibers by some lepidoptera larvae such as silkworms, spiders, scorpions, mites, and flies [331–333]. Silk proteins are usually produced within specialized glands after biosynthesis in epithelial cells, followed by secretion into the lumen of these glands where the proteins are stored before being spun into fibers. Silks differ widely in composition, structure, and properties, depending on the specific source. The most extensively characterized silks are from the domesticated silkworm, *Bombyx mori*, and from spiders (*Nephila clavipes and Araneus diadematus*). Many of the more evolutionarily advanced spiders synthesize different types of silks. Each of these different silks has a different amino acid composition and exhibits mechanical properties tailored to their specific functions: reproduction as cocoon capsular structures, lines for prey capture, lifeline support (dragline), web construction, and adhesion [334].

Fibrous proteins, such as silks and collagens, are characterized by a highly repetitive primary sequence that leads to significant homogeneity in secondary structure, that is, triple helices in the case of collagens and β-sheets in the case of many of the silks. This family of proteins has excellent mechanical properties so as to be used in the fields of CR, biomaterials, and scaffolds for tissue engineering [334].

2.3.6.4.1 Silkworm Silk

Silkworm silk, the silk from the cocoon of *B. mori* contains at least two major fibroin proteins, light and heavy chains, 25 and 325 kDa, respectively. These core fibers are encased in a sericin coat, a family of gluelike proteins that holds two fibroin fibers together to form the composite fibers of the cocoon case to protect the growing worm. Silkworm cocoon silk production, known as *sericulture*, produces high yields as the larvae can be maintained in high densities. The core sequence repeats in the fibroin heavy chain from *B. mori* include alanine–glycine repeats with serine or tyrosine [334]. It has been widely used as biomedical sutures and in textile production.

2.3.6.4.2 Spider Silk

Spider silk is a natural composite material having a molecular weight ranging from 70 to 700 kDa. The molecular weight may vary depending on the source and the method of analysis. The dragline silk from *N. clavipes* is characterized by polyalanine and glycine–glycine–X regions, where X is often tyrosine, glutamine, or leucine. Genetic engineering is being actively explored to construct, clone, and express native and synthetic genes encoding recombinant spider silk proteins to overcome limits to use of the native organisms. This strategy has provided new opportunities in fundamental studies of spider silk genetics, silk protein structure and function, and materials processing [335–337]. Silk fibroin has been used as suture material, nanofibers, film, and porous matrix formats for tissue engineering with stem cells, and for the formation of cartilage [338] and bone [339–341]. Spider silk is an interesting biomaterial for further exploration for orthopedic applications due to the impressive mechanical properties of silks, along with established biocompatibility and slow degradability [342].

2.3.7 Nucleic Acids

2.3.7.1 Natural Nucleic Acids

Natural nucleic acids include DNA and RNA, which are essential for encoding, transmitting, and expressing genetic information for a sustainable animal and plant kingdom. They can also be termed as *polynucleotides* as they are made up of nucleotide units of different origin. This terminology is incorrect because the same nucleotide units are not repeated. This is illustrated in the following section. A single nucleotide unit consists of a sugar unit, a phosphate ester unit, and a base. Each nucleotide unit can be further divided into a nucleoside and the phosphate

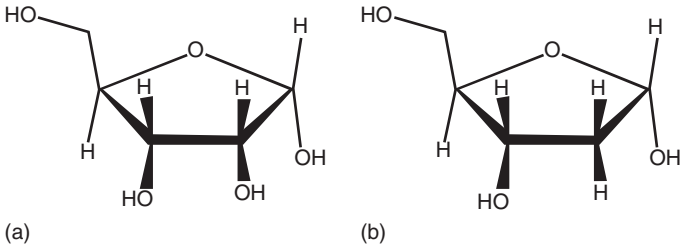

Figure 2.43 Structures of sugar units in nucleic acids. (a) Ribose and (b) deoxyribose.

ester units. This nucleoside unit comprises sugar and the various bases (purine and pyramidine bases) through the β-glycosidic linkage. Basically depending on the sugar unit present, the nucleic acid is termed *DNA* (deoxyribose as the sugar unit) and *RNA* (ribose as the sugar unit) (Figure 2.43). In addition to this, there is a small difference in the base units present in DNA and RNA. Both of them contain the purine bases adenine and guanine. For DNA, the pyramidine bases are thymine and cytosine, whereas for RNA they are uracil and cytosine. DNA has a double-stranded structure, whereas RNA is single stranded and their molecular weight is in the million scales. It is clear that DNA has higher molecular weight than RNA.

The chemical structure of DNA and RNA are depicted in Figure 2.44 and Figure 2.45. The natural nucleic acids will have a uniform code of base pairing. In DNA, the bases adenine (A) and thymine (T) are paired via two hydrogen bonds and guanine (G) and cytosine (C) via three hydrogen bonds. Similarly, in RNA, the base pairs are adenine and uracil (U) and guanine and cytosine.

There are large numbers of biological studies pertaining to the action of DNA inside and outside the cell, which is a broad and different subject area. Hence we suggest that the readers resort to the books indicated [343–345].

2.3.7.2 **Synthetic Nucleic Acids (SNA)**

The area of synthetic nucleic acids (SNAs) is quite new in the field of biopolymers and only preliminary work has been initiated by selected authors. Work in this area begins with the designing of artificial living systems with most of the cellular components being synthesized [346]. However it is to be noted that normal propagation of the system is carried out on plasmids. This is certified by companies such as Blue Heron that claim to be able to synthesize long pieces of DNA and propagate the synthesized DNA on plasmids in Escherichia *coli*. The authors could not, however, control the biological activities of this synthetic biological system efficiently, primarily because the natural system could not be completely copied owing to the presence of large number of other small and big components as promoters.

Another approach may be to use an *in vitro* replication system [347]. But *in vitro* replication eliminates many of the benefits and the built-up familiarity with cells. However, regardless of the organism used, at some point, one will want to

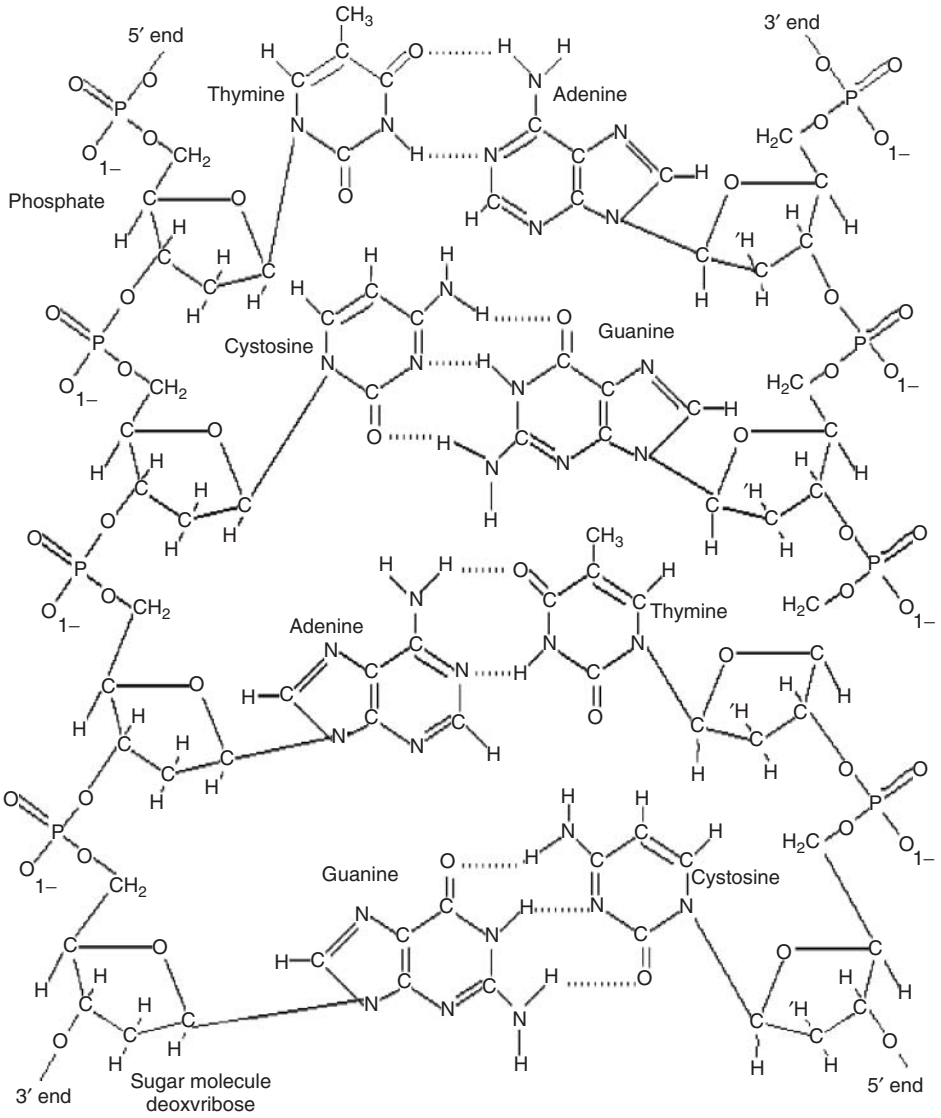

Figure 2.44 Chemical structure of DNA.

assemble components without interference with the native cell. In addition, *E. coli* is well-understood and easily manipulated.

In general, the approach would be almost like a cloning process where only the action of DNA polymerase is allowed during cell division but the role of RNA polymerase is eliminated. To achieve the previous goals, the authors used a SNA *in vivo*. SNA will be used here to represent one member from the entire family of nucleic acid analogs. The desired properties for the SNA include the following:

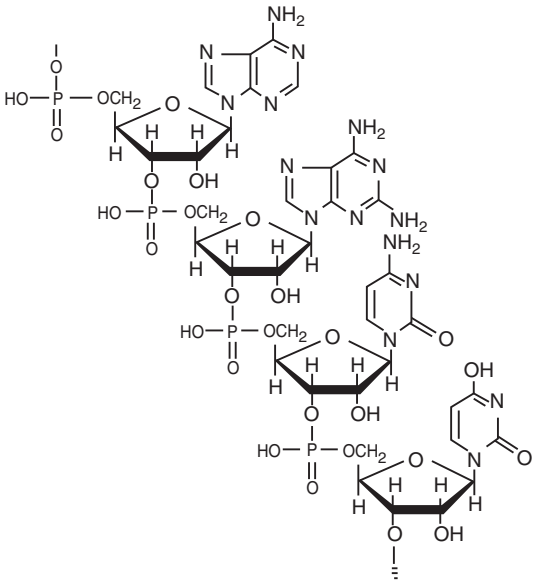

Figure 2.45 Chemical structure of RNA.

1) The SNA must be able to be easily replicated and maintained in cells. This means that the cloning strain must contain a DNA polymerase such as an enzyme that can faithfully replicate SNA to produce more SNA.
2) The SNA must not be recognized by RNA polymerase, as SNA inserts should not be expressed.
3) The SNA should be easily convertible to and from DNA to allow compatibility with other techniques.
4) Ideally, a plasmid can consist of a mix of DNA and SNA. This is to maintain a positive selection for the plasmid, and, for this, maintaining expression of an antibiotic resistance gene would be helpful.

There have been many artificially designed chemical molecules that resemble DNA, each with its own properties [348]. Changes to nucleic acids can be made in the bases used (other than A, T, U, C, G), the sugar (other than ribose or deoxyribose), or the backbone (other than a phosphodiester bond). The difficult part is not coming up with a nucleic acid analog, but rather coming up with one that has a reasonable chance of working *in vivo*. Recently, all four base pairs were replaced with larger synthetic pairs that formed a more stable and wider helix [349–352].

Other variants of SNA have also been prepared. Peptide nucleic acid (PNA) was designed by replacing the phosphate backbone of DNA with *N*-(2-amino-ethyl) glycine and connecting the base by a methylenecarbonyl group [353]. PNA has a peptidelike backbone but uses the bases found in DNA. It was designed to fit in roughly the same space as DNA, allowing PNA to form strong base pairing with DNA. PNA is comparatively easy to synthesize with manual methods or on

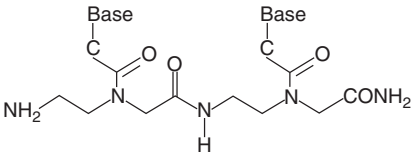

Figure 2.46 Peptide nucleic acid (PNA) consists of a peptidelike backbone joining the purines and pyrimidines of DNA, allowing it to base pair with DNA.

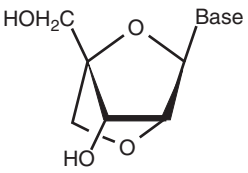

Figure 2.47 Locked nucleic acid contains an extra linkage between the 2′-O and 4′-C but is otherwise identical to RNA.

standard DNA or peptide synthesizers [354]. Figure 2.46 shows the structure of PNA.

Locked nucleic acid (LNA) consists of an extra methylene linkage between the 2′-oxygen and the 4′-carbon of the ribose sugar [355] (Figure 2.47). This extra conformation restriction increases the binding of LNA with complementary DNA. LNA is more similar to DNA than PNA. LNA has the same charged phosphodiester backbone as standard DNA, making it more soluble than PNA. LNA oligos can be also synthesized using the standard phosphoramidite chemistry and it is possible to synthesize chimeric LNA/DNA oligos [356].

Some other possibilities for nucleic acid analogs include using left-handed DNA, methylated DNA, or DNA that uses L-ribose or perhaps a completely different sugar. For example, hexitol nucleic acids (HNAs) [357, 358] have a six-membered sugar ring and can form similar helical structures with normal nucleic acids. Other nucleic acids analogs with different sugars have been shown to form much stronger base pairs than RNA and have been postulated to be part of the early evolution of nucleic acids [359, 360]. Thus, there is hope that a nonribose-based nucleic acid could function and may even function better than the existing system. Minor modifications to natural nucleic acids have also been carried out to obtain recombinant nucleic acids where one or more genes are modified to suit the required functions [361, 362].

A detailed description on this topic is beyond the scope of this chapter. Hence the readers may refer other books/articles listed in the bibliographic section for detailed analysis.

2.4 Synthetic Biopolymers

Polyesters, polyamides, PUs and polyureas, poly(amide-enamine)s, poly(anhydrides) (PAs), and so on are synthetic biopolymers. This section

mainly deals with the polymers prepared by condensation and ring-opening polymerization (ROP) methods. Synthetic biodegradable polymer materials offer more advantages than natural materials; they can be synthesized to give various properties such as predictable uniformity, no concerns regarding immunogenicity, and availability of a reliable source of raw material because the polymer materials with the fundamental building block units have simple and well-known structure and properties [15]. Synthetic materials have many advantages in their being used as scaffolds. These polymers can be tailored to produce an extensive range of mechanical properties and degradation rates and they also represent a more reliable source of raw materials with the ability to provoke an immune response in body.

2.4.1
Poly(Glycolide) PGA or Poly(Glycolic Acid)

Poly(glycolic acid) (PGA) is a rigid thermoplastic material prepared by ROP of a cyclic lactone, glycolide (Scheme 2.2). This is the simplest linear aliphatic polyester and it is not soluble in most organic solvents. It is a highly crystalline biopolymer with a crystallinity of 45–55%. It has a high melting point (220–225 °C) and a glass-transition temperature of 35–40 °C. PGA has excellent mechanical properties. Its biomedical applications are limited by its low solubility and its high rate of degradation, yielding acidic products. Consequently, copolymers of glycolide with caprolactone, lactide, or trimethylene carbonate have been prepared for medical devices [363].

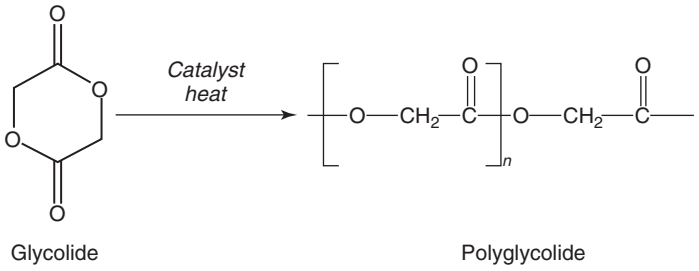

Scheme 2.2 Synthesis of poly(glycolide) or polyglycolide.

PGA can be used to fabricate into foam and porous scaffolds. The degradation and the properties can be affected by the type of processing technique; PGA is highly sensitive to degradation and it requires precise control of processing conditions. PGA is used in biomedical fields because of its degradation properties. Glycolic acid, a natural metabolite is produced by the degradation of PGA [15].

2.4.2
Poly(Lactic Acid) (PLA)

Poly(lactic acid) (PLA) is synthesized by the cyclic dimer of lactic acid (LA) that exists as two optical isomers: D- and L-lactate are the naturally occurring isomers,

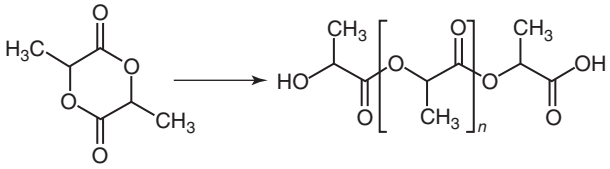

Scheme 2.3 Synthesis of poly(lactic) acid or polylactic acid.

and DL-lactide is the synthetic blend of D-lactide and L-lactide (Scheme 2.3). The semicrystalline homopolymer poly(L-lactide) (PLLA) has high tensile strength, elongation, good mechanical strength, degradation, biocompatibility, and modulus that make it more suitable for load-bearing applications such as sutures, scaffolds for tissue engineering, drug carriers, and orthopedic fixation [364]. PLA has a linear structure, and has one pendent methyl group, which makes it more amorphous and hydrophobic than PGA owing to the increase in the amorphous behavior; the solubility in the organic solvents are also amplified. PLA can be dissolved in various organic solvents, such as chloroform, methylene chloride, methanol, ethanol, benzene, acetone, and dimethylformamide (DMF) [15].

LA is the main precursor in the synthesis of PLA. There are three different routes involved in the synthesis of PLA. (i) The first route involves condensation of the L- and D-LA isomers to generate a low molecular weight prepolymer. These low molecular weight prepolymers can only be used after the addition of the external chain-coupling agents whose function is to increase the chain length of the polymer. This would prevent the polymer from becoming brittle and unusable. (ii) The second route involves ROP of the lactide, resulting in high molecular weight PLA. Solution polymerization, bulk polymerization, and melt and suspension polymerization are mainly used for the synthesis of LA-based polymers by ROP. (iii) The third route involves azeotropic dehydrative condensation of LA to yield high molecular weight PLA. This route does not require addition of chain extenders.

2.4.3 Poly(Lactide-*co*-Glycolide)

L-lactide and DL-lactide (L) have been used for copolymerization with glycolic acid monomers (G). Different ratios of poly(lactide-*co*-glycolide) (PLGA) have been commercially developed (Scheme 2.4). Amorphous polymers are obtained for a 25L : 75G monomer ratio. A copolymer with a monomer ratio of 80L : 20G is

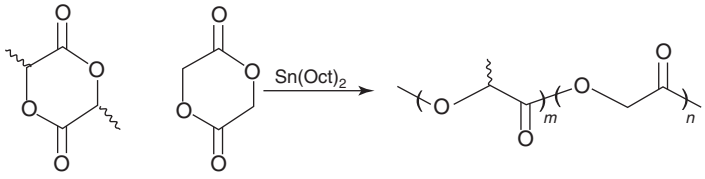

Scheme 2.4 Synthesis of poly(lactide-*co*-glycolide).

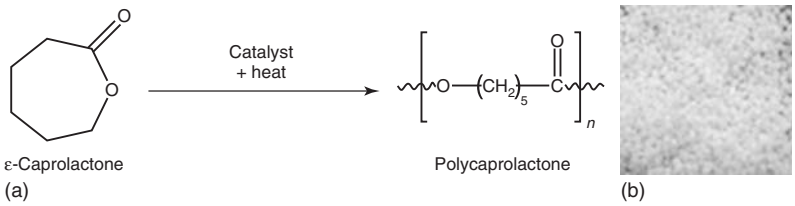

Figure 2.48 (a) Synthesis of polycaprolactone and (b) its physical appearance.

semicrystalline. The degradation rate of the copolymer decreases as the monomers L/G ratio increases [363]. This biopolymer is used in biomedical fields as resorbable suture, resorbable wound dressing, in facial augmentation, and in orthopedic fixation devices. This resorbable polymer is widely used in the biomedical field as scaffold in tissue regeneration because its degradation product is resorbed through metabolic pathways [365, 366].

2.4.4
Polycaprolactone (PCL)

Polycaprolactone (PCL), a bioresorbable and biocompatible aliphatic polyester produced by the ROP of caprolactone (Figure 2.48), has low melting point of around 60 °C and a glass-transition temperature of about −60 °C. PCL is derived by chemical synthesis from crude oil. It is generally used in pharmaceutical products. It has good water, oil, solvent, and chlorine resistance. This implantable biomaterial is degraded by hydrolysis of its ester linkages in physiological conditions (e.g., in the human body). PCL nanofibrous matrices coated with collagen support cell growth or make the three-dimensional structured multilayer of PCL nanofibers and collagen nanofibers suitable for blood-vessel engineering [367].

2.4.5
Poly(*p*-Dioxanone) (PDO)

Poly(*p*-dioxanone) (PDO) is a well-known aliphatic polyester; it is prepared by ROP of *p*-dioxanone, and shows good physical properties (Scheme 2.5). It is semicrystalline, with a low glass-transition temperature in the range −10 to 0 °C. The properties of PDO with different molecular weights have been investigated [363]. Molecular weight has a positive influence on the thermal stability of PDO. PDO has ester bonds in the polymer chains, which play a crucial role in its biodegradation [368].

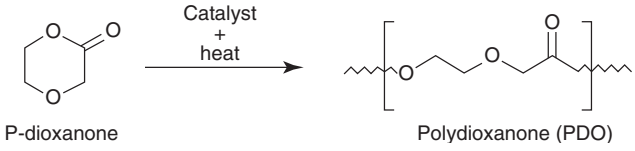

Scheme 2.5 Synthesis of poly(dioxanone).

2.4.6
Poly(Trimethylene Carbonate) (PTMC)

Poly(trimethylene carbonate) (PTMC) is a flexible polymer with high molecular weight, which is obtained by the ROP of trimethylene carbonate (Scheme 2.6). For soft-tissue regeneration, PTMC has been examined as an excellent implant material, owing to its excellent flexibility and poor mechanical strength [369]. For drug delivery applications, low molecular weight PTMC has been explored as an appropriate material. PTMC undergoes surface degradation with the rate of *in vivo* degradation was found to be much higher than *in vitro* degradation. This is most probably due to the contribution of *in vivo* enzymatic degradation process [370].

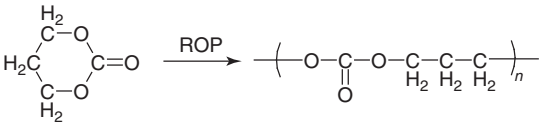

Scheme 2.6 Synthesis of poly(trimethylene carbonate).

2.4.7
Poly-β-Hydroxybutyrate (PHB)

Poly-β-hydroxybutyrate (PHB) is a linear head-to-tail homopolymer of (*R*)-β hydroxybutyric acid, which forms crystalline cytoplasmic granules in a wide variety of bacteria (Figure 2.49). After implantation, this biodegradable and biocompatible microbially produced polyester degrades slowly at body temperature and generates a nontoxic metabolite that is secreted in the urine. PHB has been used as a scaffolding device for wounds, designed to support and protect a wound against further damage, while promoting healing by encouraging cellular growth on and within the device from the wound surface. It has also been applied as a wraparound implant to guide axonal growth after peripheral nerve injury. The various applications of PHB and their copolymers are in biomedical devices and biomaterial applications, such as bone plates, sutures, rivets, staples, screws, orthopedic pins, and bone marrow scaffolds, and meniscus regeneration devices [371].

2.4.8
Poly(Glycerol Sebacic Acid) (PGS)

Poly(glycerol sebacic acid) (PGS) is a tough, biodegradable elastomer made from biocompatible monomers; it is also called *biorubber*. PGS is prepared by network condensation between glycerol and sebacic acid (Figure 2.50). It has good mechanical properties, rubberlike elasticity, and surface erosion biodegradation. PGS is

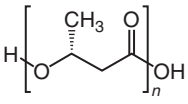

Figure 2.49 Structure of poly-β-hydroxybutyrate.

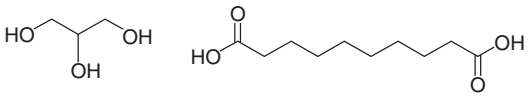

Figure 2.50 Monomers, glycerol and sebacic acid, used for making poly(glycerol sebacic acid).

proved to have similar *in vitro* and *in vivo* biocompatibility to PLGA, a widely used biodegradable polymer [372].

2.4.9
Poly(Propylene Fumarate) (PPF)

Poly(propylene fumarate) (PPF) is a synthetic, unsaturated, linear polyester. The synthesis of PPF commonly utilizes two steps: in the first step; diethyl fumarate reacts with excess propylene glycol to produce hydroxypropylfumarate in the presence of zinc chloride as acid catalyst (Scheme 2.7). PPF can be cross-linked through its fumarate double bond. PPF achieves high mechanical strength when it is properly cross-linked. Because of this property, it is highly recommended in bone replacement scaffolding. The porous PPF scaffold gives the osteoconductive surface for bone in-growth [373].

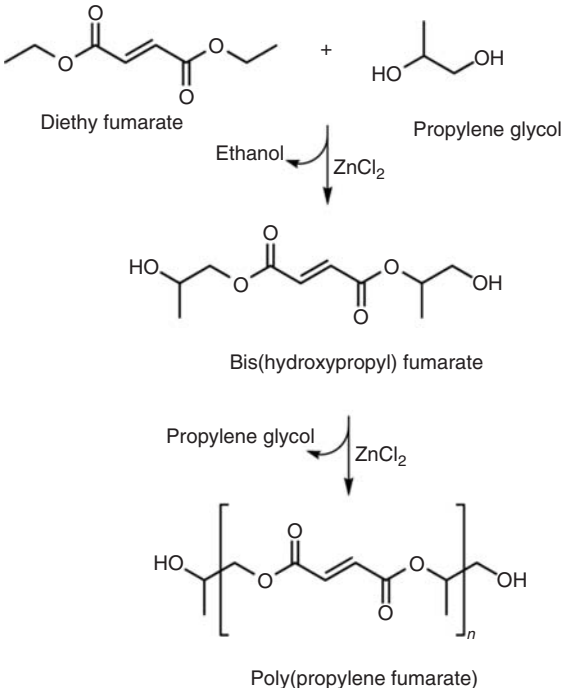

Scheme 2.7 Synthesis of poly(propylene fumarate).

PPF is soluble in methylene chloride, chloroform, tetrahydrofuran, acetone, ethanol, and ethyl acetate; it is partially soluble in toluene and insoluble in petroleum or water. Degradation can occur by hydrolytic chain scission of its ester groups.

The main by-products obtained on degradation of PPF are propylene glycol and fumaric acid. Owing to its biocompatibilty, these products can be easily removed from the body. The main characteristic of PPF is injectability into the body. The polymer becomes easy to handle as it is in the liquid form before cross-linking. It can also easily produce asymmetrically formed implants by injection molding. This characteristic makes it appropriate for the orthopedic implant in minimally persistent procedures [15].

2.4.10
Poly(Anhydrides) (PAs)

PAs are a hydrolytically unstable class of biodegradable polymers that are usually aliphatic, aromatic, or a mixture/blend of two components. PAs have demonstrated biocompatibility and excellent properties such as CR characteristics. PAs are synthesized by dehydration of the diacid or mixture of diacids by melt polycondensation photo cross-linking (Figure 2.51) [374].

2.4.11
Poly(Orthoesters) (POEs)

Poly(orthoesters) (POEs) constitute a class of amorphous, hydrophobic, biodegradable polymers. Different families of POEs have been reported (Figure 2.52). In addition to their surface wearing down mechanism, the rate of degradation of POEs is pH sensitive. They can be easily dissolved in organic solvents together with chloroform, methylene chloride, and dioxane owing to their hydrophobic nature [375].

Poly(orthoesters) can be prepared by the addition of diols to diketene acetals POE I and II. The polymer has significant potential for producing useful commercially relevant biodegradable drug delivery products (Scheme 2.8). They have great importance because of their ease of synthesis, reproducibility, and thermal stability, making possible compression, extrusion, or injection molding; they have the ability to withstand radiation sterilization without excessive loss of molecular weight. Most importantly, they can be stored under anhydrous condition at room temperature for long periods of time. They can efficiently entrap highly hydrophobic drugs such as doxorubicin or taxol because of their excellent hydrophobicity [376].

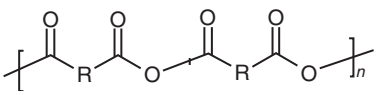

Figure 2.51 Structure of polyanhydrides.

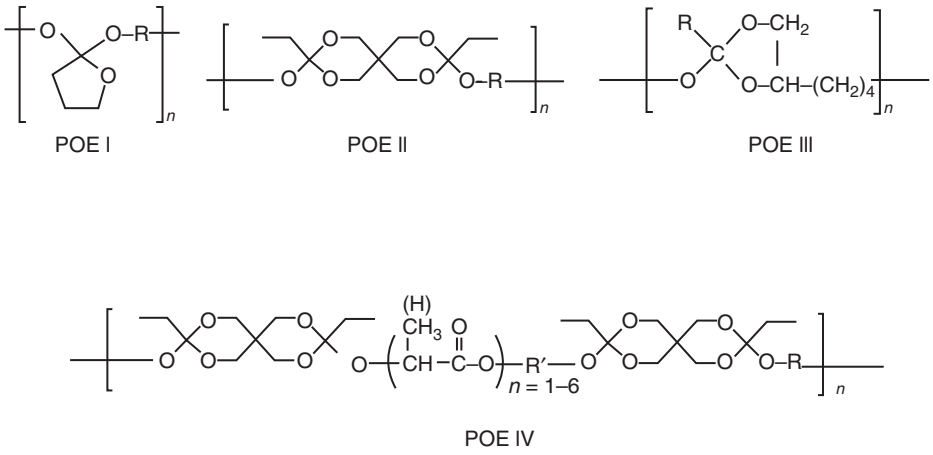

Figure 2.52 Four polymer families in poly(orthoesters).

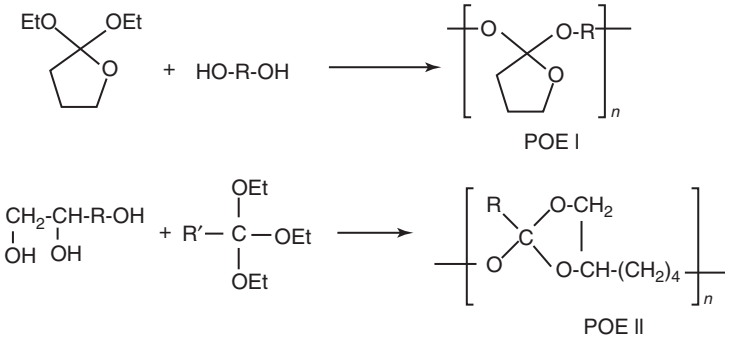

Scheme 2.8 Synthesis of poly(orthoesters).

2.4.12
Poly(Phosphazene)

Poly(phosphazenes) are prepared by the thermal ROP of hexachlorophosphazene $(Cl_2PN)_3$ (Figure 2.53) followed by esterification of the intermediate poly(dichlorophosphazene) with either amines or sodium salts of alcohols. Biodegradable polyphosphazene is synthesized by the addition of certain side groups on the phosphorous atoms that are sensitive to hydrolysis. The phosphazene polymers have aryloxy side groups functionalized with sulfonic acid, phosphonic acid, or sulfonimide groups, while alkoxy, amino (R_2N), or halogens (such as chloride or fluoride) are the other substituents. Poly(phosphazenes)

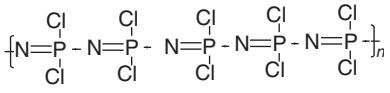

Figure 2.53 Structure of poly(phosphazene).

are excellent for drug delivery and tissue-engineering applications. They have glass-transition temperatures that range from −100 °C to more than +200 °C. Their properties include low temperature flexibility and elasticity; resistance to hydrocarbon fuels, oils, and hydraulic fluids; fire resistance, radiation resistance, and ultraviolet stability [377, 378]. Biodegradable polyphosphazene has prospective application in bone tissue engineering. The poly(phosphazene) of the amino acid ester group is an excellent biodegradable material. Amino acid is the degradation product of poly(phosphazene) [371]. Poly(phosphazene) is highly blood compatible and is studied as a material for blood-connecting devices. The decomposition products of this polymer were found to be natural and nontoxic. Poly(phosphazene) is the main component of proton-conductive polymers, which are synthesized and studied for use in polymer electrolyte fuel cells. The electrochemical stability, access to phase-separated hydrophilic/hydrophobic composite materials, and the ease of property tuning via cosubstituent groups are the major advantages of the polymer. As it is resistant to alcohol crossover, the polymer is very useful in fuel cells. Microspheres prepared from poly(phosphazene) are also used for the oral delivery of vaccines. Phosphazene elastomers are the one of the established applications of poly(phosphazenes). The major applications of phosphazenes are shock-absorbing devices for low temperature uses, and in the fabrication of O-rings, seals, and so on.

2.4.13
Poly(Vinyl Alcohol) (PVA)

Poly(vinyl alcohol) (PVA) is produced commercially from poly(vinyl acetate), usually by a continuous process. The acetate groups are hydrolyzed by ester interchange with methanol in the presence of anhydrous sodium methoxide or aqueous sodium hydroxide. PVA is an odorless and tasteless, translucent, white or cream-colored granular powder. It is widely used in pharmaceutical industry, paper coating, adhesives, and textile industries. PVA is water soluble and can dissolve in wastewater. Several microorganisms have been known to degrade PVA [379–382] (Figure 2.54). Owing to its excellent film-forming, emulsifying, and adhesive properties, PVA has broad industrial use such as water-soluble packaging films, paper adhesives, textile-sizing agent, and paper coatings [383–385]. PVA can be processed by solution casting and orientation to make high performance PVA films.

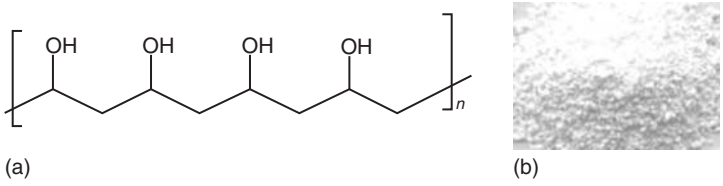

Figure 2.54 (a) Structure of poly(vinyl alcohol) and (b) its physical appearance.

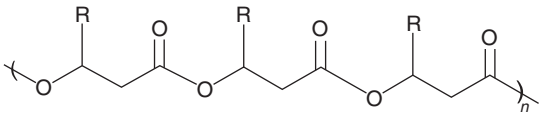

Figure 2.55 Structures of poly(hydroxyalkanoates).

2.4.14
Poly(Hydroxyalkanoates) (PHAs)

The biological polyesters, poly(hydroxyalkanoates) (PHAs) are mainly produced by microbial fermentation processes (Figure 2.55) [386]. They are lipoidic material accumulated by a variety of microorganisms in the presence of an abundant carbon source and are biochemically processed into hydroxyl alkanoates units, polymerized, and stored in the form of water-insoluble inclusions in the cell cytoplasm. They are polymers of hydroxyalkanoic acids that are accumulated intracellularly as granule inclusions by prokaryotic microorganisms (eubacteria and archaea) as carbon and energy reserves or reducing-power storage materials [387, 388]. They are synthesized in the presence of excess carbon, especially when another essential nutrient, such as nitrogen or phosphorus, is limiting [389, 390]. Their biocompatible and biodegradable nature helps them to be used in fields dominated by commodity plastics.

2.4.15
Poly(Ester Amides) (PEAs)

Poly(ester amides) (PEAs) are a class of synthetic polymers bearing both ester and amide repeat units (Scheme 2.9). These repeat units along the polymer chain can be

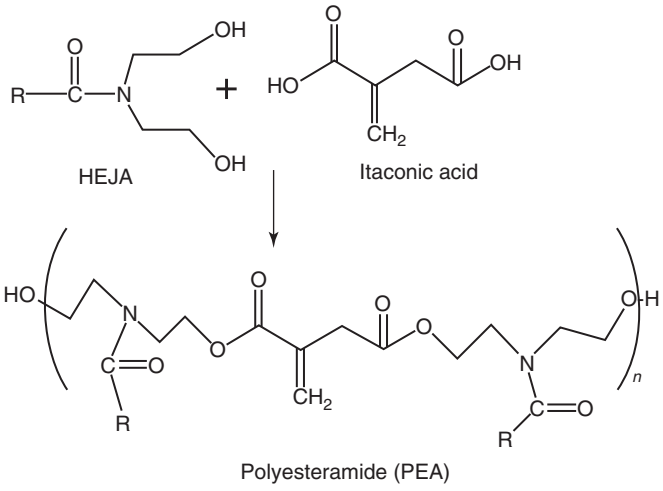

Scheme 2.9 Synthesis of poly(ester amides).

introduced using a variety of materials and methods. PEAs are vulnerable for both hydrolytic and enzymatic degradation [391–397]. The ester linkages give cleavage via hydrolysis; the hydrophobicity of the PEAs promotes enzyme adsorption, thus enhancing its surface erosion [398], which may limit a large accumulation of degradation products in the local tissue [399]. PEAs are readily biodegradable, so they can be used for the production of vascular grafts [393].

2.5 Need for Biopolymers

The growing dependence on synthetic polymers has raised a number of environmental and human health concerns. Most of the plastic materials are not biodegradable. These nonrenewable materials have high durability and strength and it is very difficult to dispose such plastic materials. In addition, the synthesis of some polymeric materials involves the use of toxic compounds or the generation of toxic by-products. These problems have focused increased attention on polymers that are derived from biological precursors or are produced by using the methods of modern biotechnology. The potential applications ranges from agriculturally or bacterially obtained thermoplastics, which are truly biodegradable, to novel medical materials that are biocompatible, to water treatment compounds that prevent mineral buildup and corrosion [400].

The uses of long-lasting polymers are broadly accepted for short-lived applications (packaging, catering, surgery, hygiene) which are not completely sufficient. The increasing concern about the preservation of ecological systems is not justified. Nowadays, synthetic polymers are produced from petrochemicals and are not biodegradable. These persistent polymers are major sources of environmental pollution, harming wildlife, when they are dispersed in the environment. For example, sea life is harmfully affected by plastic bags [401]. Plastics have an important role in waste management, and the collectivities (municipalities, regional, or national organizations) are becoming aware of the important savings that the collection of compostable wastes would provide. Energetic valorization of plastic waste leads to emission of toxic materials such as dioxin. Material valorization causes difficulties in finding appropriate and economically feasible outlets. It has also shown negative eco-balance in all cases such as waste grinding and plastic processing.

Recently, the attention of socioeconomical life has been focused on replacing conventional plastic with degradable polymers, especially for packaging applications. Biodegradable polymers and polymers derived from agro-resources such as the polysaccharides have been recognized for the applications. These agro-polymers find applications in food industry, while they have no extensive applications in packaging industry to replace conventional plastic materials. But they are likely to be used to overcome the limitation of the petrochemical resources in the future. Greener agricultural sources can be used to partially replace fossil fuel and gas and this is expected to contribute to the reduction of CO_2 emissions [401].

2.6
Exceptional Properties of Biopolymers

The extraordinary properties of the biopolymers are due to their excellent biocompatibility and biodegradability. Synthetic polymers are also attractive because they can be fabricated into various shapes with desired pore morphologic features conducive to tissue in-growth. Furthermore, the polymers can be designed with chemical functional groups that can induce tissue in-growth [402]. Polysaccharides have a surprising ability for structure formation by supramolecular interactions, and, because of this ability, they can be used to modify advanced materials.

The key advantages include the ability to tailor mechanical properties and degradation kinetics to suit various applications. Biodegradable synthetic polymers offer a number of advantages over other materials for developing scaffolds in tissue engineering. PLA and PGA can be broken down into biologically suitable molecules that are metabolized and removed from the body via normal metabolic pathways. PLA is of increasing commercial interest as it is completely made from renewable agriculture products with excellent properties comparable to many petroleum-based plastics [403].

2.7
Biomedical Polymers

Crystallinity and hydrophilic nature influence the biodegradability of a polymer. A semicrystalline nature tends to limit the accessability, effectively confining the degradation to the amorphous region of the polymer [1]. The chemical properties that are significant include (i) the chemical linkages in the polymer backbone and (ii) the pendant groups, their position, and their chemical activity.

Degradable polymeric biomaterials find useful applications in biomedical fields such as developing artificial bone, artificial tissues devices such as temporary prostheses, three-dimensional porous structures as scaffolds for tissue engineering, and as controlled/sustained release drug delivery vehicles. For providing efficient therapy, the material should have specific physical, chemical, biological, biomechanical, and degradation properties. For biomedical applications, natural or synthetic polymers degraded by hydrolytic or enzymatic route are being explored [369]. Synthetic biopolymers have become attractive alternatives for biomedical applications for the following reasons: (i) although most biologically derived biodegradable polymers possess good biocompatibility, some may trigger an immune response in the human body, possibly one that could be avoided by the use of an appropriate synthetic biopolymer; (ii) chemical modifications to biologically derived biodegradable polymers are difficult; (iii) chemical modifications likely cause the alteration of the bulk properties of biologically derived biodegradable polymers. A variety of properties can be obtained and further modifications are possible with properly designed synthetic biopolymers without altering the bulk properties.

The two major advantages of biodegradable polymer implants that are being used as a scaffold in spinal code injury (SCI) treatment are in serving as a structural scaffold for axonal growth and as a conduit for time-released delivery of therapeutic agents. Biodegradable polymer grafts are preferable to nondegradable grafts in that they do not leave behind any unnatural products in the body and are not subject to delayed immune rejection. The graft technology holds a great promise in the future of the spinal cord regeneration although it faces many obstacles [404]. The essential biomaterials that are used for tissue engineering and drug delivery are biodegradable and biocompatible polymer scaffolds [405–407].

The suitability of biomaterials in such applications has an important role in determining the molecular design of these materials. The most suitable approach of these applications is to inject the drug/polymer-cell entity to the body. Injectable systems offer specific advantages over preformed scaffolds, which include ease of application, confined delivery for a site-specific action, and improved patient compliance and comfort [408]. Various methods have been engaged for the preparation of injectable hydrogel systems. Water-soluble, thermosensitive, and pH-sensitive polymers exhibiting reversible sol–gel transition and photopolymerizable hydrogels have been tailor-made as injectables [409–412].

Hydrogels derived from naturally occurring polymers exhibit wound-healing properties and stabilize the encapsulated and transplanted cells. They mimic many features of ECM and are used to direct the migration, growth, and organization of cells during tissue regeneration. In recent years, there has been a marked increase in interest in biodegradable materials for use in packaging, agriculture, medicine, and other areas. PGA suture is gradually degraded upon hydrolysis and decreases in strength in the human body. It is completely absorbed in about 15 weeks after operation. In addition, our PGA suture has dependable knot stability and exceptional smoothness.

2.7.1 Chitosan

Chitosan has specific applications in the biomedical and biotechnological fields. It is generally more efficient in a solid nano- or microstructured morphology with respect to different soluble forms. DNA/chitosan nanospheres are used as long-term delivery vehicles (Figure 2.56) because of their intrinsic delivery properties. Chitosan has muco-adhesive properties and such molecules may be therefore efficiently employed for oral or nasal gene (or other drugs) delivery [413]. Chitosan is only soluble in aqueous solutions of some acids; therefore, the reaction of chitosan is significantly more versatile than cellulose due to the presence of NH_2 groups.

Current investigation is conducted to estimate the potential of using injectable material based on chitosan and its derivatives as a scaffold material for diverse tissue-engineering applications including cartilage, bone, and skin. Residual amount of acetyl content influences the chitosan degradation and degradation

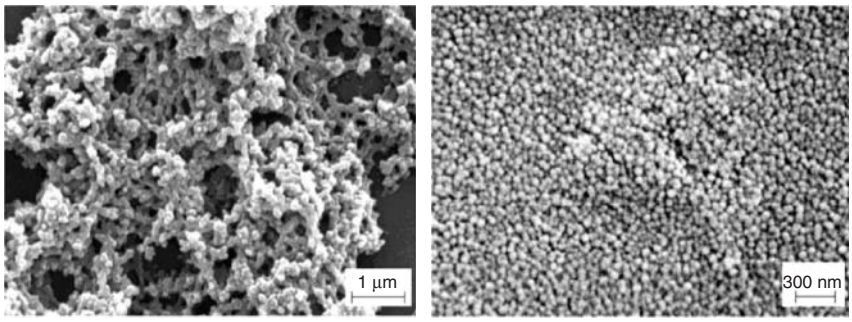

Figure 2.56 SEM images of chitosan/DNA nanospheres (H_2O/EtOH) obtained using a cellulose acetate membrane (MWCO = 12 kDa) at different magnification [414].

rate can occur rapidly *in vivo*. The mechanical properties may be influenced by controlling the porosity of the chitosan scaffold [415].

2.7.2 Poly(Lactic Acid) (PLA)

The main precursor in PLA biopolymer synthesis is LA, which is produced in large amounts by the bacterial fermentation of the hexoses (carbon source) using LA bacteria. Since it is biocompatible, it is used in biomedical applications such as implants, sutures, drug delivery, tissue engineering, and stent development. PLA can be processed using various techniques and are commercially available in the market in different grades. The biodegradability of polymers based on LA and its copolymers with ethylene glycol (EG) is used in various applications such as encapsulation and drug delivery, gene therapy, drug targeting, dental and medical devices, sutures, tissue engineering, micellar anticancer carriers, orthopedic fixation devices, formulation of artificial blood systems, and determination of cellular pathway mechanisms. PLA is biodegradable, biocompatible, and has good mechanical properties. It dissolves in common solvents and has been successfully employed as matrices for cell transplantation and tissue regeneration [32].

2.7.3 Collagen

Collagen is a protein of ECM and exists in the basal membrane of the cell. It is easily purified, and so can be proposed as a suitable substance; however, collagen has less strength to withstand long-term use and support force adhesion, as it degrades enzymatically within short periods. Therefore, using another polymer such as PCL to enhance the stability and mechanical strength of collagen would be necessary. This way, an excellent scaffold for Schwann cell adhesion, migration, orientation, and proliferation can be provided.

It has been extensively used for the regeneration of tissues, mostly for the repair of soft tissues and favors the cell adhesion and provides cellular recognition for

regulating cell attachment and function. It may lead to the concern of unfavorable immune response. Corresponding amino acids are obtained when this biopolymer undergoes enzymatic degradation, which occurs in the body via enzymes such as collagenases and metalloproteinases [32].

Degradable collagen sponges have porous structures and have been extensively studied as scaffold material for accelerated tissue reproduction. The drawbacks of collagen are its variable physical, chemical, and degradation properties, the risk of infection, and difficult-to-handle processing [416]. Absorbable collagen sponges, due to their excellent biocompatibility, biodegradability, and porous structure, have been broadly investigated as a scaffolding material for accelerated tissue regeneration. Duragen is a suture-free, three-dimensional collagen matrix graft designed for spinal dural repair and regeneration is currently undergoing late-stage clinical trial [417]. Similarly, a composite of fibrillar collagen, HAP, and TCP (Collagrafts) has been approved by the FDA for use as a biodegradable synthetic bone graft substitute. Collagen is also being used as the scaffolds for cardiovascular, musculoskeletal, and nervous tissue engineering. Collagen glycosaminoglycan (CG) scaffolds have been clinically approved as an application for skin regeneration [418].

2.7.4
Polycaprolactone (PCL)

PCL is a bioresorbable and biocompatible aliphatic polyester that is generally used in pharmaceutical products and wound dressings. In addition, PCL nanofibrous matrices coated with collagen support cell growth or make the three-dimensional structured multilayer of PCL nanofibers and collagen nanofibers suitable for blood vessel engineering [404].

2.7.5
Poly(2-Hydroxyethyl Methacrylate) (PHEMA)

Poly(2-hydroxyethyl methacrylate) (PHEMA) is particularly attractive for biomedical engineering applications (Figure 2.57). Because of its physical properties and high biocompatibility, this polymer is widely used in medical fields especially contact lenses, kerato prostheses, and as orbital implants. The PHEMA scaffold could be easily incorporated into the nerve guidance tubes [404].

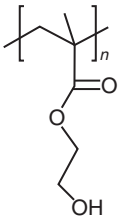

Figure 2.57 Poly(2-hydroxyethyl methacrylate) (PHEMA).

2.7.6 Carbohydrate-Based Vaccines

Carbohydrate-based vaccines, such as tumor-associated carbohydrate antigens (e.g., sTn), are a dynamic area of research. Synthetic carbohydrate polymers that are biocompatible and biodegradable are increasingly used in tissue engineering and controlled drug-release devices. Specifically, *N*-(2-hydroxypropyl) methacrylamide copolymers modified with galactosamine are known to interact with the asialoglycoprotein receptor on hepatocytes and hepatocarcinomas. Similar copolymers containing galactose, fucosylamine, and mannosamine have been targeted to hepatocytes, mouse leukemia L1210 cells, and macrophages, respectively. These specific carbohydrate-based interactions could be applied as carriers for drug or gene delivery. A sulfated-glucoside-bearing polymer activates the fibroblast growth factor, suggesting its use as an active component of tissue-engineering matrices. Modified chitosans are promising polymers as supports for hepatocyte and chondrocyte attachment, which can be applied as carrier materials for transplantation or as a scaffold for tissue engineering. The specific interactions of carbohydrates and proteins have also facilitated the application of carbohydrate polymers as specific enzyme inhibitors and in the treatment of infectious diseases [419].

2.7.7 Chitin

Chitin is found in the exoskeleton as well as in the internal structure of invertebrates. It is a nontoxic biopolymer having excellent antibacterial property, biodegradability, and biocompatibility. It is a white, hard, inelastic, nitrogeneous polysaccharide. It is highly hydrophobic and is insoluble in water and most organic solvents. Owing to these properties, it is extensively used for biomedical applications such as tissue engineering scaffolds, drug delivery, wound dressings, separation membranes and antibacterial coatings, stent coatings, and sensors. Currently, electrospinning is the most suitable technique for producing chitin fibers of high surface area and porosity and these nanofibers are extensively used in biomedical fields [419].

2.7.8 Albumin

Albumin is the protein portion of the blood, hence it is important in maintaining blood volume. It is used in the treatment of shock, burns, or low blood protein to temporarily correct or prevent a blood volume deficiency. Human body has the ability to degrade albumin.

Albumin is highly compatible with blood and therefore it is used for drug delivery applications. It is a well-characterized protein and serves important needs as a therapeutic, diagnostic agent, as well as an excipient. Recombinant albumin may also serve as a useful case study for follow-on biologics [15, 420, 421].

2.7.9 Fibrin

Fibrin is always used as carrier for cells and in conjunction with other scaffold materials. It is completely degradable and injectable, but it has the disadvantage of poor mechanical strength for articular cartilage tissue engineering applications [15]. Bioseed is a fibrin-based product obtained by mixing keratinocytes with fibrin and is used to treat chronic wounds. The matrix properties can be optimized for each different cell type and it is a unique feature of fibrin-based cell carriers [422].

2.7.10 Hyaluronic Acid (HA)

HA is used as a diagnostic marker for many diseases including cancer, rheumatoid arthritis, and liver pathologies, as well as for supplementation of impaired synovial fluid in arthritic patients by means of intra-articular injections. It is also used in certain ophthalmological and otological surgeries and cosmetic regeneration and reconstruction of soft tissue [423, 424].

2.7.11 Chondroitin Sulfate (CS)

Numerous studies have investigated the efficiency of using composite scaffolds composed of CS and other biopolymer materials, such as collagen or synthetic biodegradable polymer materials, for cartilage tissue engineering [15].

2.7.12 Alginic Acid

Alginic acid is mostly used as cell transplantation vehicles to grow new tissues as well as in wound dressing. The main drawbacks of this polymer material are slow degradation and insufficient mechanical integrity, which makes it impossible for long-term implants [15].

2.7.13 Poly(Anhydrides)

PAs are used for the orthopedic application primarily focusing on achieving good mechanical strength. They are composed of the diacid molecules and water-soluble linear methacrylicacid molecules. The hydrolytic degradation of PA is nontoxic. These nontoxic, injectable scaffolds have low degradation and high compatibility, and these properties can be modified during the manufacturing and synthesizing of scaffolds [425]. PAs have fiber-forming properties, which makes them useful in biomedical applications [363, 374, 426, 427].

2.8
Composite Material

Composite material consists of two or more materials that behave together to get the better properties of scaffold. Polymer/ceramics composite scaffolds are imitations of natural bone. Natural bone is made of HAP and organic collagen material and this HAP has better osteoconductivity. HAP, as the mineral part in the formation of composites and collagen, gelatin, chitosan, chitin, elastin, poly(methylmethacrylate), PPF, polyphosphazenes, PHB, poly(lactide-*co*-glycolide) (PCL, PLLA, PGA), PA, and POE, it can be the matrix phase for the bone replacement.

Bioactive phases in the polymer composite can also alter the degradation behavior of the polymer materials, by allowing rapid exchange of protons in water for alkali in the glass in ceramics. This behavior provides the pH-buffering effect at the polymer surface transforming the acidic polymer degradation [425].

Biodegradable polymer scaffolds may offer a number of benefits for bone tissue engineering: enhanced environment for cell seeding, survival, growth, and differentiative function because of the osteoconductive function imparted by HAP, which improves mechanical properties that are essential for load bearing [428].

2.9
Blends

Polymeric material blends, being the combination of synthetic–natural, natural–natural, and synthetic–synthetic polymers, have good mechanical characteristics and easy processability [419]. Blending synthetic and natural polymers provides a control of the degradation rate of the system as the degradation kinetics of a polymeric blend increases on increasing the amount of the natural polymer, the blend composition can be adjusted to make the scaffold degradation rate match the growth rate of the regenerating tissue. There are many polymeric blends between natural and synthetic polymers, such as PLA/chitosan, PLA/HA, PLG/gelatin/elastin [429], PLLA/starch, and PCL/starch. An easy method to improve the compatibility of PCL is by blending it with a suitable hydrophilic natural polymer [430]. For example, a blend between PCL and starch has good mechanical properties and enzymatic degradation. Synthetic/synthetic blends of polymers were developed to get ease in processability, improve mechanical and biocompatible properties, and reduce the cost [431].

Chitosan/poly(vinyl pyrrolidone) (PVP) blends are very useful for controlling the release profile of a drug with poor water solubility. Chitosan and PVA form an immiscible system, as the interactions between macromolecules of PVA are stronger than between PVA and chitosan [432, 433].

Blends of collagen with other hydrophilic polymers can be used as good-quality hydrogels [434–439] and as biodegradable polymeric scaffolds, which are widely used in medical applications [42, 439–453].

2.10 Applications of Biopolymers

Biodegradable polymers are used especially in three major areas, namely, agricultural, medical, and consumer goods packaging, of which medical device applications have developed faster than the other two because of their focused nature and greater unit value (Figure 2.58). Some of these have resulted in marketable products.

2.10.1 Medical Applications

Biodegradable plastics have broad applications as surgical implants in vascular and orthopedic surgery as implantable matrices for the controlled long-term release of drugs inside the body, as absorbable surgical sutures, and for use in the eye. Recently, the term *biomaterial* was defined as a nonviable material used in medical device applications that is intended to interact with a biological system [454]. Biocompatibility is the ability of a material to perform with an appropriate host response in a specific application [363, 374, 426, 427]. Poly(lactide), poly(glycolide), and other materials such as PDO, PTMC, PCL, and PLGA have been widely used for medical devices [455].

PLLA bone fixation devices are gradually absorbed in the human body and are used for osteotomy and osteosynthesis, thus providing effective for use in bodily regions in which surgical removal is complicated.

2.10.1.1 Surgical Sutures

Loss of structural integrity results from tissue damage and the insertion of some material or device to hold the tissue together may facilitate the healing process. The classic examples are the use of sutures to hold both deep and superficial wounds together. Once the healing is complete, the suture becomes unnecessary and can impose undesirable constraints on the healing tissues. It is preferable to remove the material from the site, either by degradation or by physical ways.

Synthetic absorbable sutures were developed in 1960s. They are now extensively used in tracheobronchial surgery as well as general surgery, because of their good biocompatibility in tissues (Figure 2.59). They are multifilament-type sutures, which have good handleability. PGA, PLLA and their copolymers, and polyglactin are the most popular and are now commercially available [363, 374, 426, 427]. PGA sutures have reliable knot stability and excellent smoothness.

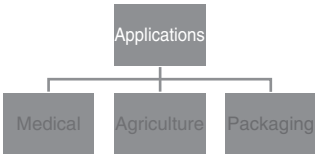

Figure 2.58 The major fields of applications of biopolymers.

Figure 2.59 Absorbable suture thread material.

2.10.1.2 **Bone Fixation Devices**

Metal fixation in fracture treatment for undisturbed bone healing is a successful procedure as the cortical bone and steel have very different mechanical properties. The elasticity constant of bone is only 1/10 that of implanted steel, while tensile strength is 10 times lower [426, 427, 456, 457]. Thus, the removal of metal implants can result in weakened bone with a danger of refracture. Biodegradable implants can meet the dynamic processes of bone healing, decreasing the weight-bearing of the material. After months, the entire material will disappear completely and no secondary surgery is necessary. PLA, PGA, and PDO have potential roles in this area. For clinical applications, PDO was recommended for ligament augmentation, for securing a ligament suture, as a kind of internal splinting suture, and as a kind of internal splinting to allow for early motion of the extremities after an operation [363, 374, 426, 427].

PLLA bone fixation devices are gradually absorbed in the human body and are used for osteotomy and osteosynthesis, thus providing efficient for use in bodily regions in which surgical removal is difficult.

2.10.1.3 **Vascular Grafts**

Small-diameter vascular prostheses with incorporated matrices can be absorbed into a growing anastomotic neointima. It was pointed out that a gelatin–heparin complex when adequately cross-linked, could simultaneously function as a temporary antithrombogenic surface and as an exceptional substructure for an anastomotic

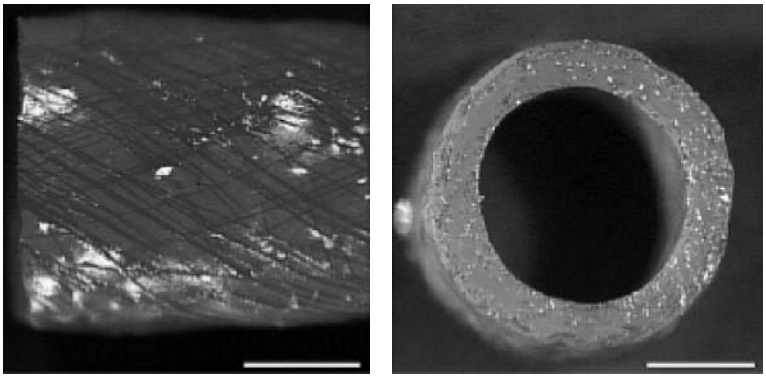

(a) (b)

Figure 2.60 Vascular grafts.

neointima [458]. Vascular grafts can also be fabricated from a recombinant elastin-like protein reinforced with collagen microfiber [459] (Figure 2.60).

2.10.1.4 **Adhesion Prevention**

Tissue adhesion after surgery is a serious complication and the materials that prevent tissue adhesion should be flexible and tough enough to offer a tight cover over the traumatized soft tissues, and should be biodegradable and reabsorbable after the injured tissue is completely regenerated [363, 374, 426, 427]. Photocurable mucopolysaccharides possess nonadherent surface characteristics such as biocompatibility and biodegradability in accordance with the wound healing property and nontoxicity. Therefore, they can be fabricated as tissue adhesion prevention material [458, 460].

2.10.1.5 **Artificial Skin**

Biodegradable polymers are used for healing burns, as skin substitutes, or for wound dressings. Now, most of the commercially developed artificial skins have utilized biodegradable polymers such as collagen [461], chitin, and poly-leucine [462], which are enzymatically degradable polymers. Fibrillar collagen (F-collagen) and gelatin combine to form a biomaterial in the form of a sponge, which can be used as artificial skin [463]. By introducing cross-links, the biomaterial was stabilized physically and metabolically.

Another progress in this area is biosynthetic wound dressing material with drug delivery capability. Chitosan-derivatized collagen is the main component of the spongy sheet that is used in medicated wound dressing. It is laminated with a gentamicin sulfate impregnated PU membrane.

2.10.1.6 **Drug Delivery Systems**

There are numerous degradable polymers that are potentially valuable for drug delivery applications. These include a collection of synthetic and natural substances. The use of intentionally degradable polymers in medicine has been brought into

importance with new innovations in drug delivery systems, for example, the use of controlled drug delivery systems [464, 465] from which the drug is released at a constant, predetermined rate, and possibly targeted to a particular site. One of the most prominent approaches is that in which the drug is contained within a polymer membrane or is otherwise encapsulated in a polymer matrix and where the drug diffuses out into the tissues following implantation. Polymer erosion or dissolution gives a way to the release mechanism in some cases. Degradable polymers such as PLA and poly(orthoesters), are used for drug delivery systems [363, 374, 426, 427].

2.10.1.7 **Artificial Corneas**

Collagen-based biopolymers, combined with synthetic cross-linkers or copolymers could be used in the field of tissue replacement in the future as scaffolds for developing prototype artificial corneas. These synthesized artificial corneas resemble the human cornea morphologically and functionally. The addition of synthetic polymers increases the suitability of the matrix scaffold for transplantation by increasing its toughness and retaining transparency and low light scattering [466, 467] (Figure 2.61).

2.10.1.8 **Artificial Blood Vessels**

PU is a strong, hard-wearing, tear-resistant, flexible, oil-resistant, and blood-compatible polymer. The functional properties of natural macromolecules can be merged with those of synthetic polymers having controllable structures and properties for the production of polymer/protein hybrids. In tissue engineering, silk fibroin/PU blend film can be used as scaffold material for artificial blood vessels [466] (Figure 2.62). Bacterial synthesized cellulose, which was designed

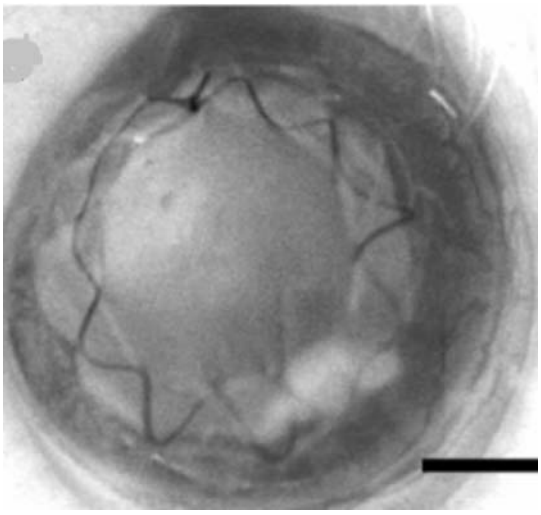

Figure 2.61 Artificial corneas.

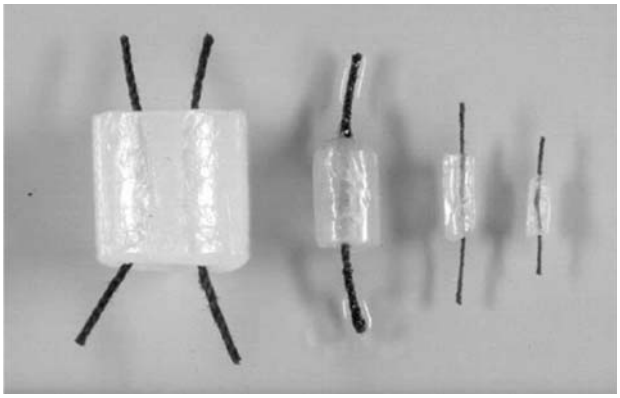

Figure 2.62 Artificial blood vessels.

directly during the culvivation, is also used as artificial blood vessel interpositions with an inner diameter of 1 mm [468].

2.10.2 Agricultural Applications

Plastics, coatings, elastomers, fibers, and water-soluble polymers are utilized in applications that comprise the CR of pesticides and nutrients, soil conditioning, seed coatings, gel plantings, and plant protection. However, degradable plastics are also of significance as agricultural mulches and agricultural planting containers. Biodegradability is also of some interest in composting as it would permit degradable plastics to be combined with other biodegradable materials and converted into useful soil-improving materials [363, 374, 426, 427].

2.10.2.1 Agricultural Mulches

Mulches allow growers to use plastic films to aid with plant growth and then photodegrade in the fields, thereby avoiding the cost of removal. Plastic films are advantageous because they conserve moisture, reduce weeds, and increase soil temperatures, thus improving the rate of growth in plants. Elimination of weeds and avoidance of soil compaction by the use of mulch eliminates the need for cultivation, therefore root damage and stunting or killing of plants is further avoided. The use of fertilizer and water is also reduced [469]. The generally used plastics for mulch films are low density polyethylene (LDPE), poly(vinyl chloride), polybutylene, or copolymers of ethylene with vinyl acetate. A particularly attractive photodegradable system consists of a mixture of ferric and nickel dibutyldithiocarbamates, the ratio of which is adjusted to provide protection for specific growing periods. The degradation is tuned so that when the growing season is over, the plastic will begin to photodegrade [470]. Polylactone and PVA films are readily degraded by soil microorganisms, whereas the addition of iron or calcium accelerates the breakdown of polyethylene [471].

2.10.2.2 Controlled Release of Agricultural Chemicals

CR is a method by which biologically active chemicals are made available to a target species at a specified rate and for a predetermined time. The polymer serves primarily to control the rate of delivery, mobility, and period of efficacy of the chemical component. The principal benefit of CR formulations is that less chemicals are used for a given time period, thus lowering the impact on nontarget species and limiting leaching, volatilization, and degradation. The macromolecular nature of polymers is the key to limiting chemical losses by these processes. The natural polymers used in CR systems are starch [472, 473], cellulose [474, 475], chitin [476–478], alginic acid, and lignin [479, 480]. These have the advantages of being abundant, relatively inexpensive, and biodegradable. Although they possess functionality for derivatization, they have the one significant disadvantage of being insoluble in standard solvents suitable for encapsulation, dispersion, and formulation. One of the largest applications for CR technology in agriculture is with fertilizers [481, 482]. A significant nitrogen source such as urea easily reacts with formaldehyde to form a polymer, and it is a simple and inexpensive system for CR.

2.10.2.3 Agricultural Planting Containers

PCL, which degrades within a rational period of time, is used as biodegradable plastic in small agricultural planting containers. These PCL planting containers have been used for automated machine planting of tree seedlings. PCL was found to undergo significant biodegradation, resulting in 48% weight loss, with 95% weight loss occurring in a year, within 6 months in the soil [483].

2.10.3 Packaging

The physical characteristics of packaging polymers are influenced by the chemical structure, molecular weight,crystallinity, and processing conditions of the polymers. The physical characteristics required in packaging depend on what item will be packaged as well as the environment in which the package will be stored. The challenge in the development of biodegradable packaging will be to combine polymers that are truly biodegradable into a laminate film or a film blend that has properties as good as those found in synthetic laminates. Several polysaccharide-based biopolymers are being used as possible coating materials or packaging films. They include starch, chitosan, and pullulan. By incorporating starch as filler, the degradation of synthetic polymer films can be accelerated. LDPE blends with up to 10% corn starch were produced using conventional techniques and were made into bags for groceries or garbage. PLLA-based packagings under consideration include grocery and garbage bags, diaper backings, six-pack rings, and fast-food containers. The purpose of food packaging is to protect the quality and safety of the food it contains from the time of manufacture to the time it is used by the consumer. An equally important function of packaging is to protect the product from physical, chemical, or biological damages [363, 374, 426, 427].

Figure 2.63 Starch-based packing materials.

2.10.3.1 **Starch-Based Packaging Materials**

Starch-based plastics are the most commonly prepared plastics from maize, sugarcane, or corn and potato starch (Figure 2.63). Nowadays, works are in progress for preparing biodegradable materials from crops and other plants for packaging their food products. Such packaging materials, which have appeared on the market for use by food companies, naturally breakdown in a garden compost heap, eradicating the need for packaging to be binned or bagged and sent to a landfill. High-amylose corn starch (HACS) can produce films with higher barrier properties and physical strength than films made from a normal corn starch. Cross-linked starch, substituted starch, acid-hydrolyzed starch, and pregelatinized starch are modified starches, which have several functional uses as viscosity modifiers, thickeners, texture enhancers, and flavor-encapsulation agents in a host of products including soups, sauces, bakery products, dairy products, and confectionery. Diminishing nonrenewable fossil fuel resources and the negative environmental impact of use of plastics has led researchers to focus efforts on utilizing starch as a biodegradable and practically inexhaustible raw material for producing packaging materials including films, foams, and molded packages [363, 374, 426, 427].

2.10.3.2 **PLA-Based Packaging Materials**

The most common use of PLA is for compostable sugarcane trays and in punnets or pallets. A starch derivative, PLA can be manufactured from maize and other plants and is a biodegradable, compostable plastic material. The material is obtainable in a range of blends and can be used in sheet or film form for a diverse range of products including food containers. It can be used for rigid thermoforms, films,

labels, and bottles, but because of its biodegradable features it cannot be used for hot-fill and gaseous drinks such as beer or sodas. PLA can also be used for noncarbonated beverages such as water, juices, and milk, as well as for edible oil products. It provides a flavor and aroma barrier comparable to that provided by poly(ethylene terephthalate) (PET) and readily accepts coatings, inks, and adhesives. Its rigidity allows for a smaller thickness than is required with materials such as PET without any loss of strength. Treofan uses PLA to make a packaging film branded as Biophan. The company intends to work on marketing Biophan to the food, cosmetics, and office materials markets and to promote Biophan as a film with ''extraordinary'' gloss and transparency, printability, and good sealing characteristics. For food packaging, Biophan-laminated film is presently used [363, 374, 426, 427].

2.10.3.3 **Cellulose-Based Packaging Materials**

Cellulose-based packaging materials incorporated with wheat gluten are biodegradable, gas selective, and permeable, and improve the shelf life of cultivated mushrooms. The disadvantages of conventional packaging materials for mushroom cultivation are short lifetime, carbon dioxide sensitivity, low moisture content that leads to opening of the cap and discoloration of mushroom. By using cellulose-based packaging materials, it should be stored at 20 °C for 4 days. The thermoplastic CA Bioceta is made up of transparent granulates processed at 170 °C and modified by addition of high amounts of liquid plant-based plasticizers to improve the complete biodegradability of acetyl cellulose. Bioceta is slowly, but fully, biologically decomposed. Its forming can be accomplished by injection, pressing, or, in the case of film production, calendaring or film blowing [363, 374, 426, 427].

2.10.3.4 **Pullulan-Based Packaging Materials**

Pullulan is composed primarily of maltotriose units linked in α-1,6 fashion and is produced as an extracellular secondary metabolite of some fungi. Because of its natural origin, pullulan was commercialized as a food source and has been accepted as a coating material for foods. It is a water-soluble polymer that provides transparent films of low oxygen permeability for foods. The film can be obtained by casting a 1–20% aqueous solution of pullulan on a metal plate roller, or, similarly to starch, pullulan can be molded with heat and pressure if a suitable amount of water is added as plasticizer [484, 485].

The development of completely biodegradable polymers for films or laminates with properties similar to those of synthetic polymers is the main challenge in biodegradable packaging materials. For food applications, pullulan can be use as a wrapping and as an edible film with limited oxygen permeability, with poly-(3-hydroxybutyrate-*co*-3-hydroxyvalerate) (PHBV) as an outside flexible cover with limited moisture permeability. The addition of pullulan to PHBV may reduce the oxygen permeability and improve product biodegradability because it increases the PHBV surface after the solution of pullulan in water.

2.10.3.5 Other Biopackaging Solution

The packaging material can be made from PHAs, polymers synthesized from organic sugars and oils that break down in soil, composting installations, waste-treatment processes, river water, and marine environments. The only products generated during decomposition are carbon dioxide and water. The successful application of PHAs indicates that fully biodegradable cosmetics packaging can be a reality. Biopol, a polymer with an ideal biodegradability profile, decomposes into carbon dioxide and water. Because of its stiff nature, it is useful for bottles and canisters [363, 374, 426, 427].

2.11 Partially Biodegradable Packaging Materials

Mixtures of synthetic polymers with added starch are an example of partly biodegradable polymers. The main disadvantage of these materials is that only the starch is biodegradable and the rest is dissipated in the environment. The degradation of the synthetic film can be accelerated by means of starch used as filling. LDPE blends containing up to 10% maize starch have been produced by conventional techniques and the end products were used in bags for shopping or garbage [486].

The biodegradable packaging industry demands a matching or superiority in physical and chemical properties of biodegradable polymers with their synthetic counterparts. Starch mixed with polyethene is also known as *biobased* (*hydrodegradable*) *material*. Microbial breakdown is controlled by the polymers that use starch, for example, PLA, PCL, and PVA. They allow breakdown in the presence of microbes, heat, moisture, and proper aeration, as found in traditional compost piles. Additive-based plastic bags are the traditional plastic bag films, whereas special chemical modification is used to make them break down under certain conditions.

2.12 Nonbiodegradable Biopolymers

2.12.1 Poly(Thioesters)

Poly(thioesters) (PTEs) are the eighth class of biopolymers in which oxygen atoms in the linkages of the polymer backbone are replaced by sulfur atoms. This results in noticeable differences in various properties of the polymers. Most of the studies carried out on their biodegradability have provided significant evidence that PTE homopolymers are nonbiodegradable. PHA-degrading bacteria or PHA depolymerases are unable to cleave the thioester bonds in the PTE backbone. PTEs are obtained *in vitro* during the enzymatic synthesis. So far, PTE homopolymers

are only obtained in a recombinant strain of *E. coli* using an unnatural pathway of PHA biosynthesis [487]. This unnatural pathway, also called the *Biotechnology Process Engineering Centre* (*BPEC*) pathway, was designed in the laboratory, because it has never been identified in bacteria. The degradation of the PTE is caused by extracellular enzymes or enzymes situated in the periplasm or at the cell surface [488]. The uptake of the polymer into the cells or into the periplasm is prevented by the molecular weight and insolubility of PTEs in water. This restricts the methods available for enzymatic PTE degradation [486].

2.12.1.1 **Poly(3-Mercaptopropionate) (Poly(3MP))**

Poly(3-mercaptopropionate) (Poly(3MP)) is known to be the first natural nonbiodegradable polymer (Figure 2.64). The inability of microorganisms to degrade poly(3MP) may be closely related to the fact that poly(3MP) homopolymer is only produced by an engineered *E. coli* strain expressing the nonnatural BPEC pathway [489]. Since 3-mercaptopropionate is only produced in relatively small quantities by the chemical industry [490] and as free 3-mercaptopropionate or other compounds, which are metabolized via 3-mercaptopropionate, occur only at low concentrations mostly in marine environments [491], exposure of bacteria to this precursor substrate for poly(3MP) biosynthesis in nature is low. Thioester bonds occurring in PTE copolymers or homopolymers were not susceptible to PHA depolymerases [492]. The failure to enrich bacteria capable of degrading the poly(3MP) homopolymer and the persistence of poly(3MP) bars in various microcosms under various conditions clearly indicate that the thioester linkages in the polymer backbone are also not hydrolyzed by other unspecific enzymes such as lipases, esterases, or proteases. It is also very unlikely that poly(3MP) exerts a general growth-inhibitory effect on microorganisms as many bacteria grew in the presence of a second substrate even if the second substrate was semicrystalline membranes of PHAs with medium change length (PHA_{SCL} or PHA_{MCL}). Utilization of the latter in the presence of poly(3MP) does also exclude inhibition or inactivation of PHA depolymerases by poly(3MP) or its degradation products.

Properties such as crystallinity or hydrophobicity prevent biodegradation of the poly(3MP), which has only thioester linkages in the backbone. Biological poly(3MP) might be very useful for some special technical applications. If poly(3MP) possesses some unique desired properties such as high thermal stability [493], which are not exhibited by other biopolymers, and if it can be shown that poly(3MP) is biocompatible, some interesting materials (i.e., medical devices) may be manufactured from this polymer for specific applications where biodegradation is undesired and they have great potential for application industries.

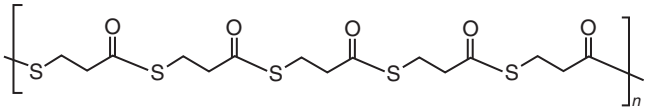

Figure 2.64 Poly(3MP).

It is extremely resistant to microbial degradation under aerobic conditions as well as under anaerobic conditions [488]. The nonbiodegradability of poly(3MP) should stimulate research to produce persistent polymers and materials from renewable resources by biotechnological processes [488].

2.13 Conversion of Nonbiodegradable to Biodegradable Polymers

Plastics can be made from LA instead of making them from conventional petroleum products. LA, which is produced via starch fermentation or as a coproduct of corn wet milling (PLA), can also be manufactured by using the starch from food wastes, cheese, whey, fruit, or grain sorghum.

Some plastics need to be durable, for example, the parts in a car. Plastics are different from organic polymers as they are feebly degraded by microbes. Environmentally degradable polymers are one of the most probable solutions for replacing petroleum-based polymers. One potential solution to replace petroleum-based polymers is environmentally degradable polymers. The main potential uses for these polymers are plastics, intended for one-time or limited use, which are used as fast-food wrappers and water-soluble polymers in detergents and cleaners, and in the printing industry.

Bioplastic bottles are the new trend in the bottled water market and it is composed of 100% plants. It opposes the mixed composition bottles that came out in the recent years. Compared to popular plastic bottles that contain petroleum and bisphenol A (BPA), the latest eco-bottles are 100% toxin-free and carbon neutral. They are also recyclable, reusable, and compostable in 80 days [494, 495].

2.14 Current Research Areas in Biopolymers and Bioplastics

The major concern for the production of plastics and bioplastics is improving usefulness. During the production process, fossil fuel is still used as an energy source. Only a few processes have emerged that actually use less energy in the production process. Therefore, researchers are still working on refining the processes used in order to make bioplastics feasible alternatives to petrochemical plastics. Energy use is not the only concern when it comes to biopolymers and bioplastics. There are also concerns about how to balance the need to grow plants for food and the need to grow plants for use as raw materials. Agricultural space needs to be shared. Researchers are looking into creating a plant that can be used for food, but also as feedstock for plastic production. One group is attempting to genetically engineer corn to contain the bacterial enzyme responsible for plastic production. The edible part of the corn would be used as food, or as livestock feed. The plastic would be removed from the remaining part of the corn plant.

Bioplastics and biopolymers and are the main constituents in creating a sustainable plastics industry. These products reduce the dependence on nonrenewable fossil fuels and are easily biodegradable. Together, this greatly limits the environmental impacts of plastic use and manufacture. In addition, features such as being biodegradable make bioplastics more acceptable for long-term use by society. It is likely that in the long-term, these products will mean plastics will remain affordable, even as fossil fuel reserves diminish.

Research on natural food biopolymers such as polysaccharides and proteins is currently at a turning point. For the past 40 years or so, research has focused on the functionality in terms of the molecules' ability to form and stabilize food structures, to impart physical stability, texture, and, to some degree, taste. However, more recently, the focus is turning toward how such biopolymers can confer health benefits.

The current center of attention in the research and development of biopolymers is to improve the properties of its products and to achieve large-scale production so as to lower costs and broaden availability, thus making it a more viable substitute for traditional polymer products. Different biopolymers have their own material-specific properties on which their possible applications are dependent. For example, bioplastics show much promise, especially for the packaging of products for in-flight catering and for dairy, as well as in pesticide soil pins. Biopolymers are beneficial for a number of reasons, the first of which is their sustainability. They are also environment friendly, a feature that is becoming increasingly important to many consumers, and can prove useful in enhancing the image of a product. This biodegradability also means easier waste management, as they can be successfully composted.

2.15
General Findings and Future Prospects

This review encompasses a detailed discussion of biopolymers in general. Here the authors gave due mention to natural and synthetic biopolymers ranging from plastics to fibers and elastomers. The method of synthesis or the process of extraction, as the case may be, is also detailed. Finally, the various applications of these materials are highlighted with specific attention to the medical field. It can be noted that the field of biopolymers is growing tremendously owing to the prime reason of, *biodegradability*. The authors foresee that in the near future, the medical field will witness the high-end utility of biopolymers in all bodily organs and parts.

Acknowledgment

The authors sincerely thank many people for the help they have received. The first and the foremost is the community in the Mahatma Gandhi University, Kottayam.

They patiently supported our efforts to complete this book chapter. PhD students, Anjaly Sivadas, and Deepa K. Baby are gratefully acknowledged for their support.

Abbreviations

BC	bacterial cellulose
BPA	bisphenol A
BPEC	Biotechnology Process Engineering Centre
FDA	US Federal Drug Administration
CS	chondroitin sulfate
ECM	extracellular matrix
EG	ethylene glycol
GD	gum damar
HA	hyaluronic acid
LA	lactic acid
LDPE	low density polyethylene
PLLA	poly(L-lactide)
PCL	polycaprolactone
PGA	poly(glycolic acid)
PGS	poly(glycerol sebacic acid)
PHB	poly-β-hydroxybutyrate
PLA	poly(lactic acid)
PTMC	poly(trimethylene carbonate)
PPF	poly(propylene fumarate)
PHEMA	poly(2-hydroxyethyl methacrylate)
PVA	poly(vinyl alcohol)
TSP	textured soy protein

References

1. Platt, K.D. (2006) *Biodegradable Polymers*, Rapra Market Report, Rapra Technology Limited.
2. Bastioli, C. (2005) *Handbook of Biodegradable Polymers*, Rapra Technology Limited, p. 533.
3. Johnson, R.M., Mwaikambo, L.Y., and Tucker, N. (2003) *Biopolymers*, Rapra Review Reports, p. 158.
4. Steinbüchel, A. (2012) *Biopolymers Online*, John Wiley & Sons, Inc., New York.
5. Steinbüchel, A. (2006) *Biopolymers*, Vol. **10**, Wiley-VCH Verlag GmbH, Weinheim, p. 5924.
6. Elnashar, M. (ed.) (2010) *Biopolymers*, Sciyo, p. 612, under CC BY-NC-SA 3.0 license.
7. Herdman, R.C. (1993) Biopolymers: making materials nature's way. US Congress, OTA-BP-E-102, NTIS order #PB94-107638.
8. Pignatello, R. (ed.) (2011) *Biomaterials Science and Engineering*, Vol. **159**, In-Tech, p. 456ISBN 978-953-307-609-6, under CC BY-NC-SA 3.0 license.
9. Walton, A.G. and Blackwell, J. (1973) *Biopolymers*, Academic Press, New York, p. 604.
10. Iqbal Sabir, M., Xu, X., and Li, L. (2009) A review on biodegradable

polymeric materials for bone tissue engineering applications. *J. Mater. Sci.*, **44**, 5713–5724.

11. Van Vlierberghe, S., Dubruel, P., and Schacht, E. (2011) Biopolymer-based hydrogels as scaffolds for tissue engineering applications: a review. *Biomacromolecules*, **12**, 1387–1408.
12. Scott, G. (ed.) (2002) *Degradable Polymers: Principles and Applications*, 2nd edn, Kluwer Academic Publishers, p. 497.
13. Kolybaba, M, Tabil, L.G, Panigrahi, S., Crerar, W.J., Powell1, T., and Wang, B. (2003) Biodegradable polymers: past, present, and future. CSAE/ASAE Annual Intersectional Meeting, Fargo, ND, October 3–4, 2003 pp. RRV03–0007.
14. Méndez-Vilas, A. (ed.) (2010) *Current Research, Technology and Education Topics in Applied Microbiology and Microbial Biotechnology*, Formatex Research Center, Badajoz.
15. Pfister, D.P. and Larock, R.C. (2010) Thermophysical properties of conjugated soybean oil/corn stover biocomposites. *Bioresour. Technol.*, **101**, 6200–6206.
16. Fraser-Reid, B.O., Flitsch, S., Tatsuta, K., Ito, Y., Thiem, J., Coté, G.L., Kondo, H., Nishimura, S., and Yu, B. (eds.) (2008) *Glycoscience: Chemistry and Chemical Biology*, 2nd edn, Vol. **1-3**, Springer, p. 2874.
17. Altman, G.H., Diaz, F., Jakuba, C., Calabro, T., Horan, R.L., Chen, J., Lu, H., Richmond, J., and Kaplan, D.L. (2003) Silk-based biomaterials. *Biomaterials*, **24**, 401–416.
18. Meinel, L., Hofmann, S., Karageorgiou, C., Kirker-Head, C., McCool, J., Gronowicz, G., Zichner, L., Langer, R., Vunjak-Novakovic, G., and Kaplan, D.L. (2005) The inflammatory responses to silk films *in vitro* and *in vivo*. *Biomaterials*, **26**, 147–155.
19. Lee, C.H., Singla, A., and Lee, Y. (2001) Biomedical applications of collagen. *Int. J. Pharm.*, **221**, 1–22.
20. Tsung, J. and Burgess, D.J. (2012) Biodegradable polymers in drug delivery systems, in *Fundamentals and Applications of Controlled Release Drug Delivery* (eds. M. Rathbone, R. Siegel, and J. Shipmann) Part 2, CRS Press, pp. 107–123doi: 10.1007/978-1-4614-0881-9-5, Springer.
21. Han, B., Huang, L.L.H., Cheung, D., Cordoba, F., and Nimni, M. (1999) Polypeptide growth factors with a collagen binding domain: their potential for tissue repair and organ regeneration, in *Tissue Engineering of Vascular Prosthetic Grafts* (eds. P. Zilla and H.P. Greisler), RG Landes, Austin, TX, pp. 287–299.
22. Mitra, T., Sailakshmi, G., Gnanamani, A., and Mandal, A.B. (2011) Cross-linking with acid chlorides improves thermal and mechanical properties of collagen based biopolymer material. *Thermochim. Acta*, **525**, 50–55.
23. Nair, L.S. and Laurencin, C.T. (2007) Biodegradable polymers as biomaterials. *Prog. Polym. Sci.*, **32**, 762–798.
24. Gordon Paul, R. and Bailey, A.J. (2003) Chemical stabilisation of collagen as a biomimetic. *Sci. World J.*, **3**, 138–155.
25. Orgel, J.P.R.O., Miller, A., Irving, T.C., Fischetti, R.F., Hammersley, A.P., and Wess, T.J. (2001) The in situ supermolecular structure of type I collagen. *Structure*, **9**, 1061–1069.
26. Orgel, J.P.R.O., San Antonio, J.D., and Antipova, O. (2011) Molecular and structural mapping of collagen fibril interactions. *Connect. Tissue Res.*, **52**, 2–17.
27. Usha, R. and Ramasami, T. (2005) Structure and conformation of intramolecularly cross-linked collagen. *Colloids Surf. B*, **41**, 21–24.
28. Nishi, Y., Doi, M., Doi, S., Nishiuchi, Y., Nakazawa, T., Ohkubo, T., and Kobayashi, Y. (2003) Stabilization mechanism of triple helical structure of collagen molecules. *Int. J. Pept. Res. Ther.*, **10**, 533 7.
29. Behring, J., Junker, R., Walboomers, X.F., Chessnut, B., and Jansen, J.A. (2008) Toward guided tissue and bone regeneration: morphology, attachment, proliferation, and migration of cells cultured on collagen barrier membranes. A systematic review. *Odontology*, **96**, 1–11.
30. Gruessner, U., Clemens, M., Pahlplatz, P.V., Sperling, P., Witte, J., and Rosen,

H.R. (2001) Improvement of perineal wound healing by local administration of gentamicin-impregnated collagen fleeces after abdominoperineal excision of rectal cancer. *Am. J. Surg.*, **182**, 502–509.

31. Erdmann, R.S. and Wennemers, H. (2011) Importance of ring puckering versus interstrand hydrogen bonds for the conformational stability of collagen. *Angew. Chem. Int. Ed.*, **50**, 6835–6838.
32. Vin, F., Teot, L., and Measume, S. (2002) The healing properties of promogran in venous leg ulcers. *J. Wound Care*, **11** (9), 335.
33. Olsen, D., Yang, C., Bodo, M., Chang, R., Leigh, S., Baez, J., Carmichael, D., Perälä, M., Hämäläinen, E.R., Jarvinen, M., and Polarek, J. (2003) Recombinant collagen and gelatin for drug delivery. *Adv. Drug Delivery Rev.*, **55**, 1547–1567.
34. Dyksterhuis, L.B., Baldock, C., Lammie, D., Wess, T.J., and Weiss, A.S. (2006) A turning point in elastin structure. *Matrix Biol.*, **25**, S17–S17.
35. Samouillan, V., Dandurand, J., Lacabanne, C., and Hornebeck, W. (2002) Molecular mobility of elastin: effect of molecular architecture. *Biomacromolecules*, **3**, 531–537.
36. Mithieux, S.M., Rasko, J.E.J., and Weiss, A.S. (2004) Synthetic elastin hydrogels derived from massive elastic assemblies of self-organized human protein monomers. *Biomaterials*, **25**, 4921–4927.
37. Woodhouse, K.A., Klement, P., Chen, V., Gorbet, M.B., Keeley, F.W., Stahl, R., Fromstein, J.D., and Bellingham, C.M. (2004) Investigation of recombinant human elastin polypeptides as non-thrombogenic coatings. *Biomaterials*, **25**, 4543–4545.
38. Bonzon, N., Carrat, X., Daminiere, C., Daculsi, G., Lefebvre, F., and Rabaud, M. (1995) New artificial connective matrix made of fibrin monomers, elastin peptides and type I + III collagens: structural study, biocompatibility and use as tympanic membranes in rabbit. *Biomaterials*, **16**, 881–885.
39. Klein, B., Schiffer, R., Hafemann, B., Klosterhalfen, B., and Zwadlo-Klarwasser, G. (2001) Inflammatory response to a porcine membrane composed of fibrous collagen and elastin as dermal substitute. *J. Mater. Sci. Mater. Med.*, **12**, 419–424.
40. Tu, Y., Mithieux, S.M., Annabi, N., Boughton, E.A., and Weiss, A.S. (2010) Synthetic elastin hydrogels that are coblended with heparin display substantial swelling, increased porosity, and improved cell penetration. *J. Biomed. Mater. Res. A*, **95A**, 4.
41. Skopinska-Wisniewska, J., Sionkowska, A., Kaminska, A., Kaznica, A., Jachimiak, R., and Drewa, T. (2009) Surface properties of collagen/elastin based biomaterials for tissue regeneration. *Appl. Surf. Sci.*, **225**, 8286–8292.
42. Sionkowska, A. (2011) Current research on the blends of natural and synthetic polymers as new biomaterials: review. *Prog. Polym. Sci.*, **36**, 1254–1276.
43. Prinsen, B.H. and de Sain-van der Velden, M.G. (2004) Albumin turnover: experimental approach and its application in health and renal diseases. *Clin. Chim. Acta*, **347** (1–2), 1–14.
44. Chuang, V.T., Kragh-Hansen, U., and Otagiri, M. (2002) Pharmaceutical strategies utilizing recombinant human serum albumin. *Pharm. Res.*, **19** (5), 569–577.
45. Uchida, M., Ito, A., Furukawa, K.S., Nakamura, k., Onimura, Y., Oyane, A., Ushida, T., Yamane, T., Tamaki, T., and Tateishi, T. (2005) Reduced platelet adhesion to titanium metal coated with apatite, albumin-apatite composite or laminin-apatite. *Compos. Biomater.*, **26**, 6924–6931.
46. Grassl, E. and Tranquillo, R.T. (2006) Fibrillar fibrin gels, in *Scaffolds in Tissue Engineering* (eds. X.P. Ma and J. Elisseeff), CRC, Taylor and Francis, Boca Raton, FL, pp. 61–70.
47. Wong, C., Inman, E., Spaethe, R., and Helgerson, S. (2003) Fibrin-based biomaterials to deliver human growth factors. *Thromb. Haemost.*, **89**, 573.
48. Hynes, R.O. (1990) *Methods for Identification of Fibronectin and Wound*

Healing Inflammation and Fibrosis Fibronectins, Springer-Verlag, New York, pp. 349–364.

49. Hynes, R.O. (1999) The dynamic dialogue between cells and matrices: implications of fibronectin's elasticity. *Proc. Natl. Acad. Sci. U.S.A.*, **96**, 2588–2590.

50. Williams, M.J., Phan, I., Baron, M., Driscoll, P.C., and Campbell, I.D. (1993) Secondary structure of a pair of fibronectin type 1 modules by two-dimensional nuclear magnetic resonance. *Biochemistry*, **32**, 7388–7395.

51. Corradini, E., de Carvalho, A.J.F., Curvelo, A.A.S., Augusto Marcondes Agnelli, J., and Henrique Capparelli Mattoso, L. (2007) Preparation and characterization of thermoplastic starch/zein blends. *Mat. Res.*, **10** (3), 227–231.

52. Sharma, K., Singh, V., and Arora, A. (2011) Natural biodegradable polymers as matrices in transdermal drug delivery. *Int. J. Drug Dev. Res.*, **3** (2), 85–103.

53. Dekov, T. (2005) The gluten-A big natural biopolymer genetic determination and general & applied genetics, supplement. *Biotechnol. Biotechnol. Equip.*, **19**, 3.

54. Attenburrow, G., Barnes, D.J., Davies, A.P., and Ingman, S.J. (1990) Rheological properties of wheat gluten. *J. Cereal. Sci.*, **12**, 1–14.

55. Pouplin, M., Redl, A., and Gontard, N. (1999) Glass transition of wheat gluten plasticized with water, glycerol or sorbitol. *J. Agric. Food Chem.*, **47**, 538–543.

56. Domenek, S., Feuilloley, P., Grataud, J., Morel, M.H., and Guilbert, S. (2004) Biodegradability of wheat gluten based bioplastics. *Chemosphere*, **54**, 551–559.

57. Jerez, A., Partal, P., Martinez, I., Callegos, C., and Guerreo, A. (2005) Rheology and processing of gluten based bioplastics. *Biochem. Eng.*, **26**, 131–138.

58. Johnston-Banks, F.A. (1990) Gelatin, in *Food Gels* (ed. P. Harris), Elsevier Applied Science Publishers, London, pp. 233–289.

59. Djabourov, M., Leblond, J., and Papon, P. (1988) Gelation of aqueous gelatin solutions. 1. Structural investigation. *J. Phys.*, **49** (2), 319–332.

60. Guenet, J.-M. (1992) *Thermoreversible Gelation of Polymers and Biopolymers*, Academic Press, New York.

61. Parker, N.G. and Povey, M.J.W. (2012) Ultrasonic study of the gelation of gelatin: phase diagram, hysteresis and kinetics. *Food Hydrocolloids*, **26**, 99–107.

62. Gomez-Guillen, M.C., Perez-Mateos, M., Gomez-Estaca, J., Lopez-Caballero, E., Gimenez, B., and Montero, P. (2009) *Trends Food Sci. Technol.*, **20**, 3–16.

63. Cao, N., Yang, X., and Fu, Y. (2009) Preparation and properties of plasticized starch modified with poly(ε-caprolactone) based waterborne polyurethane. *Food Hydrocolloids*, **23**, 729–735.

64. Ikada, Y. (1994) Surface modification of polymers for medical applications. *Biomaterials*, **15**, 725–736.

65. Yamaoka, T., Tabata, Y., and Ikada, Y. (1994) Body distribution of intravenously administered gelatin with different molecular weights. *J. Controlled Release*, **31**, 1–8.

66. Gómez-Guillén, M.C., Giménez, B., López-Caballero, M.E., and Montero, M.P. (2011) Functional and bioactive properties of collagen and gelatin from alternative sources: a review. *Food Hydrocolloids*, **25**, 1813–1827.

67. Shurtleff, W. and Aoyagi, A. (1989) *Soy Protein Isolates, Concentrates, and Textured Soy Protein Products*, Soyfoods Center, Lafayette, LA.

68. Barać, M.B., Stanojević, S.P., Jovanović, S.T., and Pešić, M.B. (2004) Soy protein modification. *APTEFF*, **35**, 3–16.

69. Lu, Y., Weng, L., and Zhang, L. (2004) Morphology and properties of Soy protein isolate thermoplastics reinforced with chitin whiskers. *Biomacromolecules*, **5**, 1046–1051.

70. Tian, H., Liu, D., and Zhang, L. (2009) Structure and properties of soy protein films, plasticized with hydroxyamine. *J. Appl. Polym. Sci.*, **111**, 1549–1556.

71. Tian, H., Wang, Y., Zhang, L., Quan, C., and Zhang, X. (2010) *Ind. Crops Prod.*, **32**, 13–20.
72. Cao, N., Fu, Y., and He, J. (2007) Preparation and physical properties of soy protein isolate and gelatin composite films. *Food Hydrocolloids*, **21**, 1153–1162.
73. Tian, H., Zhang, L., Wu, Q., Wang, X., and Chen, Y. (2010) Creation of hydrophobic materials fabricated from soy protein and natural rubber: surface, interface, and properties. *Macromol. Mater. Eng.*, **295**, 451–459.
74. Su, J., Huang, Z., Yuan, X., Wang, X., and Li, M. (2010) Structure and properties of carboxymethyl cellulose/soy protein isolate blend edible films crosslinked by Maillard reactions. *Carbohydr. Polym.*, **79**, 145–153.
75. Silva, S.S., Goodfellow, B.J., Benesch, J., Rocha, J., Mano, J.F., and Reis, R.L. (2007) Potential applications of natural origin polymer-based systems in soft tissue regeneration. *Carbohydr. Polym.*, **70**, 25–31.
76. Tang, R., Du, Y., Zheng, H., and Fan, L. (2003) Preparation and characterization of soy protein isolate–carboxymethylated konjac glucomannan blend films. *J. Appl. Polym. Sci.*, **88**, 1095–1099.
77. Monedero, F.M., Fabra, M.J., Talens, P., and Chiralt, A. (2010) Effect of calcium and sodium caseinates on physical characteristics of soy protein isolate–lipid films. *J. Food Eng.*, **97**, 228–234.
78. Monedero, F.M., Fabra, M.J., Talens, P., and Chiralt, A. (2009) Effect of oleic acid–beeswax mixtures on mechanical, optical and water barrier properties of soy protein isolate based films. *J. Food Eng.*, **91**, 509–515.
79. Kumar, P., Sandeep, K.P., Alavi, S., Truong, V.D., and Gorga, R.E. (2010) Preparation and characterization of bio-nanocomposite films based on soy protein isolate and montmorillonite using melt extrusion. *J. Food Eng.*, **100**, 480–489.
80. Kumar, R. (2010) Effect of water-mediated arylation time on the properties of soy protein films. *Ind. Eng. Chem. Res.*, **49**, 3479–3484.
81. Walzem, R.L., Dillard, C.J., and German, J.B. (2002) Whey components: millennia of evolution create functionalities for mammalian nutrition: what we know and what we may be overlooking. *Crit. Rev. Food Sci. Nutr.*, **42**, 353–375.
82. Swaisgood, H.E. (2003) Chemistry of the caseins, in *Advanced Dairy Chemistry*, Part A Volume 1- Proteins, 3rd edn (ed. P.F. Fox), Kluwer Academic, Plenum Publishers, New York, pp. 63–110.
83. Kunz, C. and Lonnerdal, B. (1990) Human-milk proteins: analysis of casein and casein subunits. *Am. J. Clin. Nutr*, **51** (1), 37–46 (The American Society for Clinical Nutrition) PMID 1688683(2011).
84. Docena, G.H., Fernandez, R., Chirdo, F.G., and Fossati, C.A. (1996) *Identification of casein as the major allergenic and antigenic protein of cow's milk. Allergy*, **51** (6), 412–416.
85. National Casein Company (2011) *The Columbia Electronic Encyclopedia Casein*, 6th edn, Columbia University.
86. Rosen, J.M., Dale, T., Gavigan, S., and Buhler, T. (1992) *Molecular Biology of Milk Proteins*, Wiley-Liss, Houston, TX, pp. 1–19.
87. Boisgard, R., Chanat, E., Lavialle, F., Pauloin, A., and Ollivier-Bousquet, M. (2001) Roads taken by milk proteins in mammary epithelial cells. *Livestock Prod. Sci.*, **70**, 49–61.
88. Linderstrom-Lang, K. and Kodama, S.C.R. (1925) Studies on casein.I.on the solubility of caseins in hydrochloric acid. *C. R. Trav. Lab. Carlsberg*, **16**, 1–47.
89. Holt, C. and Sawyer, L. (1988) Primary and predicted secondary structures of the caseins in relation to their biological functions. *Protein Eng.*, **2**, 251–259.
90. Stewart, A.F., Bonsing, J., Beattie, C.W., Shah, F., Willis, I.M., and Mackinlay, A.G. (1987) Complete nucleotide sequences of bovine alpha

S2- and beta-casein cDNAs: comparisons with related sequences in other species. *Mol. Biol. Evol.*, **4**, 231–241.

91. Swaisgood, H.E. (1992) Chemistry of the caseins, in *Advanced Dairy Chemistry* (ed. P.F. Fox), Elsevier, pp. 63–110.

92. Eigel, W.N., Butler, J.E., Ernstrom, C.A., Farrell, H.M.J., Harwalkar, V.R., Jenness, R., and Whitney, R.M. (1984) Nomenclature of proteins of cow's milk: fifth revision. *J. Dairy Sci.*, **67**, 1599–1631.

93. Alexander, L.J. and Beattie, C.W. (1992) The sequence of porcine α_{s1}-casein cDNA: evidence for protein variants generated by altered RNA splicing. *Anim. Genet.*, **23**, 283–288.

94. Devinoy, E., Schaerer, E., Jolivet, G., Fontaine, M.L., Kraehenbuhl, J.P., and Houdebine, L.M. (1988) Sequence of the rabbit alpha S1-casein cDNA. *Nucleic Acids Res.*, **16**, 11813.

95. Grusby, M.J., Mitchell, S.C., Nabavi, N., and Glimcher, L.H. (1990) Casein expression in cytotoxic T lymphocytes. *Proc. Natl. Acad. Sci. U.S.A.*, **87**, 6897–6901.

96. Hall, L., Laird, J.E., and Craig, R.K. (1984) Nucleotide sequence determination of guinea-pig casein B mRNA reveals homology with bovine and rat alpha s1 caseins and conservation of the non-coding regions of the mRNA. *Biochem. J.*, **222**, 561–570.

97. Hennighausen, L.G. and Sippel, A.E. (1982) Characterization and cloning of the mRNAs specific for the lactating mouse mammary gland. *Eur. J. Biochem.*, **125**, 131–141.

98. Hobbs, A.A. and Rosen, J.M. (1982) Sequence of rat alpha- and gamma-casein mRNAs: evolutionary comparison of the calcium-dependent rat casein multigene family. *Nucleic Acids Res.*, **10**, 8079–8098.

99. Alexander, L.J., Gupta, N.A., and Beattie, C.W. (1992) The sequence of porcine alpha s2-casein cDNA. *Anim. Genet.*, **23**, 365–367.

100. Boisnard, M. and Pe´trissant, G. (1985) Complete sequence of ovine alpha s2-casein messenger RNA. *Biochimie*, **67**, 1043–1051.

101. Bouniol, C. (1992) Sequence of the goat α_{s2}-encoding cDNA. *Gene*, **125**, 235–236.

102. Brignon, G., Ribadeau Dumas, B., Mercier, J.-C., Pe´lissier, J.P., and Das, B.C. (1977) Complete amino acid sequence of bovine alphaS2-casein. *FEBS Lett.*, **76**, 2749.

103. Dawson, S.P., Wilde, C.J., Tighe, P.J., and Mayer, R.J. (1993) Characterization of two novel casein transcripts in rabbit mammary gland. *Biochem. J.*, **296**, 777–784.

104. Hall, L., Laird, J.E., Pascall, J.C., and Craig, R.K. (1984) Nucleotide sequence determination of guinea-pig casein B mRNA reveals homology with bovine and rat ay caseins and conservation of the non-coding regions of the mRNA. *Eur. J. Biochem.*, **138**, 585–589.

105. Zivkovic, A.M. and Barile, D. (2011) Bovine milk as a source of functional oligosaccharides for improving human health. *Adv. Nutr.*, **2**, 284–289.

106. Hall, L. (1990) Nucleotide sequence of guinea-pig kappa-casein cDNA. *Nucleic Acids Res.*, **18** (20), 6129.

107. Sasaki, T., Sasaki, M., and Enami, J. (1993) Mouse gamma-casein cDNA: PCR cloning and sequence analysis. *Zool. Sci.*, **10**, 65–72.

108. Alexander, L.J. and Beattie, C.W. (1992) The sequence of porcine b-casein cDNA. *Anim. Genet.*, **23**, 369–371.

109. Blackburn, D.E., Hobbs, A.A., and Rosen, J.M. (1982) Rat beta casein cDNA: sequence analysis and evolutionary comparisons. *Nucleic Acids Res.*, **10**, 2295–2307.

110. Bonsing, J., Ring, J.M., Stewart, A.F., and Mackinlay, A.G. (1988) Complete nucleotide sequence of the bovine beta-casein gene. *Aust. J. Biol. Sci.*, **41**, 527–537.

111. Collet, C., Joseph, R., and Nicholas, K. (1992) Molecular characterization and in-vitro hormonal requirements for expression of two casein genes from a marsupial. *J. Mol. Endocrinol*, **8**, 13–20.

112. Greenberg, R., Groves, M.L., and Dower, H.J. (1984) *Human and casein amino acid sequence and identification of phosphorylation J. Biol. Chem.*, **259**, 5132–5138.

113. Jiminez-Flores, R., Klang, Y.C., and Richardson, T. (1987) Cloning and sequence analysis of bovine beta-casein cDNA. *Biochem. Biophys. Res. Commun.*, **142**, 617–621.

114. Provot, C., Persuy, M.A., and Mercier, J.C. (1989) Complete nucleotide sequence of ovine p-casein cDNA: inter-species comparison. *Biochimie*, **71**, 827–832.

115. Dumas, B.R., Brignon, G., Grosclaude, F., and Mercier, J.C. (1972) Structure primaire de la caséine β bovine: séquence complete. *Eur. J. Biochem.*, **25** (3), 505–514.

116. Richardson, B.C. and Mercier, J.C. (1979) The primary structure of the ovine p-caseins. *Eur J. Biochem.*, **99**, 285–297.

117. Thepot, D., Devinoy, E., Fontaine, M.L., and Houdebine, L.M. (1991) The structure of the gene encoding rabbit beta-casein. *Gene*, **97**, 301–306.

118. Yoshimura, M., Banerjee, M.R., and Oka, T. (1986) Transfection of 8-casein chimeric gene and hormonal induction of its expression in primary murine mammary epithelial cells. *Nucleic Acids Res.*, **14**, 8224.

119. Ginger, M.R., Piotte, C.P., Otter, D.E., and Grigor, M.R. (1999) Identification, characterisation and cDNA cloning of two caseins from the common brushtail possum (*Trichosurus vulpecula*). *Biochim. Biophys. Acta*, **1427**, 92–104.

120. Greenberg, R. and Groves, M.L. (1979) Human β-casein. *J. Dairy Res.*, **46**, 235–239.

121. Greenberg, R., Groves, M.L., and Dower, H.J. (1984) Human β-casein – amino acid sequence and identification of phosphorylation sites. *J. Biol. Chem.*, **259**, 5132–5138.

122. Kawasaki, K., Lafont, A.G., and Sire, J.Y. (2011) The Evolution of Milk Casein Genes from Tooth Genes before the Origin of Mammals, in *MBE Advance Access*, Oxford University Press on behalf of the Society for Molecular Biology.

123. Bonsing, J. and Mackinlay, A.G. (1987) Recent studies on nucleotide sequences encoding the caseins. *J. Dairy Res.*, **54**, 447–461.

124. Jolles, P., Loucheux-Lefebvre, M.H., and Henschen, A. (1978) Structural relatedness of κ-casein and fibrinogen γ-chain. *J. Mol. Evol.*, **11**, 271–277.

125. Mercier, J.C. and Vilotte, J.L. (1993) Structure and function of milk protein genes. *J. Dairy Sci.*, **76**, 3079–3098.

126. Walker, G., Cai, F., Shen, P., Reynolds, C., Ward, B., Fone, C., Honda, S., Koganei, M., Oda, M., and Reynolds, E. (2006) Increased remineralization of tooth enamel by milk containing added casein phosphopeptide-amorphous calcium phosphate. *J. Dairy Res.*, **73** (1), 74–78.

127. Dalgleish, D.G. (1998) Casein micelles as colloids: surface structures and stabilities. *J. Dairy Sci.*, **81** (11), 3013–3018.

128. (a) Robinson, R.K. (1981) *Dairy Microbiology*, Vol. **2**, Applied Science Publishers, Englewood, NJ; (b) Prins, J. (1970) Microbial rennet. *Process Biochem.*

129. Rao, M.B., Tanksale, A.M., Ghatge, M.S., and Deshpande, V.V. (1998) Molecular and biotechnological aspects of microbial proteases. *Microbiol. Mol. Biol. Rev*, **62** (3), 597–635.

130. Boirie, Y., Dangin, M., Gachon, P., Vasson, M.P., Maubois, J.L., and Beaufrere, B. (1997) Slow and fast dietary proteins differently modulate postprandial protein accretion. *Proclamations Natl. Acad. Sci.*, **94**, 14930–14935.

131. Hoffman, J.R. and Falvo, M.J. (2004) Protein - which is best? *J. Sports Sci. Med.*, **3**, 118–130.

132. Miura, Y., Kato, H., and Noguchi, T. (2007) Effect of dietary proteins on insulin-like growth factor-1 (IGF-1) messenger ribonucleic acid content in rat liver. *Br. J.Nutr.*, **67** (2), 257.

133. Sports Supplement Reviewer (2011) All About Casein.

134. Malcmacher, L. (2006) Enamel Remineralization: The Medical Model of Practicing Dentistry. *Dentistry Today* (Nov. 1).

135. Walker, G., Cai, F., Shen, P., Reynolds, C., Ward, B., Fone, C., Honda, S., Koganei, M., Oda, M., and Reynolds, E. (2006) Increased remineralization of

tooth enamel by milk containing added casein phosphopeptide-amorphous calcium phosphate. *J. Dairy Res.*, **73** (1), 74–78.

136. Steinbüchel, A. and Rhee, S.K. (2005) *Polysaccharides and polyamides in the food industry*, Vol. **1**, Wiley-VCH Verlag GmbH, Weinheim, p. 783.

137. Dumitriu, S. (2005) *Polysaccharides: Structural Diversity and Functional Versatility*, 2nd edn, Marcel Dekker, New York.

138. Marchessault, R.H., Ravenelle, F., and Xia Zhu, X. (eds.) (2006) *Polysaccharides for Drug Delivery and Pharmaceutical Applications (ACS Symposium)*, American Chemical Society, Washington, p. 934.

139. Klemm, D., Heublein, B., Fink, H.-P., and Bohn, A. (2005) Cellulose: fascinating biopolymer and sustainable raw material. *Angew. Chem. Int. Ed.*, **44**, 3358–3393.

140. Balu, B., Breedveld, V., and Hess, D.W. (2008) Fabrication of ''roll-off'' and ''sticky'' superhydrophobic cellulose surfaces via plasma processing. *Langmuir*, **24**, 4785–4790.

141. Cunha, A.G. and Gandini, A. (2010) Turning polysaccharides into hydrophobic materials: a critical review. Part 1. *Cellulose*, **17**, 875–889.

142. Song, J.-M., Zhan, Y.-J., Xu, A.-W., and Yu, S.-H. (2007) Cellulose acetate-directed growth of bamboo-raft-like single-crystalline selenium superstructures: high-yield synthesis, characterization, and formation mechanism. *Langmuir*, **23**, 7321–7327.

143. Zhao, Q., Qian, J., Gui, Z., An, Q., and Zhu, M. (2010) Interfacial self-assembly of cellulose-based polyelectrolyte complexes: pattern formation of fractal ''trees''. *Soft Matter*, **6**, 1129–1137.

144. Klemm, D., Shmauder, H.P., Heinze, T., Vandamme, E.J., De Baets, S., and Steinbüchel, A. (eds.) (2002) Cellulose, in *Biopolymers, Polysaccharides II*, Vol. **6**, Wiley-VCH Verlag GmbH, Weinheim, pp. 275–319.

145. Gu, J.D., Eberiel, D., McCarthy, S.P., and Gross, R.A. (1993) Cellulose acetate biodegradability upon exposure to simulated aerobic composting and anaerobic bioreactor environments. *J. Environ. Polym. Degrad.*, **1**, 143–153.

146. Gu, J.D., Eberiel, D., McCarthy, S.P., and Gross, R.A. (1993) Degradation and mineralization of cellulose acetate in simulated thermophilic compost environments. *J. Environ. Polym. Degrad.*, **1**, 281–291.

147. Biswas, A., Saha, B.C., Lawton, J.W., Shogren, R.L., and Willett, J.L. (2006) Process for obtaining cellulose acetate from agricultural by-products. *Carbohydr. Polym.*, **64**, 134–137.

148. Hollander, D.A., Villanueva, L., Farnes, E. Q., Attar, M., Schiffman, R.M., Chang, C., Graham, R.S., and Welty, D. F. (2011) Ketorolac compositions for corneal wound healing. US Patent 20110275688.

149. (a) Phillips, G.O. and Williams, P.A. (eds.) (2009) *Handbook of Hydrocolloids*, 2nd edn, Woodhead Press, p. 472CRC Press; (b) García-González, C.A., Alnaief, M., and Smirnova, I. (2011) Polysaccharide-based aerogels - promising biodegradable carriers for drug delivery systems- Review Article. *Carbohydr. Polym.*, **86**, 1425–1438.

150. Fredriksson, H., Silverio, J., Andersson, R., Eliasson, A.C., and Aman, P. (1998) The influence of amylase and amylopectine characteristics on gelatinization and retrogradation properties of different starches. *Carbohydr. Polym.*, **35**, 119–134.

151. Ratnayake, W.S., Hoover, R., Shahidi, F., Perera, C., and Jane, J. (2001) Composition, molecular structure and physicochemical properties of starches from four field pea cultivars. *Food Chem.*, **74**, 189–202.

152. Yukuta, T., Akira, I., and Masatoshi, K. (1990) Developments of biodegradable plastics containing polycaprolactone and/or starch. *Polym. Mater. Sci. Eng.*, **63**, 742–749.

153. Chandra, R. and Rustgi, R. (1998) Biodegradable polymers. *Prog. Polym. Sci.*, **23**, 1273–1335.

154. Netravali, A.N. and Chabba, S. (2003) Composites get greener. *Mat. Today*, **6**, 22–29.

155. F.H. Otey *et al.* (1976) Degradable starch-based agricultural mulch film.

US Patent 39,49,145, filed Feb. 27, 1975 and issued Apr. 6, 1976.

156. Chen, Y.J., Wang, Y.M., and Tsai, Y.C. (2010) Zeolite starch adhesive for corrugated cardboards and method for making the same. US Patent 20100032092.

157. Schuerch, C. (1973) Systematic approaches to the chemical synthesis of polysaccharides. *Acc. Chem. Res*, **6** (6), 184–191.

158. Reddy, N. and Yang, Y. (2009) Preparation and properties of starch acetate fibers for potential tissue engineering applications. *Biotechnol. Bioeng.*, **103** (5), 1016–1022.

159. Holloway, P.J. (1982) The chemical constitution of plant cutins, in *The Plant Cuticle* (eds. D.F. Cutler, K.L. Alvin, and C.E. Price), Academic Press, London, pp. 45–85.

160. Sevda, S. and McClure, S.J. (2004) Potential applications of chitosan in veterinary medicine. *Adv. Drug Delivery Rev.*, **56**, 1467–1480.

161. Azad, A.K., Sermsintham, N., Chandrkrachang, S., and Stevens, W.F. (2004) Chitosan membrane as a wound-healing dressing: characterization and clinical application. *J. Biomed. Mater. Res. B Appl. Biomater.*, **69**, 216–222.

162. Ueno, H., Mori, T., and Fujinaga, T. (2001) Topical formulations and wound healing applications of chitosan. *Adv. Drug delivery Rev.*, **52**, 105–115.

163. Ueno, H., Yamada, H., Tanaka, I., Kaba, N., Matsuura, M., Okumura, M., Kadosawa, T., and Fujinaga, T. (1999) Accelerating effects of chitosan for healing at early phase of experimental open wound in dogs. *Biomaterials*, **20**, 1407–1414.

164. Rao, S.B. and Sharma, C.P. (1997) Use of chitosan as a biomaterial: studies on its safety and hemostatic potential. *J. Biomed. Mater. Res.*, **34**, 21–28.

165. Shigemasa, Y. and Minami, S. (1996) Applications of chitin and chitosan for biomaterials. *Biotechnol. Genet. Eng. Rev.*, **13**, 383–420.

166. Dash, M., Chiellini, F., Ottenbrite, R.M., and Chiellini, E. (2011) Chitosan–A versatile semi-synthetic polymer in biomedical Applications. *Prog. Polym. Sci.*, **36**, 981–1014.

167. Sánchez, R., Stringari, G.B., Franco, J.M., Valencia, C., Hengameh Honarkar, C., and Barikani, M.M. (2009) Use of chitin, chitosan and acylated derivatives as thickener agents of vegetable oils for bio-lubricant applications. *Chemistry*, **140**, 1403–1420.

168. Kurita, K., Kojima, T., Nishiyama, Y., and Shimojoh, M. (2000) Preparation of nonnatural branched chitin and chitosan. *Macromolecules*, **33**, 4711–4716.

169. Ruszczak, Z. (2003) Effect of collagen matrices on dermal wound healing. *Adv. Drug delivery Rev.*, **55**, 1595–1611.

170. Green, D., Walsh, D., Mann, S., and Oreffo, R.O.C. (2002) The Potential of biomimesis in bone tissue engineering: lessons from the design and synthesis of invertebrate skeletons. *Bone*, **30** (6), 810–815.

171. Eppley, B.L. and Dadvand, B. (2006) Injectable soft-tissue fillers: clinical overview. *Plast. Reconstr. Surg.*, **118**, 98e–106e.

172. Kim G-W, Choi Y-J, Kim M-S, Park Y, Lee K-B, Kim I-S, Hwang S-J, Noh I. (2007) Synthesis and evaluation of hyaluronic acid-polyethylene oxide hydrogel via Michael-type addition reaction. Current Applied Physics, 3rd China-Korea Symposium on Biomaterials and Nano-Bio Technology 7, 2007, 28–32.

173. Kato, Y., Nakamura, S., and Nishimura, M. (2006) *Biorheology*, **43**, 347–354.

174. Yamada, M. and Honma, I. (2004) Alginic acid–imidazole composite material as anhydrous proton conducting membrane. *Polymer*, **45**, 8349–8354.

175. Klöck, G., Pfeffermann, A., Ryser, C., Gröhn, P., Kuttler, B., and Hahn, H.-J. (1997) Ulrich zimmermann biocompatibility of mannuronic acid-rich alginates. *Biomaterials*, **18** (10), 707–713.

176. Augst, A.D., Kong, H.J., and Mooney, D.J. (2006) Alginate hydrogels as biomaterials. *Macromol. Biosci.*, **6** (8), 623–633.

177. Imeson, A. (2009) *Food Stabilisers, Thickeners and Gelling Agents*, John Wiley & Sons, Ltd, Chichester.

178. Sriamornsak, P. (2003) Chemistry of pectin and its pharmaceutical uses: a review. *Silpakorn Univ. Int. J.*, **3**, 206–228.

179. Imeson, A. (2009) *Food Stabilisers, Thickeners and Gelling Agents, Sussex*, John Wiley & Sons, Ltd, Chichester.

180. Sila, D.N., Van Buggenhout, S., Duvetter, T., Fraeye, I., De Roeck, A., Van Loey, A. *et al.* (2009) Pectins in processed fruit and vegetables: part II - Structure-function relationships. *Compr. Rev. Food Sci. Food Saf.*, **8** (2), 86–104.

181. White, R.J., Budarin, V., Luque, R., Clark, J.H., and MacQuarrie, D.J. (2009) Tuneable porous carbonaceous materials from renewable resources. *Chem. Soc. Rev.*, **38** (12), 3401–3418.

182. Cardoso, S.M., Coimbra, M.A., and Lopes da Silva, J.A. (2003) Temperature dependence of the formation and melting of pectin-Ca2+ networks: a rheological study. *Food Hydrocolloids*, **17** (6), 801–807.

183. Cristiane Krause Bierhalz, A., Silva, M.A., and Guenter Kieckbusch, T. (2012) Natamycin release from alginate/pectin films for food packaging applications. *J. Food Eng.*, **110** (1), 18–25.

184. Phan, T.D., Debeaufort, F., Luu, D., and Voilley, A. (2005) Functional properties of edible agar-based and starch-based films for food quality preservation. *J. Agric. Food Chem.*, **53**, 973–981.

185. Stanley, N.F. (1995) Agar, in *Food Polysaccharides and their Applications* (ed. A.M. Stephen), Marcel Dekker, New York, pp. 187–199.

186. Belitz, H.D. and Grosch, W. (1999) *Food Chemistry Carbohydrates in Food Chemistry*, Springer, New York.

187. Freile-Pelegrín, Y., Madera-Santana, T., Robledo, D., Veleva, L., Quintana, P., and Azamar, J.A. (2007) Degradation of agar films in a humid tropical climate: thermal, mechanical, morphological and structural changes. *Polym. Degrad. Stab.*, **92**, 244–252.

188. Jhurry, D., Bhaw-Luximon, A., Mardamootoo, T., and Ramanjooloo, A. (2006) biopolymers from the mauritian marine environment. *Macromol. Symp.*, **231**, 16–27.

189. Rees, D.A. and Welsh, E.J. (1977) Secondary and tertiary structure of polysaccharides in solutions and gels. *Angew. Chem. Int. Ed. Engl.*, **16** (4), 214–224.

190. Haug, A., Larsen, B., and Smidsrod, O. (1974) Uronic acid sequence in alginate from different sources. *Carbohydr. Res*, **32**, 217–225.

191. Larsen, B., Smidsrod, O., Haug, A., and Painter, T. (1969) Determiation by a kinetic method of the nearest neighbor frequencies in a fragment of alginic acid. *Acta Chem. Scand.*, **23**, 2375–2388.

192. Strand, K.A., Boe, A., Dalberg, P.S., Sikkeland, T., and Smidsrod, O. (1982) *Macromolecules*, **15**, 570–579.

193. Timmins, P., Delargy, P., Minchom, C.M., and Howard, R. (1992) Influence of some process variables on product properties for a hydrophilic matrix controlled release tablet. *Eur. J. Pharm. Biopharm.*, **38**, 113–118.

194. Aslani, P. and Kennedy, R.A. (1996) Studies on diffusion in alginate gels. I. Effect of cross-linking with calcium or zinc ions on diffusion of acetaminophen. *J. Controlled Release*, **42**, 75–82.

195. Sabra, W. and Deckwer, W.D. (2005) in *Polysaccharides Structural Diversity and Functional Versatility* (ed. S. Dumitriu), p. 515.

196. Stanford P, Baird J, Academic Press, (1983).

197. Wang, Z.Y., Zhang, Q.Z., Konno, M., and Saito, S. (1991) Sol-gel transition of alginate solution by additions of various divalent-cations–critical-behavior of relative viscosity. *Chem. Phys. Lett.*, **186**, 463.

198. Chanda, S.K., Hirst, E.L., and Ross, A.G. (1952) The structure of alginic acid part II, percival BGV. *J. Chem. Soc.*, 1833–1837.

199. Chan, L.W., Lee, H.Y., and Heng, P.W.S. (2002) Production of alginate

microspheres by internal gelation using emulsification method. *J. Pharm.*, 242–259.

200. Smidsrod, O. (1974) *Faraday Discuss Chem. Soc.*, **57**, 263–274.

201. Grasdalen, H., Larsen, B., and Smidsrod, O. (1979) A p.m.r. study of the composition and sequence of uronate residues in alginates. *Carbohydr. Res.*, **68**, 23–31.

202. Grasdalen, H., Larsen, B., and Smidsrod, O. (1981) 13C-n.m.r. studies of monomeric composition and sequence in alginate. *Carbohydr. Res.*, **89** (2), 179–191.

203. Ouwerx, C., Velings, N., Mestdagh, M.M., and Axelos, M.A.V. (1998) Physico-chemical properties and rheology of alginate gel beads formed with various divalent cations. *Polym. Gels Netw.*, **6** (5), 393–408.

204. Bajpai, S.K. (2004) Sharma S Investigation of swelling/degradation behaviour of alginate beads crosslinked with Ca^{2+} and Ba^{2+} ions. *React. Funct. Polym.*, **59** (2), 129–140.

205. Tarun, K. and Gobi, N. (2012) Calcium alginate/ PVA blended nanofibre matrix for wound dressing. *Indian J. Fibre Tex. Res.*, **37**, 127–132.

206. Campo, V.L., Kawano, D.F., Silva Júnior, D.B., and Ivone Carvalho, I. (2009) Carrageenans: biological properties, chemical modifications and structural analysis. *Carbohydr. Polym.*, **77**, 167–180.

207. Van de Velde, F., Knutsen, S.H., Usov, A.I., Romella, H.S., and Cerezo, A.S. (2002) 1H and 13 C high resolution NMR spectroscopy of carrageenans: application in research and industry. *Trends Food Sci. Technol.*, **13**, 73–92.

208. Hoffmann, R.A., Gidley, M.J., David Cooke, D., and Frith, W.J. (1995) Effect of isolation procedures on the molecular composition and physical properties of Eucheuma cottonii carrageenan. *Food Hydrocolloids*, **9** (4), 281–289.

209. Theerkeelsen, H.G., Whistler, R.L., and BeMiller, J.N. (1993) Carrageenan, in *Industrial Gums*, Academic Press Inc., San Diego, CA.

210. Jeffree, C.E. and Kerstiens, G. (1996) Structure and ontogeny of plant cuticles, in *Plant Cuticles: An Integrated Functional Approach*, BIOS Scientific Publishers, Oxford, pp. 33–82.

211. Heredia, A. (2003) Biophysical and biochemical characteristics of cutin, a plant barrier biopolymer. *Biochim. Biophys. Acta*, **1620**, 1–7.

212. Villena, J.F., Dominguez, E., Stewart, D., and Heredia, A. (1999) Characterization and biosynthesis of non-degradable polymers in plant cuticles. *Planta*, **208**, 181–187.

213. Boom, A., Damste, J.S.D., and Leeuw, J.W. (2005) Cutan, a common aliphatic biopolymer in cuticles of drought-adapted plants. *Org. Geochem.*, **36**, 595–601.

214. Deshmukh, A.P., Simpson, A.J., Hadad, C.M., and Hatcher, P.G. (2005) Insights into the structure of cutin and cutan from *Agave americana* leaf cuticle using HRMAS NMR spectroscopy. *Org. Geochem.*, **36**, 1072–1085.

215. Shechter, M. and Chefetz, B. (2009) Decomposition and transformation of cutin and cutan biopolymers in soils: effect on their sorptive capabilities. Geophysical Research Abstracts, Vol. 11, EGU2009-2447, EGU General Assembly.

216. McKinney, D.E., Bortiatynski, J.M., Carson, D.M., Clifford, D.J., DeLeeuw, J.W., and Hatcher, P.G. (1996) Tetramethylammonium hydroxide (TMAH) thermochemolysis of the aliphatic biopolymer cutan: Insights into the chemical structure. *Org. Geochem.*, **24**, 641–650.

217. Tegelaar, E.W., DeLeeuw, J.W., Largeau, C., Derenne, S., Schulten, H.R., Müller, R., Boon, J.J., Nip, M., and Sprenkels, J.C.M. (1989) Scope and limitations of several pyrolysis methods in the structural elucidation of a macromolecular plant constituent in the leaf cuticle of *Agave Americana* L. *J. Anal. Appl. Pyrolysis.*, **15**, 29–54.

218. Schouten, S., Moerkerken, P., Gelin, F., Baas, M., de Leeuw, J.W., and Damste, J.S.S. (1998) Structural characterization of aliphatic, non-hydrolyzable biopolymers in freshwater algae and a

leaf cuticle using ruthenium tetroxide degradation. *Phytochemistry*, **49** (4), 987–993.

219. Shechter, M. and Chefetz, B. (2008) Insights into the sorption properties of cutin and cutan biopolymers. *Environ. Sci. Technol.*, **42**, 1165–1171.

220. Chefetz, B. and Xing, B. (2009) Relative role of aliphatic and aromatic moieties as sorption domains for organic compounds: a review. *Environ. Sci. Technol.*, **43** (6), 1680–1688.

221. Cutler, D.F., Alvin, K.L., and Price, C.E. (1982) *The Plant Cuticle Price*, Academic Press, London.

222. Walton, T.J. (1990) Waxes, cutin and suberin. *Methods Plant Biochem.*, **4**, 105–158.

223. Osman, S.F., Gerard, H.C., Fett, W.F., Moreau, R.A., and Dudley, R.L. (1995) Method for the production and characterization of tomato cutin oligomers. *J. Agric. Food Chem.*, **43**, 2134–2137.

224. Yan, L., Chang, P.R., Zheng, P., and Ma, X. (2012) It is an inherently biocompatible, biodegradable and nontoxic nature biopolymer. *Carbohydr. Polym.*, **87**, 1919–1924.

225. Eherton, L.E., Platz, P.E., and Cosgrove, F.P. (1955) *Drug Stand.*, **2**, 42–47.

226. Chudzikowski, R.J. (1971) Guar gum and its application. *J. Soc. Cosmt, Chem.*, **22**, 43–60.

227. Fulzele, S.V., Satturwar, P.M., and Dorle, A.K. (2003) Study of the biodegradation and in vivo biocompatibility of novel biomaterials. *Eur. J. Pharm. Sci.*, **20**, 53–61.

228. Shirwaikar, A.A. and Rosin, R.N. (2000) A polymer for micro encapsulation of diltiazem hydrochloride for sustained release by emulsion solvent evaporation technique. *Ind. J. Pharm. Sci.*, **62** (4), 308–310.

229. Sheorey, D.S. and Dorle, A.K. (1991) Effect of solvents on the characteristics of rosin walled microcapsules prepared by a solvent evaporation technique. *J. Microencapsul.*, **8** (1), 71–78.

230. Ramani, C.C., Puranik, P.K., and Dorle, A.K. (1996) Study of maleoabietic acid as matrix forming material. *Int. J. Pharm.*, **1**, 344–352.

231. Cicek, H., Tuncel, A., Tuncel, M., and Piskin, E. (1995) Degradation and drug release characteristics of Monosize polyethylcyanoacrylate microspheres. *J. Biomater. Sci. Polym. Ed.*, **6**, 845–856.

232. Mi, F.L., Lin, Y.M., Wu, Y.B., Shyu, S.S., and Tsai, Y.H. (2002) Chitin/PLGA blend microspheres as a biodegradable drug-delivery system: phase-separation, degradation and release behaviour. *Biomaterials*, **23**, 3257–3267.

233. Prakash Pal, O., Malviya, R., Bansal, V., and Kumar Sharma, P. (2010) Rosin an important polymer for drug delivery. *Dep. Pharm. Technol.*, **3**, 1.

234. Zhang, Y. and Chu, C.C. (2002) In vitro release behavior of insulin from biodegradable hybrid hydrogel networks of polysaccharide and synthetic biodegradable polyester. *J. Biomater. Appl.*, **16**, 305–325.

235. Gilbert, M.E., Kirker, K.R., Gray, S.D., Ward, P.D., Szakacs, J.G., Prestwich, G.D., and Orlandi, R.R. (2004) Chondroitin sulfate hydrogel and wound healing in rabbit maxillary sinus mucosa. *Laryngoscope*, **114** (8), 1406–1409.

236. Van Susante, J.L., Pieper, J., Buma, P., van Kuppevelt, T.H., Beuningen, H.V., van der Kraan, P.M., Veerkamp, J.H., van den Berg, W.B., and Veth, R.P.H. (2001) Linkage of chondroitin-sulfate to type I collagen scaffolds stimulates the bioactivity of seeded chondrocytes in vitro. *Biomaterials*, **22** (2359), 69.

237. Chan, P.S., Caron, J.P., Rosa, G.J., and Orth, M.W. (2005) Glucosamine and chondroitin sulfate regulate gene expression and synthesis of nitric oxide and prostaglandin E(2) in articular cartilage explants. *Osteoarthr. Cartil.*, **13**, 387–394.

238. Conelly, W.T. (1985) Copal and rattan collecting in Philippines. *Econ. Bot.*, **39**, 39.

239. Vandenabeele, P., Wehling, B., Moens, L., Edwards, H., De Reu, M., and Van Hooydonk, G. (2000) Analysis with micro-Raman spectroscopy of natural organic binding media and varnishes used in art. *Anal. Chim. Acta*, **407**, 261–274.

240. Langenheim, J. (1969) Amber: A Botanical Inquiry. *Science*, **163**, 1157.

241. Whitmore, T.C. (1980) Utilization, potential and conversation of agathis,a genus of tropical Asian conifers. *Econ. Bot.*, **34**, 1.

242. Jafarsidik, J. (1987) Damar resin-producing tree species and their distribution in Indonesia. *Duta Rimba*, **13**, 7.

243. Torquebiau, E.F. (1987) Tropical forest biology program. *Biotropia*, **1**, 42.

244. De-Foresta, H. and Michon, G. (1994) Agroforests in sumatra-where ecology meets economy. *Agroforestry Today*, **6**, 12.

245. Messer, A.C. (1990) Traditional and chemical techniques for stimulation of *Shorea javanica* (Dipterocarpaceae) resin exudation in Sumatra. *Econ. Bot.*, **44**, 463.

246. Leathers, T.D. (2003) Biotechnological production and applications of pullulan. *Appl. Microbiol. Biotechnol.*, **62**, 468–473.

247. Morris, V.J. (1995) in *Food Polysaccharides and their Applications* (ed. A.M. Stephen), Marcel Dekker, Inc., New York, pp. 341–375.

248. Tsujisaka, Y. and Mitsuhashi, M. (1993) Pullulan, in *Industrial Gums* (eds. R.L. Whistler and J.N. BeMiller), Marcel Dekker, New York, pp. 447–460.

249. Yalpani, M. (1998) in *Polysaccharides: Synthesis, Modification and Structural Property Relations* (ed. M. Yalpani), Elsevier, Amsterdam.

250. Singh, R.S., Saini, G.K., and Kennedy, J.F. (2008) Pullulan: microbial sources, production and applications. *Carbohydr. Polym.*, **73**, 515–531.

251. Yuen, S. (1974) Pullulan and its applications. *Process. Biochem.*, **9**, 7–9.

252. Rekha, M.R. and Sharma, C.P. (2007) Pullulan as a promising biomaterial for biomedical applications: a perspective. *Trends Biomater. Artif. Organs*, **20** (2), 116–121.

253. Iyer, A., Mody, K.H., and Jha, B. (2005) Biosorption of heavy metals by a marine bacterium. *Mar. Pollut. Bull.*, **50** (3), 340–343.

254. Hiji, Y. (1986) Method for inhibiting increase in blood sugar content. US Patent 4 629725.

255. Hijiya, H. and Shiosaka, M. (1975) Process for the preparation of food containing pullulan and amylase. US Patent 3 872 228.

256. Kato, K. and Shiosaka, M. (1975) Food compositions containing pullulan. US Patent 3, 875, 308.

257. Li, H., Yang, J., Hu, X., Liang, J., Fan, Y., and Zhang, X. (2011) Superabsorbent polysaccharide hydrogels based on pullulan derivate as antibacterial release wound dressing. *J. Biomed. Mater. Res. A*, **98A**, 1.

258. Krochta, J.M. and De Mulder-Johnston, C. (1997) Edible and biodegradable polymer films -challenges and opportunities (A Scientific Status Summary). *Food Technol.*, **51**, 61–74.

259. Mitsuhashi, M. and Koyama, S. (1987) Process for the production of virus vaccine. US Patent 4 659 569.

260. Yamaguchi, R., Iwai, H., Otsuka, Y., Yamamoto, S., Ueda, K., Usui, M., Taniguchi, Y., and Matuhasi, T. (1985) Conjugation of Sendai virus with pullulan and immunopotency of the conjugated virus. *Microbiol. Immunol.*, **29**, 163–168.

261. Nakashio, S., Sekine, N., Toyota, N., Fujita, F., and Domoto, M. (1976) Paper coating material containing pullulan. US Patent 3932 192.

262. Nomura, T. (1976) Paper composed mainly of pullulan fibres and method for producing the same. US Patent 3 936 347.

263. Nakashio, S, Sekine, N., Toyota, N., and Fujita, F (1975) Paint containing pullulan. US Patent 3 888 809.

264. Sano, T., Uemura, Y., and Furuta, A. (1976) Photosensitive resin composition containing pullulan or esters thereof. US Patent 3 960 685.

265. Sasago, M., Endo, M., Takeyama, K., and Nomura, N (1988) Water-Soluble photopolymer and method of forming pattern by the use of the same. US Patent 4 745 042.

266. Hikasa, E., Katakami, M., Nomura, T., Mitekura, H., Kawata, T., Matsui, F., and Fukuda, S. (2006) Application

of pullulan derivative to photographic emulsion. *J. Soc. Photogr. Sci. Technol Jpn.*, **69**, 52–53.

267. Tsukada, N., Hagihara, K., Tsuji, K., Fujimoto, M., and Nagase, T. (1978) Protective coating material for lithographic printing plate. US Patent 4 095 525.

268. Vermeersch, J. T., Coppens, P. J., Hauquier, G. I. and Schacht, E. H. (1995) Lithographic base with a modified dextran or pullulan hydrophilic layer. US Patent 5 402 725.

269. Sidebotham, R.L. (1974) Dextrans. *Adv. Carbohydr. Chem. Biochem.*, **30**, 371–444.

270. Mehvar, R.J. (2000) Dextrans for targeted and sustained delivery of therapeutic and imaging agents. *Controlled Release*, **69**, 47–55.

271. Heinze, T., Liebert, T., Heublein, B., and Hornig, S. (2006) Functional polymers based on dextran. *Adv. Polym. Sci.*, **205**, 199–291.

272. Robyt, J.F. (1987) in *Encyclopedia of Polymer Science and Technology*, 2nd edn, Vol. **3** (ed. J.I. Kroschwitz), John Wiley & Sons, Inc., New York, pp. 752–767.

273. Cade´e, J.A., van Luyn, M.J.A., Brouwer, L.A., Plantinga, J.A., van Wachem, P.B., de Groot, C.J., den Otter, W., and Hennink, W.E. (2000) In vivo biocompatibility of dextran-based hydrogels. *J. Biomed. Mater. Res.*, **50** (3), 397–404.

274. Harada, T., Terasaki, M., and Curdlan, H.A. (1993) in *Industrial Gums*, 3rd edn, (eds. R.L. Whistler and J.N. BeMiller), Academic Press, London, pp. 427–445.

275. Nishinari, K., Zhang, H., and Phillips, G.O. (2000) in *Handbook of Hydrocolloids* (ed. P.A. Williams), Woodhead Publishing Ltd, Cambridge, pp. 269–286.

276. Zhang, H., Nishinari, K., Williams, M.A.K., Foster, T.J., and Norton, I.T. (2002) A molecular description of the gelation mechanism of curdlan. *Int. J. Biol. Macromol.*, **30**, 7–16.

277. Saudagar, P.S. and Singhal, R.S. (2004) Curdlan as a support matrix for the immobilization of enzyme. *Carbohydr. Polym.*, **56**, 483–488.

278. Harada, T., Masada, M., Fujimori, K., and Maeda, I. (1966) Production of firm, resilient gel-forming polysaccharide by a mutant of *Alcaligenes faecalis* var. *myxogenes* 10C3. *Agric. Biol. Chem.*, **30**, 196–198.

279. Kim, B.D., Na, K., and Choi, H.K. (2005) Preparation and characterization of solid lipid nano particles (SLN) made of cocoa butter and curdlan. *Eur. J. Pharm. Sci.*, **24**, 199–205.

280. Baird, J.K. (1989) Xanthan, in *Encyclopedia of Polymer Science, Engineering*, Vol. **17**, John Wiley & Sons, Inc., Hoboken, NJ, pp. 901–918.

281. Katzbauer, B. (1998) Properties and applications of xanthan gum. *Polym. Degrad. Stab.*, **59**, 81–84.

282. Becker, A., Katzan, F., Puhler, A., and Ielpi, L. (1998) Xanthan gum biosynthesis and application: a biochemical/genetic perspective. *Appl. Microb. Biotechnol.*, **50**, 145–52.

283. Kennedy, J.F. and Bradshaw, I.J. (1984) Production, properties and applications of xanthan. *Prog. Ind. Microbiol.*, **19**, 319–371.

284. Margaritis, A. and Zajic, J.E. (1978) Biotechnology review: mixing mass transfer and scale up of polysaccharide fermentations. *Biotech. Bioeng.*, **20**, 939–1001.

285. Rinaudo, M. and Milas, M. (1978) Polyelectrolyte behaviour of bacterial polysaccharide from *xanthomonas campestris. Comparison with carboxymethyl cellulose. Biopolymers*, **17**, 2663–2678.

286. Flickinger, F.C. and Draw, S.W. (1999) *Encyclopedia of Bioprocess Technology: Fermentation*, Vol. **5**, John Wiley & Sons Inc., New York, pp. 2706–2707.

287. Ashtaputre, A.A. and Shah, A.K. (1995) Studies on a viscous, gel-forming exopolysaccharide from Sphingomonas paucimobilis GS1. *Appl. Environ. Microbiol.*, **61** (3), 1159–1162.

288. García-Ochoa, F., Santos, V.E., Casas, J.A., and Gómez, E. (2000) Xanthan gum: production, recovery, and properties. *Biotechnol. Adv.*, **18**, 549–579.

289. Mulchandani, A., Luong, J.H.T., and Leduy, A. (1988) Batch kinetics of microbial polysaccharide biosynthesis. *Biotechnol. Bioeng.*, **32**, 639–646.

290. Faria, S., Oliveira Petkowicz, C.L., Lemos de Morais, S.A., Gonzalo Hernandez Terrones, M., Francisca Pessoa de Franca, M.M.R., and Luiz Cardoso, V. (2011) Characterization of xanthan gum produced from sugarcane broth. *Carbohydr. Polym.*, **86**, 469–476.

291. de Mello Luvielmo, M. and Regina Pippa Scamparini, A. (2009) Xanthan gum: Production, recovery, properties and application. *Estudos Tecnológicos*, **5** (1), 50–67.

292. Shetty, K., Paliyath, G., Pometto, A., and Levin, R.E. (2005) *Food Biotechnology*, 2nd edn, CRC Press.

293. Jung, J.Y., Park, J.K., and Chang, H.N. (2005) Bacterial cellulose production by Gluconacetobactor hansenii in an agitated culture without living non-cellulose producing cells. *Enzyme Microb. Technol.*, **37**, 347–54.

294. Bielecki, S., Krystynowicz, A., Turkiewicz, M., and Kalinowska, H. (2002) Bacterial cellulose, in *Biopolymers (Polysaccharides I: Polysaccharides from Prokaryotes)*, Vol. **5** (eds. J. Vandamme, S.D. Baets, and A. Steinbüchel), Wiley-VCH Verlag GmbH, Weinheim, pp. 37–90.

295. Phisalaphong, M., Suwanmajo, T., and Tammarate, P. (2008) Synthesis and characterization of bacterial cellulose/alginate blend membranes. *J. Appl. Polym. Sci.*, **107**, 3419–3424.

296. Backdahl, H., Helenius, G., Bodin, A., Nannmark, U., Johansson, B.R., Risberg, B., and Gatenholm, P. (2006) Mechanical properties of bacterial cellulose and interactions with smooth muscles. *Biomaterials*, **27**, 2141–2149.

297. Czaja, W., Krystynowicz, A., Bielecki, S., and Brown, R.M. Jr., (2006) Microbial cellulose- the natural power to heal wounds. *Biomaterials*, **27**, 145–151.

298. Wiegand, C., Elsner, P., Hipler, U.C., and Klemm, D. (2006) Protease and OS activities influenced by a composite of bacterial cellulose and collagen type I in vitro. *Cellulose*, **13**, 689–696.

299. Oprea A.M., Neamtu A., Stoica B., Vasile C. (2009) Analele Stiintifice ale Universitii, Alexandru Ioan Cuza, Sectiunea Geneticsi Biologie Moleculara, TOM, X. p. 85–92.

300. Wu, S.C. and Lia, Y.K. (2008) Application of bacterial cellulose pellets in enzyme immobilization. *J. Mol. Catal. B: Enzym.*, **54**, 103–108.

301. Ciechanska, D. (2004) Multifunctional bacterial cellulose/ chitosan composite materials for medical applications. *Fibres Text. East Eur.*, **12**, 69–72.

302. Yoon, S.H., Jin, H.J., Kook, M.C., and Pyun, Y.R. (2006) Electrically conductive bacterial cellulose by incorporation of carbon nanotubes. *Biomacromolecules*, **7**, 1280–1284.

303. Iguchi, M., Yamadaka, S., and Budhiono, A. (2000) Bacterial cellulose-a masterpiece of nature's arts. *J. Mater. Sci.*, **35**, 261.

304. Basta, A.H. and El-Saied, H. (2009) Performance of improved bacterial cellulose application in the production of functional paper. *J. Appl. Microbiol.*, **107**, 2098–2107.

305. Nakagaito, A.N. and Yano, H. (2005) Novel High-strength biocomposites on microfibrillated cellulose having nano-order-unit web-like network structure. *Appl. Phys. A: Mater. Sci. Process.*, **80**, 155–159.

306. Yoshinaga, F., Tonouchi, N., and Watanabe, K. (1997) Research progress in production of bacterial cellulose by aeration and agitation culture and its application as new industrial material. *Biosci. Biotechnol. Biochem.*, **61**, 219–224.

307. Chibnall, A.C., Rees, M.W., and Richards, F.M. (1958) Structure of polyglutamic acid from bacillus subtilis. *Biochem. J.*, **68** (1), 129–135.

308. Sekine, T., Nakamura, T., Shimizu, Y., Ueda, H., Matsumoto, K., Takimoto, Y., and Kiyoutami, T. (2001) A new type of surgical adhesive made from porcine collagen and polyglutamic acid. *J. Biomed. Mater. Res.*, **54** (2), 305–310.

309. McLean, R.J.C., Beauchemin, D., Clapham, L., and Beveridge, T.J. (1990) Metal-binding characteristics of the gamma-glutamyl capsular polymer of

bacillus licheniformis ATCC 9945t. *Appl. Environ. Microbiol.*, **56** (12), 3671–3677.

310. Oppermann-Sanio, F. and Steinbuchel, A. (2002) Occurrence functions and biosynthesis of polyamides in microorganisms and biotechnological production. *Naturwissenschaften*, **89**, 11–22.

311. Fuser, G. (2007) Steinbuchel, Analysis of genome sequences for genes of cyanophycin metabolism: identifying putative cyanophycin metabolizing prokaryotes. *Macromol. Biosci.*, **7**, 278–296.

312. Simon, R.D. (1987) Inclusion bodies in the cyanobacteria: cyanophycin polyphosphate bodies, in *The Cyanobacteria* (eds. P. Fay and V.B.C), Elsevier, Amsterdam, pp. 199–225.

313. Lang, N.J. (1968) The fine structure of blue green algae. *Annu. Rev. Microbiol.*, **22** (1), 15–46.

314. Dembinska, M.E. and Allen, M.M. (1988) *J. Gen. Microbiol.*, **134** (2), 295–298.

315. Schwamborn, M. (1998) Chemical Synthesis of polyaspartates : a biodegradable alternative to currently used polycarboxylate homo- and copolymers. *Polym. Degrad. Stab.*, **59** (1), 39–45.

316. Shima, S. and Sakai, H. (1977) Polylysine produced by Streptomyces. *Agric. Biol. Chem.*, **41** (9), 1907–1909.

317. Shima, S. and Sakai, H. (1981) Poly-L-Lysine produced by streptomyces III. chemical studies. *Agric. Biol. Chem.*, **45** (11), 2503–2508.

318. Li, S., Li, F., Chen, X.-S., Wang, L., Jian, X., Tang, L., and Mao, Z.-G. (2012) Genome shuffling enhanced ε-poly-L-lysine production by improving glucose tolerance of streptomyces graminearus. *Appl. Biochem. Biotechnol.*, **166**, 414–423.

319. Joko, E., Tokuda, S., Kikumoto, N., Sugai, J., Hayashi, T., and Arai, M. (2002) Enzymatic function of jute fibre with various commercial enzymes. *Sen'I Gakkaishi*, **58** (1), 22–28.

320. Liu, L., Wang, Q., Cheng, L., Qian, J., and Yu, J. (2011) Modification of natural bamboo fibres for textile applications. *Fibers Polym.*, **12** (1), 95–103.

321. (2010) *Nat Prod Resour Repose*, **1** (3).

322. Sreenath, H.K., Shah, A., Yang, V., Gharia, M.M., and Jeffries, T.W. (1996) Enzymatic polishing of jute cotton blended fabrics. *J. Ferment. Bioeng.*, **81** (1), 18–20.

323. Basak, M.K., Chanda, S., Bhaduri, S.K., Mondal, S.B., and Nandi, R. (1996) Recycling of jute waste for edible mushroom production. *Ind. Crops Prod.*, **5**, 173–176.

324. Hill, C.A., Khalil, H.A., and Hale, M.D. (1998) A study of the potential of acetylation to improve the properties of plant fibres. *Ind. Crops Prod.*, **8**, 53–63.

325. Khan, F. and Ahmad, S.R. (1996) Chemical modification and spectroscopic analysis of jute fibre. *Polym. Degrad. Stab.*, **52**, 335–340.

326. Satyanarayana, K., Pillai, C.K.S., Sukumaran, K., Pillai, S.G.K., Rohatgi, P.K., and Vijayan, K. (1982) Structure property studies of fibres from various parts of the coconut tree. *J. Mater. Sci.*, **17**, 2453–2462.

327. Choudhury, A., Kumar, S., and Adhikari, B. (2007) Recycled milk pouch and virgin low-density polyethylene/linear low-density polyethylene based coir fiber composites. *J. Appl. Polym. Sci.*, **106**, 775–785.

328. Corradini, E., Morais, L.C., Rosa, M.F., Mazzetto, S.E., Mattoso, L.H., and Agnelli, J.A.M. (2006) A preliminary studies for the use of natural fibres as reinforcement in starch–gluten–glycerol matrix. *Macromol. Symp*, **245–246**, 558–564.

329. Geethamma, V.G., Thomas Mathew, K., Lakshminarayan, R., and Thomas, S. (1998) Composite of short coir fibres and natural rubber: effect of chemical modification loading and orientation of fibre. *Polymer*, **39** (6-7), 1483–1491.

330. Owolabi, O., Czvikovszky, T., and Kovacs, I. (1985) *Coconut fibre reinforced thermosetting plastics*, **30**, 1827–1836.

331. Kaplan, D.L., Mello, S.M., Arcidiacono, S., Fossey, S., Senecal, K., and Muller, W. (1998) Silk, in *Protein Based Materials* (eds. K. McGrath and D.L. Kaplan), pp. 103–131.

332. Kaplan, D.L., Adams, W.W., Farmer, B., and Viney, C. (1994) in *Silk Polymers*, ACS Symp Ser, Vol. **544** (eds. D.L. Kaplan, W.W. Adams, B. Farmer, and C. Viney), pp. 2–16.

333. Kaplan, D.L., Fossey, S., Viney, C., and Muller, W. (1992) in *Self Organization (assembly) in Biosynthesis of Silk Fibres – a Hierarchical Problem*, Vol. **255** (eds. I.A. Aksay, E. Baer, M. Sarika ya, and D.A. Tirrell), pp. 19–29*Mater. Res. Symp. Proc.*.

334. Altman, G.H., Diaz, F., Jakuba, C., Calabro, T., Horan, R.L., Chen, J., Lu, H., Richmond, J., and Kaplan, D.L. (2003) Silk based biomaterials. *Biomaterials*, **24**, 401–416.

335. Guerette, P.A., Ginzinger, D.G., Weber, B.H.F., and Gosline, J.M. (1996) Silk properties determined by gland- specific expression of a spider fibroin gene family. *Science*, **272**, 112–115.

336. Cappello, J. (1990) The biological production of protein polymers and their use. *J. Trends Biotechnol.*, **8**, 309–311.

337. Xu, M. and Lewis, R.V. (1990) Structure of a protein superfibre-spider dragline silk. *Proc. Natl. Acad. Sci. U.S.A.*, **87**, 7120–7124.

338. Meinel, L., Hofmann, S., Karageorgiou, V., Zichner, L., Langer, R., Kaplan, D., and Vunjak-Novakovic, G. (2004) Engineering cartilage-like tissue using human mesenchymal stem cells and silk protein scaffolds. *Biotechnol. Bioeng.*, **88**, 379–391.

339. Jin, H.J., Chen, J., Karageorgiou, V., Altman, G.H., and Kaplan, D.L. (2004) Human bone marrow stromal cell responses on electrospun silk fibroin mats. *Biomaterials*, **25**, 1039–1047.

340. Meinel, L., Karageorgiou, V., Fajardo, R., Snyder, B., Shinde-Patil, V., Zichner, L. *et al.* (2004) Bone tissue engineering using human mesenchymal stem cells: effects of scaffold material and medium flow. *Ann. Biomed. Eng*, **32**, 112–122.

341. Meinel, L., Kargeorgiou, V., Hofmann, S., Fajardo, R., Snyder, B., Li, C., Zichner, L., Langer, R., Vunjak-Novakovic, G., and Kaplan, D.L. (2004) Engineering bone-like tissue in vitro using human bone marrow stem cells and silk scaffolds. *J. Biomed. Mater. Res.*, **25**, 71A.

342. Sandra Hofmann, L.M., Karageorgiou, V., John McCool, C.K.H., Gronowicz, G., Zichner, L., Robert Langer, G., Vunjak-Novakovic , and Kaplan, D.L. (2005) The inflammatory responses to silk films in vitro and in vivo. *Biomaterials*, **26**, 147–155.

343. Neidle, S. (2008) *Principles of Nucleic Acid Structure*, Academic Press, Boston, MA, p. 289.

344. Michael Blackburn, G., Gait, M.J., Loakes, D., and Williams, D. (eds.) (2006) *Nucleic Acids in Chemistry and Biology*, 3rd edn, RSC publishing, Cambridge.

345. Bloomfield, V.A., Crothers, D.M., Tinoco, I., Hearst, J.E., Wemmer, D.E., Killman, P.A., and Turner, D.H. (2000) *Nucleic Acids: Structures, Properties, and Functions*, University Science Books, Sausalito, CA, p. 794.

346. (a) Pinheiro, V.B., Taylor, A.I., Cozens, C., Abramov, M., Su, M.R., Zhang, J.C., Chaput, J.W., Peak-Chew, S.Y., McLaughlin, S.H., Herdewijn, P., and Holliger, P. (2012) Synthetic genetic polymers capable of heredity and evolution. *Science*, **336**, 341–344; (b) Joyce, G.F. (2012) Toward an alternative biology. *Science*, **336**, 307–308.

347. Crooke, E. (1995) DNA synthesis initiated at oriC: *in vitro* replication reactions, in *Methods in Enzymology*, Vol. **262** (ed. J.L. Campbell), Academic Press, New York, pp. 500–506.

348. Braasch, D.A. and Corey, D.R. (2002) Novel antisense and peptide nucleic acid strategies for controlling gene expression. *Biochemistry*, **41** (14), 4503–4510.

349. Liu, H., Gao, J., Lynch, S.R., David Saito, Y., Maynard, L., and Kool, E.T. (2003) A four-base paired genetic helix with expanded size. *Science*, **302** (5646), 868–871.

350. Switzer, C.Y., Moroney, S.E., and Benner, S.A. (1993) Enzymic recognition of the base pair between isocytidine and isoguanosine. *Biochemistry*, **32** (39), 10489–10496.

351. Piccirilli, J.A., Krauch, T., Moroney, S.E., and Benner, S.A. (1990) Enzymatic incorporation of a new base pair into DNA and RNA extends the genetic alphabet. *Nature*, **343**, 33–37.

352. Bain, J.D., Switzer, C., Chamberlin, A.R., and Benner, S.A. (1992) Ribosome-mediated incorporation of a non-standard amino acid into a peptide through expansion of the genetic code. *Nature*, **356**, 537–539.

353. Ray, A. and Norden, B. (2000) Peptide nucleic acid (PNA): its medical and biotechnical applications and promise for the future. *FASEB J.*, **14**, 1041–1060.

354. Braasch, D.A. and Corey, D.R. (2001) Synthesis, analysis, purification, and intracellular delivery of peptide nucleic acids. *Methods*, **23**, 97–107.

355. Braasch, D.A. and Corey, D.R. (2001) Locked nucleic acid (LNA): fine-tuning the recognition of DNA and RNA. *Chem. Biol.*, **8**, 1–7.

356. Petersen, M. and Wengel, J. (2003) LNA: a versatile tool for therapeutics and genomics. *Trends Biotechnol.*, **21** (2), 74–81.

357. Rusk, N. (2012) Under studies of DNA and RNA. *Nat. Methods*, **9**, 530–531.

358. Lescrinier, E., Esnouf, R., Schraml, J., Busson, R., Heus, H.A., Hilbers, C.W., and Herdewijn, P. (2000) Solution structure of a HNA–RNA hybrid. *Chem. Biol.*, **7** (9), 719–731.

359. Beier, M., Reck, F., Wagner, T., Krishnamurthy, R., and Eschenmoser, A. (1999) Chemical etiology of nucleic acid structure: comparing pentopyranosyl-(2'!4') oligonucleotides with RNA. *Science*, **283**, 699–703.

360. Eschenmoser, A. (1999) Chemical etiology of nucleic acid structure. *Science*, **284** (5423), 2118–2124.

361. Jackson, D., Symons, R., and Berg, P. (1972) Biochemical method for inserting new genetic information into DNA of simian virus 40: circular SV40 DNA molecules containing lambda phage genes and the galactose operon of Escherichia coli. *Proc. Natl. Acad. Sci. U.S.A.*, **69** (10), 2904–2909.

362. Judson, H.F. (1979) *The Eighth Day of Creation: Makers of the Revolution in Biology*, Touchstone Books, 2nd edn, Cold Spring Harbor Laboratory Press, New York 1996 paperback.

363. Vroman, I. and Tighzert, L. (2009) Biodegradable polymers. *Materials*, **2**, 307–344.

364. Nair, L.S. and Laurencin, C.T. (2006) Polymers as biomaterials for tissue engineering and controlled drug delivery. *Adv. Biochem. Eng. Biotechnol.*, **102**, 47.

365. Pathiraja, A.G. and Adhikari, R. (2003) Biodegradable synthetic polymers for tissue engineering. *Eur. Cells Mater.*, **5**, 1–16.

366. Lu, H.H., Cooper, J.A. Jr., Manuel, S., Freeman, J.W., Attawia, M.A., Ko, F.K., and Laurencin, C.T. (2005) Anterior cruciate ligament regeneration using braided biodegradable scaffolds: in vitro optimization studies. *Biomaterials*, **26**, 4805–4816.

367. Tabesh, H., Amoabediny, G., Salehi Nik, N., Heydari, M., and Yosefifard, M. (2009) The role of biodegradable engineered scaffolds seeded with Schwann cells for spinal cord regeneration. *Neurochem. Int.*, **54**, 73–83.

368. Domb, A.J. and Wiseman, D.M. (1998) *Handbook of Biodegradable Polymers*, CRC Press, Boca Raton, FL.

369. Ulery, B.D., Nair, L.S., and Laurencin, C.T. (2011) Biomedical applications of biodegradable polymers. *J. Polym. Sci. B Polym. Phys.*, **49** (12), 832–864.

370. Kai, Z., Ying, D., and Guo-Qiang, C. (2003) Polyhydroxyalkanoate (PHA) scaffolds with good mechanical properties and biocompatibility. *Biochem. Eng. J.*, **16**, 115.

371. Fouda, M.M.G., Wittke, R., Knittel, D., and Schollmeye, E. (2009) Use of chitosan/polyamine biopolymers based cotton as a model system to prepare antimicrobial wound dressing. *Int. J. Diabetes Mellitus*, **1**, 61–64.

372. Vert, M., Li, S., Garreau, H., Mauduit, J., Boustta, M., Schwach, G., Engel, R., and Coudane, J. (1997) Complexity of the hydrolytic degradation of aliphatic polyesters. *J. Macromol. Mater. Eng.*, **247**, 239.

373. Li, M., Mondrinos, M.J., Chen, X., Gandhi, M.R., Ko, F.K., and Lelkes, P.I.

(2006) Co-electrospun poly(lactide-co-glycolide), gelatin, and elastin blends for tissue engineering scaffolds. *J. Biomed. Mater. Res. A*, **79** (4), 963.

374. Pouton, C.W. and Akhtar, S. (1996) Biosynthetic polyhydroxyalkanoates and their potential in drug delivery. *Adv. Drug Delivery Rev.*, **18**, 133.

375. Kumar, N., Langer, R.S., and Domb, A.J. (2002) Polyanhydrides: an overview. *Adv Drug Delivery Rev.*, **54**, 889.

376. Heller, J., Barr, J., Ng, S.Y., Abdellauoi, K.S., and Gurny, R. (2002) Poly(ortho esters): synthesis, characterization, properties and uses. *Adv. Drug Delivery. Rev.*, **54**, 1015–1039.

377. Laurencin, C.T., Norman, M.E., Elgendy, H.M., El-Amin, S.F., Allcock, H.R., Pucher, S.R., and Ambrosio, A.A. (1993) Use of polyphosphazenes for skeletal tissue regeneration. *J. Biomed. Mater.*, **27**, 963.

378. Conconi, M.T., Lora, S., Menti, A.M., Carampin, P., and Parnigotto, P.P. (2006) In vitro evaluation of Poly[Bis(ethyl alanato) Phosphazene] as a scaffold for bone tissue engineering. *Tissue Eng.*, **12** (4), 811–819.

379. Suzuki, T., Ichihara, Y., Yamada, M., and Tonomura, K. (1973) Some Characteristics of pseudomonas O-3 which utilize polyvinyl alcohol. *Agric. Biol. Chem.*, **37**, 747–756.

380. Watanabe, Y., Morita, M., Hamada, N., and Tsujisaka, Y. (1976) Purification and properties of poly(vinyl alcohol) produced by the strain of pseudomonas. *Arch. Biochem. Biophys.*, **174**, 575–581.

381. Sakazawa, C., Shimao, M., Taniguchi, Y., and Kato, N. (1981) Metabolism, growth, and industrial microbiology symbiotic utilization of polyvinyl alcohol by mixed cultures. *Appl. Environ. Microbiol.*, **41**, 261–267.

382. Hashimoto, S. and Fujita, M. (1985) Isolation of bacterium requiring three amino acids for polyvinyl alcohol degradation. *J. Ferment. Technol.*, **63**, 471–474.

383. Mori, T., Sakimoto, M., Kagi, T., and Sakai, T. (1996) Isolation and characterization of a strain of *Bacillus megaterium* that degrades poly (vinyl alcohol). *Biosci. Biotechnol. Biochem.*, **60**, 330–332.

384. Chang, J.H., Jang, T., Ihn, K.J., Lee, W., and Sur, G.S. (2003) Poly(vinyl alcohol) nanocomposites with different clays: pristine clays. *J. Appl. Polym. Sci.*, **90**, 3208–3214.

385. Ibrahim, M.M., El-Zawawy, W.K., and Nassar, M.A. (2010) Synthesis and characterization of polyvinyl alcohol/nanospherical cellulose particle films. *Carbohydr. Polym.*, **79**, 694–699.

386. Nath, A., Dixit, M., Bandiya, A., Chavda, S., and Desai, A. (2008) Enhanced PHB production and scale up studies using cheese whey in fed batch culture of Methylobacterium sp.zp24. *J. Bioresour. Technol.*, **99**, 5749–5755.

387. Steinbüchel, A. and Lütke-Eversloh, T. (2003) Metabolic engineering and pathway construction for biotechnological production of relevant polyhydroxyalkanoates in microorganisms. *Biochem. Eng. J.*, **16**, 81–96.

388. Choi, J. and Lee, S.Y. (1999) Factors affecting the economics of polyhydroxyalkanoates production by bacterial fermentation. *Appl. Microbiol. Biotechnol.*, **51**, 13–21.

389. Koller, M., Bona, R., Chiellini, E., Fernandes, E.G., Horvat, P., Kutschera, C., Hesse, P., and Braunegg, G. (2008) Polyhydroxyalkanoate production from whey by pseudomonas hydrogenovora. *Bioresour. Technol.*, **99**, 4854–4863.

390. Anderson, A.J. and Dawes, E.A. (1990) Occurrence, metabolism, metabolic role and industrial uses of bacterial polyhydroxyalkanoates. *Microbiol. Rev.*, **54**, 450–472.

391. Armelin, E., Franco, L., and Rodriguez-Galan, A. (2002) Puiggali, Study on the degradability of poly(ester amide)s related to nylons and polyesters 6,10 or 12,10. *J. Macromol. Chem. Phys.*, **203**, 48–58.

392. Bettinger, C.J., Bruggeman, J.P., Borenstein, J.T., and Langer, R.S. (2008) Amino-alcohol based degradable poly(ester amide) elastomers. *Biomaterials*, **29**, 2315–2325.

393. Pang, X. and Chu, C.C. (2010) Synthesis, characterization and biodegradation

of novel poly(ester amides) and their functionalization. *Biomaterials*, **31**, 3745–3754.

394. Paredes, N., Rodriguez-Galan, A., and Puiggali, J. (1998) Synthesis and characterization of a family of biodegradable poly (ester amide)s derived from glycine. *J. Polym. Sci., Polym. Chem.*, **36**, 1271–1282.

395. Paredes, N., Rodriguez-Galan, A., Puiggali, J., and Peraire, C. (1998) Studies on the biodegradation and biocompatibility of a new poly(ester amide) derived from L-Alanine *J. Appl. Polym. Sci.*, **69**, 1537–1549.

396. Tsitlanadze, G., Kviria, T., Katsarava, R., and Chu, C.C. (2004) Biodegradation of aminoacid based poly(ester amides): in vitro study using potentiometric titration. *J. Mater. Sci. Mater. Med.*, **15**, 185–190.

397. Tsitlanadze, G., Machaidze, M., Kviria, T., Djavakhishvili, N., Chu, C.C., and Katsarava, R. (2004) Biodegradation of amino-acid-based poly(ester amides): in vitro weight loss and preliminary in vivo studies. *J. Biomater. Sci., Polym. Ed.*, **15**, 1–24.

398. Katsarava, R., Beridze, V., Arabuli, N., Kharadze, D., Chu, C.C., and Won, C.Y. (1999) Amino acid-based bioanalogous polymers. Synthesis and study of regular poly(ester amide)s based on bis(a-amino acid) a,v-alkylene diesters, and aliphatic dicarboxylic acids. *J. Polym. Sci., Polym. Chem.*, **37**, 391–407.

399. Zhang, Z., Kuijer, R., Bulstra, S.K., Grijpma, D.W., and Feijen, J. (2006) The in vivo and in vitro degradation behaviour of poly(trimethylene carbonate). *J. Biomater.*, **27**, 1741–1748.

400. Poillon, F. (ed.) (1993) *Biopolymers: Making Materials Nature's way.*

401. Narayan, R. (2001) Drivers for biodegradable/compostable plastics and role of composting in waste management and sustainable agriculture; Report Paper. *Orbit J.*, **1** (1), 1–9.

402. Gunatillake, P.A. and Adhikari, R. (2003) Biodegradable synthetic polymers for tissue engineering. *Eur. Cells Mater.*, **5**, 1–16.

403. Sinha Ray, S., Yamada, K., Okamoto, M., and Ueda, K. (2003) Control of biodegradability of polylactide via nanocomposite technology. *Macromol. Mater. Eng.*, **288**, 203–208.

404. Langer, R. and Vacanti, J.P. (1993) Tissue engineering. *Science*, **260**, 920–926.

405. Atala, A. and Mooney, D.J. (eds.) (1997) *Synthetic Biodegradable Polymer Scaffolds*, Springer Medical, p. 258.

406. Lee, K.Y. and Mooney, D.J. (2001) Hydrogels for tissue engineering. *Chem. Rev.*, **101**, 1869–1879.

407. Mallapragada, K.S. and Narasimhan, B. (2002) Special issue. Injectable polymeric biomaterials. *Biomaterials*, **23**, 4305–4333.

408. Jeong, B., Bae, Y.H., Lee, D.S., and Kim, S.W. (1997) Biodegradable block copolymers as injectable drug-delivery systems. *Nature*, **388**, 860–862.

409. Vernon, B., Gutowska, A., Bae, Y.H., and Kim, S.W. (1996) Thermally reversible polymer gels for biohybrid artificial pancreas. *J. Macromol. Chem. Phys.*, **109**, 155–167.

410. Skjak-Braek, G., Anthonsen, T., and Sandford, P. (eds.) (1992) *Biopolymers from Renewable Resources*, Elsevier Applied Science, London.

411. Nguyen, K.T. and West, J.L. (2002) Photopolymerizable hydrogels for tissue engineering applications. *Biomaterials*, **23**, 4307–4314.

412. Balakrishnan, B. and Jayakrishnan, A. (2005) Self-cross-linking biopolymers as injectable in situ forming biodegradable scaffolds. *Biomaterials*, **26** (18), 3941–3951.

413. Masotti, A. and Ortaggi, G. (2009) Chitosan micro- and nanospheres : fabrication and applications for drug and DNA delivery. *Mini. Rev. Med. Chem.*, **9** (4), 463–469.

414. Masotti, A., Bordi, F., Ortaggi, G., Marino, F., and Palocci, C. (2008) A novel method to obtain chitosan/DNA nanospheres and a study of their release properties. *Nanotechnology*, **19**, 055302 (6pp).

415. Francis Suh, J.-K. and Matthew, H.W.T. (2000) Application of chitosan-based polysaccharide biomaterials in cartilage tissue engineering: a review. *Biomaterials*, **21**, 2589–2598.

416. Duan, X., McLaughlin, C., Griffith, M., and Sheardown, H. (2007) Biofunctionalization of collagen for improved biological response: scaffolds for corneal tissue engineering. *Biomaterials*, **28**, 78.

417. Narotham, P.K., Jose, S., Nathoo, N., Taylon, C., and Vora, Y. (2004) Collagen matrix (Duragen)in dural repair : analysis of a newly modified technique. *Spine*, **29**, 2861–2867.

418. Keogh, M.B., O' Brien, F.J., and Daly, J.S. (2010) A novel collagen scaffold supports human osteogenesis – applications for bone tissue engineering. *Cell Tissue Res.*, **340**, 169–177.

419. Min, B.M., Lee, S.W., Lim, J.N., You, Y., Lee, T.S., Kang, P.H., and Park, W.H. (2004) Chitin and chitosan nanofibers: electrospinning of chitin and deacetylation of chitin nanofibers. *Polymer*, **45**, 7137–7142.

420. Bosse, D., Praus, M., Kiessling, P., Nyman, L., Andresen, C., Waters, J., and Schindel, F. (2005) Phase I comparability of recombinant human albumin and human serum albumin. *J. Clin. Pharm.*, **45**, 57–67.

421. Halpern, W., Riccobene, T.A., Agostini, H., Baker, K., Stolow, D., Gu, M.L., Hirsch, J., Mahoney, A., Carrell, J., Boyd, E., and Grzegorzewski, K.J. (2002) Albugranin, a recombinant human granulocyte colony stimulating factor (G-CSF) genetically fused to recombinant human albumin induces prolonged myelopoietic effects in mice and monkeys. *Pharm. Res.*, **19** (11), 1720–1729.

422. Mana, M., Cole, M., Cox, S., and Tawil, B. (2006) Human U937 monocyte behaviour and protein expression on various formulations of three-dimensional fibrin clots. *Wound Repair Regen*. in press.

423. Kogan, G., Solte´s, L., Stern, R., and Gemeine, P. (2007) Hyaluronic acid: a natural biopolymer with a broad range of biomedical and industrial applications. *Biotechnol. Lett.*, **29**, 17–25.

424. Maqueta, V., Boccaccini, A.R., and Pravata, L. (2004) Porous (α- hydroxyacid/ bioglass composite scaffolds for bone tissue engineering I: preparation and in vitro characterization. *Biomaterials*, **25**, 4185.

425. Wei, G. and Ma, P.X. (2004) Structure and properties of nano-hydroxyapatite/polymer composite scaffolds for bone tissue engineering. *Biomaterials*, **25**, 4749.

426. A.J. Domb, and R.S. Langer(1988) High molecular weight polyanhydride and preparation thereof. US Patent 4757128.

427. Hirvikorpi, T., VähäNissi, M., Harlin, A., Salomäki, M., Areva, S., Korhonen, J.T., and Karppinen, M. (2011) Enhanced water vapor barrier properties for biopolymer films by polyelectrolyte multilayer and atomic layer deposited Al2O3 double-coating. *Appl. Surf. Sci.*, **257**, 9451–9454.

428. Cai, Q., Yang, J., Bei, J., and Wang, S. (2002) A novel porous cells scaffold made of polylactide–dextran blend by combining phase-separation and particle-leaching techniques. *Biomaterials*, **23**, 4483.

429. Ciardelli, G., Chiono, V., Vozzi, G., Pracella, M., Ahluwalia, A., Barbani, N., Christallini, C., and Giusti, P. (2005) Blends of poly-(E-caprolactone) and polysaccharides in tissue engineering applications. *Biomacromolecules*, **6**, 1961.

430. Kim, J.Y. and Cho, D.-W. (2009) Blended PCL/PLGA scaffold fabrication using multi-head deposition system. *Microelectron. Eng.*, **86**, 1447.

431. Williams, D.F. (1987) Advanced applications for materials implanted within the human body. *Mater. Sci. Technol.*, **3** (10), 797–806.

432. Khoo, C.G.L., Frantzich, S., Rosinski, A., Sjostrom, M., and Hoogstraate, J. (2003) Oral gingival delivery systems from chitosan blends with hydrophilic polymers. *Eur. J. Pharm. Biopharm.*, **55**, 47–56.

433. Sionkowska, A. (2011) Current research on the blends of natural and synthetic polymers as new biomaterials. *Review, Prog. Polym. Sci.*, **36**, 1254–1276.

434. Wang, X., Sang, L., Luo, D., and Li, X. (2011) From collagen–chitosan blends to three-dimensional scaffolds:

the influences of chitosan on collagen nanofibrillar structure and mechanical property. *Colloids Surf. B*, **82**, 233–240.

435. Cascone, M.G., Di Pasquale, G., La Rosa, A.D., Cristallini, C., Barbani, N., and Recca, A. (1995) Blends of synthetic and natural polymers as drug delivery systems for growth hormone. *Biomaterials*, **16**, 569–574.

436. Giusti, P., Lazzeri, L., Barbani, N., Narducci, P., Bonaretti, A., Palla, M., and Lelli, L. (1993) Hydrogels of poly(vinyl alcohol) and collagen as new bioartificial materials. Physical and morphological study. *J. Mater. Sci. Mater. Med.*, **4**, 538–542.

437. Rao, K.P. (1995) Recent developments of collagen-based materials for medical applications and drug delivery systems. *J. Biomater. Sci. Polym. Ed.*, **7**, 623–631.

438. Lopes, C.M.A. and Felisberti, M.I. (2003) Mechanical behaviour and biocompatibility of poly(1-vinyl-2-pyrrolidone)–gelatin IPN hydrogels. *Biomaterials*, **24**, 1279–1284.

439. Thacharodi, D. and Rao, K.P. (1995) Collagen–chitosan composite membranes for controlled release of propranolol hydrochloride. *Int. J. Pharm.*, **120**, 115–118.

440. Leclerc, E., Furukawa, K.S., Miyata, F., Sakai, Y., Ushida, T., and Fujii, T. (2004) Fabrication of microstructures in photosensitive biodegradable polymers for tissue engineering applications. *Biomaterials*, **25**, 4683–4690.

441. Sionkowska, A., Kaczmarek, H., Kowalonek, J., Wisniewski, M., and Skopinska, J. (2004) Surface state of UV irradiated collagen/PVP blends. *Surf. Sci.*, 566–568608–12.

442. Deng, C., Zhang, P., Vulesevic, B., Kuraitis, D., Li, F., Yang, A.F., Griffith, M., and Suuronen, E.J. (2010) A collagen–chitosan hydrogel for endothelial differentiation and angiogenesis. *Tissue Eng. A*, **16**, 3099–3109.

443. Lee, P.C., Huang, L.L.H., Chen, L.W., Hsieh, K.H., and Tsai, C.L. (1996) Effect of forms of collagen linked to polyurethane on endothelial cell growth. *J. Biomed. Mater. Res.*, **32**, 645–653.

444. Van Wachem, P.B., Hendriks, M., Blaauw, E.H., Dijk, F., Verhoeven, M.L.P.M., Cahalan, P.T., and van Luyn, M.J.A. (2002) (Electron) microscopic observations on tissue integration of collagen immobilized polyurethane. *Biomaterials*, **23**, 1401–1409.

445. Cascone, M.G., Giusti, P., Lazzeri, L., Pollicino, A., and Recca, A. (1996) Surface characterisation of collagen-based bioartificial polymeric materials. *J. Biomater. Sci. Polym. Ed.*, **7**, 917–924.

446. Shenoy, V. and Rosenblatt, J. (1995) Diffusion of macromolecules in collagen and hyaluronic acid, rigid-rod flexible polymer, composite matrices. *Macromolecules*, **28**, 8751–8756.

447. Shan, Y., Zhou, Y., Cao, Y., Xu, Q., Ju, H., and Wu, Z. (2004) Preparation and infrared emissivity study of collagen-g-PMMA/In2O3 nanocomposite. *Mater. Lett.*, **58**, 1655–1660.

448. Daamen, W.F., van Moerkerk, H.T.B., Hafmans, T., Buttafoco, L., Poot, A.A., and Veerkamp, J.H. (2003) Preparation and evaluation of molecularly defined collagen–elastin–glycosaminoglycan scaffolds for tissue engineering. *Biomaterials*, **24**, 4001–4009.

449. Ma, L., Gao, C., Mao, Z., Zhou, J., Shen, J., Hu, X., and Han, C. (2003) Collagen/chitosan porous scaffolds with improved biostability for skin tissue engineering. *Biomaterials*, **24**, 4833–4841.

450. Dai, N.T., Williamson, M.R., Khammo, N., Adams, E.F., and Coombes, A.G.A. (2004) Composite cell support membranes based on collagen and polycaprolactone for tissue engineering of skin. *Biomaterials*, **25**, 4263–4271.

451. Scotchford, C.A., Cascone, M.G., Downes, S., and Giusti, P. (1998) Osteoblast responses to collagen–PVA bioartificial polymers in vitro: the effects of cross-linking method and collagen content. *Biomaterials*, **19**, 1–11.

452. Shanmugasundaram, N., Ravichandran, P., Neelakanta, P.R., Nalini, R., Subrata, P., and Rao, K.P. (2001) Collagen–chitosan polymeric scaffolds

for the in vitro culture of human epidermoid carcinoma cells. *Biomaterials*, **22**, 1943–1951.

453. Huang, C., Chen, R., Ke, Q., Morsi, Y., Zhang, K., and Mo, X. (2011) Electrospun collagen–chitosan–TPU nanofibrous scaffolds for tissue engineered tubular grafts. *Colloids Surf. B*, **82**, 307–315.

454. Niu, S., Kurumatani, H., Satoh, S., Kanda, K., Oka, T., and Watanabe, K. (1993) Small diameter vascular prostheses with incorporated bioabsorbable matrices. A preliminary study. *ASAIO Trans.*, **39**, M750–M753.

455. Tian, H., Tang, Z., Zhuang, X., Chen, X., and Jing, X. (2012) Biodegradable synthetic polymers: preparation, functionalization and biomedical application. *Prog. Polym. Sci.*, **37**, 237–280.

456. Lawson, A.C. and Czernuszka, J.T. (1998) Collagen-calcium phosphate composites. *J. Eng. Med.*, **212**, 413–425. Proceedings of the Institution of Mechanical Engineers, Part H

457. Tencer, A.F. (2006) Biomechanics of fixation and fractures. Chapter 1, in *Rockwood and Green's Fractures in Adults*, 6th edn (eds. R.W. Bucholz, J.D. Heckman, C. Court-Brown, P. Tornetta III, K.J. Koval, and M.A. Wirth), Lippincott Williams & Wilkins, p. 2710.

458. Matsuda, T., Miwa, H., Moghaddam, M.J., and Iida, F. (1993) Newly designed tissue adhesion prevention technology based on photocurable mucopolysaccharides In vivo evaluation. *ASAIO Trans.*, **39**, M327–M331.

459. Caves, J.M., Kumar, V.A., Martinez, A.W., Kim, J., Ripberger, C.M., Haller, C.A., and Chaikof, E.L. (2010) The use of microfiber composites of elastin-like protein matrix reinforced with synthetic collagen in the design of vascular grafts. *Biomaterials*, **31**, 7175–7182.

460. M. Waki, K. Miyamoto (2000) Photocured cross-linked-hyaluronic acid gel and method of preparation thereof. US Patent 6,031,017.

461. Kuroyanagi, Y., Kim, E., and Shioya, N. (1991) Evaluation of synthetic wound dressing capable of releasing silver sulfadiazine. *J. Burn Care Rehabil.*, **12**, 106.313.

462. Koide, M., Osaki, K., Konishi, J., Oyamada, K., Katamura, T., and Takahasi, A. (1993) A new type of biomaterial for artificial skin: dehydrothermally crosslinked composites of fibrillar and denatured collagens. *Biomed. Mater.Res.*, **27**, 79.

463. Gebelein, C.G. and Carraher, C.E. (1985) *Polymeric Materials in Medication*, Plenum Press, New York, p. 321.

464. Ensuminger, W.D. and Selam, J.L. (1987) *Infusion Systems in Medicine*, Futura, New York.

465. Dubois, P. (1978) *Plastics in Agriculture*, Applied Science Publishers, London.

466. L. Zhu and W. Xu (2010) Artificial blood vessels,10.1002/spepro.003010 c , *Society of Plastics Engineers (SPE)*.

467. Liu, Y., Griffith, M., Watsky, M.A., Forrester, J.V., Kuffova, L., Grant, D., Merrett, K., and Carlsson, D.J. (2006) Properties of porcine and recombinant human collagen matrices for optically clear. *Tissue Eng. Appl. Biomacromolecules*, **7**, 1819–1828.

468. Klemm, D., Schumann, D., Udhardt, U., and Marsch, S. (2001) Bacterial synthesized cellulose – artificial blood vessels for microsurgery. *Prog. Polym. Sci.*, **26**, 1561–1603.

469. Potts, J.E. (1984) in *Kirk-Othmer Encyclopedia of Chemical Technology* (ed. M. Grayson), Wiley-Interscience, p. 626Suppl. Vol.

470. Kalia, S. and Avérous, L. (eds.) (2011) *Biopolymers: Biomedical and Environmental Applications*, John Wiley & Sons, Ltd, Chichester.

471. Shasha, B.S., Trimnell, D., and Otey, F.H. (1981) Encapsulation of pesticides in a starch-calcium adduct. *J. Polym. Sci., Polym. Chem. Ed.*, 19.

472. Scheiber, M.M. and White, M.D. (1980) Granule structure and rate of release with starch encapsulated thiocarbamates. *Weed Sci.*, **28**, 685.

473. McCormick, C.L. and Lichatowhich, D.K. (1979) Homogeneous solution reactions of cellulose, chitin and other polysaccharides to produce controlled

activity pesticide systems. *J.Polym. Sci.*, **17**, 479.347.

474. Jipa, I.M., Stoica-Guzun, A., and Stroescu, M. (2012) Controlled release of sorbic acid from bacterial cellulose based mono and multilayer antimicrobial films. *Food Sci. Technol.*, **47** (2), 400–406.

475. Paul, D.R (1976) Controlled release polymeric formulations. American Chemical Society Symposium Series No. 33. ACS, DC, p. 2

476. Mi, F.L., Tseng, Y.C., Chen, C.T., and Shyu, S.S. (1997) Preparation and release properties of biodegradable chitin microcapsules: II. Sustained release of 6-mercaptopurine from chitin microcapsules. *J. Microencapsul.*, **14** (2), 211–223.

477. Kemp, M.V. and Wightman, J.P. (1981) Interaction of 2,4-D and dicamba with chitan and chitosan: virginia. *J. Sci.*, **32**, 34.

478. Kydonieus, A.F. (ed.) (1980) *Controlled Release Technologies: Methods, Theory and Applications*, Vol. **I and II**, CRC Press, Boca Raton, FL.

479. Baumley, J.J. and IInicki, R.D. (eds.) (1981) *Combinations of flowable lignin and metribuzin for weed control in soya beans*, Proc. Annual Meeting, Northeast Weed Science Society, MD, p. 52.

480. 1981) *Chemical Economics Handbook*, SRI International, Stanford, CA, p. 8001.

481. Hauck, R.D. and Koshino, M. (1971) *Fertilizer Technology and Use*, 2nd edn, Soil Science of America, Madison.

482. Potts, J.E., Cleudinning, R.A., Ackart, W.B., and Niegich, W.D. (1973) *Polymer and Ecological Problems*, Plenum Press, New York, p. 61.

483. Boggs, W. (1959) Method of preparing polyurethane starch reaction products and product thereof. US Patent 2,908,657, filed Oct. 13, 1959.

484. Schmitt, E.E and Polistina, R.A. Surgical sutures. US Patent 3 297 033.

485. Schmitt, E. E., Epstein, M. and Polistina, R.A.. Process for polymerizing a glycolide. US Patent 3 422 871.

486. Lu tke-Eversloh, T., Fischer, A., Remminghorst, U., Kawada, J., Marchessault, R.H., Bogershausen, A., Kalwei, M., Eckert, H., Reichelt, R., Liu, S.J., and Steinbuchel, A. (2002) Biosynthesis of novel thermoplastic polythioesters by engineered Escherichia coli. *Nat. Mater.*, **1**, 236–240.

487. Doi, Y. (2002) Unnatural biopolymers. *Nat. Mater.*, **1**, 207–208.

488. Steinbuchel, A. (2005) Non-biodegradable biopolymers from renewable sources: perspectives and impacts. *Curr. Opin. Biotechnol.*, **16**, 607–613.

489. Fischer, F. (2002) 3-mercaptopropionic acid. *Synlett*, **8**, 1368.

490. Yoch, D.C. (2002) Dimethylsulfoniopropionate: its sources, role in the marine food web, and biological degradation to dimethylsulfide *Appl. Environ. Microbiol.*, **68**, 5804.

491. Elbanna, K., Lutke-Eversloh, T., Jendrossek, D., Luftmann, H., and Steinbuchel, A. (2004) Studies on the biodegradability of polymers of polythioester copolymers and homopolymers by polyhydroxyalkanoate (PHA)-degrading bacteria and PHA depolymerase. *Arch. Microbiol.*, **182**, 212.

492. Young Kim, D., Lutke-Eversloh, T., Elbanna, K., Thakor, N., and Steinbuchel, A. (2005) Poly(3-mercaptopropionate) : a nonbiodegradable biopolymer? *Biomacromolecules*, **6**, 897–901.

493. Liu, S.J., Lütke-Eversloh, T., and Steinbüchel, A. (2003) Biosynthesis of poly (3-mercaptopropionate) and poly (3-mercaptopropionate-co-3-hydroxybutyrate) with recombinant Escherichia coli. *Sheng Wu Gong Cheng Xue Bao*, **19** (2), 195–199.

494. Chua, H., Yu, P.H.F., and Ma, C.K. (1999) Accumulation of biopolymers in activated sludge biomass. *Appl. Biochem. Biotechnol.*, **78** (1-3), 389–399.

495. Chen, G. and Patel, M.K. (2012) Plastics derived from biological sources: present and future: a technical and environmental review. *Chem. Rev.*, **112**, 2082–2099.

3
Preparation, Microstructure, and Properties of Biofibers

Takashi Nishino

3.1
Introduction

Composite materials, typically glass fibers or carbon fibers embedded into epoxy resin or unsaturated polyester, show excellent mechanical and thermal properties; thus, they are widely used in various applications ranging from aerospace to vehicles to sports utensils [1]. However, these advantages cause environmental problems when disposing by incineration. Consequently, there are growing demands for environmentally friendly composites [2, 3]. A paradigm shift from energy-consuming materials to sustainable materials has brought forth the increasing importance of biomass utilization. Biofibers are among the most keenly sought after materials of the twenty-first century.

Table 3.1 summarizes kinds and origins of biomass resources that are originally obtained as fiber-shaped or bio-based materials that are spinnable into fiber. The fiber shape is significant for these materials. For example, DNA bears a function that rules the genetic code along the chain. Hair is useful to protect against the cold and for repelling water. The former function is based on the warm air preserved among the fibers. The latter is produced by the Cassie-type rough surface with random stacking of the fibers [4]. Entangled fibrin fibers are useful in stopping bleeding. Polyethylene (PE) is well known as a *typical oil-based material*; however, its industrial production from starch through bioethanol, followed by spinnability into fiber has been demonstrated recently.

In this chapter, among many biofibers, the microstructure and properties of plant-based fibers will be mainly described in comparison with other fibers. In addition, *all*-cellulose composites and nanocomposites will be discussed to show how they utilize the excellent intrinsic properties of cellulose.

Polymer Composite: Volume 3, First Edition.
Edited by Sabu Thomas, Kuruvilla Joseph, S. K. Malhotra, Koichi Goda and M. S. Sreekala.

Table 3.1 Biomass resources originally obtained as fiber shape or bio-based materials.

Species	Origins
Polysaccharides	
Cellulose	Plant stalk, leaf, branch, and seed
Starch	Plant root, seed
Chitin, chitosan	Crab, lobster, insect shell, mushroom
Protein	
Fibroin	Silkworm, spider
Keratin	Animal/bird hair, nail, skin
Actin, myosin	Muscle
Collagen, elastin	Tendon, skin, bone
Fibrin	Blood
Bionylon	
Nylon 11, Nylon 410	Natto, ricinus
Poly-γ-glutamic acid	
Nucleic acid	
DNA, RNA	Cell
Biopolyesters	
Polyhydroxyalkanoates	Microorganism
Polylactic acid	Starch
Biopolyolefins	
Biopolyethylene	Starch

3.2 Structure of Natural Plant Fibers

3.2.1 Microstructure

Natural plant fibers exist as hairs (cotton, kapok, and baobab), bast fibers (also called *soft fibers*; kenaf, ramie, flax, hemp, jute, papyrus, cordial, and Indian mallow), hard fibers (sisal, abaca (manila hemp), raffia, pineapple, and New Zealand flax), stem (bamboo, bagasse, banana stalk, and cork stalk), fruit (coconut), straw (rice, corn, and wheat), and others (seaweeds, palm). Among them, we focus here on kenaf. Kenaf, *Hibiscus cannabinus* L., family Malvaceae, is well known as a *cellulosic source* with economical and ecological advantages: within 3 months of sowing the seeds, it can grow under a wide range of weather conditions to a height of more than 3 m and a base diameter of 3–5 cm. The growing speed may reach 10 cm day^{-1} under optimum ambient conditions [5]. The stem is unbranched and straight and is composed of an outer layer (bark) and a core as shown in Figure 3.1. The optical micrograph, a scanning electron micrograph (SEM), and chemical contents of the cross-section of the interface between the bark part and the core part of the kenaf stem are seen. The bark constitutes 30–40% of the dry weight of the stem and

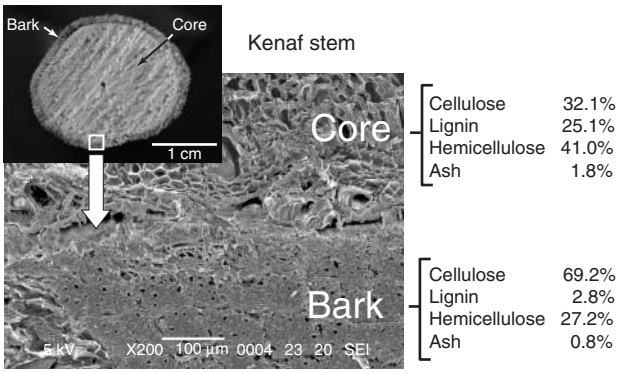

Figure 3.1 Optical and scanning electron micrographs and chemical contents of the cross-section of the interface between the bark and the core of a kenaf stem.

shows dense structure. On the contrary, the core is woodlike, and makes up the remaining 60–70% of the stem. It is easy to separate the stem into the bark and the core by chemical and/or enzymatic retting [6].

A single fiber of kenaf, which is well known to involve hierarchy microstructures with different levels down to nano sizes, is visible to the human eye.

Figure 3.2 shows the structural hierarchy of natural plant fiber. By grinding the bark, its cell wall can be separated individually. The cell wall consists of a hollow tube, which has four different layers: one primary cell wall and three secondary cell walls and a lumen. The lumen is an open channel in the center of the cell wall. Each layer is composed of cellulose microfibrils embedded in a matrix of hemicelluloses and lignin, so its structure is analogous to that of artificial fiber-reinforced composites. Hemicellulose is made up of highly branched polysaccharides including glucose, mannose, galactose, xylose, and so on. Lignin is made up of aliphatic and aromatic hydrocarbon polymers positioned around the fibers. Their composition in the bark is different from that in the core as shown

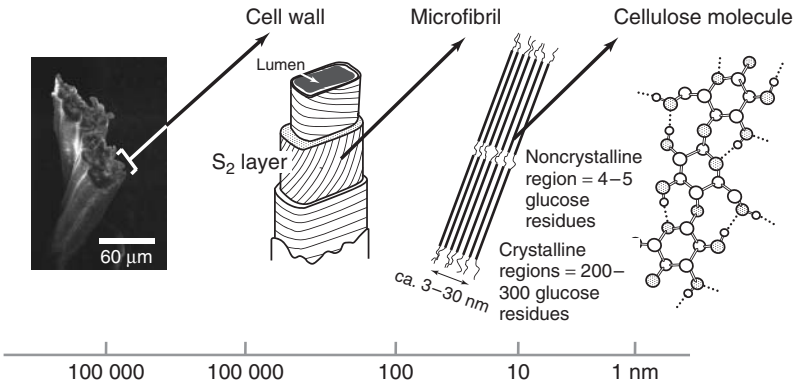

Figure 3.2 Structural hierarchy of natural plant fiber down to molecular level.

in Figure 3.1 [7]. As is usual for plant fibers, hemicellulose and lignin are easily removed by using alkali (NaOH/KOH) and $NaClO_2$, respectively.

The primary (outer) cell wall is usually very thin (<1 μm). Among the three secondary cell walls, the S_2 layer is the thickest and determines (>80%) the overall properties. The S_2 layer is formed of microfibrils, which contain large quantities of cellulose molecules. The microfibrils run fairly parallel to each other and follow a steep helix around the cell [8, 9]. Furthermore, the microfibrils are composed of alternate crystalline and amorphous regions. The size of a crystallite is about 5–30 nm in the lateral direction and up to 20–60 nm along the axis [10]. Therefore, the cellulose molecules pass through several crystallites along the axis. This structure is called a *fringed micelle structure*. This is the classic structural model and may become outdated when chain folding for synthetic polymers is found. For now, however, it is still believed to be valid for cellulose.

There are several top-down approaches to isolate cellulose microfiber from the plant cell wall. These include acid hydrolysis [11], homogenizing [12, 13], grinding [14], enzymatic hydrolysis [15], and 2,2,6,6-tetramethylpiperidine-1-oxyl radical (TEMPO)-mediated oxidation [16]. Of these, the grinding method is described here.

Figure 3.3 shows a schematic illustration of an apparatus for grinding. The aqueous suspension of breached kenaf bark fibers is introduced into the upper part of the apparatus, then the suspension is sheared between a pair of circular stones (of diameter 145 mm), one of which is rotated at high speed (1500 rpm). After grinding, the suspension, which has a cream-like texture, is poured out from the apparatus.

Figure 3.4 shows (a) the optical micrographs of as-breached bark fiber and (b) field emission FE-SEM image of kenaf nanofiber obtained by grinding. By passing the suspension through the grinder once, the bark fiber can be downsized into

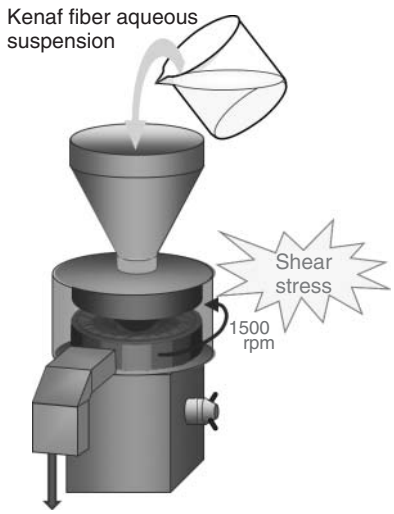

Figure 3.3 Schematic illustration of an apparatus for grinding.

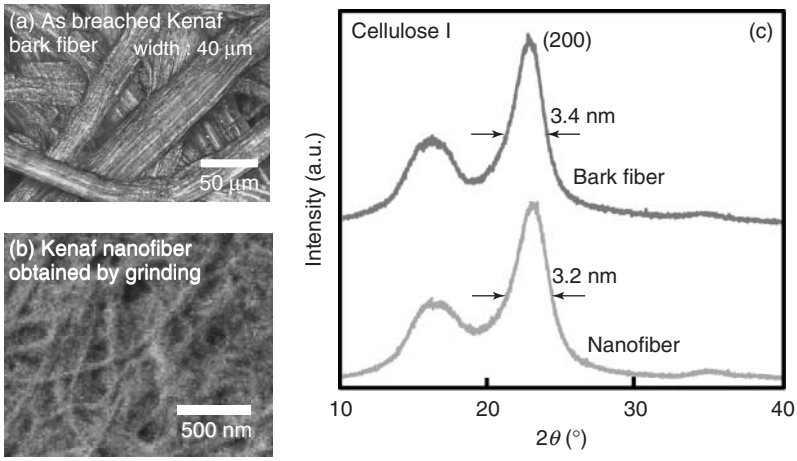

Figure 3.4 Optical micrographs of (a) as-breached bark fiber and (b) FE-SEM image of nanofiber obtained by grinding kenaf bark fiber. (c) X-ray diffraction profiles of bark fiber and nanofiber of kenaf bark.

nanofiber with a diameter of several tens of nanometers. This nanofiber almost corresponds to the microfibril shown in Figure 3.2. The crystal modification of kenaf belongs to cellulose I as is usual for plant fiber. After grinding, the crystal modification, labeled cellulose I, and the crystallite size remain almost unchanged.

Figure 3.5 shows the FE-SEM micrographs of cellulose nanofiber obtained by grinding various resources, such as bamboo, apple, coffee, and green tea residues.

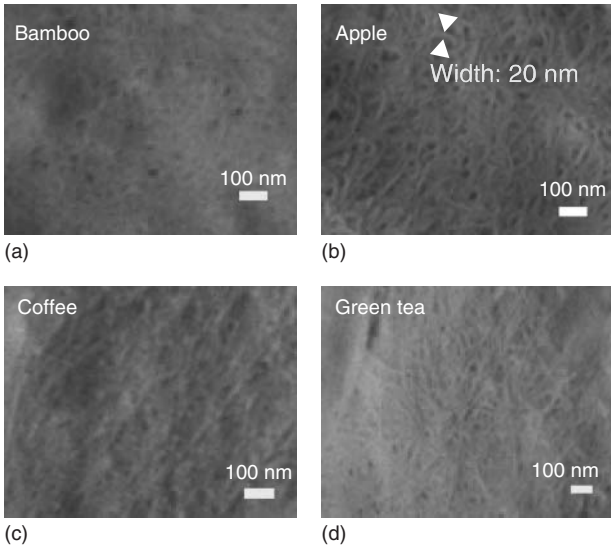

Figure 3.5 FE-SEM micrographs of cellulose nanofiber obtained by grinding from various resources: (a) bamboo, (b) apple, (c) coffee, and (d) green tea residues.

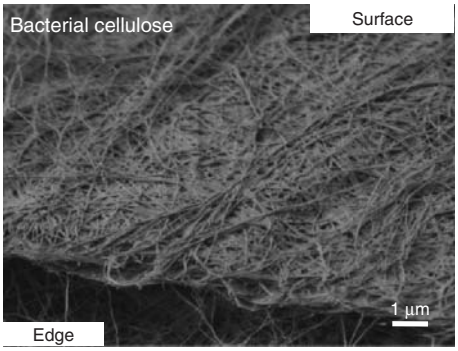

Figure 3.6 FE-SEM micrograph of bacterial cellulose.

In every case, nanofiber with a diameter of 20 nm was obtained, even after roasting of coffee beans. The annual production of 4.83 million tons of tea and 8.26 million tons of coffee in 2009 were considered waste after their use. Developments to find ways of utilizing these wastes are gaining importance and making nanofibers from them is one of the options. Electrospinning [17] of cellulose solution to get regenerated cellulose nanofiber is also reported.

Figure 3.6 shows the FE-SEM micrograph of bacterial cellulose (BC), better known as *nata de coco*, familiar as a dessert. Besides being the cell-wall component of plants, BC is also secreted extracellularly as synthesized cellulose fibers by some bacterial species, such as *Acetobacter xylinum* [18]. BC presents a unique network structure of a random assembly of ribbon-shaped nanofibers. The microfibrils extruded from bacterial cell are bundled together, forming nanofibers with naturally rectangular cross sections of dimensions of roughly 3–4 nm (thickness) × 70–130 nm (width).

3.2.2
Crystal Structure

Cellulose is a natural linear homopolymer (polysaccharide), in which D-glucopyranose rings are connected to each other with β-(1 → 4)-glycoside linkages as shown in Scheme 3.1. The degree of polymerization is 500–10 000 for natural cellulose, and 200–800 for the regenerated one. Cellulose is a crystalline polymer

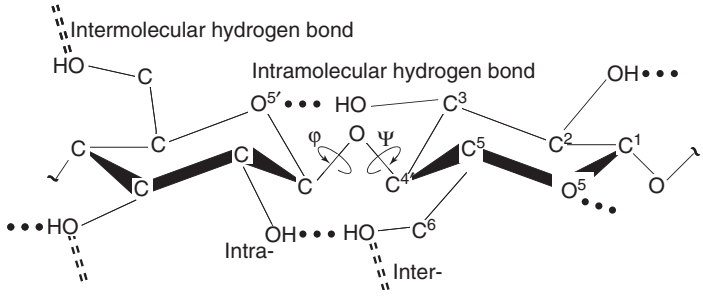

Scheme 3.1 Chemical structure of cellulose.

and there are several crystal modifications. Cellulose I, which is obtained from natural plants and woods, is the most popular of these. There have been many arguments on the crystal structure of cellulose for more than 70 years, even though cellulose is one of the most important and popular polymers. Recently, it has been clarified and concluded that cellulose I can be further divided into two crystalline modifications: the so-called cellulose I_α (triclinic) and cellulose I_β (monoclinic) [19, 20]. Natural products are a mixture of these two modifications. Cellulose I_β is dominant in plants and wood, and the percentage of cellulose present varies depending on the species and the treatments. For example, the cellulose I_β content of cotton linter and ramie is 77%. Cellulose I_α transformed into cellulose I_β by a hydrothermal treatment in an alkali solution or by heat treatment at 280 °C in an inert gas. For example, Horii et al. reported that cellulose I_β content increases to 90% by heat treatment at 260 °C in 0.1 M NaOH aqueous solution [21]. This indicates that cellulose I_β is thermodynamically more stable than cellulose I_α. Almost pure cellulose I_β is obtained from tunicates (*Halocynthia roretzi*). Cellulose I_α is reported to be the major component of bacterial and algal cellulose. The structural difference between I_α and I_β is said to be brought about by shear stress during biosynthesis of cellulose microfibrils.

Cellulose II can be obtained by swelling cellulose I samples with alkali (known as *mercerization*: typically, 21.5% NaOH aq. solution at 20 °C for 24 h) or by regeneration from cellulose solutions into precipitates, which is the typical process for the technical spinning of man-made cellulose fibers.

Cellulose III_I and III_{II} are converted from the corresponding cellulose I and II by immersing them in liquid ammonia (−78 °C). The unit cells for both crystalline structures resemble each other, but the meridional reflections especially differ in X-ray investigations. However, the molecules in these two structures pack in quite different manners: parallel arrangements in III_I and antiparallel ones in III_{II}; this is concluded from the fact that III_I and III_{II} can easily be returned to

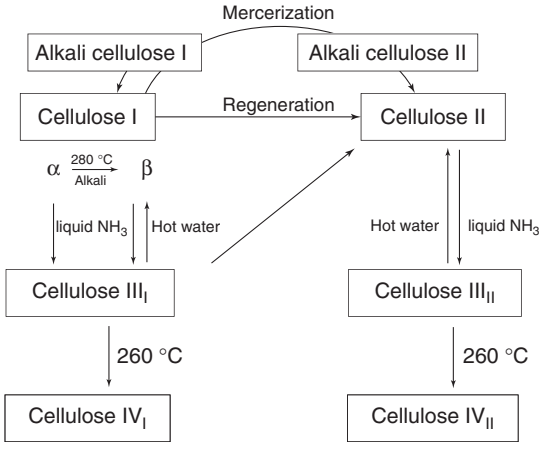

Figure 3.7 Crystal transformation map of a series of celluloses.

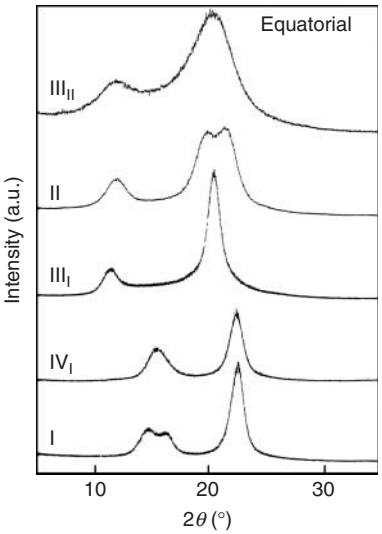

Figure 3.8 Equatorial X-ray diffraction profiles of cellulose polymorphs.

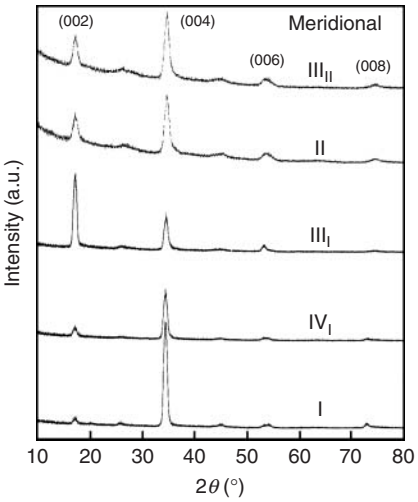

Figure 3.9 Meridional X-ray diffraction profiles of cellulose polymorphs.

their original form (parallel packed I or antiparallel packed II) by boiling water treatment.

Cellulose IV_{II} is obtained by annealing cellulose III_{II} at high temperature (260 °C). The crystal transformation map of a series of cellulose is summarized in Figure 3.7.

Figure 3.8 and Figure 3.9 show the equatorial and meridional X-ray diffraction profiles of cellulose polymorphs [22]. These modifications are said to have the same skeletal conformation as cellulose I; that is, a fairly extended zigzag conformation. However, the chain packing, chain stacking, chain direction, and intra/inter hydrogen bonds are different from one another, which is reflected in the diffraction profiles.

Table 3.2 Unit cell parameters of cellulose polymorphs.

	a	*b*	*c*	*α*	*β*	*γ*
		(nm)			(°)	
I_α	0.672	0.596	1.010	118	115	80.4
I_β	0.778	0.820	1.038	90	90	96.5
II	0.709	0.922	1.030	90	90	118.3
III_I	1.025	0.778	1.034	90	90	122.4
III_I	0.997	0.765	1.024	90	90	120.1
IV_I	0.803	0.813	1.034	90	90	90
IV_{II}	0.799	0.810	1.034	90	90	90

Table 3.2 summarizes the unit cell parameters of cellulose polymorphs. These parameters are well defined for the cellulose I series [20, 23]. However, those of the cellulose II series vary largely depending on the origins and treatment conditions.

3.3 Ultimate Properties of Natural Fibers

3.3.1 Elastic Modulus

The elastic modulus of a polymer crystal provides us with important information on the molecular conformation in the crystal lattice [24]. The elastic modulus (crystal modulus) of the crystalline regions in the direction parallel to the chain axis has been measured for a variety of polymers by X-ray diffraction [25]. Examination of the data so far accumulated enables us to relate the crystal modulus, namely, the extensivity of a polymer molecule, both to the molecular conformation and the mechanism of deformation in the crystal lattice. Furthermore, knowledge of the crystal modulus is of interest in connection with the mechanical properties of the polymer, because the crystal modulus gives the maximum attainable modulus for the specimen modulus of a polymer.

The initial slope of the stress–strain curve of the crystalline regions gives the crystal modulus, when the changes in the crystal lattice spacing under a constant stress are monitored by X-ray diffraction.

Figure 3.10 shows the stress–strain curves of the crystalline regions of cellulose I (open circles) and cellulose II (filled circles) [22]. The vertical axis directly corresponds to the extension of the cellulose chain by a tensile stress, which shows a linear function with the stress through the origin. By assuming that the stress on the crystalline regions is equal to that on the whole specimen, the inclination

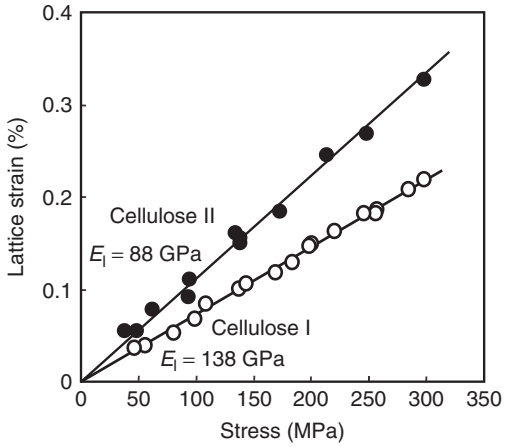

Figure 3.10 Stress–strain curves of the crystalline regions of cellulose I (open circles) and cellulose II (filled circles).

gave the crystal modulus of 138 GPa for cellulose I and 88 GPa for cellulose II. This assumption of homogeneous stress distribution has been proved to be valid for many polymers including cellulose [22, 26].

Table 3.3 shows the crystal modulus E_l, cross-sectional area S, of one molecule in the crystal lattice, f-value, and the fiber identity period (FIP) of natural fibers together with those of PE [26] and poly(*p*-phenylene terephthalamide) (PPTA, known by its commercial names Kevlar® and Twaron®, respectively [27]. The *f-value* is defined as the force needed to stretch one molecule by 1%, and could be calculated using the E_l and the S values. The E_l value of cellulose I is relatively smaller than that of PE. However, when a comparison is made based of the f-values, the f-value (4.40×10^{-10} N) of cellulose I is almost equal to or even larger than that of PE (4.28×10^{-10} N). This indicates that the extensivity of the cellulose I molecule itself is intrinsically the same as that of PE, and that the lower E_l value of cellulose I is attributed to its large S value. As shown in Scheme 3.1, the main chains are linked by intra- and intermolecular hydrogen bonds. There are two series of intramolecular hydrogen bonds: O(6′)–O(2) and O(3′)–O(5). On the basis of Northolt's calculation [28], the crystal modulus decreases drastically from 136 to 89 GPa because of the lack of O(6′)–O(2) hydrogen bonds. In contrast, Tashiro and Kobayashi [29] emphasize the importance of O(3′)–O(5) hydrogen bonds on the other side, and report that the crystal modulus decreased when hydrogen bonds vanish. Thus, the lack of intramolecular hydrogen bonds decreases the crystal modulus, and the skeleton of cellulose is not difficult to elongate in their axial direction intrinsically without intramolecular hydrogen bonds. This is manifested by the crystal moduli of cellulose trimesters (which can be synthesized by esterification of the three hydroxyl groups in the glucopyranose ring of cellulose with corresponding *n*-aliphatic acid), which are smaller than those of cellulose I. The small crystal moduli for cellulose trimesters could be explained by the lack of

Table 3.3 Crystal modulus E_1, cross-sectional area S, of one molecule in the crystal lattice, f-value, and the fiber identity period (FIP) of natural fibers together with those of polyethylene and poly(*p*-phenylene terephthalamide).

	E_1 (GPa)	S (10^{-2} nm^2)	f (10^{-10} N)	FIP (nm)
Cellulose				
I	138	31.9	4.40	1.038
II	88	32.5	2.86	1.033
III_I	87	33.9	2.95	1.034
III_{II}	58	33.4	1.94	1.024
IV_I	75	32.7	2.45	1.037
Cellulose triesters				
Acetate CTA	33.2	71.1	2.24	1.054
Propionate CTP	21.6	86.5	1.86	1.508
Butyrate CTB	17.6	97.0	1.71	1.030
Valerate CTV	17.9	113	2.03	1.043
α-Chitin	41	44.8	1.83	1.032
Chitosan	65	34.0	2.27	1.021
Silk fibroin				
Bombyx mori	23	21.7	0.50	0.697
Wild	20	25.0	0.50	0.695
Polyethylene	235	18.2	4.28	0.253
PPTA	156	20.2	3.16	1.290

intramolecular hydrogen bonds, together with large S [30]. The crystal moduli of other cellulose polymorphs (II, III_I, III_{II}, and IV_I) are smaller than that of cellulose I. These can be explained by the chain contraction in the crystal lattice.

Figure 3.11 shows the relationship between the f-value and the FIP for a series of cellulose polymorphs (open circles) and cellulose trimesters (filled circles), chitin, and chitosan. Using the f-values, instead of the E_1 value, the extensivity of the chain molecules can be directly compared to one another. The almost constant f-values for cellulose trimesters indicate that the chain contraction does not affect the f-value very much. On the contrary, hydrogen bonds play an important role, judging from the difference between the crystal moduli of these polysaccharides. The effect of the hydrogen bonds seems to be diminished for the contracted chains. The f-value decreased drastically with the chain contraction for cellulose polymorphs. This contraction is thought to be associated with the internal rotation around the main chain ether linkage between the glucopyranose rings (see φ and ψ in Scheme 3.1), which also affect the intramolecular hydrogen bonds. It is well known that the vibrational frequency of intramolecular hydrogen bonding changes depending on the crystal modifications. The crystal moduli of chitin and chitosan are low for the same reason [31]. Accordingly, the skeletal conformation and/or intramolecular hydrogen bonds change with the crystal transformation, and these

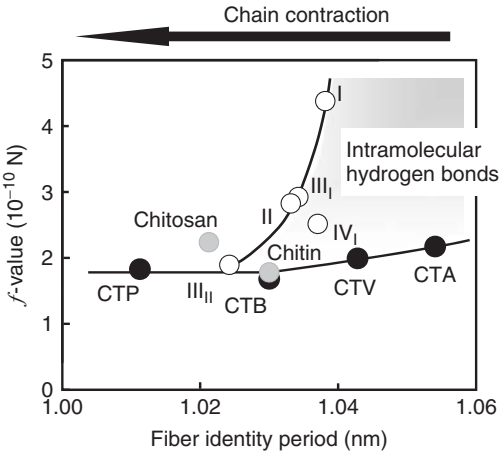

Figure 3.11 Relationship between the f-value and the FIP for a series of cellulose polymorphs (open circles) and cellulose trimesters (filled circles), chitin, and chitosan.

modifications are completely different from each other from the mechanical point of view.

Figure 3.12 shows the relationship between the crystal modulus E_1 and the maximum attained specimen modulus Y_{max} of various natural and synthetic polymers so far reported in the literature [24]. The crystal modulus (478 GPa) and Y_{max} (350 GPa) values of poly(*p*-phenylene benzobisoxazole) (PBO, commercialized with the trade name of Zylon®) are extremely high, about half of the elastic modulus (1000 GPa) of diamond [32]. Apart from them, the crystal moduli of so-called high performance polymers such as PPTA (156 GPa) and of liquid crystalline polyesters such as Vectran® (126 GPa) are comparable with that of cellulose I [33]. In addition, some plants possesses the Y_{max} more than 100 GPa, which is also comparable with those of high performance fibers and titanium alloy, and even higher than those of aluminum and glass fibers. It is clear from Figure 3.12 that so-called high modulus polymer cannot be obtained using isotactic polypropylene, chitin, and silk, because of their low E_1 value.

3.3.2 Tensile Strength

The ultimate tensile strength of a carbon–carbon single bond is calculated as 56.8 GPa on the basis of the Morse potential function [34]. This increases to 110 GPa for a C=C double bond. The calculated strength for diamond and graphite is 104 GPa, which is the maximum tensile strength among organic materials [35]. By applying this method to cellulose, the ultimate tensile strength of cellulose is reported to be 17.8 GPa, which is seven times higher than that of steel. The advantages of natural fibers over traditional reinforcing fibers such as glass or carbon fibers have been said to be their low cost, low density, and biodegradability,

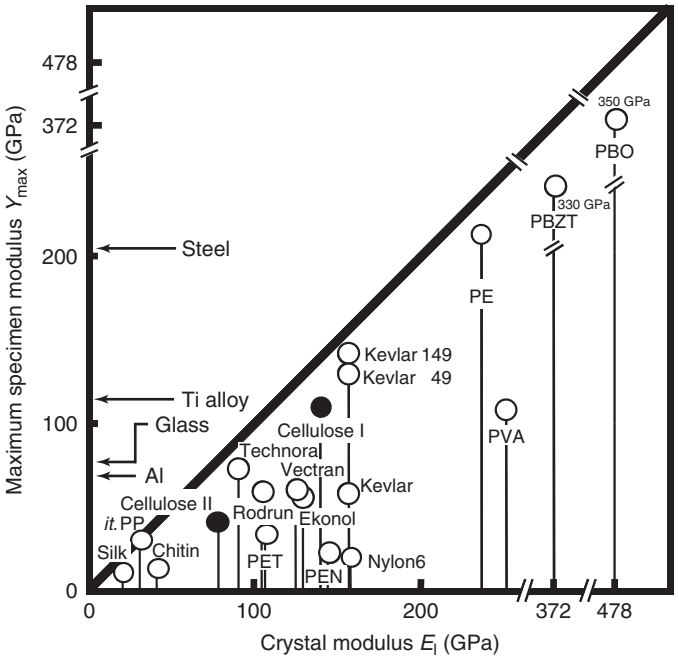

Figure 3.12 Relationship between the crystal modulus E_I and the maximum attained specimen modulus Y_{max} of various natural and synthetic polymers so far reported in the literature.

together with their high specific properties. Accordingly, the high elastic modulus and tensile strength (not specific modulus and specific strength) demonstrate that cellulose possesses a potential ability to replace glass fiber, and that it can be a good candidate for a reinforcement fiber of the composite, even without taking each density into consideration.

3.4
Mechanical and Thermal Properties of Cellulose Microfibrils and Macrofibrils

As described above, the angle between the cellulose microfibrils and the longitudinal cell axis is called the *microfibril angle*. In this spiral structure, the microfibril angle is one of the major factors in determining the mechanical properties of the macroscopic fiber [36, 37]. The average microfibril angle ranges from about 6–11 in flax to about 30 in cotton, and to more than 40 in coir and some selected leaf fibers [38].

Figure 3.13 shows the stress–strain curve of a single wood pulp fiber with different microfibril angles reported by Page and El-Hosseiny [39]. The curves show yielding followed by plastic deformation until there is breakage at 20% elongation for fibers with a high microfibril angle. On the other hand, for fibers

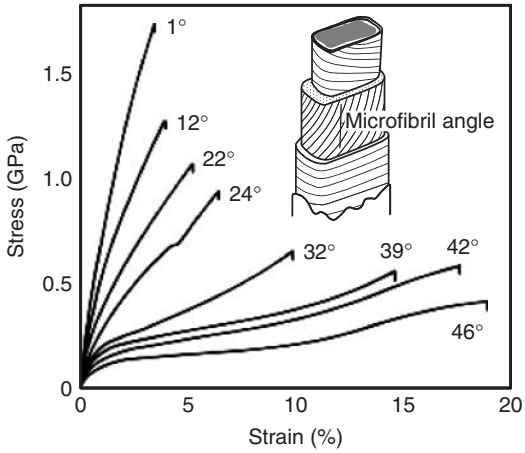

Figure 3.13 Stress–strain curves of the single wood pulp fiber with different microfibril angles.

with a low microfibril angle, the curve is steep and linear. The tensile strength and Young's modulus increased with the decrease in the microfibril angle. The tensile strength went up to 1.7 GPa and the initial inclination gave a macroscopic Young's modulus of about 90 GPa. This single fiber contains 70–80% cellulose microfibrils. Thus the macroscopic modulus for the 100% cellulose fiber can be estimated to be 113–128 GPa. Hepworth and Bruce reported a maximum elastic modulus of 130 GPa, when 1 cm^3 pieces of potato tissue were compressed [40]. Recently, Iwamoto *et al.* [41] measured the elastic modulus of a single microfibril from tunicate cellulose by a three-point bending using an atomic force microscope. Moduli from 145 to 151 GPa were obtained depending on the hydrolysis/oxidation method used to prepare the microfibrils. These values are very close to the crystal modulus of cellulose I shown above.

Figure 3.14 shows the relationship between the crystal modulus, the FIP of cellulose I, and temperature. The FIP is almost constant from room temperature up to 200 °C. This reveals that the cellulose molecule does not show any thermal expansion or contraction. This is in contrast to any other solids, including metals, polymers, and even diamond. For example, an iron crystal expands about 0.275% from 0 to 200 °C, diamond expands with a linear thermal expansion coefficient of $1.1 \times 10^{-6}\ K^{-1}$, a much larger expansion than that of the cellulose skeleton. The crystal modulus is also temperature independent, which shows that the cellulose skeleton, including intramolecular hydrogen bonds, is intrinsically thermally stable.

Figure 3.15 shows (a) Young's modulus, (b) the tensile strength, and (c) the elongation at break from numerous tensile tests on ramie single fibers. The tensile tests were performed at the initial length of 20 mm and the tensile speed of 20 mm min^{-1} at 25 °C. The fibers were dried at 120 °C prior to the tests. There is wide distribution in mechanical properties and this suggests the nonhomogeneity of natural fibers. Two measurement methods can be used to give the

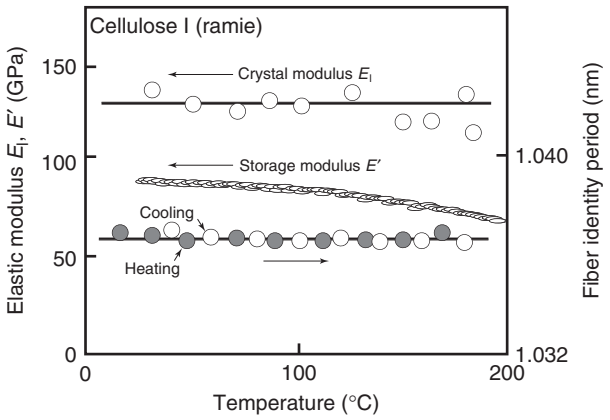

Figure 3.14 Relationship between the crystal modulus E_I, dynamic storage modulus E', the FIP of cellulose I, and temperature.

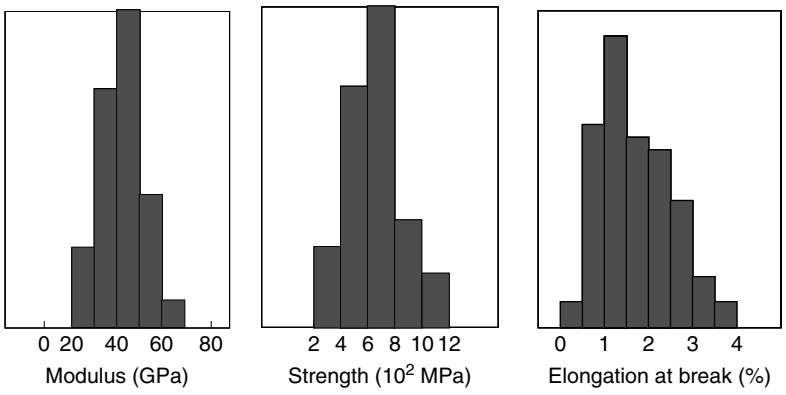

Figure 3.15 Distributions of (a) Young's modulus, (b) the tensile strength, and (c) the elongation at break from numerous tensile tests on ramie single fibers.

cross-sectional area of a single fiber: mass, length, and density can be measured (cross-sectional area = mass/(length density)) or the fiber can be directly observed using scanning electron/optical microscopy. The latter method is not adequate because of diameter fluctuation along the natural fiber, and the existence of lumen overestimating the cross-sectional area. Therefore, in order to avoid this possible cause of experimental error, the Young's modulus and the tensile strength are often expressed in terms of gram per denier (g d^{-1}) and/or gram per tex (g $dtex^{-1}$), centi N (cN $dtex^{-1}$) (one denier corresponds to the fiber fineness with 1 g of fiber per 9000 m length, and one decitex corresponds to the fiber fineness with 1 g of fiber per 10 000 m length). Many efforts have been made to obtain high modulus/high strength viscose rayon and cuprammonium rayon. Polynosic fiber is a kind of viscose rayon with a Young's modulus of 14 GPa and a tensile strength of 5 g d^{-1} [42]. Recently, a Young's modulus of 45 GPa and a strength of 1.3 GPa

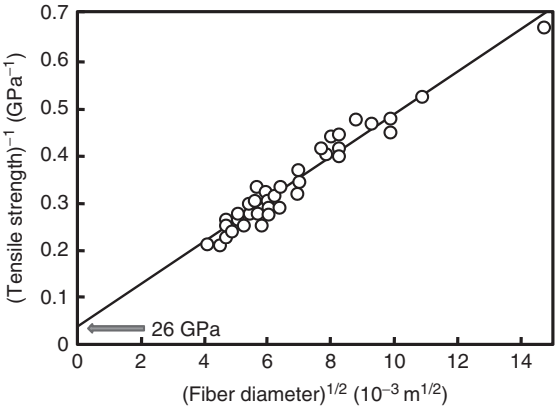

Figure 3.16 Relationship between the square root of fiber diameter and the inverse of the tensile strength, the so-called Pennings' plot, of gel-spun polyethylene fiber.

is reported for the fiber spun from an anisotropic phosphoric acid solution [43]. These values are relatively higher for regenerated cellulose fiber. However, the crystal modulus of cellulose II is intrinsically lower than that of cellulose I, which limits the production of ultrahigh modulus-regenerated cellulose fiber.

Figure 3.16 shows the relationship between the square root of fiber diameter and the inverse of the tensile strength, so-called Pennings' plot, for gel-spun PE fiber [44]. Penning assumed that the fiber fracture occurs through a crack, initiated by some defect (such as a kink band) on the fiber surface, that propagates the inside defects with fibrillation. The extrapolation to zero diameter gave the ultimate strength of 26 GPa, which is almost equal to the ultimate strength of PE (25–35 GPa) [35]. This reveals that the decrease of fiber diameter reduces the number of defects on the surface, which results in the increase of the strength to the ultimate one.

Figure 3.17 shows the stress–strain curve of kenaf microfiber and nanofiber sheets. The microfiber sheet corresponds to normal paper, which shows relatively low modulus and low strength. On the contrary, modulus and strength increases significantly for the nanofiber sheet. Besides kenaf, the stress–strain curve of cellulose nanofibrils from wood pulp by subjecting dilute wood fiber suspensions to high shear forces is shown in Figure 3.18 [45]. P_v indicates the viscosity average degree of polymerization. The curve is linear at the initial stage, followed by yielding at a stress of around 90 MPa. After that, a second linear increase in the curve stopped at a stress of 214 MPa and strain of 10.1%. Large dependence of the tensile strength on the molecular weight was observed. This curve indicates that cellulose nanofibrils in the network fracture in the second linear region; however, the large strain at break cannot be explained only by irreversible tensile deformation of the nanofibrils themselves. Instead, one may speculate that the plastic region is associated with interfibril debonding, nanofibril bending and plasticity, nanofibril slippage, and, ultimately, nanofibril tensile fracture. The work to fracture, corresponding to the area between the horizontal axis and the

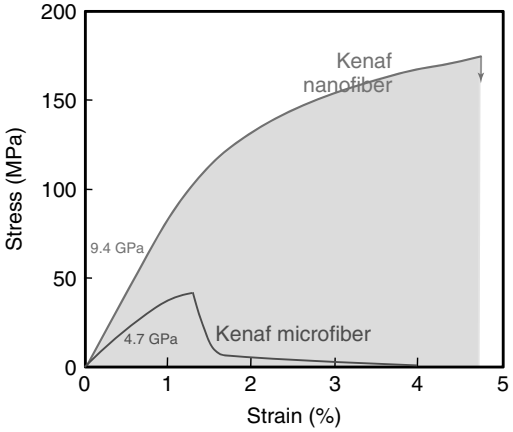

Figure 3.17 Stress–strain curves of kenaf microfiber and nanofiber.

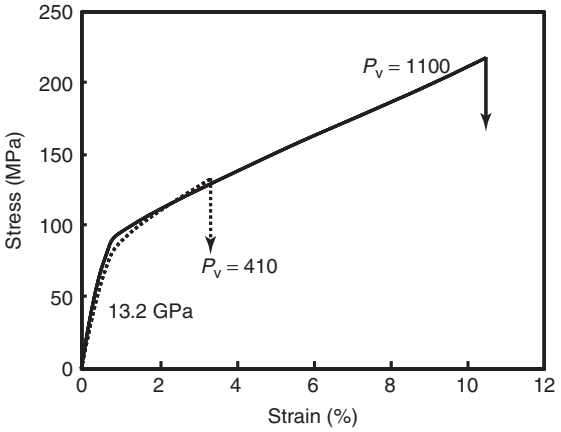

Figure 3.18 Stress–strain curve of cellulose nanopaper from wood pulp with different viscosity average degree of polymerization P_v.

stress–strain curve, reached a very large value of 15.1 MJ m^{-3} for the sheet with $P_v = 1100$. Berglund named this tough sheet, which is much tougher than cast iron, as *cellulose nanopaper*.

Table 3.4 summarizes the expected changes of structure and properties when fiber diameter is downsized to nanometer size, then applied to the composite, and so on. Nanofibers can be useful not only for composites but also for membranes, scaffolds, and so on.

Although the simultaneous attainment of both high strength and high toughness is strongly required for most structural materials, unfortunately, these are generally mutually exclusive. For high toughness, protein fibers are useful. Silk fibroin is a natural protein fibers, best known as *Bombyx mori*, which is obtained from the cocoons of the larvae of the mulberry silkworm. Normal silk fiber possesses

Table 3.4 Expected changes of structure and properties when fiber diameter is downsized to nanometers and then applied to the composite.

Specific surface area $\propto 1/d$	Increase	$\Rightarrow$ Increase; interfacial interaction Since the unit of interfacial energy is joules per square meter
Interfiber distance	Decrease	$\Rightarrow$ Increase; reinforcement, and toughness Because of the confinement of crack propagation from fiber retardation
Fiber entanglement	Increase	$\Rightarrow$ Increase; reinforcement
Structural defect	Decrease	$\Rightarrow$ Increase; reinforcement Because of increase in the strength of the fiber itself
Crystallization nuclei	Increase	$\Rightarrow$ Increase; matrix crystallinity Because the fiber surface acts as a crystallization nuclei
Bending moment	Decrease	$\Rightarrow$ Increase; malleability
Light scattering	Decrease	$\Rightarrow$ Increase; optical transparency
Porosity	Increase	$\Rightarrow$ Useful; scaffold, culture medium, and catalyst support
Mean free path of gas	Increase	$\Rightarrow$ Useful; membrane Because of high flux and low pressure loss
Curvature of fiber surface	Increase	$\Rightarrow$ Change; surface structure and properties

Young's modulus of 10 GPa and tensile strength of 0.4 GPa as shown in Figure 3.19 [46]. Silk fiber also shows low hysteresis of the stress–strain curve during loading and unloading. The relatively low modulus and high mechanical reversibility are suitable for clothes. Even with low modulus/strength, high elongation at break results in more toughness. Compared to normal silk, when silk fibroin fiber was spun from cocoons compulsively with a speed of 27 m s^{-1}, modulus and strength of the forced fiber increased [47]. Here, the stress–strain curve reached that of the crystal lattice of silk fibroin (the dotted line in Figure 3.19), from which the crystal modulus E_l is estimated as 23 GPa [46]. In addition, the tensile strength is more than 1 GPa, and the elongation at break is more than 30%, which results in very high toughness for spider silk [48]. This is a reason flying cicada can be easily caught within a web of spider silk, giving the idea of utilizing these fibers in bulletproof vests.

3.5 *All*-Cellulose Composites and Nanocomposites

In general, composites are made up of two chemically different materials. The interface between the incorporated fiber and the matrix often causes problems, such as poor compatibility, insufficient stress transfer, and high water uptake. If the fiber

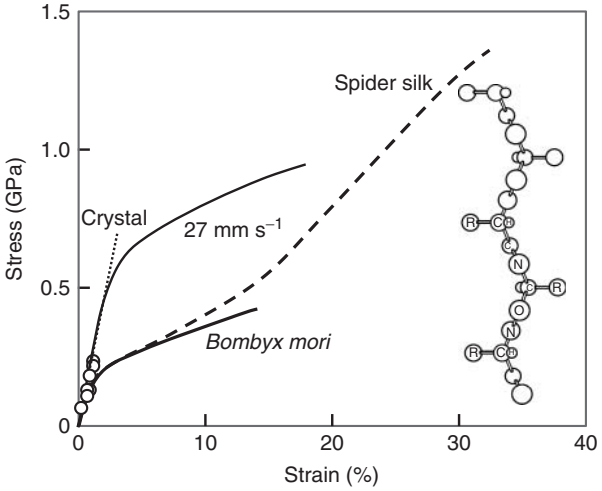

Figure 3.19 Stress–strain curves of silk fibroin. Dotted line, crystal lattice; broken line, spider silk.

and the matrix are both made of the same material, benefits such as recyclability and good adhesion through the perfect interface can be expected. A recent emerging concept of *all*-cellulose composites [49–53] and *all*-cellulose nanocomposite [54–58] within the field of macro/nano ecocomposites has received increased attention. Strong cellulose reinforcements (e.g., fibers and microcrystalline) were favorably combined with a cellulose matrix. In this way, high performance biodegradable composites can be produced from renewable resources.

Figure 3.20 shows the proposed procedures for making *all*-cellulose composites. They are (i) conventional impregnation method of the cellulose matrix into the aligned cellulose fibers [49] and (ii) selective dissolution method where the cellulose fiber skins are partially dissolved to form a matrix phase that bonds the fibers together, while the strong core fibers are retained and impart a real reinforcing effect to the composites [50]. (iii) Instead of employing the wet process using organic solvents, the cellulose fiber skins are partially esterified, which brings melt processability to the fiber surface by compression molding [59]. The range of cellulose fibers used are natural cellulosic fibers (i.e., ramie [49], kenaf, canola [55–58], and filter paper [50]), regenerated cellulose fibers such as Lyocell™ fibers as well as Bocell™ fiber spun from anisotropic phosphoric acid solution [53], together with cellulose nanofibers such as BC [52] and nanofibrillated cellulose fibers from wood [54].

Figure 3.21 shows the stress–strain curve of an *all*-cellulose composite together with those of ramie single fiber, matrix cellophane, and Mg alloy [49]. A single ramie fiber possesses a high Young's modulus (average value of 42 GPa) and high tensile strength (average value of 730 MPa). By comparison, the Young's modulus and tensile strength are lower for the *all*-cellulose composite. However, the average strength of 480 MPa for the *all*-cellulose composite was comparable or even

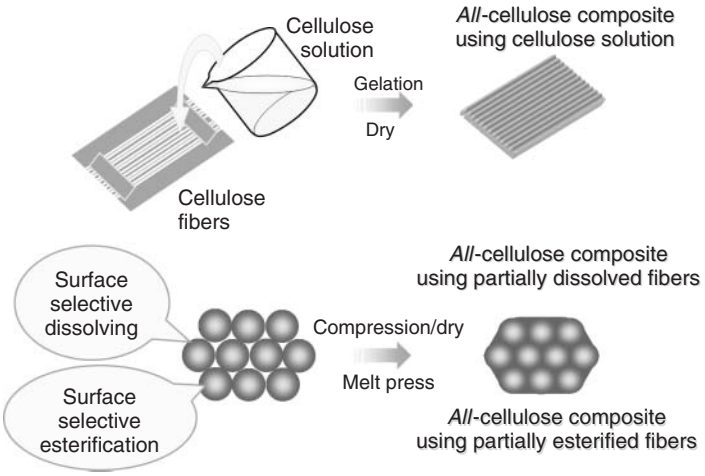

Figure 3.20 Proposed procedures for making *all*-cellulose composites.

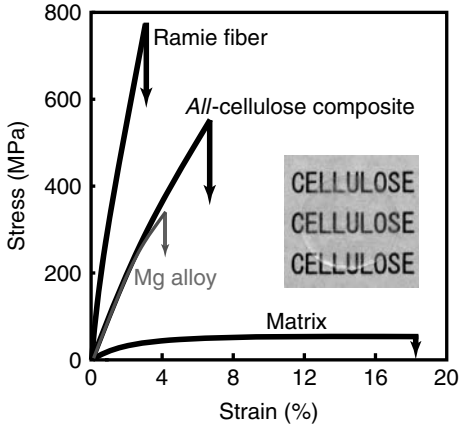

Figure 3.21 Stress–strain curve of *all*-cellulose composite together with those of ramie single fiber, matrix cellophane, and Mg alloy.

higher than that of conventional glass-fiber-reinforced composites. In addition, the modulus is comparable with that of Mg alloy, frequently used as a lightweight metal alloy for electrical devices. In addition, the *all*-cellulose composite is optically transparent because it is entirely composed of a single component (cellulose) and has an interface-free structure. The *all*-cellulose composite is entirely composed of a sustainable resource, which is biodegradable after the use and which gives it advantages with regard to disposal, composting, and incineration. It possesses excellent mechanical (high modulus/high strength), thermal (high heat resistance, low thermal expansion), and optical performance (high transparency) during use.

3.6 Conclusions

The structure and properties of biofibers, mainly of cellulose, were described in this chapter. First, the hierarchy microstructure of natural plant fiber and then a variety of crystal modifications of cellulose were mentioned. The ultimate mechanical properties (modulus of 138 GPa and strength of 17.8 GPa) and thermal properties (thermal expansion coefficient of $10^{-7}\,K^{-1}$ order) were emphasized as quite excellent for cellulosic fiber, enough for use as reinforcement in the composites. With the manifestation of these intrinsic properties in macroscopic material, the *all*-cellulose composite was shown to possess excellent mechanical properties, thermal resistance, and optical transparency, besides being composed of fully sustainable resources and hence, biodegradable. Nowadays, the interest in cellulosic nanocomposites has increased considerably [60, 61] and they are expected to be used in many fields such as electronic devices, vehicles, and windmills to replace glass and/or carbon fibers.

References

1. Hull, D. and Clyne, T.W. (1996) *An Introduction to Composite Materials*, 2nd edn, Cambridge University Press, Cambridge.
2. Baillie, C. (ed.) (2004) *Green Composites*, Woodhead Publisher, Cambridge.
3. Mohanty, A.K., Misra, M., and Drzal, L.T. (eds) (2005) *Natural Fibers, Biopolymers, and Biocomposites*, CRC Press, Boca Raton, FL.
4. Cassie, A.B.D. and Baxter, S. (1944) *Trans. Faraday Soc.*, **40**, 546.
5. Rowell, R.M. and Han, J.S. (1999) in *Kenaf Properties, Processing and Products* (eds T. Sellers and N.A. Reicher), Mississippi State University, Mississippi State, MS, p. 33.
6. Ramaswamy, G.N. (1999) in *Kenaf Properties, Processing and Products* (eds T. Sellers and N.A. Reicher), Mississippi State University, Mississippi State, MS, p. 91.
7. Inagaki, H. (2002) *High Polym.*, **51**, 597 (in Japanese).
8. Bos, H.L. and Donald, A.M. (1999) *J. Mater. Sci.*, **34**, 3029.
9. Hearle, J.W.S. (1963) *J. Appl. Polym. Sci.*, **7**, 1207.
10. Frey-Wyssling, A.V. and Muhlethaler, K. (1963) *Makromol. Chem.*, **62**, 25.
11. Ranby, B.G. (1949) *Acta Chem. Scand.*, **3**, 649.
12. Turbak, A.F., Snyder, F.W., and Sandberg, K.R. (1983) *J. Appl. Polym. Sci. Appl. Polym. Symp.*, **37**, 815.
13. Henriksson, M., Henriksson, G., Berglund, L.A., and Lindström, T. (2007) *Eur. Polym. J.*, **43**, 3434.
14. Taniguchi, T. and Okamura, K. (1998) *Polym. Int.*, **47**, 291.
15. Janardhnan, S. and Sain, M. (2006) *Bioresources*, **1**, 176.
16. Saito, T., Kimura, S., Nishiyama, Y., and Isogai, A. (2007) *Biomacromolecules*, **8**, 2485.
17. Viswanathan, G., Murugesan, S., Pushparaj, V., Nalamasu, O., and Linhardt, P.M.R.J. (2006) *Biomacromolecules*, **7**, 415.
18. Nishi, Y., Uryu, M., and Yamanaka, S. (1990) *J. Mater. Sci.*, **25**, 2997.
19. VanderHart, D.L. and Atalla, R.H. (1984) *Macromolecules*, **17**, 1465.
20. Sugiyama, J., Vuong, R., and Chanzy, H. (1991) *Macromolecules*, **24**, 4168.
21. Yamamoto, H., Horii, F., and Hirai, A. (1996) *Cellulose*, **3**, 2298.
22. Nishino, T., Takano, K., and Nakamae, K. (1995) *J. Polym. Sci., Part B: Polym. Phys.*, **33**, 1647.

23. Nishiyama, Y., langan, P., and Chanzy, H. (2002) *J. Am. Chem. Soc.*, **124**, 9074.
24. Nakamae, K. and Nishino, T. (1991) in *Integration of Fundamental Polymer Science and Technology-5* (eds P.J. Lemstra and L.A. Kleintjens), Elsevier Science, New York, p. 121.
25. Nakamae, K. and Nishino, T. (1992) *Adv. X-Ray Anal.*, **35**, 545.
26. Nakamae, K., Nishino, T., and Ohkubo, H. (1991) *J. Macromol. Sci. -Phys.*, **B30** (1).
27. Kotera, M., Nakai, A., Saito, M., Izu, T., and Nishino, T. (2007) *Polym. J.*, **39**, 1295.
28. Kroon-Batenburg, I.M.J., Kroon, J., and Northolt, M.G. (1986) *Polym. Commun.*, **27**, 290.
29. Tashiro, K. and Kobayashi, M. (1991) *Polymer*, **32**, 1516.
30. Nishino, T., Takano, K., Nakamae, K., Saitaka, K., Itakura, S., Azuma, J., and Okamura, K. (1995) *J. Polym. Sci., Part B: Polym. Phys.*, **33**, 611.
31. Nishino, T., Matsui, R., and Nakamae, K. (1999) *J. Polym. Sci., Part B, Polym. Phys.*, **37**, 1191.
32. Nishino, T., Kotera, M., Okada, K., Sakurai, H., Nakamae, K., Katsuya, Y., Kagoshima, Y., Tsusaka, Y., and Matsui, J. (2001) *Mater. Sci. Res. Int. Special Tech. Publ.*, **1**, 378.
33. Nakamae, K., Nishino, T., Shimizu, Y., and Matsumoto, T. (1987) *Polym. J.*, **19**, 451.
34. Musgrave, M.J.P. and Pople, J.A. (1962) *Proc. R. Soc. Lond.*, **A5268**, 474.
35. Ito, T. (1990) *High Performance Polymer Composites*, Maruzen, Tokyo, p. 7 (in Japanese).
36. McLaughlin, E.C. and Tait, R.A. (1980) *J. Mater. Sci.*, **15**, 89.
37. Reiterer, A., Lichtenegger, H., Tchegg, S., and Fratzl, P. (1999) *Philos. Mag.*, **A79**, 2173.
38. Wang, H.H., Drummont, J.G., Reath, S.M., Hunt, K., and Watson, P.A. (2001) *Wood Sci. Technol.*, **34**, 493.
39. Page, D.T. and El-Hosseiny, F. (1983) *J. Pulp Pap. Sci.*, **9**, 99.
40. Hepworth, D.G. and Bruce, D.M. (2000) *J. Mater. Sci.*, **35**, 5861.
41. Iwamoto, S., Kai, W., Isogai, A., and Iwata, T. (2009) *Biomacromolecules*, **10**, 2571.
42. Ohya, S. and Muraoka, Y. (1978) *Raw Materials of Fibers*, Aikawa Shobou, Tokyo.
43. Northolt, M.G., Boerstoel, H., Maatman, H., Huisman, R., Veurink, J., and Elzerman, H. (2001) *Polymer*, **42**, 8249.
44. Smook, J., Hamersma, W., and Pennings, A.J. (1984) *J. Mater. Sci.*, **19**, 1359.
45. Henriksson, M., Berglund, L.A., Isaksson, P., Lindström, T., and Nishino, T. (2008) *Biomacromolecules*, **9**, 1579.
46. Nakamae, K., Nishino, T., and Ohkubo, H. (1989) *Polymer*, **30**, 1243.
47. Shao, Z. and Vollrath, F. (2002) *Nature*, **418**, 741.
48. Osaki, S. (1996) *Nature*, **384**, 419.
49. Nishino, T., Matsuda, I., and Hirao, K. (2004) *Macromolecules*, **37**, 7683.
50. Nishino, T. and Arimoto, N. (2007) *Biomacromolecules*, **8**, 2712.
51. Soykeabkaew, N., Arimoto, N., Nishino, T., and Peijs, T. (2008) *Compos. Sci. Technol.*, **68**, 2201.
52. Soykeabkaew, N., Sian, C., Gea, S., Nishino, T., and Peijs, T. (2009) *Cellulose*, **16**, 435–444.
53. Soykeabkaew, N., Nishino, T., and Peijs, T. (2009) *Composites: Part A*, **40**, 321.
54. Nilsson, H., Galland, S., Larsson, P.T., Kristofer, E., Nishino, T., Berglund, L.A., and Iversen, T. (2010) *Compos. Sci. Technol.*, **70**, 1704.
55. Yousefi, H., Nishino, T., Faezipour, M., Ebrahimi, G., Shakeri, A., and Morimune, S. (2010) *Adv. Compos. Lett.*, **19**, 190.
56. Yousefi, H., Faezipour, M., Nishino, T., Shakeri, A., and Ebrahimi, G. (2011) *Polym. J.*, **43**, 559.
57. Yousefi, H., Nishino, T., Faezipour, M., Ebrahimi, G., and Shakeri, A. (2011) *Biomacromolecules*, **12**, 4080.
58. Yousefi, H., Nishino, T., Shakeri, A., Faezipour, M., Ebrahimi, G., and Kotera, M. (2013) *J. Adhes. Sci. Technol.* **27**, 1324.
59. Nishino, T., Kotera, M., Suetsugu, M., Murakami, H., and Urushihara, Y. (2011) *Polymer*, **52**, 830.

60. Yano, H., Sugiyama, J., Nakagaito, A.N., Nogi, M., Matsuura, T., Hikita, M., and Handa, K. (2005) *Adv. Mater.*, **17**, 153.

61. Eichhorn, S.J., Dufresne, A., Aranguren, M., Marcovich, N.E., Capadona, J.R., Weder, S.J.C., Thielemans, W., Roman, M., Renneckar, S., Gindl, W., Veigel, S., Keckes, J., Yano, H., Abe, K., Nogi, M., Nakagaito, A.N., Mangalam, A., Benight, S., Bismarck, A., Berglund, L.A., and Peijs, T. (2010) *J. Mater. Sci.*, **45** (1).

4
Surface Treatment and Characterization of Natural Fibers: Effects on the Properties of Biocomposites

Donghwan Cho, Hyun-Joong Kim, and Lawrence T. Drzal

4.1
Introduction

Recently, there has been increasing interest in natural fiber-reinforced polymer composites, referred to as *biocomposites*, also referred to as *green composites* or *ecocomposites*. Hereinafter, the word ''biocomposites'' is used. Biocomposites have been attracting much attention as an alternative to conventional glass fiber-reinforced polymer (GFRP) composites during the last decade [1–3]. Biocomposites composed of natural fibers and synthetic thermoplastic or thermosetting polymers are not sufficiently environmentally benign because most polymer matrix resins are not biodegradable. However, they can have a balance among cost, property, and environment for applications in automotive parts, building materials, electronic parts, commodities, and packaging [4]. During the last years, many research efforts on biodegradable biocomposites composed of cellulose-based natural fibers and biodegradable polymers such as polylactic acid (PLA), poly(butylene succinate) (PBS), and poly(ε-caprolactone) have been rapidly increasing in academia and industries, owing to increasing environmental awareness and social consciousness [5–8].

Industrial natural fibers have been increasingly utilized to fill and reinforce not only conventional thermoplastic and thermosetting polymers but also biodegradable polymers [9]. Their advantages and disadvantages mostly rely on those of natural fibers, which are also referred to as *biofibers*. Natural fiber reinforcements have a number of merits over conventional glass fiber reinforcement, for example, natural abundance, low cost, low density, environmental friendliness, carbon dioxide sequestration, acceptable specific mechanical properties, damping and insulation characteristics, and biodegradability. However, they also have some drawbacks, such as poor natural fiber–matrix interfacial adhesion, fiber variability, surface irregularity, finite fiber length, limited thermal stability, and restricted processing temperature [1, 10]. Natural fibers also have high moisture or water absorption characteristics due to hydroxyl and other polar groups existing therein. The moisture absorption leads to a decrease of the mechanical properties and the

Polymer Composite: Volume 3, First Edition.
Edited by Sabu Thomas, Kuruvilla Joseph, S. K. Malhotra, Koichi Goda and M. S. Sreekala.

dimensional stability, whereas it may play a positive role in the biodegradability of biocomposites [11].

The strong adhesion or bonding at the interfaces between natural fibers and a polymer matrix is critical to promote the properties and performances of biocomposites, as in GFRP and carbon fiber-reinforced polymer matrix composites [4, 12]. However, in general, such strong adhesion cannot be established in the biocomposite system using natural fibers without appropriate surface treatment or modification as natural fibers are intrinsically hydrophilic in character. Once they are used with polymer resins, which are mostly of hydrophobic character, the compatibility and wettability between the two constituents becomes poor. It may lead to biocomposites exhibiting low interfacial and mechanical properties as well as high water absorption. As a result, it may restrict their uses in many possible applications [4].

Therefore, a large number of studies on chemical and physical surface treatments of various natural fibers have been devoted not only to increasing the interfacial adhesion between the natural fiber and the polymer matrix but also to enhancing mechanical, thermal, and other properties of biocomposites consisting of different types of natural fibers and polymers [13–20]. Meanwhile, a few excellent papers have reviewed the surface modification of natural fibers for biocomposites [4, 11, 21, 22]. Many research results dealing with surface treatment of natural fibers and characterizing various properties of biocomposites with different modification methods as well as with different natural fibers and polymers have been reported in recent years.

Consequently, it is worth overviewing extensively current research efforts on the effects of surface treatment of natural fibers on the properties of biocomposites in terms of interfacial, static mechanical, dynamic mechanical, impact, thermal, physical, morphological, fracture behavior, and water absorption. In the present chapter, the description and information focus mostly on the results reported in recent years.

4.2 Why Is Surface Treatment of Natural Fibers Important in Biocomposites?

Right selections of polymer resins and natural fibers are, first of all, substantially important for targeting properties and performances of a biocomposite material. As with traditional fiber-reinforced polymer composites [23], the mechanical, thermal, and impact properties, water absorption, and so on, of biocomposites generally depend on various factors such as fiber–matrix adhesion, fiber treatment/modification, fiber loading, fiber aspect ratio, fiber orientation, and composite processing method, as well as fiber and matrix types [24, 25]. Among them, interfacial adhesion between the natural fiber and the polymer matrix is a key factor in a biocomposite system using natural fibers as reinforcement [10, 11, 21]. The improvement of interfacial adhesion between hydrophilic natural fibers and a hydrophobic polymer matrix through surface treatment of natural fibers

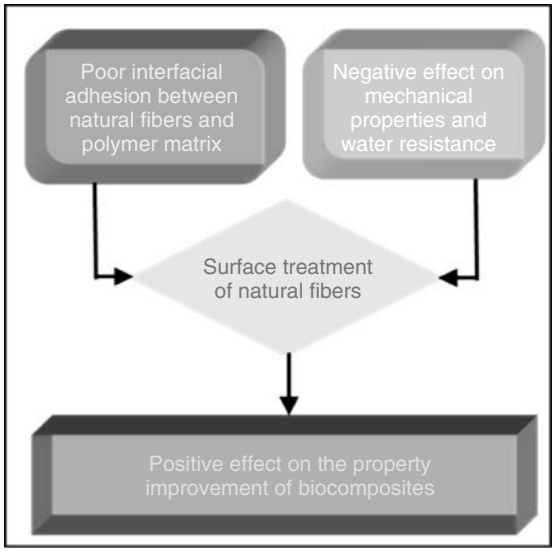

Figure 4.1 A schematic indicating the importance of surface treatment of natural fibers for fabricating biocomposites with improved properties and performances.

before composite processing contributes to a greater or less extent to an increase in the properties of the biocomposite. Poor wetting and bonding of the fiber with the polymer result in a negative effect on the mechanical and thermal properties as well as on the water resistance of the biocomposites, limiting their potential and extensive uses. An appropriate surface treatment of natural fibers may provide a positive effect on the improvement of the properties of the resulting biocomposites, as illustrated in Figure 4.1. Therefore, such shortcomings have to be overcome to make biocomposites with improved properties and performance.

Figure 4.2 illustrates the fundamental concept of interface and interphase in a fiber-reinforced polymer matrix composite material system, as proposed by Drzal in 1983 [26]. This schematic concept may also be applied for a biocomposite system. Once a sizing or coating material is applied to the region between the fiber and the matrix, there exists an interphase, which may be referred as a *third phase*. Two interfaces can exist between the reinforcing fiber and the polymer matrix. One is a fiber-size interface and the other is a polymer-size interface.

Once a composite is subject to an external mechanical load, the stress or load transfer at the interfaces plays a critical role not only in sustaining the material properties but also in prolonging the lifetime of the material. The interfacial adhesion or bonding between the fiber and the matrix may determine how effectively the external stress can be transferred to neighboring fibers and matrix. A strong fiber–matrix adhesion at the interfaces is necessary for effective stress transfer and load distribution from the matrix to the neighboring fibers and vice versa. It is also critical for attaining acceptable mechanical properties of resulting biocomposites. There would be an optimal level of the fiber–matrix

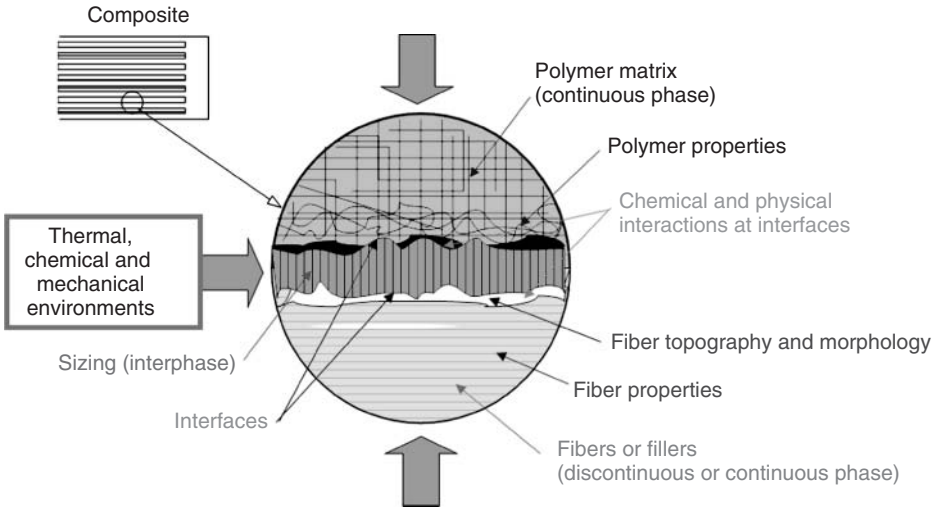

Figure 4.2 A schematic illustrating the importance of interface–interphase in a composite material. (After L.T. Drzal *et al.* [26].)

adhesion, which can result in the best mechanical properties of biocomposites [27]. From this viewpoint, research and development of the science and technology of surface treatment of natural fibers is necessary. Hence, studies on the property improvement on the basis of the fiber–matrix adhesion of biocomposites are important.

A composite material may often be exposed to thermal, chemical, mechanical, and hygrothermal environments. The polymer matrix, which may be a continuous and domain phase, can chemically and/or physically interact with and without the sizing interphase at the interfaces. Chemical bonding, molecular interdiffusion, interpenetration, and so on, may be involved during composite processing. In addition, the fiber or filler, which may be a discontinuous or occasionally continuous phase, can chemically or physically interact with and without the sizing interphase at the interfaces. Fiber characteristics such as stiffness, fiber diameter, fiber shape, fiber topography, fiber morphology, and wettability may be importantly considered as well. If the interface and interphase can be designed properly considering an engineering viewpoint, the mechanical and thermal properties of a composite material would be managed well from external environments.

The polymer matrix resin cannot perform its fundamental duties in the composite unless the fibers have been well wetted to the matrix [23]. Dry fibers do not transfer external loads effectively. Therefore, a critical function of a polymer matrix resin is simply to wet out and to bond it to the fibers and to form a continuous phase that interconnects all constituents of the composite. The hydrophilic polar character of natural fibers results in inherently low compatibility with hydrophobic nonpolar character of polymer matrices. It may cause insufficient wetting of a polymer resin to the fiber surfaces, providing poor interfacial adhesion, low mechanical properties,

and high water absorption. The presence of waxes, surface impurities, and weak boundary surface layers also provide poor surface wetting. Therefore, appropriate natural fiber treatment is surely beneficial in order to enhance the water absorption resistance as well as the wettability and to promote the interfacial properties. In particular, reducing water or moisture absorption is extremely important, because high water absorption may cause dimensional instability (swelling or plasticizing) and poor mechanical properties of the resulting biocomposite products [4, 28].

Many research efforts to enhance the interfacial properties of biocomposites and ultimately to improve the mechanical and thermal properties and so forth have been performed more extensively by treating or modifying natural fibers before composite processing than by modifying polymer matrices. Natural fibers can be treated by chemical and physical approaches.

4.3
What Are the Surface Treatment Methods of Natural Fibers?

In order to obtain biocomposites with good properties and high performances, it is very important to utilize an appropriate and efficient processing and fabrication technique, depending on the kinds of polymer resins that are going to be used, thermoplastics or thermosetting [29]. Once a thermoplastic polymer resin is selected as the matrix for making a biocomposite with short or chopped natural fibers, one can adopt the extrusion, injection, or compression molding technique according the work objective. On the other hand, once a thermosetting resin is selected as matrix, one can adopt traditional composite processing techniques such as compression molding, thermoforming, sheet molding compounding, bulk molding compounding, or resin transfer molding (RTM) technique although the limited length of natural fibers may restrict use of some other traditional thermosetting composite techniques such as pultrusion and filament winding (Figure 4.3).

Again, it may be recalled that the surface treatment or modification of natural fibers is critically important to obtain successful biocomposites with improved properties and performances. It would be desirable to use cost-effective, efficient, labor-friendly, environment-friendly, and energy-saving methods for the surface treatment of natural fibers. Traditionally, the chemical methods for natural fiber treatment were more commonly adopted than the physical methods, probably due to low cost, simple and easy handling, less skill, and so on. There are a variety of chemical methods, as introduced in the following section. Among them, the most frequently used chemical methods are alkali and silane treatments [21, 22]. In natural fiber/polymer biocomposite systems, chemical or physical treatments for modifying natural fiber surfaces are normally carried out before composite fabrication and processing. There are several methods that can be adopted appropriately according the work aim to treat cellulose-based natural fibers chemically or physically. Chemical treatments are alkali treatment, silane treatment, acetylation treatment, benzoylation/benzylation treatment,

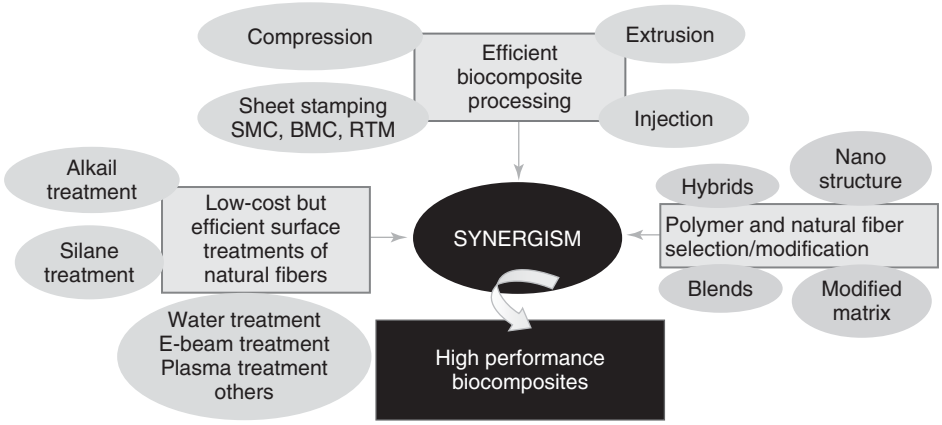

Figure 4.3 Schematic diagram indicating diverse approaches to design high performance biocomposites by combination of processing, surface treatment, and polymer modification.

maleic anhydride-*grafted*-polypropylene (MAPP) treatment, peroxide treatment, graft copolymerization, isocyanate treatment, etherification, permanganate treatment, and so on. Physical treatments are plasma treatment, corona treatment, electron beam treatment, UV treatment, thermal treatment, and so on. In addition, water treatment can be utilized.

The improvement of the properties of biocomposites can also be attained by polymer matrix modification as well as by natural fiber modification. A right combination of natural fiber and polymer matrix modifications may give rise to a synergetic effect. For instance, the incorporation of organic–inorganic hybrid polymer matrix, nanostructured polymer matrix, blended polymer matrix, or chemically or physically modified polymer matrix into natural fiber reinforcement may be considered.

4.3.1 Chemical Treatment Methods

4.3.1.1 Alkali Treatment

Alkali treatment of natural fibers, also referred to as *mercerization*, is an old and most widely used method for modifying cellulose-based natural fibers [30–36]. The most favorable alkali solution for mercerization is sodium hydroxide (NaOH) aqueous solution. The effect of alkali treatment on the properties of the composite as well as on the natural fibers strongly depends on alkali solution type, alkali concentration, treatment time, treatment temperature, and treatment tool. Alkali treatment may cause fibrillation of pristine natural fibers, resulting in the breakdown of individual fibers with smaller fiber diameter. This phenomenon can not only increase the aspect ratio of reinforcing natural fibers but also roughen the fiber surfaces. As a result, the fiber–matrix interfacial adhesion may be enhanced and the

mechanical properties of the resulting composites may be improved as well [37]. The effectiveness of the treatment, of course, depends on the alkali treatment condition adopted. Uses of excessive alkali concentration, extended time, and high temperature can accelerate the extent of treatment but may depolymerize the cellulose component and damage the pristine natural fibers, resulting in the deterioration of the fiber strength [4].

The following scheme represents the established chemical reaction scheme of NaOH with hydroxyl groups in natural fibers.

$$\text{Natural fiber-OH} + \text{NaOH} \rightarrow \text{Natural fiber-O}^{-}\text{Na}^{+} + \text{H}_2\text{O}$$

During alkali treatment, cementing substances such as hemicelluloses and lignin, which lead to better packing of the cellulose chains and to maintain the fiber architecture, these can be removed by appropriate alkali treatment. As a result, the interfibrillar region becomes less dense and less rigid and thereby allows the fibrils some rearrangement themselves [38]. Some waxes, oils, and surface impurities existing on the fiber surfaces can also be removed during the treatment. Therefore alkali treatment may influence the chemical composition, degree of polymerization, molecular orientation, crystallinity, and cellulose structure [4, 37, 39]. The alkali treatment may increase the degree of crystallinity by the removal of cementing substances.

After NaOH treatment, natural fibers of interest are normally washed or rinsed sufficiently with tap or distilled water in order to remove the excess of NaOH or unreacted NaOH for neutralization and then dried before use [8, 16, 19]. A large number of studies [12, 40–50] on the effect of alkali treatment on the properties of biocomposites consisting of various natural fibers and polymer matrices have been extensively performed by many research groups. Some papers [51–53] explored the combination effect of alkali treatment and silane treatment to improve the mechanical properties through the interfacial modification between natural fibers and polymer matrix.

4.3.1.2 **Silane Treatment**

As the basis of one of the major chemical treatment methods, silanes are chemical substances capable of reacting with both natural fiber reinforcement and polymer matrix of a biocomposite material [5]. Silane plays an important role as an interphase between the bulk polymer phase and the bulk fiber phase forming chemical bridges between the two phases. As a matter of fact, silane compounds have been widely utilized as efficient coupling agents in GFRP composites [54] and mineral filler/polymer composites [55]. In addition, silanes have also been used as adhesion promoters in adhesive formulations, giving rise to strong adhesion. An excellent book extensively dealing with silane coupling agents, their chemistry, and applications, was published in 1991 [56].

Since both glass fibers and natural fibers have reactive hydroxyl groups, extensive research efforts on silane coupling agents for processing composites have been performed [18, 57–66]. Additional silane treatment done to the fiber after alkali

treatment of natural fibers may provide higher efficiency in enhancing the properties of resulting biocomposites than the alkali-treated or untreated cases [51–53]. This may be due mainly to the presence of more reactive sites generated during the silane reaction. Therefore, natural fibers were pretreated with sodium hydroxide at appropriate concentration and time before coupling the fibers with silane, washed sufficiently, and then dried [37].

The general chemical formula of silanes is X3Si-R, which is an organofunctional (bifunctional) molecule that can react with the cellulose-based natural fiber surfaces at one end and with the polymer matrix resin at the other end. Here R designates a chemical group that can react with the polymer resin and X designates a functional group that can hydrolyze to generate a silanol group in aqueous silane solution and react with hydroxyl groups on the natural fiber surfaces. The R groups must be able to react with the functional groups in the polymer resin under given processing or curing conditions for producing biocomposites. Vinyl, γ-glycidoxypropyl, γ-aminopropyl, γ-methacryloxypropyl, and so on, can act as R groups. The X groups must be able to hydrolyze to allow reactions to take place between the silane and the hydroxyl groups located on the natural fiber surfaces. Methoxy, ethoxy, trimethoxy, triethoxy, and chloro can act as X groups [22].

Silane coupling agents may decrease the number of cellulose hydroxyl groups existing in the natural fiber–matrix interfacial region. In the presence of water or moisture, via hydrolysis, hydrolyzable alkoxy groups can form silanol groups, as seen in Scheme 4.1. The silanol groups are able to react with the hydroxyl groups of natural fibers, forming stable covalent bonds to the fiber surfaces and/or to the cell wall and providing a macromolecular network [28]. The hydrolysis of silanes may depend on the hydrolytic condition, for instance, solvent, temperature, pH, and silane concentration [28, 67].

Once silane-treated natural fibers come in contact with the polymer, the R groups located on the natural fiber surfaces may react with the functional groups in the polymer matrix resin, generating chemically stable and strong covalent bonds and bridging the natural fibers to the matrix resin. Therefore, it may lead to an increase in the degree of cross-linking in the interfacial region between the natural fibers and the matrix. As a result, silane treatment may play a contributing role in improving the mechanical and thermal properties and water resistance of biocomposites as well as in enhancing the interfacial adhesion between the fibers and the matrix. In general, several interactions between silane coupling agents and natural fibers may occur through hydrolysis, self-condensation, adsorption, and grafting, as illustrated in Scheme 4.1 [28, 68–70].

By silane treatment under proper experimental conditions, natural fibers, which are normally hydrophilic or hygroscopic, can be converted into hydrophobic fibers for nonpolar polymer matrices [28], reducing the water absorption rate. Silane treatment of natural fibers may more or less increase the thermal stability of natural fibers depending on the treatment conditions. Silane treatment normally does not damage the natural fibers because no fiber-damaging elements such as an acidic catalyst are present in the silane solution and high temperature treatment

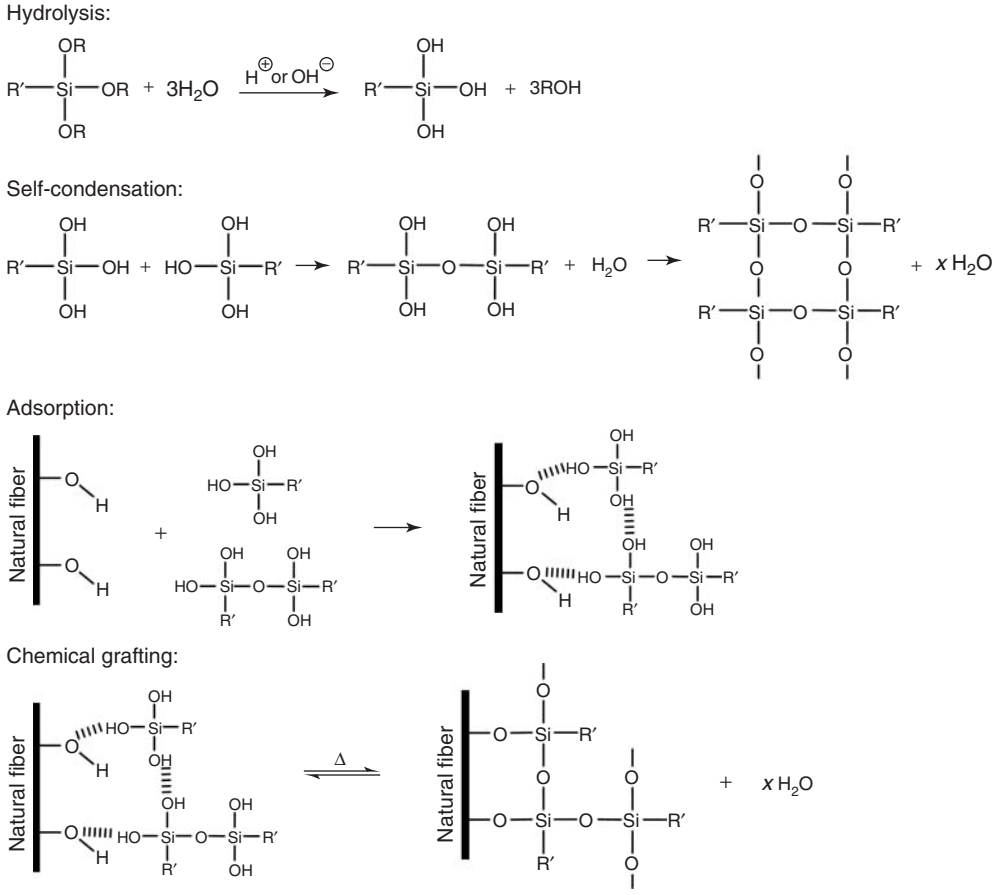

Scheme 4.1 Reaction schemes showing possible interaction between silane coupling agents and natural fibers by hydrolysis. (After Y. Xie [28].)

is not used. Therefore it is noted that the tensile strength of natural fibers should be little influenced by the silane itself [36].

The chemical and/or physical interaction between the silane-treated natural fibers and the polymer matrix is an important factor for improving the mechanical properties of biocomposites. Physical mixing of silane-treated natural fibers with thermoplastic resins can enhance the fiber–matrix interaction through intermolecular entanglement or acid–base interaction [56]. In this case, limited improvement in the mechanical properties may be expected. The mechanical properties may be marginally increased by the increased wettability and the uniform dispersion of silane-treated natural fibers into the thermoplastic matrices [71]. The molecular chains may be interdiffused into the natural fiber surfaces, forming a (semi)interpenetrating polymer network [65, 72].

In order to increase the mechanical properties of silane-treated natural fiber/thermoplastic biocomposites effectively, some chemical bonds should be formed between the silane-treated natural fibers and the nonpolar thermoplastic matrix during composite processing, including compounding, extrusion, or injection. Unfortunately, most nonpolar thermoplastics resins do not have enough functionality to react and make covalent bonds between them during composite processing. In these cases, some other chemical or physical approaches to modify the silane-treated natural fiber surfaces in order for them to bond covalently to the thermoplastic matrix resin are necessary. In contrast with thermoplastics, thermosetting polymer resins, which are usually in liquid state before cured, are quite reactive with the organofunctional groups of silanes and they can easily wet out short or long natural fibers without any fiber damage during composite processing. Scheme 4.2 and Scheme 4.3 present the possible acid–base reaction between γ-aminopropyltriethoxysilane (APS)-treated natural fibers and poly(vinyl chloride) (PVC) matrix and coupling reaction between APS-treated natural fibers with epoxy resin, respectively. One can find examples of silane compounds possibly usable for natural fiber-reinforced polymer matrix biocomposites [28].

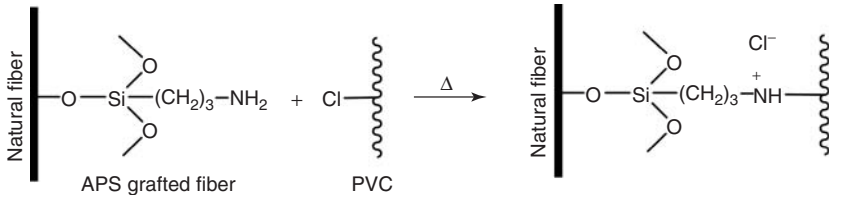

Scheme 4.2 Acid–base reaction between APS-treated natural fiber and PVC. (After I.M. Matuana [71].)

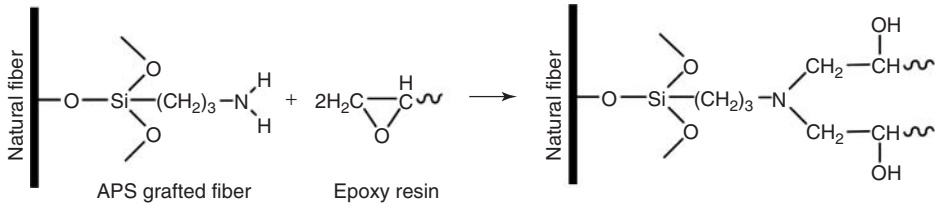

Scheme 4.3 Coupling reaction scheme between APS-treated natural fiber and epoxy resin. (After Y. Xie [28].)

4.3.1.3 **Acetylation Treatment**

Acetylation treatment of natural fibers is originally applied to wood cellulose to stabilize cell walls against moisture, improving dimensional stability and environmental degradation [73]. Therefore, acetylation may contribute toward decreasing the moisture absorption of natural fibers [37]. Plasticization of cellulose-based natural fiber can be introduced by this treatment, which is related to an esterification method. During the treatment of natural fibers with acetic anhydride, the hydroxyl groups

in the cell wall can be substituted with acetyl groups, modifying the surfaces to make them more hydrophobic [74]. Acetylation is based on the reaction of hydroxyl groups in the cell wall of lignocellulosic materials with acetic or propionic anhydride at elevated temperature. Acetylation can be carried out in the presence or absence of acid catalysts such as H_2SO_4 and $(CH_3CO)_2O$, as displayed in Scheme 4.4.

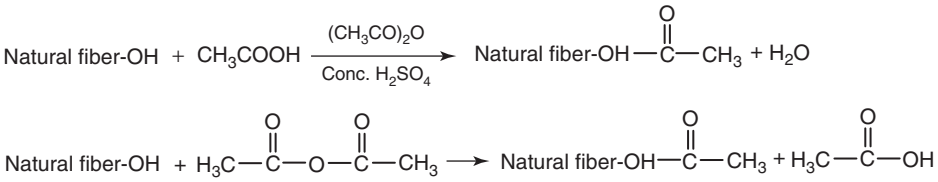

Scheme 4.4 Reaction scheme of acetylation of natural fibers with (a) and without (b) catalyst. (After A.K. Mohanty [4].)

Acetic anhydride is preferable for acetylation with cellulose because it has more reactive hydroxyl groups than acetic acid. Experimentally, natural fibers of interest are normally first soaked in acetic acid and subsequently treated with acetic anhydride. This is to promote the reaction as acetic anhydride does not swell enough cellulose for the reaction. In order to provide a combination effect of the treatment, alkali treatment may be carried out before treating natural fibers with glacial acetic acid followed by acetic anhydride [75–77].

4.3.1.4 Benzoylation and Benzylation Treatments

Benzoylation treatment is also a useful method to change the hydrophilic character of natural fibers. Benzoyl chloride (C_6H_5COCl) has been most frequently used in the treatment. The benzoyl groups ($C_6H_5C{=}O$) incorporated in natural fibers contribute to reducing the hydrophilicity of treated natural fibers, making the fiber more compatible with the hydrophobic polymer matrix [78]. In general, alkali treatment of natural fibers in NaOH solution at appropriate concentrations can be done before adding benzoyl chloride [75, 79, 80], similarly to that in the acetylation treatment. Similarly, with other chemical treatment cases, the natural fibers should be washed with water and then sufficiently dried. Benzyl chloride ($C_6H_5CH_2Cl$) may be used for benzylation of natural fibers [81, 82]. The hydroxyl groups existing in natural fibers can be substituted by benzyl groups ($C_6H_5CH_2$) during the treatment, producing benzylated natural fibers.

4.3.1.5 MAPP Treatment

Among commercial coupling agents, MAPP has been recognized to be most efficient in enhancing the fiber–matrix adhesion at the interfaces in natural fiber–polypropylene (PP) biocomposites [83–85]. Therefore MAPP, which is often also called *maleated PP*, is useful for increasing the compatibility between the natural fibers and the polymer matrix. MAPP plays the role of a coupling agent or compatibilizer in natural fiber-reinforced PP composites [86–88]. The covalent bonds between the maleic anhydride and the hydroxyl groups of cellulose-based

natural fibers can be formed across the interfaces between the fiber and the matrix. The surface energy of the fibers may be increased, resulting in improved wettability and interfacial adhesion [4]. The high molecular weight and anhydride content play a significant role not only in enhancing the natural fiber–matrix interfacial adhesion but also in increasing the properties because they influence the molecular diffusion with the polymer matrix and the chemical composition in the interphase created by the MAPP. Too high molecular weight MAPP may cause some entanglement with PP molecules so that the polar groups on MAPP have difficulties in finding the hydroxyl groups located on the natural fiber surfaces [4]. Scheme 4.5 shows a possible reaction scheme of natural fibers with MAPP.

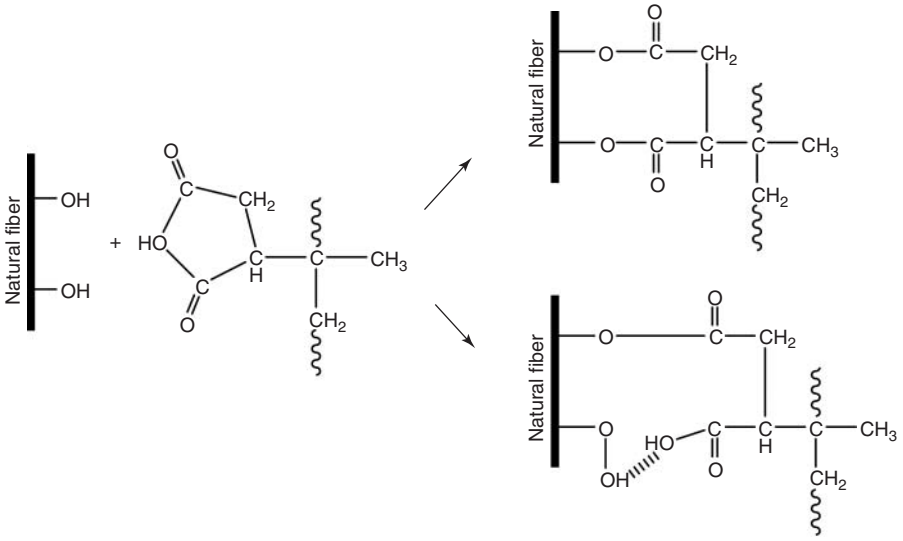

Scheme 4.5 Reaction scheme of natural fibers with MAPP. (After A.K. Mohanty [4].)

Hence, it is noted that the effect of MAPP on the enhancement of biocomposite properties depends on MAPP type, molecular weight, miscibility between MAPP and PP, PP grade, biocomposite processing condition, and so on. It was investigated that the molecular weight of MAPP was more important than the maleic anhydride content in MAPP for increasing the coupling efficiency in natural fiber/PP composites produced by injection molding [89]. The explanation for this was that the backbone structure of MAPP influenced the interfacial adhesion of the composites because of miscibility in the PP matrix. It was also reported that the mechanical properties of the composites were increased on increasing the amount of MAPP, but the effect was leveled off or began decreasing at higher MAPP contents.

4.3.1.6 **Peroxide Treatment**

Peroxide treatment using organic peroxides such as benzoyl peroxide, dicumyl peroxide, or hydrogen peroxide has attracted attention in the treatment of natural

fibers for producing the biocomposites because of easy processability and mechanical property enhancement [37, 90]. Organic peroxides may decompose easily to free radicals (RO·), which further react with the hydrogen atoms of the polymer matrix and natural fibers. The treatment is often conducted at high temperature (e.g., 70 °C) after alkali pretreatment [70, 91]. Use of high temperature helps peroxide molecules to decompose easily. A saturated solution of the peroxide in acetone can be used. Of course, the treated natural fibers should be washed with water and sufficiently dried before biocomposite processing.

4.3.2 Physical Treatment Methods

Physical methods for treating natural fibers before biocomposite processing involve electrical discharges such as cold plasma and corona, electron beam irradiation, ultraviolet (UV) treatment, and ultrasonic treatment, . Such physical approaches are of great interest because, in general, the processes are dry, clean, labor-friendly, environment-friendly, and fast in comparison with most of the chemical methods, which are wet processes. Under appropriate treatment conditions, they can effectively modify structural and surface characteristics of natural fibers, thereby improving the mechanical and thermal properties of biocomposites as well as enhancing the interfacial adhesion between the natural fibers and the polymer matrix.

4.3.2.1 Plasma Treatment

Plasma treatment is a simple process without any pollution problems. Physical treatment such as cold plasma treatment is a clean, dry, and environmentally friendly method [92]. Cold (low temperature) plasma process, which can be generated under atmospheric pressure in the presence of helium [93], is carried out by utilizing particles such as electrons, ions, radicals, and excited molecules produced by electrical discharge. They may modify the fiber surfaces without influencing the bulk properties, depending on the treatment power and time. Under appropriate conditions, cold plasma treatment of the natural fibers before composite fabrication may enhance the interfacial adhesion between the natural fibers and the polymer matrix, depending on the type of natural fibers and polymer matrices used [94]. According to the type and nature of plasma gas applied, surface energy may be increased or decreased, reactive free radicals may be formed, and the polymer may be cross-linked [95]. Figure 4.4 illustrates a proposed reaction mechanism for the surface treatment by plasma [11]. Plasma treatment may result in the following phenomena on the natural fiber surfaces, more or less influencing the interfacial bonding between the natural fibers and the polymer matrix consisting of biocomposites:

1) surface cleaning and topological and morphological changes of surfaces;
2) surface etching resulting in an increase of roughness;
3) cross-linking at the surfaces;
4) chemical structure change and free radical formation at the surfaces.

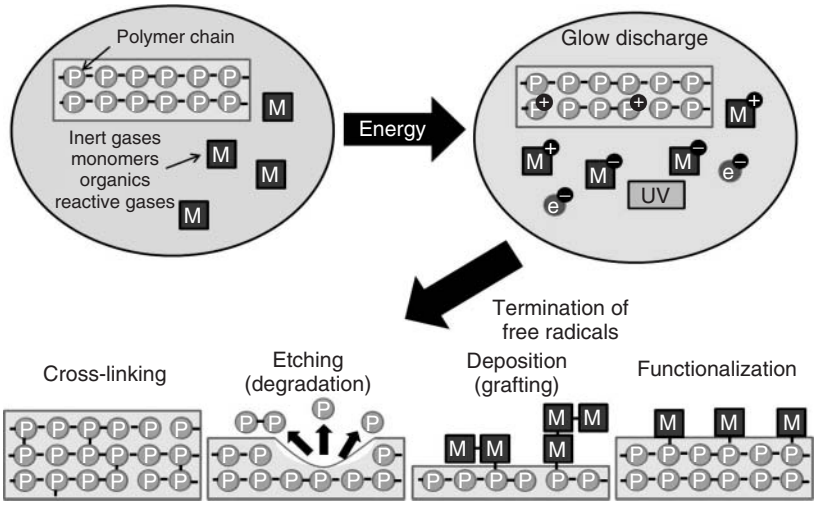

Figure 4.4 A proposed reaction mechanism for the surface treatment by plasma. (After S. Mukhopadhyay [11].)

There are a number of papers reporting the surface treatment of cellulose-based natural fibers and the property improvement of biocomposites through the surface modification of natural fibers by means of plasma treatment [96–99].

4.3.2.2 **Corona Treatment**

As one of the electrical discharges, corona discharges are relatively low power electrical discharges that occur at or near atmospheric pressure [11]. Corona treatment is one of the most interesting methods for surface oxidation. It has been known that electrical discharge methods like plasma and corona treatments are effective for modifying nonactive polymer surfaces such as polyethylene, PP, and polystyrene [100]. In addition, they may change the surface energy of cellulose-based natural fibers, decreasing the melt viscosity of polymer and natural fiber mixture [101]. Corona treatment can alter the surface composition and the surface properties of resulting composites. It has been reported that the polarity of natural fibers like jute was increased by the corona treatment and the increase of the polarity may be attributed to an increase of the number of carboxyl (–COOH) and hydroxyl (–OH) groups on the fiber surfaces [101]. The increase of carboxyl and hydroxyl groups leads to an increase of the natural fiber–polymer adhesion at the interfaces. However, similar to the plasma treatment, overtreatment may cause the lowering of the composite properties towing to the deterioration of the mechanical properties and the fracture energy of overtreated individual natural fibers.

A few papers have reported that cellulose-based natural fiber surfaces can be modified with corona treatment and that the resulting polymer composites exhibited the improved properties through the surface modification of natural fibers [102, 103].

4.3.2.3 Electron Beam Treatment

The electron beam technique has often been utilized for surface modification and property improvement of polymer materials like fibers, films, plastics, and composites in recent decades [104–107]. It may remove surface impurities and alter surface chemical characteristics at an appropriate irradiation condition. Electron beam processing is a dry, clean, and cold method with advantages such as energy-saving, high throughput rate, uniform treatment, and environmental safety.

The cellulose component of natural fibers may be degraded or cross-linked upon electron beam irradiation of high energy [108]. The chain scission of cellulose may occur at higher irradiation dosage and it may cause deterioration in the mechanical properties of natural fibers [14, 109, 110]. The irradiation may considerably change the structure, reactivity, physicochemical, and mechanical properties of cellulose. It was reported [111] that with increasing electron beam dosage up to 500 kGy, the α-cellulose content of kenaf fibers was decreased due to cellulose degradation, resulting in decreased maximum thermal decomposition temperature of cellulose and little change of the functional groups of kenaf. Also, it was found that electron beam irradiation maintains the inner pore structure of cellulose-based henequen fibers, as compared to some destruction or damage of the inner structure of henequen by alkali treatment [112].

Electron beam treatment of natural fibers of interest is carried out before biocomposite fabrication. A relatively large amount of raw natural fibers, bundles, and/or woven fabrics contained and spread in a polyethylene bag can be irradiated separately or simultaneously. Different levels of electron beam dosages, for example, from 1 to 100 kGy, or even higher, may be applied. Use of too high intensity of electron beam may cause some damages and microstructural defects of the natural fibers, resulting in deterioration of their mechanical properties. Eventually, the treatment effect on the property improvement of biocomposites may depend on the treatment level, as reported earlier with different natural fiber/polymer biocomposite systems by Cho *et al.* [105, 107–110, 112]. The electron beam irradiation processes can normally be performed at ambient temperature in air. Each irradiation process can be done when natural fiber-containing bags resting on a conveying cart are passed through the electron beam channel under prescheduled treatment conditions, as illustrated in Figure 4.5. The electron beam dosages can be controlled by the number of sample irradiations exposed in the electron beam channel. The treated natural fibers can be utilized directly to make composites with polymer resins without any additional processes such as washing and drying.

4.3.2.4 Ultraviolet Treatment

The energy and frequency of UV radiation are smaller than those of X-rays but greater than those of visible light. UV energy, which ranges from approximately 200–400 nm, can also be used to modify the natural fiber surfaces [113]. UV treatment may lead to an increase of the polarity of the fiber surfaces. As a result, the wettability of the fibers can be increased and the interfacial and mechanical properties of biocomposites can be increased.

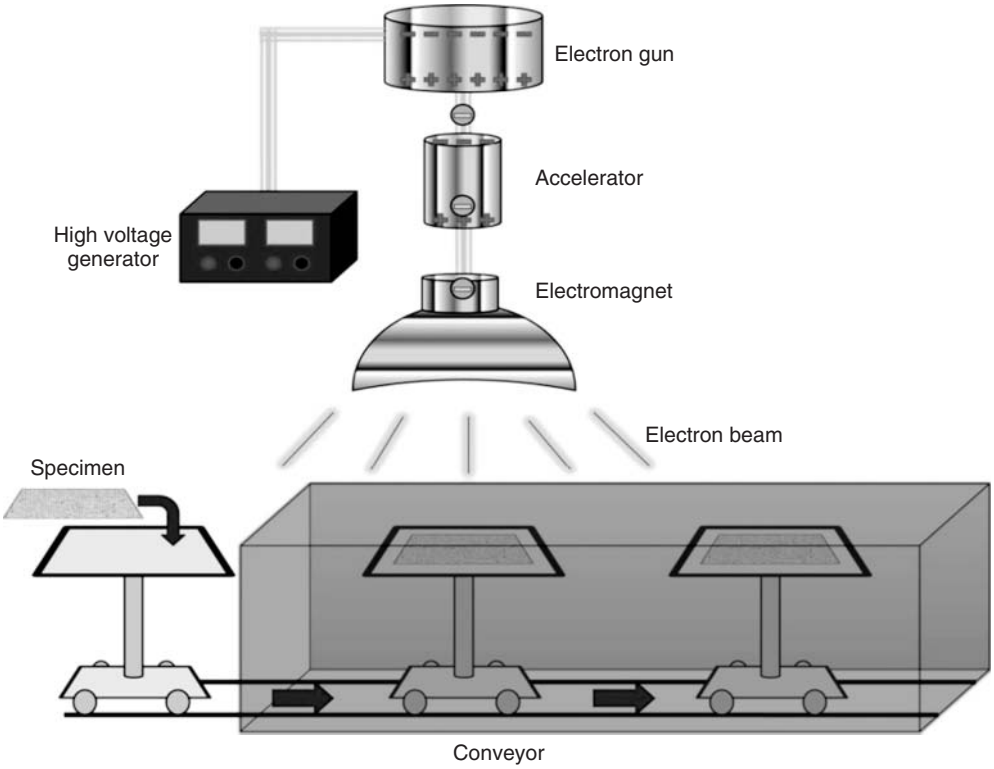

Figure 4.5 Illustration of electron beam irradiation processing for treating natural fibers. (After S.G. Ji [107].)

The fiber polarity and the properties of fibers and composites substantially depend on the UV treatment time and the distance from the UV lamp to the fiber substrate [11]. Gassan and Gutowski [103] insisted that a balance between the increased polarity of fiber surface and the decreased fiber strength is necessary for improving the mechanical properties of jute/epoxy (JEP) composites by the UV oxidation of jute fibers. Rahman and Khan [114] reported that UV pretreatment of coir showed an increase in tensile properties with increasing radiation dosage and the result may be due to the cross-linking between the neighboring cellulose molecules occurred under UV radiation.

4.3.2.5 **Ultrasonic Treatment**

Ultrasonic treatment or ultrasound treatment deals with very high frequencies of sound, generally higher than 20 kHz. Early uses of ultrasound were in pulp and paper technology for various processes such as debarking, defibrillation, beating, and bleaching [115]. Such a technique may also be applied for treating cellulose-based natural fibers by means of ultrasonic equipment containing aqueous or organic media with varying frequency. Cho *et al.* reported that jute fibers were

dynamically treated with tap water and sodium hydroxide solutions using an ultrasonic method. They studied the effect of ultrasonic treatment on the interfacial and mechanical properties of jute/PLA [8] and henequen/unsaturated polyester (UPE) biocomposites [116]. The result showed that the ultrasonic treatments of natural fibers at 40 kHz contributed to improving the interfacial adhesion between the natural fiber and the PLA matrix. The PLA biocomposite reinforced with jute fibers ultrasonic-treated with tap water exhibited the increased storage modulus in the temperature range of 25–150 °C. Their results suggested that the ultrasonic treatment of natural fibers with water play a positive role in enhancing the properties of biocomposites and the treatment may accelerate the treatment efficiency at low alkali concentration as well as for a short period of alkali treatment time. On the other hand, the treatment at high alkali concentrations and/or for a long period of time may adversely affect the properties because of possible fiber damages and deterioration of intrinsic fiber strength.

4.4
How Does the Surface Treatment Influence the Properties of Biocomposites?

4.4.1
Chemical Changes of Natural Fibers

The chemical changes of natural fibers have often been investigated by means of attenuated total reflectance Fourier transform infrared spectroscopy (ATR-FTIR) in order to examine the presence and absence (or disappearance) of functional groups of interest on the surfaces. Alkali treatment may change the surface chemistry of cellulose-based natural fibers such as kenaf, jute, flax, hemp, henequen, and sisal. For instance, the absorption peaks of 3400–3200 cm^{-1} due to hydrogen-bonded O–H stretching vibration and 1373 cm^{-1} due to O–H in-plane bending vibration may be decreased with the formation of glycosidic bonds by alkali treatment of kenaf, depending on the alkali concentration [43]. The stretching band near 1736 cm^{-1} due to C=O groups decreases or disappears due to the hemicellulose component removed by alkali treatment, depending on the concentration [43, 117–119]. The band near 1240 cm^{-1} may be ascribed to axial asymmetric strain of =C–O–C group, where =C–O– occurs in ether, ester, and phenol. Some ether bonds in the lignin molecules can probably be broken by alkali treatment, resulting in the disappearance of this band [120].

No significant spectral changes in raw and electron beam-treated kenaf and henequen fibers were observed from ATR-FTIR measurement [43, 113]. However, from the earlier study using elemental analysis [111] and X-ray photoelectron spectroscopy (XPS) [15] by Cho *et al.*, it was pointed out that the [O]/[C] ratio of the electron beam-treated jute and henequen fibers was lower than that before the irradiation (0 kGy). The ratio exhibited the lowest value at 10 kGy [15, 111]. The decrease of the ratio after the irradiation indicated that the treated jute fibers have more hydrophobic character than the treated. It was suggested that the combination

of physical and chemical effects induced by optimal electron beam irradiation can contribute to increasing the interfacial adhesion between the natural fibers (jute and henequen) and the matrices (PLA and poly(butylene succinate)) and further to improving the mechanical and thermal properties of the resulting biocomposites.

Cho *et al*. [121] also studied the presence and absence of some functional groups on the flax fiber surfaces unmodified (dewaxed), acetylated, and plasma-treated, using ATR-FTIR. In the unmodified flax, there was a broad band near 3400 cm^{-1} due to stretching vibration of the hydrogen-bonded OH groups on the surfaces. By plasma treatment, it was likely that the O–H band was more or less sharper than that of the unmodified one. The explanation for this was that some hydroxyl groups in the flax were changed to ether linkages by ethylene plasma treatment. The changed hydroxyl groups may lead to the reduction of intramolecular and intermolecular hydrogen bonds [122]. In the case of acetylated flax, the O–H band between 3100 and 3600 cm^{-1} almost disappeared, indicating that most of hydroxyl groups existing on the surface were modified by acetylation, resulting in esterification. In the acetylated flax, there was also a strong absorption band near 1740 cm^{-1} due to stretching vibration of carbonyl groups in the ester bonds, indicating the hydrophobicity of the fiber surface. The esterification reaction can also be confirmed by the presence of a new absorption peak near 1200 cm^{-1} due to the C–O stretching vibration of the ester carbonyl groups.

Sever *et al*. [123] analyzed the effect of oxygen plasma treatment on the functional groups of jute fibers using XPS. It was found that with an oxygen plasma, various oxygen-containing groups such as –C–OH, –C=O, –COOH, and $-CO_2$ were introduced by the surfaces of treated jute fibers.

4.4.2
Morphological and Structural Changes of Natural Fibers

Alkali treatment can clean the surfaces by removing surface impurities and low molecular weight waxes existing on raw natural fibers and also remove all or some of hemicellulose and lignin components of the fiber, depending on the alkali concentration and treatment time used [124, 125]. It may lead to morphological and topological changes of natural fibers. Uses of elevated temperature and ultrasonic frequency during the alkali treatment may accelerate the treatment efficiency but they may cause some fiber defects or damages under excessive conditions [8, 126], as described earlier. It was obvious that the alkali-treated jute fibers had rougher surfaces and more crevices on the surfaces than the untreated. The fiber surface undulation with striations became more pronounced at a higher alkali concentration and a longer treatment time [8]. The alkali treatment may result in fibrillation with more detailed topography. Sodium hydroxide can react with hydroxyl groups of the hemicellulose component. Excessive treatment may cause the destruction of the cellular structure and consequently the natural fibers split into finer fibrils by the dissolution of hemicellulose, called *fibrillation* [14, 41, 127], leading to an increase of the fiber surface area. As a result, the alkali treatment can contribute to making the fiber surface rougher and consequently to improving the

interfacial adhesion between the natural fiber and the polymer matrix, depending on the treatment time and concentration. Many papers have dealt with the alkali treatment to increase the mechanical properties of various types of biocomposites [47, 128–133].

It was revealed in an earlier report [111] that the morphology of jute fiber surfaces strongly depends on the electron beam treatment done at different intensities. The surface impurities and waxes were removed somewhat from the fiber surfaces by the treatment at 5 kGy. At 10 kGy, the surfaces became cleaner, revealing surface unevenness, and striations. The irradiation of 30 kGy may cause formation of defects on the surfaces. At 50 kGy, jute exhibited flat surfaces that lacked roughness. Then, the surface damage and cleavage took place at a relatively high intensity of 100 kGy (Figure 4.6).

Dynamic contact angle measurement indicated that the surfaces of flax fibers treated with ethylene plasma exhibited greater water contact angle than the untreated and the acetylated flax, reflecting that the plasma-treated flax surfaces became more hydrophobic [122]. The contact angle was increased on increasing the ethylene flow rate to 0.5 $cm^3\ s^{-1}$ and the plasma power to 50 W.

The effect of surface treatment on the crystallinity of natural fiber has been explored by means of X-ray diffraction analysis [134]. It was reported that the crystallinity index of untreated hemp fiber was 84.7%. The value was increased to 89.6% for NaOH-treated hemp and 89.1% for $NaOH/Na_2SO_3$-treated hemp. The explanation for this result was that NaOH treatment was responsible for the removal of a greater amount of amorphous component from natural fiber than $NaOH/Na_2SO_3$ treatment.

It was found from the Thomas' research group [77] that the surfaces of alkali-treated natural fiber have more available hydroxyl groups due to the opening up, resulting from the removal of hemicellulose and lignin therein by alkali treatment. With the alkali treatment, the interfibrillar structure was likely to be less dense and less rigid and made the fibrils more capable of rearranging themselves along the direction of tensile deformation [38]. Alkali treatment gave rise to the process of swelling and dissolution, increasing the accessibility of the cellulose hydroxyl groups for a subsequent reaction [77]. The rough surface morphology due to the removed hemicellulose and lignin played a contributing role in the interfacial adhesion between the natural fiber and the matrix, preventing interfacial slippage.

4.4.3
Mechanical Changes of Natural Fibers

In many studies, it has been reported that alkali treatment may decrease the mechanical properties of many natural fibers [44, 86, 134]. On the contrary, in some cases, it has been noted that alkali treatment may increase the mechanical properties depending on the NaOH concentration and treatment time [135, 136]. A decrease of the fiber strength may be due to cellulose degradation during the treatment. More likely, alkali treatment may cause an increase of surface roughness, including striations and the structural defects, resulting in an increase of stress

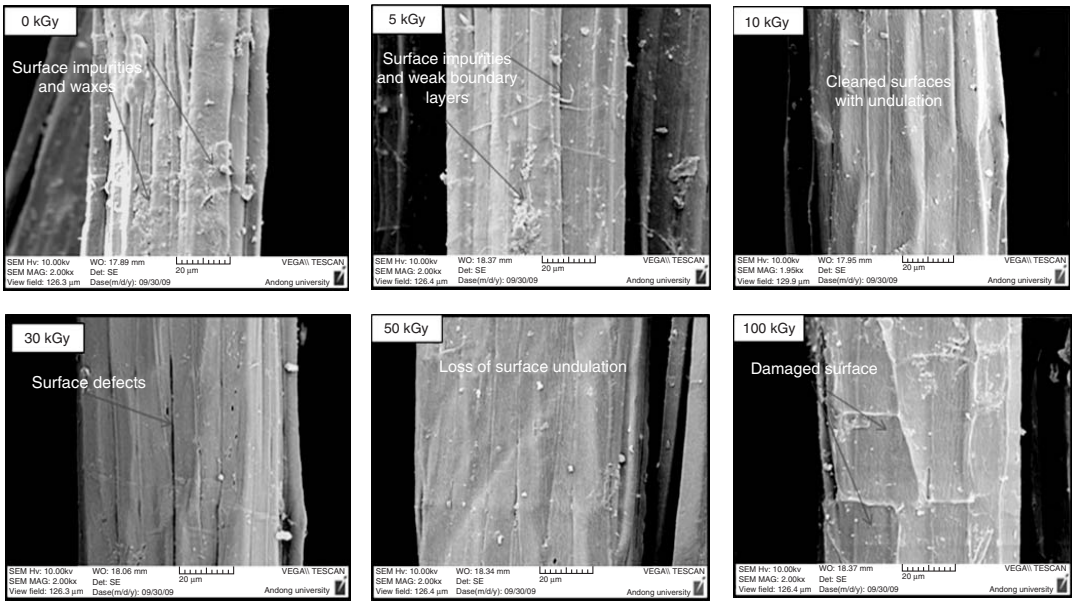

Figure 4.6 Morphological changes in jute fiber surfaces by electron beam treatment at various intensities. (After S.G. Ji [110].)

concentration and therefore a decrease of the fiber strength [44]. An increase of the crystallinity index of alkali-treated natural fibers, which can be achieved by the removal of cementing component like lignin and/or amorphous components like lignin and hemicellulose, gives rising to an increase in the packing density of crystalline chains [44, 120]. This leads to an increase in mechanical strength and modulus. Consequently, optimal conditions of alkali treatment should be adopted to obtain improved tensile properties of natural fibers. In other words, care must be taken in using appropriate alkali concentration and treatment time, temperature, and tools.

It has been reported that $NaOH/Na_2SO_3$ treatment resulted in increased strength and modulus of hemp fiber than the untreated counterpart [134]. In addition, there was a paper reporting that a combined alkali and fungi treatment increased about 32% of tensile strength of hemp, compared to the untreated [44].

Silane treatment normally does not damage the natural fibers because fiber-damaging elements such as an acidic catalyst are not present in the silane solution nor is high temperature treatment used, as mentioned above. Therefore, it is noted that the tensile strength of natural fibers should be little affected by the silane itself [36]. MAPP treatment may slightly increase the fiber strength due to the deposition of MAPP copolymer on the fiber surfaces, leading to more or less uniform and smooth surfaces [86]

As studied earlier using single-fiber tensile tests [111], the tensile strength and modulus of jute were noticeably decreased with increasing the electron beam intensity above 30 kGy. A significant decrease of both tensile strength and modulus at 50 kGy and higher may be due to the defects and damages of α-cellulose structure of the fiber by the irradiation [43]. No significant loss of the tensile properties of jute fibers was found below 10 kGy. It may be expected that the electron beam treatment may influence similarly the mechanical properties of other types of cellulose-based natural fibers.

Han *et al*. [15] investigated, using dynamic mechanical analysis (DMA), that the storage modulus of single henequen fibers treated with electron beam at various dosages gradually decreased on increasing both electron beam dosage and temperature, as shown in Figure 4.7. The storage modulus of the untreated raw henequen fiber was reduced by about 20% at 100 kGy. The lowest storage modulus was observed at 500 kGy, resulting from the degradation of henequen due to high energy of electron beam, leading to breakage of the fiber at 200 °C during DMA measurement.

4.4.4
Interfacial Properties of Biocomposites

It was demonstrated by the Cho *et al*. [16] that the natural fiber–polymer matrix adhesion at the interfaces of biocomposites can be effectively enhanced by both soaking (static) and ultrasonic (dynamic) treatments with tap water and NaOH and the effect can be more profound with ultrasonic treatment at a given frequency, as seen in Figure 4.8. In their study, the effect of natural fiber surface treatment on

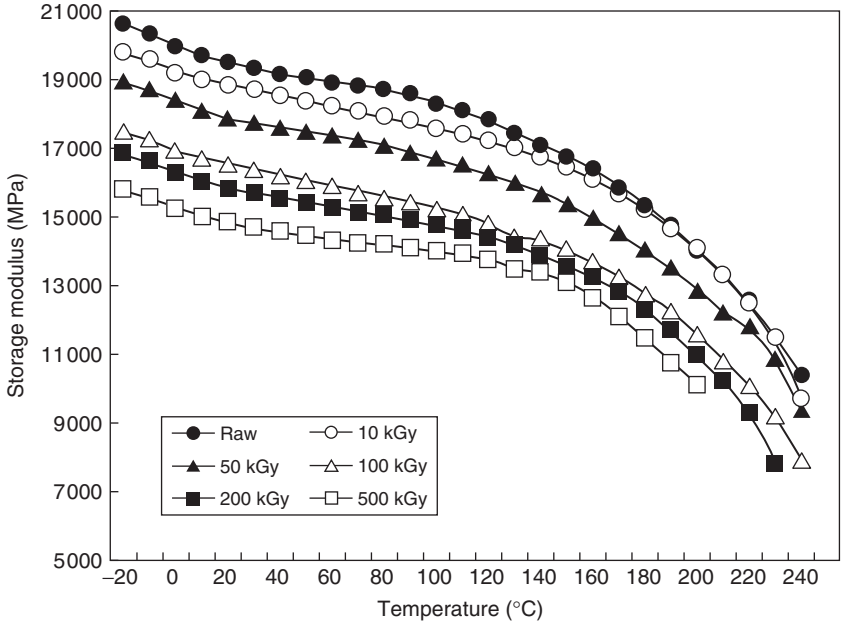

Figure 4.7 Variation of the storage modulus as a function of temperature observed for single henequen fibers treated at various electron beam dosages. (After S.O. Han *et al.* [15].)

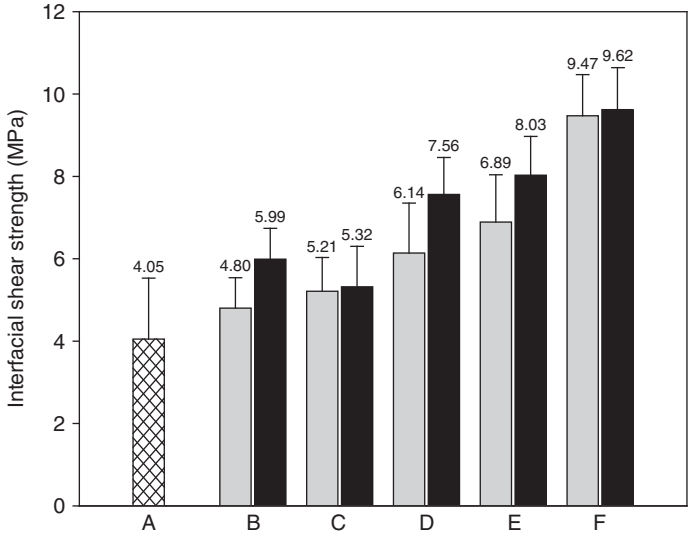

Figure 4.8 Interfacial shear strengths of henequen/PP biocomposites untreated (A) and treated by soaking (gray) and ultrasonic (black) treatments with tap water (B) and NaOH (C: 1 wt%, 10 min; D: 1 wt%, 60 min, E: 6 wt%, 10 min, F: 6 wt%, 60 min). (After H.S. Lee *et al.* [16].)

the interfacial shear strength (IFSS) was investigated by means of microbonding tests with a large number of composite specimens with a single henequen fiber embedded in a PP microdroplet. They insisted that in both static and dynamic methods, the IFSS of henequen/PP biocomposites increased with increasing NaOH concentration and treatment time.

An inspection of the fracture surfaces of composites composed of reinforcing fibers and polymer matrices provides qualitatively useful information on the interfacial adhesion between the fiber and the matrix and also gives rise to an indication of the effect of fiber surface treatment on the mechanical and thermal properties of resulting composites [137–139].

Figure 4.9 displays the scanning electron micrographs of the fracture surfaces of untreated and treated henequen/PP biocomposites. It was found that the untreated composite exhibited poor interfacial adhesion between the henequen fiber and the PP matrix. The interfacial adhesion was more or less enhanced by soaking treatment with tap water and also by 1 wt% NaOH for 60 min. The biocomposite with ultrasonic treatment with 6 wt% NaOH for 60 min exhibited the best interfacial adhesion, showing the henequen fiber broken upon fracture [16].

Figure 4.10 presents the effect of electron beam dosage irradiated to jute fibers on the IFSS of jute/PLA green composites, as reported earlier by Ji *et al.* [110]. A significant increase of the IFSS was obtained at 10 kGy, indicating an improvement of about 22% on the interfacial adhesion between the jute fibers and the PLA in comparison to the untreated one. They demonstrated that such interfacial improvement significantly contributed to the increase of the mechanical and thermal properties of jute/PLA green composites [140].

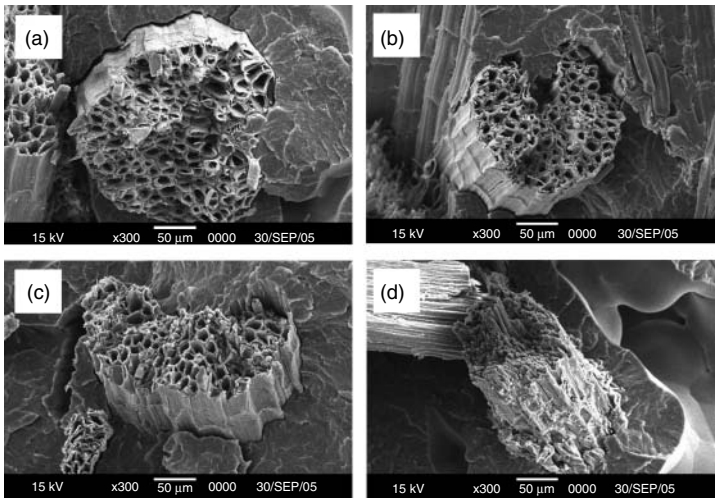

Figure 4.9 SEM micrographs (×300) showing the fracture surfaces of henequen/PP biocomposites (a) untreated and (b) treated with tap water, (c) 1 wt% NaOH by soaking, and with (d) 6 wt% NaOH by ultrasonic treatment, respectively. (After H.S. Lee [16].)

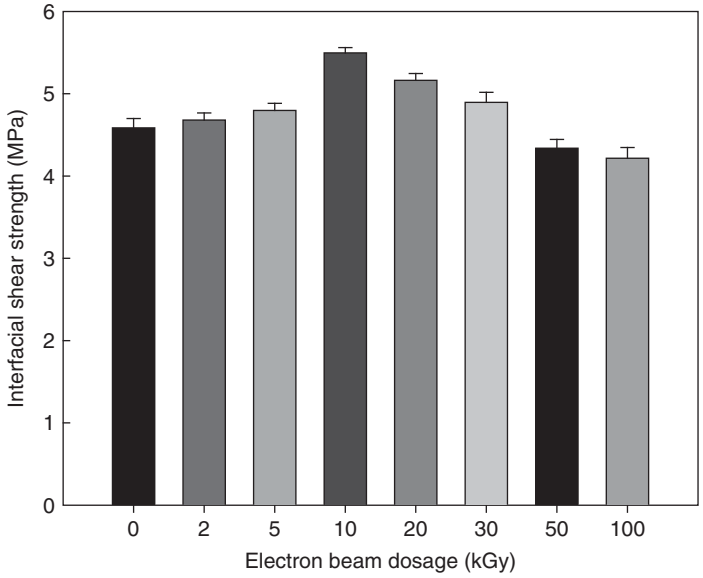

Figure 4.10 Variation of interfacial shear strength of jute/PLA green composites as a function of electron beam dosage treatment of jute fibers [110].

Interlaminar shear strength (ILSS) depends primarily on the matrix properties and fiber–matrix interfacial adhesion rather than on the fiber properties [141]. The ILSS, measured by the short-beam shear test, can be enhanced by increasing the tensile strength and volume fraction of the matrix as well as by increasing the interfacial adhesion in the laminates.

It was reported that the effect of surface modification of flax on the ILSS of two-directional flax fabric/poly(3-hydroxybutyrate-*co*-3-hydroxyvalerate) (PHBV) biocomposites [121]. The ILSS values of the surface-treated flax fabric/PHBV biocomposites were greater than that of with untreated fabric. The plasma-treated specimen exhibited ILSS values greater than those for the acetylated one in comparison with the untreated specimens. The explanation for this was that aliphatic moieties with greater hydrophobicity may be formed on the fiber surfaces by ethylene plasma. It was noted that both acetylation and plasma treatment played an important role in improving the interfacial properties of flax/PHBV biocomposites, suggesting that the ethylene plasma treatment was more effective.

It was also found from dynamic contact angle measurements in an earlier study [122] that fiber surfaces became more hydrophobic on treatment with ethylene plasma rather than by acetylation. It was also reported that plasma treatment resulted in hydrophobicity in jute fibers, indicating an increase of contact angle with water and the rough surfaces formed after plasma treatment, leading to better fiber–matrix adhesion [94]. Sever *et al.* [142] investigated the effect of oxygen plasma power on the ILSS of jute/high density polyethylene (HDPE) composites. They pointed out that the ILSS was increased from 30 to 60 W, showing about 32–47%

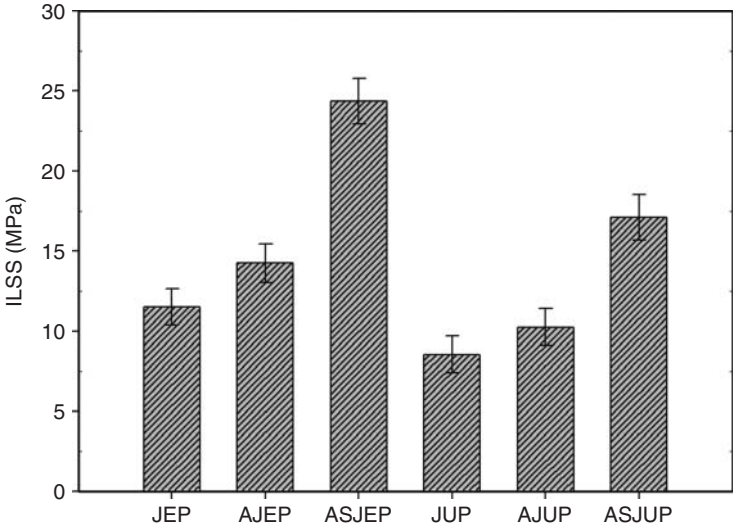

Figure 4.11 Comparison of ILSS of jute/thermoset composites with surface treatments. (After Y. Seki [53].)

improvement. The maximum ILSS value was obtained at plasma power of 60 W, beyond which the ILSS was decreased with increasing power to 90 W.

Figure 4.11 compares the ILSS values of JEP, alkali-treated jute/epoxy (AJEP), siloxane-alkali-treated jute/epoxy (ASJEP), jute/unsaturated polyester (JUP), alkali-treated jute/unsaturated polyester (AJUP), and siloxane-alkali-treated jute/unsaturated polyester (ASJUP) composites [52]. Both alkali (5 wt% NaOH, 2 h) and oligomeric siloxane (1 wt%) treatments increased the ILSS but the combined treatment (siloxane treatment additionally done after alkali treatment) improved the interfacial strength of the composite significantly. It was suggested that siloxane treatment of jute fabrics contributed more to enhance the jute fiber–thermosetting matrix adhesion.

It has been concluded from a number of studies that cellulose-based natural fibers must be chemically or physically surface treated to improve the interfacial properties of the biocomposites and consequently to increase their mechanical, thermal, and/or other relevant properties.

4.4.5
Mechanical Properties of Biocomposites

The effect of silane treatment of kenaf fibers on the mechanical properties of kenaf/PP and kenaf/UPE composites was studied, comparing with E-glass fiber composites (GFRP) fabricated under the same fiber loading, fiber length, and processing conditions [17]. Figure 4.12 shows the variation of the tensile properties measured for various kenaf/PP and kenaf/UPE composites with kenaf fibers treated at different γ-glycidoxypropyltrimethoxy silane (GPS) concentrations. The tensile

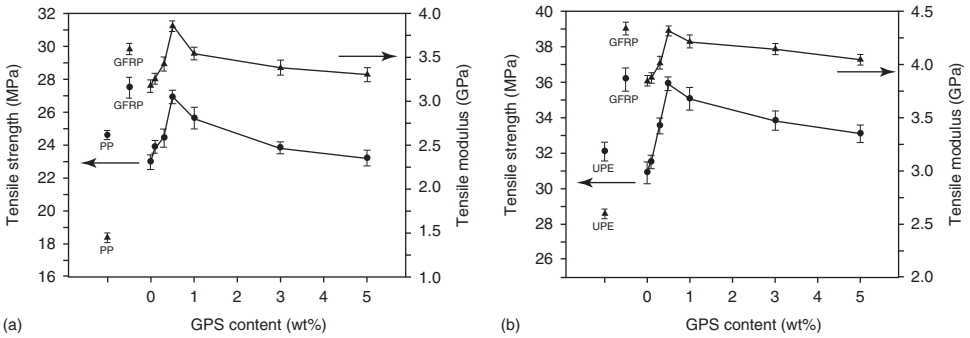

Figure 4.12 Variation of the tensile strength and modulus for (a) kenaf/PP and (b) kenaf/UPE biocomposites with kenaf fibers treated at various GPS concentrations. Each figure includes the data for PP, GFRP (E-glass/PP), and UPE, GFRP (E-glass/UPE), respectively. (After D. Cho *et al.* [17].)

strength of untreated kenaf/PP and kenaf/UPE biocomposites increased with silane treatment. The greatest improvement was attained from both composites made using kenaf fibers treated with 0.5 wt% GPS. The flexural result exhibited a similar tendency. The mechanical properties of kenaf/PP and kenaf/UPE biocomposites strongly depended on the GPS concentration. It was also noted that the greatest mechanical strength and modulus of kenaf/PP and kenaf/UPE biocomposites were comparable to those of E-glass composites with corresponding fiber length and loading.

Huda *et al.* [51] reported that the flexural modulus of kenaf/PLA biocomposites was greatly improved by incorporating kenaf fibers into PLA and further increased by using surface-treated kenaf fibers, whereas the flexural strength was decreased with kenaf fibers and it was enhanced by surface treatment, exhibiting lower strength than the untreated fibers. It was found that both silane-treated (5 wt% APS, 3 h) and alkali-treated (5 wt%, 2 h) kenaf/PLA biocomposites exhibited superior mechanical properties compared to the untreated ones. Alkali treatment followed by silane treatment of kenaf fibers showed greater improvement in mechanical properties than that achieved by a single chemical treatment (Figure 4.13).

The superior mechanical properties of biocomposites with appropriate alkali-treated natural fibers are ascribed to the increased fiber–matrix adhesion on removing the natural and artificial impurities, thereby forming roughened surfaces. As described earlier, alkali treatment may lead to fiber fibrillation, resulting in the increase surface area contactable with the polymer. Such surface roughness and increased aspect ratio by fibrillation offer better natural fiber–polymer matrix bonds [4]. In another paper [143], the effect of the addition of silane-treated- and untreated talc as filler on the mechanical properties of PLA/recycled newspaper cellulose fiber/talc hybrid composites was evaluated.

Thomas *et al.* [144] studied extensively the effect of fiber surface modification on the mechanical properties of sisal/UPE composites fabricated by RTM. Alkali,

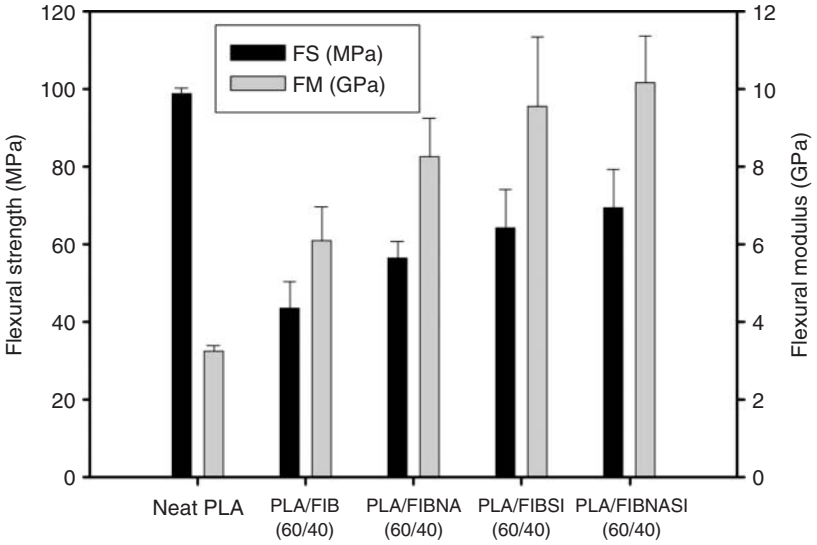

Figure 4.13 Effect of fiber treatment on the flexural properties of neat PLA and kenaf/PLA laminated biocomposites. FIB, untreated kenaf; FIBNA, alkali-treated kenaf; FIBSI, silane-treated kenaf; and FIBNASI, alkali + silane-treated kenaf. (After M.S. Huda *et al.* [51].)

permanganate, benzoylation, and silane treatments were carried out on the sisal fibers, respectively. The treatments caused a decrease in the elongation, resulting in a decrease in the ductility of the resulting composites. The tensile and flexural properties of the composites were enhanced after every treatment of sisal owing to the improvement of sisal–UPE interfacial interaction. Alkali-treated sisal/UPE composites exhibited 36% increase in tensile strength and 53% increase in Young's modulus. Silane treatment also increased the tensile strength and modulus of the composites but the increase was lower than with alkali treatment. Permanganate treatment increased the flexural strength by about 25%, whereas alkali and silane treatments showed an increase of 21% in the flexural strength. The flexural modulus was greatest in the case of silane treatment.

It was found that alkali and silane treatments also increased the tensile and flexural strength of PLA/ramie composites, exhibiting that alkali treatment (5 wt%, 3 h) is more effective than silane treatment (APS and GPS, 24 h) [145]. Oxygen plasma treatment of jute fibers improved the tensile and flexural properties of jute/HDPE composites, showing that radio frequency (RF) plasma treatment was more effective than low frequency (LF) plasma treatment up to 60 W [139]. Oligomeric siloxane treatment after alkali treatment of jute fibers resulted in an additional increase in both tensile and flexural strengths of JEP and JUP composites, compared with either alkali or silane treatment alone, resulting from the increase of fiber–matrix adhesion by surface treatment, as mentioned earlier [53].

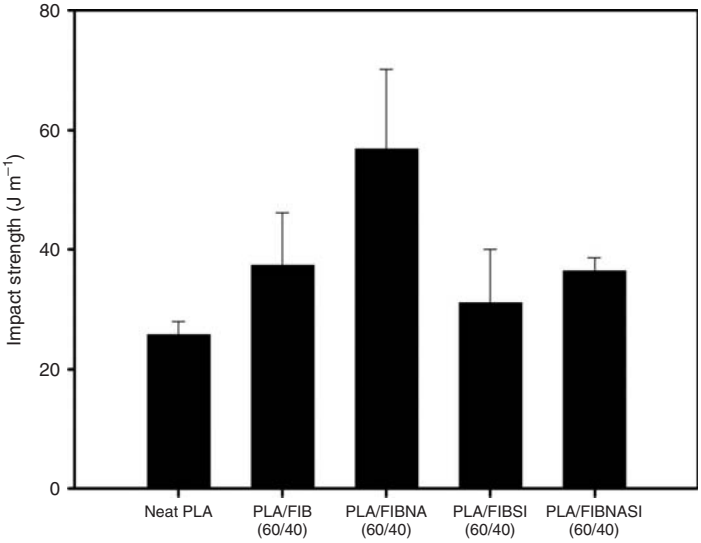

Figure 4.14 Effect of fiber treatment on the notched Izod impact strength of neat PLA and kenaf/PLA laminated biocomposites. FIB, untreated kenaf; FIBNA, alkali-treated kenaf; FIBSI, silane-treated kenaf; and FIBNASI: alkali + silane-treated kenaf. (After M.S. Huda *et al.* [51].)

4.4.6
Impact Properties of Biocomposites

The impact strength of a material is the ability of the material to absorb energy without breaking or rupture under stress applied at high speed, which is directly related to the toughness of a material. Such impact toughness is correlated with the equilibrium toughness, which is related to the area under the tensile stress–strain curve because energy absorption is the summation of all the force resistance effects within the material. In a fiber-reinforced polymer composite material, as well as in the matrix, the fibers play a very important role in impact resistance because they can interact with crack formation in the polymer matrix and act as a stress-transferring medium [19]. Therefore, the impact strength and toughness of the composites strongly depend on the reinforcing fiber, polymer matrix resin, and fiber–matrix interfacial adhesion strength and frictional work involved in pulling out the fiber from the matrix [146, 147].

Figure 4.14 indicates that the incorporation of kenaf fibers increased the Izod impact strength compared to neat PLA and the alkali treatment of kenaf further increased the strength of kenaf/PLA biocomposites with 40 wt% kenaf fiber content [51]. Silane treatment did not contribute to the enhancement of the impact strength in the case studied. The explanation for this was that the superior impact property of PLA/FIBNA was attributed to the increased fiber–matrix adhesion, the removed surface impurities, and thereby the formation of rough fiber surfaces.

Goda *et al.* [133] studied the effect of water content on the impact energy of green composites with ramie fibers and biodegradable thermoplastic resin made

from polycaprolactone and cornstarch by means of a drop weight impact testing machine. They reported that the higher the water contents, the greater the impact energy of the composites. Softening of the polymer matrix resin with increasing water content was responsible for the decreased impact strength, leading to the reduced deformation resistance and mechanical strength of the composites. In the study of kenaf fiber-reinforced soy-based biocomposites by Liu *et al.* [148], the notched Izod impact strength of compression-molded biocomposites was higher than that of injection-molded specimens; this was ascribed to the fiber-bridging effect through fiber pullout. Injection-molded specimens exhibited less fiber-bridging effect because of fiber damage by extrusion and injection moldings, whereas compression molding did not damage the fibers, resulting in a greater bridging effect and thereby a greater extent of fiber pullout.

From a large number of studies on biocomposites [19, 47, 51, 145–147], it has been understood that the impact strength may be enhanced by appropriate chemical and physical treatments of natural fibers. In fact, the improvement of the interfacial adhesion in natural fiber/polymer composite systems, which can be achieved by surface treatment, does not necessarily increase the impact properties [51, 149] as well. The impact behavior also depends on the type of natural fibers, which have different internal or cellular structures. It was reported [49, 144] that in the cases of sisal/UPE composites, various surface modifications such as alkali, silane, permanganate, and benzoylation can result in the lowering of the impact strength. Ray *et al.* [150] also observed that in composites having weak interfacial bonding the crack propagated along the fiber–matrix interface caused debonding, which could lead to a significant increase of the energy absorption ability of the composites.

4.4.7
Dynamic Mechanical Properties of Biocomposites

DMA is a very powerful method capable of providing information on the thermal mechanical behavior of polymer composites as well as viscoelastic polymer materials and the blends due to the temperature dependence of the storage modulus, loss modulus, and tan δ. The glass transition behavior, which is sensitive to molecular mobility, material stiffness, and damping behavior of a polymeric material, can be studied using DMA.

A number of dynamic mechanical studies with various biocomposites have been performed in the Drzal's group [19, 51, 143]. The storage modulus of biocomposites with reinforcing natural fibers is normally higher than that of neat polymer matrix, owing to the reinforcement effect imparted by natural fibers. In addition, appropriate surface treatments of natural fibers normally enhance the dynamic mechanical properties of biocomposites because of the increased interfacial adhesion between the fibers and the matrix, depending on the treatment method and conditions. Figure 4.15 indicates that the kenaf/PLA biocomposite specimen FIBNASI, which is alkali-treated followed by silane treatment, exhibits the greatest storage modulus

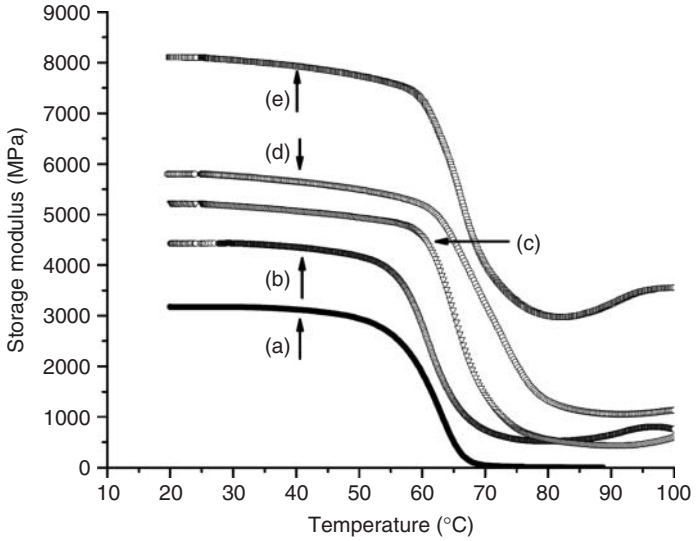

Figure 4.15 Effect of fiber treatment on the dynamic mechanical properties of neat PLA and kenaf/PLA laminated biocomposites. FIB, untreated kenaf; FIBNA, alkali-treated kenaf; FIBSI, silane-treated kenaf; and FIBNASI, alkali + silane-treated kenaf. (After M.S. Huda *et al.* [51].)

among the specimens with different types of surface treatment, reflecting agreement with the flexural modulus. Most effectively improved interfacial adhesion between the kenaf and the PLA matrix in the FIBNASI was responsible for the largely improved modulus [51].

Cho *et al.* [110] explored the effect of electron beam treatment on the dynamic mechanical properties of henequen/PP biocomposites. They reported the variation of the storage moduli measured at specified measuring temperatures (−30 °C, T_g, 25, 50, and 100 °C), as indicated in Figure 4.16. The reason for selecting such specified temperatures is as follows: −30 °C in the glassy region, T_g at glass transition temperature, 25 °C at room temperature, and also at above the glass transition, and at 50 and 100 °C, which may be possibly usable temperatures for the composite. At all the specified temperatures, the storage modulus of PP was significantly increased by incorporating chopped henequen fibers and the storage modulus of untreated henequen/PP biocomposite was obviously enhanced by the electron beam treatment of henequen at 10 kGy. Above 100 kGy, the intrinsic characteristics of natural fibers were more or less deteriorated by the given electron beam irradiation, although the moduli were likely increased because of increased fiber stiffness accompanying chain scission and severe damages at high electron beam energy. In this paper, the authors implied that raw henequen fibers should be modified with electron beam at an appropriate intensity to improve the dynamic mechanical property of henequen/PP composites as well as their interfacial and static mechanical properties. They also clarified that the electron beam treatment of the henequen fibers influenced the storage modulus of the biocomposites,

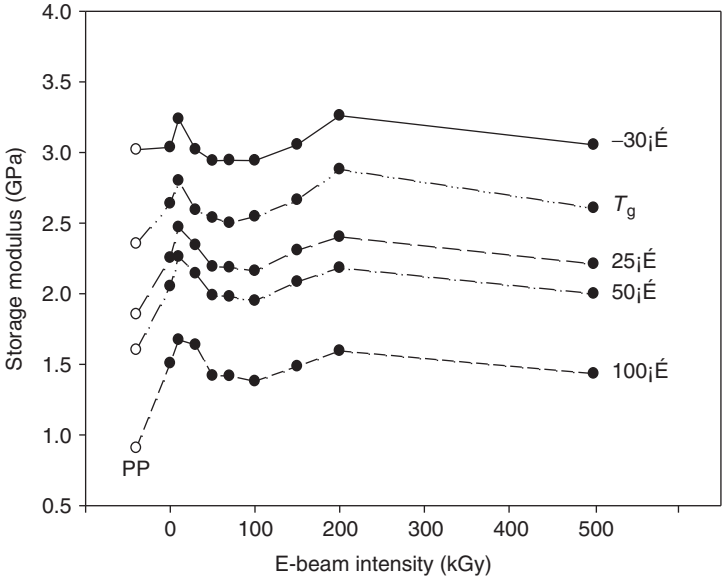

Figure 4.16 Variation of the storage moduli measured at specified measuring temperatures as a function of electron beam intensity.

displaying a similar tendency over the entire temperature range below, at, and above the T_g.

They also reported in another paper [8] that the storage modulus of PLA was largely increased by incorporating chopped jute fibers into PLA and the modulus was further increased by ultrasonic treatment with tap water. Ultrasonic treatment was more effective than soaking treatment with aqueous or alkali media. They confirmed a similar effect of the fiber treatment method with henequen/PP biocomposites [16].

Drzal *et al*. [19] studied the increasing effect on the dynamic mechanical properties of nonwoven industrial hemp fiber mat/UPE biocomposites by various chemical treatments. They also suggested that the gap in the properties between performance of glass fiber-based composites and natural fiber-based biocomposites may be bridged by fabricating a hybrid composite comprising of glass and hemp fibers. Recently, it was reported that alkali treatment was more effective than silane treatment to increase the dynamic storage modulus as well as the interfacial adhesion of ramie/PLA composites [145]. Acha *et al*. [139] studied the dynamic mechanical behavior of jute fabric/PP composites focusing on the interfacial adhesion effect of MAPP coupling agent and esterification treatment of jute with alkenyl succinic anhydride. The role of fiber–matrix interactions on the DMA properties of UPE composites chemically treated with NaOH and acetylation was also investigated at different frequencies [77]. Many other dynamic mechanical studies on different biocomposite systems were found elsewhere [6, 41, 54, 57, 139]

4.4.8
Thermal Properties of Biocomposites

It was reported that alkalization led to an increase of relative cellulose content of wheat straw fiber and exhibited increased crystallinity due to a rearrangement of the crystalline regions, resulting in an increase of degradation temperature [124]. In this paper, it was also described that acetylation had more effect on the thermal and chemical stabilities of wheat straw fiber, contributing to the formation of ester bonding, compared with alkalization.

Biocomposites comprising of natural fibers and a polymer matrix often exhibited an intermediate level of thermal stability between the natural fiber and the matrix as the thermal stability of typical cellulose-based natural fibers was lower than that of the polymer matrix used, as seen in Figure 4.17 and in other biocomposite systems [24, 52, 121]. The thermal stability of raw natural fibers may be further enhanced by surface treatments [124, 145, 151, 152]. Zhou *et al.* [18] investigated the effect of silane treatment of jute fibers on the thermal stability of jute/polycardanol biocomposites. Here polycardanol, which can be obtained from natural resources via enzymatic polymerization [153], has no volatile organic compounds (VOCs) so that it has potential as a glossy formaldehyde-free coating material and a biocomposite matrix resin. Polycardanol is normally dark brown, highly viscous, and thermally curable [154, 155]. As seen in Figure 4.17, silane-treated jute/polycardanol biocomposite exhibited slightly higher thermal stability than the untreated jute/polycardanol biocomposite. This was due mainly

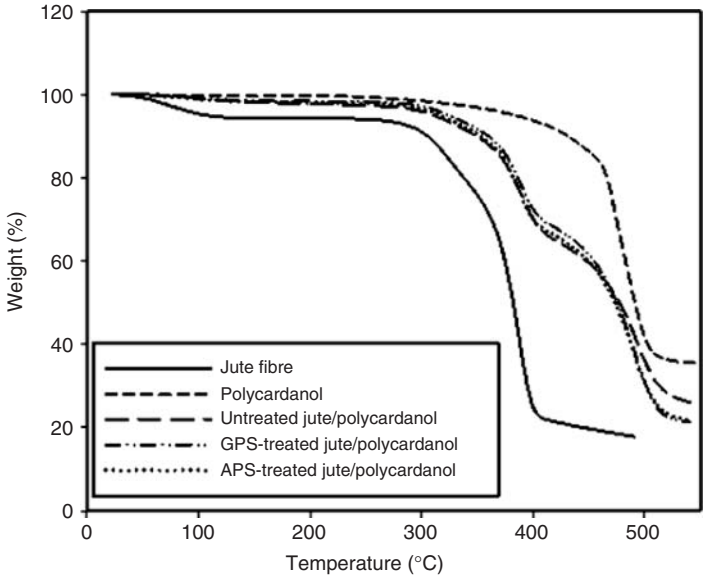

Figure 4.17 TGA curves measured for jute, polycardanol, and jute/polycardanol biocomposites with untreated and silane-treated jute fibers. (After Q. Zhou *et al.* [18].)

to the increased interfacial adhesion between the silane-treated jute fibers and the polycardanol. GPS-treated jute biocomposite showed slightly increased stability than APS-treated counterpart. The initial weight loss of about 7% starting below 100 °C was ascribed to the removal of intrinsically bound water molecules in jute fibers as likely found in other natural fibers.

It was observed that the weight losses about 310–320 °C and near 380 °C were ascribed to the thermal decomposition of hemicellulose and α-cellulose, respectively. The TGA result indicated that the hemicellulose component of natural fiber was not removed by silane treatment, unlike in alkali treatment [18].

Heat deflection temperature (HDT) is defined as the temperature at which a plastic or composite material deflects by 0.25 mm under the application of a load of 66 psi [148]. HDT is a key property in selecting materials for commercial and industrial applications. Therefore, manufacturers often optimize fiber size and length, fiber content, and the processing method to improve the HDT of composites. One of the main drawbacks of PLA is low heat HDT of about 55–65 °C depending on the grade version. The HDT can be significantly improved by introducing natural fibers into the PLA resin. Generally, a greater aspect ratio of the fiber may lead to a greater improvement of HDT. It was reported [156] that the HDT of neat PLA was markedly increased from 56 to 136–142 °C by incorporating jute fibers or fabrics into the PLA, as indicated in Figure 4.18. Such a large improvement of HDT was

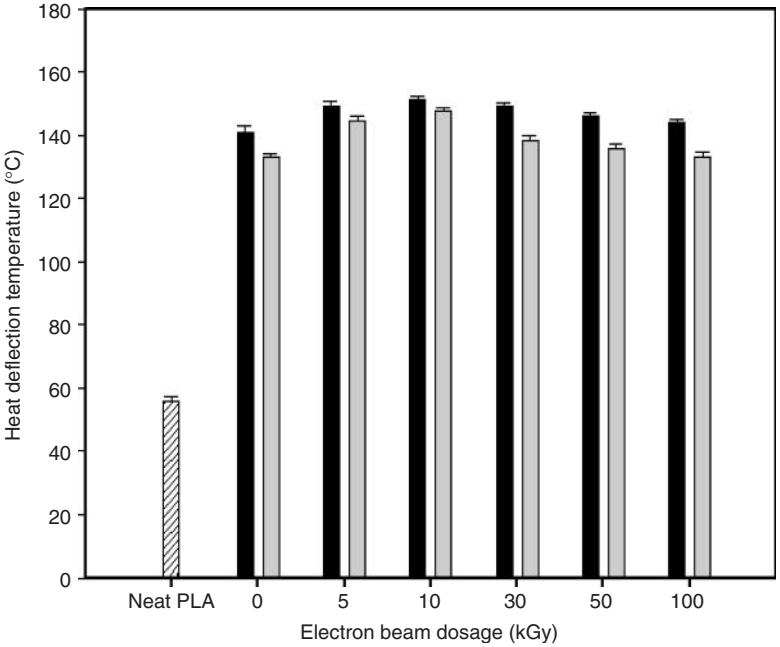

Figure 4.18 A comparison of heat deflection temperatures measured for neat PLA and random and 2D jute/PLA green composites with jute treated at different electron beam dosages. (After S.G. Ji *et al.* [156].)

due mainly to the reinforcing effect of jute fibers and fabrics distributed in the PLA matrix. In addition, the HDT of PLA biocomposites reinforced with chopped jute fibers or woven jute fabrics was further increased by the electron beam treatment of jute, particularly at 10 kGy. It was also found that randomly oriented jute/PLA biocomposites exhibited slightly greater HDT than two-directionally oriented jute/PLA counterparts, reflecting that the HDT result showed the dependence of the chopped jute fibers distributed in the through-the-thick direction of the specimen.

The HDT of PLA was also greatly improved up to about 170 °C by introducing and surface treating kenaf fibers into PLA, as found by the Drzal's research group [51]. They also reported that the HDT of soy flour-based biocomposites can be increased about 36 °C based on the processing methods, compared to the control. A paper [145] reported that the Vicat softening temperatures of ramie/PLA composites with alkali or silane treatment are higher than that of composites with untreated fibers. The explanation for this was that the improvement was ascribed mainly to the increase in modulus as well as the fiber–matrix interaction by surface treatment of ramie fibers.

It was reported that the thermal stability of ramie/PLA biocomposites treated with flame-retardant ammonium polyphosphate (APP) of 5 wt% was increased with a greater char formation in the high temperature region above about 360 °C but was decreased in the low temperature region below about 350 °C because of removed gases from APP during the measurement [157].

It was found by Cho's research group [24] that the thermal expansion of neat poly(butylene succinate) dramatically reduced by reinforcing it with chopped silk fibers, which are animal-based natural fibers, without any surface treatment or modification, indicating much improved dimensional stability of silk/PBS biocomposites, as seen in Figure 4.19. The linear coefficients of thermal expansion (CTE) were 294×10^{-6} °C^{-1} for neat PBS and 10×10^{-6} to 52×10^{-6} °C^{-1} for silk/PBS biocomposites, depending on the fiber content incorporated. This result implied that such a reduction of the CTE may be further performed by enhancing the fiber–matrix adhesion through optional surface modification of raw silk fibers.

4.4.9 Water Absorption Behavior of Biocomposites

All polymer composites absorb substantial amounts of moisture or water in humid environment as well as in water. The most important concern in indoor and outdoor applications of natural fiber-based biocomposites with polymer matrices is their sensitivity to water absorption, which can reduce considerably their mechanical, physical, and thermal properties and performances. The water absorption of biocomposites results in the debonding or gap in the natural fiber–polymer matrix interfacial region, leading to poor stress transfer efficiency from the matrix to the fiber and reduced mechanical and dimensional stabilities as well [158]. It has been known that the hemicellulose component in cellulose-based natural fibers may be mainly responsible for water absorption because it is more susceptible to water molecules than the crystalline cellulose component. Also, poor interfacial adhesion

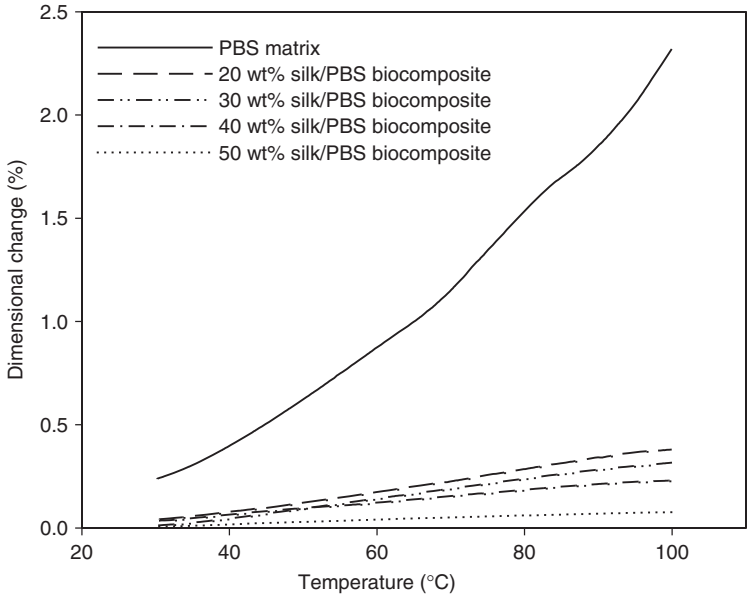

Figure 4.19 Thermal expansion behavior of PBS and silk/PBS biocomposites with various silk fiber contents as a function of temperature, measured using thermomechanical analysis (TMA). (After S.M. Lee *et al.* [24].)

between hydrophilic natural fibers, with polar nature, and hydrophobic polymer matrices, with nonpolar nature, is the main reason for poor water absorption resistance of biocomposites. As a result, a number of studies [60, 76, 120, 147, 152, 158, 159] have been performed to understand the water absorption behavior and also to alleviate the extent of water uptake in different types of biocomposites.

In hemp/UPE composites studied by Dhakal *et al.* [158], moisture uptake increased with increasing the fiber volume fraction because of increased voids and cellulose content therein. The authors pointed out that the higher and faster weight gain due to the water absorbed upon exposure to boiling water or elevated temperature water than to room temperature water may be attributed to the different diffusivity of water into the composite material, resulting in moisture-induced interfacial cracks at an accelerated rate and thereby degradation in the fiber–matrix interfacial region and significant drops in the tensile and flexural properties.

In order to eliminate the hemicellulose component and, consequently, to increase the water absorption resistance, alkali treatment of natural fibers has often been conducted in diverse biocomposite systems, for example, sisal/phenolic [120] and natural fiber/glass fiber hybrid UPE [76]. Mishra *et al.* [76] reported that the water absorption of pineapple leaf fiber/glass hybrid and sisal/glass hybrid composites was 7% less than that of the unhybridized composites and the absorption was further reduced by 6% by fiber surface treatments before composite processing, compared with the untreated fiber/glass hybrid composites.

In addition, many other approaches for treating the surfaces of natural fibers such as coupling agents, polymer coating, enzyme modification, and acetylation to increase the water absorption resistance through the improvement of fiber–matrix interfacial properties have been attempted [60, 147, 152, 159].

Qin *et al*. [152] reported that poly(butyl acrylate) (PBA), adsorbed and coated on rice straw fibers, reduced the water absorption of the PLA/rice straw fiber composite as PBA is hydrophobic. They suggested that there was an optimal content of the PBA coating and too high amount of coating may result in the poor interfacial adhesion between PLA and rice straw fibers. Bledzki *et al*. [147] stressed that the equilibrium moisture contents of enzyme (fungamix)-modified abaca fiber/PP and coupling agent MAPP-modified abaca fiber/PP composites were respectively 45% and 35% lower than that of the unmodified counterpart, respectively, after a long period of testing time for 90 days.

Lee and Wang [159] studied the water absorption characteristics of PLA/bamboo and PBS/bamboo biocomposites with the bio-based coupling agent, lysine-based diisocyanate (LDI). They reported that the LDI treatment made the water absorption difficult, this being evidenced by the improvement of the interfacial adhesion between the hydrophobic PLA and PBS polymers and hydrophilic bamboo fibers due to the coupling effect of LDI and the reaction of LDI with hydroxyl groups in the polymers, resulting in less hydrophilicity of bamboo fibers. The increase in the content of bamboo fiber, which has stronger hydrophilicity, increased the water absorption rate.

4.5 Concluding Remarks

There have been a large number of papers and reports on research and development of biocomposite materials predominantly with plant-based natural fibers such as kenaf, jute, hemp, flax, ramie, sisal, henequen, bamboo, and wood and occasionally with animal-based natural fibers such as silk and wool. The main polymer resins utilized in biocomposites are PP, polyethylene, UPE, phenolic, epoxy, rubbers, PLA, PBS, and so on. In fact, the properties and performances of biocomposites are quite variable with polymer matrix, natural fiber type, fiber quality, fiber length, fiber orientation, fiber loading, surface treatment method and condition, processing technique, and so on. Biocomposites have potential to replace glass fiber composites on both a performance and cost basis [4]. The potential may not be satisfactorily established without further property improvement. With proper natural fiber treatments, biocomposites may provide increased stiffness and thermomechanical properties but, on the other hand, the ductility and the tensile strength may be reduced [160]. Lack of good interfacial adhesion between the natural fibers and the polymers, low mechanical properties, and high water absorption make the use of biocomposites less attractive. Consequently, research has been focused on the surface treatment or modification of natural fibers to improve their mechanical, thermal, and physical properties as well as their interfacial properties. Chemical

treatment methods, which are most widely used, are a rewarding way to improve the properties of biocomposites whereas physical treatment methods, which may be currently used in the lab scale, are a promising way to improve the properties. Each method has some advantages and disadvantages, as noted. Industries are interested in simpler, cheaper, and faster processes, suitable for industrial adoption. With increasing social consciousness and global awareness, both academia and industries should also consider labor-friendly, environmentally friendly, and high-valued processes for the twenty-first century materials. In addition, it is necessary to maintain a constant product quality. Less expensive surface treatment should be used for biocomposites to replace glass fiber composites in current and potential applications in the future [161].

In recent years, a considerable amount of research and development on biodegradable polymer resins and the biocomposites has been performed in many research laboratories all over the world. At present, the major applications of biocomposites are in the automobile and construction sectors. With the development of high performance biocomposites, their applications will be extended to many more areas. Designing desirable biocomposite materials through optimal surface treatment or modification of natural fibers is a necessity from the engineering viewpoint.

References

1. Cho, D., Lee, S.G., Park, W.H., and Han, S.O. (2002) Eco-friendly biocomposite materials using biofibers. *Polym. Sci. Technol.*, **13**, 460–476.
2. Joshi, S.V., Drzal, L.T., Mohanty, A.K., and Arora, S. (2004) Are natural fiber composites environmentally superior to glass fiber reinforced composites? *Composites Part A*, **35**, 371–378.
3. Fisher, R. (2006) Natural fibers and green composites. *Compos. Manuf.*, **March**, 20–23.
4. Mohanty, A.K., Misra, M., and Drzal, L.T. (2001) Surface modifications of natural fibers and performance of the resulting biocomposites: an overview. *Compos. Interfaces*, **8** (5), 313–343.
5. Mohanty, A.K., Misra, M., and Hinrichsen, G. (2000) Biofibers, biodegradable polymers and biocomposites: an overview. *Macromol. Mater. Eng.*, **276–277**, 1–24.
6. Nishino, K., Hirao, K., Kotera, M., Nakamae, K., and Inagaki, H. (2003) Kenaf reinforced biodegradable composite. *Compos. Sci. Technol.*, **63**, 1281–1286.
7. Oksman, K., Skrifvars, M., and Selin, J.-F. (2003) Natural fibres as reinforcement in polylactic acid (PLA) composites. *Compos. Sci. Technol.*, **63**, 1317–1324.
8. Seo, J.M., Cho, D., Park, W.H., Han, S.O., Hwang, T.W., Choi, C.H., and Jung, S.J. (2007) Fiber surface treatments for improvement of the interfacial adhesion and flexural and thermal properties of jute/poly(lactic acid) biocomposites. *J. Biobased Mater. Bioenergy*, **1**, 331–340.
9. Müssig, J. (2010) *Industrial Applications of Natural Fibres: Structure, Properties and Technical Applications*, John Wiley & Sons, Ltd, Chichester.
10. Mohanty, A.K., Misra, M., and Drzal, L.T. (2005) *Natural Fibers, Biopolymers, and Biocomposites*, Taylor & Francis, Boca Raton, FL.
11. Mukhopadhyay, S. and Fangueiro, R. (2009) Physical modification of natural fibers and thermoplastic films for composites–a review. *J. Thermoplast. Compos. Mater.*, **22**, 135–162.

12. Lackey, E., Inamdar, K., Vaughan, J., and O'Haver, J. (2008) Fiber treatment for hemp fiber using pultrusion. *SAMPE J.*, **44** (3), 67–77.
13. Herrera-Franco, P.J. and Valadez-González, A. (2005) in *Fiber-Matrix Adhesion in Natural Fiber Composites in Natural Fibers, Biopolymers, and Biocomposites* (eds A.K. Mohanty, M. Misra, and L.T. Drzal), Taylor & Francis, Boca Raton, FL, pp. 177–230.
14. Aziz, S.H., Ansell, M.P., Clarke, S.J., and Panteny, S.R. (2005) Modified polyester resin for natural fibre composites. *Compos. Sci. Technol.*, **65**, 525–535.
15. Han, S.O., Cho, D., Park, W.H., and Drzal, L.T. (2006) Henequen/poly(butylene succinate) biocomposites: electron beam irradiation effects on henequen fiber and the interfacial properties of biocomposites. *Compos. Interfaces*, **13**, 231–247.
16. Lee, H.S., Cho, D., and Han, S.O. (2008) Effect of natural fiber surface treatments on the interfacial and mechanical properties of henequen/polypropylene biocomposites. *Macromol. Res.*, **16**, 411–417.
17. Cho, D., Lee, H.S., and Han, S.O. (2009) Effect of fiber surface modification on the interfacial and mechanical properties of kenaf fiber-reinforced thermoplastic and thermosetting polymer composites. *Compos. Interfaces*, **16**, 711–729.
18. Zhou, Q., Cho, D., Song, B.K., and Kim, H.-J. (2009) Novel jute/polycardanol biocomposites: effect of fiber surface treatment on their properties. *Compos. Interfaces*, **16**, 781–795.
19. Mehta, G., Drzal, L.T., Mohanty, A.K., and Misra, M. (2006) Effect of fiber surface treatment on the properties of biocomposites from nonwoven industrial hemp fiber mats and unsaturated polyester resin. *J. Appl. Polym. Sci.*, **99**, 1055–1068.
20. Arbelaiz, A., Cantero, G., Fernandez, B., Mondragon, I., Ganan, P., and Kenny, J.M. (2005) Flax fiber surface modifications: effects on fiber physico mechanical and flax/polypropylene interface properties. *Polym. Compos.*, **February**, 324–332.
21. Bledzki, A.K., Reihmane, S., and Gassan, J. (1996) Properties and modification methods for vegetable fibers for natural fiber composites. *J. Appl. Polym. Sci.*, **59**, 1329–1336.
22. George, J., Sreekala, M.S., and Thomas, S. (2001) A review on interface modification and characterization of natural fiber reinforced plastic composites. *Polym. Eng. Sci.*, **41**, 1471–1485.
23. Strong, A.B. (2008) *Fundamentals of Composites Manufacturing: Materials, Methods, and Applications*, 2nd edn, Society for Manufacturing Engineer, Dearborn.
24. Lee, S.M., Cho, D., Park, W.H., Lee, S.G., Han, S.O., and Drzal, L.T. (2005) Novel silk/poly(butylene succinate) biocomposites: the effect of short fiber content on their mechanical and thermal properties. *Compos. Sci. Technol.*, **65**, 647–657.
25. Lee, S.M., Han, S.O., Cho, D., Park, W.H., and Lee, S.G. (2005) Influence of chopped fiber length on the mechanical and thermal properties of silk fiber-reinforced poly(butylene succinate) biocomposites. *Polym. Polym. Compos.*, **13**, 479–488.
26. Drzal, L.T., Rich, M.J., and Lloyd, P.F. (1983) Adhesion of graphite fibers to epoxy matrices. Part I. The role of fiber surface treatment. *J. Adhes.*, **16**, 1–30.
27. Drzal, L.T. and Madhukar, M. (1993) Fiber-matrix adhesion and its relationship to composite mechanical properties. *J. Mater. Sci.*, **28**, 569–610.
28. Xie, Y., Hill, C.A.S., Xia, Z., Militz, H., and Mai, C. (2010) Silane coupling agents used for natural fiber/polymer composites: a review. *Composites Part A*, **41**, 806–819.
29. Cho, D. and Kim, H.-J. (2009) Naturally cyclable biocomposites. *Elast. Compos.*, **44** (1), 13–21.
30. Prasad, S.V., Pavithran, C., and Rohatgi, P.K. (1983) Alkali treatment of coir fibres for coir-polyester composites. *J. Mater. Sci.*, **18**, 1443–1454.

31. Owolabi, O., Ozvikovzki, T., and Kovacs, I. (1985) Coconut-fiber-reinforced thermosetting plastics. *J. Appl. Polym. Sci.*, **30**, 1827–1836.
32. Chand, N. and Rohatgi, P.K. (1986) Adhesion of sisal fiber-polyester system. *Polym. Compos.*, **27**, 157–160.
33. Tsuji, W., Nakao, T., Ohigashi, K., Maegawa, K., Kobayashi, N., Shukri, S., Kasai, S., and Miyanaga, K. (1986) Chemical modification of cotton fiber by alkali-swelling and substitution reactions-acetylation, cyanoethylation, benzoylation, and oleoylation. *J. Appl. Polym. Sci.*, **32**, 5175–5192.
34. Bisanda, E.T.N. and Ansell, M.P. (1991) The effect of silane treatment on the mechanical and physical properties of sisal-epoxy composites. *Compos. Sci. Technol.*, **41**, 165–178.
35. Geethamma, V.G., Joseph, R., and Thomas, S. (1995) Short coir fiber-reinforced natural rubber composites: effects of fiber length, orientation, and alkali treatment. *J. Appl. Polym. Sci.*, **55**, 583–594.
36. Sreekala, M.S., Kumaran, M.G., and Thomas, S. (1997) Oil palm fibers: morphology, chemical composition, surface modification, and mechanical properties. *J. Appl. Polym. Sci.*, **66**, 821–835.
37. Kalia, S., Kaith, B.S., and Kaur, I. (2009) Pretreatments of natural fibers and their application as reinforcing material in polymer composites-a review. *Polym. Eng. Sci.*, **49**, 1253–1272.
38. Gassan, J. and Bledzki, A.K. (1999) Possibilities for improving the mechanical properties of jute/epoxy composites by alkali treatment of fibres. *Compos. Sci. Technol.*, **59**, 1303–1309.
39. Sreenivasan, S., Bahama, I.P., and Krishnan, K.R.I. (1996) Influence of delignification and alkali treatment on the fine structure of coir fibres (Cocos Nucifera). *J. Mater. Sci.*, **31**, 721–726.
40. de Albuquerque, A.C., Joseph, K., de Carvalho, L.H., and d'Almeida, J.R.M. (2000) Effect of wettability and ageing conditions on the physical and mechanical properties of uniaxially oriented jute-roving-reinforced polyester composites. *Compos. Sci. Technol.*, **60**, 833–844.
41. Ray, D., Sarkar, B.K., Das, S., and Rana, A.K. (2002) Dynamic mechanical and thermal analysis of vinylester-rein-matrix composites reinforced with untreated and alkali-treated jute fibres. *Compos. Sci. Technol.*, **62**, 911–917.
42. Cao, Y., Shibata, S., and Fukumoto, I. (2006) Mechanical properties of biodegradable composites reinforced with bagasse fibre and after alkali treatments. *Composites Part A*, **37**, 421–429.
43. Han, Y.H., Han, S.O., Cho, D., and Kim, H.-I. (2007) Kenaf/polypropylene biocomposites: effects of electron beam irradiation and alkali treatment on kenaf natural fibers. *Compos. Interfaces*, **14**, 559–578.
44. Ishiaku, U.S., Yang, X.Y., Leong, Y.W., Hamada, H., Semba, T., and Kitagawa, K. (2007) Effects of fiber content and alkali treatment on the mechanical and morphological properties of poly(lactic acid)/poly(caprolactone) blend jute fiber-filled biodegradable composites. *J. Biobased Mater. Bioenergy*, **1**, 78–86.
45. Pickering, K.L., Li, Y., Farrell, R.L., and Lay, M. (2007) Interfacial modification of hemp fiber reinforced composites using fungal and alkali treatment. *J. Biobased Mater. Bioenergy*, **1**, 109–117.
46. Balnois, E., Busnel, F., Baley, C., and Grohens, Y. (2007) An AFM study of the effect of chemical treatments on the surface microstructure and adhesion properties of flax fibres. *Compos. Interfaces*, **14**, 715–731.
47. Kushwaha, P. and Kumar, R. (2009) Enhanced mechanical strength of BFRP composites using modified bamboos. *J. Reinf. Plast. Compos.*, **28**, 2851–2859.
48. Suizu, N., Uno, T., Goda, K., and Ohgi, J. (2009) Tensile and impact properties of fully green composites reinforced with mercerized ramie fibers. *J. Mater. Sci.*, **44**, 2477–2482.
49. Favaro, S.L., Lopes, M.S., de Carvalho Neto, A.G.V., de Santana, R.R., and Radovanovic, E. (2010) Chemical, morphological, and

mechanical analysis of rice husk/post-consumer polyethylene composites. *Composites Part A*, **41**, 154–160.
50. Athijayamani, A., Thiruchitrambalam, M., Natarajan, U., and Pazhanivel, B. (2010) Influence of alkali-treated fibers on the mechanical properties and machinability of roselle and sisal fiber hybrid polyester composites. *Polym. Compos.*, **31**, 723–731.
51. Huda, M.S., Drzal, L.T., Mohanty, A.K., and Misra, M. (2008) Effect of fiber surface-treatments on the properties of laminated biocomposites from poly(lactic acid) (PLA) and kenaf fibers. *Compos. Sci. Technol.*, **68**, 424–432.
52. Threepopnatkul, P., Kaerkitcha, N., and Athipongarporn, N. (2009) Effect of surface treatment on performance of pineapple leaf fiber-polycarbonate composites. *Composites Part B*, **40**, 628–632.
53. Seki, Y. (2009) Innovative multifunctional siloxane treatment of jute fiber surface and its effect on the mechanical properties of jute/thermoset composites. *Mater. Sci. Eng., A*, **508**, 247–252.
54. Wu, H.F., Dwight, D.W., and Huff, N.T. (1997) Effects of silane coupling agents on the interphase and performance of glass-fiber-reinforced polymer composites. *Compos. Sci. Technol.*, **57**, 975–983.
55. Park, J.M., Subramanian, R.V., and Bayoumi, A.E. (1994) Interfacial shear strength and durability improvement by silanes in single-filament composite specimens of basalt fiber in brittle phenolic and isocyanate resins. *J. Adhes. Sci. Technol.*, **8**, 133–150.
56. Plueddemann, E.P. (1991) *Silane Coupling Agents*, 2nd edn, Plenum Press, New York.
57. Abdelmouleh, M., Boufi, S., Belgacem, M.N., Dufresne, A., and Gandini, A. (2005) Modification of cellulose fibers with functionalized silanes: effect of the fiber treatment on the mechanical performances of cellulose-thermoset composites. *J. Appl. Polym. Sci.*, **98**, 974–984.
58. Herrera-Franco, P.J. and Valadez-González, A. (2004) Mechanical properties of continuous natural fibre-reinforced polymer composites. *Composites Part A*, **35**, 339–345.
59. Salon, M.-C.B., Abdelmouleh, M., Boufi, S., Belgacem, M.N., and Gandini, A. (2005) Silane adsorption onto cellulose fibers: hydrolysis and condensation reactions. *J. Colloid Interface Sci.*, **289**, 249–261.
60. Abdelmouleh, M., Boufi, S., Belgacem, M.N., and Dufresne, A. (2006) Short natural-fibre reinforced polyethylene and natural rubber composites: effect of silane coupling agents and fibres loading. *Compos. Sci. Technol.*, **67**, 1627–1639.
61. Maziad, N.A., El-Nashar, D.E., and Sadek, E.M. (2009) The effect of a silane coupling agent on properties of rice husk-filled maleic acid anhydride compatibilized natural rubber/low-density polyethylene blend. *J. Mater. Sci.*, **44**, 2665–2673.
62. Kushwaha, P. and Kumar, R. (2009) Effect of silanes on mechanical properties of bamboo fiber-epoxy composites. *J. Reinf. Plast. Compos.*, **29**, 718–724.
63. Xu, Y., Kawata, S., Hosoi, K., Kawai, T., and Kurota, S. (2009) Thermomechanical properties of the silanized-kenaf/polystyrene composites. *Express Polym. Lett.*, **3**, 657–664.
64. Marsyahyo, E., Rochardjo, H.S.B., and Seokrisno (2009) Preliminary investigation on bulletproof panels made from ramie fiber reinforced composites for NIJ Level II, IIA, and IV. *J. Ind. Text.*, **39**, 13–26.
65. Herrera-Franco, P.J. and Valadez-González, A. (2005) A study of the mechanical properties of short natural-fiber reinforced polymer composites. *Composites Part B*, **36**, 597–608.
66. Towo, A.N. and Ansell, M.P. (2008) Fatigue evaluation and dynamic mechanical thermal analysis of sisal fibre-thermosetting resin composites. *Compos. Sci. Technol.*, **68**, 925–932.
67. Tesoro, G. and Wu, Y. (1991) Silane coupling agents: the role of the organofunctional group. *J. Adhes. Sci. Technol.*, **5**, 771–784.

68. Salon, M.C.B., Gerbaud, G., Abdelmouleh, M., Bruzzese, C., Boufi, S., and Belgacem, M.N. (2007) Studies of interactions between silane coupling agents and cellulose fibers with liquid and solid-state NMR. *Magn. Reson. Chem.*, **45**, 473–483.

69. Arkles, B., Steinmetz, J.R., Zazyczny, J., and Mehta, P. (1992) Factors contributing to the stability of alkoxysilanes in aqueous solution. *J. Adhes. Sci. Technol.*, **6**, 193–206.

70. Sreekala, M.S., Kumaran, M.G., Joseph, S., Jacob, M., and Thomas, S. (2000) Oil palm fibre reinforced phenol formaldehyde composites: influence of fibre surface modifications on the mechanical performance. *Appl. Compos. Mater.*, **7**, 295–329.

71. Matuana, I.M., Woodhams, R.T., Balatinecz, J.I., and Park, C.B. (1998) Influence of interfacial interactions on the properties of PVC/cellulosic fiber composites. *Polym. Compos.*, **19**, 446–455.

72. Pothan, L.A. and Thomas, S. (2003) Polarity parameters and dynamic mechanical behaviours of chemically modified banana fiber reinforced polyester composites. *Compos. Sci. Technol.*, **63**, 1231–1240.

73. Anderson, M. and Tillman, A.M. (1989) Acetylation of jute: effects on strength, rot resistance, and hydrophobicity. *J. Appl. Polym. Sci.*, **37**, 3437–3447.

74. Hill, C.A.S., Khalil, A., and Hale, M.D. (1998) A study of the potential of acetylation to improve the properties of plant fibre. *Ind. Crops. Prod.*, **8**, 53–63.

75. Nair, K.C.M., Thomas, S., and Groeninckx, G. (2001) Thermal and dynamic mechanical analysis of polystyrene composites reinforced with short sisal fibres. *Compos. Sci. Technol.*, **61**, 2519–2529.

76. Mishra, S., Mohanty, A.K., Drzal, L.T., Misra, M., Parija, S., Nayak, S.K., and Tripathy, S.S. (2003) Studies on mechanical performance of biofibre/glass reinforced polyester hybrid composites. *Compos. Sci. Technol.*, **63**, 1377–1385.

77. Pothan, L.A., Thomas, S., and Groeninckx, G. (2006) The role of fibre/matrix interactions on the dynamic mechanical properties of chemically modified banana fibre/polyester composites. *Composites Part A*, **37**, 1260–1269.

78. Paul, S.A., Boudenne, A., Ibos, L., Candau, Y., Joseph, K., and Thomas, S. (2008) Effect of fiber loading and chemical treatments on thermophysical properties of banana fiber/polypropylene commingled composite materials. *Composites Part A*, **39**, 1582–1588.

79. Nair, K.C.M., Diwan, S.M., and Thomas, S. (1996) Tensile properties of short sisal fiber reinforced polystyrene composites. *J. Appl. Polym. Sci.*, **60**, 1483–1491.

80. Nair, K.C.M. and Thomas, S. (2003) Effect of interface modification on the mechanical properties of polystyrene-sisal fiber composites. *Polym. Compos.*, **24**, 332–343.

81. Lu, X., Zhang, M.Q., Rong, M.Z., Shi, G., and Yang, G.C. (2002) All-plant fiber composites. I: unidirectional sisal fiber reinforced benzylated wood. *Polym. Compos.*, **23**, 624–633.

82. Lu, X., Zhang, M.Q., Rong, M.Z., Yue, D.L., and Yang, G.C. (2004) Environmental degradability of self-reinforced composites made from sisal. *Compos. Sci. Technol.*, **64**, 1301–1310.

83. Feng, D., Caulfield, D.F., and Sanadi, A.R. (2001) Effect of compatibilizer on the structure–property relationships of kenaf-fiber/polypropylene composites. *Polym. Compos.*, **22**, 506–517.

84. Fung, K.L., Li, R.K.Y., and Tjong, S.C. (2002) Interface modification on the properties of sisal fiber-reinforced polypropylene composites. *J. Appl. Polym. Sci.*, **85**, 169–176.

85. Rana, A.K., Mandal, A., and Bandyopadhyay, S. (2003) Short jute fibre reinforced polypropylene composites: effect of compatibilizer, impact modifier and fibre loading. *Compos. Sci. Technol.*, **63**, 801–806.

86. Arbelaiz, A., Cantero, G., Fernández, B., and Mondragon, I. (2005) Flax fiber surface modifications: effects on fiber physic mechanical and flax/polypropylene interface properties. *Polym. Compos.*, **26**, 324–332.

87. Doan, T.-T.-L., Gao, S.-L., and Mäder, E. (2006) Jute/polypropylene composites I. Effect of matrix modification. *Compos. Sci. Technol.*, **66**, 952–963.
88. Mechraoui, A., Riedl, B., and Rodgrigue, D. (2007) The effect of fibre and coupling agent content on the mechanical properties of hemp/polypropylene composites. *Compos. Interfaces*, **14**, 837–848.
89. Snijder, M.H.B. and Bos, H.L. (2000) Reinforcement of polypropylene by annual plant fibers. Optimization of the coupling agent efficiency. *Compos. Interfaces*, **7**, 69–75.
90. Lee, S., Shi, S., Groom, L.H., and Xue, Y. (2010) Properties of unidirectional kenaf fiber-polyolefin laminates. *Polym. Compos.*, **31**, 1067–1074.
91. Sreekala, M.S., Kumaran, M.G., and Thomas, S. (2002) Water sorption in oil palm fibre reinforced phenol formaldehyde composites. *Composites Part A*, **33**, 763–777.
92. Mittal, K.L. (ed.) (2000) *Polymer Surface Modification: Relevance to Adhesion*, Vol. 2, VSP, Utrecht.
93. Wakida, T. and Tokino, S. (1996) Surface modification of fiber and polymeric materials by discharge treatment and its application to textile processing. *Ind. J. Fiber Text. Res.*, **21**, 69–79.
94. Sinha, E. and Panigrahi, S. (2009) Effect of plasma treatment on structure, wettability of jute fiber and flexural strength of its composites. *J. Compos. Mater.*, **43**, 1791–1802.
95. Yuan, X., Jayaraman, K., and Bhattacharyya, D. (2004) Mechanical properties of plasma-treated sisal fibre-reinforced polypropylene composites. *J. Adhes. Sci. Technol.*, **18**, 1027–1045.
96. Ahlbad, G. and Kron, A. (1994) Effect of plasma treatment on mechanical properties of rubber/cellulose fibre composites. *Polym. Int.*, **33**, 103–109.
97. Chu, B.Y., Kwon, M.Y., Lee, S.G., Cho, D., Park, W.H., and Han, S.O. (2004) Interfacial adhesion of silk/PLA biocomposites by plasma surface treatment. *J. Adhes. Interface*, **5** (4), 9–16.
98. Marias, S., Gouanve, F., Bonnesoeur, A., Grenet, J., Poncin-Epaillard, F., Morvan, C., and Metayeret, M. (2005) Unsaturated polyester composites reinforced with flax fibers: effect of cold plasma and autoclave treatments on mechanical and permeation properties. *Composites Part A*, **36**, 975–986.
99. Sinha, E. (2009) Effect of cold plasma treatment on macromolecular structure, thermal and mechanical behavior of jute fiber. *J. Ind. Text.*, **38**, 317–339.
100. Goa, S. and Zeng, Y. (1993) Surface modification of ultrahigh molecular weight polyethylene fibers by plasma treatment. I. Improving surface adhesion. *J. Appl. Polym. Sci.*, **47**, 2065–2071.
101. Belgacem, M.N., Bataille, P., and Sapieha, S. (1994) Effect of corona modification on cellulose/PP composites. *J. Appl. Polym. Sci.*, **53**, 379–385.
102. Dong, S., Sapieha, S., and Schreiber, H.P. (1992) Effect of corona discharge on cellulose polyethylene composites. *Polym. Eng. Sci.*, **32**, 1737–1741.
103. Gassan, J. and Gutowski, S. (2000) Effects of corona discharge and UV treatment on the properties of jute-fiber epoxy composites. *Compos. Sci. Technol.*, **60**, 2857–2863.
104. Zenkiewicz, M. (2004) Effects of electron-beam irradiation on some mechanical properties of polymer films. *Radiat. Phys. Chem.*, **69**, 373–378.
105. Pang, Y., Cho, D., Han, S.O., and Park, W.H. (2005) Interfacial shear strength and thermal properties of electron beam-treated henequen fibers reinforced unsaturated polyester composites. *Macromol. Res.*, **13**, 453–459.
106. Kondo, Y., Miyazaki, K., Yamaguchi, Y., Sasaki, T., Irie, S., and Sakurai, K. (2006) Mechanical properties of fiber reinforced styrene-butadiene rubbers using surface-modified UHMWPE fibers under EB irradiation. *Eur. Polym. J.*, **42**, 1008–1014.
107. Ji, S.G., Cho, D., and Lee, B.C. (2010) Chemical and thermal characterization of electron beam irradiated jute fibers. *J. Adhes. Interface*, **11** (4), 162–167.

108. Pruzinec, J., Kadlecik, J., Varga, S., and Pivovarnicek, F. (1981) Study of the effect of high-energy radiation on cellulose. *Radiochem. Radioanal. Lett.*, **49**, 395–404.

109. Cho, D., Lee, H.S., Han, S.O., and Drzal, L.T. (2007) Effects of E-beam treatment on the interfacial and mechanical properties of henequen/polypropylene biocomposites. *Adv. Compos. Mater.*, **16** (4), 315–334.

110. Ji, S.G., Park, W.H., Cho, D., and Lee, B.C. (2010) Electron beam effect on the tensile properties and topology of jute fibers and the interfacial strength of jute-PLA green composites. *Macromol. Res.*, **18**, 919–922.

111. Takacs, E., Wojnarovits, L., Foldvary, C., Hargittai, P., Borsa, J., and Sajo, I. (2000) Effect of combined gamma-irradiation and alkali treatment on cotton-cellulose. *Radiat. Phys. Chem.*, **57**, 399–403.

112. Han, Y.H., Han, S.O., Cho, D., and Kim, H.-I. (2006) Henequen/unsaturated polyester biocomposites: electron beam irradiation treatment and alkali treatment effects on the henequen fiber. *Macromol. Symp.*, **245–246**, 539–548.

113. Khan, M.A., Shehrzade, S., and Hassan, M.M. (2004) Effect of alkali and ultraviolet (UV) radiation pretreatment on physical and mechanical properties of 1,6-hexanediol diacrylate-grafted jute yarn by UV radiation. *J. Appl. Polym. Sci.*, **92**, 18–24.

114. Rahman, M.M. and Khan, M.A. (2007) Surface treatment of coir (Cocos nucifera) fibers and its influence on the fibers' physic-mechanical properties. *Compos. Sci. Technol.*, **67**, 2369–2376.

115. Willems, P. (1962) Kinematic high-frequency and ultrasonic treatment of pulp. *Pulp Pap. Mag. Can.*, **63**, T455–T462.

116. Cho, D., Yoon, S.B., and Drzal, L.T. (2009) Cellulose-based natural fiber topography and the interfacial shear strength of henequen/unsaturated polyester composites: influence of water and alkali treatments. *Compos. Interfaces*, **16**, 769–779.

117. Ouajai, S. and Shanks, R.A. (2005) Composition, structure and thermal degradation of hemp cellulose after chemical treatments. *Polym. Degrad. Stab.*, **89**, 327–335.

118. Han, S.O. and Jung, Y.M. (2008) Characterization of henequen natural fiber by using two-dimensional correlation spectroscopy. *J. Mol. Struct.*, **883–884**, 142–148.

119. Oh, S.Y., Yoo, D.I., Shin, Y., and Seo, G. (2005) FRIR analysis of cellulose treated with sodium hydroxide and carbon dioxide. *Carbohydr. Res.*, **340**, 417–428.

120. Botaro, V.R., Siqueira, G., Megiatto, Jr., J.D., and Frollini, E. (2010) Sisal fibers treated with NaOH and benzophenonetetracarboxylic dianhydride as reinforcement of phenolic resin. *J. Appl. Polym. Sci.*, **115**, 269–276.

121. Cho, D., Lee, S.M., Lee, S.G., and Park, W.H. (2006) Effect of acetylation and plasma treatment on the interfacial and thermal properties of poly(3-hydroxybutyrate-co-3-hydroxyvalerate)/woven flax fabric biocomposites. *Am. J. Appl. Sci.* (Special Issue: Bio-compatible and Bio-composite Materials), 17–24.

122. Lee, S.G., Choi, S.-S., Park, W.H., and Cho, D. (2003) Characterization of surface modified flax fibers and their biocomposites with PHB. *Macromol. Symp.*, **197**, 89–99.

123. Sever, K., Erden, S., Gülec, H.A., Seki, Y., and Sarikanat, M. (2011) Oxygen plasma treatments of jute fibers in improving the mechanical properties of jute/HDPE composites. *Mater. Chem. Phys.*, **129**, 275–280.

124. Pan, M.-Z., Zhou, D.-G., Deng, J., and Zhang, S.Y. (2009) Preparation and properties of wheat straw fiber-polypropylene composites. I. Investigation of surface treatments on the wheat straw fiber. *J. Appl. Polym. Sci.*, **114**, 3049–3056.

125. Liu, L., Yu, J., Cheng, L., and Qu, W. (2009) Mechanical properties of poly(butylene succinate) (PBS) biocomposites reinforced with surface modified jute fibre. *Composites Part A*, **40**, 669–674.

126. Seo, J.M., Cho, D., and Park, W.H. (2008) Alkali treatment of kenaf fibers on the characteristics of kenaf/PLA biocomposites. *J. Adhes. Interface*, **9** (4), 1–11.

127. Rong, M.Z., Zhong, M.Q., Liu, Y., Yang, G.G., and Zheng, H.M. (2001) The effect of fiber treatment on the mechanical properties of unidirectional sisal-reinforced epoxy composites. *Compos. Sci. Technol.*, **61**, 1437–1447.

128. Rout, J., Misra, M., Tripathy, S.S., Nayak, R.K., and Mohanty, A.K. (2001) Novel eco-friendly biodegradable coir-polyester amide biocomposites: fabrication and properties evaluation. *Polym. Compos.*, **22**, 770–778.

129. Alawar, A., Hamed, A.M., and Al-Kaabi, K. (2009) Characterization of treated date palm tree fiber as composite reinforcement. *Composites Part B*, **40**, 601–606.

130. Haque, M.M., Hasan, M., Islam, M.S., and Ali, M.E. (2009) Physic-mechanical properties of chemically treated palm and coir fiber reinforced polypropylene composites. *Bioresour. Technol.*, **100**, 4903–4906.

131. Okubo, K., Fujii, T., and Thostenson, E.T. (2009) Multi-scale hybrid biocomposite: processing and mechanical characterization of bamboo fiber reinforced PLA with microfibrillated cellulose. *Composites Part A*, **40**, 469–475.

132. Paul, S.A., Joseph, K., Mathew, G.D.G., Pothen, L.A., and Thomas, S. (2010) Influence of polarity parameters on the mechanical properties of composites from polypropylene fiber and short banana fiber. *Composites Part A*, **41**, 1380–1387.

133. Goda, K., Sreekala, M.S., Gomes, A., Kaji, T., and Ohgi, J. (2006) Improvement of plant based natural fibers for toughening green composites–effect of load application during mercerization of ramie fibers. *Composites Part A*, **37**, 2213–2220.

134. Beckermann, G.W. and Pickering, K.L. (2008) Engineering and evaluation of hemp fibre reinforced polypropylene composites: fibre treatment and matrix modification. *Composites Part A*, **39**, 979–988.

135. Ganan, P. and Mondragon, I. (2002) Surface modification of fique fibers, effects on their physic-mechanical properties. *Polym. Compos.*, **23**, 383–394.

136. Ray, D. and Sarkar, B.K. (2001) Characterization of alkali-treated jute fibers for physical and mechanical properties. *J. Appl. Polym. Sci.*, **80**, 1013–1020.

137. Cho, D., Choi, Y., and Drzal, L.T. (2003) Characterization, properties, and processing of LaRC PETI-5 as a high-temperature sizing material. III. Adhesion enhancement of carbon/BMI composites. *J. Adhes.*, **79**, 1–23.

138. Cho, D., Yun, S.H., Kim, J., Lim, S., Park, M., Lee, S.-S., and Lee, G.-W. (2004) Influence of silane coupling agents on the interlaminar and thermal properties of woven glass fabric/nylon 6 composites. *Macromol. Res.*, **12**, 119–126.

139. Acha, B.A., Reboredo, M.M., and Marcovich, N.E. (2007) Creep and dynamic mechanical behavior of PP-jute composites: effect of the interfacial adhesion. *Composites Part A*, **38**, 1507–1516.

140. Ji, S.G., Hwang, J.H., Cho, D., and Lee, B.C. (2010) A role of modification of jute fibers by electron beam irradiation in jute/PLA green composites. Proceedings of the Sixth International Workshop on Green Composites (IWGC-6), Gumi, Korea, September 8–10, 2010, p. 139–142.

141. Ahmed, K.S. and Vijayarangan, S. (2008) Tensile, flexural and interlaminar shear properties of woven jute and jute-glass fabric reinforced polyester composites. *J. Mater. Process. Technol.*, **207**, 330–335.

142. Sever, K., Erden, S., Gülec, H.A., Seki, Y., and Sarikanat, M. (2011) Oxygen plasma treatments of jute fibers in improving the mechanical properties of jute/HDPE composites. *Mater. Chem. Phys.*, **129**, 275–280.

143. Huda, M.S., Drzal, L.T., Mohanty, A.K., and Misra, M. (2007) The effect of silane treated- and untreated-talc on the mechanical and physic-mechanical properties of poly(lactic acid)/newspaper fibers/talc hybrid

composites. *Composites Part B*, **38**, 367–379.

144. Sreekumar, P.A., Thomas, S.P., Saiter, J.M., Joseph, K., Unnikrishnan, G., and Thomas, S. (2009) Effect of fiber surface modification on the mechanical and water absorption characteristics of sisal/polyester composites fabricated by resin transfer molding. *Composites Part A*, **40**, 1777–1784.

145. Yu, T., Ren, J., Li, S., Yuan, H., and Li, Y. (2010) Effect of fiber surface-treatments on the properties of poly(lactic acid)/ramie composites. *Composites Part A*, **41**, 499–505.

146. Huda, M.S., Drzal, L.T., and Misra, M. (2005) A study on biocomposites from recycled newspaper fiber and poly(lactic acid). *Ind. Eng. Chem. Res.*, **44**, 5593–5601.

147. Bledzki, A.K., Mamun, A.A., Jaszkiewicz, A., and Erdmann, K. (2010) Propylene composites with enzyme modified abaca fibre. *Compos. Sci. Technol.*, **70**, 854–860.

148. Liu, W., Drzal, L.T., Mohanty, A.K., and Misra, M. (2006) Influence of processing methods and fiber length on physical properties of kenaf fiber reinforced soy based biocomposites. *Composites Part B*, **38**, 352–359.

149. Pinho, S.T., Iannucci, L., and Robinson, P. (2006) Physically-based failure models and criteria for laminated fiber reinforced composites with emphasis on fiber kinking: part I: development. *Composites Part A*, **37**, 63–73.

150. Ray, D., Sarkar, B.K., Rana, A.K., and Bose, N.R. (2001) The mechanical properties of vinylester resin matrix composites reinforced with alkali-treated jute fibers. *Composites Part A*, **32**, 119–127.

151. Han, Y.H., Han, S.O., Cho, D., and Kim, H.-I. (2008) Dynamic mechanical properties of natural fiber/polymer biocomposites: the effect of fiber treatment with electron beam. *Macromol. Res.*, **16**, 253–260.

152. Qin, L., Qin, J., Liu, M., Dong, S., Shao, L., Lu, S., Zhang, G., Zhao, Y., and Fu, X. (2011) Mechanical and thermal properties of poly(lactic acid) composites with rice straw fiber modified by poly(butyl acrylate). *Chem. Eng. J.*, **166**, 772–778.

153. Kim, Y.H., Won, K., Kwon, J.M., Jeong, H.S., Park, S.Y., An, E.S., and Song, B.K. (2005) Synthesis of polycardanol from a renewable resource using a fungal peroxidase from Coprinus cinereus. *J. Mol. Catal. B: Enzym.*, **34**, 33–38.

154. Zhou, Q., Cho, D., Song, B.K., and Kim, H.-J. (2010) Curing behavior of polycardanol by MEKP and cobalt naphthenate using differential scanning calorimetry. *J. Therm. Anal. Calorim.*, **99**, 277–284.

155. Zhou, Q., Cho, D., Park, W.H., Song, B.K., and Kim, H.-J. (2011) FT-IR studies on the curing behavior of polycardanol from naturally renewable resources. *J. Appl. Polym. Sci.*, **122**, 2774–2778.

156. Ji, S. G., Hwang, J. H., Cho, D., Kim, H.-J. (2013) Influence of electron beam treatment of jute on the thermal properties of random and two-directional jute/poly(lactic acid) green composites. *J. Adhes. Sci. Technol.*, **27**, 1359–1373.

157. Li, S., Ren, J., Yuan, H., Yu, T., and Yuan, W. (2009) Influence of ammonium polyphosphate on the flame retardancy and mechanical properties of ramie fiber-reinforced poly(lactic acid) biocomposites. *Polym. Int.*, **59**, 242–248.

158. Dhakal, H.N., Zhang, Z.Y., and Richardson, M.O.W. (2007) Effect of water absorption on the mechanical properties of hemp fibre reinforced unsaturated polyester composites. *Compos. Sci. Technol.*, **67**, 1674–1683.

159. Lee, S.-H. and Wang, S. (2006) Biodegradable polymers/bamboo fiber biocomposite with bio-based coupling agent. *Composites Part A*, **37**, 80–91.

160. La Mantia, F.P. and Morreale, M. (2011) Green composites: a brief review. *Composites Part A*, **42**, 579–588.

161. Fowler, P.A., Hughes, J.M., and Elias, R.M. (2006) Biocomposites: technology, environmental credentials and market forces. *J. Sci. Food Agric.*, **86**, 1781–1789.

5
Manufacturing and Processing Methods of Biocomposites

5.1
Processing Technology of Natural Fiber-Reinforced Thermoplastic Composite

Tatsuya Tanaka

5.1.1
Background

Global measures for reducing the levels of CO_2 gas, which has been identified as a cause of global warming, have begun to be implemented as discussed in the Session of the Conference of the Parties to the United Nations Framework Convention on Climate Change (COP). Since resin parts are manufactured from fossil fuels in most processes, the regulations that control the use of the fossil fuels are being enforced. For example, the resin waste produced in a factory has to be necessarily recycled. Furthermore, once poly(ethylene terephthalate) (PET) bottles and automobile bumpers are commercially marketed, they are collected again at the end of their useful life for recycling in factories. They are used as raw materials for other products by being combined with other materials or by modifying and improving their properties.

In recent years, biodegradable resins have been manufactured at plants without the use of fossil fuels. These biodegradable resins take in CO_2 from the atmosphere by photosynthesis at the time of growth, and after being used, they are decomposed and return to the soil. Therefore, these resins are also called *cyclical form materials*, an example being poly(lactic acid) (PLA), which is beginning to be adopted in the manufacture of resin products. This move toward a sustainable society is primarily taking place in the automobile industry.

As shown in Figure 5.1, Toyota Motor has a developed a concept for the manufacture of a nuclear fuel from the ethanol extracted from plants. This concept includes polymerization of biomaterials to PLA resin, followed by the fabrication of automobile parts [1]. However, when only PLA resin is used with the substitution of polypropylene resin (PP), which is currently in wide use in the manufacture of automobile parts, results in limitations to mechanical properties, such as shock resistance and heat resistance. Therefore, as it is difficult to apply the PLA resin to automobile parts, there has been little increase in demand.

Polymer Composite: Volume 3, First Edition.
Edited by Sabu Thomas, Kuruvilla Joseph, S. K. Malhotra, Koichi Goda and M. S. Sreekala.

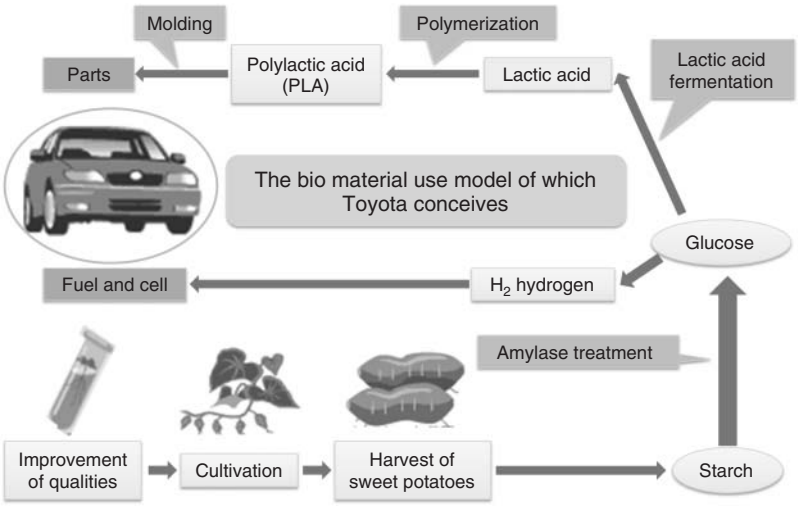

Figure 5.1 The using model biomaterial as conceived by Toyota.

On the other hand, natural fiber (NF), which uses plant materials and fixes CO_2 similarly to the PLA resin, has attracted attention as a reinforcement fiber that can substitute the conventional glass fiber (GF). It is for this reason that compounding an NF and PLA resin does not deviate from the carbon-neutral concept. Jute fiber, kenaf fiber, and bamboo fiber (BF) are examples of NFs. An example of the use of a composite material with PLA resin reinforcement with the kenaf fiber for automobile parts is shown in Figure 5.2 [2–8]. If the technology for obtaining nuclear fuel from ethanol and manufacturing automobile parts from PLA resin in considerable quantities takes off successfully, it is expected that this will enable the construction of a sustainable society.

Figure 5.2 PLA compound material parts reinforced with kenaf fiber.

5.1.2
NF- Reinforced PLA Resin Composite Material

The methods for improving the mechanical properties of Natural fiber-reinforced PLA resin matrix composite materials (NFRTP) are discussed later. We now take up the issue of hydrolysis, which is the cause for reduction in the mechanical properties of PLA resin. The molecular weight of PLA resin decreases during hydrolysis and a decrease in molecular weight of the resin reduces its mechanical properties considerably. Generally, in the case of a polyester resin system, the amount of moisture needs to be less than 50 ppm for preventing hydrolysis. However, NF is made from plant materials and plants usually contain about 10% of moisture. As mentioned above, when NF is used as the strengthening fiber of a PLA resin, it can easily be imagined how the influence of the moisture contained in the NF initiates hydrolysis in the PLA resin.

On the other hand, it is possible to use BF which is also NF, as a reinforcement fiber for the PLA resin, using the conventional compound technology. However, there is almost no literature in which improvement in the mechanical properties of BF-reinforced PLA resin composite material is reported [9, 10]. In addition, hydrolysis of the PLA resin is not discussed in these articles, either. One reason that the mechanical properties of the composite material did not improve is the degradation owing to decrease in molecular weight of PLA resin, and this is considered to have greater influence rather than reinforcement of the PLA resin by BF. However, there is very little research that has offered clarification into the influence that hydrolysis of the PLA resin has on a composite material.

Usually, when mixing other substances (e.g., particles and a fiber) with a resin, the resin is heated to a temperature higher than its melting point and its viscosity is lowered. Here, the melting temperature of PLA resin is 170 °C. So, in order to make the resin distribute NF well, it is necessary to heat the resin to about 200 °C more than its melting temperature. However, NF, which consists of a cellulose, a hemicellulose, and lignin starts thermal decomposition above 200 °C [11]. This is the main causes for degradation of the NF and reduction in its strength. For these two reasons, if an NF-reinforced PLA resin compound material is manufactured by the conventional mixing method, it turns out that heating to the temperature required poses a the big problem.

5.1.3
Pellet Production Technology of Continuation Fiber-Reinforced Thermoplastic Resin Composite Material

The filament pellet (hereafter referred to as *LFP*) reinforced with the continuous fiber was invented at ICI (Britain) in the early 1980s [12]. GF and carbon fiber (CF) were used as a continuous fibers. Furthermore, as flexibility was high, nylon (PA, polyamide) and PP resin were applied to the matrix resin. In the late 1980s, many resin and GF manufacturers in Japan, the United States, and Europe started to develop an epoch-making fiber-strengthening resin compound material. However,

on the technical side, the problem was that the strength of the mold used for production was insufficient to overcome for the fiber breakage that took place when injection molding was carried out. On the other hand, in the legal field, there were ongoing disputes over the basic patent for this technology. Therefore, as expected, the status quo during which there was no expansion into the commercial scene continued for 20 years or more. In the meantime, there was a global integration of the resin manufacturing industry. As a result, reexamination of the technological strategy was made by the individual companies. Since expansion of the commercial scene of LFP was not acceptable, many makers gave up the idea of development. However, expansion of the global market started at the same time that the right of the basic patent expired in 2002. In addition, by coincidence, in Japan, the front-end modular component, which is one of the large-sized automobile parts, began to be manufactured by LFP [13]. The mold production of LFP was beginning to be applied focusing on lightweight automobile parts and aiming at energy savings [14, 15]. The difference in the fiber distribution states of LFP and short fiber pellet (SFP) is typically shown in Figure 5.3.

The NF-LFP production method introduced here was developed in Kobe Steel Ltd. In Kobe Steel, development of the process began in mid-1980s with the objective of manufacturing GF- or CF-reinforced thermoplastic (TP) resin pellets. In addition, Kobe Steel became a commercial supplier of LFP material from the middle of the 1990s to around 2000. However, since the market expansion of GF- or CF-strengthening LFP as mentioned above, a new business development in this area was given up. On the other hand, market research for considering the development of other reinforcement fibers began around the year 2000. As a result,

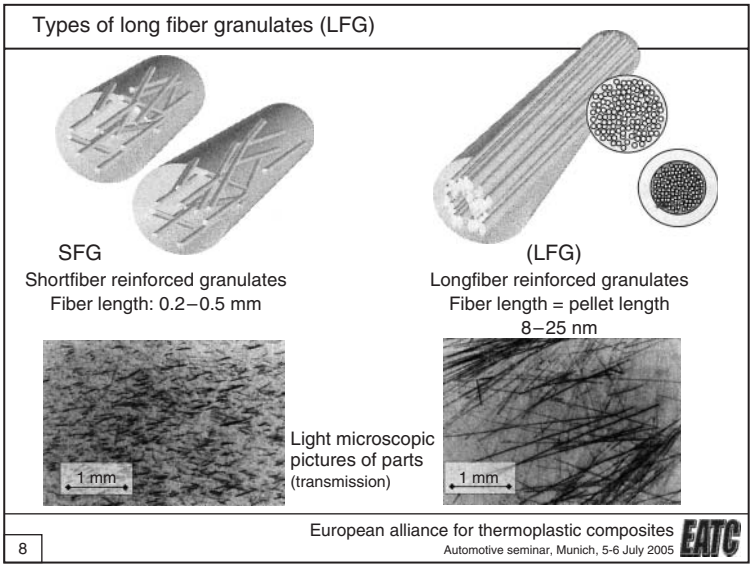

Figure 5.3 The mimetic diagram of the difference in the fiber distribution states of LFP (LFG, long fiber-reinforced granulates) and SFP (SFG, short fiber-reinforced granulates) [14].

the development of organic fibers such as nylon or PET fibers as well as NF such as jute and kenaf fibers was considered. The manufacturing technology of the TP resin pellet (NF-LFP) was strengthened with the manufacture of continuous NF, which is cotton yarn, by an original twist technology [16, 17].

5.1.4 Pellet Manufacturing Technology of the Continuous Natural Fiber–Reinforced Thermoplastic Resin Composite Material

In this section, the review of the manufacturing technology of NF-LFP is described [18, 19]. First, the different fiber reinforcement configurations in the resin and the relationship between the aspect ratio of the fiber and the mechanical properties are shown in Figure 5.4. The feature of LFP is that the strengthening fiber is arranged along the direction of the long axis of the pellet. The fundamental manufacturing process is described in the following.

5.1.4.1 Process Outline

The LFP manufacturing system developed by Kobe Steel makes use of injection molding. LFP is also manufactured by the strand (rod)-cutting method, in which the reinforcement fiber is arranged along the direction of a long axis to predetermined arbitrary length (usually 3–15 mm). The feature of this process is that it carries impregnation of the TP resin into various reinforcement fibers. When NF is especially made into a reinforcement fiber, the resin temperature control during impregnation is important because of the low heat resistance of NF.

5.1.4.2 Review of Mechanical Apparatus

This LFP manufacturing process consists of six main steps described below. Although the process by which a strand is taken over in parallel is the same as in the conventional system (as shown in Figure 5.5 [17]), the configuration of the impregnation die head and the taking over system are quite different. Here, the

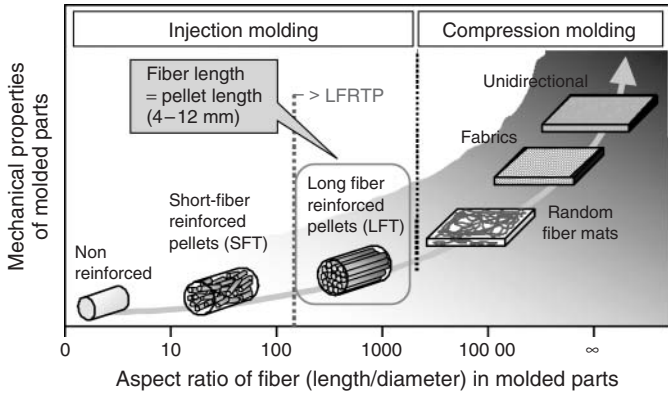

Figure 5.4 Effect of fiber aspect ratio on mechanical properties of FRTP.

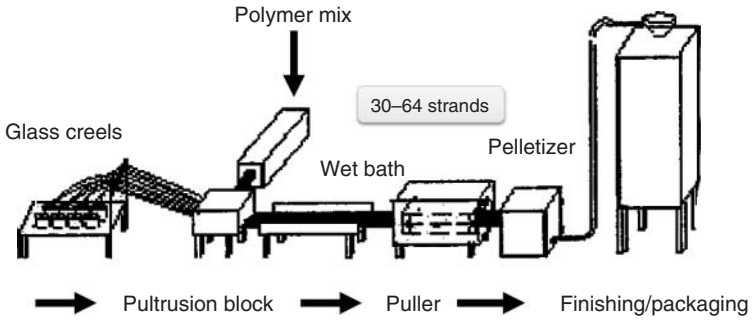

Figure 5.5 Conventional LFP manufacture system (parallel taking over system).

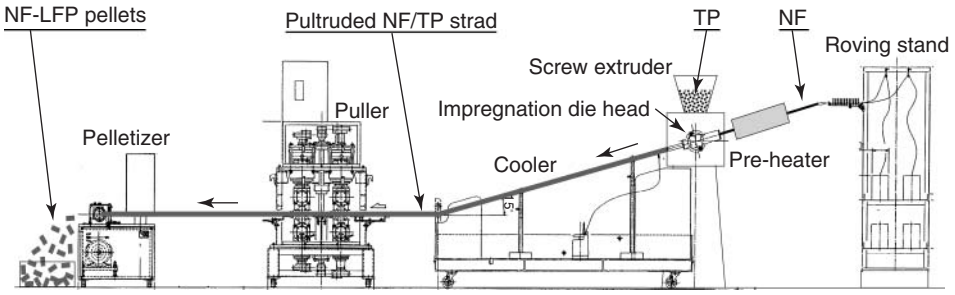

Figure 5.6 Flow chart of the reinforced NF (natural fiber) and TP (thermoplastic) resin.

system for labs aiming at material development and its process flow (Figure 5.5) are shown in Figure 5.6. In this figure, the steps by with which a reinforcement fiber and resin are united are shown. A photograph of the trial production system is shown in Figure 5.7. The parts that constitute the system by which LFP is manufactured continuously are described below.

1) Roving stand table (the step of sending out reinforcement fiber)
2) Twin-screw extruder (TSE) (the step of melting and a refining for TP resin by the kneading action)
3) Impregnating die head (the step of impregnating TP resin to reinforcement fiber)
4) Cooling water tank (the step of cooling a strand)
5) Takeover equipment (the step of applying a twist to a strand while applying a tension regulator to the reinforcement fiber)
6) Pelletizer (the step of cutting a strand into pellets).

As shown in Figure 5.7, the reinforcement fiber is sent out from (1). On the other hand, the resin, which is melted by (2), is impregnated into the space between the reinforcement fibers by passing it through (3). The strand that comes out of (3) has an internal structure in which the reinforcement fiber is arranged in one direction. The strand is the solidified simultaneously with cooling during passage through (4). The strand is then twisted by the twist mechanism of (5). Finally, the strand

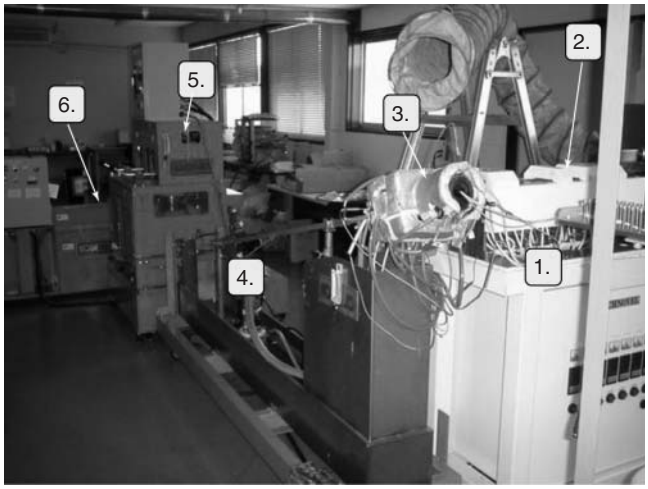

Figure 5.7 Photograph of the trial production system for LFP manufacture. (1) Roving stand, (2) twin screw extruder, (3) impregnation die head, (4) cooler, (5) puller, and (6) pelletizer.

is cut into pellets of arbitrary lengths in (6) and the LFP for injection molding is obtained.

5.1.4.3 Main Equipment

5.1.4.3.1 Twin-Screw Extruder

The intermeshing, noncounter-rotating TSE is used to melt the resin. The advantage of using TSE is that the LFP to which resin materials are applied are used for the manufacture of a wide range of general engineering plastics.

1) Since the screw speed can be adjusted regardless of the throughput of resin, the resin is kneaded at the optimal temperature.
2) If a peroxide is added to a PP of high viscosity, a PP of low viscosity, which has improved mobility, will be obtained. As a result, it becomes possible to lower the cost of resin materials.
3) It is possible to add a denaturing agent to the resin in order to improve the wettability of the resin–reinforcement fiber interface.
4) Since a compound of the resin and filler is possible, the resin is refined simultaneously.
5) If the direct dry extrusion technology by degassing is used, the dry step involving hydrolytic resin is skipped.

5.1.4.3.2 Impregnating Die Head

Kobe Steel have developed a unique special impregnation die head, whereby impregnation can also use twisted NF, such as cotton yarn, which had been difficult to use as reinforcement fiber in the conventional impregnation processes.

During the process of impregnation of the resin into the reinforcement fiber, the surface of each fiber is enough covered by the resin. Very good resin impregnation of LFP is possible as a result. Since the resin has fully adhered to the fiber, its mechanical properties improve. Furthermore, as a nonimpregnated fiber does not disperse, LFP does cause problems in the hopper of an injection-molding machine. Since the parts that constitute an impregnation writing head can be substituted, the maintenance process of changing a resin or dealing with a break in the fiber is quite simple. This means that normal operation can be resumed in a short time, without cessation in the manufacturing process in the case that there are two or more production lines.

5.1.4.3.3 The Taking over System and Pelletizer

Kobe Steel originally developed originally the strand takeover system to which the twist function was subsequently attached. By development of this system, the tow rope resistance in which the reinforcement fiber passes through the outlet of an impregnation die head was reduced. As a result, the high-speed takeover of the stable strand became possible. For example, in the assembly consisting of GF content 50 wt% and PP, a track record, in which the strand was taken over at the rate of 100 m min^{-1}, has been demonstrated. The details of the takeover method are described elsewhere.

Thus, by attaining a high throughput, even if the manufacturing cost of LFP is high compared with that of the TP resin pellet strengthened with the conventional short fiber, its production was sufficiently competitive.

5.1.4.4 Process Features

If the Kobe Steel LFP manufacture system is used, even if it uses cotton yarn such as NF, LFP such as GF and CF, which are mono filaments, can be easily manufactured. The reason is that the TP resin is of high viscosity and can easily impregnate inside NF as described in detail in the following.

There are two kinds of direction in cotton yarn twisting – the S-twist and the Z-twist. In S-twist, the fiber bundle is twisted in the direction of the right screw, whereas in the Z-twist, it is twisted in the direction of the left screw. The method developed in the impregnation system uses the difference between the S-twist and the Z-twist. The steps of the resin impregnation method into cotton yarn are shown in Figure 5.8. The case where jute fiber is used as the NF is especially illustrated here. This is because the productivity of jute fiber is high and it is inexpensive. Moreover, it is imported in stable condition and its mechanical properties are also excellent.

Generally, jute fiber bundle is made of the Z-twist. Therefore, when the rotation direction of a strand is taken over as that of an S-twist, the fiber bundle is twisted in the reverse direction and is thus loosened within the impregnation diehead. The NF then simultaneously unites with TP resin within the impregnation diehead. As a result, the resin impregnates into the inside of the fiber bundle. Furthermore, as a twist is added in the direction of S, a strand of S-twist is obtained.

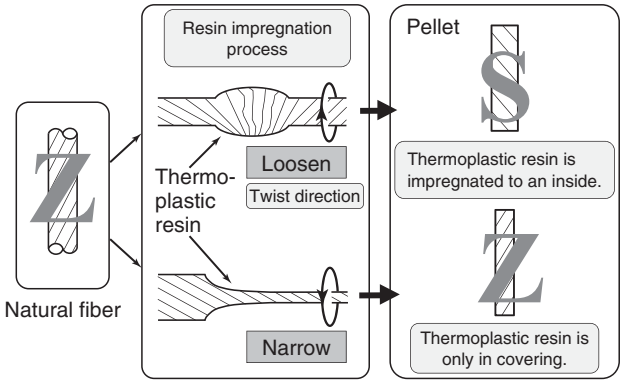

Figure 5.8 Comparison of PP resin impregnated by the difference in the twist direction of the fiber.

The fiber bundle does not get loosened when the rotation direction of a strand taken is in the direction of a Z-twist. Therefore, the resin is not impregnated in the inside of the fiber bundle.

In that case, a strand of Z-twist with which only the surface covered with resin is obtained.

In the production method of the TP resin compound material in which NF is the reinforcement fiber, the difference between the conventional system and this system is illustrated in Figure 5.9. The big difference between the two systems is the holding time for which the reinforcement fiber is exposed to high temperature within the resin. NF is composed of cellulose, hemicellulose, and lignin. Moreover, these clearly begin a thermal decomposition at around 200 °C, which is the general melting temperature of a TP resin. If the conventional system is used, NF will

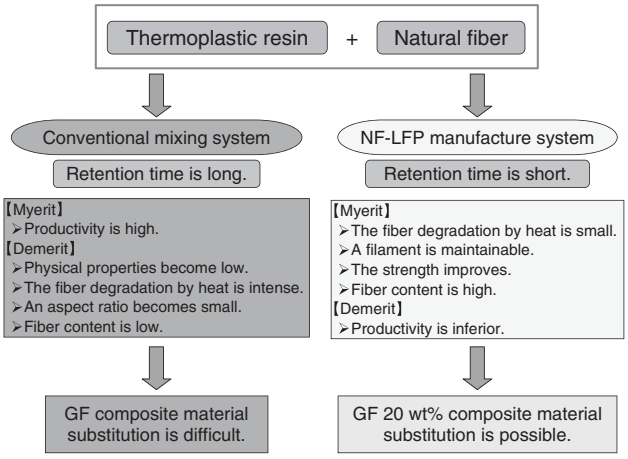

Figure 5.9 Comparison of the conventional mixing system and the NF-LFP manufacture system.

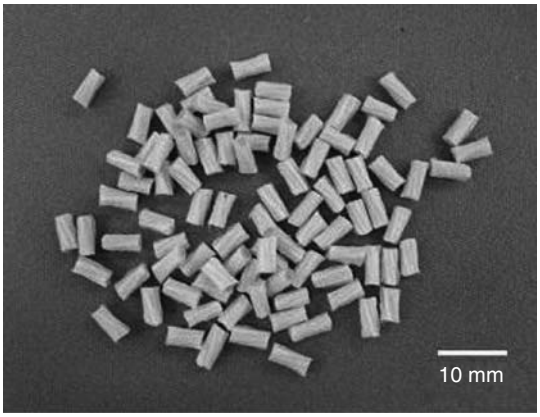

Figure 5.10 NF-LFP of the thermoplastic resin (PP) reinforced with the jute filament.

stagnate for several minutes in the temperature zone of more than 200 °C. As a result, NF is degraded by heat and the strength of the fiber is reduced. Moreover, the impregnation of resin to the inside of the NF bundle of cotton yarn becomes difficult in the conventional system currently used in the manufacture of GF, LFP, of CF. Therefore, the pellet for injection molding with the configuration of an LFP, using cotton yarn as the reinforcement fiber has not been manufactured.

For the above reason, after conventional NF reinforcement, the TP resin is used as a mat blank by dry blending it into the fiber, avoiding the steps of manufacture using heating press molding (see Figure 5.2). Thus, NF-LFP, with reinforcement by cotton yarn, has recently come to be manufactured. The parts of NF reinforcement by TP resin composite came to be manufactured using the injection molding process. As a result, we are now certain that the scope of NF reinforcement by TP resin composite can be extended further. A photograph of an NF-LFP is reproduced in Figure 5.10.

5.1.4.5 **Mechanical Properties of NF-LFP**

The influence of the manufacturing conditions and injection molding conditions of NF-LFP on its tensile strength was investigated. To show the complicated parts that are molded using NF-LFP, a sample photograph of a breaker case is shown in Figure 5.11. The following points are understood from Figure 5.11.

- If jute fiber is the NF used as reinforcement for the TP resin, sufficient improvement is expected in the mechanical properties of the composite material.
- If the content of jute fiber becomes high, the mechanical properties will also improve. Therefore, it is molded with still higher NF content and the positive result of obtaining materials of cyclical form is expected.
- The mechanical properties of both PP and PLA, whose jute fiber content is 51 wt% are shown in Figure 5.12. When the mechanical properties of PP and PLA reinforced by 51 wt% jute fiber are compared, the PLA shows improved properties rather than the PP. The mechanical properties, in this case, become

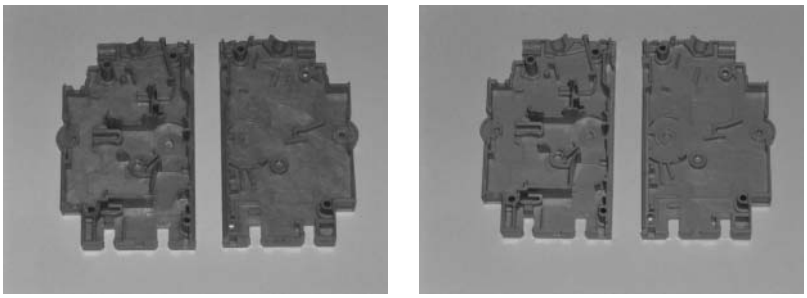

Figure 5.11 The product molded using colored NF-LFP (breaker case). (a) NF-LFP reinforced with the white jute fiber and (b) NF-LFP colored cream.

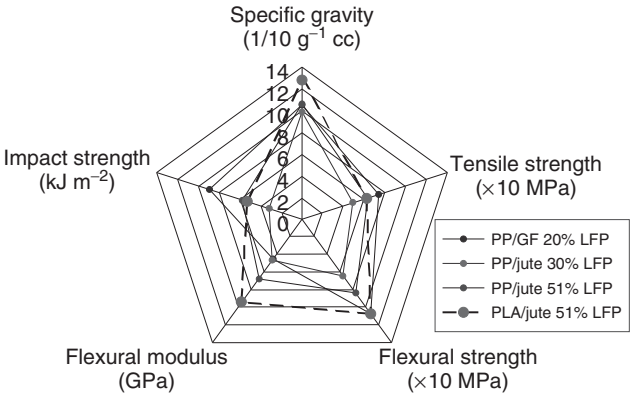

Figure 5.12 The mechanical properties of NF-LFP which use PP and PLA as the matrix.

comparable to those of the 20 wt% GF-reinforced PP composite material that is at present being widely used in automobile parts.

- On the other hand, the big problem with PLA is that its heat resistance is low compared to that of PP. Furthermore, PLA produces hydrolysis in the presence of moisture and the molecular weight becomes low.
- Hereinafter, we consider the dry method for the removal of moisture from NF and the surface treatment method for improvement in the NF–matrix resin interface adhesiveness.

5.1.5
Pellet Manufacturing Technology of the Distributed Type Natural Fiber–Reinforced Thermoplastic Resin Composites

5.1.5.1 Process Development

Since the mechanical properties fibers are excellent in NF-reinforced composites, increased use of BF as a reinforcement fiber should be expected. However, it is

difficult to carry out the spinning of continuous fiber using BF, the length of whose staple is only about 10 mm. Therefore, NF-LFP cannot be manufactured from BF. (In China and Southeast Asia, there is a BF-corded yarn of the same configuration as cotton yarn.)

On the other hand, composite material made of TP resin distributes the staple (short fiber) of GF or CF, which is manufactured using the TSE; this has already been put into practical use. However, when applying this method to BF, the stable feeding to TSE is difficult because of the bulky nature of the fibers and the low coefficient of friction between fibers. Therefore, only the composite material with low BF content has been experimentally manufactured [9, 10]. In order to mix BF of high content, BF and TP resin are kneaded using the batch-type mixer. The massive composite material is ground and pellets are manufactured. However, when a batch-type mixer is used, there is the problem of breakage of fibers owing to high shear stress as well as that of the degradation of the fibers owing to the high temperature. As a result, TP resin composite material strengthened with BF is difficult to be manufactured, and is hardly used (Figure 5.13).

For the above reason, Doshisha University and Kobe Steel started joint development of the continuous granulation method by NF, which is not used in the manufacture of cotton yarn, but used with short fibers such as BF. First, NF of the short fiber is wrapped in the TP resin nonwoven fabric similar to the ingredients in rolled sushi. Simultaneously, a denaturing agent is also mixed in order to improve the interface adhesiveness of the NF and TP resin. In addition, a cohesive force is directly supplied by the screw of the TSE. The nonwoven fabric made of TP resin is melted by the shear stress of the TSE. As a result, the short fibers of the NF are compounded with the TP resin. PP, PET, and PLA are used as the nonwoven fabric [20, 21].

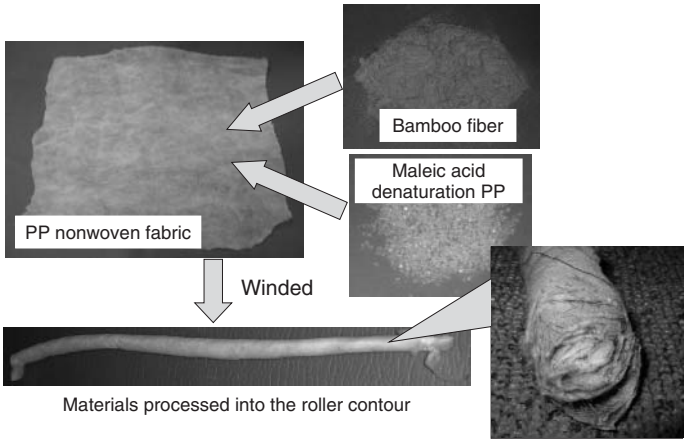

Figure 5.13 The production method of the roller materials using BF and nonwoven fabric.

5.1.5.1.1 Sample Trial Production

The nonwoven fabric made from PP was used in the sample trial production experiment. A 5 wt% of PP was denatured with maleic acid and simultaneously mixed in the nonwoven fabric. The NF materials in the nonwoven fabric are called *roller materials*. These roller materials were manually injected into the screw of TSE and the pellet with 50–60 wt% BF was manufactured. The extruding machine used for the trial production is Kobe Steel KTX-30 and has the following technical specifications.

- Intermeshing-type counter-rotating screw
- Aspect ratio $L/d = 42$
- Screw diameter = 31 mm
- Maximum screw speed = 800 rpm.

The photographs of roller material and the pellets are shown in Figure 5.13 and Figure 5.14, respectively.

5.1.5.2 Automatic Material-Supplying System

While checking the effectiveness of the process, the job of wrapping the NF around the nonwoven fabric was performed manually in advance [22]. However, for practical purposes, it is imperative that the material-provisioning method is automated. So, a system that continuously manufactures the nonwoven fabric wrapped in NF was developed. This system was then attached to the material supply port of the TSE. A sketch of the model and a photograph of the system developed are shown in Figure 5.15 and Figure 5.16, respectively.

This system consists of the four following parts.

1) the delivery part of a continuous nonwoven fabric sheet;

Figure 5.14 Bamboo fiber reinforced thermo plastics (BFRTP) manufactured using roller materials.

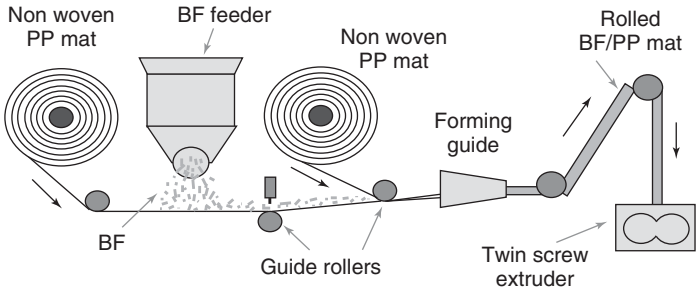

Figure 5.15 The mimetic diagram of the system that continuously feeds the resin nonwoven fabric with BF.

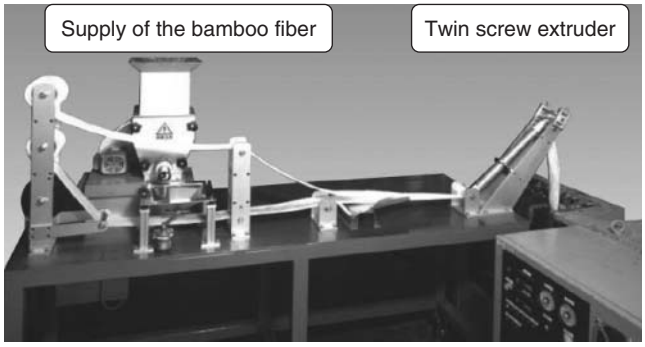

Figure 5.16 The photograph of a system that continuously feeds the resin nonwoven fabric with BF.

2) the feeder of the inverter control that supplies required amount of NF automatically to wrap the nonwoven fabric;
3) the guide-plate part from which the nonwoven fabric wrapped in NF is formed into roller material;
4) the crane part by which the roller material is supplied to the TSE.

Roller materials are supplied to the inner side of the resin under the driving force provided by the rotation of the screw of the TSE. If nonwoven fabric of considerable length is used, a pellet of uniform composition will be manufactured by continuous running.

5.1.5.2.1 The Example and Process Evaluation

Using this system, roller materials were adjusted so that the ratio of the weight of BF and PP could be set at 50 : 50. Roller materials were supplied to the TSE and BF-reinforced PP pellets were manufactured. The screw rotated at a speed of 180 rpm and the sleeve temperature was set as 180 °C. In order to check the effectivity of this system, the tensile and flexural strengths with and without the system were compared. The results obtained are shown in Figure 5.17. Bamboo fiber reinforced thermo plastics-automatically (BFRTP-AT)shows the case where

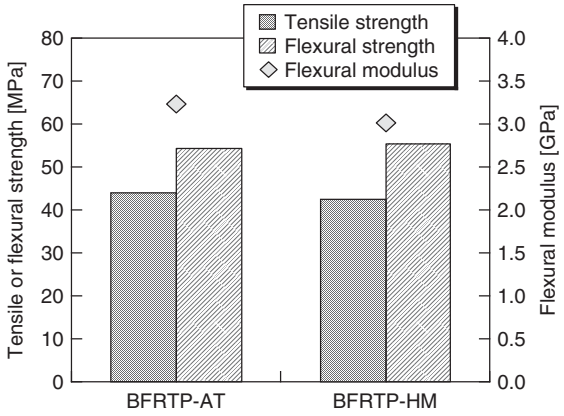

Figure 5.17 Comparison of the mechanical properties between the manual and the automatic methods of supplying roll materials.

an extruding machine is automatically supplied using this system, and bamboo fiber reinforced thermo plastics-hand made (BFRTPHM) shows the case where roller materials were prepared in advance and supplied to an extruding machine. The opening of the BF was carried out mechanically. The BF used according to the diameter classification of the fiber was in the range 88–125 μm. The BF content was about 50 wt%. As shown in the figure, in both methods the mechanical properties acquired were almost equal.

5.1.5.3 Optimal Screw Configuration and Influence of BF Fiber Diameter

Roller materials are placed in positions A and B, shown in Figure 5.18. Two kinds of pellets were manufactured. These pellets were called *Type A* and *Type B*, respectively. First, the position of B is closer to the outlet than the position of A. The screw

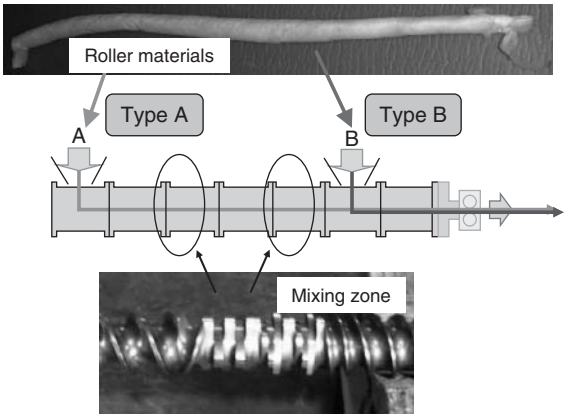

Figure 5.18 Evaluation of the mechanical properties depending on the different supply positions of the roll materials.

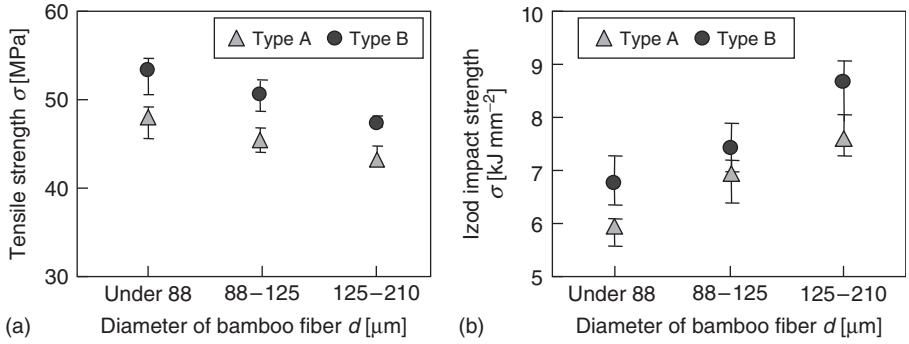

Figure 5.19 The influence of the mechanical properties on BFRTP by change in diameter of the BFs. (a) Tensile strength and (b) Izod impact strength.

composition has a kneading part for mixing that is positioned between A and B. Therefore, in Type B, the roller materials do not pass the kneading part. As for the barrel temperatures of the extruder, both were set as 190 °C. Thus, the tensile strength and the Izod impact strength were evaluated using the pellet manufactured by the two methods. The diameter and filling factor of BF were evaluated simultaneously.

The BF was first classified by a sorter into three kinds according to the diameters of the fibers. The diameters were ~88, 88–125, and 125–210 μm. As a result, six kinds of pellets were compared. Here, the number of types of material at the entrance slot is two, and that of the BF diameter is three. However, all fiber content was made into 60 wt% in these cases.

The relationship between BF diameter and the tensile strength and between BF diameter and the Izod impact strength are shown in Figure 5.19. The difference in the screw configuration is also shown in this figure. The strength in Type B was shown to be higher than that in Type A. Even if the BF diameter is changed, the difference between Type B and Type A showed the same tendency. In addition, even though the screw configuration of Type B had few kneading parts, the fiber was sufficiently dispersed and its degradation was also prevented. Preventing fiber degradation was shown clearly to be of primary importance for the improvement in mechanical properties of BFRTP.

On the other hand, BFRTP whose fiber diameter is smaller than 88 μm indicated the highest tensile strength. However, BFRTP of the highest impact strength was found in the case of fibers of diameter larger than 125 μm. This resulted in a conflict. In order to investigate the reason for this, the SEM photograph of the fracture after the tension test on the BFRTP specimen in which the diameters of the BFs differ is shown in Figure 5.20. The fiber diameter of Figure 5.20a is smaller than 88 μm and Figure 5.20b is from 125 to 210 μm. It is understood from Figure 5.20b that the fiber has fractured. Past results show that the fiber–resin interface strength falls as the diameter of the BF increases. Therefore, in the method that used the fiber with a small diameter, the fiber–resin interface strength is strong. It is thought that, as a result, the tensile strength became high. Similarly, the SEM

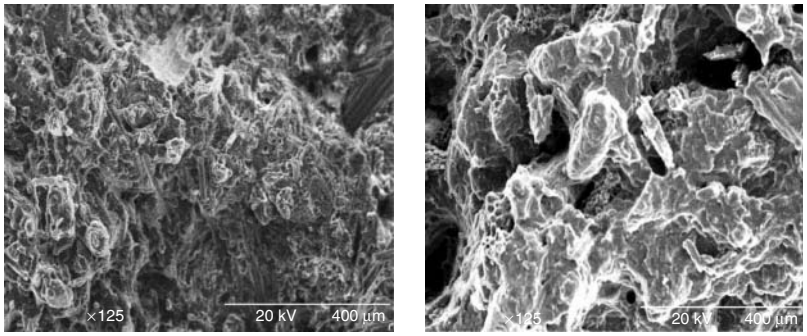

Figure 5.20 The SEM photographs of the fracture surface of the tensile test specimen. (a) Under 88 μm and (b) 125–210 μm.

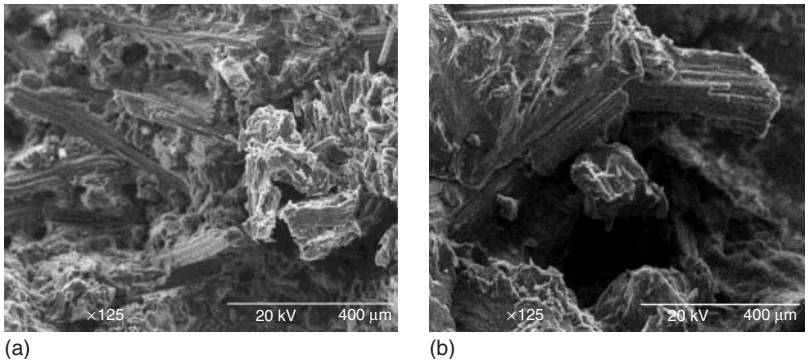

Figure 5.21 The SEM photographs of the fracture surface for the Izod impact test specimen. (a) Under 88 μm and (b) 125–210 μm.

photograph of the fracture after an impact test is shown in Figure 5.21. The marks which show the pullout of the fibers to fracture are seen in both photographs. Moreover, the irregularity of the fracture is greater if the diameter of a fiber is large. In that case, as the fracture was complicated, it was surmised that the energy of the fracture became large. Furthermore, as hardness of the fiber–resin interface decreased, it was also concluded that this was because the friction energy spent in drawing out the fiber was large.

5.1.5.4 **Influence of BF Content**

The strong point of this method is that it can make the BF content higher. Therefore, the influence of the mechanical property on BFRTP was considered for change in fiber content. When the fiber diameter was smaller than 88 μm, the maximum BF content was 80 wt%. Therefore, the change of content was evaluated by using BF with diameter smaller than 88 μm. The screw configuration used was that of Type B, which resulted in tensile strength for fibers of all diameters. The content of BF was changed to 80, 70, and 60 wt%. The relationship between the content of BF and

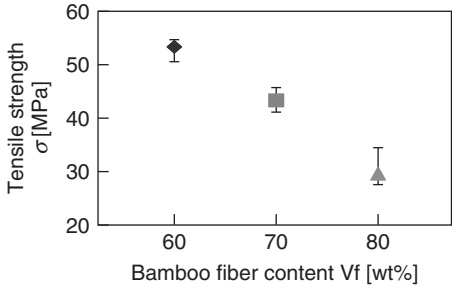

Figure 5.22 The influence of the tensile strength on BFRTP by change in BF contents.

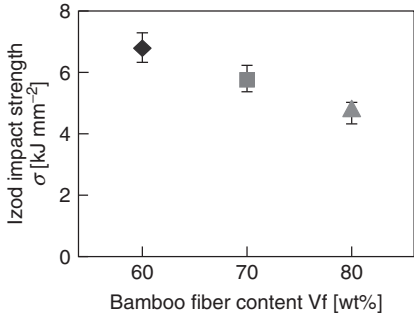

Figure 5.23 The influence of Izod impact strength on BFRTP by change of BF contents.

the tensile strength is shown in Figure 5.22. Moreover, the relationship between BF content and Izod impact strength is shown in Figure 5.23. Both tensile strength and Izod impact strength fall as BF content increases. In order to investigate the cause, the fracture photograph after tensile and Izod impact tests for BF content 80 wt% is shown in Figure 5.24. BF content 80 wt% (Figure 5.24a) was compared with BF content 60 wt% (Figure 5.20) using the fracture photograph after the tensile test. In

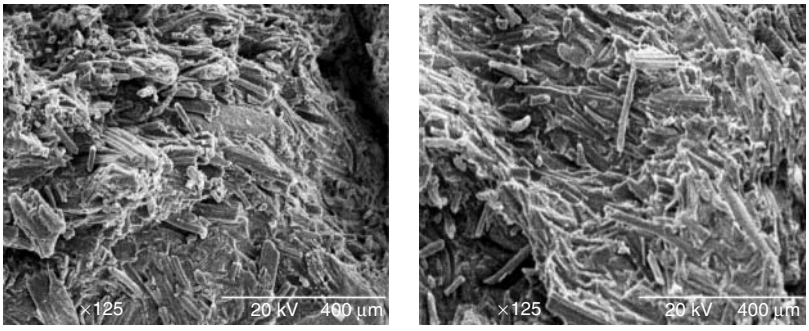

(a) (b)

Figure 5.24 The SEM photographs of the fracture surface (fiber contents Vf: 80 wt%). (a) After tensile strength and (b) after Izod impact test.

the case of BF content 80 wt%, it was possible to see many fibers to which the resin had not adhered. This is true for the fracture face after an impact test (Figure 5.23b and Figure 5.21). For this reason, if BF content increases to 80 wt%, the number of parts into which fibers lay upon one another will increase. As a result, this will produce a range in which the resin has not been fully impregnated by fibers. Another reason is that the mixing of resin and fiber may have been insufficient in Type B. Therefore, when a pellet with high BF content is manufactured, the entrance slot of materials is set to that of Type A. Therefore, development of an optimal screw configuration that can sufficiently mix the fibers by the difference in BF content without breaking is needed in the near future.

From the above result, this system is effective for pellet manufacture in the case where BF is made the reinforcement fiber. However, the present conditions are restricted to BF of limited size and the configuration. Therefore, even whatever the kind of NF used, the problem of manufacturing a stable pellet remains. This system is being improved, by attempting pellet manufacture using various NFs at high filling rates.

5.1.6
Future Outlook

Two main issues in the method of manufacturing NF-impregnated PLA composites were described. One is the mixing technology to prevent heat degradation of the NFs adapting long fiber-reinforced TP composites pellet manufacturing technology. The other is the mixing technology for preventing hydrolysis of PLA. However, even if the two kinds of mixing technology introduced here are used as the manufacturing method of the NF-reinforced TP composite pellets, these issues are not necessarily resolved completely.

As the solution to this problem, it is necessary to perform optimal processing on the surface of NF by the continuous technique before compounding the resin and NF. It is desirable to specifically process the NF, before it is supplied to the extruder. Moisture inside the NF is removed during processing. Furthermore, the wettability and adhesiveness between resin and NF surface are improved. In addition, an improvement in many more mechanical properties will also be achieved [23, 24].

5.2
Processing Technology of Wood Plastic Composite (WPC)
Hirokazu Ito

Wood plastic composites (WPCs), which are produced from wood flour and TP, are used widely as industrial material in the field of biocomposites. WPC is included under the category of the filler for filling plastic material, which includes inorganic materials, such as silica, talc, and calcium carbonate. Therefore, its method of production is also based on the method used for fillers for filling plastic, divided into the compounding process that makes molten mixture of wood flour as filler and

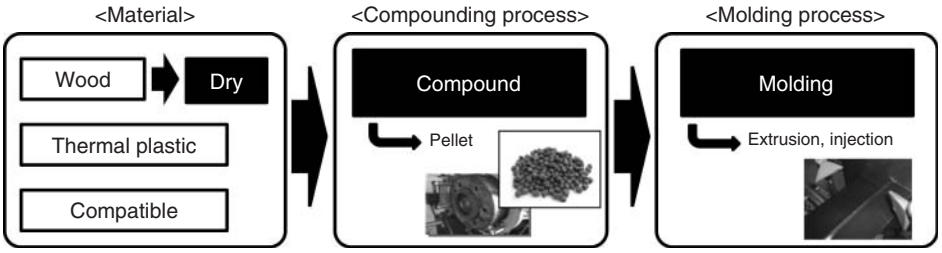

Figure 5.25 The process outline for the production of WPCs.

plastic, and the molding process that carries out extrusion molding and injection molding (Figure 5.25). This section describes these processes in WPC production. Moreover, the characteristics of wood flour as raw material are also explained as it has the characteristic features as filler for plastic.

5.2.1 Raw Materials

5.2.1.1 Manufacture of Woody Materials

There are many kinds of woody material that can be used for a WPC. Moreover, it is also known widely that various characteristics can be obtained depending on the kind of woody materials used. However, in the industry, woody materials are selected from what is conveniently availability on the supply side rather than what the characteristic is, in many cases. Its low density and volume makes long distance transportation of woody material disadvantageous in terms of cost. Although, hemp, ramie, kenaf, and so on, are used in WPCs in Southeast Asia, where they are produced abundantly, wood flour is used more often [25–31]. So, this section explains the use of wood flour for the manufacture of WPCs.

The wood flour particle size for WPC ranges from 100 μm to 1 mm in general, the range most in demand being 300–100 μm. Although, wood flour of a larger size is advantageous in terms of cost of pulverization and high filler content in a composite, there are drawbacks such as lack of water resistance of the composite and difficulties in fabrication by injection molding. On the other hand, when the size of wood flour particles is small, mechanical properties and durability of the composite are improved, but problems arise in terms of cost of pulverization and filler content. Since many of the uses of WPC are as exterior materials, the wood flour size that can respond to the demands in quality required for exterior use is in the range 300–100 μm.

Wood flour of 100 μm or more is manufactured by dry pulverization of wood material with 10% or less of water content using a hammer mill or cutter mill (Figure 5.26). In dry pulverization, manufacture of wood flour of 100 μm or less is difficult, and there is a limitation on the size of finely powdered wood flour because of its reflocculation. The graph for pulverization time versus wood flour size for pulverizing 300 μm, using a planet-type ball mill is shown in Figure 5.27. Wood

Figure 5.26 Pulverization machine (cutter mill, Masukou Sangyou).

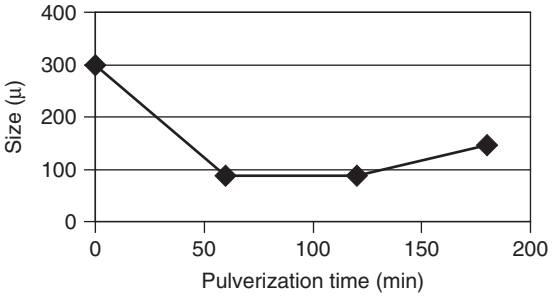

Figure 5.27 Correlation between wood flour size and pulverization time (wood flour; a Japan cedar, the number of rotations; 300 rpm).

flour size is stabilized at about 100 μm, and wood flour size increases with further pulverization. Moreover, the risk of dust explosion also increases for fine powders. Wet milling is suitable to obtain wood flour of 100 μm or less. Although, the final water content depends on the size of the wood flour, the pulverization equipment, and the conditions for pulverization, it is possible to prepare fine powder of nano size levels. The wood flour manufactured with wet milling needs drying process, as the wood flour for WPC is used in dry conditions.

Five percent or less moisture content in the wood flour is desirable for WPC. If the wet wood flour containing more moisture is used, molding becomes unstable in the WPC production process. Furthermore, in the process of preparing melt mixture with a plastic (compounding), flocculation of wood flour takes place because of rapid drying and pressuring (Figure 5.28). The flocculation generated in the compounding process is hard, and is not broken during the molding process.

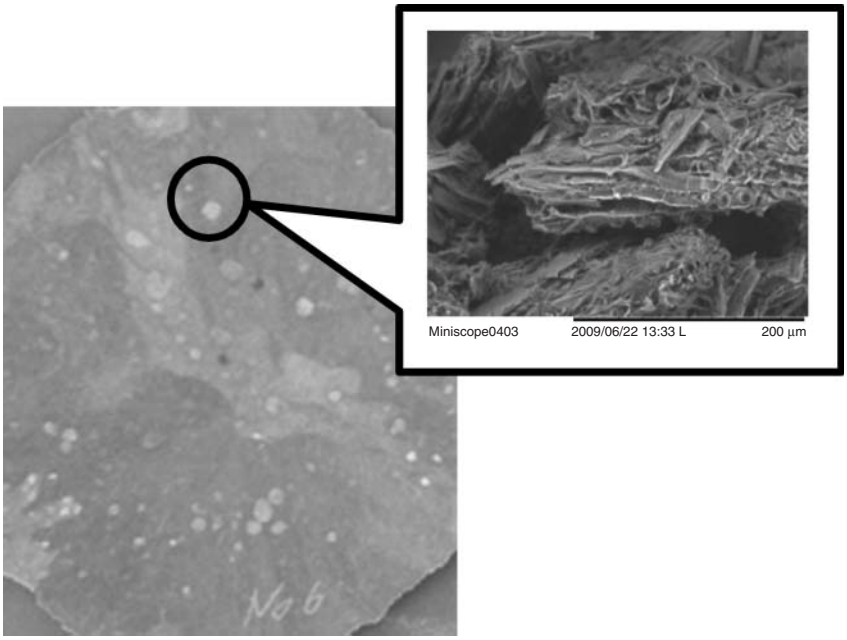

Figure 5.28 The wood flour flocculation produced in WPC.

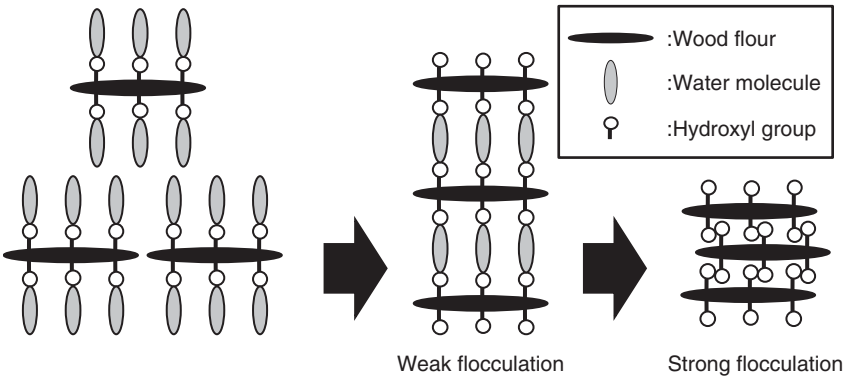

Figure 5.29 Flocculation of the wood flour in compound process.

It is held strongly by the hydrogen bond (Figure 5.29) and, although flocculation has no influence on the strength (Figure 5.30) of the WPC, it has a negative effect on water resistance of the composite (Figure 5.31) [32]. Since many WPC goods are manufacture for exterior use, water resistance is an important factor. Therefore, it is necessary to avoid flocculation of wood flour.

Although the wood species influence the characteristics of the WPC, it is difficult to choose the best species because of lack of availability on the supply side in industrial production.

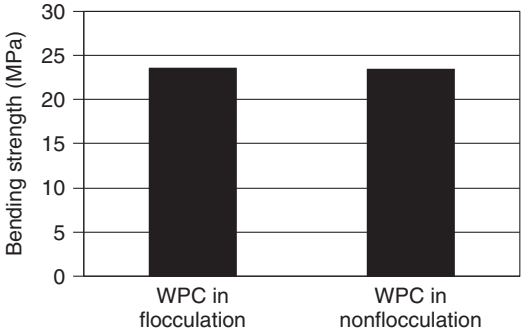

Figure 5.30 Bending strength of WPC produced by wood flour flocculation produced. WPC of PE resin 50%.

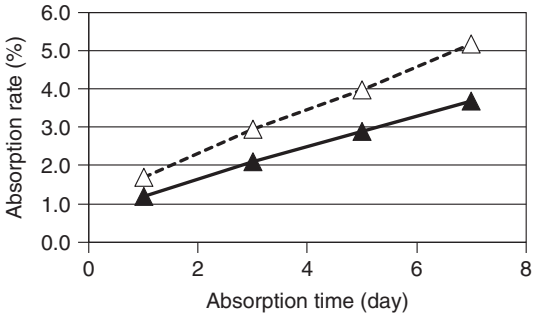

Figure 5.31 Water absorption of WPC produced by wood flour flocculation. WPC of PE resin 50%. Symbols; △, WPC in flocculation and ▲, WPC in nonflocculation.

5.2.1.2 **Plastic**

Wood flour starts to deteriorate at over 200 °C. Therefore, it is desirable for the plastic of a WPC to have a melting point of 200 °C or less. A general-purpose plastic for this use is olefinic resin (polyethylene and PP). The plastic material is selected according to the use of WPC. The plastic that is suitable for abundant exterior use, that is olefinic resin, is generally used. In addition, styrene-type resin (acrylonitrile butadiene styrene (ABS), AS, etc.) and vinyl chloride resin are also used. Moreover, as wood flour is a natural material, a plastic of vegetal origin is used for manufacturing a completely bio-based material.

The fluidity of plastic is chosen on the basis of the molding method (molded machine and type of mold) and composition (content of wood flour). In extrusion molding, low fluidity has a bad influence on the productivity, and high fluidity induces the problem of stability of forming. Furthermore, depending on the fluidity of the plastic and the shape of wood flour, the orientation of wood flour must be also taken into account. In the case of wood/olefinic resin composite with wood flour content of 50%, the plastic with fluidity (melt flow rate, MFR) of 0.1–10 g/10 min is general used.

In WPC, recycled plastic material is often used. Use of a recycled plastic has merits not only in terms of cost but also in terms of properties of the material. Usually a recycled plastic has low mechanical properties. Since mechanical properties are improved with increased wood flour content in WPC, WPC with the wood flour content of 50% or more can make good the demerits of recycled plastic.

5.2.1.3 **Compatibilizer**

Since wood flour is hydrophilic and plastic used in WPC is hydrophobic, the compatibility of these two is low. Low compatibility of components has a bad influence on the mechanical properties or durability of the composite. Generally, for WPCs, a plastic material in which the base plastic is modified with maleic acid is used [33–38]. The maleic acid-modified plastic is prepared by adding maleic acid in a side chain within the main chain of the base plastic (the model of maleic acid modified PP is shown in Figure 5.32). Since the main chain of a maleic acid-modified plastic is the same as that of the base plastic, compatibility is high. On the other hand, the maleic acid-modified portion of the side chain acts on the hydroxyl group on the surface of wood flour and modifies the wood flour surface (Figure 5.32). Thus compatibility between the wood flour and the base plastic is improved [39, 40].

Although the amount of addition depends on the state of the modification of maleic acid, it is 1–5% of wood flour, in general. Since the base plastic of a maleic acid-modified plastic has a low molecular weight, if the quantity added becomes too high, the composite is influenced by the base plastic. Moreover, if the amount of addition exceeds a certain limit, further addition has no effect. The reason that maleic acid-modified plastic is widely used in WPC is not only due to the ease of treating. Inorganic fillers such as silica and calcium carbonate are also hydrophilic, and a compatibilization processing is needed similarly to a WPC. In inorganic fillers, coupling processing is common. However, as there is considerable void,

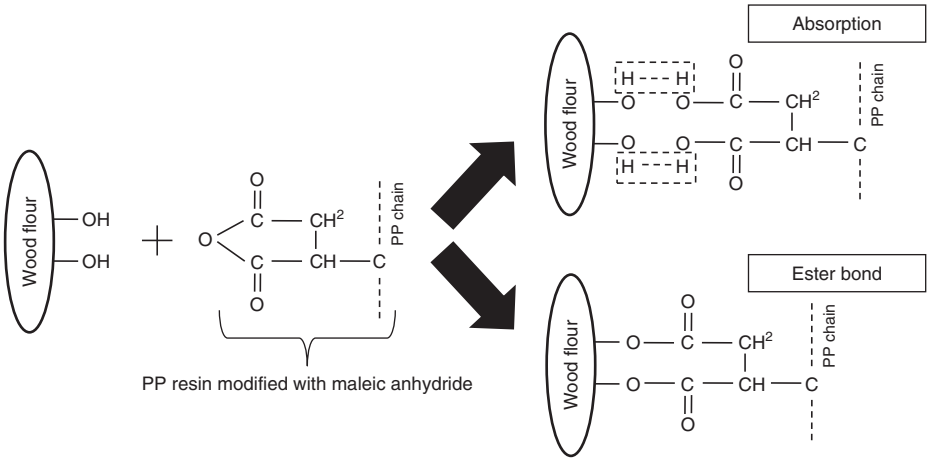

Figure 5.32 Wood flour surface modification by a maleic acid-modified plastic.

coupling processing is less effective for wood flour, and it is not used widely in the industry.

About compatibilization technology, acetylation and various heat treatments are also possible. But these processing methods have problems in respect of cost in industrial use. However, as chemical processing is not too difficult for wood flour compared with that for inorganic fillers, it is a potential technical domain of development of WPC at present.

5.2.2 Compounding Process

The compounding process is very important in the manufacture of WPCs. The performance of a compound has big influence on the properties or productivity of the WPC. So, in this section, not only the technique but also the purpose and some points of attention are included in the discussion of a compounding process.

5.2.2.1 Compounding Using an Extrusion Machine

The technique widely used in compound manufacture of WPCs is the compound process using an extrusion machine. Since continuous production of compound using an extrusion-molding machine is possible, it can secure high productivity. Furthermore, as a pellet-shaped compound is handled easily at molding (extrusion or injection), it is easy prepared by compounding by extrusion molding.

There are various kinds of extrusion-molding machines, such as the single-screw extrusion machine, twin-screw extrusion machine, conical twin-screw extrusion machine, or combination-type machine, depending on the form of the screw. Which machine is most suitable for compound production of a wood plastic depends on the formulation, required quality, and allowed costs of the compound. Although a single-screw extrusion machine has an advantage of cheap equipment cost, a weak point is the dispersion of the wood flour in the base plastic. Although the TSE provides good dispersion, it tends to show low productivity when the wood flour content becomes high (fluidity is low). Although the conical twin-screw extrusion machine can secure high productivity even in a formulation with low fluidity, there is a problem with dispersion. Moreover, although there are also composition-type machines that combine the features of these extrusion machines, the cost of the equipment poses a problem, since it is a special-purpose machine. Therefore, when manufacturing a compound of WPC, it is necessary to understand these merits and demerits before carrying out equipment selection.

Although the type of machine is important in the compounding process, the biggest point is the screw design. The wood flour is easy to flocculate in the compounding process. Furthermore, flocculation becomes more marked when the compounding formulation is of high filler content. Flocculation can be suppressed by not only making the moisture content of wood flour low but also by giving high shear in the early stages of the compounding process. However, since high shear induces the heat of shear by friction of wood flour, causing it to deteriorate in some cases, it is necessary to pay attention to the proper processing

temperature. Low bulk density of wood flour tends to greatly affect increase in the filling weight into a screw, and the productivity of the compound is usually low. This drawback can be overcome by reducing the wood flour volume before feeding it into the screw, or by enlarging the feeding cross-section area of the screw. As shown in some examples, the screw design that can overcome such problems needs to be considered while using wood flour, as many of the issues are characteristics peculiar to wood flour.

Wood flour contains volatile components. If some volatile components remain in the compound, various problems arise during the molding process. It is therefore desirable to remove these volatile components to the extenet possible in the compounding process. Usually, this can be effected by carrying out the compounding process at a temperature higher than the molding process, as the volatile components include some acidic gases that can induce corrosion of equipment. A vent mechanism that discharges the volatile component is required in a machine.

5.2.2.2 **Compounding Using a Henschel Type Mixer**

Flocculation can be prevented to some extent by sufficiently drying the wood flour before starting the compounding process. However, wood flour absorbs moisture easily up to about 10% according to the storage environment. Although, there are methods of keeping wood flour in a damp-proof container and/or drying it up with a hopper dryer, it will be impossible to maintain the moisture content near 0% on an industrial scale. However, there is a compounding method that uses the Henschel type mixer (Figure 5.33), a technique that does not flocculate wood flour containing a certain amount of moisture.

Compounding by the Henschel type mixer is a method that uses the heat of friction by the collision of materials during high-speed stirring for compounding the molten plastic and wood flour. Although, flocculation of wood flour is generated transiently with reduction in moisture content during processing, flocculation is not rigid because high pressure is not applied and wood flour collides and redisperses.

Figure 5.33 Henschel type mixer (Kawata).

It may be stated that the technique is a suitable compounding method that prevents flocculation.

However, Henschel-type mixing is a batch-type processing method and not suitable for mass production. Therefore, the process is adopted in WPC production of many kinds of products in small quantities. Furthermore, it must be kept in mind that a fiber is cut by collision and fiber length becomes short, when this process is used for fibrous wood flour. Moreover, there may be cases in which the removal of volatile components is incomplete, when the content of wood flour is low.

The compound obtained by the Henschel-type mixer has powder or granule shape in many cases. Although, there is no problem in using this compound in extrusion or injection molding, dust dispersion to the circumference may be noticed at the time of handling. In a molder's factory, various products are molded using many molding lines, and dispersed dust may mix in other products and the risk of powder explosion increases. Therefore, the presence of powder in factory surroundings is not welcome. The drawback can be overcome if a compound obtained by the Henschel-type mixer is processed into pellets by using a granulator.

5.2.2.3 **Evaluation of Compounds**

In a compound, important evaluation criteria are fluidity and dispersion. The common fluidity evaluation in the plastic material is the MFR, carried out by a melt indexer (Figure 5.34). However, in WPC of high content of wood flour, the usual MFR measurement is difficult, as fluidity becomes low; in such cases, a capillary rheometer (Figure 5.35) is suitable. On the other hand, as MFR is simple, measurement can be improved by enlarging the diameter of the orifice of the melt indexer and increasing the load applied. However, at present, this measuring method only provides relative evaluation instead of absolute evaluation.

Regarding dispersion, an evaluation method consisting of press molding the compound into a sheet form and then detecting the existence of flocculation by

Figure 5.34 Melt indexer (Ekoseiki).

Figure 5.35 Capillary rheometer (Ekoseiki).

visible evaluation is common. However, when the wood flour content increases, evaluation of the dispersion by sheeting becomes difficult. For evaluation of the dispersion in a WPC compound with wood flour content that is greater than 70%, a cone rheometer (Figure 5.36) may be effective [41]. Since the distance between wood flour particles is very small in such compounds, the interaction of wood flour develops in WPCs with high wood flour content. There is a technique (Figure 5.37) for measuring the interaction by measuring the storage modulus. There is individual specificity according to the size of the wood flour particles, and the kind of resin; this technique is also a relative evaluation method. Furthermore,

Figure 5.36 Cone rheometer (Ekoseiki).

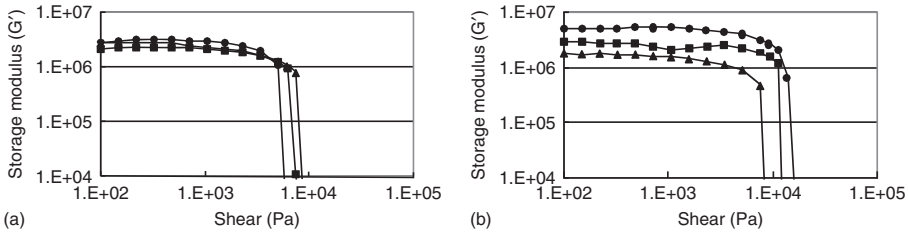

Figure 5.37 The difference in the wood flour dispersion state, and the relation of the storage modulus. WPC used was PP resin and cellulose fiber. (a) Poor dispersion and (b) good dispersion. Symbols; ●, resin content 10%; ■, resin content 20%; and ▲, resin content 30%.

evaluation of dispersion is possible from the water absorption characteristic. With compounds of the low dispersion in which flocculation takes place, quick water absorption is observed and the strength after water absorption is low.

5.2.3 Molding Process

The molding of WPCs can be done by using various molding methods, such as extrusion molding, injection molding, press molding, and blow molding, as in the case of a general plastic. In WPC, extrusion molding is used for the general purposes. Although this chapter has mainly focused on extrusion molding, a short description of injection molding has been included as injection molding, which takes advantage of the functional characteristics of WPC, is also finding widespread use in recent years.

5.2.3.1 Extrusion Molding

There are several kinds of extrusion molding machines as described in Section 5.2.2. However as discussed, the most suitable extrusion molding machine varies, depending on the shape of the molded object, content of wood flour, kind of plastic, states of the compound, and so on. Since WPC can contain wood flour in higher content than the usual filled filling plastic material, there is a close relationship between content of wood flour and selection of the extrusion machine. WPC, which shows fluidity of general filler filled plastic (the wood flour content is generally 30% or less), can be processed with a general-purpose extrusion machine. However, WPC of low fluidity needs to have its fluidity raised by an extrusion machine, and the conical twin-screw extrusion machine, which has high feeding ability, is used. On the other hand, there are also uses for which good dispersion of filler is requested for the quality of the composite rather than the productivity. In such cases, the twin-screw extrusion machine, which ensures high mull, is used. In the case of WPC of high wood flour content, when mixing is increased, the shear between wood flours increases, with unusual heating inside the extrusion machine, causing deterioration of the wood flour. Therefore, careful control of temperature conditions is also important.

As an important point common to all the extrusion machines, it is desirable to have a vent (gas emission outlet). The vent serves to remove the gas that evolves from the wood flour itself, such as moisture and other volatile components. If these components remain in the extrusion machine, the molding speed becomes unstable, or it becomes difficult to maintain the molded form because of swelling.

Usually the compound described in the preceding section is used for molding of WPC. The merit of using the compound is not only the dispersion of wood flour and plastic, but also the amount of discharge per one rotation of screw (productivity). Productivity is increased by volume reduction and the amount of compound filled in the extrusion machine screw is increased. Moreover, compound helps in reduction of the volatile component of wood flour mentioned above.

A direct extrusion process without wood flour and plastic having to pass through the compound process was introduced in recent years (Figure 5.38). This process is characterized by the presence of a zone of full mixing inside the extruder. It is expected that the development of the extrusion machine will move forward corresponding to the specific features of the WPCs, with an expansion of the WPC market.

Multilayer molding is another characteristic of extrusion molding. This technology can also be used in the extrusion molding of WPCs. For example, for WPCs for exterior use, a two-layer molded object is available, in which the inside material takes charge of functionality, such as mechanical properties and dimensional stability, and the outside material contributes to the durability and design.

Compared with injection molding, control of the anisotropy by orientation of wood flour is difficult in extrusion molding. Anisotropy has many demerits, except for some properties such as use in a sound component. In order to overcome these demerits, cross-sectional design of the composite is elaborated in many cases rather than controlling the orientation by molding conditions.

5.2.3.2 **Injection Molding**

The products obtained by extrusion molding are mainly used in present day WPCs. Since WPC has been developed as alternatives for wood products, extrusion

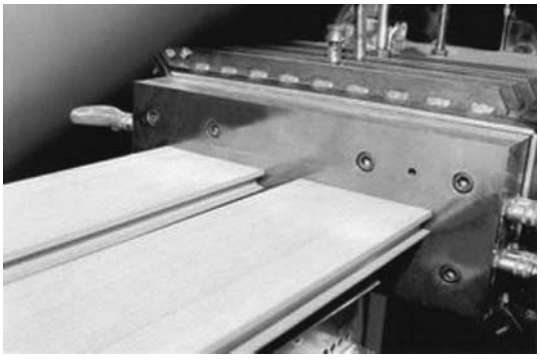

Figure 5.38 Direct extrusion-molding machine (Reifenhoiser).

molding is selected as a suitable molding process to prepare woodlike products. However, the injection molding, which utilizes the important function of high moldability of WPCs, has attracted attention in recent years. Although the special-purpose injection molding machine specific to WPCs is also put into the practical use, WPCs molded with conventional injection molding machines in many cases. When a general-purpose injection molding machine is used for WPCs, as there is no vent, it is necessary to dry the raw material well and mold it at a temperature lower than that of the compounding process so that gas evolution may be surpassed at the time of molding. Since good flow is indispensable for injection molding, compared with extrusion molding, the content of wood flour in the moldable compound becomes low. The model design should include the removal of forms, since there is little contraction after molding.

Although the anisotropy of molded WPC is more remarkable in injection than extrusion molding, an improvement is possible by the design of a gate. The erosion of the machine by the organic acid (formic acid, acetic acid, etc.) generated from wood poses a more serious problem in injection molding, as an injection molder is not generally equipped with a vent. Since the emission control of organic acids is difficult, frequent cleaning is necessary in injection molding.

5.2.4 The Future Outlook for WPC in Industry

It is certain that the uses of WPCs will expand as alternatives to the use of wood material in building materials and exteriors, and so on, forming he background of supplying materials of long life. Compared with the general filled filling plastic, the WPCs have specific features that the filler content can be very high and the wood flour as filler is lightweight, compared with inorganic fillers. In the near future, taking advantage of the feature of weight saving and the dimensional stability by the high filling effect, the production is expected to expand into the use in transport and machinery, and so on. Therefore, it is highly encouraged to develop products with new uses that are not just wood substitutes.

References

1. Nikkei Biotechnology and Business *http://www.toyota.co.jp/jp/environmental_rep/03/special02.html*..
2. Saheb, D.N. and Jog, J.P. Natural fiber polymer composites: a review *Adv. Polym. Technol.* **18** (4) 351–363 (1999).
3. Jiang, J. Okubo, K., and Fujii, T. (2000) Fabrication of eco-composites using natural fiber. 45th FRP CON-EX 2000, pp. A.8/1–A.8/2.
4. Hasegawa, T., Composite goods of a natural fiber and a plastic, *Jpn. Plast.*, **51** (11), 62–69, (2000).
5. Daimler Chrysler (2000) Daimler Chrysler-News-The Environmental Patent 2000, *http://www.daimlerchrysler.com/news/top/2000/t00717_e.htm*. Japanese Patent 10-219000.
6. Unitika, Ltd (2005) About Practical Use Development of Kenaf Addition Poly-lactic Acid and Application on the NEC

Personal Computer Parts, January 13, 2005 *http://www.unitika.co.jp/news/io-pdf/00039.pdf* (accessed 30 March 2013).
7. Nikkei Biotechnology & Business (2005) Kenaf Reinforcement Kenaf, No. 1, pp. 74–75, *http://biobiz.nikkeibp.co.jp/*.
8. Nikkan Kogyo Shinbun, Ltd (2004) Doshisha University: Advanced Use of a Bamboo, July 9, 2004.
9. Nakamura, M. *et al.* (2006) Effect of fiber surface modification on mechanical properties of injection molded bamboo fiber reinforced biodegradable composites. Proceeding of the 55th JSMS Annual Meeting, pp. 164–165.
10. Nakamura, M. *et al.* (2007) Fiber surface treatment and mechanical properties in bamboo fiber/biodegradable polymer composites by injection molding. Proceeding of JCOM-36, pp. 13–16.
11. The Society of Fiber Science and Technology, Japan (2004) Basic Knowledge of a Fiber, The Nikkan Kogyo Shinbun, Ltd, pp. 46–47.
12. Cogswell, F.N. *et al.* (1982) Method for impregnating filaments with thermoplastic. US Patent 4,549,920, filed Jan. 20, 1982 and issued Oct. 29, 1985.
13. Tochioka, T.. The present status and the prospect of the plastic material and processing in the automotive industry. *J. Jpn. Soc. Polym. Process.* **20** (8) 589–594 (2008).
14. The European Alliance for Thermoplastic Composites (EATC) *http://www.eatc-online.org/* (accessed 30 March 2013).
15. Deaver, D. and Mcllvaine, J. Use of structural long glass fiber composites to replace steel in automotive running boards *Spec. Publ. Soc. Automot. Eng.* **SP-1960** 121–125 (2005).
16. Tanaka, T., Long fiber pellet production plants and their application to natural fiber composites. (Eco-composites), *Ind. Mach.*, **631**, 13–15 (2003).
17. Tanaka, T. and Tashiro, N., Production apparatus for long-fiber pellet and ecological composite, *Jpn. Plast.*, **56** (7), 95–104 (2005).
18. Tanaka, T. and Hirano, Y., Long fiber pellet production plants and their application to natural fiber composites. (Eco-composites), *R&D Kobe Steel Eng., Rep.*, **51** (2), 62–66 (2001).
19. Tanaka, T., Hirano, Y. and Nagaoka, T., Long fiber pellet production plants and their application to natural fiber composites. (Eco-composites), *Plast. Molding Tech.*, **19** (10), 25–31 (2003).
20. Tanaka, T., Fujiura, T., Fujii, T., Okubo, K., and Okuno, K. (2005) Development of Long-Fiber Reinforced TP Pellets Using White Jute Fiber. (NF-LFP). JSPP '05 Technical Papers, Vol. 16, pp. 213–214.
21. Tanaka, T., Fujiura, T., Fujisawa, K., Fujii, T., and Okubo, K. (2004) How to Fabricate TP Pellets Containing Bamboo Fibers more than 50% in Weight for Injection Molding. JSPP '04 Technical Papers, Vol. 15, pp. 139–140.
22. Fujiura, T. Tanaka, T. Fujii, K. Okubo, T., and Nagatani, A. (2005) Development of Fabrication Method for TP Pellets Containing Bamboo Fibers More than 50% in Weight for Injection Molding (II), JSPP '05 Technical Papers Vol. 16, pp. 199–200.
23. Fujiura, T., Sakamoto, K., Tanaka, T., and Imaida, Y., A study on preparation and mechanical properties of long jute fiber reinforced polylactic acid by the injection molding process, *WIT Trans. Built Environ.*, **97**, 231–240 (2008).
24. Fujiura, T., Okamoto, T., Tanaka, T. and Imaida, Y., Improvement of mechanical properties of long jute fiber reinforced polylactide prepared by injection molding process. *WIT Trans. Built Environ.*, **138**, 181–188 (2010).
25. Lamy, B., Baley, C., Stiffness prediction of flax fibers-epoxy composite materials, *J. Mater. Sci. Lett.*, **19** (11), 979–980 (2000).
26. Sampath, A. and Martin, G.C. (2000) Enhancement of natural fiber-epoxy interaction using bi-functional surface modifiers. ANTEC 2000 Conference Proceedings, pp. 458.
27. Dash, B.N., Rana, A., Kmishra, H.K., Nayak, S.K., Tripathy, S.S., Novel low-cost jute-polyester composite. III. Weathering and thermal behaviour, *J. Appl. Polym. Sci.*, **78** (9), 1671–1679 (2000).

28. M.Gowda, T., Naidu, A.C.B., Chhaya, R., Some mechanical properties of untreated jute fabric-reinforced polyester composites, *Appl. Sci. Manuf.*, **30A** (3), 277–284 (1999).
29. Saha, A.K., Das, S., Bhatta, D., Mitra, B.C., Jute fiber reinforced polyester composites by dynamic mechanical analysis, *J. Appl. Polym. Sci.*, **71** (9), 1505–1513 (1999).
30. Zimmerman, J.M., Losure, N.S., Mechanical properties of kenaf bast fiber reinforced epoxy matrix composite panels, *J. Adv. Mater.*, **30** (2), 32–38 (1998).
31. Zhu, W.H., Tobias, B.C., Coutts, R.S.P., Banana fiber strands reinforced polyester composite, *J. Mater. Sci. Lett.*, **14** (7), 508–510 (1995).
32. Ito, H., Hattori, H., Okamoto, T., Takatani, M., Physical properties of wood plastic composites with MDF, *Wood Ind.*, **64** (6), 268–272 (2009).
33. Xiaoya, C., Qipeng, G., Yongli, M., Bamboo fiber-reinforced polypropylene composites: a study of the mechanical properties, *J. Appl. Polym. Sci.*, **69** (10), 1891–1899 (1998).
34. Bledzki, A.K., Faruk, O., Huque, M., Physico-mechanical studied of wood fiber reinforced composites, *Polym. Plast. Technol. Eng.*, **41** (3), 435–451 (2002).
35. Rana, A.K., Mitra, B.C., Banerjee, A.N., Soft jute fiber-reinforced polypropylene composites: dynamic mechanical study, *J. Appl. Polym. Sci.*, **7** (4), 531–539 (1999).
36. Rozman, H.D., Penng, G.B., Effect of compounding techniques on the mechanical properties of oil palm empty fruit bunch-polypropylene composites, *J. Appl. Polym. Sci.*, **70** (13), 2647–2655 (1998).
37. Qiu, W., Endo, T., Hirotsu, T., Interfacial interaction, morphology, and tensile properties of a composite of highly crystalline cellulose and maleated polypropylene, *J. Appl. Polym. Sci.*, **10** (4), 3830–3841 (2006).
38. Qiu, W., Zhang, F., Endo, T., Hirotsu, T., Effect of maleated polypropylene on performance of polypropylene/cellulose composite, *Polym. Compos.*, **26** (4), 448–453 (2005).
39. Simonsen, J., Jacobsen, R., Rowell, R., Wood-fiber reinforcement of styrene-maleic anhydride copolymer, *J. Appl. Polym. Sci.*, **68** (10), 1567–1573 (1998).
40. Coutinho, F.M.B., Costa, T.H.S., Carvalho, D.L., Polypropylene-wood fiber composites: effect of treatment and mixing conditions on mechanical properties, *J. Appl. Poly. Sci.*, **65** (6), 1227–1235 (1997).
41. Ito, H., Kumari, R., Takatani, M., Okamoto, T., Viscoelastic evaluation of effect of fiber size and composition on cellulose-polypropylene composite of high filler content, *Polym. Eng. Sci.*, **48** (2), 415–423 (2008).

6
Biofiber-Reinforced Thermoset Composites

Masatoshi Kubouchi, Terence P. Tumolva, and Yoshinobu Shimamura

6.1
Introduction

One way of generally classifying natural fiber-reinforced plastic (NFRP) composites is according to the type of polymeric resin used as matrix. The thermoplastic-based NFRP composites are presently being used in a continually expanding range of applications; however, the major portion of the NFRP market is still comprised of biofiber-reinforced thermoset-based composites. Thermoset matrix systems dominate the composites industry because they are more reactive and easier to impregnate with fillers. They also play an important role in the industry owing to their high flexibility for tailoring desired ultimate properties. Various thermosetting resins have been utilized in the manufacture of composites for their excellent chemical stability, which allows the possibility of long-term applications such as pipes and chemical tank linings. They are also suitable for high temperature applications such as insulators. However, thermosetting resins are brittle at room temperature and have low fracture toughness – hence the necessity for reinforcements such as fibers.

This chapter reviews the recent studies on the manufacture of thermoset biocomposites, which may be produced either by using biothermoset matrices or by using biofiber reinforcements. Because natural fibers, although highly eco-friendly, have poor mechanical strength and low stability, the use of thermosetting matrices offers a distinct advantage when it comes to fabricating NFRP composites designed for very long service lifetime applications.

6.2
Materials and Fabrication Techniques

6.2.1
Thermosetting Resins

The IUPAC defines thermosetting polymers, or thermosets, as ''prepolymers in a soft solid or viscous state that changes irreversibly into an infusible, insoluble

Polymer Composite: Volume 3, First Edition.
Edited by Sabu Thomas, Kuruvilla Joseph, S. K. Malhotra, Koichi Goda and M. S. Sreekala.

polymer network by curing'' [1]. Unlike the linear molecules of thermoplastic polymers, the adjacent molecular chains in a thermoset undergo a chemical reaction during polymerization and become cross-linked during the curing process, which is most often thermally activated, resulting in the production of complex networks that restrict the movement of the polymeric chains past each other at any given temperature. However, because of this high cross-linking density, thermosetting resins possess an inherently low impact resistance and also cannot be reshaped post cure. Therefore, in order to satisfy the requirements of high-performance industrial applications, such as civil infrastructure and transportation, a variety of fillers are often added to the resin matrix to form composite materials. Most thermosets are incorporated with particulate fillers or fiber reinforcements to (i) modify their physical properties to develop other useful functions, (ii) reduce shrinkage while curing, (iii) improve flame retardance, and, to some extent, and (iv) reduce cost. In addition, as thermosetting polymers cannot be melted and reshaped because of the cross-linking network formed upon curing, they also cannot be directly processed as plastic materials, except by grinding them and converting them into fillers.

With a history that predates that of thermoplastics (the earliest known use being for wood veneering in the Sculpture of Thebes circa 1500 BC), the development of thermosets have long since progressed from their typical application as adhesives or molding compounds [2]. Advances in polymer science research have led to the synthesis of novel thermosets and thermoset-based composites that possess additional functionalities and advantages, such as thermally reworkable epoxide resins as removable adhesives in electronics [3], phenylethynyl-terminated polyimide nanocomposites for aircraft engine components and aerospace applications [4], phthalonitrile/novolac resin blends with high thermal stability and low melting point and curing temperatures [5], and a variety of functional thermosets derived from plant oils such as soybean and corn oil.

6.2.1.1 **Synthetic Thermosets**

Similar to all commercial plastics, the traditional and more commonly used thermosetting resins are considered as ''petrochemicals,'' having been manufactured from petroleum. Some of the primary distillation products of crude oil, which can be classified either as olefins or aromatics, serve as precursors for the synthesis of thermosets. For example, epoxy resins are manufactured by the reaction of epichlorohydrin, a chloro-oxirane, and a derivative of propylene, with bisphenol A, which is a derivative of cumene. Another example would be the unsaturated polyesters (UPs), which are derivatives ultimately originating from ethylene (ethylene glycol) and benzene (maleic acid) [6]. Epoxies and polyesters constitute more than 95% of the thermoset composite market; of the two, polyester-based systems predominate in volume by about 10-fold [6, 7]. Other thermoset resins used in reinforced form are phenolics, vinyl esters, and polyimides. Details of the properties and applications of these thermoset systems will be further discussed in the following section.

Owing to their petrochemical nature, production of synthetic thermosets is largely dependent on the status of the oil industry. Currently, the market for

conventional plastics is expecting a dramatic rise in production cost owing to the continuing increase in oil price, as well as the growing concerns regarding the uncertain future of the world's oil reserve. The production of plastics is also significantly affected by global environmental concerns such as nonbiodegradable landfill impact and emission of toxic pollutants and greenhouse gases; in response, the petroleum-based plastic industry is compelled to seek and utilize alternative sources of raw materials.

6.2.1.2 **Biosynthetic Thermosets**

Renewable resources can provide a significantly sustainable platform to substitute petroleum-based polymers through the design of bio-based polymers that can compete or even surpass the existing petroleum-based materials on a cost-performance basis with high eco-friendliness values. These eco-friendly composites fabricated using crop-derived bioplastics are considered novel materials of the twenty-first century gaining mainstream applications and importance in the materials world [8]. At present, plant oils, polysaccharides (primarily cellulose and starch), and vegetable proteins are most widely utilized plant-based resources for nonfood applications. Over the past decades, a number of efforts have been made to partially, or in some cases totally, substitute these renewable-based analogs for petroleum-based thermosetting materials like epoxy resins and polyurethane (PU) resins and, in some cases, the comparable levels of performances starting from these ''green'' precursors are achieved as compared with petroleum-based thermosetting materials. However, it is difficult to establish a generalized comparison between the properties of these bio-based materials and those of the traditional thermosets, as these properties (glass transition temperature, impact strength, stiffness, water absorptivity, etc.) vary extensively with respect to their origin and, consequently, their structure; for instance, the impact strength of lignophenolic bagasse fiber composites is comparable to that of its phenol formaldehyde counterpart, but they exhibit higher moisture affinity [9]. Recently, renewable resources have being viewed not as a substitute for the existing thermosetting materials, but as resources to produce novel thermosetting materials in more specific applications. Details on the preparation and the properties of bio-based thermosetting materials are discussed in Section 6.3.

6.2.2
Natural Fibers

Cellulosic fibers, which are currently viewed as viable alternatives to synthetic fibers in the manufacture of NFRPs, have already established their place in the infrastructure and commercial products market. Currently, many types of natural fibers, derived from either wood and agricultural fibrous plants (such as flax, hemp, jute, and kenaf) or vegetable wastes (such as bagasse, rice husk, and grass), have already been investigated for use with plastics. Table 6.1 shows a list of biofibers and their sources [10]; a more detailed discussion on natural fiber reinforcements can be found in Chapter 3 of this book. In general, biofibers can be considered

Table 6.1 List of important biofibers [10].

Fiber source	Species	Origin
Abaca	*Musa textilis*	Leaf
Bagasse	—	Grass
Bamboo	(>1250 species)	Grass
Banana	*Musa indica*	Leaf
Broom root	*Muhlenbergia macroura*	Root
Cantala	*Agave cantala*	Leaf
Caroa	*Neoglaziovia variegata*	Leaf
China jute	*Abutilon theophrasti*	Stem
Coir	*Cocos nucifera*	Fruit
Cotton	*Gossypium* sp.	Seed
Curaua	*Ananas erectifolius*	Leaf
Date palm	*Phoenix dactylifera*	Leaf
Flax	*Linum usitatissimum*	Stem
Hemp	*Cannabis sativa*	Stem
Henequen	*Agave fourcroydes*	Leaf
Isora	*Helicteres isora*	Stem
Istle	*Samuela carnerosana*	Leaf
Jute	*Corchorus capsularies*	Stem
Kapok	*Ceiba pentranda*	Fruit
Kenaf	*Hibiscus cannabinus*	Stem
Kudzu	*Pueraria thunbergiana*	Stem
Mauritius hemp	*Furcraea gigantea*	Leaf
Nettle	*Urtica dioica*	Stem
Oil palm	*Elaeis guineensis*	Fruit
Piassava	*Attalea funifera*	Leaf
Pineapple	*Ananus comosus*	Leaf
Phormium	*Phormium tenas*	Leaf
Roselle	*Hibiscus sabdariffa*	Stem
Ramie	*Boehmeria nivea*	Stem
Sansevieria (bowstring hemp)	*Sansevieria*	Leaf
Sisal	*Agave sisilana*	Leaf
Sponge gourd	*Luffa cylinderica*	Fruit
Straw (cereal)	=	Stalk
Sun hemp	*Crorolaria juncea*	Stem
Cadillo/urena	*Urena lobata*	Stem
Wood	>10 000 species	Stem

to be composites of hollow cellulose fibrils held together by a matrix of lignin – a complex hydrocarbon polymer with aliphatic and aromatic components – and heteropolysaccharides collectively known as *pentosans*.

One important technical reason for this preference for NFRP is that they offer less damage to tools and molding equipment and provide relatively better finishing. The higher degree of flexibility, as well as low density and nonabrasive surface of

natural fibers offer practical advantages for reinforcing polymer–matrix composite components in comparison to glass fibers. Additionally, the relatively greater toughness of NFRP allows for absorbing high impact energy.

From a practical point of view, bio-based fibers are limited by the largely varying dimensions provided by the source plant's anatomy, that is, it is rather almost impossible to specify a given length or diameter for a specific natural fiber and one must simply accept what nature provides. The statistically significant dispersion in dimensional values is also quite accentuated, which, technically, is an undesirable feature. Therefore, these fibers, like all other lignocellulosics, can be considered nonuniform in comparison with synthetic fibers that are fabricated within precise dimensional values. However, in terms of length, it has been shown that many lignocellulosic fibers such as abaca and kenaf have average values that are sufficient to be considered as long and continuous fiber reinforcement and assure effective strengthening of the composites. One possible solution for the limitation in length of lignocellulosic fibers is to weave the fibers into a continuous thread that could then be wound on a spool (as done with cotton, flax, and ramie): in this way, uniformly distributed NFRPs could be automatically fabricated by pultrusion, prepreg, or filament-winding processes. However, a weave operation adds supplementary cost to the fiber processing and diminishes its economical advantage. Moreover, highly stiff fibers such as bamboo and coir are difficult to weave in automated fabrication equipment.

6.2.3
Fabrication Techniques

Basically, the fabrication of fiber-reinforced thermoset composites involves five distinct procedures: (i) alignment of reinforcing fibers, (ii) mixing the matrix resin with the hardening agent, (iii) dispensing the mixture into the product mold, (iv) fiber impregnation with the resin, and (v) curing. However, although thermosets are the simplest of the plastic materials to process, some deformities may still occur during the molding process. Some common problems that must be considered are (i) the air bubbles that may potentially get trapped in the molded plastic, (ii) the complexity of the mold design from which the product must be extracted, and (iii) thermal-induced volume shrinkage, which can cause cracking or high residual stress when it occurs rapidly and unevenly.

Fabrication techniques suitable for manufacturing natural fiber-reinforced thermoset composites include the (i) hand layup for unidirectional fibers/mats/fabrics; (ii) sheet molding compound (SMC)/bulk molding compound (BMC) for short and chopped fibers; (iii) filament winding, and (iv) pultrusion for continuous fibers. However, in natural fibers, there are really no ''continuous'' fibers such as in the case of man-made fibers – the length of some natural fibers reaches up only to several meters (for fibers bundles connected along the length direction, then the fiber length can be longer). Prepregs are also sometimes used, although they are limited by the irreversible curing of thermosets.

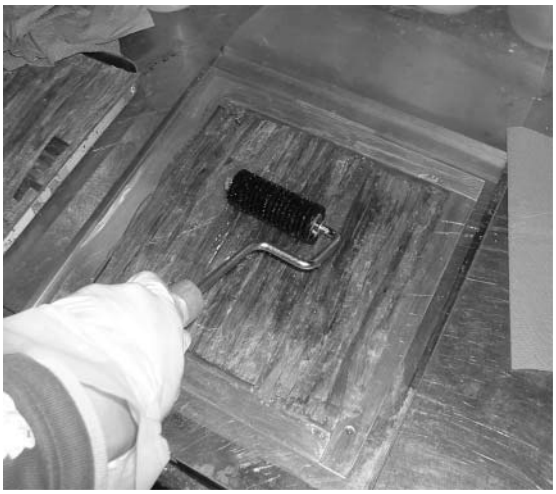

Figure 6.1 Lab-scale fabrication of multi-ply, unidirectional kenaf, and fiber-reinforced ortho-UP composites by hand layup [12].

6.2.3.1 **Hand Layup**

Hand layup is by far the most widely used processing method for fiber-reinforced materials [11]. In this method, the mold is first prepared with a sufficient degree of finish. A release agent is applied to the mold to get a resin-rich top surface. Then the resin is mixed with suitable proportions of accelerator, promoter, and catalyst. The resin-impregnated fibers are laid on the prepared mold to a desired thickness, and the material is pressed with a hand roller to eliminate any entrapped air bubbles and extra resin (Figure 6.1). The product is then subjected to postcuring treatment. The extent of fiber loading is restricted by their anatomical features – particularly by the intrafiber voids called *lumen*. If the natural fiber being used has large lumens and small cell walls, then higher fiber loading can only be achieved with increased compression.

One major advantage of hand layup is that it is a very simple process so that very little special equipment is needed, and the required molds may be made from plaster, wood, sheet metal, or even FRP. However, while it is the simplest and easiest fabrication method, because it is an open mold process, its final product shape is not readily controllable, and there is an undesirable release of volatile organic compounds (VOCs) during curing. VOC emissions from polyester resin operations occur when the cross-linking agent, such as styrene and methyl methacrylate monomer, contained in the liquid resin evaporates from fresh resin surfaces into air during application curing, as well as from the use of solvents for cleanup of hands, tools, molds, and the application equipment [13]. Therefore, for better dimensional accuracy and safer work conditions, the other liquid composite molding processes are preferred.

6.2.3.2 Compression Molding

Compression molding is the most common method of forming thermosetting resins prior to the advent of injection molding. It includes sheet molding, bulk molding, and cold press and hot press methods – all of which are done by compressing the material in a mold cavity of the desired shape with the application of heat. The procedure is similar to the hand layup technique, except for the set of matched dies used, which are closed upon application of pressure before cure takes place – thus producing less VOC emissions than hand layup. Also, by applying this method, up to 70 wt% of fiber loading could be attained and the thickness of the product can be around 1–10 mm. The much larger volume of fiber loading is possible compared to the hand layup process because the applied pressure compresses the intrafiber voids or lumens more effectively. Pressure is usually at 7–14 MPa, although some thermosets may require pressures down to 345 kPa or even just plain contact. Majority of thermosets are heated to about 150–200 °C for optimum cure, but can go as high as 650 °C (but not if they are used as matrix resins) [14].

6.2.3.3 Filament Winding

Filament winding is another way to continuously manufacture NFRP composites for hollow parts (such as pipes and vessels). Here, the continuous fibers are impregnated in a bath of the resin mix (resin + accelerator + catalyst + promoter) and then wound on a rotating mandrel. After impregnation, the fibers are continuously conveyed to a rotating mandrel. In comparison to thermoplastic polymer composites – in which fibers are inserted in a polymer melt, followed by forming the composite to the desired shape at an elevated temperature – the use of thermosets provides better impregnation and higher reactivity with the fibers during curing, leading to finer morphological structures. Because the fiber coating and layer forming procedure for this method is very intricate, filament winding has the capability to yield high-strength FRP materials – thus, it is mostly applied to fabricating material parts for aerospace and other engineering applications of highly demanding requirements [15].

6.2.3.4 Pultrusion

Thermoset-based composites parts (called *profiles*) with a constant cross-sectional shape may be manufactured through a continuous technique called *pultrusion*. This continuous process consists of impregnating a fiber as a reinforcing material into a resin bath, and then passing the impregnated fiber toward a shaping die where the resin is subsequently cured. The predried fibers are mixed with the resin mixture and pulled through a hollow tube to produce composites in the form of rods. Continuous profiles of any dimension can be manufactured by this method. While this technique is very popular for manufacturing synthetic fiber-reinforced composites, there still remains an immense scope in utilizing this method for manufacturing biocomposites for widespread applications. The applicability of this method is limited by the shape of the forming dies available for usage, and special modifications must be added to the equipment to allow for cross-linking [16].

6.2.3.5 Resin Transfer Molding

Resin transfer molding (RTM), also called *resin injection molding* (*RIM*), uses a set of dies encapsulating a preform, followed by resin injection into the preform. Inserts and core can be encapsulated into the molded laminate, if necessary. RTM is suitable for low- to mid-volume production with constant and high quality. Recently, vacuum-assisted resin transfer molding (VaRTM) has been developed for cost saving. VaRTM uses only one mold whose material is not limited only to metals, and the preform placed on the mold is sealed with a vacuum bag. The prepolymeric and liquid resin is then injected (or compressed) with vacuum pressure into a closed mold containing a fibrous preform. The mold is then heated, and the resin cures/polymerizes into a cross-linked network, entrapping the fibers. As an alternative, preimpregnation of fabrics with the prepolymeric resin may be carried out. In that case, curing/polymerization are generally activated by heat in an autoclave after compressing the mixture into a closed mold. Because of the high fiber volume (55–60%) that can be achieved with this method, RTM is also employed when fabricating parts for aerospace applications [17].

6.3 Biofiber-Reinforced Synthetic Thermoset Composites

6.3.1 Polyester-Based Composites

UP-based green composites have been a subject of several investigations. Vilay *et al.* [18] reported the positive effects of chemical fiber treatment and increased fiber loading on the mechanical strength of bagasse fiber-reinforced UP composites. Fiber surface modification is essential in improving interfacial adhesion between the hydrophilic natural fibers and the hydrophobic polymer matrix. This is achieved either (i) by fibrillation upon separation of cellulose fibrils from lignin and other components or (ii) by activation of cellulosic hydroxyl groups using coupling agents and replacing them with moieties that are thermodynamically compatible with the thermoset resin, thereby forming strong fiber–matrix links made of hydrogen bonds and covalent bonds. The most traditional form of fiber treatment is mercerization, which can effectively increase the mechanical strength of any NFR composite, provided that optimum treatment conditions are established (Figure 6.2). NFRP strength can also be increased by incorporating fibers at high weight fractions and configurations, as shown in Figure 6.3 [12]. It is clearly evident that by increasing the fiber content in the polyester matrix, the tensile strength also increases because the polyester resin transmits and distributes the applied stress to the fibers, resulting in higher strength [19, 20].

One major drawback of fabricating NFRPs with high fiber loading is the increase in water absorption, which is the primary focus of some of the research endeavors. The contribution of natural fibers to the overall water affinity of the NFRP can be evaluated by measuring the mechanical performance of composites in wet

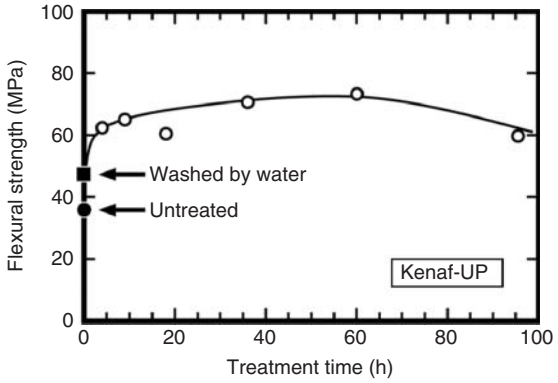

Figure 6.2 Effect of alkali treatment time on the tensile properties of continuous kenaf fiber-reinforced ortho-UP composites. The alkali solution bath temperature is set at 80 °C [12].

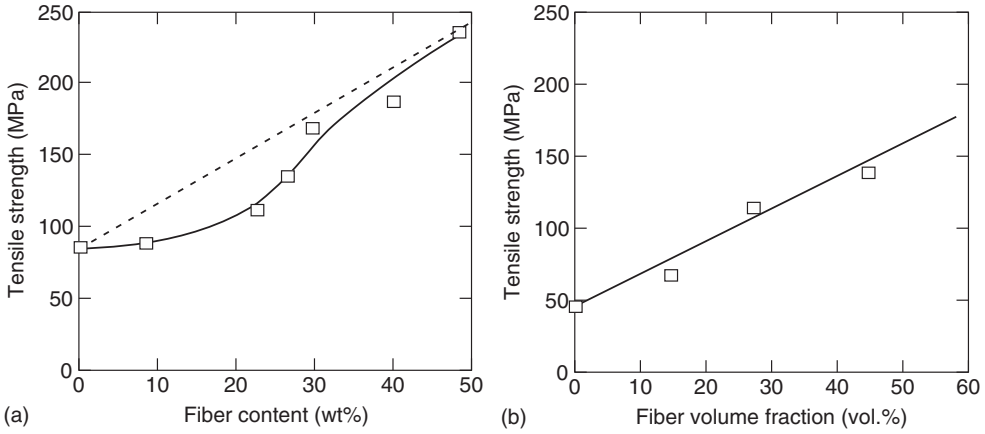

Figure 6.3 (a) Flexural and (b) tensile strength of unidirectional kenaf fiber-UP composites [12].

environment. Dhakal *et al*. [21] have discussed the NFRP failure due to water degradation based on their study on water sorption properties and wet mechanical properties of hemp fiber–UP composites. For brittle thermosetting resins such as UP, moisture uptake can easily reduce mechanical strength by fiber swelling-induced microcracking. This leads to increased water diffusion by capillary action along the fiber–matrix interface, which further degrades owing to the hydrophilicity of cellulose and a decline in mechanical strength and stiffness. It must be noted that water sorption behavior differs for different types of NFR composites, as illustrated in Figure 6.4, which also shows that the combination of two different fibers would yield a hybrid with an intermediary set of properties [22]. The source of the natural fiber reinforcement also has a vital impact on the composites' water

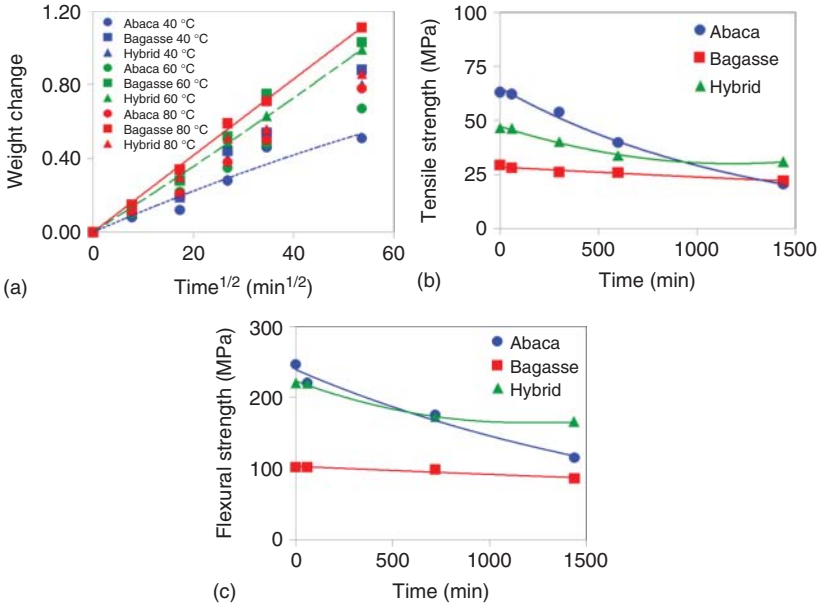

Figure 6.4 Water sorption curves (a), postimmersion tensile (b), and flexural strength (c) for abaca and bagasse FRP composites [22].

sorption properties, which is an important quality of long-lasting, degradation-resistant polymeric materials. However, while each type of NFRP has its own water sorption tendency, they all tend to observe the same Fickian diffusion behavior [23]. This is because of their varying structure (specifically the cell wall-to-lumen ratio) and composition (the O/C ratio is an indication of hydrophilicity). The lumen density, which determines fiber porosity and, consequently, the resulting NFRP's equilibrium moisture content, is characteristic of each natural fiber's morphology and may not be altered by chemical treatment. The lumen density is also dependent on which part of the plant the fibers were extracted: the porosity of bagasse fibers, for example, depends on whether they were extracted from the sugarcane rind or pith [24]. On the other hand, the fiber's O/C ratio is easily subject to lowering by the activation of the cellulose hydroxyl groups, such as in alkali and silane treatment. In any case, this problem can be attenuated using an appropriate fiber treatment operation, although this implies additional processing cost and decreases the economical competitiveness of the bio-based fibers.

6.3.2 Epoxy-Based Composites

Epoxy-based biocomposites have been a significant topic in the continually growing field of research on green composite design for long-term applications. As a potential viable replacement to traditional glass fiber-reinforced plastics (GFRPs),

it is imperative to evaluate the major factors contributing to the performance of NFR epoxy resins – particularly those that dictate the reinforcing capability of natural fibers. Aside from extent of chemical treatment and volume fraction, other important fiber parameters are fiber source, length, and orientation, and type of fiber mat fabricated. For instance, in the case of unidirectional fibers, composite strength depends upon the failure strains of both the fiber (ε_f) and the matrix (ε_m); however, if the fiber content of the composite is high enough ($V_f > 11\%$), then the ultimate stress of the composite (σ_{uc}) can be estimated as a linear function of the volume fraction ($\sigma_{uc} = \sigma_{uf} V_f$) [25]. Scanning electron microscopy (SEM) may be used to directly observe the composite structure – particularly the fiber–matrix interface – to study adhesion strength and determine the cause of a composite's failure. For instance, if it has been noticed that the fiber failed by tearing but no interfacial failure is observed, and that there are traces of matrix is still adhered to the fiber, then it is a clear indication that the fiber–matrix adhesion is not lost and that failure is predominantly due to the matrix properties [26].

6.3.3
Vinyl Ester-Based Composites

Vinyl ester resins, which are synthesized by the reaction of a diepoxide with an acrylic acid, are relatively recent additions in the family of thermosetting resins used for manufacturing NFR composites. They combine the excellent chemical resistance and the thermal and mechanical properties of epoxy resins, making them highly applicable for FRP pipes and tanks, but with the ease of processing and the rapid curing characteristics of UP resins. Compared to other thermosets, these resins show a more superior moisture resistance and wet mechanical strength, as illustrated in Figure 6.5 [27]. Vinyl esters have given way to broad new set of applications for thermoset resins because of the following reasons: (i) they can be cured at room temperature using relatively nontoxic catalysts much like polyester resins; (ii) they have excellent wetting characteristics, owing to the presence of the epoxy group; (iii) they possess very high dimensional stability because of their controlled cross-linking structure; and (iv) they have very good thermal aging properties when novolac-type epoxy becomes a part of the basic structure.

Ray *et al.* [28] have reported the effect of the degree of mercerization of jute fibers on the mechanical strength of jute/vinyl ester composites. From the data presented, it can be deduced that fiber treatment conditions may significantly affect the mechanical strength of the NFRP, which implies the necessity to determine optimum treatment parameters. The same observation has been reported by Botaro *et al.* [29] on vinylester reinforced with esterified *Luffa cylindrica* fibers. Another mechanical property that must also be evaluated with the application of natural fiber treatments is impact strength, which is an essential fracture property of the green composite. Li *et al.* [30] have reported that while chemical agents such as silane and permanganate helps strengthen the fiber–matrix interfacial strength, it considerably decreases the ability of the composite to absorb impact energy during fracture. This is because the stronger the interfacial bond between the fiber and

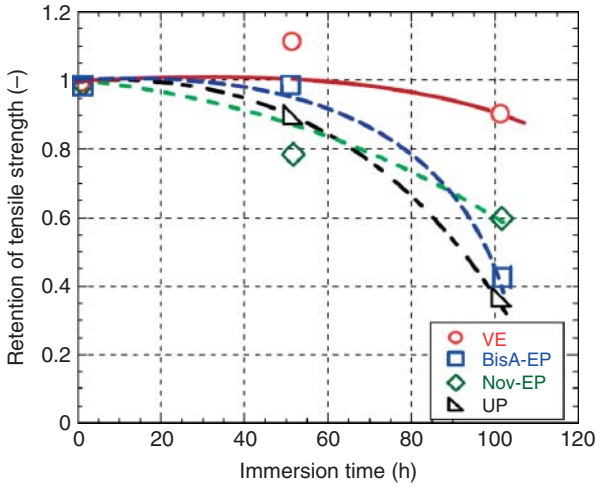

Figure 6.5 Retention of tensile strength of different kenaf fiber-reinforced thermosets after immersion test in water at 80 °C [27].

the resin is, the more rigid the material becomes, and therefore the mobility of the polymer matrix and its ability to dissipate energy gets more restricted.

6.3.4 Phenolic Resin-Based Composites

Phenolic resins, also widely known as *phenol–formaldehyde* (*PF*) resins and phenoplasts, work well with natural fibers in the production of biocomposites as they do not require a high processing temperature (<200 °C); this allows for the manufacture of NFR composites without the risk of thermal degradation of the fibers, which innately have low thermal stability and low coefficient of thermal expansion. They also have polar functional groups that can easily form a bond with the lignocellulosic fibers. For sisal fiber-reinforced phenolic thermosets, De Paiva and Frollini [31] showed that the PF matrix resin can effectively protect the incorporated fibers from large thermal degradation, based on the lower mass loss incurred by the treated sisal fiber-reinforced PF composites. However, Kalia and Kaith [32] showed that the mechanical properties of the composites may be further increased by grafting the fibers to the polymer matrix. Another important thermal property of thermoset systems such as PF composites is their thermomechanical behavior, which is usually measured by performing a dynamic mechanical thermal analysis (DMTA). The addition of the fibers increases the glass transition temperature (T_g) of the system, and fiber treatment can further increase the biocomposites' ability to dissipate energy by improving the fiber–matrix interfacial strength and, consequently, the load transfer efficiency. There is an observable increase in storage modulus because the fibers' cellulose is a highly crystalline material that can act as an internal link in the matrix [33].

6.3.5
Other Thermoset-Based Composites

PU-based green composites have already shown promise in the automotive industry, using fibers such as jute and ramie to manufacture parts such as door linings. However, PUs, one of the most versatile thermosetting materials, have been used as a biocomposite matrix in only a limited number of research reports: Bledzki *et al*. [34], for instance, have come up with an experiment-based approximation model relating the static mechanical properties of jute and flax fabric-reinforced PU microfoams with microvoid content. The mechanical performance and properties of other thermoset biocomposites, such as coir fiber-reinforced ethylene glycol dimethacrylate (EGDMA) [35] and oil palm fiber-reinforced poly(allyl methacrylate) [36], are even more scarce. Recently, a lot of research efforts are given to the synthesis and application of thermosetting resins derived from renewable sources, the details of which are discussed further in the following sections.

6.4
Biofiber-Reinforced Biosynthetic Thermoset Composites

6.4.1
Lignin-Based Composites

Lignin is the most abundant natural polymer next to cellulose and it exists as one of the major constituents in plant cell walls; however, it is also considered as a by-product in the pulp and paper industry, which is the primary source of commercially available lignins. The lignosulfates, which are obtained from the sulfite process, are the most commonly available type of lignin. Lignin has a variety of interunit linkage and an amorphous three-dimensional network polymer; they have an aromatic and cross-linked structure, together with a great variety of functional groups such as ether and hydroxyl groups, depending on the origin of lignin and the extraction technology applied [37]. In general, however, it is widely accepted that the biosynthesis of this complex macromolecule stems from the polymerization of three types of phenylpropane units, also referred to as *monolignols*. These units are coniferyl, sinapyl, and *p*-coumaryl alcohol (see Figure 6.6) [38]. Owing to its phenolic nature, lignin has mostly been considered as the most natural substitute for phenol in PF-based resins [39], therefore, the same preparation may be adopted, such as the prepolymer synthesis involving lignin methylolation presented by Paiva and Frollini [9]. However, in PF formulation, it introduces highly substituted aromatic rings bearing less free sites and more steric restrictions; thus, modifications such as the one presented by Mikame and Funaoka [40] must be employed to increase phenolic content and reactivity.

Guigo *et al*. [41] have reported that, based on TGA and DMTA, the incorporation of plasticized lignin to polyfurfural alcohol, another biosynthetic thermoset, effectively increases impact strength and stiffness. Because of its high compatibility with

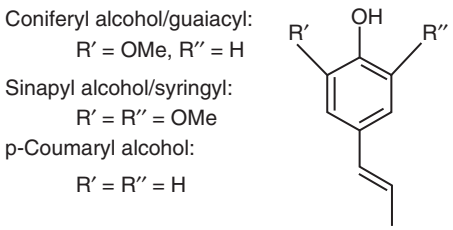

Figure 6.6 Chemical structure of the main components of lignin [38].

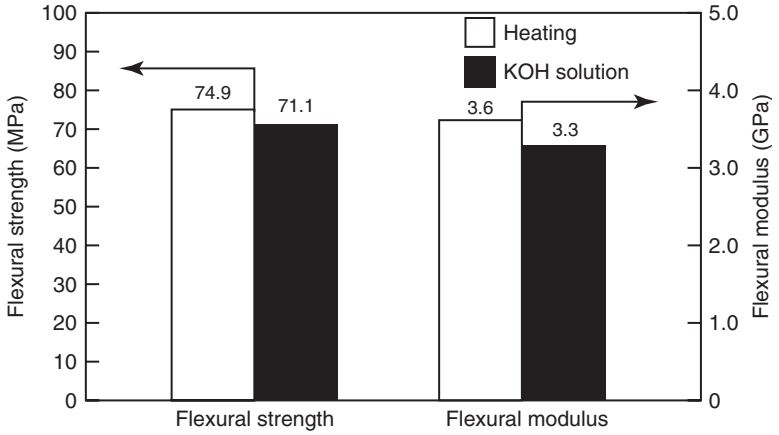

Figure 6.7 Effect of KOH solution as catalyst on the flexural strength and modulus of lignin-filled epoxy composites [43].

lignin, furfuryl alcohol is also reported to be a suitable fiber treatment (coupling agent) for preparing lignophenolic-based NFR composites [42]. However, other thermosets may be investigated for evaluating the applicability of lignin as particle filler. For epoxy/lignin composites, Tamura *et al.* [43] studied the acceleration effects of heat, amine, and KOH addition to the reaction of lignophenols to epoxy groups, which determines the mechanical strength of the polymer blend (see Figure 6.7).

Recently, lignin esters have also been proposed for use as UP thermosets, using anhydrides to render them more soluble in styrene, which is a commonly used diluent in unsaturated thermosetting materials [44]. The use of lignin esters as an additive in unsaturated thermosetting materials provides several advantages by acting as a toughening agent that improves the cross-link network connectivity and offers additional stiffening groups.

6.4.2 Protein-Based Composites

Recent years have witnessed a particular attention on protein-based thermosetting materials owing to the depletion of petrochemical resources. Vegetable proteins

such as soybean-based protein are now regaining more attention as substitute to synthetic polymers in specific applications, where these macromolecules are processed as thermosets by extrusion at high temperature. Yang *et al.* [45] has presented the synthesis of a thermosetting material for food packaging, using a blend of wheat gluten powder and rice protein powder mixed with formaldehyde as a cross-linking agent and glycerol as plasticizer. As a biocomposite matrix, its low mechanical strength calls for the need to reinforce it with natural fibers.

There are several available reports focusing on the NFR soybean protein-based composites: for example, Liu *et al.* [46] evaluated the mechanical properties of grass-reinforced soy-based bioplastic, while Lodha and Netravali [47] evaluated the interfacial strength for ramie fiber-reinforced soy protein isolate (SPI). It must be noted, however, that the long-term performance of soy proteins is limited because of their high sensitivity to moisture as a result of the presence of amine, amide, carboxyl, and hydroxyl groups. To reduce their hygroscopicity, the soy proteins are cross-linked with aldehydes such as formaldehyde.

6.4.3
Tannin-Based Composites

Tannin compounds, extracted from the wood, bark, leaves, and galls of plants and used mainly in the leather industry, are now considered as another raw renewable material in the design of phenolic resins. Tannins are natural polyphenolic materials that can be classified by their chemical structure and properties into two groups: hydrolyzable tannins and condensed tannins (see Figure 6.8); between the two, the condensed tannins show better reactivity with formaldehyde, owing to the presence of a larger number of free phenolic rings [48]. Circumstantial evidence strongly suggests that their repeat unit is structured as illustrated in Figure 6.9 [49]. Extraction of tannin is done using water at an elevated temperature (~95 °C)

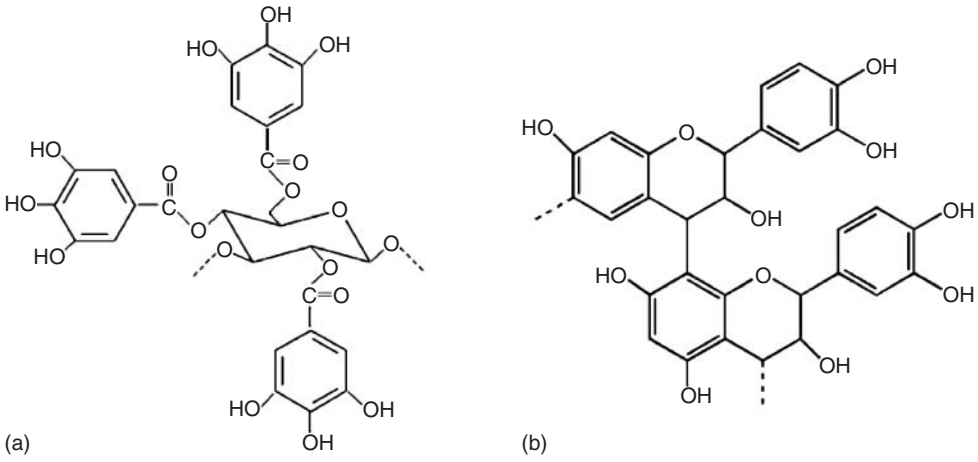

Figure 6.8 Chemical structure of the hydrolyzable (a) and condensed (b) tannins [48].

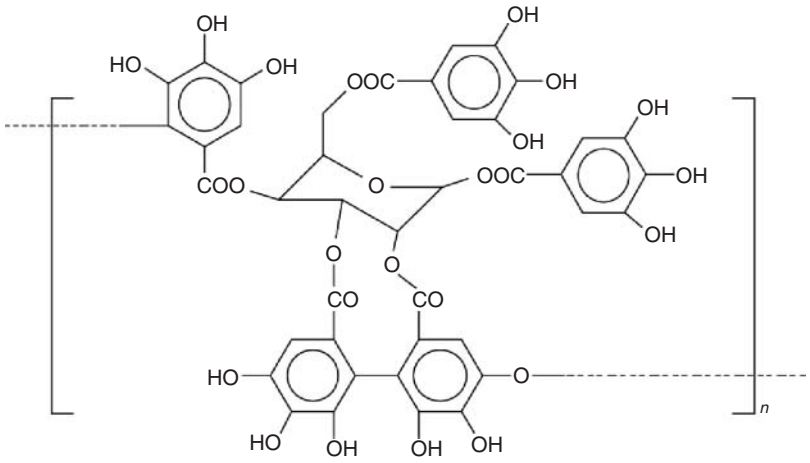

Figure 6.9 Generalized chemical structure of a tannin polymer [49].

followed by fractionation and isolation in an acetone/water mixture (6 : 4); curing is similar to that of a PF resin. Examples of tannin use as thermoset include adhesive applications with partial or full replacement of PF resin in plywood and composite panels, and the partial substitution of resorcinol in phenol resorcinol formaldehyde (PRF) adhesives in ambient temperature curing, cold-set finger jointing, or laminating applications [50].

A limited number of research papers focusing on tannin biocomposites have been published, which is indicative of the degree of novelty of tannin–phenolic thermoset systems. Barbosa *et al.* [48] showed, using a coir fiber-reinforced tannin–phenolic thermoset, that fiber length can have a significant effect on the biocomposite's fracture strength, thermal stability, and water affinity. Much like in the case of lignophenolics, further investigation on the properties and potential applications of tannin-based biocomposites can be foreseen in the near future.

6.4.4 Triglyceride-Based Composites

In the formation of sustainable thermoset resins, epoxidized and acrylated epoxydized plant oils and fatty acids have been largely utilized, as reported from literature [51]. For composite applications, acrylated epoxydized soy bean oil (AESO) resin is mainly used because it is commercially accessible [52]. The synthesis of AESO is shown Figure 6.10: the carbon–carbon double bonds in the fatty acid chains are modified to append different polymerizable functionalities, such as epoxides and acrylates, to increase the reactivity of the vegetable oils [53]. AESO can be cured at room and high temperatures, depending on the initiator, and can be blended with a reactive diluent such as styrene in order to improve the processing flowability and the mechanical performance. Structural applications such as sandwich beams

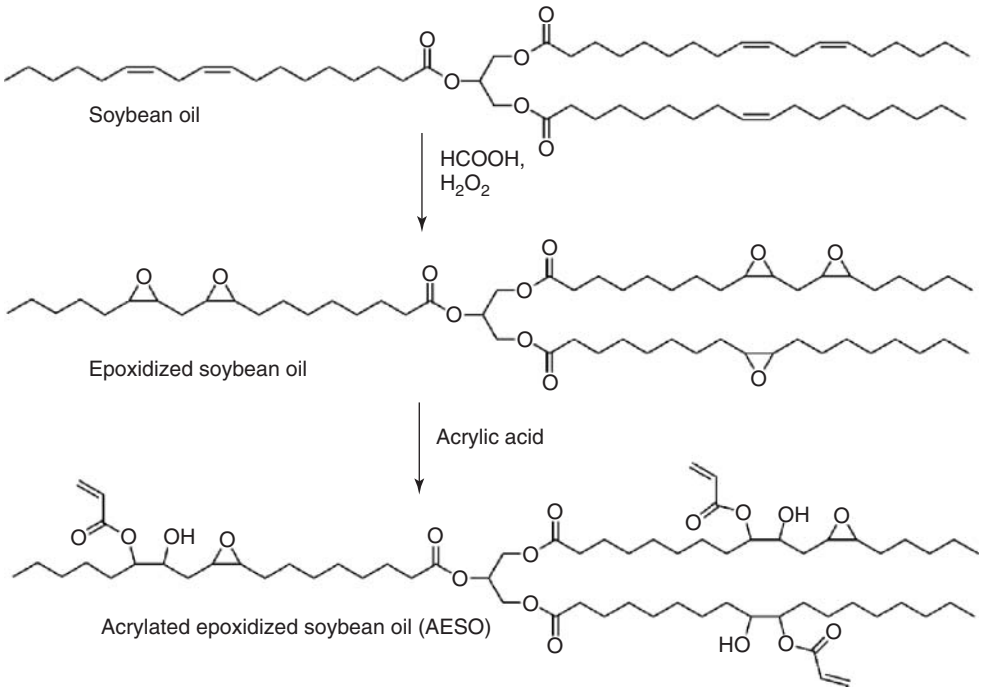

Figure 6.10 Synthesis of acrylated epoxidized soybean oil (AESO) [53].

using natural fibers and AESO resin with VaRTM technique have already been investigated [54, 55].

Epoxidized plant oils such as castor oil can also be converted into polyols and copolymerized with isocyanates such as toluenediisocyanate (TDI) or methylene-4,49-diphenyldiisocyanate (MDI) to obtain PUs. Meier *et al.* [56] reported that canola, corn, soybean, and sunflower oil-derived polyols yield PU resins of similar cross-linking densities (and, consequently, similar glass transition temperatures) and mechanical properties, despite differences in fatty acid distribution.

6.4.5
Other Thermoset-Based Composites

Recently, UP made partly from biomass resources have been developed for commercial applications. For example, Japan U-PICA Co. Ltd [57] has recently patented the synthesis of UP resin made partly of monomers from inedible biomass resources. The resulting resin is proven to exhibit better processability and performance comparable to that of conventional UP. Bamboo, hemp, and kenaf fiber mat-reinforced composites of this particular resin have exhibited high specific bending strength and stiffness comparable to those of glass fiber mat-reinforced composites. Another biosynthetic resin that has been recently gaining more attention in the biocomposite industry is poly(furfuryl alcohol) (PFA), or furan resin,

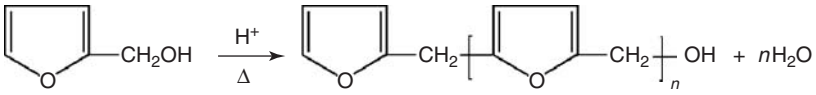

Figure 6.11 Polycondensation reaction of furfuryl alcohol into furan resin [58].

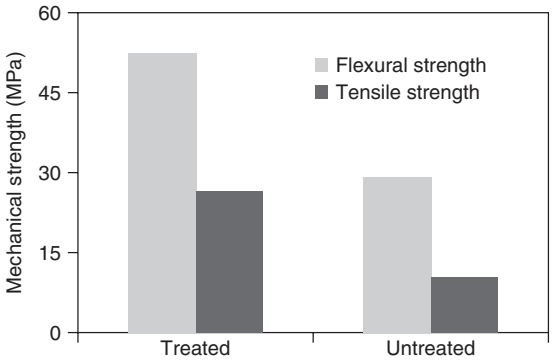

Figure 6.12 Mechanical strength of untreated and alkali-treated continuous abaca fiber-reinforced furan resin composites [60].

which is a highly brittle but extremely corrosion-resistant thermoset derived from the destructive distillation of agricultural wastes such as corn cobs and oat hulls. Furan resin is a linear condensation polymer (see Figure 6.11 [58]) derived from agricultural by-products such as corn cobs and rice hulls. This biosynthetic resin exhibits excellent resistance to most acids, alkalis, and solvents, with the exception of strong oxidizing agents such as peroxides and very strong acids. It also possesses a strong heat resistance and fire-retardant property, making it suitable for application in elevated temperatures. As one of the most stable thermosetting plastics, furan resin is highly resistant to biodegradation; however, because it is synthesized from agricultural by-products, this bio-based polymer resin still offers a certain degree of environment friendliness. Its use in the production of such renewable materials, combined with its excellent corrosion resistance, makes furan one of the major commercially available resin mortars and chemical linings [59]. As a biocomposite matrix, it is currently used by the European automotive industry for making car parts because of its excellent fire-retardant quality, but it is also an excellent lining material for chemical storage tanks and pipelines because of its anticorrosion properties. Owing to its low mechanical strength, it is important to establish a proper curing procedure for the resin and ensure that the natural fiber incorporated into the resin provides sufficient reinforcement; this can be achieved by using proper fiber treatment procedures (see Figure 6.12) [60] – making its mechanical performance comparable to that of a UP-based biocomposite (see Figure 6.13). In addition, because it is derived from biomass, the use of furan resin as a matrix allows for an increase in long-term carbon fixation compared to the traditional petrochemical resins [61].

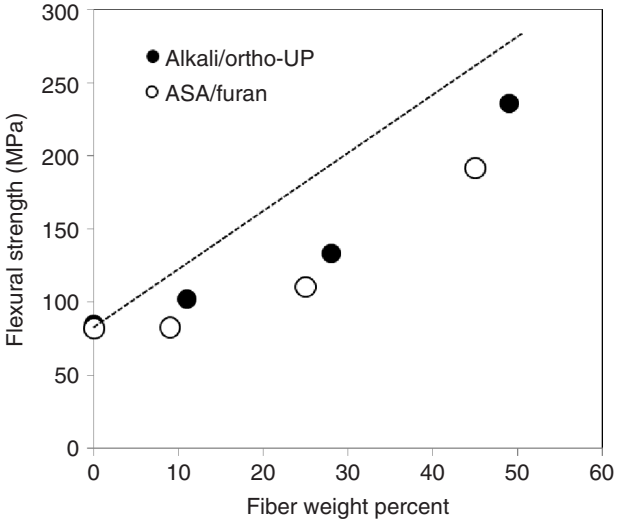

Figure 6.13 Flexural strength of abaca/furan composite and abaca/ortho-UP composite at different fiber weight fractions [61].

6.5
End-of-Life Treatment of NFR Thermoset Composites

Because of their lack of biodegradability, it is necessary to determine the proper methods for dealing with thermoset-based materials at the end of their service lives. Currently, there are four established treatment procedures that can be applied to thermoset composites: (i) recycling as composite fillers, (ii) pyrolysis, (iii) chemical recycling, and (iv) energy recovery.

6.5.1
Recycling as Composite Fillers

This mechanical recycling approach, also known as *comminution*, is widely used owing to its lower energy requirement in comparison to the other methods. When the thermoset-based composites are recycled, they are typically subjected to a grinding process to break the composites into fragments that may then be used directly as a filler or reinforcement fiber in a new component. Thermoset composites are milled into very fine powders and are used as filler materials for polymers [62]. A regrinding process is also generally used on uncontaminated composites: the finer the material is ground, the better the finish that can be obtained. It must be noted that when using recycled filler for compression and injection molding of new components, simple molds, and higher pressures are often required.

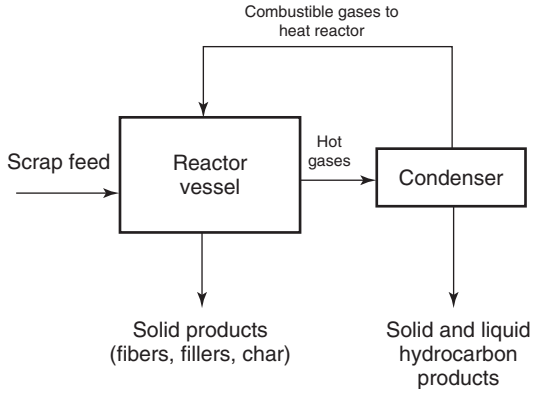

Figure 6.14 Schematic representation of the pyrolysis process [63].

6.5.2 Pyrolysis

Pyrolysis can be considered as an alternative method of recycling plastic materials and is especially appropriate for thermoset composites which cannot be remolded. Figure 6.14 illustrates the scheme for the process: it shows the thermal decomposition of materials at high temperature without the presence of oxygen [63]. This technology has already been widely applied over the years to convert wood, coal, and other carbonaceous materials into secondary fuels [64]. The pyrolysis of a polymeric composite produces various hydrocarbons that can be used mainly to produce energy but can also be ingredients in the synthesis of new polymers; therefore, pyrolysis can be considered as an indirect way of using plastic wastes as fuels. On the downside, the remaining pyrolysis product is considered solid waste – made more significant by composites having a significant amount of mineral content – that must still be disposed at a cost; thus this method is not always as cost effective as other treatment methods.

6.5.3 Chemical Recycling

Chemical recycling, also known as *feedstock recycling*, involves breaking down the polymer matrix into smaller molecules that can be easily separated from impurities and fillers, after which the obtained products are used to synthesize raw materials for petrochemical processes [65]. Examples of such recycling technique are cracking, hydrogenation, and solvolysis: (i) alcoholysis, (ii) glycolysis, (iii) ammonolysis, and (iv) hydrolysis. Polymeric composites made from PUs, epoxy, polyester, and other resins systems are immersed in a chemical environment, where they undergo depolymerization for the recovery of their base monomers. The procedures are described in several reports, such as the one presented by Behrendt and Naber for PUs [66], and the degradation mechanisms are subjects of several investigations

such as the one presented by Dilafruz *et al*. [67]. For solvolysis, the solvent to be used depends on the resin's solubility; it is therefore imperative to perform segregation prior to treatment as each polymer degrades at a different rate. In addition, because the reinforcing fibers still require disposal after the process, chemical recycling is still preferred to be implemented on unreinforced plastic wastes; however, for biofiber-reinforced polymer resins, this issue is minimal because of the fibers' biodegradability.

6.5.4 Energy Recovery

Direct usage of waste thermosets may be considered as a form of recycling that follows the waste-to-fuel scheme. Aside from base monomers, the used biocomposites can also be considered as direct substitute or supplement to fossil fuel as energy source, as they may have heating values to comparable to that of low grade coal. The shredded residues can either be incinerated, or they can be burnt in pure oxygen to form steam. The use of pure oxygen, however, can raise some cost and safety concerns. One advantage of using incineration for energy recovery is that it allows the feeding of mixed plastics, and even mixed materials, without the need to segregate. Spent composites can easily be disposed by this method, although the nature of their contamination must be taken into account during their handling and processing, to ensure environmental safety. One major disadvantage of this technique is that the energy requirement to completely consume the waste thermoset materials are considerably high and not all countries can afford to maintain the continuous operation of an incineration facility.

6.6 Conclusions

Natural fiber-reinforced biocomposites have been gaining popularity as alternative to GFRP owing to their higher specific properties as well as their easier and less expensive processing. While the current trend in biocomposites is directed toward biodegradable polymer matrices, some of these eco-friendly polymeric materials must be continually developed for long-term applications such as needed in the chemical industries. Thermosetting resins not only provide very stable matrices with very long service lifetimes but also allow for long-term carbon fixation when used to laminate natural fibers in biofiber-reinforced composites. The use of biothermosets such as lignophenolics and furan resins can even further increase the carbon storage potential of these composites because of the additional bio-based carbon content. They are also proven to possess thermal and mechanical properties comparable to those of the commercially used petrochemical resins, as demonstrated by the plethora of research investigations over the recent decades.

Various molding techniques can be employed to fabricate biofiber thermoset composites with relative ease even if continuous fiber reinforcements are preferred,

which gives them a distinct advantage over thermoplastic composites; on the other hand, thermoset-based composites are not readily recyclable unlike their thermoplastic counterparts. However, at high fiber loading, they can be directly utilized as fuel for energy recovery; otherwise, they can be subjected to thermal and chemical treatment to degrade the macromolecules of the resin into simpler hydrocarbons such as oils and monomers.

References

1. McNaught, A.D. and Wilkinson, A. (1997) *Compendium of Chemical Terminology*, 2nd edn, Blackwell Scientific Publications, Oxford.
2. Peng, W. and Riedl, P. (1995) Thermosetting resins. *J. Chem. Educ.*, **72** (7), 587–592.
3. Khosravi, E. and Musa, O.M. (2011) Thermally degradable thermosetting materials. *Eur. Polym. J.*, **47**, 465–473.
4. Liu, H., Wang, T., and Wang, Q. (2012) In situ synthesis and properties of PMR PI/SiO_2 nanocomposites. *J. Appl. Polym. Sci.*, **125**, 488–493.
5. Guo, H., Lei, Y., Zhao, X., Yang, X., Zhao, R., and Liu, X. (2012) Curing behaviors and properties of novolac/bisphthalonitrile blends. *J. Appl. Polym. Sci.*, **125**, 649–656.
6. Mathews, F.L. (1994) Techniques for manufacture of composites, in *Handbook of Polymer Composites for Engineers* (ed. L. Hollaway), Woodhead Publishing, Cambridge.
7. Brydson, J.A. (1999) *Plastics Materials*, 7th edn, Butterworth-Heinemann, Oxford.
8. Vaidya, U.R. and Nadkarni, V.M. (1987) Unsaturated polyester resins from poly(ethylene terephthalate) waste. 1. Synthesis and characterization. *Ind. Eng. Chem. Res.*, **26**, 194–198.
9. Paiva, J.M.F. and Frollini, E. (2002) Sugarcane bagasse reinforced phenolic and lignophenolic composites. *J. Appl. Polym. Sci.*, **83**, 880–888.
10. John, M.J. and Thomas, S. (2008) Biofibres and biocomposites. *Carbohydr. Polym.*, **71**, 343–364.
11. Crawford, R.J. (2002) *Plastics Engineering*, 3rd edn, Butterworth-Heinemann, Oxford.
12. Kubouchi, M., Tamura, K., Yajima, M., Sembokuya, H., Sakai, T., and Tsuda, K. (2005) Development of high strength Kenaf fiber reinforced UP resin. Proceedings of the Third International Workshop on Green Composites, Kyoto, Japan, March 16–17, 2005.
13. South Coast Air Quality Management District (2007) Guidelines for Calculating Emissions from Polyester Resin Operations, *http://www.aqmd.gov* (accessed 28 March 2013).
14. Rosato, D.V. and Rosato, D. (2003) *Plastics Engineered Product Design*, Elsevier Advanced Technology, Oxford.
15. Groover, M.P. (2007) *Fundamentals of Modern Manufacturing – Materials, Processes, and Systems*, 3rd edn, John Wiley & Sons, Inc., Hoboken, NJ.
16. Starr, T.F. (ed.) (2000) *Pultrusion for Engineers*, Woodhouse Publishing Ltd, Cambridge.
17. Tong, L., Mouritz, A.P., and Bannister, M.K. (2002) *3D Fibre Reinforced Polymer Composites*, Elsevier Science Ltd, Oxford.
18. Vilay, V., Mariatti, M., Taib, R.M., and Todo, M. (2008) Effect of fiber surface treatment and fiber loading on the properties of bagasse fiber-reinforced unsaturated polyester composites. *Compos. Sci. Technol.*, **68**, 631–638.
19. Ramanaiah, K., Ratna Prasad, A.V., and Hema Chandra Reddy, K. (2012) Effect of fiber loading on mechanical properties of Borassus seed shoot fiber reinforced polyester composites. *J. Mater. Environ. Sci.*, **3** (3), 374–378.
20. Dedeepya, M., Dharma Raju, T., and Jayananda Kumar, T. (2012) Effect of alkaline treatment on mechanical and thermal properties of Typha angustifolia fiber reinforced composites. *Int. J. Mech. Ind. Eng.*, **1** (4), 12–14.

21. Dhakal, H.N., Zhang, Z.Y., and Richardson, M.O.W. (2007) Effect of water absorption on the mechanical properties of hemp fibre-reinforced unsaturated polyester composites. *Compos. Sci. Technol.*, **67**, 1674–1683.
22. Tumolva, T., Kubouchi, M., Aoki, S, and Sakai, T. (2010) Water sorption in abaca and bagasse fiber-reinforced NFR composites. Proceedings of the First Japan Conference on Composite Materials, Kyoto, Japan, March 9–11, 2010.
23. Sgriccia, N., Hawley, M.C., and Misra, M. (2008) Characterization of natural fiber surfaces and natural fiber composites. *Composites. Part A*, **39**, 1632–1637.
24. Lee, S.C. and Mariatti, M. (2007) The effect of bagasse fibers obtained (from rind and pith component) on the properties of unsaturated polyester composites. *Mater. Lett.*, **62**, 2253–2256.
25. Rong, M.Z., Zhang, M.Q., Liu, Y., Yang, G.C., and Zeng, H.M. (2001) The effect of fiber treatment on the mechanical properties of unidirectional sisal-reinforced epoxy composites. *Compos. Sci. Technol.*, **61**, 1437–1447.
26. Raghavendra, S., Balachandrashetty, P., Mukunda, P.G., and Sathyanarayana, K.G. (2012) The effect of fiber length on tensile properties of epoxy resin composites reinforced by the fibers of banana. *Int. J. Eng. Res. Technol.*, **1** (6).
27. Kobayashi, H., Kubouchi, M., Sakai, T., Tumolva, T., and Tsuda, K. (2007) Effect of matrix on the water resistance of kenaf fiber reinforced plastic. Proceedings of the 10th Japan International SAMPE Symposium and Exhibition, Tokyo, Japan, November 27–30, 2007.
28. Ray, D., Sarkar, B.K., Rana, A.K., and Bose, N.R. (2001) Effect of alkali treated jute fibres on composite properties. *Bull. Mater. Sci.*, **24** (2), 129–135.
29. Botaro, V.R., Novack, K.M., and Siqueira, É.J. (2012) Dynamic mechanical behavior of vinylester matrix composites reinforced by Luffa cylindrica modified fibers. *J. Appl. Polym. Sci.*, **124** (3), 1967–1975.
30. Li, Y., Mai, Y.W., and Ye, L. (2005) Effects of fiber surface treatment on the fracture-mechanical properties of sisal-fiber composites. *Compos. Interfaces*, **12**, 141–163.
31. De Paiva, J.M.F. and Frollini, E. (2006) Unmodified and modified surface sisal fibers as reinforcement of phenolic and lignophenolic matrices composites: thermal analyses of fibers and composites. *Macromol. Mater. Eng.*, **291**, 405–417.
32. Kalia, S. and Kaith, B.S. (2008) Mechanical properties of phenolic composites reinforced with flax-g-copolymers prepared under different reaction conditions – a comparative study. *E-J. Chem.*, **5** (1), 177–184.
33. Silva, C.G., Benaducci, D., and Frollini, E. (2011) Lyocell fiber-thermoset composites. *BioResources*, **7** (1), 78–98.
34. Bledzki, A.K., Zhang, W., and Chate, A. (2001) Natural-fibre-reinforced polyurethane microfoams. *Compos. Sci. Technol.*, **61**, 2405–2411.
35. Khan, M.A., Bhattacharia, S.K., Hassan, M.M., and Sultana, A. (2006) Effect of pretreatment with detergent on mechanical properties of photocured coir (Cocos nucifera) fiber with ethyleneglycol dimethacrylate. *J. Appl. Polym. Sci.*, **101**, 1630–1636.
36. Rahman, M.M., Malik, A.K., and Khan, M.A. (2007) Influences of various surface pretreatments on the mechanical and degradable properties of photografted oil palm fibers. *J. Appl. Polym. Sci.*, **105**, 3077–3086.
37. Raqueza, J.M., Deléglise, M., Lacrampea, M.F., and Krawczak, P. (2010) Thermosetting (bio)materials derived from renewable resources: a critical review. *Prog. Polym. Sci.*, **35**, 487–509.
38. Lisperguer, J., Perez, P., and Urizar, S. (2009) Structure and thermal properties of lignins: characterization by infrared spectroscopy and differential scanning calorimetry. *J. Chil. Chem. Soc.*, **54** (4), 460–463.
39. Kaplan, D.L. (1998) *Biopolymers from Renewable Resources*, Springer, New York.
40. Mikame, K. and Funaoka, M. (2006) Polymer structure of lignophenol I: structure and function of fractionated lignophenol. *Polym. J.*, **38** (6), 585–591.
41. Guigo, N., Mija, A., Vincent, L., and Sbirrazzuoli, N. (2010) Eco-friendly

composite resins based on renewable biomass resources: polyfurfuryl alcohol/lignin thermosets. *Eur. Polym. J.*, **46**, 1016–1023.

42. Hoareau, W., Oliveira, F.B., Grelier, S., Siegmund, B., Frollini, E., and Castellan, A. (2006) Fiberboards based on sugarcane bagasse lignin and fibers. *Macromol. Mater. Eng.*, **291**, 829–839.
43. Tamura, K., Kubouchi, M., Sakai, T., and Tsuda, K. (2005) Study on lignin particle filled epoxy composite. Proceedings of the Fourth International Workshop on Green Composites, Tokyo, Japan, September 14–15, 2006.
44. Thielemans, W. and Wool, R.P. (2005) Lignin esters for use in unsaturated thermosets: lignin modification and solubility modeling. *Biomacromolecules*, **6**, 1895–1905.
45. Yang, Y., Zhang, K., Song, Y., and Zheng, Q. (2011) Preparation and properties of wheat gluten/rice protein composites plasticized with glycerol. *Chin. J. Polym. Sci.*, **29** (1), 87–92.
46. Liu, W., Mohanty, A.K., Drzal, L.T., and Misra, M. (2005) Novel biocomposites from native grass and soy based bioplastic: processing and properties evaluation. *Ind. Eng. Chem. Res.*, **44**, 7105–7112.
47. Lodha, P. and Netravali, A.N. (2002) Characterization of interfacial and mechanical properties of ''green'' composites with soy protein isolate and ramie fiber. *J. Mater. Sci.*, **37**, 3657–3665.
48. Barbosa, V. Jr., Ramires, E.C., Razera, I.A.T., and Frollini, E. (2010) Biobased composites from tannin–phenolic polymers reinforced with coir fibers. *Ind. Crops Prod.*, **32** (3), 305–312. doi: 10.1016/j.indcrop.2010.05.007
49. Pizzi, A. (2008) Tannins: major sources, properties and applications, in *Monomers, Polymers and Composites from Renewable Resources* (eds M.N. Belgacem and A. Gandini), Elsevier Ltd., Oxford, pp. 179–200.
50. Grigsby, W. and Warnes, J. (2004) Potential of tannin extracts as resorcinol replacements in cold cure thermoset adhesives. *Eur. J. Wood Wood Prod*, **62** (6), 433–438.
51. Sharma, V. and Kundu, P.P. (2006) Addition polymers from natural oils-a review. *Prog. Polym. Sci.*, **31**, 983–1008.
52. Wool, R.P. and Khot, S.N. (2001) in *ASM Handbook*, Composites, 10th edn, Vol. 21 (eds D.B. Miracle and S.L. Donaldson), ASM International, Ohio, pp. 184–193.
53. Xia, Y. and Larock, R.C. (2010) Vegetable oil-based polymeric materials: synthesis, properties, and applications. *Green Chem.*, **12**, 1893–1909.
54. Dweib, M.A., Hu, B., O'Donnell, A., Shenton, H.W., and Wool, R.P. (2004) All natural composite sandwich beams for structural applications. *Compos. Struct.*, **63**, 147–157.
55. Dweib, M.A., Hu, B., Shenton, H.W. III, and Wool, R.P. (2006) Bio-based composite roof structure: manufacturing and processing issues. *Compos. Struct.*, **74**, 379–388.
56. Meier, M.A.R., Metzgerb, J.O., and Schubert, U.S. (2007) Plant oil renewable resources as green alternatives in polymer science. *Chem. Soc. Rev.*, **36**, 1788–1802.
57. Yoshida, N. (2009) Biomass-based unsaturated polyester. *Reinf. Plast.*, **55** (12), 89–92(in Japanese).
58. Song, C., Wang, T., Wang, X., Qiu, J., and Cao, Y. (2008) Preparation and gas separation properties of poly(furfuryl alcohol)-based C/CMS composite membranes. *Sep. Purif. Technol.*, **58**, 412–418.
59. Walters, J.M. (1986) in *Furan Resins, Corrosion and Chemical Resistant Masonry Materials Handbook* (ed. W.L. Sheppard Jr.,), Noyes Publications, Park Ridge, NJ.
60. Tumolva, T., Kubouchi, M., and Sakai, T. (2009) Development of abaca/furan green composites. Proceedings of the 17th International Conference on Composite Materials, Edinburgh, U.K., July 27–31, 2009.
61. Tumolva, T., Kubouchi, M., Aoki, S., and Sakai, T. (2011) Evaluating the carbon storage potential of furan resin-based green composites. Proceedings of the 18th International Conference on Composite Materials, Jeju, South Korea, August 21–26, 2011.
62. Thomas, R., Vijayan, P., and Thomas, S. (2011) in *Recent Developments in*

Polymer Recycling (eds A. Fainleib and O. Grigoryeva), Transworld Research Network, Kerala, pp. 121–153.

63. Pickering, S.J. (2006) Recycling technologies for thermoset composite materials-current status. *Composites: Part A*, **37**, 1206–1215.

64. Torres, A., de Marco, I., Caballero, B.M., Laresgoiti, M.F., Legarreta, J.A., Cabrero, M.A., González, A., Chomón, M.J., and Gondra, K. (2000) Recycling by pyrolysis of thermoset composites: characteristics of the liquid and gaseous fuels obtained. *Fuel*, **79**, 897–902.

65. Goodship, V. (2007) *Introduction to Plastics Recycling*, 2nd edn, Smithers Rapra Technology Ltd, Shropshire.

66. Behrendt, G. and Naber, B.W. (2009) The chemical recycling of polyurethanes (review). *J. Univ. Chem. Technol. Metallurgy*, **44** (1), 3–23.

67. Dilafruz, K., Kubouchi, M., Dang, W., Sembokuya, H., and Tsuda, K. (2003) Chemical recycling bisphenol a type epoxy resin based on degradation in nitric acid. Proceedings of EcoDesign 2003: Third International Symposium on Environmentally Conscious Design and Inverse Manufacturing, Tokyo, Japan, December 8–11, 2003.

7
Biofiber-Reinforced Thermoplastic Composites

Susheel Kalia, Balbir Singh Kaith, Inderjeet Kaur, and James Njuguna

7.1
Introduction

Synthetic materials made their appearance in the beginning of the last century and slowly replaced the bio-based products. Thus, owing to the change in the starting material, utilization combined with an increase in energy, the world community is facing the challenge of decreasing pollution levels with simultaneous increase in industrial output. Sustainability, industrial ecology, eco-friendliness, and the concept of green chemistry are guiding factors for the next generation materials and processes.

Fibers are hairlike materials consisting of continuous filaments or they are present as discrete elongated pieces. The earliest evidence of human use of fiber is the discovery of wool and dyed flax fiber, found in prehistoric caves back in 36 000 BP, in what is today the Republic of Georgia. Fibers can be spun into ropes, thread, or can be matted into sheets to make paper. On the basis of their origin, they are classified as natural, cellulosic, and synthetic fibers. Despite the vast applications of synthetic fibers, their nonbiodegradable nature makes them less attractive. These are petroleum-based products, so continuous depletion of petroleum reserves results in the demand for sustainable and renewable raw materials to replace these nonbiodegradable products [1–4].

Agro-based and other bio-based materials can form the bases for the development of biodegradable and eco-friendly products, which can compete and capture the market currently dominated by petroleum-based products. The annual global production of biofibers is about 4 billion tons of which 60% are agricultural crops and 40% are from the forest [5]. Biofibers, such as flax and hemp, have potential as a raw material for the production of various types of composites that are of great importance in automotive, building, packaging, paper, and furniture industries. Biofibers are fast emerging as viable alternatives to glass fiber for the preparation of composites. The utilization of biofibers such as bamboo, hemp, flax, jute, and sisal as reinforcing materials for the preparation of composites is competitive with synthetic ones. However, the use of biofibers as a reinforcing material requires special attention such as biofiber–matrix interface interaction,

Polymer Composite: Volume 3, First Edition.
Edited by Sabu Thomas, Kuruvilla Joseph, S. K. Malhotra, Koichi Goda and M. S. Sreekala.

uniformity of the fiber, shape, size, and novel processing techniques. Natural fiber-reinforced polypropylene (PP) composites have attained commercial significance especially in automotive industries. Use of biofibers with polymer matrix is the answer to many environmental issues raised by environmentalists from time to time [6].

7.2 Source of Biofibers

The biofiber-based composite concept consists of two components: ''biofiber'' means that the material is extracted from the renewable plant resources and the word ''composite'' means a material prepared by combining at least two ground materials in order to give a new material with special desired properties. Another term is *biocomposite*, which means the material comprising of one or more phase(s) derived from a biological origin. The reinforcing agent could be a plant fiber such as from sisal, bamboo, cotton, flax, and hemp or the fibers derived from recycled paper waste, wood waste, by-products of food crops, and regenerated fiber.

The use of plant fiber can be traced back in history, when they were used for fishing and trapping purposes. Over the last few years, various research groups have been involved in the investigation of including natural fibers as a constituent of the composites. The growing interest in natural fibers is due to their low cost production from renewable resources, safer handling, and positive environmental impacts. Cotton, jute, flax, ramie, sisal, and hemp are the suitable candidates to replace glass fiber in the composites as environmental-friendly strengthening agents [7].

Vegetable fibers have considerable variation in the properties depending upon the variety, climate maturity, and processing methods for the extraction of fibers. Properties such as density, tensile strength, Young's modulus, and elongation at break depend upon the internal structure and chemical composition of the fiber. Vegetable fibers can be considered as composites having cellulose embedded in lignin matrix. The other components are hemicelluloses, pectin, and waxes. Cellulose is a polymer of D-anhydroglucose having β-1,4-glycosidic linkages. The reinforcing efficiency of fiber depends on the nature of the cellulose and its crystallinity. Hemicellulose forms a matrix for the support of cellulose microfibrils. Hemicellulose consists of sugar units having pendant side groups resulting in its noncrystalline nature. Lignin is a hydrocarbon polymer having an amorphous nature. It provides rigidity to the plant. Pectins are heteropolysaccharides and provide flexibility to the plant. Waxes consist of different types of alcohols [8, 9].

Flax is one of the oldest fiber crops in world. Canada, China, and India are the largest producers of flax. Flax has high tensile strength in the range of 345–1100 MPa due to high cellulose content and low microfibril angle. Jute, the golden fiber, is one of the most affordable natural fibers and second most produced and used fiber after cotton. Ramie, one of the strongest natural fibers, is native to China and Japan and exhibits even greater strength when wet. Coir shows the least

tensile strength among natural fibers. Fiber strength not only depends on cellulose content but also gets affected by lignin content in the fiber. The strength of natural fibers is comparable with that of glass fibers [10–12].

Animal hair fibers consists of a protein known as *keratin*, which has a composition similar to human hair. Animal tendons consist of collagen, a fibrous protein with a complex hierarchical structure. Keratin proteins are actually crystalline copolymers of nylon, where amino acids are the repeating units. They get cross-linked through disulfide bonds present in the cystine amino acid [13].

Silk fibers are partially crystalline protein fibers. Silk is a continuous protein filament spun by the silkworm to form its cocoon. Mulberry silkworm, silk moth larva, *Bombyx mori* is the main specie used for the commercial production of silk. It belongs to the order Lepidoptera. Silk and sericulture probably began in China more than 4000 years ago. Silk has been used for clothing, wall hangings, paintings, religious ornamentation, interior decoration, and to maintain religious records. Silk fibers have uniform fiber properties–they are continuous fibers with high toughness, high crystallinity, and high tensile strength [14, 15].

Wool forms the protective covering of sheep. Wool has a length of 2.54–35.56 cm (1–14 in.) or more and diameter of 0.04–0.008 mm (1/600–1/3000 in.). The average chemical composition of wool is 50% carbon; 7% hydrogen; 22–25% oxygen; 16–17% nitrogen; and 3–4% sulfur. Wool is extremely flexible and can be bent 20 000 times without breaking. It is naturally resilient and is capable of trapping air, providing insulation, and absorbing moisture up to 30% of their weight. Wool is thermally stable and decomposition starts at about 100 °C.

Among three mineral fibers, only asbestos is a true natural fiber. Glass and aluminum silicate fibers require human intervention in their processing, and might be better considered as man-made fibers.

7.3
Types of Biofibers

On the basis of their life cycle, biofibers are divided into two types: annual biofibers and perennial biofibers. Further, these biofibers are divided into different categories such as plant-based, animal-based, and mineral-based biofibers, depending upon their origin. Most plant fibers are composed of celluloses, hemicelluloses, lignins, pectins, and waxes, whereas animal fibers consist of proteins, for example, hair, silk, and wool. Plant fibers include stem fibers, leaf fibers, seeds, fruit wood, cereal crops, and other grass fibers.

7.3.1
Annual Biofibers

Nonwood fibers are annual fibers obtained from various monocotyledonous and dicotyledonous plants. Nonwood fibers include straw, grass, bast, leaf, and fruit fibers. During 1996–1997, world paper consumption was about 300 million tons

and it was expected to 400 million tons in 2010 [16]. In view of the increased demand for paper products, nonwood plants and agricultural residues have attracted attention worldwide. Such raw materials offer several advantages like low cost irrigation and fertilization, short growth cycles, and low lignin content, resulting in a reduction in the requirement of energy and chemicals for processing [16–18].

7.3.1.1 Straw

Straw, obtained after the removal of grain and chaff from the dry stalks of cereal plants, is an agricultural by-product. Straw has various applications such as fuel, animal feed, bedding for livestock like horses, packaging and decoration material, and construction materials. About half of the yield of cereal crops such as barley, oats, rice, rye, and wheat is straw. Straws are the main agricultural waste materials and by-products of agricultural plants and are rich resources of biofibers. Its wide utilization in different fields draws the attention of researchers to make useful industrial products from such agriculture by-products [19–23].

Straw has a more complicated constitution than wood. Straw contains a relatively large number of cell elements. It contains fiber, vessel elements, the parenchyma cells, and epidermic cells, having high amount of ash and silica. The epidermic cells form the outermost surface cells, which are covered by a very thin layer of wax. This surface layer reduces the moisture absorbance of straw. Wheat straw has higher cellulose, ash, and silica content as compared to that of wood. The wax content of straw is higher than that of wood. Rice straw has been found to possess higher wax content [24].

Wheat straw is one of the most important agricultural residues. It is available worldwide and is annual renewable source of biofiber. Only a very small part of wheat straw has been used as feedstock and energy production whereas most of it remains unused. During the past 20 years, the potential of wheat straw for papermaking and composite preparation along with other applications has been explored [25, 26].

The world's second largest cereal after wheat is rice but it results in more residues (straw) as compared to wheat. Eastern and southeastern countries are the major producers of rice. The whole rice straw fiber consists of rice husk, leaf sheath, straw leaf blade, straw stem, and straw root. Rice straw is a good source of carbohydrates for ruminants but its nutritive value is compensated by its high lignin and low nitrogen contents. Rice straw being lignocellulosic in nature is a good candidate as reinforcing agents for thermoplastic composites [24, 27–29].

7.3.1.2 Bast Fiber

Bast fiber plants have been grown throughout the world for centuries. Bast fibers, as their name suggests, are the outer portion of the plants' stem, having long and strong fiber bundles. Bast plants include flax, hemp, kenaf, ramie, jute, and so on. Bast is stringy, with the vascular portion of the stem comprising 10–40% of the mass of the stem. Bast fibers have high tensile strength and relatively low specific gravity. Various bast fibers such as sisal, flax, and coconut have been explored as reinforcing agents in polymeric matrices [30–33].

Flax is an annual plant native to the region extending from the Mediterranean to India. Flax fiber is a soft, flexible, and lustrous fiber extracted from the bast or skin of the stem of the flax plant. It has about 80% cellulose, 13% hemicellulose, 3% lignin, and 4% pectin. It is stronger than cotton and has low elasticity. Flax has been used for making linen fabrics, twine, and ropes. Flax is a raw material for the paper industry. The high tensile strength, high specific strength, low cost, and renewability are the reasons for its wide use in composites [34–36].

Hemp fiber is an inexpensive bast natural fiber, which has attracted considerable attention of researchers all over the world. It is cultivated from the plants of *Cannabis* genus. Industrial hemp has been produced all over the world almost by 30 countries. Canada, France, and China are the major producers of hemp. Hemp contains about 61% cellulose (by weight), 24% hemicellulose, 10% lignin, and 3% extractives. The use of hemp dates back over 7000 years to the Stone Age. Old pottery shards in China and Taiwan have imprints of hemp fiber. It has been used for industrial purposes including paper, clothing, animal bedding, construction, fuel, and many more. The high strength, high durability, and low level of lignin content make it a suitable for use in composites. Several researchers have worked with hemp fibers for developing thermoplastic and thermoset composites. It has been used as a reinforcing agent for soy oil-based resin, novolac resin, epoxy resin, acrylic resin, unsaturated polyester resin, PP, and polystyrene [37–45].

Ramie is a bast fiber obtained from the perennial herbaceous plant, *Boehmeria nivea*. It is mainly grown in China, India, Japan, Korea, and Philippines. Ramie plants are one of the fast-growing plants and can be harvested within an interval of a few months. Three crops of this plant can be harvested every year. Sisal is a hard fiber extracted from the leaves of the sisal plant (*Agave sisalana*). The length of sisal fiber is between 1.0 and 1.5 m and the diameter is about 100–300 μm.

Next to cotton, jute is the second most common natural fiber cultivated in the world. It is an annual plant that flourishes in monsoon climates and grows to 2.5–4.5 m in height. It is primarily cultivated in Bangladesh, Brazil, China, India, and Indonesia. Traditionally, jute is used as a textile fiber because of its better strength due to the presence of cellulose and lignin. But today jute is a viable candidate for application in paper, automobile, and furniture industries. Jute-based thermoplastic matrix composites have been developed for making building and automobile products [46, 47]. *Hibiscus cannabinus* is a native plant of Africa. It is a warm-season, annual, herbaceous fiber plant. It has been cultivated since around 4000 BC for food and fiber. It is also known as *mesta* in India and Bangladesh, *ambari* in Taiwan, *stokroos* in Africa, and *till* in Egypt. The plant has high cellulose content (46–57%) and low lignin content (6.9%). It is similar to jute in many of its properties and used for ropes, paper, clothing, animal bedding, and so on [48, 49].

The bamboo fiber (BF) is abundant, especially in Asia and South American countries. Its reproducibility is better than that of other trees. It has several advantages including small environment load, rapid growth, renewability, relatively high strength, and good flexibility. It offers good potential as a reinforcement material in composites as it is a renewable resource with high biomass efficiency, high specific strength, and stiffness. It is believed that, for some applications, a

high fiber volume content of BFs can be competitive with the strength of synthetic fibers such as E-glass and other kinds of natural fibers such as jute, flax, and hemp. Owing to its excellent physical and mechanical properties, such as density, tensile strength, stiffness, and strain at break, bamboo has been used as a reinforcing agent in polymer composites. It is a widespread plant found in almost all continents. It has been traditionally used for various household items and tools. Bamboo has 45.3% of cellulose and 25.5% of lignin, with tensile strength of 150–520 MPa. Scientists have studied the tensile and flexural properties of bamboo-reinforced composites. The flexural strength of mortar laminates can be improved to greater than 90 MPa on reinforcement with BF [50–53].

7.3.1.3 Grasses

Corn stalk, rice stalk, and grasses are the agricultural by-products that are emerging as new eco-friendly materials having low cost as well as environmental acceptability. These materials are an abundant resource for natural fibers as they are inexpensive, eco-friendly, sustainable, recyclable, and biodegradable. Grasses are mainly used as feed for livestock and for modification of contaminated soil. Grasses have the potential to replace traditional fibers in green composites. Elephant grass-based biocomposites are being investigated for automotive applications. Elephant grass requires very little supplement for growth. It has the potential of being used as a renewable-energy source and has been explored for its conversion to high calorific-value fuel. Most native grasses such as big bluestem, little bluestem, and Indian grass have not being explored much for polymer-based composites [54–56].

7.3.1.4 Residues

Among various natural fibers, fibers obtained from waste products/residues of plants form an important section of fibers used for various applications. They are available in abundance and without any additional cost inputs; they can be used for industrial purposes. The residual fibers can be obtained from the leaf residues of leaves (sisal, pineapple leaf fiber, and henequen), seeds (cotton), or fruits (coir). Pineapple leaf fibers are obtained from the leaves of plant *Ananas cosomus*. Pineapple fibers contain 70–82% of cellulose and 5–12% of lignin. High cellulose content results in good tensile strength (400–1600 MPa) and modulus (59 GPa), because of which it has been used as a reinforcing agent in polycarbonates, low density polyethylene (LDPE), and soy-based bioplastics. Sisal is an important fiber extracted from the leaves of the plant *A. sisalana* by a process called *decotication*. Apart from being used for making ropes and twines, sisal is also used in making low cost papers, dartboards, geotextiles, mattresses, carpets, and so on. In recent years, it has been developed as an environmental-friendly reinforcing agent in composites to replace traditional glass fiber [57–59].

Henequen (*Agave fourcroydes*) is commonly used in the manufacture of textile products. Henequen fibers contain 60% cellulose, 28% hemicellulose, 8% lignin, and 4% extractives. The tensile strength of henequen fiber is 500 MPa, strain at break is 4.8%, and the Young's modulus is 13.2 GPa; these properties make it suitable for its use as a reinforcement in composites [60, 61].

7.3.2 Perennial Biofibers (Wood Fibers)

Wood is a hard, fibrous tissue found in many plants. It is an organic natural material and can be treated as a natural composite of cellulosic fibers embedded in the lignin matrix. It is a heterogeneous, hygroscopic material composed of cells and cell walls. It contains 40–50% cellulose, 15–25% hemicellulose, and 15–30% lignin.

In the first half of nineteenth century, the use of perennial or wood fibers was more common for the production of pulp and paper. At present, only about 7.5% of world's pulp comes from the nonwoody fiber. Wood can be softwood, obtained from softwood coniferous trees such as pine or hardwood obtained from hardwood deciduous dicotyledons trees such as oak. Wood is unsuitable for construction in its native form but may be broken down into fibers and used as raw material for building clipboards, hardboards, medium-density fiber boards, oriented standard boards, and so on. Wood fibers are important components of most papers [62, 63].

7.3.2.1 Tree Plantation Products

Tree plantation technology has the potential for the development in the field of pulp wood and biomass. It also involves development of unutilized forest lands. Tree plantation is a well-developed technology resulting in the production of rubber, coconut, tea, lumber, and paper pulp [64, 65].

Tree plantations are not a natural ecosystem and they are, therefore, also sometimes known as *man-made forests* or *tree farms*. Tree plantations generally utilize fast-growing trees either to replace already logged forest trees or to substitute their absence. The plantations include hybrid trees or genetically modified trees. They involve trees of industrial importance, for example, pine, spruces, and eucalyptus, because of their fast growth rate and good properties for paper and timber production. Eucalyptus plantations have been developed vastly for the last 30 years in subtropical and tropical zones [66–68].

Wood production from tree plantations is generally higher than that from natural forests. The yield of wood production from forests is 1–3 m^3 ha^{-1} $year^{-1}$ whereas plantations of tropical species commonly yield 5–20 m^3 wood ha^{-1} annually. Eucalyptus plantations can have growth rate of 25 m^3 ha^{-1} $year^{-1}$ or higher. Throughout the world, only 5% of total forest area is that of the plantations but it contributes 20% of total wood production [69, 70].

Mangium is a fast-growing teak tree. It reaches a height of 10–12 ft in just one year. It can grow in adverse climate conditions and in arid soil as well. Mangium yields best quality pulp and is used for particle board manufacturing. Mangium plantations in India are mainly found in West Bengal, Maharashtra, Goa, Andhra Pradesh, Karnataka, Tamilnadu, Kerala, Pondicherry, and some parts of Gujarat [71].

7.3.2.2 Forest Plant Products

Forests cover the 30% of the world's land. Forest trees form an important part of human society. Forests not only stabilize the environment but also provide essential components as well as protect landscapes. Forest trees nourish wild life, support industries, and aid rural economies. Forest plants provide a wide variety of products resulting in direct and indirect benefits to society. Leaves, bark, flowers, roots, seeds, and wood are used to manufacture various industrial products such as fibers, resins, medicines, construction and building material, food, fuel, pulp, and paper [72, 73].

Pines are coniferous trees native to the northern hemisphere and grow well in acidic soil. These are the most important tree species for timber and wood pulp throughout the world. In Chile, Brazil, South Africa, Australia, and New Zealand, pines are the sources of timber. Pinewood is widely used in furniture, flooring, roofing, and other interior decoration work.

7.3.2.3 Agro-Forestry Products

The term *agro-forestry* is used to describe the incorporation of trees and other woody species of plants that find use in different types of agricultural activities. Earlier, the term *agriculture* was used instead of *agro-forestry*, but agro-forestry has a much broader definition, which, other than agriculture, also includes other combinations such as livestock production and even aquaculture. Agro-forestry systems might produce firewood, biomass feedstocks, and fodder for grazing animals, pine straw, and other forestry products [74]. This means agro-forestry plays an important role in the development and enhancement of either biological productivity or economic returns, or both.

In ancient times, there was a system of single-purpose crops, that is, monocrops, but agro-forestry involves multipurpose activities such as tree planting with another enterprise that includes grazing animals or producing mushroom or a diversity of special forest products. Trees provide shelter for livestock and protect them from wind or sun. They are also the source of habitat for wildlife. Moreover, agro-forestry controls soil erosion and improves soil fertility by using leguminous species for nitrogen fixation [75].

7.3.2.3.1 Biological Basis of Agro-Forestry

Agro-forestry practices may enhance biological productivity in many ways. With the help of agro-forestry, soil fertility may be enhanced by planting nitrogen-fixing woody species between the rows of crops. The waste or foliage of many woody species provides ''green manure'' to crop plants and such woody species also act as wind breakers [76].

7.3.2.3.2 Economic Basis of Agro-Forestry

Agro-forestry practices in use include alley cropping, silvopastures, wind breakers and shelterbelts, riparian buffer strips, and forest farming. In addition to enhancing the biological productivity, agro-forestry also plays a role in the enhancement of economic returns. The woody foliage used as fodder may reduce the cost of feeding

livestock or it may also prevent the economic damage caused to livestock during famine or drought. In addition, agro-forestry plants also provide fruits, fibers, nuts, building and craft materials, medicines, timbers, charcoal, and many other commercial products [77].

7.3.2.3.3 Alley Cropping

In this system, crops such as grains, forage, vegetables are grown between trees planted in rows. The spacing between the rows is designed in such a way that it accommodates the mature tree plants without harming the crops. Once the trees are fully grown, they cover the most of the ground surface and provide shaded for shade-tolerant crops such as mushrooms and ornamental ferns [78].

7.3.2.3.4 Silvopasture

A combination of trees and pasture is called *silvopasture agro-forestry*. In this system, hardwoods are planted in single or multiple rows and livestock graze between them. In this way, both are managed for production, and, depending upon the requirements, one is dominant over the other. In the first year of establishment, crops are harvested from the plantings and grazing generally starts after 2 or 3 years because at that time trees are large enough and are not damaged by the livestock. Grazing enhances the nutrient value of the soil and also reduces costs of commercial fertilizer [78].

7.3.2.3.5 Wind breaks or Shelterbelts

In this system, trees and grasses are planted in areas along streams or rivers. These are designed in such a way that they can bind the excess nutrients and chemical pesticides that are lying on the land surface to the soil before their entry into the waterways [79].

7.3.2.3.6 Forest Farming

In this system, natural forest area fulfills the requirements of wood products and other additional enterprises. Proper knowledge of thinning, pruning, harvesting practices and market options for the products are given by qualified specialists to enhance the productivity [80].

Bamboos are long-lived, woody, stemmed perennial grasses. There are approximately 87 genera and over 1500 species of bamboo, out of which 100 species are of economical importance. Bamboo is used for domestic purposes in farms. Commercially, bamboos are used in the production of construction materials, concrete reinforcements, fishing poles, furniture, crafts, and musical instruments. They are also used in ornamental works, landscaping, and conservation of soil. Bamboo furniture and craft have long durability and high strength. Musical instruments such as flutes, wind chimes, pan pipes, and xylophones are made from bamboo parts. Moreover, some uses of bamboo that are of prime importance are as riparian vegetation filters, in the development of wetlands, as living screens, and in permaculture [81].

7.4 Advantages of Biofibers

Use of biofibers as reinforcements in plastics because of their good mechanical performance and perceived environmental advantages has received increased interest. The environmental advantages of natural fibers have an important influence, particularly in Europe. Natural fibers are derived from renewable resources and often from industrial by-products. Wood and other natural fibers derived from renewable resources do not have a large energy requirement to process and are biodegradable [82]. The following are the main advantages of biofibers [83, 7]:

- a renewable resource, with production requiring little energy; CO_2 is used up, while oxygen is given back to the environment;
- possibility of thermal recycling, where glass causes problems in combustion furnaces;
- good thermal and acoustic insulating properties;
- abundant availability and therefore low costs;
- biodegradability;
- flexibility during processing;
- minimal health hazards;
- low density;
- desirable fiber aspect ratio;
- relatively high tensile and flexural modulus.

Table 7.1 gives a comparison of the properties of natural and glass fibers that clearly shows that natural fibers have distinct advantages over the glass fibers.

Table 7.1 Comparison between natural and glass fibers.

	Natural fibers	Glass fibers
Density	Low	Twice that of natural fibers
Cost	Low	Low, but higher than that of natural fibers
Renewability	Yes	No
Recyclability	Yes	No
Energy consumption	Low	High
Distribution	Wide	Wide
CO_2 neutral	Yes	No
Abrasion to machines	No	Yes
Health risk when inhaled	No	Yes
Disposal	Biodegradable	Not biodegradable

''Source: Reprinted from [84], Copyright 2003, with permission from Elsevier.''

7.5 Disadvantages of Biofibers

The hydrophilic nature of cellulose fibers often results in poor compatibility with hydrophobic polymer matrices. Therefore, it becomes necessary to modify the surface of natural fiber for better binding between fiber and matrix.

The use of biofibers as reinforcing agents for composites is one of the most promising areas of composite development, although biofibers have some inherent limitations that have to be looked into before their use in any material production. The following are the main disadvantages of biofibers [85–90]:

- Before the chemical extraction process, the biofibers in their natural state have waxes and other encrusting extractions such as hemicelluloses, lignin, and pectin that form a thick outer layer to protect the cellulose inside. The presence of encrusting substances and other impurities causes the fibers to have an irregular appearance and also affects the processability of the fibers.
- Biofibers do not show the general relationship between crystallinity and strength observed in pure cellulose fibers such as cotton and rayon, that is, the higher the crystallinity, the higher the strength. The presence of substantial amounts of noncellulosics, mainly lignin, which contributes to the strength of fibers and variations in the dimensions of the unit cells, is the major reason for the absence of the good relationship between crystallinity and strength. Therefore the amount of noncellulosics and dimensions of the unit cells fiber are to be considered when designing products from biofibers.
- The inherent polar and hydrophilic nature of the lignocellulosic fibers and the nonpolar (hydrophobic) characteristics of most of the thermoplastics results in compounding difficulties to bond together that leads to nonuniform dispersion of fibers in the matrix, which impairs the efficiency of the composites.
- Another limitation of the use of agro-fibers for composites is the lower processing temperature, restricted to 200 °C, owing to the possibility of degradation of the lignocellulosic fibers at higher temperatures. This limits the processing temperatures and the types of the thermoplastics that can be used with agro-fibers to produce composites.
- The high moisture absorption of natural fibers leads to swelling and to the presence of voids at the interface that result in poor mechanical properties affecting dimensional stability of the composites.
- Successful exploitation of the use of biofibers for durable composite applications is restricted by low microbial resistance and susceptibility to rotting. These properties pose serious problems during shipping, storage, and composite processing.
- The nonuniformity and variations in the dimensions and the mechanical properties of the plants (even between individual plants in the same cultivation) pose another serious problem.
- Another drawback is the lack of established collection, storage, and handling systems that would prevent the degradation of the lignocellulosics when stored for a considerable period.

- Ash present in the lignocelluloses, especially straw contains silica that has many undesirable effects. Silica blunts cutting machinery, reduces the digestibility of the straw, interferes with the pulping process by forming scales on the surface of the reactors, and makes combustion more difficult. In paper and pulp manufacture, silica present in fiber (rice and wheat straw) accumulates and causes scaling in evaporators, reducing the efficiency of the pulping process.

However, it is quite evident that the advantages of the biofibers overweigh the disadvantages/limitations and most of the shortcomings have remedial measures in the form of chemical treatment. Biofibers have an advantage over the synthetic ones since they buckle rather than break during processing and fabrication.

7.6 Graft Copolymerization of Biofibers

Desirable and targeted properties can be imparted to natural polymers through graft copolymerization in order to meet the requirement of specialized applications. It is a convenient and clean means for altering the properties of numerous polymer backbones. Graft copolymerization is one of the best methods for modifying the properties of biofibers. Different binary vinyl monomers and their mixtures have been graft copolymerized onto cellulosic material for modifying the properties of numerous polymer backbones [12, 91].

During the last decades, several methods have been suggested for the preparation of graft copolymers by conventional chemical techniques. Creation of an active site on the preexisting polymeric backbone is the common feature of most methods for the synthesis of graft copolymers. The active site may be either a free-radical or a chemical group that may get involved in an ionic polymerization or in a condensation process. Polymerization of an appropriate monomer onto this activated backbone polymer leads to the formation of a graft copolymer. Ionic polymerization has to be carried out in the presence of anhydrous medium and/or in the presence of considerable quantity of alkali metal hydroxide. Another disadvantage with the ionic grafting is that low molecular weight graft copolymers are obtained, while in case of free radical grafting, high molecular weight polymers can be prepared. C_2, C_3, and C_6 hydroxyls and C–H groups are the active sites for grafting in cellulosics (Figure 7.1) [12].

The conventional technique of grafting and chemical modification of natural fibers requires significant time and energy. The use of the microwave radiation (MWR) technique to modify the properties of natural fibers within the textile industry, although somewhat slow and still rather limited, is finding its way into numerous uses in production plants. The MWR technique reduces the extent of physicochemical stresses to which the fibers are exposed during the conventional techniques. Microwave technology uses electromagnetic waves, which pass through a material and causes its molecules to oscillate. Microwave energy is not absorbed by nonpolar materials to any degree, while polar water molecules held within a polymer matrix do absorb energy very proficiently, thus becoming heated [92, 93].

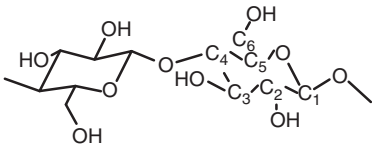

Figure 7.1 Structure of cellulose.

The following properties can be achieved by graft copolymerization of various monomers onto biofibers [91, 93–94]:

- Chemical resistance in biofibers
- Enhancement in thermal stability of biofibers
- Enhancement in strength of biofibers
- Enhancement in crystallinity of biofibers
- Rough fiber surface, which results in better compatibility with polymer matrices
- Moisture resistance in biofibers.

Graft copolymerization of methyl methacrylate (MMA) onto flax fiber is carried out under three different reaction methods: in air, under pressure, and under the influence of MWRs. Grafting through the MWR technique is an effective method in terms of time consumption and cost effectiveness. Maximum percentage grafting has been observed in case of grafting carried out in air followed by grafting under pressure and under the influence of MWRs. Flax faces less surface deformations (Figure 7.2) during the grafting process under the influence of

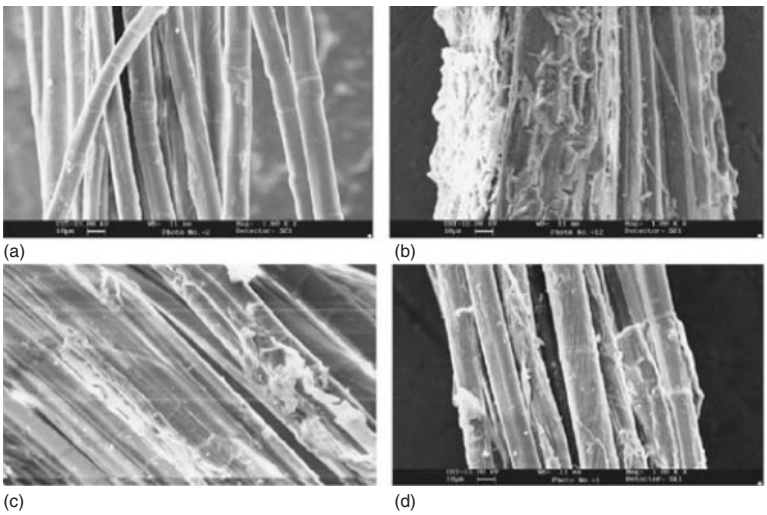

Figure 7.2 (a) SEM of flax fiber, (b) flax-*g*-poly(MMA) in air, (c) flax-*g*-poly(MMA) under pressure, and (d) flax-*g*-poly(MMA) under microwave radiations. (Reprinted from [94], Open access 2008.)

MWRs as compared to grafting in air and under pressure, thereby retaining better crystalline structure [94].

The grafting of ethyl acrylate (EA) onto sunn hemp cellulose (SHC) is supposed to follow the following mechanism (Scheme 7.1): morphological and thermal studies showed that the surface of sunn hemp fibers becomes rough through graft copolymerization and thermal stability has been found to increase. MWR-induced grafting showed a diminutive effect on the crystalline behavior of the sunn hemp fibers as the optimum time to get maximum grafting is very short (40 min) in comparison to that in conventional grafting [95].

7.7 Surface Modifications of Biofibers Using Bacterial Cellulose

The hydrophilic nature of cellulose fibers often results in poor compatibility with hydrophobic polymer matrices. Therefore, it becomes necessary to modify the surface of natural fiber for better binding between fiber and matrix. Chemicals are commonly used for the modification of cellulosic materials but large amount of solvents are also usually involved. Surface modification of biofibers using bacterial cellulose (BC) is one of the best methods for greener surface treatment of biofibers.

BC has gained attention in the research area for the encouraging properties it possesses, such as significant mechanical properties in both dry and wet states, porosity, water absorbency, moldability, biodegradability, and excellent biological affinity [96]. Because of these properties, BC has a wide range of potential applications.

The introduction of BC onto biofibers provides new means of controlling the interaction between natural fibers and polymer matrices. Coating of biofibers with BC does not only facilitate good distribution of BC within the matrix but also results in an improved interfacial adhesion between the fibers and the matrix. This enhances the interaction between the biofibers and the polymer matrix through mechanical interlocking. BC-coated natural fibers introduced nanocellulose at the interface between the fibers and the matrix, leading to increased stiffness of the matrix around the natural fibers [97, 98].

Acetobacter xylinum (or *Gluconacetobacter xylinus*) is the most efficient producer of BC. BC is secreted as a ribbon-shaped fibril, less than 100 nm wide, which is composed of much finer 2–4 nm nanofibrils [99, 100]. In comparison to the methods for obtaining nanocellulose through mechanical or chemo-mechanical processes, BC is produced by bacteria through cellulose biosynthesis and the building up of bundles of microfibrils [101].

Figure 7.3 shows the cultivation of the cellulose-producing bacteria in the presence of natural fibers such as sisal and hemp, resulting in the coating of natural fiber surfaces by BC [97]. Strong and highly crystalline BC fibrils preferentially attached to the surface of natural fibers, thereby creating "hairy fibers" (Figure 7.4), leading to a nanostructured natural fiber surface. Simply weighing the fibers before and after the BC fermentation process confirmed that between 5 and 6 wt% of BC adhered to the fibers after the surface modification. The strength of attachment of

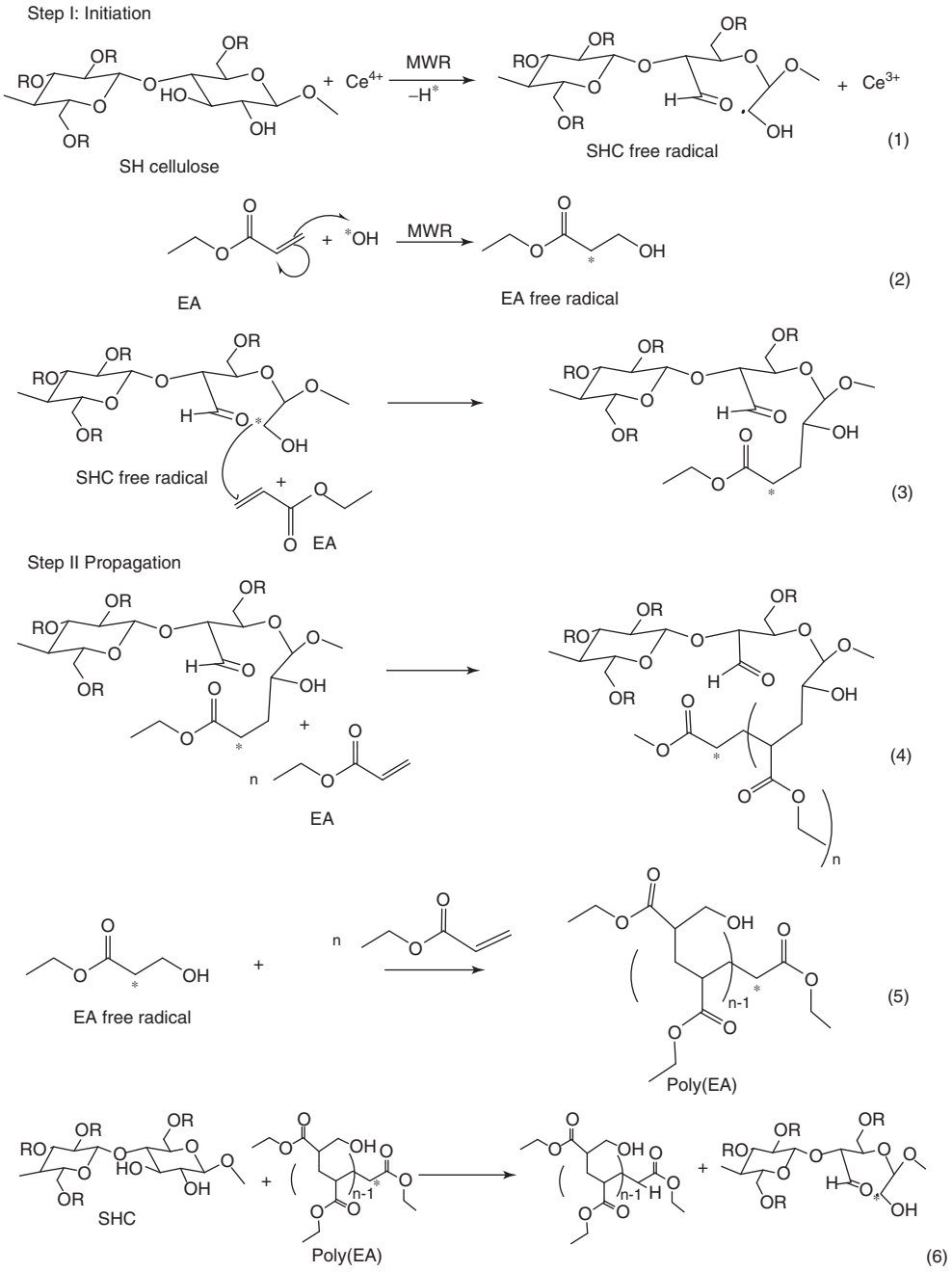

Scheme 7.1 Mechanism of grafting of ethyl acrylate onto sunn hemp fibers (Reprinted from [95], Open access 2011.)

Step III Termination

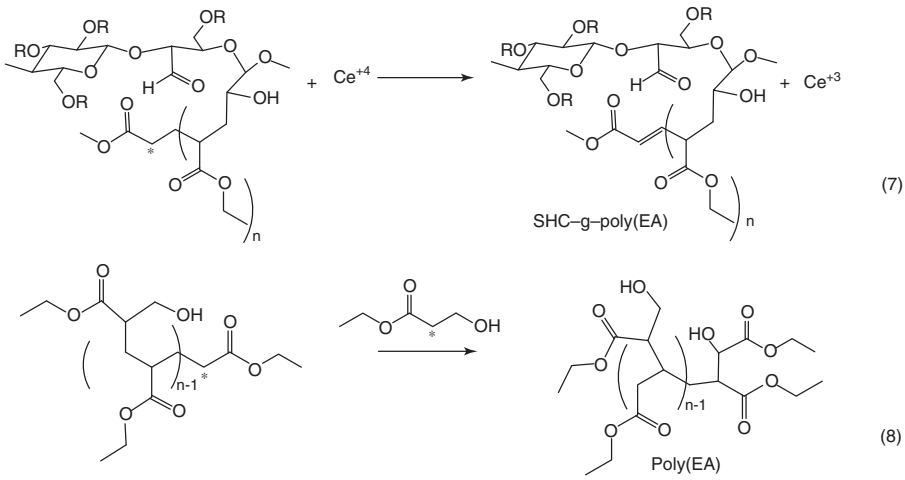

(7)

(8)

Scheme 7.1 (*continued*)

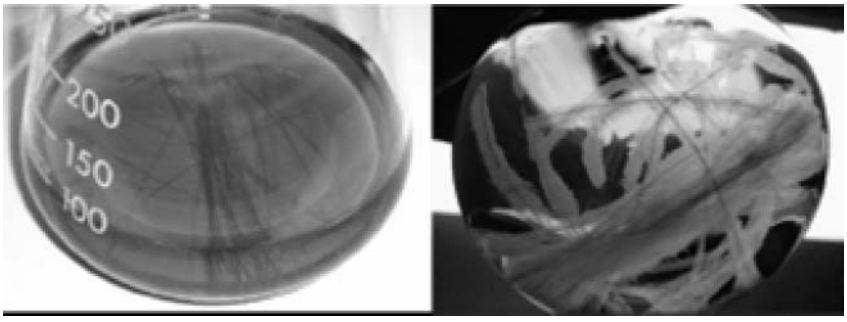

(a) (b)

Figure 7.3 Photographs of sisal fibers before (a) and after (b) bacterial culture (Reprinted from [97], Copyright 2008, with permission from American Chemical Society.)

the nanocellulose coating to the natural fibers can be attributed to strong hydrogen bonding between the hydroxyl groups present in BC and the lignocellulose in natural fibers [102]. The modification process does not affect the mechanical properties of sisal fibers but it significantly reduces the mechanical properties of hemp fibers [97]. Figure 7.5 shows the surface modification of hemp fibers by coating with BC.

7.8 Applications of Biofibers as Reinforcement

In most of the applications, general plants or vegetable fibers (biofibers) are used for the preparation of reinforced plastic materials. The commonly used biofibers

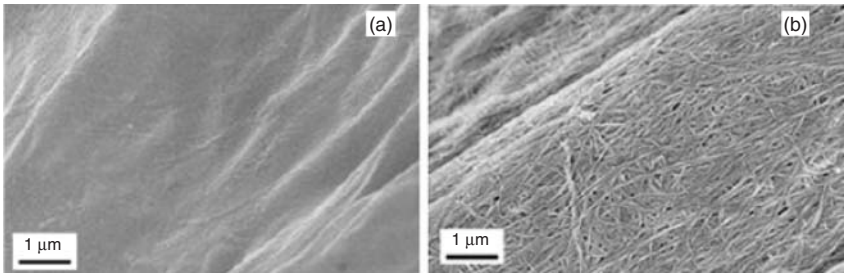

Figure 7.4 SEM micrographs (a) sisal fiber and (b) bacterial cellulose coated sisal fiber (Reprinted from [97], Copyright 2008, with permission from American Chemical Society.)

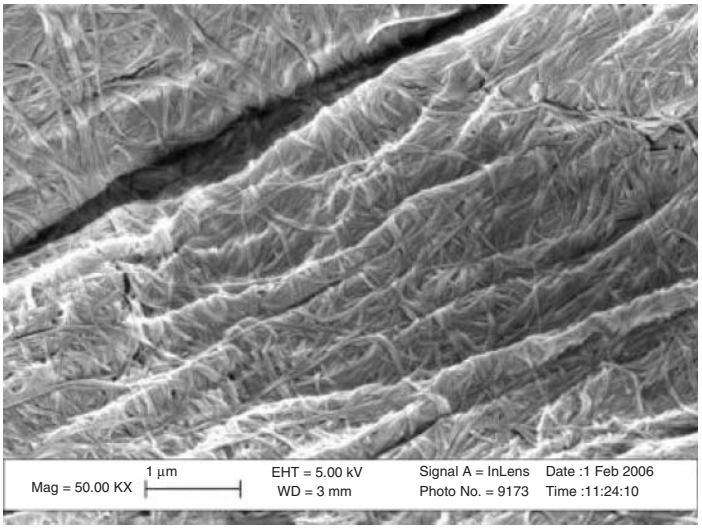

Figure 7.5 Hemp fiber after bacterial cellulose modification (Reprinted from [97], Copyright 2008, with permission from American Chemical Society.)

are wood, bamboo, ramie, flax, sisal, jute, and hemp. The use of these biofibers as reinforcing material for the preparation of composites in commercial products is desirable from an environmental point of view. The availability of a large quantity of biofibers with well-defined mechanical properties is a prerequisite for the successful applications of these materials.

7.8.1 Composite Boards

Composite boards are fabricated by using a heat press machine with the biofibers as the reinforcement and the polymer resin as the matrix. These composite boards fall into two main categories based on the physical configuration of the

Table 7.2 Raw materials and bonding agents for composite boards.

Type of boards	Reinforcements	Bonding agents
Particleboards	Wood particles, shives of flax flakes, saw dust, bagasse, hemp, kenaf, jute, cereal straw, coconut coir, corn and cotton stalks, rice husks, vetiver roots, and other fiber sources	Urea, melamine, phenol formaldehyde resin, isocyanate, resorcinol, vinyl polyacetate resins and natural polymers, tannins, protein, casein, soybeans, modified starch, lignin activated by enzymatic system polylactic and polyhydroxybutyric acid
MDFB	Lignocellulosic fibers	As above
OSB	Lignocellulosic strands	As above

MDFB, medium-density fibreboards; OSBs, oriented strand boards.
''Source: Reprinted from [105], Copyright 2004, with Permission from Springer.''

lingo-cellulosic fibers. Both wet and dry processes are used for the preparation of conventional composite boards [103]. These boards have very low water absorption and negligible swelling. Composite boards can be used as wood substitute for paneling, cladding, surfacing and partitioning, and other interior applications. These composite boards can partially or completely replace wood-based insulation materials [104]. The composite boards were used as roof and wall sheathing, subflooring, interior surfaces for walls and ceiling, as bases for plaster, and as insulation strips for foundation walls and slab floors. The raw materials, polymers, and bonding agents for composite boards are listed in Table 7.2 [105].

7.8.1.1 **Particleboards**

There is a growing demand for high performance, low maintenance, and low cost building materials. Biofiber-thermoplastic composites are being used to produce products such as decking, window and door elements, panels, roofing, and siding [106]. The use of agricultural and industrial residues to replace wood as raw materials for particleboard has received considerable attention in recent years [107, 108]. There are different process lines for particleboard production. One of them is a production line using a combination of wood fibers (on the surface) and wood particles (in the core) [109]. Figure 7.6 presents a diagram of a three-layer particleboard production with paper sludge as a face layer [110].

Paper sludge is mainly composed of fibrous fines; therefore, it may have potential application in particleboard production as an alternative to wood fiber. The process of particleboard production with paper sludge as a surface layer is similar to that of particleboard production using a combination of wood fibers and wood particles. Removal of inorganic materials and dirt from paper sludge using pretreatments may be important before use in particleboard production [110].

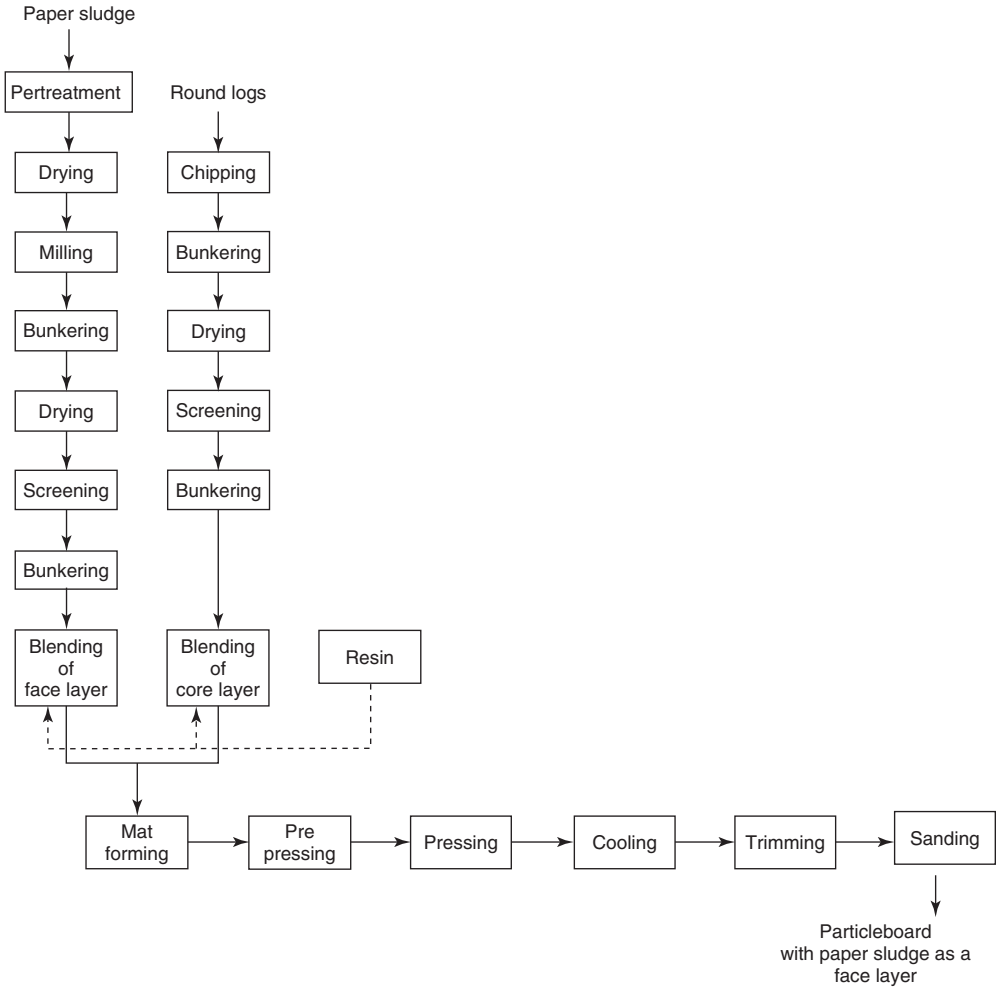

Figure 7.6 Particleboard manufacturing with paper sludge as a face layer (Reprinted from [110, Copyright 2007, with permission from Elsevier].)

Lignocellulosic materials used for the preparation of particleboard are wood, flax and hemp shives, jute stalks, bagasse, reed stalks, cotton stalks, grass like miscanthus, vetiver roots, rape straw, oil flax straw, small grain straw, peanut husks, rice husks, grapevine stalks, and palm stalks. These are cheap and valuable materials for lingo-cellulosic board production [105]. One of the most important properties of these boards is that a wide range of densities (300–750 kg m^{-3}) could be attained. Annual plant-based boards are mainly used in the buildings, furniture, and transportation industries [111].

Different thermoplastics in conjunction with isocyanate and bagasse lignin have been used as the binder for particleboards. Bagasse particleboards offer superior

mechanical properties compared to those made of only thermoplastic or a coupling agent. The mechanical strength of particle boards depends on the concentration of polymers and the coupling agent, nature of the fiber, polymer and coupling agent, and lignin content of the bagasse. Mechanical properties and dimensional stability of coupling agent-treated particle boards are superior to those of the nontreated ones [112].

7.8.1.2 **Fiberboards**

Manufacturing of medium-density fiberboards (MDFBs) from lingo-cellulosic fibers has been increasing in recent years [113–115]. Structural fiberboards are being made from wood, other plant materials, and wastepaper. They are classified by density and can be prepared by dry or wet processes. These boards fall into two main categories: high density (hardboard) fiberboards and MDFBs. The fiberboards are prepared by the dry process method, whereas the wet process method is applied to both hardboards and low density insulation boards [103].

MDFBs consist of 82% fiber, 9% gluing amino resin, 1% paraffin, and 8% water. Crumbled hemp, flax, and kenaf straw and shives are excellent materials for the preparation of these boards. These boards offer several advantages over particleboards [105]:

1) Higher structural homogeneity
2) Less roughness and closed surface
3) Higher dimensional stability
4) Easier and more uniform dyeability
5) Higher bending and tensile strength.

MDFB has a large number of advantages over solid wood:

1) Drying and seasoning are not necessary.
2) Fiber orientation is of no importance to frontal processing.
3) Varnishability is similar to that of wood.
4) Yield relative to material is higher.

Agricultural residues are plentiful, widespread, and easily accessible, so fiberboard manufacturers are now studying their use as raw material substitutes [115, 116]. The strength properties in the MDFBs are mainly attributable to the physical and mechanical properties of individual wood fibers, fiber orientation, and the manner in which these components are combined in the structure. The chemical characteristics of peanut husks are found to be similar to those of other crop residues. The lower mechanical properties of MDFB panels with peanut husk could be due to the small size of peanut husk particles in the structure, which results in lower fiber aspect ratios, ultimately leading to poor fiber-to-fiber contact [116].

The hot waste oil vapor from sunflowers has some effects on the physical and bending properties of commercially manufactured thin MDFB panels. The water absorption and thickness swelling of the samples are improved by the treated panels with hot vapor oil and heat. The thermal conductivity of the panels is enhanced

by such treatment. Panel products treated with these processes could have some promising potential in various applications including outdoor use [117].

Fiberboards are prepared mainly for use as panels, insulation, and cover materials in buildings and construction where flat sheets of moderate strength are required. They are also used to a considerable extent as components in doors, cabinets, cupboards, and millwork [118]. They have frequently replaced solid wood, plywood, and particleboard for many furniture applications. They also have potential use in other interior and exterior markets such as moldings, exterior trim, and pallet decking [119].

7.8.2 Biofiber-Reinforced Thermoplastic Composites

Many researchers have studied the development of advanced composites using biofibers as reinforcements and thermoplastics as resins for aerospace and automotive applications. There has been a growing interest among various researchers to utilize biofibers as reinforcement in thermoplastic composites because of the low cost, lightweight, and biodegradable properties. In this section, use of various biofibers such as bamboo, ramie, flax, sisal, jute, and hemp as reinforcements in the preparation of composites have been discussed.

7.8.2.1 Bamboo Fiber-Reinforced Thermoplastics

Crystallization and interfacial morphology using differential scanning calorimetry, wide-angle X-ray diffraction, and optical microscopy of BF-reinforced PP composites were studied using PP and two maleated polypropylenes (*s*-MAPP and *m*-MAPP) as matrices. The addition of BF to any of the three polymers causes an increase in the overall crystallization rate [120]. Bamboo cellulose crystals (BCCs) were prepared using a combined HNO_3–$KClO_3$ treatment and sulfuric acid hydrolysis. Nanoscaled crystals showed typical cellulose I structure, and the morphology was dependent on concentration in the suspension. The tensile strength and Young's modulus of the starch/BCC composite films (SBC) were enhanced by the incorporation of the crystals because of reinforcement of the BCCs and reduction of water uptake. BCCs at the optimal 8% loading level exhibited a higher reinforcing efficiency for plasticized starch plastic than at any other loading level [121].

Flexural tests with two fiber orientations were performed for unidirectional BF thermoplastic composites. The consolidation temperature has a clear effect on the final behavior of the unidirectional BF thermoplastic composites with PP and maleic anhydride-*grafted*-polypropylene (MAPP) loaded in the longitudinal direction of the fibers. There is no clear difference in maximum strength between PP and MAPP, as all samples are roughly situated on one line as a function of processing temperature. In both cases, not only a shift to the left part of the spectrum is observed when the temperature is raised by 10° but also there is a reduction in strain at maximum stress. The combination of both results in a modulus increase (Figure 7.7). The Young's modulus for PP composites increases

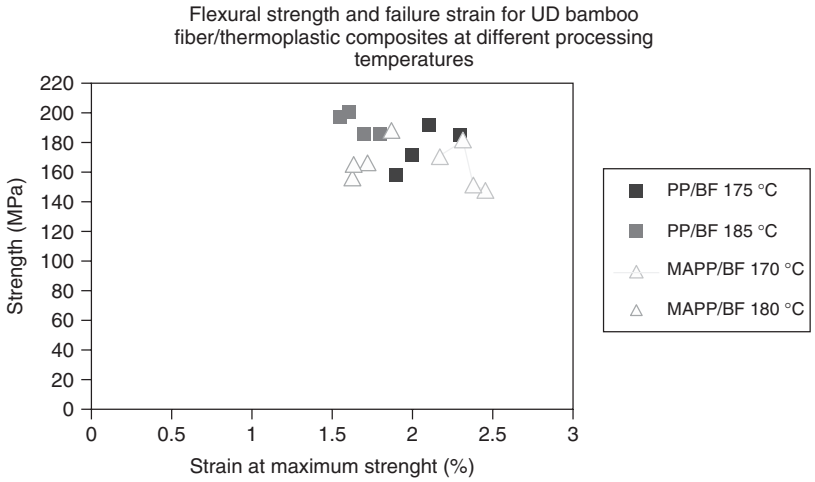

Figure 7.7 Strength and failure strain results of bamboo fiber thermoplastic composites (Reprinted from [122]. Open access 2010.)

from 15.6 to 19.3 GPa and for MAPP composites from 11.8 to 16.4 GPa, improving by 24% and 39%, respectively, again for the same increase in temperature [122].

BF-reinforced polylactic acid (PLA) composites improve the impact strength and heat resistance of PLA. Composite samples were fabricated using three different types of BFs designated as short fiber bundle, alkali-treated filament, and steam-exploded filament by injection molding using PLA/BF pellets prepared by a twin-screw extruding machine. The impact strength of PLA was not greatly improved by the addition of short fiber bundles as well as both filaments. PLA composites fabricated by hot pressing using medium length bamboo fiber bundles (MFB) increase the impact strength. The impact strength of the PLA/MFB composite, in which long fiber bundles were pulled out from the matrix, significantly increased. The addition of BF improves thermal properties and heat resistance of PLA/BF composites [123, 124].

7.8.2.2 **Ramie Fiber-Reinforced Thermoplastics**

Owing to their excellent properties, ramie fibers have high potential as reinforcing fiber for thermoplastic composites. Ramie contains 67–76% cellulose and 13–16.7% hemicellulose. It is a perennial plant and its stem height is about 2 m. Its reported stiffness (modulus) of up to 128 GPa is much greater than those reported for cotton and silk, which range between 5.5 and 12.6 GPa. The tensile fracture stress, Young's modulus, and fracture strain of ramie fibers have been reported to be in the ranges of 400–938 MPa, 61–128 GPa, and 1.2–3.8%, respectively [125, 126].

Biofiber-reinforced PP composites have received lot of attention because of their light weight, good mechanical properties, recyclability, and environmental-friendly features. The mechanical properties of ramie fiber-reinforced PP composites

were studied and the results show that the increase of fiber length and fiber content can improve the tensile, flexural, and compressive strengths of composites. However, impact strength and elongation behavior of composites have been found to decrease [127]. Comparing the mechanical properties of ramie and cotton fiber-reinforced PP it was observed that the ramie fiber-reinforced PP was stronger than cotton fiber-reinforced PP, but the breaking elongation of composites of cotton fiber-reinforced PP was superior to that of ramie fiber-reinforced PP because of the character of natural fiber [128]. The effect of the ramie fiber, flame retardant, and plasticizer on the sound absorption property of ramie fiber-reinforced poly(L-lactic acid) (PLLA) composites has been investigated. The composites with short ramie fiber have better sound absorption property than the ramie fabric-reinforced PLLA composites. The addition of flame retardant and plasticizer has a positive effect on the sound absorption property of the ramie fabric–PLLA composites. A morphological study reveals the microphase separation in the plasticizer poly(butylene adipate-*co*-terephthalate)–PLLA composites, the porosity of the single ramie fiber bundle, and the distribution of short ramie fiber and ramie fabric in the PLLA composites [129].

Ramie fiber-reinforced thermoplastic biodegradable composites were manufactured using the *in situ* polymerization method. Ramie fibers were treated with coupling agents to improve their compatibility and to strengthen the interface. The effect of fiber length and fiber content on tensile and impact strength of these composites was studied and the results showed that both tensile and impact strength were highest when the ramie fiber length was 5–6 mm and the fiber content was 45% [130]. The effect of ramie fiber surface treatments on the properties of PLA composites was investigated. Treatment of ramie fiber with alkali and silane (3-amino propyl triethoxy silane and γ-glycidoxy propyl trimethoxy silane) shows significant improvement in the tensile (Figure 7.8), flexural (Figure 7.9), and impact strengths (Figure 7.10). Increase in the storage modulus was observed for the composites from the treated ramie fiber in comparison to that of the plain PLA and the composites with untreated fiber by dynamic mechanical analysis (DMA). Thermogravimetric analysis shows that fiber treatment can improve the degradation temperature of the composites. Morphology of the fracture surface indicates that surface treatment can result in better adhesion between the fiber and the matrix [131].

7.8.2.3 Flax Fiber-Reinforced Thermoplastics

The mechanical properties of flax fiber-reinforced thermoplastic composites depend on the nature and orientation of the fibers, the nature of the matrix, and mainly on the adhesion between the fiber and polymer matrix [132]. Flax fiber (including 58% flax shives by weight) was used as a reinforcing material in polyethylene (PE), both high density polyethylene, HDPE and linear low density polyethylene, LLDPE, biocomposites. Five different methods of surface modification of flax fibers were carried out and the surface characteristics were analyzed by scanning electronic microscopy. Surface modifications increases tensile strength and decreases moisture absorption of the biocomposite to varying degrees. Acrylic acid treatment showed a relatively good result in reducing moisture absorption and enhancing

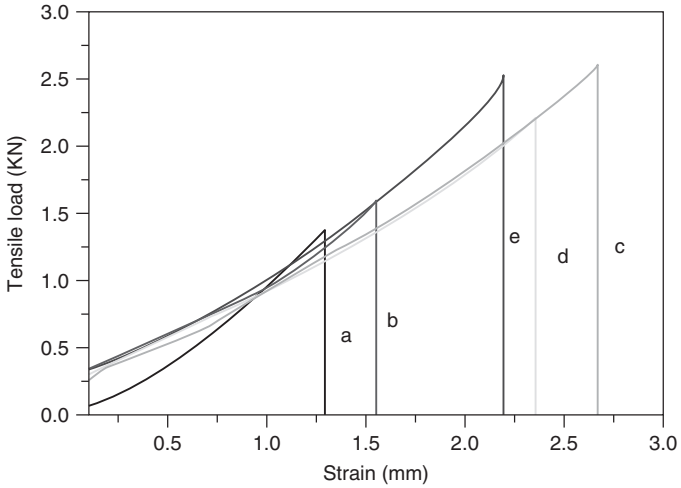

Figure 7.8 Tensile load–strain curves of neat PLA and ramie fiber-reinforced PLA composites: (a) neat PLA, (b) untreated fiber–PLA, (c) alkali-treated fiber–PLA, (d) 3-aminopropyltriethoxy silane treated fiber–PLA, and (e) γ-glycidoxypropyltrimethoxy silane treated fiber – PLA (Reprinted from [131], Copyright 2010, with permission from Elsevier.)

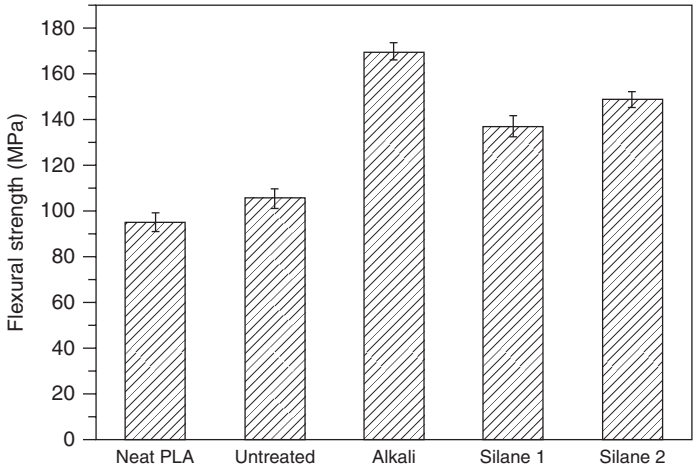

Figure 7.9 Flexural strength of neat PLA and ramie fiber-reinforced PLA composites (Reprinted from [131], Copyright 2010, with permission from Elsevier.)

tensile properties of biocomposites. The tensile strength and moisture absorption of biocomposites increased with increase in fiber content (from 10% to 30%) in the composites [133].

The main problems associated with the use of biofibers as reinforcements in thermoplastics are the poor wettability and weak interfacial bonding with the polymer because of the inherently poor compatibility of the hydrophilic

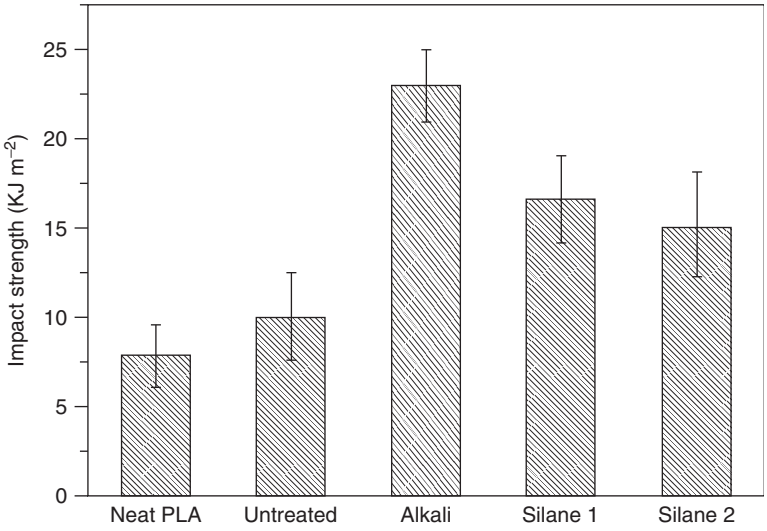

Figure 7.10 Impact strength of neat PLA and ramie fiber-reinforced PLA composites (Reprinted from [131], Copyright 2010, with permission from Elsevier.)

biofibers with the hydrophobic thermoplastics. Various chemical treatments of biofibers can improve the interface between the fibers and matrix. The effects of mercerization, silane treatment, benzoylation, and peroxide treatments of flax fibers on the performance of the fiber-reinforced HDPE, LLDPE, or HDPE/LLDPE mix composites have been investigated. Tensile properties can be improved with a suitable fiber surface treatment as compared to the untreated fiber composite. Silane-, benzoyl-, and peroxide-treated fiber composites offer superior physical and mechanical properties. The water absorption of the treated flax fiber composites is lower than that of untreated flax fiber composites. The incorporation of 10% chemically treated flax fiber into LLDPE, HDPE, or LLDPE/HDPE can considerably increase the melting point compared with untreated fiber composites [134]. Maleic acid anhydride-*grafted*-polypropylene (MAA-PP) has been reported to be a successful coupling agent for flax/PP composites. The interfacial adhesion between the flax fibers and maleic acid anhydride (MAA)-modified PP was studied with fiber pullout tests. The highest increase in apparent shear stress was obtained by treatment of the flax fiber with MAA-PP [135]. Acetylation has significant effect on the properties of flax fiber-reinforced PP composites. The mechanical properties of flax fiber-reinforced PP composites were investigated. The tensile and flexural strengths of the composites were found to increase with increasing degree of acetylation up to 18% and then decrease [136]. The mechanical properties of flax fiber-reinforced PP composites were also investigated. PP composites reinforced with zein coupling agent modified flax fibers were found to possess improved mechanical properties. Zein coating was found to increase the storage modulus owing to enhanced interfacial adhesion [137]. The mechanical properties of polystyrene composites reinforced with chemically treated flax fiber were

investigated and it has been found that mercerization of flax fiber improves the mechanical properties of the composites [138].

The use of thermoplastic composites offers several advantages compared to thermoset materials. Their useful properties include high impact resistance, damage tolerance, low price, and recyclability. Hybrid yarns containing both reinforcing fibers such as flax fiber and the thermoplastic matrix in the form of fibers such as PP filaments are easier and quicker to manufacture [139–141].

7.8.2.4 **Sisal Fiber-Reinforced Thermoplastics**

Sisal fiber is a promising reinforcing material for use in polymer composites on account of its better properties. Sisal fiber-reinforced thermoplastics composites have gained much more interest among material scientists and engineers than thermosets because of their low cost and recyclable properties. There has been an increasing interest in finding new applications for sisal fiber-reinforced composites that are traditionally used for making ropes, mats, carpets, fancy articles, and so on [142].

The tensile properties of short sisal fiber/PE composites in relation to processing methods and the effects of fiber content, length, and orientation were studied. The tensile properties show a gradual increase with fiber length, reaching a maximum at about 6 mm (12.5 MPa) and thereafter showing a decrease (10.24 MPa at 10 mm). Unidirectional short fibers achieved by extrusion enhance the tensile strength and elastic modulus of the composites along the axis of fiber alignment by more than twofold compared to randomly oriented fiber composites [143]. Sisal fibers could effectively reinforce PP matrix when used in optimal concentration of fibers and coupling agents. Maleic anhydride polypropylene (MAPP) is an effective coupling agent for sisal–PP composites. The mechanical tests revealed that the tensile, flexural, and impact strengths of the composites are significantly improved by the addition of MAPP in comparison to other treatment techniques. The morphology of the interface region and the thermal analysis also confirmed an efficient interfacial adhesion in the MAPP-treated composites [144].

Processing methods have different effects on the mechanical properties of sisal fiber-reinforced polypropylene (SF/PP) composites. Under optimum mixing conditions, melt-mixed composites showed better tensile properties than those of solution-mixed composites. The effect of different chemical treatments on the properties of sisal/PP composites was investigated and it was found that the tensile properties of the composites were enhanced considerably [145].

PP is a thermoplastic matrix material that received attention for the production of biofiber-reinforced thermoplastic composites. The problems encountered in relation to injection molding of SF/PP composites are increased melt flow viscosity as sisal fibers were introduced [145, 146] and poor interfacial bonding between sisal fiber and PP. A high injection temperature is needed to overcome the high melt viscosity of the SF/PP composites. The elevated injection temperature can cause severe thermal degradation of the reinforcing sisal fibers. This gives rise to the darkening color and odor emission of the molded SF/PP composites. A number of fiber pretreatments such as alkaline, heat, and coupling agent treatments are

necessary to overcome the poor interfacial bonding between the sisal fiber and PP. Maleic anhydride can serve as an effective compatibilizer for cellulosic fiber and polyolefin matrices [146–148]. By using a maleic anhydride-*grafted*-polypropylene (MA-g-PP) as the compatibilizer for SF/PP composites, the melt-blending torque could also be reduced [146].

The aging of sisal fibers has different effects on the properties of sisal/PP composites. Fresh sisal fiber shows better tenacity, breaking strength, and elongation when compared to aged fiber. This may be due to oxidation of cellulose in aged fiber, which results in degradation of strength; this does not happen for fresh fiber. However, aged sisal fiber-reinforced composites show better mechanical properties than fresh sisal fiber composites. The mechanical properties of sisal/PP composites not only depend upon the fiber strength alone but also on the interfacial adhesion between the fiber and the matrix. Aged sisal fiber has less moisture absorption, which results in better adhesion between the sisal fiber and PP matrix [149].

Table 7.3 shows the tensile properties of solution-mixed SF/PP, LDPE, and polystyrene composites (fiber length 6 mm) [143]. In the case of both PP/sisal and sisal/LDPE composites, the tensile strength and modulus go on increasing as the percentage of fiber content increases (from 0% to 30%), whereas the values changes in an irregular manner in the case of sisal/polystyrene composites. Since PP is more crystalline compared to LDPE, the increase in tensile strength by the addition of sisal fiber is less in the case of PP compared to LDPE. But the strength of the composite formed by the addition of fiber is more in the case of PP as compared

Table 7.3 Comparison of the tensile properties of longitudinally and randomly oriented solution-mixed sisal fiber-reinforced polypropylene (PP), polystyrene composites, and low density polyethylene (LDPE) (fiber length 6 mm).

Fiber content (%)	Composite type	Tensile strength (MPa)		Young's modulus (MPa)		Elongation at break (%)	
		L	R	L	R	L	R
0	PP	35.00	35.00	498	489	15.00	15.00
	PS	34.90	34.90	390	390	9.00	9.00
	PE	9.20	9.20	140	140	200.00	200.00
10	PP	36.00	29.00	730	605	7.82	8.00
	PS	21.30	18.16	629	516	9.00	7.00
	PE	15.61	10.80	1429	324	4.00	27.00
20	PP	39.10	31.14	971	798	7.11	7.33
	PS	43.20	25.98	999	553	8.00	6.00
	PE	21.66	12.50	2008	453	3.00	10.00
30	PP	44.40	33.84	1040	940	8.33	8.50
	PS	45.06	20.42	9998	624	7.00	4.00
	PE	31.12	14.70	3086	781	2.00	7.00

L, longitudinal; R, random.
''Source: Reprinted from [145], Copyright 1999, with permission from Elsevier.''

to LDPE. In the case of polystyrene at 10% fiber loading, the tensile strength is decreased by 40% but in the case of PP, it is increased by 3%. However, at high fiber loading, the tensile strength values are comparable for both PP and polystyrene. Thus, PP was found to be a good matrix for sisal/polyolefin composites [145, 150].

7.8.2.5 Jute Fiber Reinforced-Thermoplastics

Among the biofiber-reinforced composites, jute turns out to be quite promising because it is relatively inexpensive and commercially available in a required form. Jute fiber is an important agricultural product. It is the second most important fiber in the world. Among the naturally occurring lingo-cellulosic fibers, jute contains the highest proportion of the stiff natural cellulose that forms its main structural component. In recent years, considerable attempts have been made on the use of thermoplastic matrices for jute composites in making low cost items such as automotive components, door profiles and window frames, pellets, and furniture. There are several reports about the use of jute as reinforcing fibers for thermoplastics [151, 152]. The studies on jute fiber composites were carried out mostly in India in the early years of research.

Pretreatment of jute fibers and interfacial modification are frequently studied issues aiming to improve the properties of short or long fiber-reinforced composites. Maleic anhydride-*grafted*-PP has been widely used as a coupling agent to improve the adhesion between jute fiber and PP, and the effect of maleic anhydride-*grafted*-PP and fiber length on the performance of a jute/PP composite system has been investigated. Treatment of jute fibers with alkali treatment and MAPP emulsion has been found to be very efficient in improving the fiber–matrix adhesion in jute fiber mat-reinforced PP composites [153]. It has been shown that treatments changed not only the surface topography but also the distribution of diameter and strength of the jute fibers, which was analyzed by using a two-parameter Weibull distribution model. Consequently, the interfacial shear strength, flexural, and tensile strength of the composites all increased, but the impact strength decreased slightly.

Alkali treatment of jute fibers also improves the mechanical properties of thermoplastics. The vinyl ester resin reinforced with alkali-treated fibers shows improved mechanical properties. The maximum improvement was noted for the composites prepared with 4 h alkali-treated fibers at 35% fiber loading. The flexural strength improved by 20% and the modulus by 23%. The strength and modulus of the composites were found to be lower than the values estimated from the general rule of mixtures. For the jute/vinyl ester composites with 35% fiber content, the strength was decreased by 29% and 16% for the untreated and 4 h alkali-treated fibers and the modulus was lower by 51% and 37% for the untreated and 4 h alkali-treated fibers, respectively [154].

A silane-coupling agent improves the suitability of jute fibers as a reinforcing material. The reaction mechanism of silane treatment of jute fibers and silane treated jute–PP composites is shown in Scheme 7.2. Silane treatment of the jute fibers increased the fiber–matrix interaction through a condensation reaction between hydrolyzed silane and hydroxyl groups of jute cellulose. During the fracture process of silanized composites, the jute fibers were broken without complete

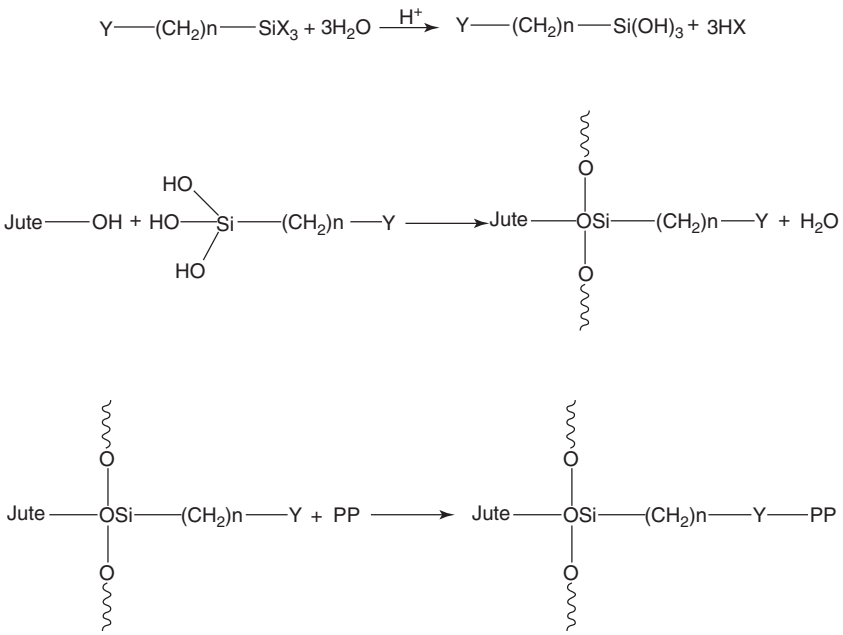

Scheme 7.2 Silane treated jute-PP composites (Reprinted from [155], Copyright 2008, with permission from Elsevier.)

pullout and much of the PP matrix remained surrounding the fibers. Silane treatment increased the tensile properties of the jute–PP composites (Figure 7.11), caused by improved adhesion between the silanized jute fiber and the PP matrix. The silanized jute composites exhibited greater dynamic mechanical properties in comparison to the untreated jute–PP composites [155].

Gamma radiation treatment of jute fibers and matrix material has considerable effect on the properties of thermoplastic composites. The mechanical properties of the composites made of different combinations of gamma treatment were measured and the effect of gamma radiation on the PP composites was investigated. Investigation showed that irradiated jute fabrics/irradiated PP-based composite produced the highest mechanical properties at 500 krad of total dose compared to the nonirradiated jute fabrics/irradiated PP and irradiated jute fabrics/nonirradiated PP-based composites [156].

Matrix modification based on MA-*g*-PP, affects the interfacial adhesion and mechanical properties of jute/PP composites. The effect of maleic anhydride-*grafted*-PP (MA-*g*-PP) coupling agents on the properties of jute fiber/PP composites has been studied. The addition of 2 wt% MAPP to PP matrices can significantly improve the adhesion strength with jute fibers and in turn the mechanical properties of the composites.

MA-*g*-PP improved the interaction between jute fibers and PP matrices. A hypothetical model of the interface between MA-*g*-PP with hydroxyl groups of jute

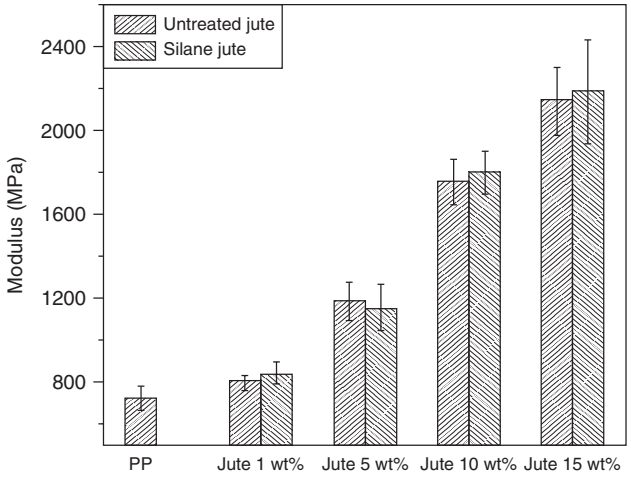

Figure 7.11 Tensile moduli of untreated and silanized jute–PP composites (Reprinted from [155], Copyright 2008, with permission from Elsevier.)

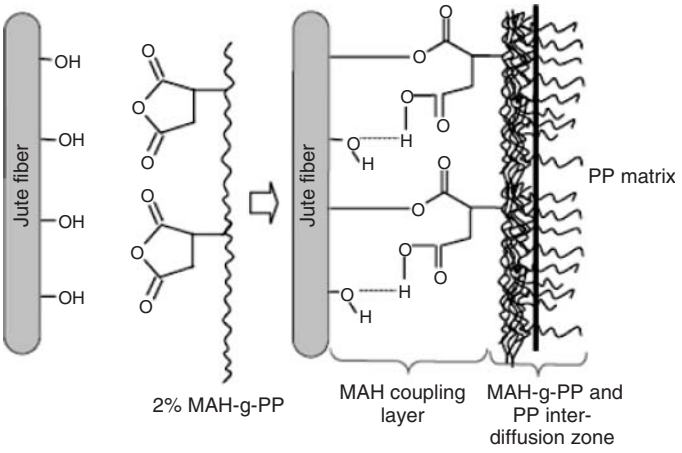

Figure 7.12 Hypothetical model of the interface between MAPP with hydroxyl groups of jute (Reprinted from [157], Copyright 2006, with permission from Elsevier.)

fiber is shown in Figure 7.12. The strong interfacial adhesion between the jute fiber and MA-*g*-PP treated PP matrices can be understood from this model, in which both chemical (ester bond) and physical interactions (hydrogen bond) should be formed between the biofiber and coupling agent. The PP chain of MA-*g*-PP diffuses into the PP matrix through interchain entanglements. On the other hand, the maleic anhydride group forms both covalent and hydrogen bonds with the hydroxyl groups of the fiber. These cause better adhesion between the fiber and the matrix. Therefore, the transfer of stress from the matrix to the fibers is improved and leads to higher tensile strengths [157].

The effects of various surface modifications of jute on the performance of jute–biodegradable polyester composites have received growing interest. Bacterially derived biodegradable polyester is a thermoplastic and has tensile strength comparable to that of PP. Among the various chemically modified jute (dewaxed, bleached, alkali-treated, cyanoethylated, and grafted), the alkali-treated, cyanoethylated, and low percent grafted samples based biodegradable polyester amide matrix composites produce comparatively better properties than untreated and dewaxed sample counterparts [158].

7.8.2.6 Hemp Fiber-Reinforced Thermoplastics

Hemp has found use in the production of specialty papers and also as reinforcement for composites. Hemp is one of the highest yielding and least intensive crops, which grows in temperate countries. It is highly self-compatible so that there is no need for crop rotation. Similar to other lingo-cellulosic fibers, hemp is biodegradable and environmentally friendly, and its Young's modulus is one of the highest among biofibers [159].

Several research studies have shown the effectiveness of hemp fiber-reinforced thermoplastic matrices [160–162]. Among the thermoplastic matrices, PP is one of the commodity thermoplastics with better properties such as low density, high Vicat softening point, good surface hardness, good flex life, scratch resistance, abrasion resistance, and very good electrical properties [163].

Hemp strands and cane straw of hemp have been used as reinforcement and filler in PP composites. Hemp straw–PP composites have low tensile properties. However, the tensile stress of hemp straw composites showed a slight increase for composites containing MAPP, which means that hemp straw could be used as filler. Moreover, the Young's modulus of hemp straw composites was higher than that of the PP matrix and achieved 70% of the Young's modulus of hemp strand composites. So, hemp plant derivates (hemp strands and hemp straw) can be used as reinforcement for polymeric matrices that give composites with remarkable tensile properties at very attractive economic costs [164]. The operating temperature of composite formulations has a noticeable effect on the mechanical properties of hemp fiber–PP composites. Flexural strength, flexural modulus, tensile strength, and tensile modulus of the composites drop remarkably at higher temperatures. The effect of temperature has been observed to be the highest on stiffness of the composites (both flexural and tensile) compared with that of strength values. Impact strength has been found to be independent of temperature [165].

For the polar hemp fiber and nonpolar PP matrix, physical and chemical treatments of hemp fibers have to be used to avoid the different and incompatible surface polarities. In order to improve the fiber–matrix adhesion, initial hemp strands were submitted to low cost processes, such as refining process and surface modification with alkyl ketene dimer (AKD), commonly used in the paper-making industry. Hemp strands comprising about 15% of cane straw have been used to reinforce the PP matrix. Refining or AKD sizing of hemp fiber results in composites with higher tensile and flexural strength and the stiffness of composites is also greatly enhanced. The tensile and flexural strength at yield of hemp and glass

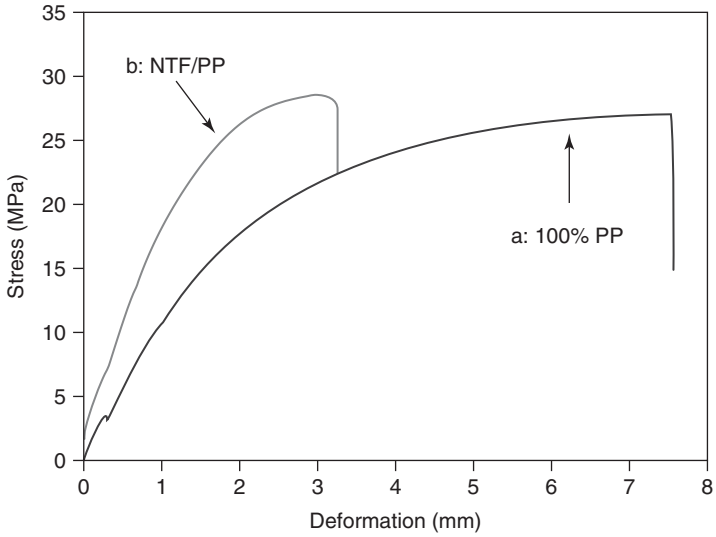

Figure 7.13 Tensile behavior of (a) PP matrix and (b) nontreated fiber (NTF)–PP composites (Reprinted from [44], Copyright 2010, with permission from Elsevier.)

fiber-reinforced (GFR) composites were even closer. Thus, due to the lower density of hemp strands, specific properties at yield of hemp strands composites offer a good perspective as glass fiber substitutes, as the specific properties at yield of hemp composites may increase 80% of the mechanical properties of glass fiber composites [166].

Corona discharge treatment represents a valuable technique for the surface modification of cellulosic fibers used for manufacturing composites. It is an efficient and eco-friendly treatment that enhances the fiber–matrix interaction in composites. The treatment of hemp fiber by means of corona discharge permits to obtain greater characteristics (Young's modulus, stiffness, elastic density energy). Hemp–PP composites properties were found to be highly sensitive to interfacial phenomena. Modification of hemp fiber rather than the PP matrix allows a greater improvement in the composites properties [44].

Figure 7.13 displays the stress–strain behavior of 100% PP and a 20 wt% content hemp fibers composite. The addition of hemp fibers increases the tensile strength at failure by 30% as compared to the 100% PP material and reduces significantly the deformation at break (until 50% of reduction). Figure 7.14 shows the tensile curves for the different composites reinforced with nontreated and corona-treated hemp fibers. In the case of treated fibers (corona treatment), the strength at break is significantly increased (37.8 against 28.6 MPa), whereas the deformation is nearly unchanged [44].

The adhesion between the fibers and matrix can be improved by either modifying the surface of the fibers to make them more compatible with the matrix, or by modifying the matrix with a coupling agent that adheres well to both the fibers and the matrix. The addition of a sufficient amount of Na_2SO_3 to NaOH can assist

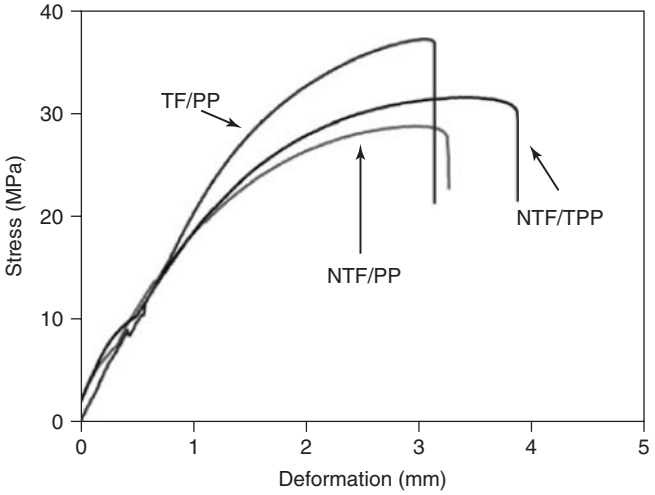

Figure 7.14 Tensile curve for composites materials reinforced with 20 wt% hemp fiber (Reprinted from [44], Copyright 2010, with permission from Elsevier.)

in the removal of lignin, and can also shorten the treatment time required to remove the lignin from biofibers. An injection-molded hemp fiber-reinforced PP composite consisting of 40 wt% $NaOH/Na_2SO_3$-treated fiber, 4% MAPP and PP had the highest tensile strength (50.5 MPa) and Young's modulus (5.31 GPa) of all the composites tested, due to the inclusion of the strongest fibers and an optimum MAPP content. TGA and DTA analysis (Figure 7.15) showed that untreated hemp fiber composites and $NaOH/Na_2SO_3$ treated hemp fiber composites (each with a matrix of 4% MAPP and PP) were less thermally stable than PP matrix alone. The thermal stabilities of composites containing untreated fiber and $NaOH/Na_2SO_3$-treated fiber were found to be similar to each other [167].

7.9 Biofiber Graft Copolymers Reinforced Thermoplastic Composites

In order to develop composites with better mechanical properties and environmental performance, it becomes necessary to increase the hydrophobicity of the biofibers and to improve the interface between matrix and biofibers. Graft copolymerization of biofibers is one of the best methods to attain these improvements. As of now, only few studies have reported the use of biofiber graft copolymers as reinforcing material in the preparation of composites [33]. Mechanical properties of thermoplastic composites reinforced with acrylate-*grafted* henequen cellulose fibers were studied. It has been found that best results could be obtained with poly(methyl methacrylate) (PMMA)-*grafted* cellulose fibers because of better fiber–matrix adhesion. The modulus of poly(vinyl chloride) (PVC) composites is increased when grafted or ungrafted cellulose are used as reinforcement but the composites with

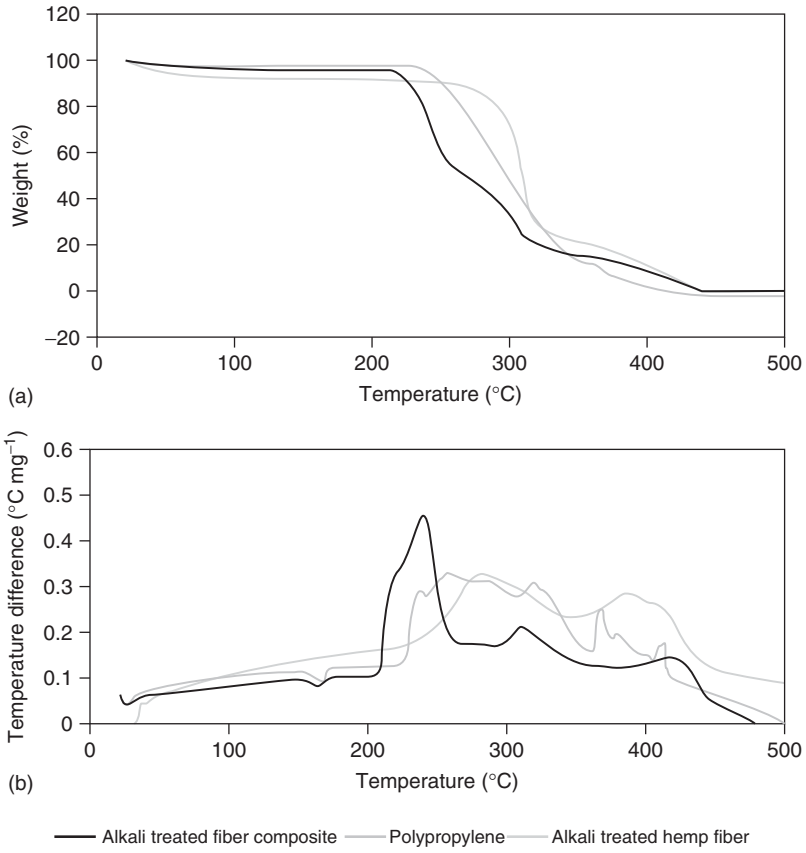

Figure 7.15 (a) TGA and (b) DTA curves for polypropylene, alkali-treated hemp fiber, and composites containing alkali-treated hemp fiber (Reprinted from [167], Copyright 2008, with permission from Elsevier.)

PMMA-*grafted* cellulose present the higher modulus. The better adhesion between the PMMA-*grafted* cellulose fiber and the PVC matrix results in an increase in the tensile strength at fiber content up to 15 wt% [61].

Green composites reinforced with *Saccharum spontaneum* fiber and its different graft copolymers were fully biodegradable and environment friendly. Mechanical properties including tensile strength, compressive strength, and wear resistance of different reinforced samples were significantly improved in comparison to pure cornstarch matrix. Maximum compressive strength and wear resistance was found in case of fibers grafted with MMA. The three-dimensional network of the composites and its breaking down due to biodegradation at Stage-I, Stage-II, Stage-III, and Stage-IV are also shown in (Figure 7.16a–h). These SEM images show the morphological changes occurred on cornstarch composites reinforced with *S. spontaneum* and different graft copolymers at different stages of biodegradation. At an intermediate stage (after 15 days of degradation), sample surfaces became

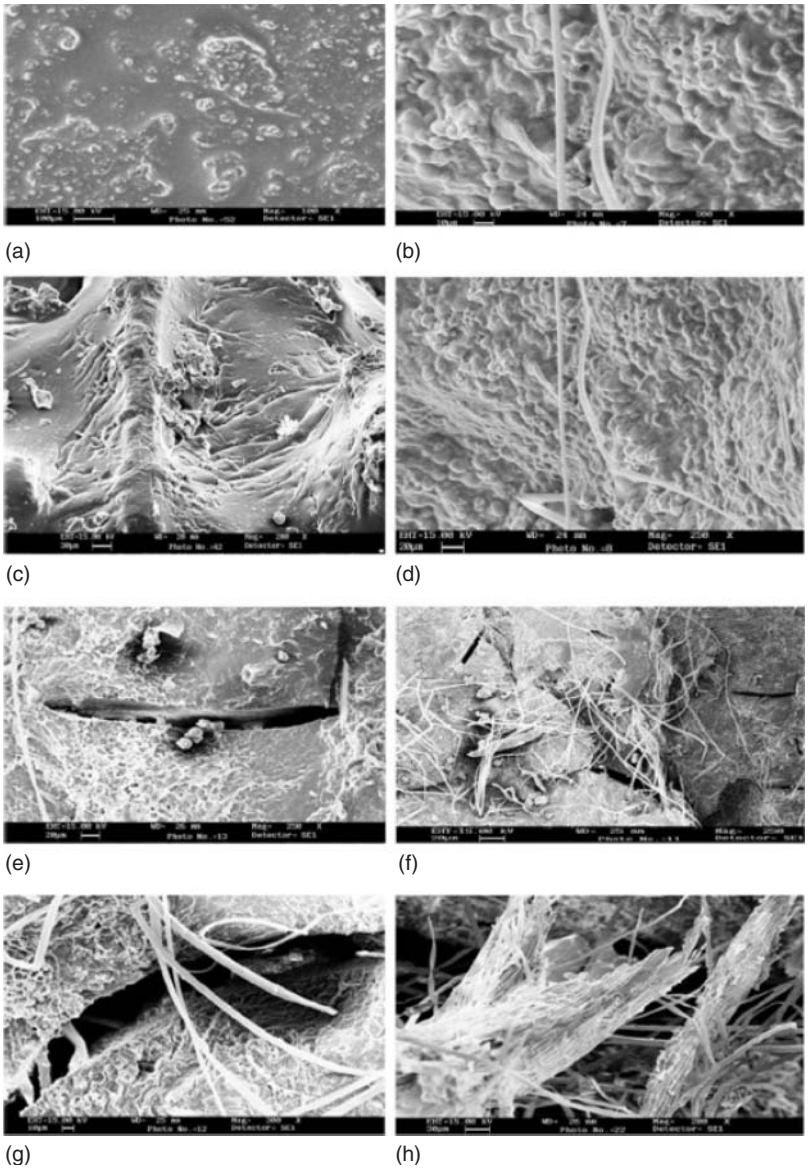

Figure 7.16 SEM of cornstarch matrix-based composites (a–d); biodegradation (I, II, III, and IV stages) of cornstarch matrix-based composites (e–h) (Reprinted from [168], Copyright 2010, with permission from Elsevier.)

heterogeneous and rough. However, after 30 days of degradation, the surfaces became more heterogeneous and reinforced fibers came out of the composites because of rupture of the matrix. At the final stage of degradation (after 60 days), the matrix totally disappeared and only the reinforced fibers were left behind [168].

Agave fiber-reinforced polystyrene composites were prepared by the compression-molding technique in which good interfacial adhesion is generated by fiber surface modification. The agave fibers were modified through graft copolymerization with MMA. The short grafted fibers were then spread between the alternate layers of polystyrene resin by hand layup method to obtain the thermoplastic composites. Polystyrene composites reinforced with graft copolymers of agave fibers showed better mechanical properties [169].

Graft copolymers of PP and maleic anhydride (MA–PP) have shown to be very effective additives for cellulose fiber–PP composites. The treatment of biofibers with hot MA-PP copolymers provides covalent bonds across the interface. After this treatment, the surface energy of biofibers is increased to a level much closer to the surface energy of the matrix. Thus, a better wettability and higher interfacial adhesion is obtained. The PP chain permits segmental crystallization and cohesive coupling between the modified fiber and the PP matrix. All mechanical properties of composites were improved when treated fibers were used. SEM studies of the tensile fracture surfaces of the composites showed that composites containing treated fibers showed better dispersion of fibers in the matrix, a more effective wetting of fibers by the matrix, and a better adhesion between the two phases [170, 171].

7.10 Bacterial Cellulose and Bacterial Cellulose-Coated, Biofiber-Reinforced, Thermoplastic Composites

BC produced by *A. xylinum* is becoming an excellent reinforcing agent for polymeric materials and composites because of its high mechanical strength, high crystallinity, and a highly pure nanofibrillar network structure [172–174].

The small dimensions of BC fibrils enable them a direct contact between cellulose and matrix polymers, allowing for a large contact surface and thus excellent adhesion. BC films present a good reinforcement for cellulose acetate butyrate (CAB) composites. These composites exhibit phenomena such as stiffening after straining in tension; this is widely observed in plant tissues, emphasizing the usefulness of BC-reinforced composites as easily controllable and well-defined model systems for cellulosic composites. Composites reinforced with BC may also find practical application where special properties such as biodegradability are desired [175].

BC produced by *A. xylinum* was used as reinforcement in composites with a starch thermoplastic matrix. BC acts efficiently as reinforcement, even in relatively low quantities, since 5% produced a significant increase in both modulus and tensile strength. BC-reinforced composites displayed better mechanical properties

than those with vegetable cellulose fibers. The Young's modulus of composites increased by 30- and 17-fold (with 5% fibers), while the elongation at break was reduced from 144% to 24% and 48% with increasing fiber content of bacterial and vegetable cellulose, respectively [176]. BC and plasticized starch combination proved to have much better mechanical properties than the plasticized starch alone. An enzyme treatment using *Trichoderma reesei* endoglucanases enhanced the reinforcement properties of BC nanofibers. The enzymatic treatment also had the advantage of causing less material loss in comparison to other nanofiber production processes, such as acid hydrolysis or mechanical fibrillation. The elastic modulus of composite reinforced with treated BC was 17 times higher than that of the starch matrix and four times higher than that of the film containing untreated fibers. Tensile strength was increased eight times that of the starch matrix and almost double that of the film containing untreated fibers [177].

Green nanocomposites were produced using functionalized BC to improve the interfacial adhesion between BC and biodegradable and hydrophobic aliphatic thermoplastic polyester PLLA. BC was functionalized using various organic acids such as acetic, hexanoic, and dodecanoic acid. The mechanical properties of the surface-functionalized, BC-reinforced PLLA nanocomposites showed significant improvements when compared to neat PLLA and BC-reinforced PLLA. The thermal degradation and viscoelastic behavior of the nanocomposites were also improved over neat PLLA [178]. Tensile properties of the BC–starch biocomposites were tested and compared with those of the unreinforced starch. The presence of BC nanofibers improves the tensile properties and the resistance to moisture and microorganism attacks. The higher resistance to water absorption for the biocomposites than the unreinforced matrix is believed to be attributable to the higher resistance of BC fibers and the strong hydrogen bonding formed at the fiber–matrix interfaces [179].

The coating of biofibers provides strength and will make the composites more durable without affecting their biodegradability. These composites are more suitable for recycling (or composting) than commonly used petroleum-based composites. Hemp and sisal fibers were coated with nanosized BC through a special fermentation process. The coated sisal fibers showed much better adhesion properties than the original fibers, without losing their mechanical properties and the properties ideal for their use in PLLA and CAB composites. The practical adhesion between the modified fibers and the renewable polymers CAB was quantified using the single-fiber pullout test (Figure 7.17). The modified hemp fibers also had improved adhesion properties [97].

Figure 7.18 shows exemplarily the pullout data for the hemp and sisal fibers from CAB. The gradient corresponds to the apparent interfacial shear strength. The steeper slope for the BC-modified fibers indicates a stronger apparent adhesion. This stronger interface presumably arises from the increase in roughness associated with the presence of nanoscale cellulose on the surface and the entanglement between the BC fibrils and the polymer molecules. Strong interactions are expected due to the potential for hydrogen bonding between the hydroxyl groups present on the modified fiber surface and in CAB [97].

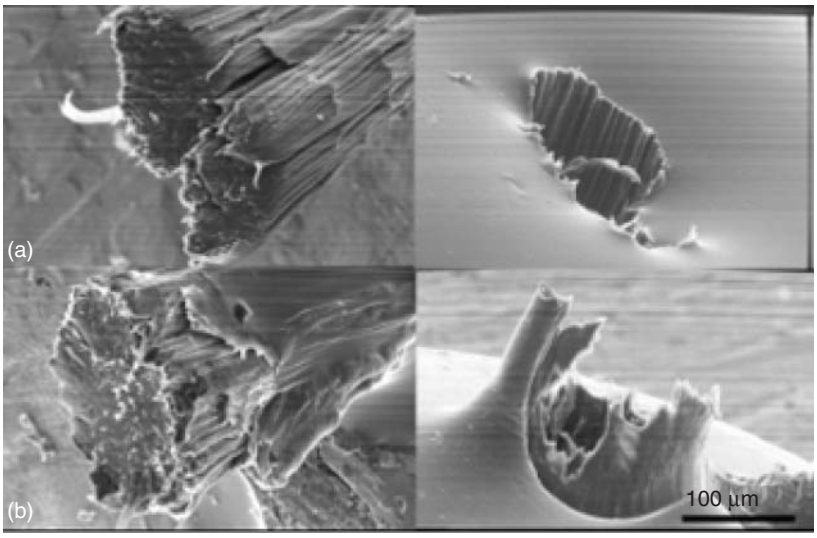

Figure 7.17 SEM micrographs of (a) bacterial cellulose-modified sisal and (b) acetone-treated and bacterial cellulose-modified sisal fibers and the corresponding CAB matrix cavities after single fiber pullout testing (Reprinted from [97], Copyright 2008, with permission from American Chemical Society.)

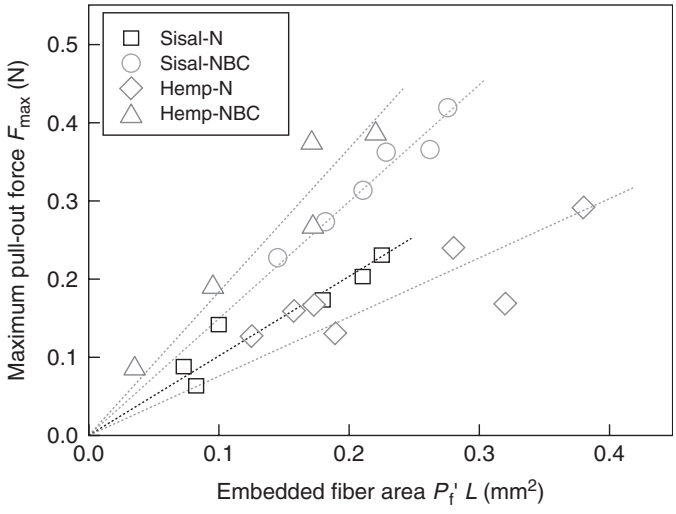

Figure 7.18 Single fiber pullout results for hemp and sisal fibers in CAB matrix; (□) natural sisal fiber (Sisal-N); (○) sisal fiber modified with bacterial nanocellulose (Sisal-NBC); (◊) natural hemp fiber (Hemp-N); and (Δ) hemp fiber modified with bacterial cellulose (Hemp-NBC) (Reprinted from [97], Copyright 2008, with permission from American Chemical Society.)

7.11
Applications of Biofiber-Reinforced Thermoplastic Composites

Biofiber-reinforced polymer composites have received much attention because of their mechanical and biodegradable properties. Nowadays, glass fibers represent 85% of the materials used for the reinforcement of polymers. Nevertheless, because of a stronger and stronger political will to reduce the environmental impact of human industrial activities, the development and use of natural fibers will indubitably follow an exponential growth. This trend is already well initiated in the automotive field since the European parliament issued in September 2000 a directive setting the objectives related to the end-of-life recycling of vehicles: no later than January 2015–after which vehicles have to be made out of 95% recyclable materials. This directive coupled with environmental concerns has contributed to the increased use of natural fiber composites in the automotive sector. At present, all the major auto makers utilize these materials to make nonstructural components of the vehicles such as headliners, luggage compartments, door panels, and seat backs.

Car manufacturers are now using biocomposites in various applications [180]. All these so-called ''biocomposites'' use natural fibers but the resin matrix is always an oil-derived synthetic material. As of now, many of the major car manufacturers such as Daimler Chrysler, Mercedes, Volkswagen, Audi Group, BMW, Ford, and Opel use biocomposites in various applications [8]. Interior trim components such as dashboards and door panels using PP and natural fibers have been produced for Daimler Chrysler for a while. The use of flax fibers in car disk brakes to replace asbestos fibers is another example. In 2000, Audi launched the A2 midrange car in which door trim panels were made of polyurethane reinforced with mixed flax/sisal mat. Daimler Chrysler has been increasing its research and development in flax-reinforced polyester composites for exterior applications for a number of years now [181]. Mercedes also used jute-based door panels in its E-class vehicles in 1996 [182]. Cotton fibers embedded in polyester matrix were used in the body of the East German ''Trabant'' car [183]. Some other applications include underfloor protection trim of Mercedes A class made from banana fiber-reinforced composites, and the Mercedes S class automotive components made from different biofiber-reinforced composites [184]. Lotus manufactured ''Eco Elise'' bodyworks, which contains hemp fibers, while sisal fibers are used for interior trimmings, whereas the inner door panels for the BMW 7 Series contain 70% sisal fibers. Plant fiber-reinforced PLA composites with improved rigidity and reduced processing times have been applied in the Toyota Lexus HS 250h hybrid vehicle recently.

It is, therefore acknowledged that natural fiber production requires much less nonrenewable energy than glass fiber production. The nonrenewable energy consumed by the production of glass fiber mats (54.7 MJ kg^{-1}) is more than five times higher than the value estimated for the flax fiber mats (9.55 MJ kg^{-1}) [185]. While natural fiber growth mainly demands solar energy, glass fiber production process including melting stages at extreme temperatures depends on intensive consumption of fossil fuels. The only trouble spot of natural fibers crops is related to the use

of fertilizers that could potentially lead to increased nitrate emissions and result in eutrophication effects. Nevertheless, even if the contributions of atmospheric NO_x emissions to eutrophication phenomenon are taken into account, production environmental impact of GFR composites is more severe [186]. Moreover, to facilitate wide-scale applications, a better understanding is required to properly quantify the added benefit of green composites. For mass production in applications such as the automobile industry, special consideration needs to be given for damage tolerance, impact behavior (failure and resistance), fatigue life, and vehicle safety margins.

Biofibers are manufactured using many of the composite-manufacturing processes such as hand layup, compression molding, and resin transfer molding. It is possible to make fully biodegradable composites if natural fibers can be used to reinforce natural resins. Environmentally friendly composites find applications in interior door and ceiling panels because of their superior insulation against noise and heat. Research has focused on how to make green composites strong enough to meet the requirements of durability. Biodegradable composites can save landfill space and boost the country's economy.

Wood ash can be used as filler or reinforcement for PP, PE, or PVC to make environmentally friendly composites. The resulting products can replace wood in the building industry. Other applications for wood–plastic composites are door frames, roofs, fences, window frames, and furniture. The diversification of the composite products has a direct effect on the number of different jobs that can be created, the dual advantage of cost and performance being the main selling factors.

If current research efforts for the development of fully biodegradable green composites are of utmost importance, use of biocomposites represents a necessary intermediate step. Mechanical properties and strengths of widespread thermoset or thermoplastic resins (PP, PE, PEEK, polyetheretherketone, etc.) can be significantly increased by employing natural fibers as reinforcement. Biofibers present the advantage to have a higher specific strength when compared to common glass fibers; besides, they are carbon dioxide neutral. Most of them are vegetal, extracted from leaves (abaca, banana, sisal, pineapple), stem (jute, flax, hemp, kenaf, ramie), fruits (coir, oil palm), seeds (cotton), grasses (bamboo), or roots (broom), but some fibers of animal (wool, silk) and mineral (basalt) origin are also produced. Another alternative consists in mixing synthetics and biofibers or different types of biofibers to obtain hybrid composites (basalt/glass/PP, basalt/hemp/PP, etc.) and make the most of the specific properties of each constituent. Up to now, biofiber-reinforced polymeric composites are used for applications such as particleboards, printed circuit boards, window frames, and asbestos replacement in car disk brakes, car door panels, interior trim boards, or dashboards.

7.12 Conclusions

Biofibers have received much attention as reinforcements for composites due to many advantages such as annually renewable, sustainable, low cost, high specific

modulus, lightweight, and biocompatible features. Biofiber-reinforced composites have lightweight, nonabrasive, combustible, nontoxic, low cost, and biodegradable properties.

In order to develop composites with better mechanical properties and environmental performance, it becomes necessary to increase the hydrophobicity of the biofibers and to improve the interface between matrix and biofibers. Graft copolymerization of biofibers is one of the best methods to attain these improvements. The introduction of BC onto biofibers provides new means of controlling the interaction between biofibers and polymer matrices. BC is becoming an excellent reinforcing agent for polymeric materials and composites due to high mechanical strength, high crystallinity, and a highly pure nanofibrillar network structure. Coating of biofibers with BC not only facilitates good distribution of BC within the matrix but also results in an improved interfacial adhesion between the fibers and the matrix. The coating of biofibers provides strength and will make composites more durable without affecting their biodegradability.

Biofiber-reinforced polymeric composites are used in applications such as particleboards, printed circuit boards, window frames, and asbestos replacement in car disk brakes, car door panels, interior trim boards, or dashboards.

References

1. Balter, M. (2009) Clothes make the (Hu) man. *Science*, **325**, 1329.
2. Kvavadze, E., Bar-Yosef, O., Belfer-Cohen, A., Boaretto, E., Jakeli, N., Matskevich, Z., and Mashvelian, T. (2009) 30,000 year old wild flax fibres. *Science*, **325**, 1359.
3. Rao, K.M.M. and Rao, K.M. (2007) Extraction and tensile strength of natural fibres: vakka, date and bambo. *Compos. Struct.*, **77**, 288–295.
4. Ghoreishi, S.R., Davies, P., Cartraud, P., and Messager, T. (2007) Analytical modeling of synthetic fiber ropes. Part II: a linear elastic model for 1 + 6 fibrous structures. *Int. J. Solids Struct.*, **44**, 2943–2960.
5. Svennerstedt, M. (2002) Durability and life cycle aspects on bio-fibre composite materials. 9th International Conference on the Durability of Building Materials and Components, Paper 025, Brisbane, Australia, March 17–21, 2002.
6. Barghoorn, P., Stebani, U., and Balsam, M. (1998) Trends in applied polymer chemistry. *Adv. Mater.*, **10**, 635–641.
7. Xie, Y., Hill, C.A.S., Xiao, Z., Militz, H., and Mai, C. (2010) Silane coupling agents used for natural fiber/polymer composites: a review. *Composites Part A*, **41**, 806–819.
8. John, M.J. and Thomas, S. (2008) Biofibres and biocomposites. *Carbohydr. Polym.*, **71**, 343–364.
9. Bledzki, A.K. and Gassan, J. (1999) Composites reinforced with cellulose based fibres. *Prog. Polym. Sci.*, **24**, 221–74.
10. Sreenath, H.K., Shah, A., Yang, V., Gharia, M.M., and Jeffries, T.W. (1993) Enzymatic polishing of jute/cotton blended fabrics. *J. Ferment. Bioeng.*, **84**, 18–20.
11. Angelini, L.G., Lazzeri, A., Levita, G., Fontanelli, D., and Bozzi, C. (2000) Ramie and spanish broom fibres for composite materials: agronomical aspects, morphology and mechanical properties. *Ind. Crops Prod.*, **11**, 145–161.
12. Kalia, S., Kaith, B.S., and Kaur, I. (2009) Pretreatments of natural fibers

and their application as reinforcing material in polymer composites–a review. *Polym. Eng. Sci.*, **49** (7), 1253–1273.
13. Fries, W. (1998) Collagen-biomaterial for drug delivery. *Eur. J. Pharm. Biopharma.*, **45**, 113–136.
14. Han, S.O., Lee, S.M., Park, W.H., and Cho, D. (2006) Mechanical and thermal properties of waste silk fiber-reinforced poly (butylene succinate) biocomposites. *J. Appl. Polym. Sci.*, **100**, 4972–4980.
15. Perez-Rigueiro, J., Viney, C., Llorca, J., and Elices, M. (1998) Silkworm silk as an engineering material. *J. Appl. Polym. Sci.*, **70**, 2439–2447.
16. Hurter, R.W. and Riccio, F.A. (1998) Why CEOS don't want to hear about nonwoods-or should they? TAPPI Proceedings, NA Nonwood Fiber Symposium, Atlanta, Georgia, pp. 1–11.
17. Ververis, C., Georghiou, K., Christodoulakis, N., Santas, P., and Santas, R. (2004) Fiber dimensions, lignin and cellulose content of various plant materials and their suitability for paper production. *Ind. Crops Prod.*, **19**, 245–254.
18. Han, J.S. (1998) Properties of nonwood fibers. Proceedings of the Korean Society of Wood Science and Technology Annual Meeting.
19. White, N.M. and Ansell, M.P. (1983) Straw reinforced polyester composites. *J. Mater. Sci.*, **18**, 1549–1556.
20. Hornsby, P.R., Hinrichsen, E., and Trivedi, K. (1997) Preparation and properties of polypropylene composites reinforced with wheat and flax straw fibres: part II analysis of composite microstructure and mechanical properties. *J. Mater. Sci.*, **32**, 1009–1015.
21. Tsai, W.T., Chang, C.Y., and Lee, S.L. (1998) A low cost adsorbent from agricultural waste corn cob by zinc chloride activation. *Bioresour. Technol.*, **64**, 211–217.
22. Ishak, Z.A., Yow, B.N., Ng, B.L., Khalil, H.P.S.A., and Rozman, H.D. (2001) Hygrothermal aging and tensile behavior of injection-molded rice husk-filled polypropylene composites. *J. Appl. Polym. Sci.*, **81**, 742–753.
23. Wang, D. and Sun, X.S. (2002) Low density particleboard from wheat straw and corn pith. *Ind. Crops Prod.*, **15**, 43–50.
24. Yang, H.S., Kin, D.J., and Kim, H.J. (2003) Rice straw–wood particle composite for sound absorbing wooden construction materials. *Bioresour. Technol.*, **86**, 117–121.
25. Pradhan, R., Misra, M., Erickson, L., and Mohanty, A. (2010) Compostability and biodegradation study of PLA–wheat straw and PLA–soy straw based green composites in simulated composting bioreactor. *Bioresour. Technol.*, **101**, 8489–8491.
26. Sain, M. and Panthapulakkal, S. (2006) Bioprocess preparation of wheat straw fibres and their characterization. *Ind. Crops Prod.*, **23**, 1–8.
27. Soest, P.V.J. (2006) Rice straw, the role of silica and treatments to improve quality. *Anim. Feed Sci. Technol.*, **130**, 137–171.
28. Agbagla-Dohnani, A., Nozière, P., Clément, G., and Doreau, M. (2001) In sacco degradability, chemical and morphological composition of 15 varities of European rice straw. *Anim. Feed Sci. Technol.*, **94** (1–2), 15–27.
29. Yao, F., Wu, Q., Lei, Y., and Xu, Y. (2008) Rice straw fiber-reinforced high-density polyethylenecomposite: effect of fiber type and loading. *Ind. Crops Prod.*, **28**, 63–72.
30. Kozłowskiy, R. and Przybylak, M.W. (2008) Flammability and fire resistance of composites reinforced by natural fibres. *Polym. Adv. Technol.*, **19**, 446–453.
31. Jacob, M., Varughese, K.T., and Thomas, S. (2006) A study on the moisture sorption characteristics in woven sisal fabric reinforced natural rubber biocomposites. *J. Appl. Polym. Sci.*, **102**, 416–423.
32. Rosa, M.F., Chiou, B., Medeiros, E.S., Wood, D.F., Mattoso, L.H.C., Orts, W.J., and Imam, S.H. (2009) Biodegradable composites based on starch/EVOH/glycerol blends and coconut fibres. *J. Appl. Polym. Sci.*, **111**, 612–618.

33. Kalia, S., Kaith, B.S., Sharma, S., and Bhardwaj, B. (2008) Mechanical properties of flax-g-poly(methyl acrylate) reinforced phenolic composites. *Fibers Polym.*, **9**, 416–422.
34. Chabba, S. and Netravali, A.N. (2005) 'Green' composites part 2: characterization of flax yarn and glutaraldehyde/poly(vinyl alcohol) modified soy protein concentrate composites. *J. Mater. Sci.*, **40**, 6275–82.
35. Summerscales, J., Dissanayake, N.P.J., Virk, A.S., and Hall, W. (2010) A review of bast fibres and their composites. Part 1, fibres as reinforcements. *Composites Part A*, **41**, 1329–1335.
36. Baley, C. (2002) Analysis of the flax fibres tensile behaviour and analysis of the tensile stiffness increase. *Composites Part A*, **33**, 939–948.
37. Panthapulakkal, S. and Sain, M. (2007) Injection-molded short hemp fiber/glass fiber-reinforced polypropylene hybrid composites–mechanical, water absorption and thermal properties. *J. Appl. Polym. Sci.*, **103**, 2432–2441.
38. Mohanty, A.K., Tummala, P., Liu, W., Misra, M., Mulukutla, P.V., and Drzal, L.T. (2005) Injection molded biocomposites from soy protein based bioplastic and short industrial hemp fiber. *J. Polym. Environ.*, **13**, 279–283.
39. Williams, G.I. and Wool, R.P. (2000) Composites from natural fibers and soy oil resins. *Appl. Compos. Mater.*, **7**, 421–432.
40. Mehta, G., Drzal, L.T., Mohanty, A.K., and Misra, M. (2006) Effect of fiber surface treatment on the properties of biocomposites from nonwoven industrial hemp fiber mats and unsaturated polyester resin. *J. Appl. Polym. Sci.*, **99**, 1055–1068.
41. Mishra, S., Naik, J.B., and Patil, Y.P. (2004) Studies on swelling properties of wood/polymer composites based on agro-waste and novolac. *Adv. Polym. Technol.*, **23**, 46–50.
42. Bledzki, A.K., Fink, H.P., and Speecht, K. (2004) Unidirectional hemp and flax EP- and PP-composites: influence of defined fiber treatments. *J. Appl. Polym. Sci.*, **93**, 2150–2156.
43. Behzad, T. and Sain, M. (2005) Cure simulation of hemp fibre acrylic based composites during sheet molding process. *Polym. Polym. Compos.*, **13**, 235–244.
44. Ragoubia, M., Bienaiméb, D., Molinaa, S., Georgea, B., and Merlina, A. (2010) Impact of corona treated hemp fibres onto mechanical properties of polypropylene composites made thereof. *Ind. Crops Prod.*, **31**, 344–349.
45. Mishra, S. and Naik, J.B. (1998) Absorption of water at ambient temperature and steam in wood–polymer composites prepared from agrowaste and polystyrene. *J. Appl. Polym. Sci.*, **68**, 681–686.
46. Plackett, D., Andersen, T.L., Batsberg, W., and Nielsen, P.L. (2003) Biodegradable composites based upon L-polylactic acid and jute fibre. *Compos. Sci. Technol.*, **63**, 1287–1296.
47. Singh, B., Gupta, M., and Verma, A. (1996) Influence of fiber surface treatment on the properties of sisal-polyester composites. *Polym. Compos.*, **17**, 910–918.
48. Dobreva, T., Peren, J.M., Perez, E., Benavente, R., and Garcıa, M. (2009) Crystallization behavior of poly(L-lactic acid)-based ecocomposites prepared with kenaf fiber and rice straw. *Polym. Compos.*, **30** (1), 1–11.
49. Amaducci, S., Amaducci, M.T., Benati, R., and Venturi, G. (2000) Crop yield and quality parameters of four annual fibre crops (hemp, kenaf, maize and sorghum) in the North of Italy. *Ind. Crops Prod.*, **11**, 179–186.
50. Reis, J.M.L. (2006) Fracture and flexural characteristics of natural fiber reinforced polymer concrete. *Constr. Build. Mater.*, **20**, 673–678.
51. Okubo, K., Fujii, T., and Yamamoto, Y. (2004) Development of bamboo-based polymer compositesand their mechanical properties. *Composites Part A*, **35**, 377–383.
52. Li, S.H., Zeng, Q.Y., Xiao, Y.L., Fu, S.Y., and Zhou, B.L. (1995) Biomimicry of bamboo bast fiber with engineering composite materials. *Mater. Sci. Eng., C*, **3**, 125–130.

53. Yoa, W. and Li, Z. (2003) Flexural behaviour of bamboo fiber reinforced mortar laminates. *Cem. Conrcr. Res.*, **33**, 15–19.
54. Phillips, T.A., Belden, J.B., Henderson, K.L.D., and Coats, J.R. (2002) Phytoremediation of pesticide-contaminated soil using a mixture and individual prairie grasses. 224th ACS National Meeting, Boston, Massachusetts , August 2002.
55. Ekpenyong, K.I., Arawo, J.D.E., Melaiye, A., Ekwenchi, M.M., and Abdullahi, H.A. (1995) Biogas production potential of unextracted, nutrient-rich elephant-grass lignocelluloses. *Fuel*, **74**, 1080–1082.
56. Stokke, D.D., Kuo, M., Curry, D.G., and Gieselman, H.H. (2001) Grassland flour/polyethylene composites. Sixth International Conference on Woodfiber–Plastic Composites, Madison, Wisconsin, pp. 43–53.
57. George, J., Bhagawanb, S.S., and Thomas, S. (1998) Effects of environment on the properties of low-density polyethylene composites reinforced with pineapple-leaf fibre. *Compos. Sci. Technol.*, **58**, 1471–1485.
58. Liu, W., Misra, M., Askelanda, P., Drzala, L.T., and Mohanty, A.K. (2005) 'Green' composites from soy based plastic and pineapple leaf fiber: fabrication and properties evaluation. *Polymer*, **46**, 2710–2721.
59. Chand, N., Tiwari, R.K., and Rohtangi, P.K. (1998) Bibliography resource structure properties of natural cellulosic fibres –an annotated bibliography. *J. Mater. Sci.*, **23**, 381–387.
60. Herrera-Franco, P.J. and Valadez-Gonzalez, A. (2005) A study of the mechanical properties of short natural-fiber reinforced composites. *Composites Part B*, **36**, 597–608.
61. Canche-Escamilla, G., Cauich-Cupula, J.I., Mendizabalb, E., Puigb, J.E., Vazquez-Torres, H.E., and Herrera-Francoa, P.J. (1999) Mechanical properties of acrylate-grafted henequen cellulose fibers and their application in composites. *Composites Part A*, **30**, 349–359.
62. Barnett, R. and Bonham, V.A. (2004) Cellulose microfibril angle in the cell wall of wood fibres. *J. Biol. Rev.*, **79**, 461–472.
63. Bledzki, A.K., Reihmane, S., and Gassang, J. (1998) Thermoplastics reinforced with wood fillers: a literature review. *Polym. Plast. Technol. Eng.*, **37** (4), 451–468.
64. Clapp, R.A. (2001) Policy review tree farming and forest conservation in chile: do replacement forests leave any originals behind? *Soc. Nat. Resour.*, **14**, 341–356.
65. Balis, J.S. (1977) Tree plantations as resources for renewable energy production. Presentation at the 1977 Winter Meeting American Society of Agricultural Engineers.
66. Bowyer, J. (2001) Environmental implications of wood production in intensively managed plantations. *Wood and Fiber Science*, **33**, 318–333.
67. Sedjo, R. (1999) The potential of high-yield plantation forestry for meeting timber needs. *New Forests*, **17**, 339–359.
68. Sedjo, R. and Botkin, D. (1997) Using forest plantations to spare national forests. *Environment*, **39**, 14–20.
69. Bhatia, C.L. (1984) Eucalyptus in India–its status and research needs. *Indian Forester*, **110**, 91–96.
70. Martin, B. (2003) in *Eucalyptus Plantations: Research, Management and Development* (eds R.-P. Wei and D. Xu), World Scientific, Singapore, pp. 3–18.
71. Kudus, K.A., Kimber, A.C., and Lapongan, J. (2006) A parametric model for the interval censored survival times of acacia mangium plantation in a spacing trial. *J. Appl. Stat.*, **33** (10), 1067–1074.
72. Myers, N. (1983) Tropical moist forest: over-exploited and under-utilized? *For. Ecol. Mamage.*, **6** (1), 59–79.
73. Myers, N. (1988) Tropical forests: much more than stocks of wood. *J. Trop. Ecol.*, **4**, 209–221.
74. Young, A. (1997) *Agroforestry for Soil Management*, CAB International, New York, p. 320.
75. Auclair, D. and Dupraz, C. (eds) (1999) *Agroforestry for Sustainable Land-Use*,

Kluwer Academic Publishers, Hardbound, p. 266.
76. Cornell, J.D. and Miller, M. (2007) Agroforestry, in *Encyclopedia of Earth* (ed. C.J. Cleveland), Island Press, Washington.
77. Encyclopaedia of Earth *www.eoearth.org/article/agroforestry* (accessed 2 April 2013).
78. Beetz, A. (2002) Agroforestry Overview, Appropriate Technology Transfer for Rural Areas, pp. 1–6.
79. Near.org *www.attra.neat.org/attra.pub/PDF/agrofor.pdf* (accessed 2 April 2013).
80. American Bamboo Socity *http://www.bamboo.org/abs/SpeciesSourceList.html* (accessed 2 April 2013).
81. American Bamboo Socity *http://www.bamboo.org/abs/BooksOnBamboo.html* (accessed 2 April 2013).
82. Suddell, B.C. and Evans, W.J. (2003) The increasing use and application of natural fibre composite materials within the automotive industry. Proceeding 7th International Conference on Woodfiber-Plastic Composites, Forest Products Society, Madison, Wisconsin.
83. Brouwer, W.D. Natural Fibre Composites in Structural Components: Alternative Applications for Sisal? Delft University, Buizerdlaan, *http://www.fao.org/docrep/004/y1873e/y1873e0a.htm* (accessed 2 April 2013).
84. Wambua, P., Ivens, J., and Verpoest, I. (2003) Natural fibres: can they replace glass in fibre reinforced plastics? *Compos. Sci. Technol.*, **63**, 1259–1264.
85. Staniforth, A.R. (1979) *Cereal Straw*, Clarendon Press, pp. 116–123.
86. Reddy, N. and Yang, Y. (2004) Structure and novel cellulose fiber from corn husk. *Polym. Preprints Amer. Chem. Soc., Div. Polym. Sci.*, **45** (2), 411.
87. Eichhorn, S.J., Baillie, C.A., Zafeipouls, N., Mwaikambo, L.Y., and Ansell, M.P. (2001) Current international research into cellulosic fibers and composites. *J. Mater Sci.*, **36**, 2107–2131.
88. Netravali, N. and Chabba, S. (2003) Composites get greener. *Mater. Today*, **6**, 22–29.
89. Geethamma, V.G., Mathew, K.T., Lakshminarayanan, R., and Thomas, S. (1998) Composites and short coir fibers and natural rubber: effect of chemical modification, loading and orientation of fibre. *Polymer*, **39**, 1483–1491.
90. Burger, H. *et al.* (1995) Use of natural fibers and environmental aspects. *Int. Polym. Sci. Technol.*, **22** (18), T/25–T/34.
91. Kaith, B.S., Singha, A.S., Kumar, S., and Misra, B.N. (2005) FAS-H2O2 initiated graft polymerization of methylmethacrylate onto flax and evaluation of some physical and chemical properties. *J. Polym. Mater.*, **22**, 425–432.
92. Tsukada, M., Islam, S., Arai, T., Boschi, A., and Freddi, G. (2005) Microwave irradiation technique to enhance protein fibre properties. *Autex Res. J.*, **5**, 40–48.
93. Kaith, B.S. and Kalia, S. (2008) Preparation of micro-wave radiation induced graft copolymers and their applications as reinforcing material in phenolic composites. *Polym. Compos.*, **29**, 791–797.
94. Kaith, B.S. and Kalia, S. (2008) Graft copolymerization of MMA onto flax under different reaction conditions: a comparative study. *Express Polym. Lett.*, **2**, 93–100.
95. Kalia, S., Kumar, A. and Kaith, B.S. (2011) Sunn hemp cellulose graft copolymers polyhydroxybutyrate composites: morphological and mechanical studies. *Adv. Mat. Lett.*, **2**, 17–25.
96. Shoda, M. and Sugano, Y. (2005) Recent advances in bacterial cellulose production. *Biotechnol. Bioprocess Eng.*, **10**, 1–8.
97. Pommet, M., Juntaro, J., Heng, J.Y.Y., Mantalaris, A., Lee, A.F., Wilson, K., Kalinka, G., Shaffer, M.S.P., and Bismarck, A. (2008) Surface modification of natural fibers using bacteria: depositing bacterial cellulose onto natural fibers to create hierarchical fiber reinforced nanocomposites. *Biomacromolecules*, **9**, 1643–1651.
98. Eichhorn, S.J., Dufresne, A., Aranguren, M., Marcovich, N.E., Capadona, J.R., Rowan, S.J., Weder,

C., Thielemans, W., Roman, M., Renneckar, S., Gindl, W., Veigel, S., Keckes, J., Yano, H., Abe, K., Nogi, M., Nakagaito, A.N., Mangalam, A., Simonsen, J., Benight, A.S., Bismarck, A., Berglund, L.A., and Peijs, T. (2010) Review: current international research into cellulose nanofibres and nanocomposites. *J. Mater. Sci.*, **45**, 1–33.

99. Iguchi, M., Yamanaka, S., and Budhiono, A. (2000) Bacterial cellulose-a masterpiece of nature arts. *J. Mater. Sci.*, **35**, 261–270.

100. Brown, E.E. and Laborie, M.P.G. (2007) Bioengineering bacterial cellulose/poly(ethylene oxide) nanocomposites. *Biomacromolecules*, **8**, 3074–3081.

101. Nakagaito, A.N. and Yano, H. (2005) Novel high-strength biocomposites based on microfibrillated cellulose having nano- order-unit web-like network structure. *Appl. Phys. A: Mater. Sci. Process.*, **80**, 155–159.

102. Gardner, D.J., Oporto, G.S., Mills, R., and Samir, M. (2008) Adhesion and surface issues in cellulose and nanocellulose. *J. Adhes. Sci. Technol.*, **22**, 545–567.

103. English, B., Chow, P., and Bajwa, D.S. (1997) Processing into composites, in *Paper and Composites from Agro-Based Resources* (eds R.M. Rowell *et al.*), CRC/Lewis Publishers, Boca Raton, FL.

104. Mo, X., Wang, D., and Sun, X.S. (2005) Straw-based biomass and biocomposites, in *Natural Fibers, Biopolymers, and Biocomposites* (eds A.K. Mohanty, M. Misra, and L.T. Drzal) Chapter 14, CRC Press, Boca Raton, FL.

105. Kozlowski, R. and Wladyka-Przbylak, M. (2004) in *Natural Fibers, Plastics and Composites* (eds F.T. Wallenberger and N. Weston), Kluwer Academic Publisher, New York, pp. 249–274.

106. Falk, R.H., Vos, D.J., Cramer, S.M., and English, B.W. (2001) Performance of fasteners in wood flour-thermoplastic composite panels. *For. Prod. J.*, **51**, 55–61.

107. Papadopoulos, A.N. and Hague, J.R.B. (2003) The potential for using Flax (Linum usitatissimum L.) shiv as a lingo-cellulosic raw material for particleboard. *Ind. Crops Prod.*, **17**, 143–147.

108. Kim, S., Kim, H.J., and Park, J.C. (2009) Application of recycled paper sludge and biomass materials in manufacture of green composite pallet. *Resour. Conserv. Recycl.*, **53**, 674–679.

109. Maloney, T.M. (1977) *Modern Particleboard and Dry-Process Fiberboard Manufacturing*, Miller Freeman Publications, San Francisco, CA, p. 688.

110. Taramian, A., Doosthoseini, K., Mirshokraii, S.A., and Faezipour, M. (2007) Particleboard manufacturing: an innovative way to recycle paper sludge. *Waste Manage.*, **27**, 1739–1746.

111. Kozlowski, R., Mieleniak, B., and Przepiera, A. (1994) A Plant residues as materials for particleboards. Proceedings of the 28th International Particleboard/Composite Materials Symposium, Washington State University, Pullman, Washington.

112. Maldas, D. and Kokta, B.V. (1991) Studies on the preparation and properties of particle boards made from bagasse and PVC: II. Influence of the addition of coupling agents. *Bioresour. Technol.*, **35**, 251–261.

113. Akgul, M. and Camlibel, O. (2008) Manufacture of medium density fiberboard (MDF) panels from rhododendron (R. ponticum L.) biomass. *Build. Environ.*, **43**, 438–443.

114. Hiziroglu, S., Jarusombuti, S., Bauchongkol, P., and Fueangvivat, V. (2008) Overlaying properties of fiberboard manufactured from bamboo and rice straw. *Ind. Crops Prod.*, **28**, 107–111.

115. Yousefi, H. (2009) Canola straw as a bio-waste resource for medium density fibreboard (MDF) manufacture. *Waste Manage.*, **29**, 2644–2648.

116. Akgul, M. and Tozluoglu, A. (2008) Utilizing peanut husk (Arachis hypogaea L.) in the manufacture of medium-density fibreboards. *Bioresour. Technol.*, **99**, 5590–5594.

117. Çavdar, A.D., Ertas, M., Kalaycıoglu, H., and Alma, M.H. (2010) Some properties of thin medium density

fiberboard panels treated with sunflower waste oil vapour. *Mater. Des.*, **31**, 2561–2567.

118. Food and Agriculture Organization of the United Nations (FAO) (1958) *Fiberboard and Particle Board Report of an International Consultation on Insulation Board, Hardboard and Particle Board*, Food and Agriculture Organization of the United Nations, Rome.

119. P.Ye, X., Julson, J., Kuo, M., Womac, A., and Myers, D. (2007) Properties of medium density fiberboards made from renewable biomass. *Bioresour. Technol.*, **98**, 1077–1084.

120. Mi, Y., Chen, X., and Guo, Q. (1997) Bamboo fiber-reinforced polypropylene composites: crystallization and interfacial morphology. *J. Appl. Polym. Sci.*, **64**, 1267–1273.

121. Liu, D., Zhong, T., Chang, P.R., Li, K., and Wuc, Q. (2010) Starch composites reinforced by bamboo cellulosic crystals. *Bioresour. Technol.*, **101**, 2529–2536.

122. Trujillo, E., Osorio, L., Van Vuure, A.W., and Ivens, J., and Verpoest, I. (2010) Characterization of polymer composite materials based on bamboo fibres. 14th European Conference on Composite Materials, Budapest, Hungary, June 7–10, 2010.

123. Tokoro, R., Vu, D.M., Okubo, K., Tanaka, T., Fujii, T., and Fujiura, T. (2008) How to improve mechanical properties of polylactic acid with bamboo fibers. *J. Mater. Sci.*, **43**, 775–787.

124. Avella, M., Buzarovska, A., Errico, M.E., Gentile, G., and Grozdanov, A. (2009) Eco-challenges of bio-based polymer composites. *Materials*, **2**, 911–925.

125. Cook, J.G. (1964) *Handbook of Textile Fibers*, Merrow Publishing Co. Ltd., Watford.

126. Kim, J.T. and Netravali, A.N. (2010) Effect of protein content in soy protein resins on their interfacial shear strength with ramie fibers. *J. Adhes. Sci. Technol.*, **24**, 203–215.

127. Li-Ping, H., Yong, T., and Lu-Lin, W. (2008) Study on ramie fiber reinforced polypropylene composites (RF-PP) and its mechanical properties. *Adv. Mater. Res.*, **41–42**, 313–316.

128. Mizuta, K., Ichihara, Y., Matsuoka, T., Hirayama, T., and Fujita, H. (2006) Mechanical properties of loosing natural fiber reinforced polypropylene, in *High Performance Structures and Materials III* (ed. C.A. Brebbia), WIT Press, Boston, MA.

129. Chen, D., Li, J., and Ren, J. (2010) Study on sound absorption property of ramie fiber reinforced poly(L-lactic acid) composites: morphology and properties. *Composites Part A*, **41**, 1012–1018.

130. Xu, H., Wang, L., Teng, C., and Yu, M. (2008) Biodegradable composites: ramie fiber reinforced PLLA-PCL composite prepared by in situ polymerization process. *Polym. Bull.*, **61**, 663–670.

131. Yu, T., Ren, J., Li, S., Yuan, H., and Li, Y. (2010) Effect of fiber surface-treatments on the properties of poly(lactic acid)/ramie composites. *Composites Part A*, **41**, 499–505.

132. Panigrahy, B.S., Rana, A., Panigrahi, S., and Chang, P. (2006) Overview of flax fiber reinforced thermoplastic composites. ASAE Annual Meeting, American Society of Agricultural and Biological Engineers, St. Joseph, Michigan.

133. Li, X., Panigrahi, S., and Tabil, L.G. (2009) A study on flax fiber-reinforced polyethylene biocomposites. *Appl. Eng. Agric.*, **25**, 525–531.

134. Wang, B., Panigrahi, S., Tabil, L., and Crerar, W. (2007) Pre-treatment of flax fibers for use in rotationally molded biocomposites. *J. Reinf. Plast. Compos.*, **26**, 447–463.

135. Van de Velde, K. and Kiekens, P. (2001) Influence of fiber surface characteristics on the flax/polypropylene interface. *J. Thermoplast. Compos. Mater.*, **14**, 244–260.

136. Bledzki, A.K., Mamun, A.A., Lucka-Gabor, M., and Gutowski, V.S. (2008) The effects of acetylation on properties of flax fibre and its polypropylene composites. *Express Polym. Lett.*, **2**, 413–422.

137. John, M.J. and Anandjiwala, R.D. (2009) Chemical modification of flax

reinforced polypropylene composites. *Composites Part A.*, **40**, 442–448.

138. Kaith, B.S., Singha, A.S., Kumar, S., and Kalia, S. (2008) Mechanical properties of polystyrene composites reinforced with chemically treated flax fiber were investigated. Mercerization of flax fiber improves the mechanical properties of polystyrene composites. *Int. J. Polym. Mater.*, **57**, 54–72.

139. Sala, G. and Cutolo, D. (1996) Heater chamber winding of thermoplastic powder impregnated composites: part 1. Technology and basic thermochemical aspects. *Composites Part A*, **27**, 387–392.

140. Svensson, N. and Shishoo, R. (1996) Fabrication and mechanical response of commingled GF/PET composites. *Polym. Compos.*, **19**, 360–369.

141. Gu, H. and Liyan, L. (2008) Research on properties of thermoplastic composites reinforced by flax fabrics. *Mater. Des.*, **29**, 1075–1079.

142. Li, Y., Mai, Y.W., and Ye, L. (2000) Sisal fibre and its composites: a review of recent developments. *Compos. Sci. Technol.*, **60**, 2037–2055.

143. Joseph, K., Thomas, S., Pavithran, C., and Brahmakumar, M. (1993) Tensile properties of short sisal fibre-reinforced polyethylene composites. *J. Appl. Polym. Sci.*, **47**, 1731–1739.

144. Mohanty, S., Nayak, S.K., Verma, S.K., and Tripathy, S.S. (2004) Effect of MAPP as coupling agent on the performance of sisal–PP composites. *J. Reinf. Plast. Compos.*, **23**, 2047–2063.

145. Joseph, P.V., Joseph, K., and Thomas, S. (1999) Effect of processing variables on the mechanical properties of sisal-fiber-reinforced polypropylene composites. *Compos. Sci. Technol.*, **59**, 1625–1640.

146. Fung, K.L., Li, R.K.Y., and Tjong, S.C. (2002) Interface modification on the properties of sisal fibre reinforced polypropylene composites. *J. Appl. Polym. Sci.*, **85**, 169–176.

147. Tjong, S.C., Xu, Y., and Meng, Y.Z. (1999) Composites based on maleated polypropylene and methyl cellulosic fiber: Mechanical and thermal properties. *J. Appl. Polym. Sci.*, **72**, 1647–1653.

148. Li, T.Q., Ng, C.N., and Li, R.K.Y. (2001) Impact behavior of sawdust/recycled-PP composites. *J. Appl. Polym. Sci.*, **81**, 1420–1428.

149. Mukhopadhyay, S. and Srikanta, R. (2008) Effect of ageing of sisal fibres on properties of sisal –polypropylene composites. *Polym. Degrad. Stab.*, **93**, 2048–2051.

150. Joseph, K., Dias, R., Filho, T., James, B., Thomas, S., and Hecker de Carvalho, L. (1999) A review on sisal fiber reinforced polymer composites. *Rev. Bras. Eng. Agríc. Ambient. Campina Grande*, **3**, 367–379.

151. Karmaker, A.C. and Youngquist, J.A. (1996) Injection moulding of polypropylene reinforced with short jute fibers. *J. Appl. Polym. Sci.*, **62**, 1147–1151.

152. Gassan, J. and Bledzki, A.K. (2000) Possibilities to improve the properties of natural fiber reinforced plastics by fiber modification–jute polypropylene composites. *Appl. Compos. Mater.*, **7**, 373–385.

153. Liu, X.Y. and Dai, G.C. (2007) Surface modification and micromechanical properties of jute fiber mat reinforced polypropylene composites. *Express Polym. Lett.*, **1**, 299–307.

154. Ray, D., Sarkar, B.K., Rana, A.K., and Bose, N.R. (2001) Effect of alkali treated jute fibers on composite properties. *Bull. Mater. Sci.*, **24**, 129–135.

155. Hong, C.K., Hwang, I., Kim, N., Park, D.H., Hwang, B.S., and Nah, C. (2008) Mechanical properties of silanized jute–polypropylene composites. *J. Ind. Eng. Chem.*, **14**, 71–76.

156. Haydar, U.Z., Khan, R.A., Khan, M.A., Khan, A.H., and Hossain, M.A. (2009) Effect of gamma radiation on the performance of jute fabrics-reinforced polypropylene composites. *Radiat. Phys. Chem.*, **78**, 986–993.

157. Doan, T.T.L., Gao, S.L., and Mader, E. (2006) Jute/polypropylene composites I. Effect of matrix modification. *Compos. Sci. Technol.*, **66**, 952–963.

158. Mohanty, A.K., Khan, M.A., and Hinrichsen, G. (2000) Influence of

chemical surface modification on the properties of biodegradable jute fabrics–polyester amide composites. *Composites Part A*, **31**, 143–150.

159. Government of Manitoba (2000) Manitoba Industrial Hemp Association Market Opportunity for Industrial Hemp Fibre-based Products, December 2000, *http://www.gov.mb.ca/agriculture/crops/hemp/bko07s01.html* (accessed 2 April 2013).

160. Wielage, B., Lampke, T., Utschick, H., and Soergel, F. (2003) Processing of natural fibre reinforced polymers and the resulting dynamic-mechanical properties. *J. Mater. Process Technol.*, **139**, 140–146.

161. Keller, A. (2003) Compounding and mechanical properties of biodegradable hemp fibre composites. *Compos. Sci. Technol.*, **63**, 1307–1316.

162. Vilaseca, F., Lopez, A., Llauro, X., Pelach, M.A., and Mutje, P. (2004) Hemp strands as reinforcement of polystyrene composites. *Chem. Eng. Res. Des.*, **82**, 1425–1431.

163. Brydson, J.A. (1975) *Plastic Materials*, 3rd edn Chapter 11, Newnes Butterworths, London.

164. Mutje, P., Lopez, A., Vallejos, M.E., Lopez, J.P., and Vilaseca, F. (2007) Full exploitation of cannabis sativa as reinforcement/filler of thermoplastic composite materials. *Composites Part A*, **38**, 369–377.

165. Tajvidi, M., Motie, N., Rassam, G., Falk, R.H., and Felton, C. (2009) Mechanical performance of hemp fiber polypropylene composites at different operating temperatures. *J. Reinf. Plast. Compos.*, **29**, 664–674.

166. Mutje, P., Girones, J., Lopez, A., Llop, M.F., and Vilaseca, F. (2006) Hemp strands: PP composites by injection molding: effect of low cost physico-chemical treatments. *J. Reinf. Plast. Compos.*, **25**, 313–327.

167. Beckermann, G.W. and Pickering, K.L. (2008) Engineering and evaluation of hemp fibre reinforced polypropylene composites: fibre treatment and matrix modification. *Composites Part A*, **39**, 979–988.

168. Kaith, B.S., Jindal, R., Jana, A.K., and Maiti, M. (2010) Development of corn starch based green composites reinforced with saccharum spontaneum L fiber and graft copolymers–evaluation of thermal, physico-chemical and mechanical properties. *Bioresour. Technol.*, **101**, 6843–6851.

169. Singha, A.S., Rana, R.K., and Rana, A. (2010) Natural fiber reinforced polystyrene matrix based composites. *Adv. Mater. Res.*, **123–125**, 1175–1178.

170. Bledzki, A.K., Reihmane, S., and Gassan, J. (1996) Properties and modification methods for vegetable fibers for natural fiber composites. *J. Appl. Polym. Sci.*, **59**, 1329–1336.

171. Felix, J.M. and Gatenholm, P. (1991) The nature of adhesion in composites of modified cellulose fibers and polypropylene. *J. Appl. Polym. Sci.*, **42**, 609–620.

172. Klemm, D., Schumann, D., Udhardt, U., and Marsch, S. (2001) Bacterial synthesized cellulose – artificial blood vessels for microsurgery. *Prog. Polym. Sci.*, **26**, 1561–1603.

173. Chawla, P.R., Bajaj, I.B., Survase, S.A., and Singhal, R.S. (2009) Microbial cellulose: fermentative production and applications. *Food Technol. Biotechnol.*, **47**, 107–124.

174. Pecoraro, E., Manzani, D., Messaddeq, Y., and Ribeiro, S. (2008) Bacterial cellulose from glucanacetobacter xylinus: preparation, properties and applications, in *Monomers, Polymers and Composites from Renewable Resources* (eds M.N. Belgacem and A. Gandini), Amsterdam, Elsevier.

175. Gindl, W. and Keckes, J. (2004) Tensile properties of cellulose acetate butyrate composites reinforced with bacterial cellulose. *Compos. Sci. Technol.*, **64**, 2407–2413.

176. Martins, I.M.G., Magina, S.P., Oliveira, L., Freire, C.S.R., Silvestre, A.J.D., Neto, C.P., and Gandini, A. (2009) New biocomposites based on thermoplastic starch and bacterial cellulose. *Compos. Sci. Technol.*, **69**, 2163–2168.

177. Woehl, M.A., Canestraro, C.D., Mikowski, A., Sierakowski, M.R., Ramos, L.P., and Wypych, F. (2010)

Bionanocomposites of thermoplastic starch reinforced with bacterial cellulose nanofibres: effect of enzymatic treatment on mechanical properties. *Carbohydr. Polym.*, **80**, 866–873.

178. Lee, K.Y., Blaker, J.J., and Bismarck, A. (2009) Surface functionalisation of bacterial cellulose as the route to produce green polylactide nanocomposites with improved properties. *Compos. Sci. Technol.*, **69**, 2724–2733.

179. Wan, Y.Z., Luo, H., He, F., Liang, H., Huang, Y., and Li, X.L. (2009) Mechanical, moisture absorption, and biodegradation behaviours of bacterial cellulose fibre-reinforced starch biocomposites. *Compos. Sci. Technol.*, **69**, 1212–1217.

180. Njuguna, J., Pena, I., Zhu, H. *et al.* (2009) Opportunities and environmental health challenges facing integration of polymer nanocomposites: technologies for automotive applications. *Int. J. Polym. Technol.*, **1**, 113–122.

181. Automotive Industries (2000) *Daimler-Chrysler "Goes Natural" for Large Body Panel*, DaimlerChrysler, p. 9.

182. Pervaiz, M. and Sain, M.M. (2003) Sheet-molded polyolefin natural fiber composites for automotive applications. *Macromol. Mater. Eng.*, **288**, 553–557.

183. Suddell, B.C., Evans, W.J., Mohanty, A.K., Misra, M., and Drzal, L.T. (2005) Natural fiber composites in automotive applications, in *Natural Fibers, Biopolymers and Biocomposites* (eds A.K. Mohanty, M. Misra, and L.T. Drzal) Chapter 7, CRC Press, Boca Raton, FL.

184. Bledzki, A.K., Faruk, O., and Sperher, V.E. (2006) Cars from bio-fibres. *Macromol. Mater. Eng.*, **291**, 449–457.

185. Diener, J. and Siehler, U. (1999) Ökologischer vergleich von NMT- und GMT-bauteilen. *Angew. Makromol. Chem.*, **272**, 1–1.

186. Jolliet, O. (2001) Life cycle assessment of biofibres replacing glass fibres as reinforcement in plastics. *Resour. Conserv. Recycl.*, **33**, 267–287.

8
Biofiber-Reinforced Natural Rubber Composites

Parambath Madhom Sreekumar, Preetha Gopalakrishnan, and Jean Marc Saiter

8.1
Introduction

Composites are one of the most advanced and adaptable engineering materials known to man. They are heterogeneous in nature, and consist of filler and matrix. Composites possess exceptional mechanical properties, which are not attainable by individual components acting alone. At present, composites based on natural fibers as reinforcement are receiving wide interest because of their specific advantages such as good mechanical performance in combination with better eco-performance at lower price and renewability. Recent reports indicate that plant-based natural fibers such as henequen, sisal, coir, jute, palm, bamboo, and wood, as well as several waste cellulosic products such as shell flour, wood flour, and pulp can be used as the reinforcing agents for different thermosetting and thermoplastic polymers as well as in elastomers. Moreover, natural fibers can, to some extent, replace the more expensive and nonrenewable synthetic fibers.

8.2
Natural Rubber (NR)

Natural rubber (NR), the most fascinating material known to mankind, is extracted from the latex of *Hevea braziliensis*. NR is a linear, long-chain polymer chemically known as *cis-1,4 polyisoprene*. Like other high polymers, it is made up of molecules of different sizes with molecular weight ranging from 30 000 to about 10 million. Polyisoprene exists naturally in the form of two stereoisomers, namely *cis*-1,4-polyisoprene and *trans*-1,4-polyisoprene (Figure 8.1).

Owing to the high structural regularity of *cis*-1,4 polyisoprene, NR tends to crystallize when stored at low temperatures or when stretched. NR has an intrinsic density of about 0.92 g cm^{-3}. Raw NR contains about 93% rubber hydrocarbons. The rest consists of inorganic salts and organic materials some of which are natural antioxidants and accelerators (Table 8.1).

Polymer Composite: Volume 3, First Edition.
Edited by Sabu Thomas, Kuruvilla Joseph, S. K. Malhotra, Koichi Goda and M. S. Sreekala.

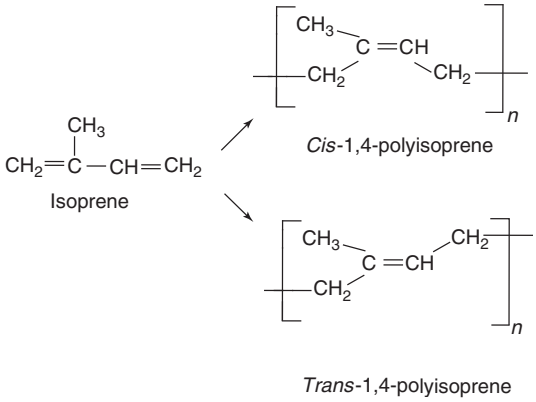

Figure 8.1 Structure of natural rubber.

Table 8.1 Typical analysis of natural rubber.

Constituents	Percentage
Rubber hydrocarbon	93.3
Protein	2.8
Acetone extract	2.9
Moisture	0.6
Ash	0.4

NR has excellent abrasion resistance, especially under mild abrasive conditions. It has high resilience, with values exceeding 90% in well-cured gum vulcanizates. Hence it can be used in many applications such as heavy vehicle tires where cyclic stressing is involved. Compression set and related processes such as creep are lower in NR than in synthetic polyisoprene. In addition to this, NR has excellent tensile and tear properties, good green strength, and building tack. NR is not resistant to oxidation, to ozone weathering, to many solvents, mainly due to its unsaturated chain structure and non polarity. At present, a variety of synthetic rubbers such as acrylonitrile butadiene rubber (NBR), styrene butadiene rubber (SBR), butyl rubber (IIR), butadiene rubber, ethylene propylene diene rubber, silicon rubber, and chloroprene rubber are produced for various applications.

8.3 Biofibers

Biofibers are among the world's renewable materials that contribute significantly to the world's economy. They can be classified as vegetable, animal, and mineral fibers as shown in Figure 8.2.

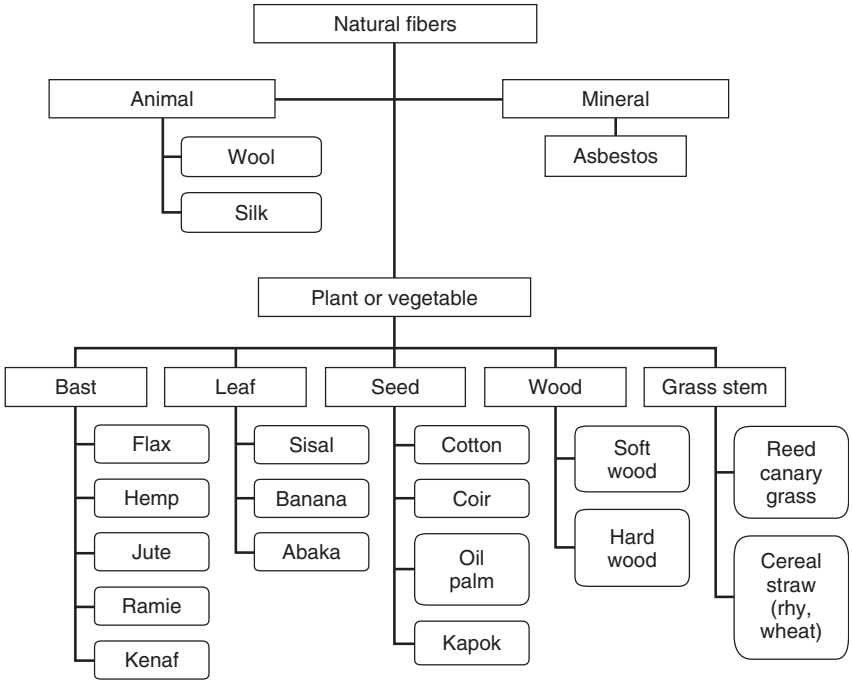

Figure 8.2 Classification of biofibers based on origin.

Natural fibers are basically rigid and possess both crystalline and amorphous regions. They are composed of cellulose, hemicellulose, lignin, waxes, and some water-soluble compounds, where cellulose, hemicellulose, and lignin are the major constituents. The hydrogen bonds and other linkages provide the necessary strength to the fibers. Plant fibers consist of bundles of elongated thick-walled cells. The cell walls are formed from oriented reinforcing semicrystalline cellulose microfibrils embedded in hemicelluloses–lignin matrices of varying composition. Such microfibrils have typically a diameter of about 10–30 nm, each composed of 30–200 cellulose molecules in extended-chain conformation, providing mechanical strength to the fiber. The diameters of these fibers can also play significant role in the mechanical properties [1, 2].

The chemical composition and structure are influenced by the climatic conditions where rubber grows, the age of the plant, and the digestion process used for fiber separation. The microfibrillar angle, cellulose, and moisture content determine the mechanical properties of the natural fibers. They can be used as reinforcing agents for many polymers owing to their relative high strength, stiffness, and low density. Table 8.2 displays the mechanical properties of different natural fibers as compared to various synthetic fibers.

Table 8.2 Comparison of various properties of natural fibers with synthetic fibers [3].

Fiber	Density ($g\ cm^{-3}$)	Elongation (%)	Tensile strength (MPa)	Young's modulus (GPa)
Cotton	1.5–1.6	7.0–8.0	287–597	5.5–12.6
Jute	1.3	1.5–1.8	393–773	26.5
Flax	1.5	2.7–3.2	345–1035	27.6
Hemp	—	1.6	690	—
Ramie	—	3.6–3.8	400–938	61.4–128
Sisal	1.5	2.0–2.5	511–635	9.4–22.0
Coir	1.2	30.0	175	4.0–6.0
Viscose	—	11.4	593	11.0
Softwood kraft	1.5	—	1000	40.0
OPEFB	1.4	14	248	2
E-glass	2.5	2.5	2000–3500	70.0
S-glass	2.5	2.8	4570	86.0
Aramid (normal)	1.4	3.3–3.7	3000–3150	63.0–67.0
Carbon (standard)	1.4	1.4–1.8	4000	230.0–240.0

OPEFB, oil palm empty fruit bunch.

8.4 Processing

Short fibers can be easily incorporated into rubber during compounding. They provide high green strength and dimensional stability during fabrication. Almost all standard rubber-processing operations such as extrusion, calendaring, compression molding, injection molding, and transfer molding can be used for the fabrication of composites.

8.5 Biofiber-Reinforced Rubber Composites

Elastomers are known for their rubberlike elasticity, high flexibility, and abrasion resistance; however their low strength and stiffness restricts these materials in many applications. Short fibers can be used to strengthen these elastomers, which leads to the formation of a new class of materials known as *short fiber-reinforced elastomeric composites*. The main attraction of these materials is they possess the strength and stiffness of the fibers and the elasticity of the matrix. They are easily processable, have high green strength, and possess enormous possibilities in product design. According to O'Connor [4], the limitations of short fibers in rubber-compounding applications are the difficulties in achieving uniform dispersion in the matrix, fiber breakage during processing, and adhesion with the rubber matrix. Hence researchers are mainly concentrating on the effect of fiber length, fiber

Table 8.3 Vulcanization characteristics of PALF–NR composites with various fiber loadings [8].

Concentration of untreated PALF (phr)	Properties			
	Scorch time (min)	Cure time (min)	Minimum torque (dN m)	Maximum torque (dN m)
0	7.21	13.48	2.5	20.7
10	4.46	11.53	2.1	23.8
20	4.32	11.24	1.1	21.63
30	4.06	9.06	1.1	24.3
40	3.48	11.02	2.3	32.90

orientation, fiber loading, type of bonding agent, and fiber–matrix interaction on the properties of composites, which include mechanical properties, viscoelastic properties, rheological behavior, thermal aging, γ-irradiation, and ozone resistance.

8.5.1 Cure Characteristics

Scorch time and cure time (t_{90}) are the measures of time at which vulcanization begins and when it reaches 90% of complete cure. Maximum torque is a measure of cross-link density and stiffness in the rubber, while the minimum torque is a measure of initial viscosity of rubber compounds. Generally, when biofibers are incorporated into rubber, initially the torque decreases, then increases, and finally levels off. The softening of the rubber matrix causes an initial decrease in torque to a minimum value while the cross-linking of rubber increases the torque values. The leveling off is an indication of the completion of curing. In composites, the maximum torque increases as a function of fiber concentration and fiber length [5, 6]. For example, in the isora–NR composites, Lovely and Joseph [7] reported that maximum torque is for the composites having a fiber length of 10 mm due to the entanglement and breakage during mixing. Lopattananon *et al.* [8] showed that the processing parameters of the short pineapple leaf fiber (PALF)-filled NR composites are independent of fiber loading, but the maximum torque increases with increase in the concentration of fibers (Table 8.3).

Moreover, for the fiber-filled composites, the scorch, and cure time is low when compared to those of an unfilled one because of the increase in the mixing time [8, 9]. Ismail *et al.* [10] investigated the particle size on the processing parameters of the oil palm wood flour (OPWF)/NR composites. They found a decrease in the scorch time with increase of OPWF content. At any filler loading, OPWF with larger particle size shows shorter torque value and scorch time. The cure enhancement for these composites is attributed to the filler-related parameters such as surface area, surface reactivity, particle size, and moisture content. Comparison of the cure

characteristics of rice husk ash (RHA)-filled NR composites to that of silica and carbon black-filled NR were conducted by Arayapranee *et al*. [11]. The increase in the loading of carbon black and RHA slightly decreased the optimum curing time of the composites. However, at a similar filler loading, carbon black-filled NR exhibited the shortest value for t_{90} compared to RHA-filled NR composites. The lowest value for Mooney viscosity of RHA–NR also indicates that it could be processed more easily than the others.

The addition of a bonding agent and fiber surface modification can affect the cure characteristics of the composites. In the bamboo–NR composites, Ismail *et al*. [12] indicated that at constant fiber loading, the scorch and cure times of composites with a bonding agent are lower than those of composites without bonding agent. The addition of a bonding agent increased the Mooney viscosity owing to the increased stiffness of the composites. Ismail *et al*. [9] reported that at similar fiber loading of silane-treated oil palm–NR composites, the scorch time and cure time are shorter than for the untreated composite. Geethamma *et al*. [13] showed that fiber modifications such as acetylation and γ-ray irradiation can also affect the melt viscosity, flow behavior index, and extrudate deformation of the composites with shear rate.

8.5.2 Mechanical Properties

The degree and type of adhesion can be measured by using micromechanical or spectroscopic methods. The main parameters affecting the performance of a fiber-reinforced rubber composite are fiber concentration, fiber aspect ratio, direction and extent of fiber orientation, degree of fiber dispersion, rubber matrix adhesion to the fiber, and void content.

8.5.2.1 Effect of Fiber Length

In the composites, extent of stress transfer varies on the basis of fiber length and the fiber–matrix interaction. Hence it is essential to conserve fiber length as much as possible during rubber compounding. At a critical fiber length, the load transmittance from the matrix to the fiber is at a maximum. If critical fiber length is greater than the length of the fiber, the stressed fiber debonds from the matrix and the composite fails at a lower load. To study the effect of aspect ratio of fiber on the mechanical properties of composites, Lovely and Joseph [7, 14] fabricated a series of short isora fiber–NR composites having fiber length 6, 10, and 14 mm at 15 phr (parts per hundred resin) loading. The details of the mechanical properties obtained for these composites are given in Table 8.4.

Composites having fiber length of 10 mm with bonding agent (resorcinol–formaldehyde resin) showed maximum mechanical properties compared to all other composites. Similarly, in oil palm–NR composites Joseph *et al*. [15] indicated that the mechanical properties will depend upon the fiber length. In the case of sisal–oil palm hybrid NR composites, all mechanical properties were at a maximum when the length of the sisal and oil palm fibers were 10 and 6 mm, respectively [5].

Table 8.4 Mechanical properties of vulcanizates with various fiber lengths [7].

Property	Orientation	Gum	L_1	L_2	L_3
Tensile modulus (300% *E*; MPa)	L	23(0.28)	2.71(1.18)	2.95(0.55)	2.80(1.05)
	T	23(0.22)	2.30(0.95)	2.40(0.73)	2.30(0.91)
Tensile strength (MPa)	L	25.9(0.48)	14.0(1.02)	16.2(0.87)	15.9(0.90)
	T	25.0(0.39)	12.1(0.98)	13.8(0.97)	14.0(0.95)
Elongation break (%)	L	1050(0.29)	700(1.15)	625(0.45)	695(0.77)
	T	1045(0.31)	725(1.06)	650(0.88)	715(1.11)
Tear strength (kN m^{-1})	L	35.1(0.42)	37.5(0.92)	42.0(0.65)	42.5(0.61)

L, longitudinal; T, transverse; Mixes L_1, L_2, and L_3 contained fibers 6, 10, and 14 mm in length before mixing.

The breakage of fiber during the processing increases the difficulties in controlling its length and aspect ratio in NR. The extent of fiber breakage depends mainly on the type of fiber, initial aspect ratio, and the magnitude of stress and strain experienced by the fibers during processing. This breakage of fibers during mixing can be indicated by a fiber length distribution curve. The distribution of fiber lengths can be represented in terms of moments of the distribution. The number- and weight-average fiber lengths can be defined as

$$L_n = \frac{\sum N_i \; L_i}{\sum N_i} \tag{8.1}$$

$$L_w = \frac{\sum N_i \; L_i^2}{\sum N_i \; L_i} \tag{8.2}$$

where L_n is the number-average fiber length, L_w is the weight-average fiber length, and N_i the number of fibers with length L_i. The value of L_w/L_n, the polydispersity index, can be taken as a measure of the fiber length distribution. Jacob *et al.* [5] showed that after mixing, the breaking of both sisal and oil palm fibers was low. As both fibers are lignocellulosic, they undergo bending and curling rather than breaking during milling.

8.5.2.2 Effect of Fiber Orientation

Similarly to the aspect ratio, fiber orientation has a greater influence on the properties of composites. During processing, the fibers will tend to orient along the flow direction, which results in variation of the mechanical properties in different directions. The extent of fiber orientation in short fiber–NR composites can be measured using the solvent-swelling method [8]. In this test, the swelling of the matrix containing preferred aligned fibers is anisotropic, leading to the progressive increase in swelling upon increasing the angle (θ) relative to fiber orientation and

can be expressed as follows:

$$a_\theta^2 = (a_T^2 - a_L^2)\ \sin^2\theta + a_L^2 \tag{8.3}$$

where a_θ, a_L, and a_T are dimensional swelling ratios in the angle (θ), longitudinal, and transverse directions, respectively. For all fiber-filled samples, the increase in value of θ causes an increase in swelling and the high extent of swelling is found at an angle of 90°. The swelling of NR matrix is isotropic in the absence of fibers. As the fiber content increases at any fixed angle, the swelling of NR obviously becomes lesser. In the case of PALF–NR composites [8] the maximum preferred orientation was obtained for composites having 20 phr fibers. At lower loading, the movement of fiber occurs in any direction in the mold owing to the action of shear flow during compression molding, which results in poor fiber alignment. For higher fiber loading (i.e., 30 and 40 phr), agglomeration of fibers might occur, leading to a lower level of alignment than that of 20 phr fiber loading. From the green strength measurement, the extent of fiber orientation in the coir–NR composite was calculated by Geethamma *et al*. [16] and was high for the composite having 40 phr fibers. The rate of relaxation of the longitudinally oriented coir fiber–NR composites was lower than that of the transverse composites because of the decreased plastic flow of the former [17]. A similar trend was observed for the tensile strength by Jacob *et al*. [5] in sisal–oil palm hybrid NR composites. This is because in the longitudinal direction, the fibers were oriented in the direction of the applied force, and in the transverse direction, the fibers were aligned in the perpendicular direction. In the latter case, the fiber–rubber interface had only a small role in the stress transfer, and the majority of relaxation was due to the rubber molecules alone. However, in the longitudinal fiber-reinforced composite, the relaxation was a combined effect of the rubber molecules and the fiber–rubber interface. As a result, the increase in entropy was reduced; hence, the stress relaxation rate was lower for the longitudinal fiber-reinforced composites.

8.5.2.3 **Effect of Fiber Loading**

In NR, poor fiber dispersion will lead to decrease the reinforcing effect. In addition, the strength of the bundle may be low due to poor adhesion. Both these factors will cause a reduction in the properties of composites. Generally, in the case of biofiber–NR composites the tensile strength initially drops to a certain amount of fiber and then increases. There is a minimum volume of fiber above which the fiber reinforces the matrix. This critical volume will depend upon the nature of the fiber and the matrix, fiber aspect ratio, and fiber–matrix interfacial adhesion. At lower fiber concentrations, the fiber acts as a flaw in NR. The matrix is not restrained by enough fibers, causing highly localized strains in the matrix at low stress. As a result, the bond between fiber and rubber breaks, leaving the matrix diluted by nonreinforcing debonded fibers. As the fiber concentration increases, the stress is more evenly distributed and the strength of the composite increases. The incorporation of fiber into rubber matrix increases the hardness of the composite, which is related to strength and toughness. The same trend has been observed in PALF–NR composites (Figure 8.3) [8].

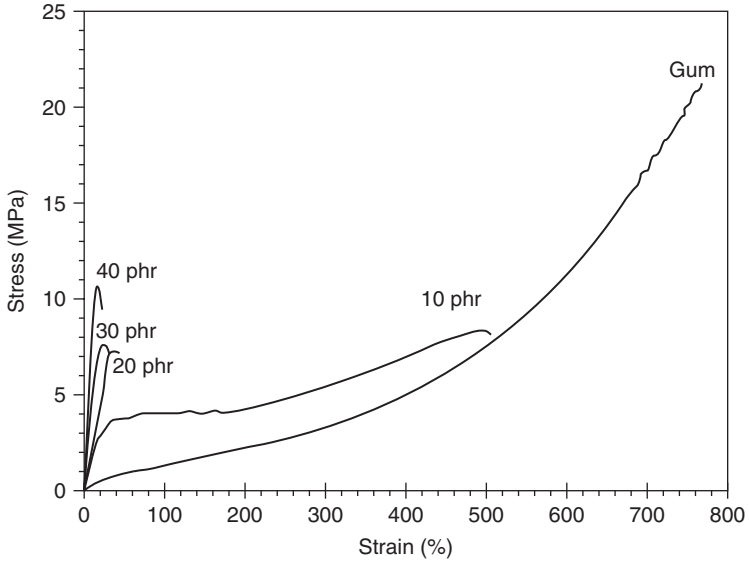

Figure 8.3 Longitudinal forces–extension curve of PALF–NR composites with various fiber loading [8].

The reinforcing effect of coir in NR matrix has been extensively studied by Geethamma *et al.* [17]. Upon incorporation of coir fiber, the tensile strength decreased sharply with increase in fiber loading up to 30 phr and then showed a slight increase for composites containing 40 and 60 phr fiber loading. In the case of kenaf–NR composites, Ismail *et al.* [6] found a decreasing trend in the mechanical properties when the fiber loading increased from 0 to 40 phr. El Sabbagh *et al.* [19] studied the physicomechanical properties of NR vulcanizates loaded with kenaf fibers. An increase in the rheometric and mechanical properties was observed. The fiber-loaded composites also possessed good thermal stability and swelling resistance. Details of the work conducted by several groups on the physical properties of biofiber–NR composites are given in Table 8.5.

Another interesting area in the biofiber–NR composites is that of hybrid composites. The material obtained by the incorporation of two or more types of fibers within a single matrix is known as a *hybrid composite*. The behavior of hybrid composites is the weighted sum of the individual components in which there is a more favorable balance between the inherent advantages and disadvantages. The mechanical properties of biofiber–NR hybrid composites have been well documented by Jacob et al. [33–35]. Increase in the concentration of fibers resulted in the reduction of tensile strength and tear strength, but increased the modulus of composites. In addition, the treatment of both sisal and oil palm fibers resulted in an increase of tensile strength and modulus. For the partial replacement of silica in rubber composites, microcrystalline cellulose (MCC) can also be added to the NR matrix [36]. This significantly reduced the energy required for dispersion of fillers in rubber matrix and lowered the internal temperature during the compounding.

Table 8.5 Physical properties of biofiber–NR composites.

Composites	Measurements	Conclusions	References
Rice husk–NR	Mechanical properties	Resulted in improved hardness but decreased tensile strength and tear strength. Better resilience property than that of silica and carbon black.	[11]
Coir–NR	Stress relaxation behavior	Rate of relaxation was high for the NR compound, and decreased when fiber loading increased from 30 to 60 phr.	[17]
Oil palm–wood flour–NR	Tensile properties tear strength elongation at break hardness	Increasing OPWF loading in NR resulted in the reduction of tensile strength, tear strength, and elongation at break while there was an increase in the tensile modulus and hardness.	[20]
Sisal fiber–NR	Mechanical properties	Tensile strength decreased up to 17.5 vol% loading and then increased. The tear strength and modulus values showed a consistent increase.	[21]
Oil palm–NR	Mechanical properties	Increase in the oil palm fiber content resulted in the reduction of tensile strength and tear strength, while there was an increase in modulus and hardness.	[22]
Oil palm–wood flour–NR	Fatigue and hysteresis behavior	Stress at any strain decreased with increase in fiber loading. Thermal aging reduced the fatigue life and increased the hysteresis of the composites.	[23]
MHR–NR	Mechanical properties	Except for abrasion resistance, MHA-filled vulcanizates with 20 phr exhibited physical properties not much inferior to commercial carbon black or silica-filled vulcanizates.	[24]
Oil palm–ENR	Mechanical properties	Increasing OPWF content in ENR resulted in the reduction of tensile strength and elongation at break but increased tensile modulus, tear strength, and hardness. Smaller sized OPWF-filled composites showed higher tensile strength, tensile modulus, and tear strength.	[10]

Table 8.5 (*Continued*)

Composites	Measurements	Conclusions	References
Cocoa pod husks, rubber-seed shell–NR	Tensile properties, hardness, abrasion resistance, flex fatigue, and compression set	Composites containing up to 40 wt% of the raw agricultural waste products and more than 60 wt% of the carbonized waste products gave comparable physicomechanical properties with compound obtained with N330 carbon black.	[25]
RHA–NR	Mechanical properties	RHA having low and high carbon contents, provided inferior mechanical properties compared to those of composites filled with silica and carbon black.	[26]
RHA–NR	Dynamic mechanical analysis	The better wetting and dispersion property of RHA was not enough to cause an enhancement in the dynamic mechanical performance.	[27]
Bamboo fiber–NR	Mechanical properties	Tensile modulus and hardness of composites increase with increasing filler loading and in the presence of bonding agents.	[12]
Sisal–coir–NR	Mechanical properties	At 30 phr fiber loading, the composites exhibited higher tensile properties.	[28]
Silk fiber–NR	Mechanical properties	Introduction of silk fibers into NR vulcanizates increases the hardness, heat buildup, compression set, tear resistance, and decreases resilience, and elongation at break.	[29]
Grass fiber–NR	Mechanical properties	Increase in the amount of fibers reduced the tensile strength and increased the modulus.	[30]
Newsprint fiber–NR–NBR	Mechanical and electrical properties	Addition of treated newsprint fiber waste at a concentration of 40 phr could lead to an end product characterized by good electrical and mechanical properties.	[31]
Acaı´ fiber–NR	Mechanical and thermal properties	Composites with 5% of fibers show the best values for mechanical properties. Addition of the fibers did not influence its thermal stability.	[32]

MHR, milled rice husk ash; ENR, epoxidized natural rubber; RHA, rice husk ash.

Moreover Mooney viscosity, apparent shear stress, and apparent shear viscosity of the rubber composites reduced, which facilitated the manufacturing process of the rubber composites.

8.5.3 Viscoelastic Properties

Rubber products generally undergo dynamic stress during service. Therefore their behavior in dynamic load application is highly important. Dynamic mechanical analysis (DMA) is a very useful technique to investigate the viscoelasticity behavior of a composite as it can cover a wide range of temperatures and frequencies, which is not possible with other techniques. The viscoelastic properties of composites depends on the fiber content, fiber–matrix interphase, presence of additives, the compatabilizer, fiber orientation, and the mode of testing of the composites. It gives us information regarding the stiffness, load-bearing capability, amount of energy that can be dissipated as heat, and the damping nature of the material.

Several studies have been conducted about the viscoelastic behavior of natural fiber-reinforced rubber composites [37–43]. For example, in the coir–NR composites, Geethamma *et al.* [37] observed an increase in loss modulus and damping factor, which indicates lower heat dissipation in the gum. The composites with poor interfacial bonding tend to dissipate more energy than those with good interfacial bonding. For sisal–oil palm hybrid fiber-reinforced NR composites, Jacob *et al.* [39] showed that the storage modulus value will increase with increase in the fiber loading. Moreover, to investigate the effect of fiber surface modification, these fibers were subjected to silanization reactions with various silanes such as silane F8261 [1,1,2,2-perfluorooctyl triethoxy silane], silane A1100 [γ-aminopropyltriethoxy silane], and silane A151 [vinyl triethoxy silane]. Incorporation of the treated fibers in the NR matrix increased the storage modulus (E') and loss modulus, while there was a decrease in the damping property. The maximum value for E' was exhibited by the composite prepared using silane F8261-treated fibers and the minimum by composites containing fibers treated with silane A151. The silanization reduced the moisture-absorbing capacity of fibers, leading to improved wetting. This in turn produced a strong interfacial interface, giving rise to a much stiffer composite with higher modulus. The reduction in the damping properties was due to the hindered molecular motion of the rubber macromolecular chains. The values of loss modulus and damping factor of gum, treated, and untreated sisal–oil palm–NR hybrid composite is given in Table 8.6.

Treatments such as mercerization/acetylation of fibers will result in an increase in the dynamic mechanical properties of composites, which was observed by Martins and Mattoso [40]. The stabilizing effect of lignin filler on NR was examined by Kosikova *et al.* [41], using DMA. Addition of lignin improved the dynamic mechanical properties of NR vulcanizates. In another study, Da Costa *et al.* [27] found that addition of RHA to NR causes a shift in T_g values of filled rubber vulcanizates toward higher temperatures, showing the presence of cross-links,

Table 8.6 Loss modulus and damping values of gum, untreated, and treated sisal–oil palm–NR composites [39].

Sample	Loss modulus (MPa)	Damping factor (tan δ)
Gum	415	2.1
Untreated	634.2	0.965
Silane F8261	694.3	0.85
Silane A151	644.3	0.92
Silane A1100	669.2	0.89

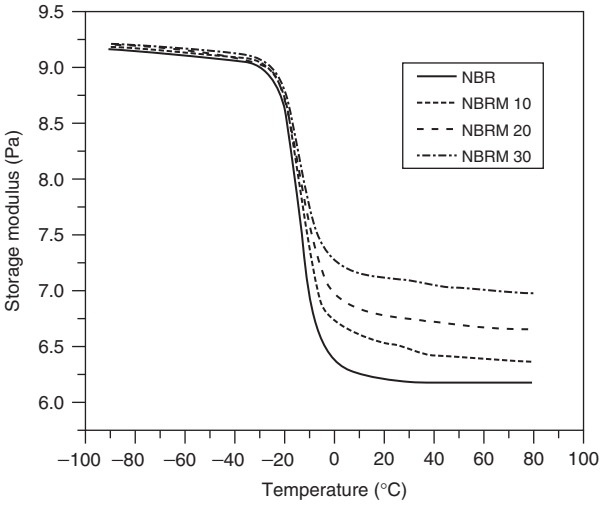

Figure 8.4 Storage modulus versus temperature curves of untreated oil palm microfibril–NBR composites having various fiber contents [42].

which restrict the mobility of polymer chains. The interactions between fillers and rubber phase also account for the higher properties. A more interesting study was by Joseph *et al*. [42], incorporating the oil palm fiber in the micro-level to the NBR matrix. Similarly to macro-fiber-reinforced rubber composites, here the storage modulus was found to increase with the weight fraction of microfibrils because of the increased stiffness imparted by the strong adhesion between the polar matrix and the hydrophilic microfibrils. The damping properties were found to decrease with increase in the fiber loading (Figure 8.4).

The viscoelastic properties of short melamine fiber-reinforced NBR composites were studied by Rajeev *et al*. [43]. Usage of resorcinol–hexa–silica bonding system in the composites also causes a significant improvement in the storage and loss modulus values.

8.5.4
Diffusion and Swelling Properties

Diffusion and swelling studies of biofiber-reinforced rubber composites are very important as they provide information about its interface and the service performance in liquid environment. On absorption of liquid, the composite undergoes a diffusion process, which involves transfer of liquid to its interior. Hence, the material swells as a whole, which leads to gradual deterioration in its physical and mechanical properties and subsequent premature failure. Several factors such as chemical structure and composition of the rubber compound, solvent, test piece size and shape, rubber–liquid ratio, temperature, time, presence of fillers affect the swelling behavior of elastomers.

To know the effect of fiber loading, chemical treatment, and bonding agent on liquid sorption, Geethamma *et al*. [44] conducted diffusion of water and artificial seawater through cross-linked coir–NR composites. On the basis of the experiments, it was suggested that the probable mechanism of transport in gum compound is Fickian and that, in composites, this is anomalous. The liquid uptake of all the composites is higher in water than that in artificial seawater. Moreover, the mercerization of coir fiber reduced the swelling behavior of the composites. Swelling behavior of NR vulcanizates loaded with kenaf fibers were studied using hydrated silica, resorcinol, and hexamethylene tetramine as the adhesion system, and compared with those of NR composites loaded with synthetic polyester short fibers [45]. Water absorption characteristics of the sisal–oil palm hybrid NR composites were evaluated with reference to fiber loading and fiber surface modifications [46]. Similarly to the coir–NR system, here also the mechanism of diffusion in the gum sample was found to be Fickian in nature, while in the loaded composites, it was nonFickian. The chemical modification of fiber reduced the water abruption nature of the composites (Figure 8.5).

Another interesting study was by Jacob *et al*. [47], which used woven sisal fabric as reinforcement in NR. The sisal fabric was subjected to various chemical modifications such as mercerization, silanization, and thermal treatment. It was found that water uptake mainly depends on the properties of the woven fabric and the diffusion followed a Fickian nature in the composites. Among all the chemically treated composites, mercerized samples exhibited the maximum sorption, while the composite containing bonding agent alone showed minimum water uptake. This was attributed to the fact that the mercerization of fiber will promote the activation of hydroxyl groups of the cellulose units. These activated hydroxyl groups can effectively form hydrogen bonds with water, which increases the water uptake of mercerized fiber-reinforced composites. The high adhesion power given by the presence of bonding agents to the rubber matrix reduces the water uptake in composites when compared to all other samples. The rate of diffusion was seen to increase with temperature for all composites.

Rather than water, the solvent-swelling characteristics of NR composites containing both untreated and mercerized isora fibers were investigated in aromatic and aliphatic solvents such as toluene and *n*-hexane [48]. The uptake of aromatic

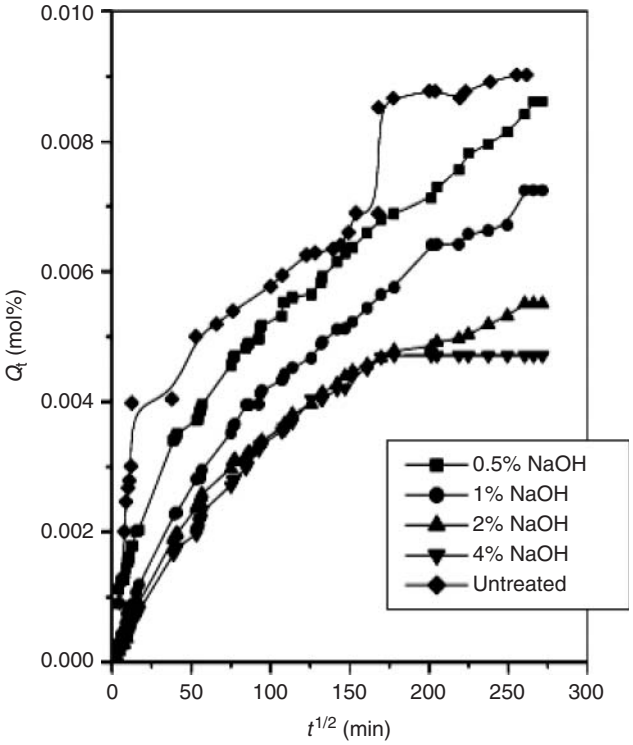

Figure 8.5 Water absorption characteristics of the sisal–oil palm hybrid NR composites with reference to fiber surface modifications [46]. with permission from ACS.

solvent is higher than that of aliphatic solvent for the composites cured at all temperatures. The effect of fiber loading on the swelling behavior of the composite was also investigated in oils like petrol, diesel, and lubricating oil. The percentage of swelling index and swelling coefficient of the composite were found to decrease with increase in fiber loading (Table 8.7).

This is due to the increased hindrance exerted by the fibers at higher fiber loadings and also due to the good fiber–rubber interactions. Among petrol, diesel, and lubricating oils, the maximum uptake of solvent was observed with petrol followed by diesel and then lubricating oil. The strong interfacial adhesion imparted by the bonding agent and mercerization in the composites restricted the swelling considerably. Haseena *et al*. [49] investigated the interfacial adhesion of sisal–coir hybrid fiber-reinforced NR composites by this method with special reference to fiber loading, orientation, and bonding agent in three aromatic solvents, namely; benzene, toluene, and xylene. As the fiber content and penetrant size increases, the solvent uptake has been found to decrease because of the increased hindrance and good fiber–rubber interaction. The addition of a bonding agent to the NR also decreased the swelling of the composites. They also observed that, in strongly

Table 8.7 Swelling coefficient of the isora–NR composites in various oils.

Mixes	Petrol	Diesel	Lubricating oils
Gum	3.46	1.93	0.808
X10	2.71	1.65	0.626
X10b	2.57	1.28	0.561
X20	2.58	1.35	0.540
X20b	2.32	1.11	0.423
X30	2.42	1.09	0.451
X30b	2.31	1.02	0.387
X40	2.41	0.96	0.41
X40b	1.91	0.88	0.369

X represents the conventionally cured composites; b represents the bonding agent.

bonded composites, the swelling has been mainly observed to take place in the thickness direction.

8.5.5 Dielectric Properties

The dielectric constant of a material depends upon the polarizability of the molecules. The polarizability of nonpolar molecules arises from electronic polarization and atomic polarization. In the case of polar molecules, a third factor also comes into play, which is orientation polarization. NR is nonpolar and has only instantaneous atomic and electronic polarization. The presence of biofibers in NR leads to an overwhelming presence of polar groups giving rise to dipole or orientation polarizability. The overall polarizability of a biofiber-reinforced composite is therefore the sum of electronic, atomic, and orientation polarization, giving rise to a higher dielectric constant. Therefore, the dielectric constant increases with increase in fiber loading at all frequencies. The increase in frequency increases the dielectric constant of these composites because of the decrease in the orientation polarization. At lower frequencies, complete orientation of the molecule is possible, while at medium frequencies there is only little time for orientation. Orientation of the molecules is not possible at very high frequencies. A similar trend has been observed by Jacob *et al*. [50] in the dielectric characteristics of sisal–oil palm hybrid fibe-reinforced NR composites (Figure 8.6).

Ismail *et al*. [51] conducted the electrical property analysis of lignocellulosic–NR composites at a frequency range of 10^2–10^5 Hz at room temperature. It was noticed that dielectric loss (ε') for bagasse pulp is higher than that for cotton stalks pulp, because of the higher hemilignin content in bagasse pulp, which is characterized by a low degree of polarization. An abrupt increase of ε'' at a higher content of bagasse pulp was also noticed.

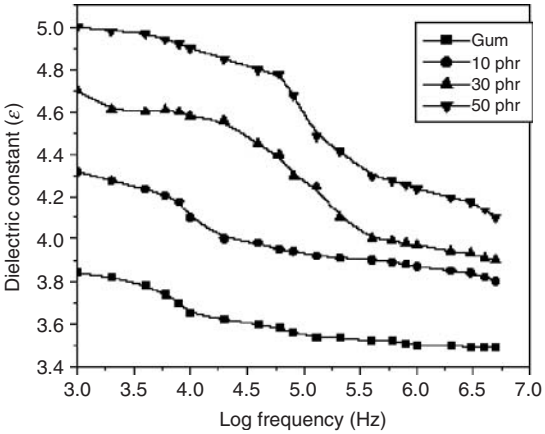

Figure 8.6 Dielectric characteristics of sisal–oil palm hybrid fiber-reinforced natural rubber composites [50]. with permission from Springer Science + Business Media.

The chemical modification of fibers causes a decrease in orientation polarization, which results in low values for the dielectric constant of composites. Chemical treatment also results in a reduction in the moisture absorption capacity of fibers owing to the reduced interaction between polar –OH groups of fibers with water molecules. This decrease in hydrophilicity of the fibers lowers the orientation polarization and subsequently dielectric constant. The dielectric properties of surface-modified oil palm–NR composites were characterized by Marzinotto *et al*. [52], who observed an increase of the loss factor after fiber treatment. The effect of fiber loading, fiber ratio, frequency, chemical modification of fibers, and the presence of a bonding agent on the dielectric properties of sisal–coir hybrid fiber-reinforced NR composites have been studied by Haseena *et al*. [53]. The dielectric constant values have been found to be higher for fiber-filled systems than for pure NR. The volume resistivity of the composites was found to decrease with fiber loading and a percolation threshold has been obtained at 16% volume of fibers. The dielectric constant values were lower for systems consisting of fibers subjected to chemical treatments. The addition of a two-component dry bonding agent consisting of hexamethylene tetramine and resorcinol, used for the improvement of interfacial adhesion between the matrix and fibers, reduced the dielectric constant of the composites. When the weight percentage of sisal fiber was increased in the total fiber content of the hybrid composites, the dielectric constant was found to increase. The added fibers and different chemical treatments for them increased the dielectric dissipation factor.

8.5.6
Rheological and Aging Characteristics

Rubber reinforced with short fibers generally shows a highly pseudoplastic viscosity, obeying the power law relationship over a wide range in shear rates. The effect of

fiber reinforcement is more exaggerated as the shear rate is reduced. A number of rheological studies have been carried out on specific types of fiber-reinforced rubber alone [16, 54, 55]. The melt flow behavior of NR composites containing untreated, acetylated, and γ-ray irradiated coir fibers were studied by Geethamma *et al.* [16]. It was found that the pseudoplasticity of the melt increased with fiber loading. Incorporation of fibers decreased the extrudate deformation and this reduction was more prominent at higher fiber loading. The die swell of composites containing coir fibers was lower than that of gum compound and it was negligible for composites containing 20 and 30 phr of fibers. Prasantha Kumar *et al.* [55] studied the rheological behavior of short fiber-reinforced SBR composites and found that the fibers present in the matrix will prevent the shape distortion of the extrudates and an increase in the fiber content will also decrease the shape distortion.

NR will retain its double bonds in the vulcanized structure and is sensitive to heat, light, and oxygen. Unless protected with antioxidants, NR ages by an autocatalytic process accompanied by an increase in oxygen content. As a result of aging, either softening or embrittlement of rubber occurs. NR is far more sensitive than other rubbers to oxygen and ozone attack owing to the presence of the reactive double bond in the main chain. The effects of degrading agents such as oxygen, ozone, heat, and high-energy radiation depend mainly upon the chemical structure of the polymer chain [56]. The mechanical properties such as tensile strength, elongation, modulus, and hardness are decreased as a result of chain scission, while cross-linking has the opposite effect on these properties. The action of different degrading agents on the properties of sisal–NR composites was investigated by Varghese *et al.* [57]. The authors reported that at low irradiation, the retention in tensile strength was almost constant beyond 6 vol% fiber loading. On prolonged irradiation, degradation of polymer chains was the main reaction taking place at low fiber loading, whereas at higher fiber loading, retention of tensile properties is higher. Unsaturated elastomers, especially those containing activated double bonds in the main chain are severely attacked by ozone, resulting in deep cracks in a direction perpendicular to the applied stress. Protection against ozone attack can be achieved by blending with any saturated elastomers or by mixing with antiozonants. In the case of composites, the fibers incorporated in the mixes prevent crack initiation and also hinder crack propagation. The thermal-aging properties of NR can be improved by the presence of untreated fibers and can be further improved with treated fibers [8]. In PALF–NR systems, the incorporation of fibers in NR resulted in an increased level of retention of tensile strength. These results indicated that the rubber degradation was restricted to some extent by incorporated fibers. Furthermore, the increase in retention was greater in composites containing both 5% NaOH- and 1% benzoyl peroxide (BPO)-treated pineapple fibers. This is because decomposition of volatile extractables present on the fiber surfaces upon heating at 100 °C during aging, leads to the formation of voids at the fiber–matrix interface, and this would weaken the fiber–matrix bond strength and, thereby, the composite performance. Thus, in the case of NaOH and BPO-treated fiber composites, the existence of good interfacial adhesion will provide the protection against void formation during aging, and an improvement of retention of tensile strength.

8.6
Approaches to Improve Fiber–Matrix Adhesion

Natural fiber is hydrophilic and possesses hydroxyl groups on its surface. The brittle nature and low cellulose content makes it a less effective reinforcement. The compatibility of hydrophobic rubber matrix and hydrophilic cellulose fiber can be enhanced through the modification of the polymer or fiber surface. For that, natural fiber can be subjected to some sort of pretreatment. The extent of adhesion is usually increased by the use of bonding/coupling agents and chemical modification of fibers. Most of the fiber surface modifications used in rubber compounding are as follows: mercerization, acetylation, benzoylation, toluene diisocyanate (TDIC) treatment, peroxide treatment, isocyanate treatment, permanganate treatment, coupling agents such as silanes, and titanates, and bonding agents. The most commonly used bonding agents are resorcinol-based adhesives such as resorcinol–formaldehyde latex (RFL) or resorcinol–hexamethylene tetramine–hydrated silica (HRH).

8.6.1
Mercerization

Several investigations were conducted to know the effectiveness of mercerization on the biofiber–NR interface [29, 58–61]. The effectiveness depends upon the type and concentration of the alkaline solution, temperature, time of treatment, tension of the material, as well as on the additives. Lopattananon *et al.* [8] studied the effect of mercerization on the tensile properties of PALF–NR composites. The alkali-treated fiber-reinforced composites exhibited higher elongation at break in comparison to unmodified fiber-reinforced composites. When the concentration of NaOH solution increased from 3% to 5% (w/v), the tensile strength of treated fiber composites increased by 28% over that of untreated fiber composites. This improvement in tensile properties was attributed to an increase in effective surface area and roughness of the pineapple fibers, which increased the interfacial bond strength through mechanical interlocking between the fiber and NR (Figure 8.7a,b).

Acetylation is a well-known esterification method to introduce plasticization to cellulosic fibers. Pretreatment of fibers with acetic anhydride substitutes the polymer hydroxyl groups of the cell wall with the acetyl group so that they become hydrophobic. Acetylation is based on the reaction of cell wall hydroxyl groups of lignocellulosic materials with acetic or propionic anhydride at elevated temperature. The hydroxyl groups of cellulose (crystalline material) are closely packed with hydrogen bonds, preventing the diffusion of reagent and thus resulting in very low extents of reaction. Varghese *et al.* [57] studied the effect of acetylation and bonding agent on the aging properties of sisal fiber-reinforced NR composites, which included thermal aging, γ-radiation, and ozone resistance. High fiber-volume fraction showed better resistance to aging, especially with fiber surface treatment. Increasing the dosage of γ-radiation was found to increase the extent of the aging process.

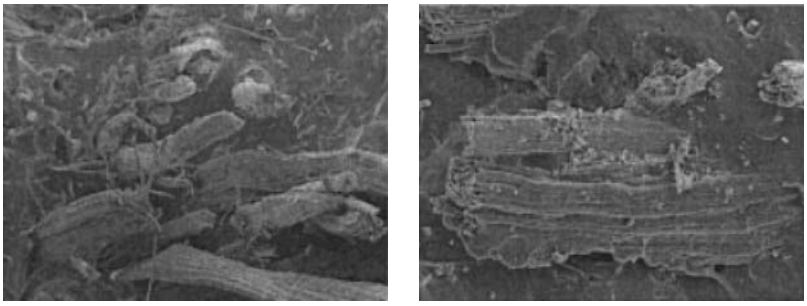

(a) (b)

Figure 8.7 SEM photomicrographs of fracture surfaces of PALF–natural rubber composites containing (a) untreated (b) 5% NaOH-treated pineapple fibers [8].

8.6.2
Benzoylation

Benzoylation is a chemical method where an aryl radical (C_6H_5CO) is reacted with the cellulosic –OH group of natural fibers making them more compatible with polymers, by decreasing their polarity. In this treatment, natural fibers are soaked in NaOH solution and then treated with benzoyl chloride. The treated fibers are soaked in ethanol to remove the unreacted benzoyl chloride for a specified length of time and finally washed with water and dried before compounding. Peroxide treatment of biofibers has attracted the attention of various researchers owing to its ease of processability and improvement in mechanical properties. Organic peroxides tend to decompose easily to free radicals, which further react with the hydrogen group of the matrix and biofibers. In this treatment, fibers were treated with BPO or dicumyl peroxide in acetone solution for about 30 min after alkali pretreatment. A saturated solution of the peroxide in acetone was used. High-temperatures were favored for decomposition with the peroxide. The composites reinforced with BPO-treated PALF fibers showed an increase in both tensile and elongation at break relative to untreated composites [8]. This is attributed to the increase in hydrophobic character of these fiber surfaces, making them more compatible with NR. However, the increase in the amount of BPO will decrease the tensile strength of composites. Pretreatments with permanganate can be used to modify the fiber surface. For that, the fibers were soaked in different concentrations of potassium permanganate ($KMnO_4$) in acetone solution from 1 to 3 min after alkaline pretreatment.

8.6.3
Coupling Agents

Coupling agents usually improve the degree of cross-linking in the interface region and offer a perfect bonding. Isocyanate coupling agents can be an effective way of improving the interface through urethane linkage formation between isocyanate

(—N=C=O) and hydroxyl groups present on the fiber surface. The main advantage of using isocyanates as coupling agents is the hydrolytic stability of the urethane groups formed and the availability of several isocyanates with different chemical structures, which make them compatible with a wide range of polymeric matrices, thereby providing better interaction with these matrices and resulting in composite materials with superior properties. Among the other coupling agents, silane coupling agents were found to be effective in modifying the natural fiber–matrix interface. Efficiency of silane treatment was high for the alkaline-treated fiber than for the untreated fiber because more reactive sites can be generated with the silane reaction. Therefore, the fibers were pretreated with NaOH for about half an hour before coupling with silane. The fibers were then washed many times in distilled water and finally dried. Zeng *et al.* [58] used bis(3-triethoxysilylpropyl) tetrasulfide (TESPT) to improve the interfacial adhesion between cotton fiber and NR. Composites with TESPT had higher cross-link density, better mechanical properties, higher initial modulus, and higher yield strength than the composites without TESPT because of the difference in interfacial adhesion. The results of an interfacial adhesion evaluation, namely, the high storage modulus, low damping values of the composites with TESPT, and the coarse surfaces of the pullout fibers implied the enhancement of interfacial adhesion.

8.6.4
Bonding Agents

As mentioned earlier, the commonly used bonding systems are phenol–formaldehyde, silica–phenol–formaldehyde, resorcinol–formaldehyde, and resorcinol–hexamethylene tetramine–silica. In these, silica is believed to act as controller for resin formation and help in developing adhesion between rubber and fiber. The importance of silica is still a matter of controversy. Another interesting report [16] claimed that silica was not essential in producing good adhesion between coir fiber and NR. It was observed that the tensile strength of mixes that did not contain silica was significantly higher than that of the mixes containing silica. Thus, it is clear that the nature of both the rubber matrix and the reinforcing fiber determines whether silica is needed or not as one of the components. The adhesion of short oil palm–NR was investigated [59] using various bonding agents like phenol–formaldehyde; resorcinol formaldehyde–silica; hexamethylene tetramine–resorcinol formaldehyde–silica. However Ismail *et al.* [10] reported that addition of bonding agent will prolong the cure time of oil palm–NR composites. The treated fiber-reinforced composites show less difference in the cure time of the composites when compared to untreated ones. Better mechanical properties were obtained for the bonding system RF : Sil : Hex (5 : 2 : 5). The effectiveness of bonding systems were found to follow the order: RF : Sil : Hexa (5 : 2 : 0) > RF : Sil (5 : 2) > PF (10 phr). Arumugam *et al.* [60] studied the effects of fiber content and bonding agent on the physical properties and aging characteristics of coir fiber-reinforced NR composites. It was observed that coir fibers acted as a reinforcing agent only above 10 phr loading and that the adhesion between coir

Table 8.8 Summary of the studies performed in the improvement of fiber–matrix adhesion.

Composites	Measurements	Treatment of biofibers	Conclusion	References
Isora/NR	Mechanical properties	Mercerization, acetylation, benzoylation TDI, silane	Increased the tensile strength, tensile modulus, tear strength, and hardness.	[7, 14]
Bamboo–NR	Cure characteristics, mechanical properties	Silane coupling agent	Scorch time and cure time decreased with increasing filler loading. Mechanical properties improved with the addition of Si-69.	[9]
Oil palm–NR	Mechanical properties	Mercerization	Increased the tensile strength, tensile modulus, tear strength, and hardness.	[15]
Coir fiber–NR	Mechanical properties	Mercerization TDI HR	Good adhesion for composite containing fibers subjected to a chemical treatment with alkali, TDI, and NR solutions along with the HR system.	[17]
Oil palm–NR	Mechanical properties, processing characteristics	Mercerization	Increased the tensile properties, tear strength, and hardness. Scorch and curing time was found to be independent of modification of fiber surface.	[22]
Rice husk–NR	Mechanical properties	Bis(3-triethoxy silyl propyl)-tetrasulfane (Si 69)	Addition of Si-69 silane coupling agent resulted in little improvement in the performance of all filled vulcanizates.	[24]
Grass fiber–NR	Cure characteristics mechanical properties	Mercerization, RFL	Rubber–fiber interface was improved by the addition of RFL. The optimum cure time of vulcanizates having RFL-treated fibers was higher than that of the other vulcanizates, it decreased with fiber loading in the presence of RFL. This value was lower than that of the rubber composite with out RFL.	[30]
Sisal/oil palm–NR	DMA	Mercerization	Resulted in higher storage modulus and lowered the tan δ values due to increased cross-linking and formation of a strong fiber–matrix interface.	[34]

Table 8.8 (*Continued*)

Composites	Measurements	Treatment of biofibers	Conclusion	References
Sisal/oil Palm–NR	Vulcanization parameters, processability, tensile properties, swelling characteristics	Mercerization, silane coupling agent	Composites containing chemically treated fibers were found to possess enhanced mechanical properties.	[35]
Coir/NR	DMA	Mercerization bleaching TDI	Composite containing fibers subjected to bleaching exhibited very high tan δ values in the low temperature region but the lowest values at high temperature region.	[37]
Sisal/coir–NR	Dielectric properties	Mercerization acetylation, benzoylation, peroxide, permanganate	Dielectric constant values were lower.	[49]
Cellulose whiskers and microfibrillated cellulose–NR	DMA and mechanical properties		The stiffness of the natural rubber was significantly increased above its glass–rubber transition temperature upon nanoparticles addition. The reinforcing effect was shown to be higher for nanocomposites with MFC compared to whiskers.	[61]

HR, hexaresorcinol; RFL, resorcinol–formaldehyde latex.

fibers and the rubber matrix was enhanced by a bonding agent. The composites had a superior antiaging property for fiber loading of 30 phr in the presence of bonding agents. In the grass fiber–NR composite, the rubber–fiber interface was improved by the addition of RFL as bonding agent [30]. A reduction in scorch time and increment in optimum torque values with increase in concentration of bonding agent was observed. The HRH bonding system was found to be effective for silk fiber-reinforced NR composites too [29]. The modulus values of kenaf fiber-reinforced NR was found to increase in the presence of HRH bonding system [21]. O'Connor [4] investigated the effect of bonding agents on the properties of cellulose fiber–NR composites. The bonding agents studied were an HRH system, a resorcinol hydrated(RH) silica system that omitted silica and a resin-bonding agent. Better composite properties were obtained with the RH system. A summary of the studies performed in this area is given in Table 8.8.

8.7 Applications

NR-based composites can be used for several applications from household to industrial products. The main advantage of these composites is that they have both the elastic behavior of rubber and the strength and stiffness of reinforcing fibers. Good resistance to flexing and fatigue together with high resilience of NR makes their use more attractive in the automobile industry especially in the area of tires and tubes. Short fiber-reinforced rubber composites can be used for the manufacturing of moderate-performance hose or in cord constructions. The natural fibers can provide stiffening to soft inner tubes for the application of metal braids and can extend hose life by bridging the stresses across weakened filaments. Other uses are as belts diaphragms and gaskets. Some of the other applications are roofing, dock and ship fenders, and general uses such as belts and other industrial articles.

8.8 Conclusions

In recent years, there is a paradigm shift in the field of materials science with the usage of natural fibers for a spectrum of applications. They are extensively being used to reinforce polymer matrices to get composites with many desirable properties. Most of the studies indicated that natural fibers can be used to reinforce NR. However, the properties of the product will depend upon various factors such as fiber length, fiber orientation, fiber loading, and fiber–matrix adhesion. Usage of pretreated fibers by various chemical and physical methods in NR improves static and dynamic mechanical properties, while there is a decrease in the solvent uptake owing to the increased fiber–matrix adhesion. Literature survey also shows that more studies should be concentrated on the usage of the nanofiller-reinforced NR matrix as well as on other elastomers in order to develop composites with superior performance.

References

1. Charlet, K., Eve, S., Jernot, J.P., Gomina, M., and Breard, J. (2009) Tensile deformation of a flax fiber. *Procedia Eng.*, **1**, 233–236.
2. Baley, C. (2002) Analysis of the flax fibres tensile behaviour and analysis of the tensile stiffness increase. *Composites Part A*, **33**, 939–948.
3. Bledzki, A.K., Reihmane, S., and Gassan, J. (1996) Properties and modification methods for vegetable fibers for natural fiber composites. *J. Appl. Polym. Sci.*, **59**, 1329–1336.
4. O'Connor, J.E. (1977) Short-fiber-reinforced elastomer composites. *Rubber Chem. Technol.*, **50**, 945–958.
5. Jacob, M., Thomas, S., and Varughese, K.T. (2004) Natural rubber composites reinforced with sisal/oil palm hybrid fibers: tensile and cure characteristics. *J. Appl. Polym. Sci.*, **93**, 2305–2312.
6. Ismail, H., Norjulia, A.M., and Ahmad, Z. (2010) The effects of untreated and treated kenaf loading on the properties

of kenaf fiber-filled natural rubber compounds. *Polym. Plast. Technol. Eng.*, **49**, 519–524.

7. Lovely, M. and Joseph, R. (2007) Mechanical properties of short-isora-fiber-reinforced natural rubber composites: effects of fiber length, orientation, and loading; alkali treatment; and bonding agent. *J. Appl. Polym. Sci.*, **103**, 1640–1650.
8. Lopattananon, N., Panawarangkul, K., Sahakaro, K., and Ellis, B. (2006) Performance of pineapple leaf fiber-natural rubber composites: The effect of fiber surface treatments. *J. Appl. Polym. Sci.*, **102**, 1974–1984.
9. Ismail, H., Shuhelmy, S., and Edyham, M.R. (2002) The effects of a silane coupling agent on curing characteristics and mechanical properties of bamboo fiber filled natural rubber composites. *Eur. Polym. J.*, **38**, 39–47.
10. Ismail, H., Rozman, H.D., Jaffri, R.M., and Mohd Ishak, Z.A. (1997) Oil palm wood flour reinforced epoxidized natural rubber composites: the effect of filler content and size. *Eur. Polym. J.*, **33**, 1627–1632.
11. Arayapranee, W., Na-Ranong, N., and Rempel, G.L. (2005) Application of rice husk ash as fillers in the natural rubber industry. *J. Appl. Polym. Sci.*, **98**, 34–41.
12. Ismail, H., Edyham, M.R., and Wirjosentono, B. (2002) Bamboo fiber filled natural rubber composites: the effects of filler loading and bonding agent. *Polym. Test.*, **21**, 139–144.
13. Geethamma, V.G., Ramamurthy, K., Janardhan, R., and Thomas, S. (1996) Melt flow behavior of short coir fiber reinforced natural rubber composites. *Int. J.Polym. Mater.*, **32**, 147–161.
14. Mathew, L., Joseph, K.U., and Joseph, R. (2004) Isora fibers and their composites with natural rubber. *Prog. Rubber Plast. Recycl. Technol.*, **20**, 337–349.
15. Joseph, S., Joseph, K., and Thomas, S. (2006) Green composites from natural rubber and oil palm fiber: physical and mechanical properties. *Int. J. Polym. Mater.*, **55**, 925–945.
16. Geethamma, V.G., Mathew, K.T., Lakshminarayanan, R., and Thomas, S. (1998) Composite of short coir fibers and natural rubber: effect of chemical modification, loading and orientation of fiber. *Polymer*, **39**, 1483–1491.
17. Geethamma, V.G., Pothen, L.A., Rhao, B., Neelakantan, N.R., and Thomas, S. (2004) Tensile stress relaxation of short-coir-fiber-reinforced natural rubber composites. *J. Appl. Polym. Sci.*, **94**, 96–104.
18. Nassar, M.M., Ashour, E.A., and Washid, S.S. (1996) Thermal characteristics of bagasse. *J. Appl. Polym. Sci.*, **61**, 885–890.
19. El Sabbagh, S.H., El Hariri, D.M., and Abd. El Ghaffar, M.A. (2000) Proceedings from the 3rd International Symposium on Natural Polymers and Composites: ISNa Pol/May 14–17, pp. 469–483.
20. Ismail, H. and Jaffri, R.M. (1999) Physico-mechanical properties of oil palm wood flour filled natural rubber composites. *Polym. Test.*, **18**, 381–388.
21. Varghese, S., Kuriakose, B., Thomas, S., and Koshy, A.T. (1994) Mechanical and viscoelastic properties of short fiber reinforced natural rubber composites: effects of interfacial adhesion, fiber loading, and orientation. *J. Adhes. Sci. Technol.*, **8**, 235–248.
22. Ismail, H., Rosnah, N., and Ishiaku, U.S. (1997) Oil palm fiber-reinforced rubber composite: effects of concentration and modification of fiber surface. *Polym. Int.*, **43**, 223–230.
23. Ismail, H., Jaffri, R.M., and Rozman, H.D. (2000) Oil palm wood flour filled natural rubber composites: fatigue and hysteresis behaviour. *Polym. Int.*, **49**, 618–622.
24. Da Costa, H.M., Visconte, L.L.Y., Nunes, R.C.R., and Furtado, C.R.G. (2000) The effect of coupling agent and chemical treatment on rice husk ash–filled natural rubber composites. *J. Appl. Polym. Sci.*, **76**, 1019–1027.
25. Okieimen, F.E. and Imanah, J.E. (2006) Studies in the utilization of agricultural waste products as filler in natural rubber compounds. *J. Appl. Polym. Sci.*, **100**, 2561–2564.
26. Saeoui, P., Rakdee, C., and Thanmathorn, P. (2002) Use of rice husk ash as filler in natural rubber

vulcanizates: in comparison with other commercial fillers. *J. Appl. Polym. Sci.*, **83**, 2485–2493.

27. Da Costa, H.M., Visconte, L.L.Y., Nunes, R.C.R., and Furtado, C.R.G. (2002) Mechanical and dynamic mechanical properties of rice husk ash–filled natural rubber compounds. *J. Appl. Polym. Sci.*, **83**, 2331–2346.
28. Haseena, A.P., Priyadasan, K., Unnikrishnan, G., and Thomas, S. (2005) Mechanical properties of sisal/coir hybrid fiber reinforced natural rubber. *Prog. Rubber Plast. Recycl. Technol.*, **21**, 155–181.
29. Setua, D.K. and De, S.K. (1983) Short silk fiber reinforced natural rubber composites. *Rubber Chem. Technol.*, **56**, 808–826.
30. Debasish, D., Debapriya, D., and Adhikari, B. (2006) Curing characteristics and mechanical properties of alkali-treated grass-fiber-filled natural rubber composites and effects of bonding agent. *J. Appl. Polym. Sci.*, **101**, 3151–3160.
31. Nashar, D.E.E., Abd-El-Messieh, S.L., and Basta, A.H. (2004) Newsprint paper waste as a fiber reinforcement in rubber composites. *J. Appl. Polym. Sci.*, **91**, 469–478.
32. Martins, M.A., Pessoa, J.D.C., Goncalves, P.S., Souza, F.I., and Mattoso, L.H.C. (2008) Thermal and mechanical properties of the açaí fiber/natural rubber composites. *J. Mater. Sci.*, **43**, 6531–6538.
33. Jacob, M., Thomas, S., and Varughese, K.T. (2001) Lignocellulose–material of the millenium: technology and application. Proceedings from USM-JIRCAS Joint International Symposium, Penang, Malaysia, March 20–22, 2001.
34. Jacob, M., Francis, B., Thomas, S., and Varghese, K.T. (2006) Dynamical mechanical analysis of sisal/oil palm hybrid fiber-reinforced natural rubber composites. *Polym. Compos.*, **27**, 671–680.
35. Jacob, M., Francis, B., Varghese, K.T., and Thomas, S. (2008) Effect of chemical modification on properties of hybrid fiber biocomposites. *Composites Part A*, **39**, 352–363.
36. Bai, W. and Li, K. (2009) Partial replacement of silica with microcrystalline cellulose in rubber composites. *Composites Part A*, **40**, 1597–1605.
37. Geethamma, V.G., Kalaprasad, G., Groeninckx, G., and Thomas, S. (2005) Dynamic mechanical behavior of short coir fiber reinforced natural rubber composites. *Composites Part A*, **36**, 1499–1506.
38. Murty, V.M. and De, S.K. (1982) Effect of particulate fillers on short jute fiber-reinforced natural rubber composites. *J. Appl. Polym. Sci.*, **27**, 4611–4622.
39. Jacob, M., Francis, B., Varghese, K.T., and Thomas, S. (2006) The effect of silane coupling agents on the viscoelastic properties of rubber biocomposites. *Macromol. Mater. Eng.*, **291**, 1119–1126.
40. Martins, M.A. and Mattoso, L.H.C. (2004) Short sisal fiber-reinforced tire rubber composites: dynamic and mechanical properties. *J. Appl. Polym. Sci.*, **91**, 670–677.
41. Kosikova, B., Osvald, A., and Krajcovicova, J. (2007) Role of lignin filler in stabilization of natural rubber-based composites. *J. Appl. Polym. Sci.*, **103**, 1226–1231.
42. Joseph, S., Sreekumar, P.A., Kenny, J.M., Puglia, D., Thomas, S., and Joseph, K. (2010) Dynamic mechanical analysis of oil palm microfibril-reinforced acrylonitrile butadiene rubber composites. *Polym. Compos.*, **31**, 236–244.
43. Rajeev, R.S., Bhowmick, A.K., De, S.K., and Bandyopadhyay, S. (2003) Short melamine fiber filled nitrile rubber composites. *J. Appl. Polym. Sci.*, **90**, 544–558.
44. Geethamma, V.G. and Thomas, S. (2005) Diffusion of water and artificial seawater through coir fiber reinforced natural rubber composites. *Polym. Compos.*, **26**, 136–143.
45. El-Sabbagh, S.H., El-Hariri, D.M., and El-Ghaffar, M.A. (2001) Effect of kenaf fibers on the properties of natural rubber vulcanizates. *Polym. Polym. Compos.*, **9**, 549–560.
46. Jacob, M., Varughese, K.T., and Thomas, S. (2005) Water sorption studies of hybrid biofiber-reinforced

natural rubber biocomposites. *Biomacromolecules*, **6**, 2969–2979.

47. Jacob, M., Varughese, K.T., and Thomas, S. (2006) A study on the moisture sorption characteristics in woven sisal fabric reinforced natural rubber biocomposites. *J. Appl. Polym. Sci.*, **102**, 416–423.
48. Mathew, L., Joseph, K.U., and Joseph, R. (2006) Swelling behaviour of isora/natural rubber composites in oils used in automobiles. *Bull. Mater. Sci.*, **29**, 91–99.
49. Haseena, A.P., Priyadasan, K., Namitha, R., Unnikrishnan, G., and Thomas, S. (2004) Investigation on interfacial adhesion of short sisal/coir hybrid fiber reinforced natural rubber composites by restricted equilibrium swelling technique. *Compos. Interfaces*, **11**, 489–513.
50. Jacob, M., Varughese, K.T., and Thomas, S. (2006) Dielectric characteristics of sisal–oil palm hybrid biofibers reinforced natural rubber biocomposites. *J. Mater. Sci.*, **41**, 5538–5547.
51. Ismail, M.N., Turky, G.M., and Nada, A.M.A. (2000) Electromechanical behavior of natural rubber-lignocellulosic material composites. *Polym. Plast. Technol. Eng.*, **39**, 249–263.
52. Marzinotto, M., Santulli, C., and Mazzetti, C. (2007) Dielectric properties of oil palm-natural rubber biocomposites. Electrical Insulation and Dielectric Phenomena, CEIDP 2007. Annual Report–Conference on Issue Date: 14–17 October, 2007, pp. 584–587.
53. Haseena, A.P., Unnikrishnan, G., and Kalaprasad, G. (2007) Dielectric properties of short sisal/coir hybrid fiber reinforced natural rubber composites. *Compos. Interfaces*, **14**, 763–786.
54. Goettler, L.A., Leib, R.I., and Lambright, A.J. (1979) Short fiber reinforced hose: a new concept in production and performance. *Rubber Chem. Technol.*, **52**, 838–863.
55. Prasantha Kumar, R., Manikandan Nair, K.C., Thomas, S., Schit, S.C., and Ramamurthy, K. (2000) Morphology and melt rheological behaviour of short-sisal-fiber-reinforced SBR composites. *Compos. Sci. Technol.*, **60**, 1737–1751.
56. Razumovskii, S.D. and Zaikov, G.E. (1982) in *Developments in Polymer Stabilisation*, 6th edn (ed. G. Scott), Applied Science Publishers, London.
57. Varghese, S., Kuriakose, B., and Thomas, S. (1994) Short sisal fiber reinforced natural rubber composites: high-energy radiation, thermal and ozone degradation. *Polym. Degrad. Stab.*, **44**, 55–61.
58. Zeng, Z., Ren, W., Xu, C., Lu, W., Zhang, Y., and Zhang, Y. (2009) Effect of bis(3-triethoxysilylpropyl) tetrasulfide on the crosslink structure interfacial adhesion, and mechanical properties of natural rubber/cotton fiber composites. *J. Appl. Polym. Sci.*, **111**, 437–443.
59. Ismail, H., Rosnah, N., and Rozman, H.D. (1997) Curing characteristics and mechanical properties of short oil palm fiber reinforced rubber composites. *Polymer*, **38**, 4059–4064.
60. Arumugam, N., Tamare Selvy, T., and Venkata Rao, K. (1989) Coconut-fiber-reinforced rubber composites. *J. Appl. Polym. Sci.*, **37**, 2645–2659.
61. Bendahou, A., Kaddami, H., and Dufresne, A. (2010) Macromolecular nanotechnology investigation on the effect of cellulosic nanoparticles' morphology on the properties of natural rubber based nanocomposites. *Eur. Polym. J.*, **46**, 609–620.

9
Improvement of Interfacial Adhesion in Bamboo Polymer Composite Enhanced with Microfibrillated Cellulose

Kazuya Okubo and Toru Fujii

9.1
Introduction

Polymer matrix composites using natural fiber have been the focus for many applications because of their low impact on the environment. Natural fibers such as bamboo, jute, and cotton have excellent mechanical properties such as high specific strength as well as high specific modulus [1, 2]. Bamboo fiber (BF), especially, has excellent mechanical proprieties in comparison with its weight due to the longitudinally aligned fibers in its body (Figure 9.1). However, such excellent mechanical properties have not been well utilized by the polymer composite because of poor interfacial strength between the BF and thermoplastic matrix [3] (especially when short fibers are used as reinforcement). It should be stated that the strength of the natural fiber composites is not sufficient to be used even for semistructural members. Therefore, a novel approach is required to improve the interfacial strength. Some reports have been published showing that the development of composites can be improved by modification of the surface of the natural fibers by suitable chemical and other treatments [4–17].

Another method to improve the mechanical properties such as interfacial strength is to add nanosized carbon fiber-reinforced particles into the composite [18–20]. A strong influence of a uniform dispersion of the small-sized fibers or particles on the composite properties of advanced nanocomposites, such as carbon nanotube-reinforced composites was also reported [21–24]. However, few papers mention the enhancing method for improving the interfacial adhesion between fiber and matrix in a natural BF composite.

In this study, microfibrillated cellulose (MFC), which is a nanosized natural material fiber with high aspect ratio and high strength, was used as an enhancer for a polylactic acid (PLA)-based composite using BF, to increase mechanical properties such as bending strength and fracture toughness. The effect of weight content of the MFC on those properties was also discussed.

Polymer Composite: Volume 3, First Edition.
Edited by Sabu Thomas, Kuruvilla Joseph, S. K. Malhotra, Koichi Goda and M. S. Sreekala.

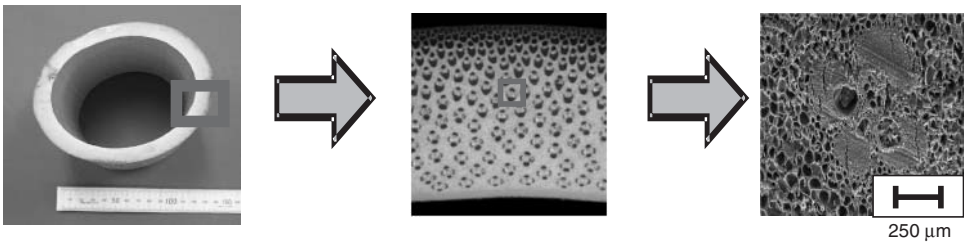

Figure 9.1 Microstructure of bamboo.

9.2 Materials

9.2.1 Matrix

PLA, which is a typical biodegradable polymer (PL-1000: Miyoshi Oil and Fat Co., Ltd) was used as matrix. Fine particles of the PLA with 4.5 μm average diameter are dispersed in a water-based solution.

9.2.2 Bamboo Fibers

BF was extracted from raw bamboo by using the steam explosion method. Table 9.1 lists the condition for the stream explosion method. Figure 9.2 shows the BF bundles after the steam explosion. The surface of the BF bundles was still covered with xylem (soft-wall cells). In order to remove the xylem, the fiber bundles were washed and rubbed in water, and then dried at 100 °C for 5 h. The fiber bundles were finally put into a mixing machine. As shown in Figure 9.3, almost all the BF bundles were separated into single fibers during the process. The aspect ratio was about 56, while the average length of BFs was 1145 μm, estimated on the Weibull distribution assumption.

Table 9.1 Conditions for the steam explosion method.

Contents	Time (min)	Temperature (°C)	Pressure (MPa)	Number of explosions in one process
Bamboo	120	175	0.8	9

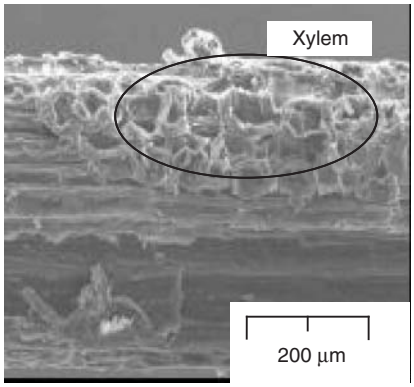

Figure 9.2 Surface of bamboo fiber bundles extracted by steam explosion.

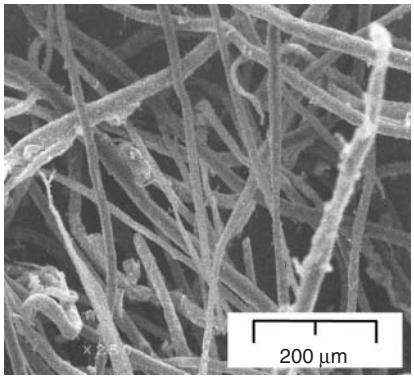

Figure 9.3 Modified bamboo fiber.

9.2.3
Microfibrillated cellulose (MFC)

MFC used in this study was obtained from wood pulp (not bamboo), supplied by Daicel Chemical Industry in Japan. Figure 9.4 shows an appearance of the MFC.

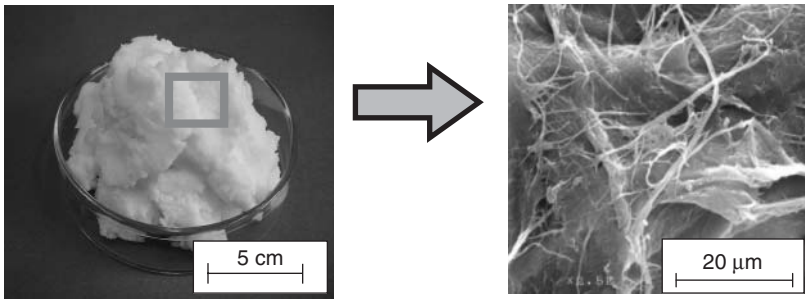

Figure 9.4 Appearance of MFC.

9.3 Experiments

9.3.1 Fabrication Procedure of Developed Composite Using PLA, BF, and MFC (PLA/BF/MFC Composite)

The PLA, BF, and liquid-based MFC were put together into water and they were mixed for 15 min. Then, the immersion was filtered under vacuum pressure (0.06 MPa). The sheets obtained on the filter were dried at 105 °C in an electric oven to remove moisture. The obtained sheets were laminated and pressed at 190 °C under 120 MPa pressure for 3 min. Figure 9.5 shows the PLA/BF/MFC composite fabricated through the process.

Five kinds of samples having different MFC contents in weight were prepared to evaluate the effect of weight content of the MFC on the mechanical properties of the composite, as shown in Table 9.2. The content of the PLA was set to 50% in weight.

Figure 9.5 PLA/BF/MFC composite.

Table 9.2 Type of test specimens.

	PLA	BF : MFC	PLA BF MFC
50 : 50 : 0	50	50 : 0	50 50
50 : 45 : 5		45 : 5	50 45 5
50 : 40 : 10		40 : 10	50 40 10
50 : 35 : 15		35 : 15	50 35 15
50 : 30 : 20		30 : 20	50 30 20

in weight

9.3.2
Three-Point Bending Test

Specimens whose dimensions were 1.5 mm thick, 40 mm long, and 3 mm wide, were fabricated to measure the bending properties. The cross-head speed was 2 mm min^{-1} while the span was 30 mm, according to JIS (Japanese Industrial Standard) K7171-1994. The fractured surfaces were also observed by scanning electron microscope (SEM).

9.3.3
Microdrop Test

To evaluate the effect of MFC content on the interfacial shear strength, the microdrop test was conducted at a test speed of 1 mm min^{-1} with the specimen shown in Figure 9.6. The interfacial strength was calculated by Eq. (9.1):

$$\tau_{\text{interface}} = \frac{P}{\pi d l} \tag{9.1}$$

where P, d, and l denote the critical load, nominal diameter of the BF, and the length of embedded BF in the resin, respectively.

9.3.4
Fracture Toughness Test

Critical energy release rate under Mode I loading was also evaluated for the PLA/MFC and PLA/BF/MFC composites. Figure 9.7 shows the dimensions of the specimens for the fracture toughness tests. The critical energy release rate was calculated by Eq. (9.2):

$$\begin{aligned} G &= \frac{1-\nu^2}{E}K^2 \\ K &= \frac{FS}{BW^{3/2}}f(a/W) \\ f(a/W) &= \frac{3(a/W)^{1/2}\left[1.99-(a/W)(1-a/W)\left(2.15-3.93a/W+2.7a^2/W^2\right)\right]}{2(1+2a/W)(1-a/W)^{3/2}} \end{aligned} \tag{9.2}$$

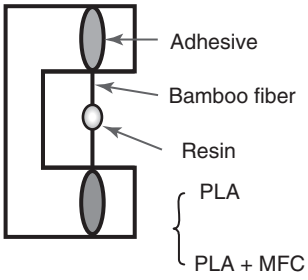

Figure 9.6 Geometry of microdrop test specimen.

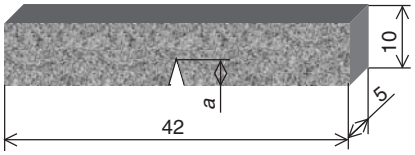

Figure 9.7 Dimensions of fracture toughness test.

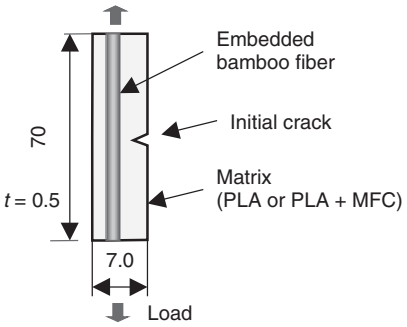

Figure 9.8 Embedded test specimens.

where F, ν, S, B, W, and a denote the critical load, Poisson's ratio, span length, thickness, width, and initial crack length of the specimen, respectively.

9.3.5
Bamboo Fiber Embedded Test

Crack propagation behavior was observed for a special specimen of the PLA/BF and PLA/BF/MFC composite in which a single long fiber was longitudinally embedded in the matrix as shown in Figure 9.8. In this test, constraint strain was applied to the specimen, having initiated transverse crack in the matrix.

9.4
Results and Discussion

9.4.1
Internal State of PLA/BF/MFC Composite

Figure 9.9 shows the internal state and the magnified pictures of some PLA/BF/MFC specimens. It was observed that the BFs were well dispersed in the matrix and the resin-rich regions remarkably decreased for the specimen having an elevated content of the MFC.

9.4.2
Bending Strength of PLA/BF/MFC Composite

Figure 9.10 shows typical stress–strain curves of neat PLA resin, PLA/BF, and PLA/MFC composites. The bending strength and elastic modulus of the PLA/BF

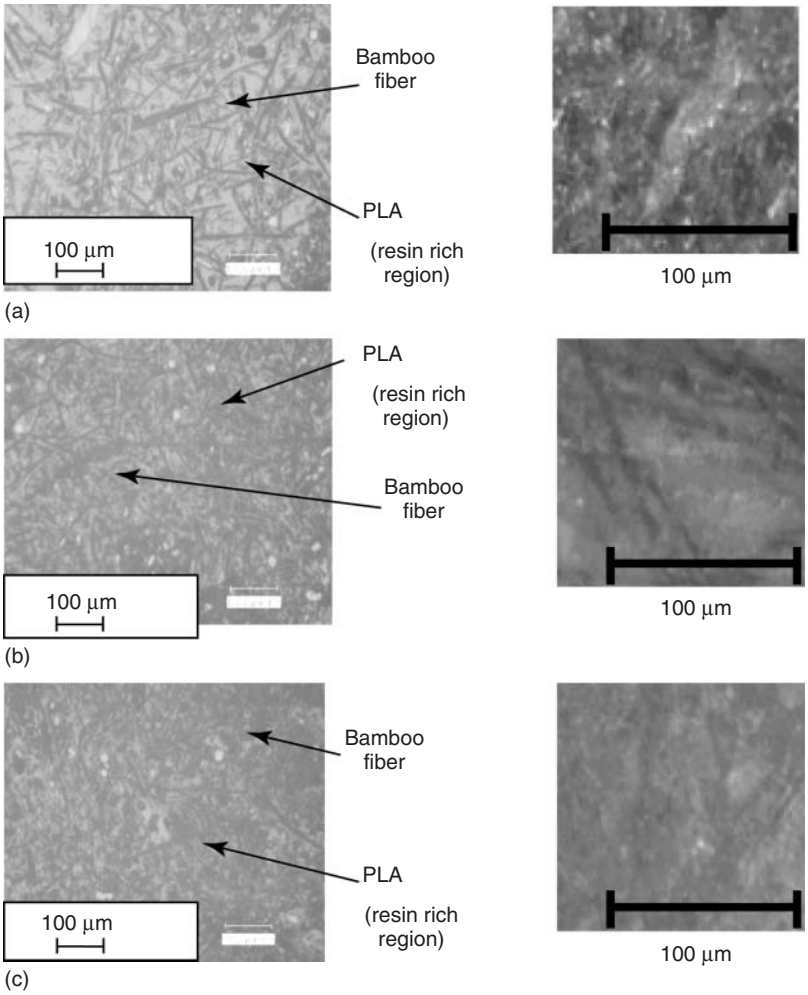

Figure 9.9 Internal state of PLA/BF/MFC composites. (a) PLA : BF : MFC = 50 : 50 : 0, (b) PLA : BF : MFC = 50 : 40 : 10, and (c) PLA : BF : MFC = 50 : 30 : 20.

composite were increased in comparison with those of neat PLA resin. It is confirmed that the BFs reinforce the PLA material. Figure 9.11 shows the bending strengths with respect to the MFC content in weight. If the BF composite (PLA/BF composite) has a small amount of MFC (less than 10% in weight), the strengths were improved on increasing the MFC content. However, the increasing ratio was not significant for the specimen with high content of MFC (over the 10% in weight).

Figure 9.12 shows the fractured surface of the PLA/BF and PLA/BF/MFC composite. Many fiber pullouts were observed in the PLA/BF composite, while a few were found in the fractured surface of the PLA/BF/MFC composite. On the other hand, cohesive failure was observed in the PLA/BF/MFC composite. For

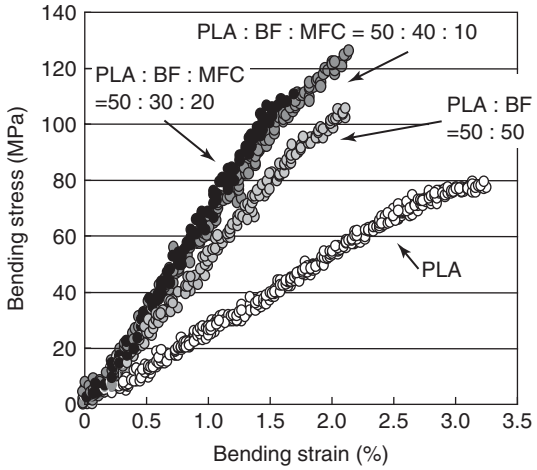

Figure 9.10 Typical stress–strain curves of neat PLA, PLA/BF, and PLA/BF/MFC composite.

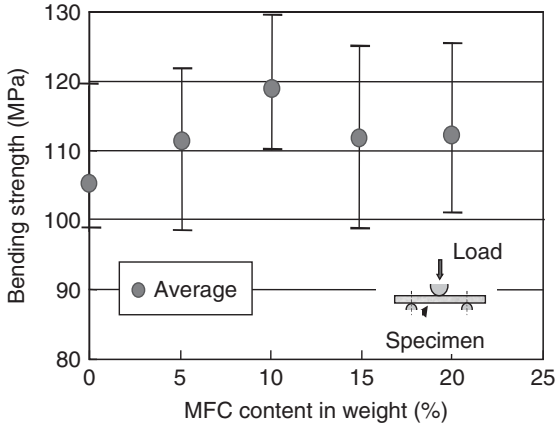

Figure 9.11 Bending strength with respect to MFC contents in weight.

the composite investigated in the current study, interfacial failure determines fatal failure of the PLA/BF composite.

Figure 9.13 also shows interfacial shear strength between fiber and resin, measured by microdrop tests. In this case, the content ratio of the MFC to matrix was 10 : 50 in weight. High interfacial strengths were observed if a small amount of the MFC was added to the resin drop. It was found that enhanced MFC prevents interfacial failure between the BF and resin in the PLA/BF/MFC composite.

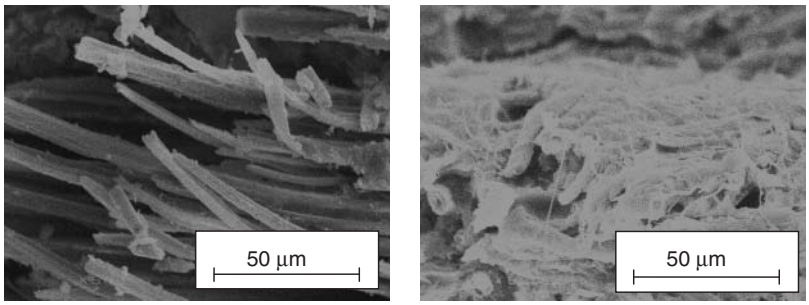

Figure 9.12 Fractured surface after bending test. (a) PLA : BF = 50 : 50 and (b) PLA : BF : MFC = 50 : 40 : 10.

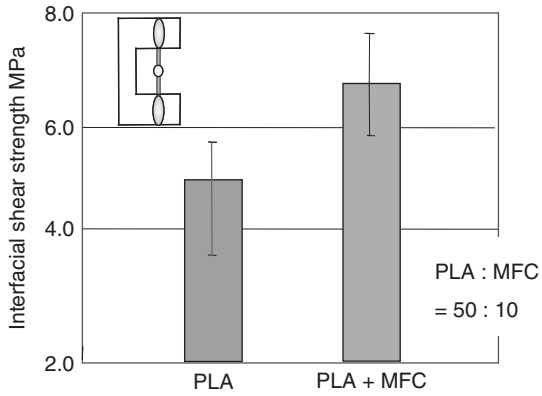

Figure 9.13 Interfacial shear strength.

9.4.3
Fracture Toughness of PLA/BF/MFC Composite

Figure 9.14 shows the result of the fracture toughness test. The critical energy release rate was considerably improved, even when 10% of the MFC in weight was put into the PLA/BF composite.

Figure 9.15a,b also shows the fractured surface after the toughness test for the PLA/BF and PLA/BF/MFC composites, respectively. These results indicate that if a small amount of MFC is put into BF composite, tangled MFC fibers prevent crack growth along the interface between the BF and the resin.

9.4.4
Crack Propagation Behavior

Figure 9.16 shows simply observed behavior of crack propagation in the PLA/BF and PLA/BF/MFC composite, respectively. In the figure, $\varepsilon/\varepsilon_{max}$ denotes the ratio of applied strain to fracture strain of the specimen.

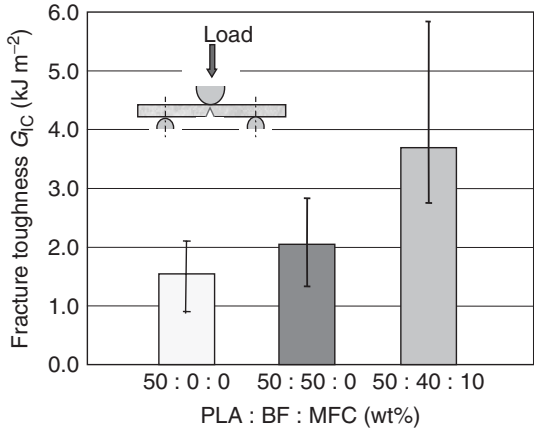

Figure 9.14 Fracture toughness of neat PLA, PLA/BF, and PLA/BF/MFC composite.

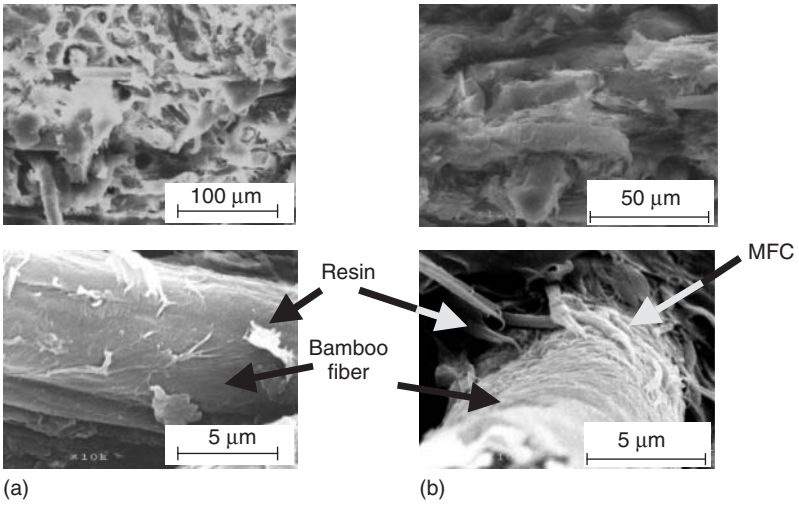

Figure 9.15 SEM photographs of fractured surface after fractured toughness test. (a) PLA/BF composite and (b) PLA/BF/MFC composite.

The initiated crack propagated from the right surface of the specimen in the photograph. As soon as the crack reached the BF, it propagated along the interface between the BF and the matrix in the PLA/BF composite. On the other hand, debonding was not observed even after the crack reached the BF in the PLA/BF/MFC. If the 10% MFC in weight content was used as enhancer, the MFC adequately improved interfacial shear strength because it prevented the crack growth along the interface between the BF and matrix. However, in case of MFC

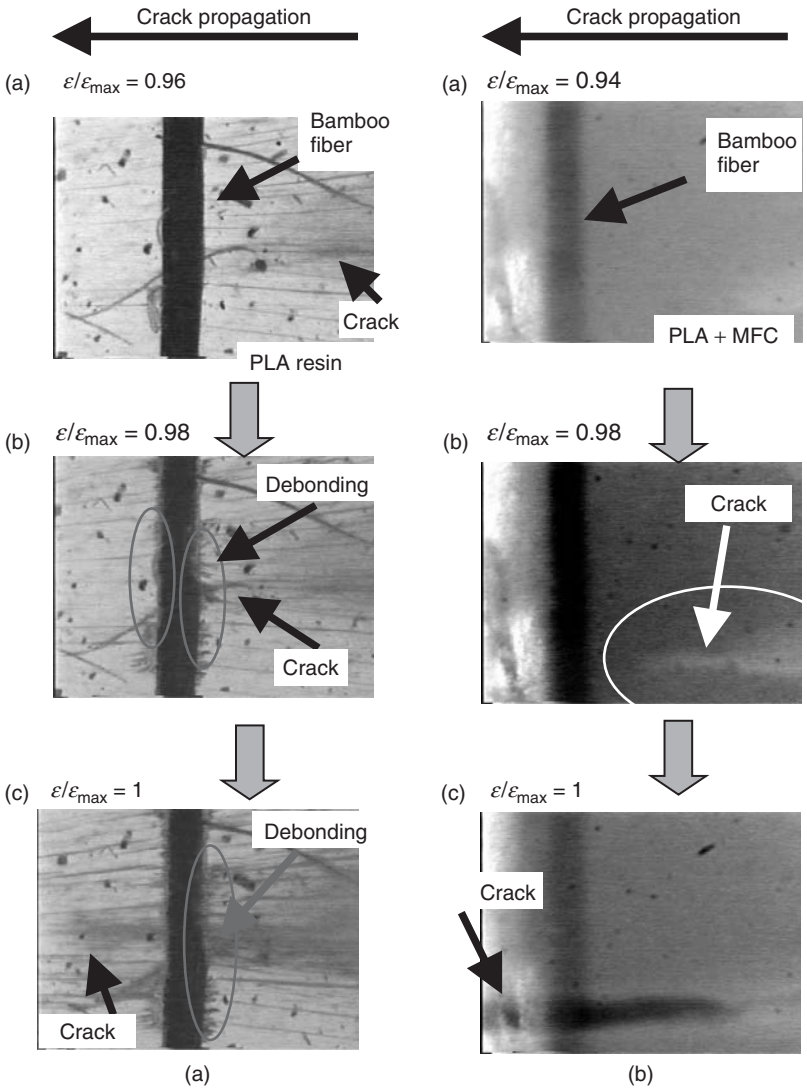

Figure 9.16 Crack propagation process for (a) PLA/BF and (b) PLA/BF/MFC composite.

content exceeding 10% in weight, fiber breakage of the BF might be promoted because a large amount of MFC produced excessive interfacial shear strength compared to that having adequate content. As a result, the bending strength of the PLA/BF/MFC composite has a maximum value at particular content of the MFC.

This paper revealed the existence of adequate MFC content for the BF composite (PLA/BF composite), to improve the mechanical properties.

9.5 Conclusion

In this study, MFC was used as an enhancer for a PLA-based composite using BF to increase mechanical properties such as bending strength and fracture toughness. The effect of weight content of MFC on those mechanical properties was examined.

1) If MFC is used as enhancer in a biodegradable composite reinforced by BF, the bending strength as well as fracture toughness are improved.
2) When a low fraction by weight of MFC is added to the original BF composite (PLA/BF composite), tangled MFC fibers prevent crack growth along the interface between the BF and the resin.

Acknowledgments

This study was supported by the high technology research project on ''Research and Development Center for Advanced Composite Materials'' of Doshisha University and the Ministry of Education, Culture, Sports, Science, and Technology, Japan. This study was possible also because of the contribution from Mr Naoya Yamashita (former graduate student of Doshisha University).

References

1. Shito, T., Okubo, K., and Fujii, T. (2002) Development of eco-composites using natural bamboo fibers and their mechanical properties. *High Perform. Struct. Compos.*, **4**, 175–182.
2. Yamamoto, Y., Okubo, K., and Fujii, T. (2002) Development of eco-composite using bamboo fibers – FRPP using bamboo fibers extracted by the steam explosion method. Proceedings of the International Workshop on Green Compo, Society of Material Science, Japan, pp. 30–34.
3. Tanahashi, M., Takada, S., Aoki, T., Goto, T., Higuchi, T., and Hanai, S. (1982) Characterization of explosion wood. *Wood Res.*, **69**, 36–51.
4. Tanahashi, M., Higuchi, T., Kobayashi, H., Togamura, Y., and Shimada, M. (1985) Characterization and nutritional improvement of steam-explosion wood as ruminant feed. *Cellul. Chem. Technol.*, **19**, 687–696.
5. Shin, F.G., Xian, X.-J., Zheng, W.-P., and Yipp, M.W. (1989) Analysis of the mechanical properties and microstructure of bamboo-epoxy composites. *J. Mater. Sci.*, **24**, 3483–3490.
6. Jain, S., Kumar, R., and Jindal, U.C. (1992) Mechanical behavior of bamboo and bamboo composite. *J. Mater. Sci.*, **27**, 4598–4604.
7. Li, S.H., Fu, S.Y., Zhou, B.L., Zeng, Q.Y., and Bao, X.R. (1994) Reformed bamboo and reformed bamboo/aluminium composite. *J. Mater. Sci.*, **29**, 5990–5996.
8. Jain, S., Jindal, U.C., and Kumar, R. (1993) Development and fracture mechanism of the bamboo/polyester resin composite. *J. Mater. Sci. Lett.*, **12**, 558–560.
9. Rajulu, A.V., Baksh, S.A., Reddy, G.R., and Chary, K.N. (1998) Chemical resistance and tensile properties of short bamboo fiber reinforced epoxy composites. *J. Reinf. Plast. Compos.*, **17**, 1507.
10. Chen, X., Guo, Q., and Mi, Y. (1998) Bamboo fiber-reinforced polypropylene

composites: a study of the mechanical properties. *J. Appl. Polym. Sci.*, **69**, 1891–1899.

11. Gassan, J. and Blendzki, A.K. (1999) Influence of fiber surface treatment on the creep behavior of jute fiber-reinforced polypropylene. *J. Thermoplast. Compos. Mater.*, **12**, 388–397.
12. Goda, K., Gomes, A., Asahi, T., and Yamane, T. (2002) Development of biodegradable natural fiber composites by press forming method. Proceedings of the International Workshop on Green Compo, Society of Material Science, Japan, pp. 8–11.
13. Takagi, H., Winoto, C.W., and Netravali, A.N. (2002) Tensile properties of starch-based green-composites reinforced with randomly oriented discontinuous MAO fibers. Proceedings of the International Workshop on Green Compo, Society of Material Science, Japan, pp. 4–7.
14. Lodha, P. and Netravali, A.N. (2002) Characterization of interfacial and mechanical properties of "green" composites with soy protein isolate and ramie fiber. *J. Mater. Sci.*, **37**, 3657–3665.
15. Osman, K., Skrifvars, M., and Selin, J.–.F. (2003) Natural fibers as reinforcement in polylactic acid (PLA) composites. *Compos. Sci. Technol.*, **63**, 1317–1324.
16. Pothan, L.A. and Thomas, S. (2003) Polarity parameters and dynamic mechanical behavior of chemically modified banana fiber reinforced polyester composites. *Compos. Sci. Technol.*, **63**, 1231–1240.
17. Gomes, A., Matsuo, T., Goda, K., and Ohgi, J. (2007) Development and effect of alkali treatment on tensile properties of curaua fiber green composites. *Composites Part A*, **38**, 1811–1820.
18. Pallone, E.M.J.A., Botta, F.W.J., and Tomasi, R.B. (1999) Alumina–niobium composites. *British Ceram. Proc.*, **58**, 461–462.
19. Elloappan, V., El-aasser, M.S., Klein, A., Daniels, E.S., Roberts, J.E., and Pearson, R.A. (1994) Effect of the core/shell latex particle interphase on the mechanical behavior of rubber-toughened poly(methyl methacrylate). *J. Appl. Polym. Sci.*, **65**, 581–593.
20. Bruneel, E., Degriec, J., van Driessche, I., Hoste, S., and Oku, T. (2002) *Key Eng. Mater.*, **206** (2), 637–640.
21. Thostenson, E.T. and Chou, T.W. (2002) Aligned multi-walled carbon nanotube-reinforced composites: processing and mechanical characterization. *J. Phys. D: Appl. Phys.*, **35**, L77–L80.
22. Thostenson, E.T. and Chou, T.W. (2003) On the elastic properties of carbon nanotube-based composites: modelling and characterization. *J. Phys. D: Appl. Phys.*, **36**, 573–582.
23. Thostenson, E.T. and Chou, T.W. (2001) Advances in the science and technology of carbon nanotubes and their composites: a review. *Compos. Sci. Technol.*, **61**, 1899–1912.
24. Thostenson, E.T. and Chou, T.W. (2005) Nanocomposites in context. *Compos. Sci. Technol.*, **65**, 491–516.

10
Textile Biocomposites

A textile composite reinforced by woven or nonwoven fabrics, knits, or braids is a material of great interest. Conventional textile composites are developed as the combination of various synthetic fibers and resins. On the other hand, material developed by the combination of natural fibers and natural-resource-based resin may be called a *textile biocomposite*. Natural fibers are first changed into bundle form, known as *slivers*, and then spun into a continuous yarn. Spun yarns are often twisted around each other to make a heavier yarn, called a *twisted* or *plied* yarn. Such spun yarns are processed into final textile products such as woven fabrics, knits, and braids. The textile biocomposites described in this chapter are natural-resource-based resin composites reinforced by such spun yarns or textile products. Section 10.1 describes the elastic properties of twisted yarn biocomposites of ramie, and Section 10.2 introduces the development and evaluation of bladed yarn composites made from jute.

10.1
Elastic Properties of Twisted Yarn Biocomposites

Koichi Goda and Rie Nakamura

10.1.1
Introduction

Cellulose-based natural fibers are limited in length, and therefore, in the textile industry, the fibers are spun into a continuous yarn, called a *spun yarn*. Spun yarns are often twisted to obtain a stronger yarn, called a *twisted* or *plied* yarn, which corresponds to the filament yarn of synthetic fibers. Although there is no chemical bond between fibers, each fiber in spun yarn can present its intrinsic strength and stiffness through interfiber friction. Natural fiber twisted yarns can furthermore be controlled in mechanical and other properties by changing the twist number per unit length, for example, twist per inch, and/or the number of spun yarns. Such structural changes in twisted yarns are deeply related to the texture, suppleness, and contraction in textile products, and thus quite important in terms of practical use [1].

Polymer Composite: Volume 3, First Edition.
Edited by Sabu Thomas, Kuruvilla Joseph, S. K. Malhotra, Koichi Goda and M. S. Sreekala.

On the other hand, natural fiber twisted yarns can be embedded in resin and may be applied as reinforcement for composite materials. One such practical natural fiber yarn composite is that of the tire cords for automobile tires, for which cotton fibers were applied in the past, and, nowadays, synthetic fibers such as nylon and polyester are often used. To reduce the environmental impact, natural fiber twisted yarns should positively be applied as reinforcement of a thermoset or thermoplastic resin composite, in place of synthetic yarns. The advantage of the twisted yarns lies in a continuous fibrous structure, which brings higher strength and stiffness to the resultant composite as compared with short natural fiber composites. The magnitudes of strength and stiffness often depend on the twist number per unit length, as mentioned above. The Young's modulus, which is a representative elastic property of twisted yarn composites, is closely related to the twist number [2]. In this section, theoretical models for predicting such elastic moduli of twisted yarn composites are introduced and compared with experimental results of ramie twisted yarn-reinforced biodegradable resin composites.

10.1.2 Classical Theories of Yarn Elastic Modulus

For simplicity, in this section, twisted or filament yarns are denoted as *yarns*, and spun yarns or synthetic fibers are denoted as *fibers*, because these constituents are treated as the same element in theory. Yarn strength and stiffness depend on the degree of twist. However, even if the twist number is the same, the twist angle is not the same when the number of individual fibers is different. Thus, the relation between stiffness and twist angle is of interest in the field of textile engineering, in which an elastic constant called *yarn modulus* is used to denote the magnitude of stiffness, similarly to the Young's modulus in the field of mechanical engineering. In general, the yarn modulus decreases with increasing twist angle. Yarns with a relatively low twist angle behave nonlinearly at the initial stages, as evidenced by the stress–strain diagram. As strain increases, the yarn gradually exhibits a linear behavior because all the fibers sustain the applied load. This is the second stage of the stress–strain behavior, and yarn modulus is often measured in this stage. In this sense, yarn modulus is different from Young's modulus, which is defined at the initial stage.

Gegauff [3] assumed an ideal arrangement of each fiber, as shown in Figure 10.1a, in which the tangent of twist angle θ, that is, fiber orientation angle, is proportional to radius r of the yarn as follows:

$$\tan\theta = \frac{2\pi r}{h} \quad \text{and} \quad \tan\Theta = \frac{2\pi R}{h} \tag{10.1}$$

where, R is the yarn radius, Θ is the twist angle at the yarn surface and h is the yarn length for one turn. Assuming that the yarn does not contract along the radial direction during extension, the cylindrical plane at the radius r shows an open-out structure in Figure 10.1b. Figure 10.1c shows an open-out structure at the radius R. Then, the yarn strain ε_1 along the longitudinal direction is given as $\varepsilon_1 = \delta h/h$.

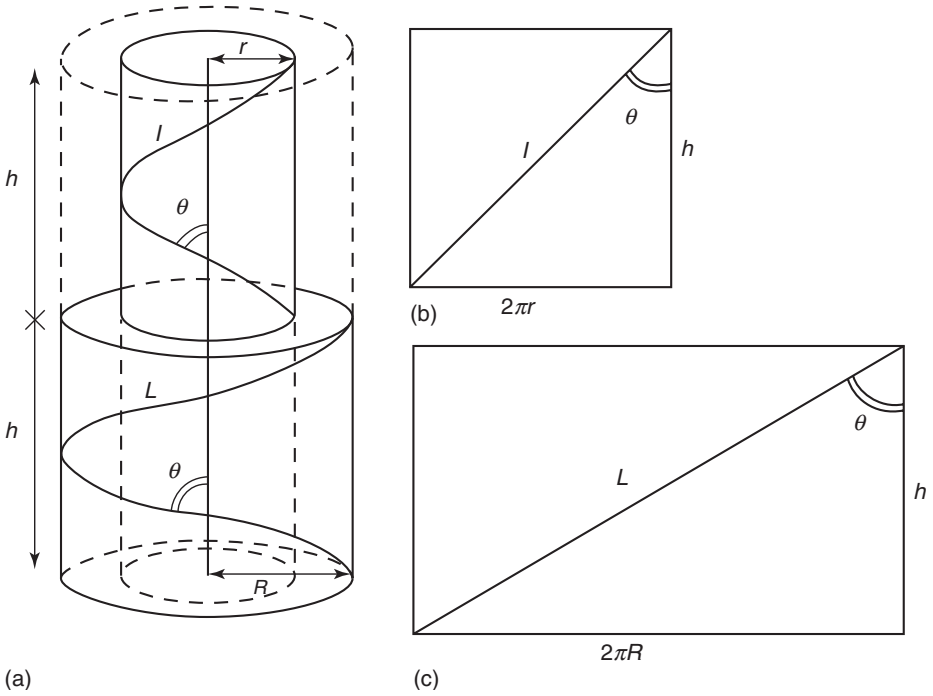

Figure 10.1 Idealized helical yarn geometry. (a) Idealized geometry; (b) ''opened-out'' diagram of cylinder at radius *r*; and (c) ''opened-out'' yarn surface.

Where, δh is an elongation along the longitudinal direction. Since the fiber length l and its elongation δl are given as $h/\cos\,\theta$ and $\delta h \times \cos\,\theta$, respectively, the fiber strain ε_f is $\varepsilon_f = \delta\, l/l = \delta h \cos^2\theta/h$. Thus, the yarn strain is as follows:

$$\varepsilon_1 = \frac{\varepsilon_f}{\cos^2\theta} \tag{10.2}$$

Tensile stress σ_f of the fiber is $\varepsilon_f \times E_f$ (E_f: Young's modulus of the fiber). An equivalent area perpendicular to the fiber axis is given by $2\pi r\mathrm{d}r\,\cos\theta$. Then the component of tensile load parallel to the yarn axis at the radius r is $E_f\varepsilon_f$ ($2\pi r\mathrm{d}r\,\cos\theta$) $\cos\theta = E_f\,2\pi r\mathrm{d}r\,\varepsilon_1\cos^4\theta$. Therefore, integration of $E_f\,2\pi r\mathrm{d}r\,\varepsilon_1\cos^4\theta$ in the range of 0 to R yields the total yarn tensile load Y, through the change of variables, $2\pi r = h\tan\theta$, as follows:

$$Y = \pi R^2 E_f \varepsilon_y \cos^2\Theta \tag{10.3}$$

Then, the yarn modulus $\hat{E}$ is given as by

$$\hat{E} = E_f \cos^2\Theta \tag{10.4}$$

This equation is often called a *power cosine* rule. Thus, the yarn modulus following this model is strongly dependent on the elastic modulus of fibers.

In the above cosine rule, as is obviously seen, the lateral deformation perpendicular to the yarn axis is not taken into consideration. In order to extend the power

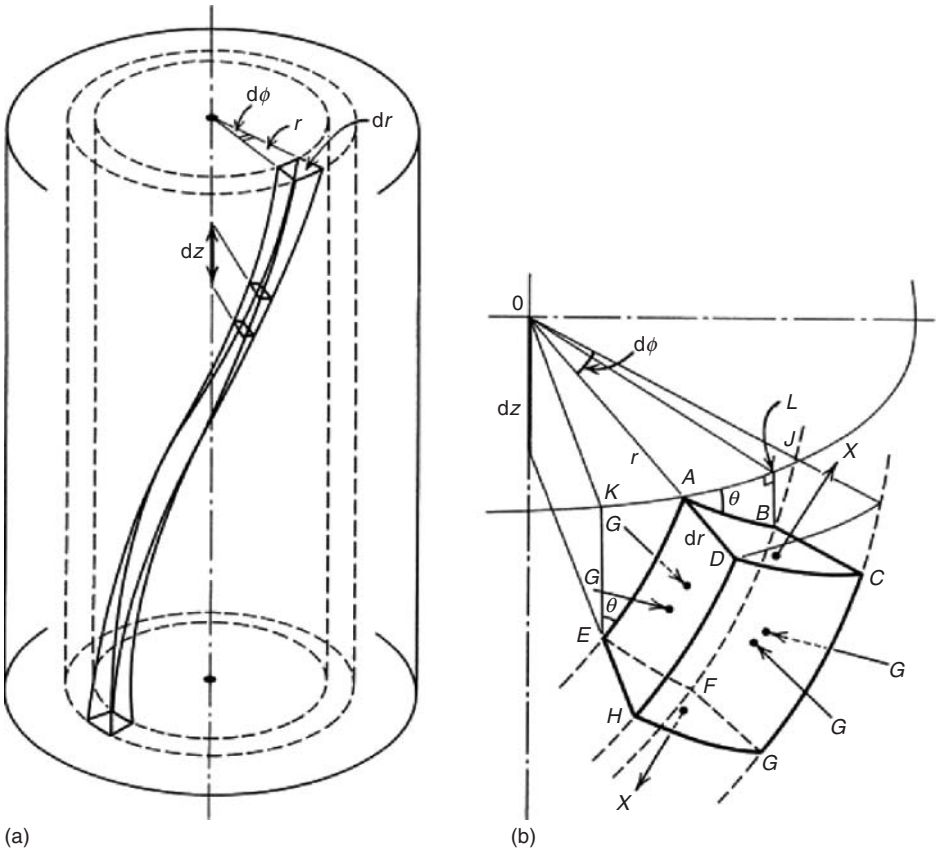

Figure 10.2 (a) Helically twisted yarn showing element by dr, dϕ, and dz. (b) Exaggerated view of element.

cosine rule, Hearle *et al.* [1] introduced the lateral forces applied for an element in the fiber as shown in Figure 10.2. First, they obtained the fiber strain from the yarn strain through coordinate transformation, leading to an equation on the relation between the fiber tensile stress and compressive transverse stress from the stress–strain relation in the fiber. Next, they proposed a force equilibrium equation in the radial direction, in which a radial force resolved from the tensile forces at the fiber axis on the element as well as a radial force resolved from the circumferential direction of the yarn are taken into account. As the above two equations were given as simultaneous differential equations, analytical solutions were obtained as follows:

$$g = \frac{1+\nu_y}{(1+2\nu_1)}\frac{c^2}{u^2}(1-u^{1+2\nu_1}) - \nu_y\frac{1-u^{2\nu_1-1}}{(2\nu_1-1)} \tag{10.5}$$

$$x = \frac{(1+\nu_y)c^2}{(1+2\nu_1)u^2}(1+2\nu_1 u^{1+2\nu_1}) + \nu_y\frac{1-2\nu_1 u^{2\nu_1-1}}{(2\nu_1-1)} \tag{10.6}$$

where, g is the normalized radial stress of the fiber, and x is the longitudinal tensile stress of the fiber. c is cos Θ, and u is the ratio of fiber length l at radius r to fiber length L at radius R, that is, $u = l/L$. ν_y is the Poisson's ratio of the yarn and ν_1 is the axial Poisson's ratio of the fiber. By integrating the force components parallel to the yarn axis derived from Eqs. (10.5) and (10.6), the mean normalized stress $\overline{\sigma}_{yarn}$ is obtained as follows:

$$\overline{\sigma}_{yarn} = \frac{2c}{(1+2\nu_1)(1-c^2)}\left\{\left(1+\nu_y\right)\left[\ln c + \frac{2\left(1+\nu_1\right)}{1+2\nu_1}(1-c^{2\nu_1+1})\right] - \frac{\nu_y}{2}\left[\frac{3\left(1+2\nu_1\right)}{2\nu_1-1} - \frac{4(1+\nu_1)}{2\nu_1-1}c^{2\nu_1-1} - \frac{1}{c^2}\right]\right\} \tag{10.7}$$

By multiplying the elastic modulus of the fiber by Eq. (10.7), the yarn modulus $\hat{E}$ is obtained. When $\nu_y = \nu_1 = 0.5$, Eq. (10.7) is simplified as

$$\overline{\sigma}_{yarn} = \frac{1}{4} + \frac{9}{4}c^2 + \frac{3c^2}{1-c^2}\ln c \tag{10.8}$$

Hearle *et al.* also complemented Platt's model and listed several patterns of yarn moduli, as shown in the pages 196–197 of Ref. [1]. The above model proposed by Hearle *et al.* was analytically solved under the condition that radial and circumferential stresses perpendicular to the fiber axis are equal. Although this condition is not correct necessarily, the derived solution given by Eq. (10.8) is in good agreement with many experimental data, as shown in Figure 10.3.

10.1.3
Orthotropic Theory for Twisted Yarn-Reinforced Composites

10.1.3.1 Yarn Modulus Based on Orthotropic Theory

It is difficult to apply the orthotropic theory to a twisted yarn consisting of natural fiber-spun yarns or filament yarn consisting of carbon or aramid fibers, because these posses a strong anisotropy. In this section, the same terms, namely, *yarns* for twisted or filament yarns and *fibers* for spun yarns or synthetic fibers, are used. The whole modulus of elasticity of a yarn is gradually affected by the transverse modulus of the fiber with increasing twist angle; as a result, it does not agree well with experimental data because the fiber is treated as an isotropic body in the above-mentioned theories. Anisotropy also appears in a composite reinforced with yarns, so an anisotropic model has been newly developed in the field of textile composites. According to Madhavan and Naik [4] and Rao and Farris [5], the yarn composite is regarded as a column, composed of thin cylindrical layers, as shown in Figure 10.4. Each fiber is placed in the layer with the angle θ, which increases with increasing radius r of the column. According to the orthotropic theory, the stress–strain relation of a lamina is given by

$$\begin{Bmatrix}\sigma_x\\ \sigma_y\\ \tau_{xy}\end{Bmatrix} = [\overline{Q}_{ij}]\begin{Bmatrix}\varepsilon_x\\ \varepsilon_y\\ \gamma_{xy}\end{Bmatrix} \tag{10.9}$$

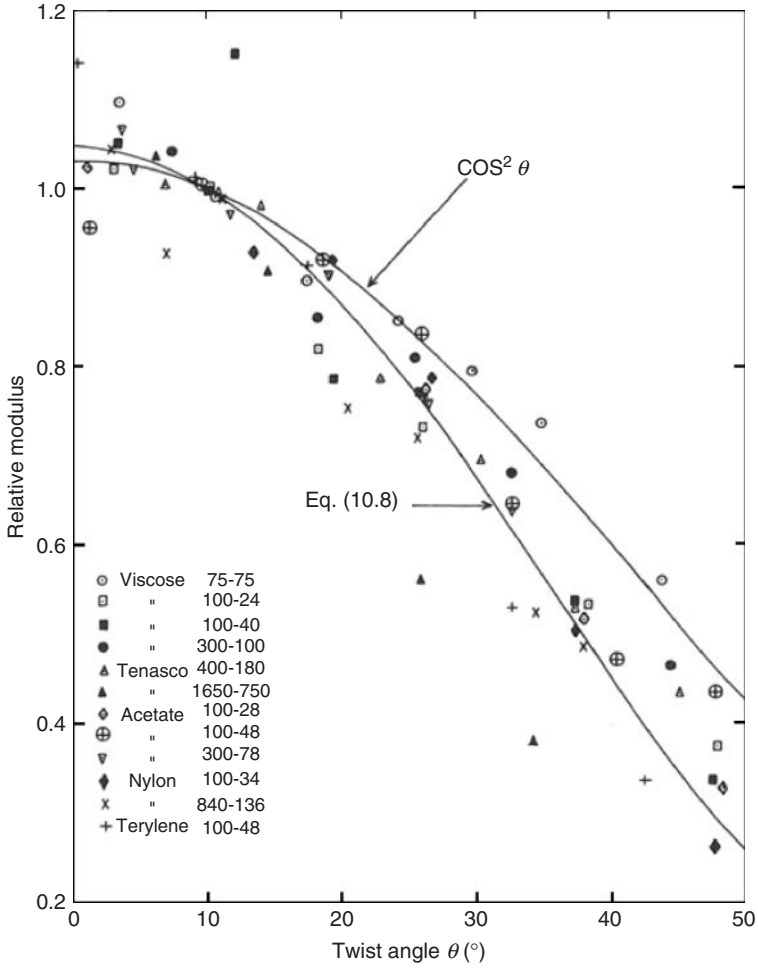

Figure 10.3 Comparison of experimental values of modulus with theoretical relations, namely, $\cos^2\Theta\,\alpha$ from Eq. (10.4) and Eq. (10.7) with $\nu_1 = 0.5$ and $\nu_y = 0.5$, i.e. Eq. (10.8) [1]. (Note: According to our calculation, both $\cos^2\Theta$ and Eq. (10.8) approach to 1.0 with decreasing twist angle Θ.)

where, $\overline{Q}_{ij}$ ($i = 1, 2, 3$ and $j = 1, 2, 3$) are the reduced stiffness, each of which is given from material constants and an angle θ, that is,

$$\overline{Q}_{11} = l^4 Q_{11} + 2l^2 m^2 (Q_{12} + 2Q_{66}) + m^4 Q_{22}$$
$$\overline{Q}_{22} = m^4 Q_{11} + 2l^2 m^2 (Q_{12} + 2Q_{66}) + l^4 Q_{22}$$
$$\overline{Q}_{66} = l^2 m^2 (Q_{11} + Q_{22} - 2Q_{12}) + (l^2 - m^2)^2 Q_{66}$$
$$\overline{Q}_{12} = l^2 m^2 (Q_{11} + Q_{22} - 4Q_{66}) + (l^4 + m^4) Q_{12}$$
$$\overline{Q}_{16} = -l^3 m (2Q_{66} - Q_{11} + Q_{12}) + l m^3 (2Q_{66} - Q_{22} + Q_{12})$$

$$\overline{Q}_{26} = -lm^3(2Q_{66} - Q_{11} + Q_{12}) + l^3m(2Q_{66} - Q_{22} + Q_{12}) \tag{10.10}$$

where, $l = \cos\theta$, $m = \sin\theta$ and

$$\begin{aligned} Q_{11} &= \frac{E_1}{1 - \nu_{12}\nu_{21}} \\ Q_{22} &= \frac{E_2}{1 - \nu_{12}\nu_{21}} \\ Q_{12} &= \frac{\nu_{12}E_2}{1 - \nu_{12}\nu_{21}} = \frac{\nu_{21}E_1}{1 - \nu_{12}\nu_{21}} \\ Q_{66} &= G_{12} \end{aligned} \tag{10.11}$$

The yarn composite is thus modeled by concentrically piling up each lamina. By considering the transformed reduced stiffness and the area of each lamina, a new

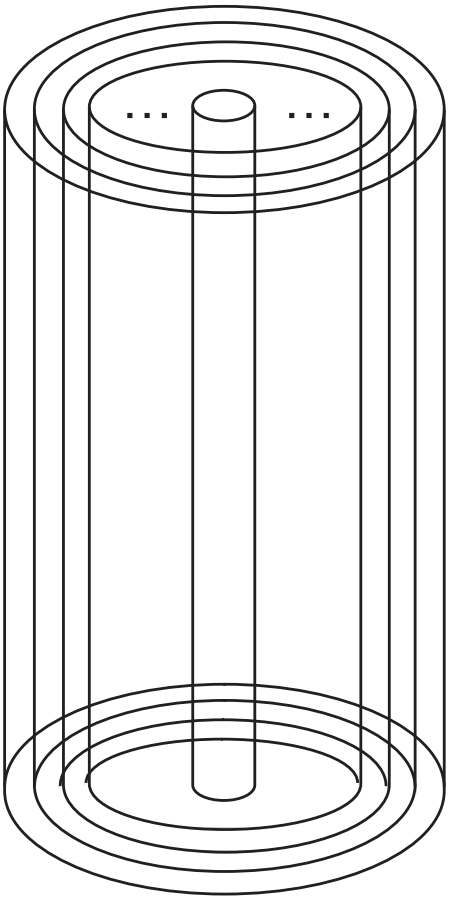

Figure 10.4 Cylindrical model for twisted yarn composite.

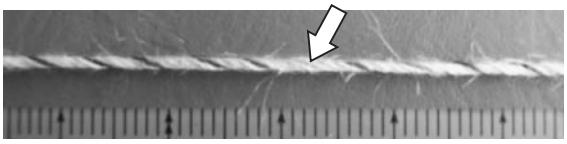

Figure 10.5 Migration in a ramie twisted yarn.

reduced stiffness for the twisted yarn is proposed as follows [4]:

$$\begin{Bmatrix} \sigma_x \\ \sigma_y \\ \tau_{xy} \end{Bmatrix} = \left[\frac{1}{\pi R^2} \int_0^R \overline{Q}_{ij}(\theta)\, 2\pi r dr \right] \begin{Bmatrix} \varepsilon_x \\ \varepsilon_y \\ \gamma_{xy} \end{Bmatrix} \tag{10.12}$$

This stiffness is termed the *two-dimensional off-axis reduced stiffness* for twisted yarn, because each lamina is loaded in-plane. According to the ideal twist geometry, the twist angle is given as a function of the radius r of the laminated cylinder as shown in Eq. (10.1) or as follows:

$$\tan\theta = \tilde{r}\tan\Theta$$

where $\tilde{r} = r/R$. The fiber orientation angle θ is expressed as a function of r, as follows:

$$\theta = \tan^{-1}(\tilde{r}\tan\Theta) \tag{10.13}$$

Through the above ideal relation, the Young's modulus of the lamina can be obtained as an exact solution [5] (see Box 10.1). On the other hand, actual fibers migrate irregularly inward and outward in a yarn, so that the relation between θ and r is more complicated. As shown in a single yarn colored black in Figure 10.5 (see the arrow), this means that each constituent is irregularly placed along the yarn axis in a complicated path, because they occupy their position at the site of lower mechanical energy during twisting process. This is the ''migration.''We consider, because of this phenomenon, the relation between r and θ is not actually given as Eq.(10.13). According to Nakamura *et al.* [6], the relation between θ and r is determined experimentally through a power-law function as:

$$\theta = \Theta\,\tilde{r}^{\beta} \tag{10.14}$$

where, β is a constant, experimentally obtained. Equation (10.14) agrees approximately with Eq. (10.13) when $\Theta \ll \pi/2$ and $\beta = 1$. Equation (10.12) can numerically be calculated by substituting Eq. (10.12). Finally, Young's modulus of the lamina can be obtained from the inverse form of Eq. (10.14) under the condition $\sigma_y = \tau_{xy} = 0$.

10.1.3.2 Relation between Mechanical Properties and Twist Angle

To validate the ''two-dimensional off-axis reduced stiffness'' described in Section 10.1.3.1, Nakamura *et al.* [6] fabricated ramie twisted yarn-reinforced biodegradable resin matrix composites through a compression molding method. According to this study, the single yarn used was a ramie single yarn (No. 5, supplied

Table 10.1 Tensile properties of unidirectional composites with various yarn twist angles.

Matrix type	Yarn type	Volume fraction (%)	Young's modulus (GPa)	Tensile strength (MPa)	Fracture strain (%)	E/V_f (GPa)	σ/V_f (MPa)
CPR	SY	41.1	16.7	187.5	1.76	40.6	456.1
	ST	47.6	16.9	237.8	1.63	35.5	500.1
	MT	53.8	11.7	196.7	2.90	21.9	365.6
	LT	34.7	6.09	104.6	2.06	17.6	301.4
PLA	SY	40.0	20.9	194.4	1.65	47.7	486.0
	ST	47.0	19.6	201.7	2.04	41.7	373.6
	MT	41.3	16.7	170.9	2.11	40.5	414.4
	LT	52.3	15.6	172.7	2.51	29.8	340.7

by TOSCO Co., Japan) and two types of biodegradable resin, cornstarch-based resin (CPR) and polylactic acid (PLA), were used. Table 10.1 shows tensile test results for the composites. In this table, twisted yarns of 0, 1.5, 3.5 and 6.5/inch are denoted as SY, ST, MT and LT. Thus, the spun yarn-reinforced composite means a composite reinforced with twistless yarns (zero twist angle), while LT has the largest twist angle with the yarn axis. These data clearly indicate that the normalized Young's moduli (E/V_f) of CPR and PLA composites decrease with increasing twist angles. In addition, the Young's modulus of PLA composites is higher in the all-yarn types than that of CPR composites. Regarding tensile strength, its value decreases with an increase in the twist angle of both CPR and PLA composites except for SY composites, of which the normalized strengths (σ/V_f) are slightly lower than that of ST composites. Fracture strains of CPR and PLA composites tend to increase with an increase in twist angle.

Elastic constants, E_1, E_2, and υ_{12} used in the calculation were obtained from the tensile test of SY composites along 0° and 90° directions. Shear modulus G_{12} was estimated through the following equation:

$$G_{12} = \frac{1}{\frac{4}{E_{45}} - \frac{1}{E_1} - \frac{1}{E_2} + \frac{2\upsilon_{12}}{E_1}} \tag{10.20}$$

where, E_{45} is the elastic modulus obtained from the tensile test of SY composites along 45° direction. The above elastic constants are listed in Table 10.2.

Table 10.2 Elastic constants used in the calculation.

	CPR composite	PLA composite
Longitudinal elastic E_1 (GPa)	16.7	20.9
Transverse elastic modulus E_2 (GPa)	1.98	3.77
Poisson's ratio υ_{12}	0.4	0.3
Shear modulus of elasticity G_{12} (GPa)	0.71	1.33

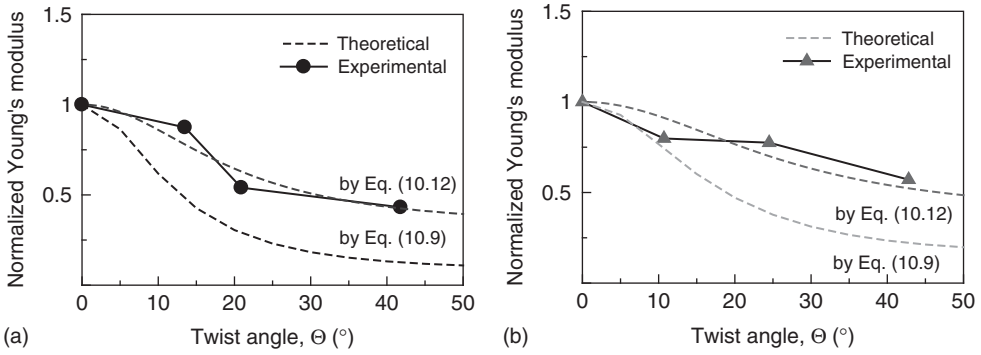

Figure 10.6 Relations between twist angle and normalized Young's modulus of (a) CPR composites, and (b) PLA composites.

Once a relation between θ and r as in Eq. (10.14) is obtained, the Young's modulus of the twisted yarn composites can be calculated numerically from Eq. (10.12), on the basis of the elastic constants in Table 10.2. Thus, β was decided to be 1.87 as a fitting curve to Young's modulus data plots of CPR composites, as shown in Figure 10.6(a). Figure 10.7 shows the plots for fiber orientation angle versus the distance r from the center of twisted yarn. The results indicate that the angle θ changes largely when close to the surface area of twisted yarns. This physical meaning is that an inner single yarn nearer to the center runs with a smaller angle along the axis, but an outer single yarn nearer to the surface runs with a larger angle. Thus, the composite with a larger twist angle Θ yields a lower Young's modulus.

Next, the Young's modulus of a PLA composite was calculated using $\beta = 1.87$ in the same way as that of CPR composites. The elastic constants used are listed in

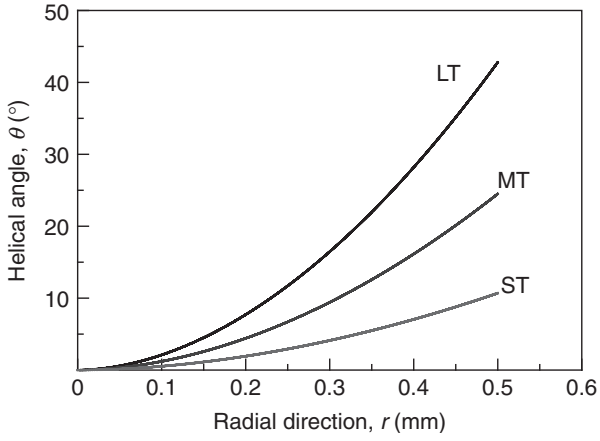

Figure 10.7 Distribution of fiber orientation angle (helical angle) of single yarn in twisted yarns.

Table 10.2. The result calculated from Eq. (10.9) is illustrated by the broken line in Figure 10.6(b). As seen in this figure, the line seems to be fitting the experimental results, that is to say, an estimation of the single yarn orientation angle as given in Eq. (10.14) is suitable to calculate the Young's modulus. It is concluded that the Young's modulus can be predicted through two-dimensional off-axis reduced stiffness for twisted yarn composites.

10.1.3.3 Extension of Theory to Off-Axis Loading

Two-dimensional off-axis reduced stiffness for twisted yarn was developed to "three-dimensional reduced stiffness." As described earlier, if the migration structure in the twisted yarn is stationary along the yarn axis, in other words, the yarn axis is the same as the loading axis, the Young's modulus can be calculated through Eq. (10.14) as the orientation angle of each cylindrical element is invariable.

When the twisted yarn leans against the loading axis at an angle ψ, the orientation angle of single yarns to the loading axis varies along the circumferential direction as well as the radial one, as shown in Figure 10.8. Hereinafter, ψ is denoted as off-axis angle. Under this condition, the single yarn orientation angles to the loading axis change along the circumferential direction at each cylindrical element. As a result, the three-dimensional off-axis reduced stiffness for twisted yarn composites is given as

$$\begin{Bmatrix} \sigma_x \\ \sigma_y \\ \tau_{xy} \end{Bmatrix} = \left[\frac{1}{\pi} \int_0^{\pi} \frac{1}{\pi R^2} \int_0^{R} \overline{Q}_{ij}(\psi)\, 2\pi r \mathrm{d}r \mathrm{d}\eta \right] \begin{Bmatrix} \varepsilon_x \\ \varepsilon_y \\ \gamma_{xy} \end{Bmatrix} \tag{10.21}$$

where, ϕ is the relative orientation angle, which is the angle between the loading axis and the single yarn orientation, and η is a variation of the angle along the circumferential direction of the twisted yarn, which is divided into a fine element $\mathrm{d}\eta$. As known from Eq. (10.21), the three-dimensional off-axis reduced stiffness is expressed by the integration of the two-dimensional off-axis reduced stiffness from 0 to π. ϕ is estimated by the geometric relation of a tetrahedron as

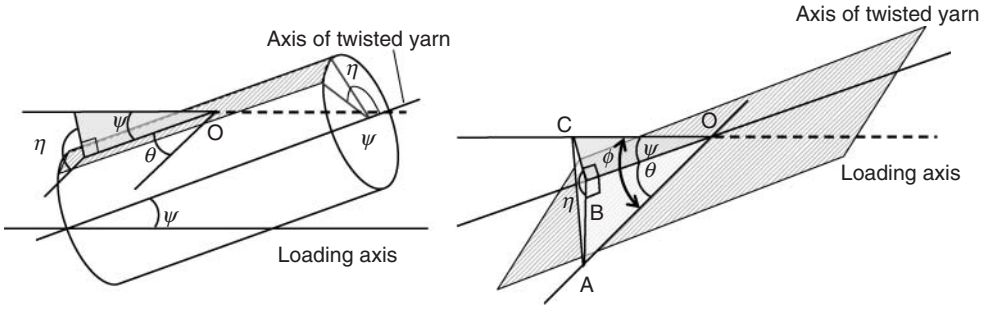

Figure 10.8 Schematics of relationship between off-axis angle and twist angle of a longitudinal yarn.

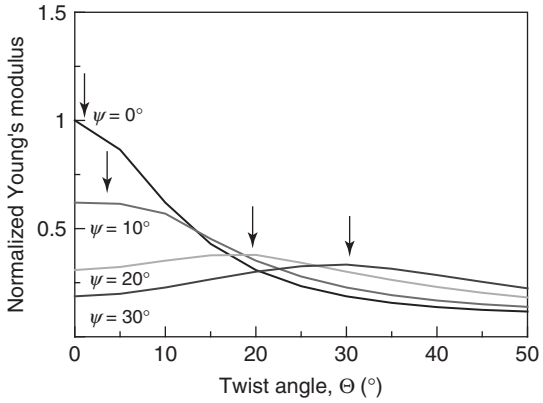

Figure 10.9 Relationship between Young's modulus of off-axis angle and twist angle, without taking account Eq. (10.14) (CPR composite).

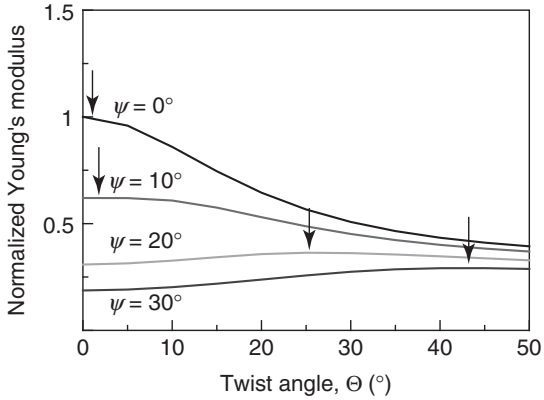

Figure 10.10 Relationship between Young's modulus of off-axis angle and twist angle, taking account Eq. (10.14) (CPR composite).

follows:

$$\phi = \cos^{-1}\{\cos\theta(r)\cos\psi + \sin\theta(r)\sin\psi\cos\eta\} \ldots \tag{10.22}$$

The results considered without and with Eq. (10.14) are respectively shown in Figure 10.9 and Figure 10.10. In the former, the orientation angle is given as $\theta{=}\Theta$. When the off-axis angle is the same as the twist angle, the peak of the modulus tends to appear, as shown in Figure 10.9 because the single yarn is oriented along the loading axis. On the other hand, this tendency is not observed in Figure 10.10 because various relative orientation angles act on the twisted yarn. It is found from Figure 10.10 that every Young's modulus tends to converge approximately on a constant, as ψ increases. At 30° off-axis angle, the Young's modulus increases

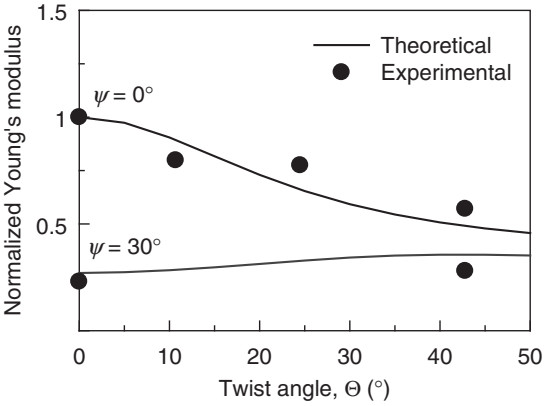

Figure 10.11 Comparison between theoretical and experimental values in PLA composites.

gradually with increase in twist angle. In other words, even if twisted yarns in a composite are placed under the condition of a large off-axis angle, the Young's modulus is expected to be improved by choosing an optimal twist angle.

As shown in Figure 10.11, the theoretical and experimental results were compared at 30° off-axis angle. As can be seen, the Young's modulus of PLA composites is in good agreement with the theoretical results. Thus, it is concluded that the Young's modulus can be predicted through three-dimensional off-axis reduced stiffness for twisted yarn composites.

Box 10.1 (According to reference [5]. The twist angle Θ is here denoted as α.)

In case only the stress σ_x is working at an off-axis composite lamina with the angle θ, under the condition $\sigma_y = \tau_{xy} = 0$, the strain ε_x is given as follows:

$$\varepsilon_x = \overline{S}_{11} \cdot \sigma_x \tag{10.15}$$

The modulus of elasticity of the off-axis composite lamina is then estimated as

$$\frac{\varepsilon_x}{\sigma_x} = \overline{S}_{11} = \frac{1}{E(\theta)} = \frac{l^4}{E_1} + \frac{m^4}{E_2} + \left(\frac{1}{G_{12}} - \frac{2\nu_{12}}{E_1}\right) l^2 m^2 \tag{10.16}$$

The off-axis angle θ in each lamina is corresponding to the twist angle, if we change it to the shape of a thin cylinder. According to the ideal twist geometry, the twist angle is given as a function of the radius r of the laminated cylinder as shown in Eq. (10.1). By taking account of Eq. (10.1) and integrating Eq. (10.16), the modulus of elasticity E of the twisted yarn composite is given as

$$E = \frac{2}{\tan^2 \alpha} \int_0^{\alpha} \frac{1}{S_{11}} \tan\theta \sec^2\theta \, d\theta \tag{10.17}$$

After integration, an exact solution is obtained as

$$E(\alpha) = \frac{1}{\tan^2\alpha}\left[\frac{b}{2c^2}\ln\frac{(a+b+c)\,T_0^2}{(aT_0^2+bT_0+c)} - \frac{T_0-1}{cT_0} + \frac{(b^2-2ac)}{2c^2\sqrt{b^2-4ac}}\ln\frac{(2a+b-\sqrt{b^2-4ac})\times(2aT_0+b+\sqrt{b^2-4ac})}{(2aT_0+b-\sqrt{b^2-4ac})\times(2a+b+\sqrt{b^2-4ac})}\right] \tag{10.18}$$

where,

$$T_0 = \cos^2\alpha, \quad a = \frac{1}{E_z} + \frac{1}{E_y} - \frac{1}{E_s} + \frac{2\nu_{yz}}{E_z},$$

$$b = \frac{1}{E_s} - \frac{2}{E_y} - \frac{2\nu_{yz}}{E_z}, \quad c = \frac{1}{E_y}$$

They also obtained the approximation solution given as

$$\text{Yarn modulus, } \hat{E}(\alpha) = E_z \times \left[\left(\frac{3T_0+1}{2dT_0}\right) + \frac{(1-d)^2}{d^3\tan^2\alpha}\ln\frac{(1-d)T_0+d}{T_0}\right] \tag{10.19}$$

10.1.4 Conclusion

Natural fibers are often used as reinforcement of green composites, but morphology of the fibers is a short filament which sustains a lower load in a resin, as compared to long fibers. Thus, single and plied (twisted) yarns composed of natural fibers produced in textile industry, are expected as reinforcement with a continuous morphology in the research of biocomposites. In the field of textile engineering, the relation between elastic moduli of the fiber and yarn has been clarified. In this section, therefore, we focused on the relation between elastic properties of single and twisted yarn composites. Both yarns and yarn composites decrease in elastic modulus with an increase in twist angle. However, each theoretical model introduced in this section is clearly different in a point that the orthotropic and lamination theories are a basis of yarn composite models, while the conventional textile models assume an isotropy for the fiber and yarn. This means, elastic properties of textile biocomposites are discussed under the theoretical system of general composite materials. On the other hand, modeling of yarn morphology is undoubtedly based on knowledge of textile engineering. Thus, although we are likely to face various mechanical issues in the development of textile biocomposites in the near future, these can be solved through the fields of textile engineering as well as composite engineering.

10.2
Fabrication Process for Textile Biocomposites

Asami Nakai and Louis Laberge Lebel

10.2.1
Introduction

Continuous natural fiber-reinforced thermoplastic composites have excellent mechanical properties compared with short fiber-reinforced thermoplastic composites. However, the impregnation of the resin into the fiber bundle is difficult because of the high melt viscosity of the thermoplastic resin compared to thermosetting material. Especially for the fiber assembly of textile biocomposite such as woven, knitted, and braided fabrics, macroscopic flow of resin through the surface of the fabrics is the dominant rather than the microscopic flow of resin as impregnation into the fiber bundle. To solve this problem, various intermediate materials like the preimpregnated tape, or intermediate yarn precursors such as the powder-impregnated yarn, the commingled, yarn and the microbraided yarn (MBY) have been developed.

In this section, intermediate materials are introduced, which can be applied to the fabrication process for textile biocomposites. By combining the textile technique for making intermediate materials and textile reinforcements, the textile biocomposite was realized. Incorporation of jute fibers into PLA resin has been previously carried out with good impregnation quality and mechanical properties, using compression molding of MBYs [7]. This concept was applied into the manufacturing of a Jute/PLA L-shaped beam using the braid-trusion method. This method combines the braiding preforming technique to the pultrusion process to produce multiaxially reinforced continuous beams [8]. A geometrical model is first presented and used to understand the phenomena involved in the braid-trusion experiments.

10.2.2
Intermediate Materials for Continuous Natural Fiber-Reinforced Thermoplastic Composites

Figure 10.12 shows a schematic of the preimpregnated tape structure. This material allows the manufacture of products with complete impregnation, good fiber alignment, and uniform distribution using short molding cycles. However, the high stiffness of the preimpregnated tape restricts their application to flat or simply curved parts. Moreover, the cost of preimpregnated tape is generally prohibitive [9].

This method simply uses a reinforcement fabric sandwiched between thermoplastic films as shown in Figure 10.13. The composite material is consolidated by applying pressure and temperature. This method is attractive because of its simplicity and the availability of matrix films. However, the preforms have low drapeability and the process is difficult to apply to complex shapes. It should consider the stacking between reinforcement and thermoplastic film as well as

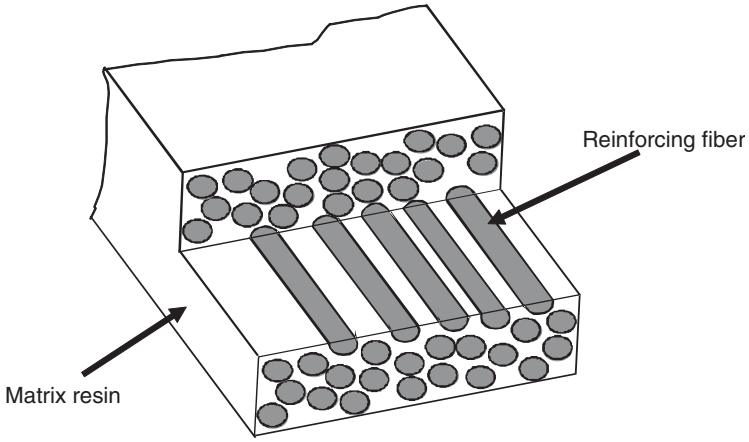

Figure 10.12 Schematic drawing of preimpregnated tape.

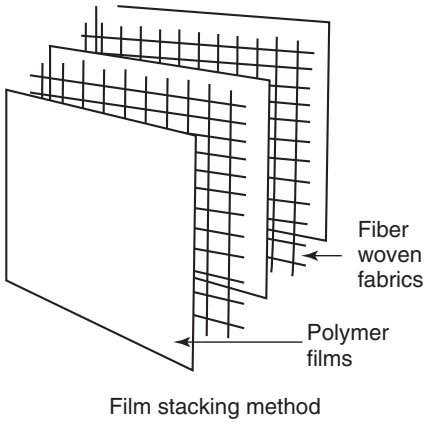

Figure 10.13 Schematic drawing of film-stacking method.

impregnation of resin into the reinforcement fiber. The impregnation distance is in the order of millimeters, which is quite large for thermoplastic matrices, leading to difficulties in impregnation [10, 11].

To overcome the drawbacks of preimpregnated tape or film stacking, intermediate fibers for continuous fiber-reinforced thermoplastic composites have been developed. Intermediate fibers have flexibility and are developed for textile applications. As shown in Figure 10.14, the powder-impregnated yarn contains fibers impregnated with fine thermoplastic particles [12–16]. The incorporation of the matrix powder into the reinforcement yarn is performed by the fluidized-bed

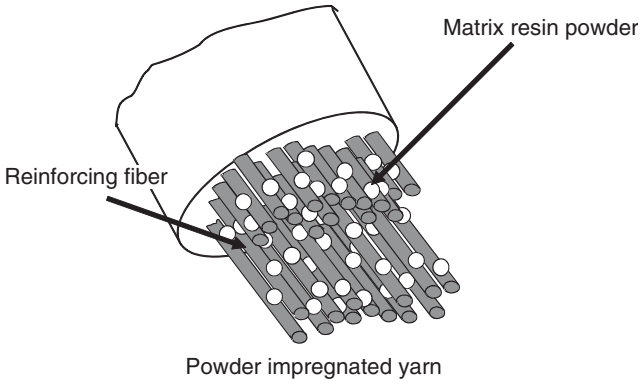

Figure 10.14 Schematic drawing of powder-impregnated yarn.

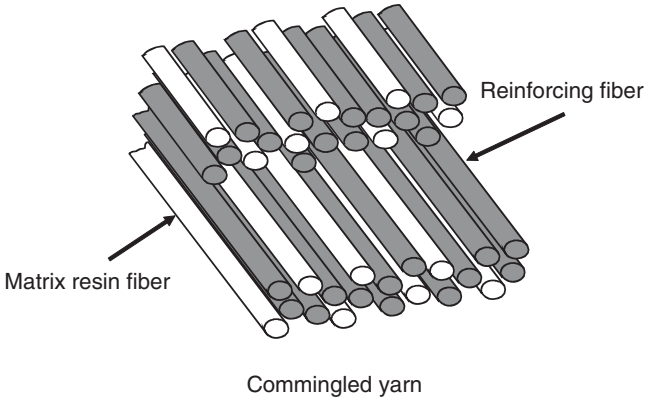

Figure 10.15 Schematic drawing of commingled yarn.

or fluid-slurry methods. A yarn preform can then be manufactured using weaving, knitting, or braiding. The advantage of powder-impregnated yarns is the versatility of the fiber/matrix combination because of the wide availability of thermoplastic powders. However, it is difficult to control the powder distribution. Moreover, owing to higher friction of particles, the textile process is quite difficult.

Figure 10.15 shows schematic of the commingled yarns. This yarn is a mix of reinforcement and matrix filaments at desired fiber volume content [17–26]. The commingled yarn provides a high degree of fiber/matrix mixing, resulting in a short impregnation distance in the order of micrometers. The commingled yarn is also flexible and exhibits low friction. However, the reinforcing fibers are usually damaged during the process of mingling and filaments can be damaged during further processing such as weaving or braiding. Availability also makes commingled yarns and fabrics a difficult choice when dealing

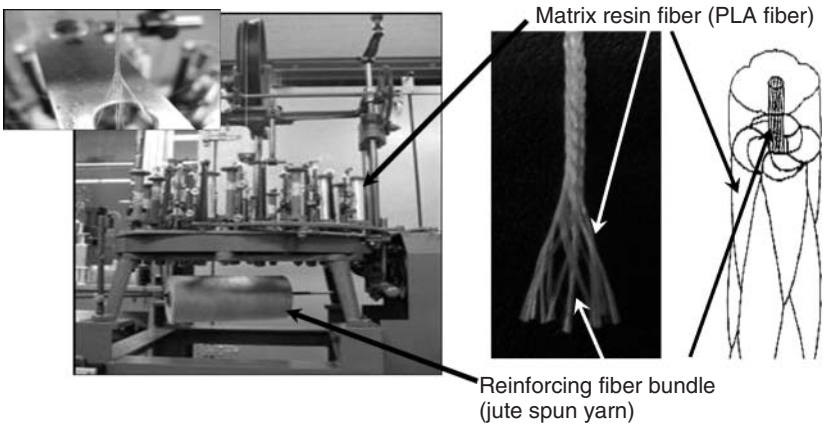

Figure 10.16 Schematic drawing and photograph of microbraided yarn.

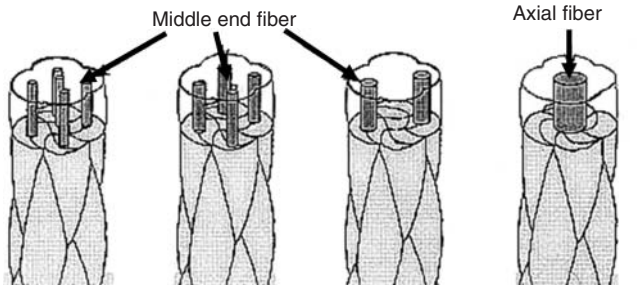

Figure 10.17 Types of microbraided yarn.

with thermoplastic composites owing to the scarcity of matrix/reinforcement combinations on the market and the high cost of the commingled form of material.

The MBY has been developed on the basis of the traditional braiding technique [27–29]. MBY, as shown in Figure 10.16, is fabricated by a tubular braiding machine without damaging the reinforcing fiber bundles. In the microbraiding process, the reinforcement fiber bundle is directly inserted and the matrix resin fiber bundles are braided around it. Since resin fibers are located adjacent to the reinforcement fiber bundle, better impregnation during melt molding is expected. Various types of MBY can be fabricated as shown in Figure 10.17. The impregnation distance and the degree of fiber dispersion can be easily controlled by changing the number and location of the reinforcing yarns. Moreover, MBY is preferred in textile process because of its high drapeability, excellent handling ability, and better protection for the reinforcing fibers than is available for the other types of intermediate fibers during manufacture and further preforming operations such as woven fabric, braided fabric, and knitted fabric (see Figure 10.18).

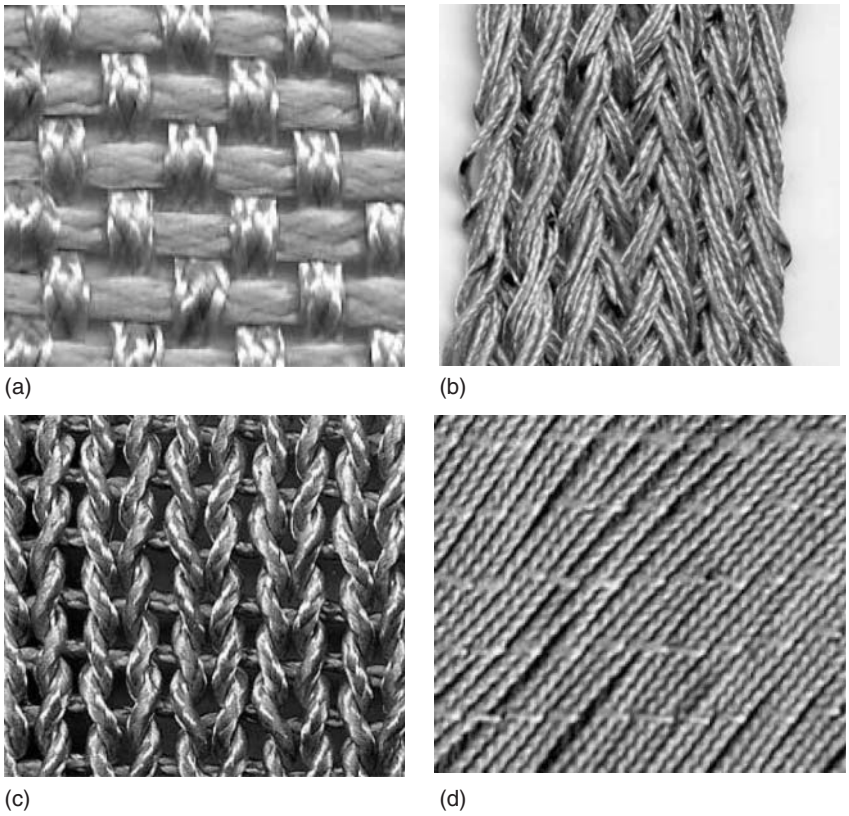

Figure 10.18 Application of microbraided yarn to textile. (a) Woven fabric, (b) flat braided fabric, (c) plain knitted fabric, and (d) multiaxial warp knitted fabric.

10.2.3
Braid-Trusion of Jute/Polylactic Acid Composites

10.2.3.1 Braid Geometry

The three-axial, tubular, braided fabric possesses yarns continuously spiraling along the braid axis, which are known as the *braiding yarns* (*BYs*). The BYs are divided into two sets intertwined in opposite directions along the braid axis. Another set of yarns, called the *middle-end yarns* (*MEYs*), are laid inside the braid along the axis direction and are locked in by the two sets of BYs. Finally, a third set of yarns, called the *core yarns* (*CYs*) can be placed inside the braid along the braid axis. All the yarns are assumed to have an elliptic cross-section characterized by a width and a thickness (a_Y, b_Y). In the regular braided fabric, each BY continuously passes under two other yarns and then over two yarns of the opposing set. Figure 10.19 shows the braid architecture and a representation of the BY path.

The pitch length (p) is the distance for one BY to execute a complete rotation around the braid axis (see Figure 10.19a). The BY orientation is found using the

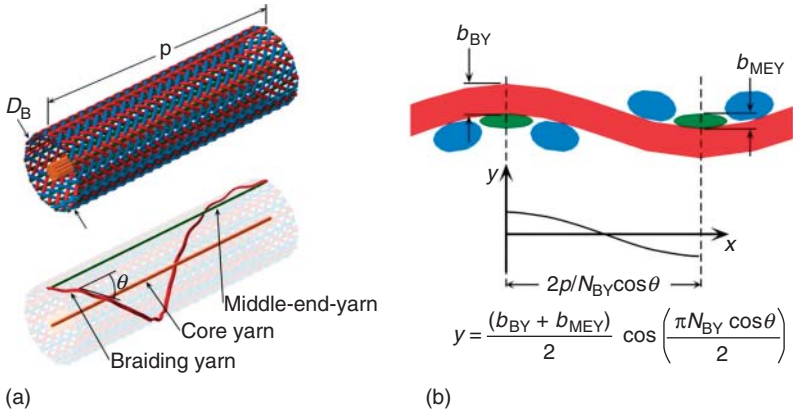

Figure 10.19 Braid architecture: (a) Localization of the braiding yarn, middle-end yarn, and core yarn for one pitch length. (b) The fiber path for one braid plait is represented by a cosine.

pitch length and the braid diameter (D_B) (Eq. (10.23)).

$$\theta = \arctan\left(\frac{\pi D_B}{p}\right) \tag{10.23}$$

One repeat of the braid fabric along the braid axis is called a *plait* [30]. For a regular braid, the plait length is calculated according to Eq. (10.24).

$$l_{pl} = \frac{2p}{N_{BY}} \tag{10.24}$$

Figure 10.19b shows the BY path in one braid plait projected onto the braid angle. The BY path is assumed here to be constituted by a cosine. The cosine part can then be expressed using (Eq. (10.25)).

$$y = \frac{(b_{BY} + b_{MEY})}{2} \cos\left(\frac{\pi B_{BY} \cos\theta}{2}\right), \quad \text{with } 0 \le x \le = \frac{2p}{N_{BY}\cos\theta} \tag{10.25}$$

The maximum crimp angle α is calculated at the middle plait length from the derivative of the BY cosine path, as shown by Eq. (10.26).

$$\alpha = \arctan\left(\frac{N_{BY}}{4p}(b_{BY} + b_{MEY})\,\pi\cos\theta\right) \tag{10.26}$$

The length of the cosine braiding yarn centerline (L_{BY}) can be calculated using numerical integration. The crimp ratio of the BY can be calculated using the length cosine braiding yarn path divided by the straight plait length projected on the braid angle direction (Eq. (10.27)).

$$R_c = \frac{L_{BY}\ N_{BY}\ \cos\theta}{2p} \tag{10.27}$$

It is generally accepted that the specific volume of the yarns inside the fabric remains constant, but the cross-section dimensions of the yarn are assumed to

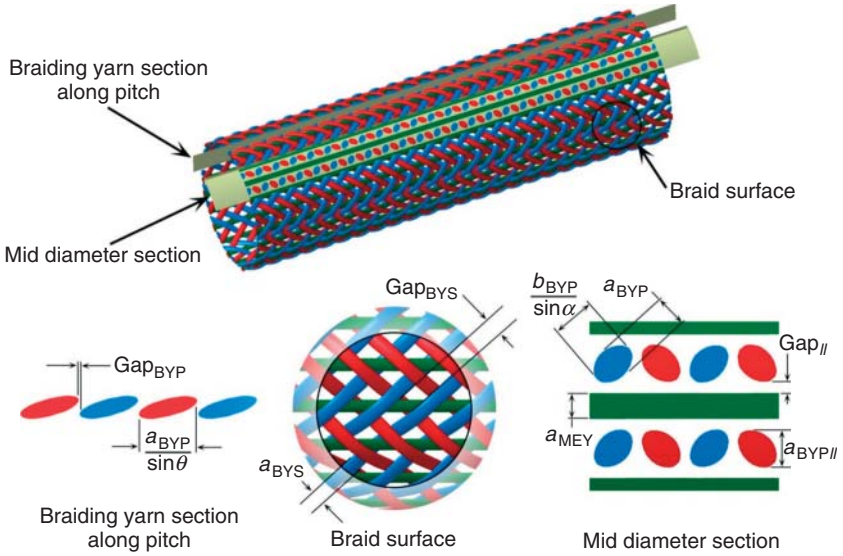

Figure 10.20 Description of the gaps between yarns in the braid.

vary depending on its position inside the fabric [31]. The dry yarn cross-section area (S_Y) can be found using the material properties and can also be calculated by the equation of an ellipse. In Eq. (10.28), the parameter R_{YComp} is the yarn fiber packing and is assumed here to be 0.7.

$$S_Y = \frac{A_Y}{R_{YComp}} = \frac{\pi a_Y b_Y}{4} \tag{10.28}$$

Owing to the constraints applied on one fiber by the fibers surrounding it, the cross-section dimensions of one braiding yarn will change depending on its position in the braid. The constraints applied on one yarn are from several sources such as tension, bending, and friction. Several models, based on the energy minimization, have been developed to calculate the yarn deformations and positions inside a fabric [32, 33]. However, the approach chosen here will be purely geometric and rely on the critical points inside the braid where the yarns are subjected to contact themselves. At these critical points, the yarn cross-section dimensions will be modified in the event of a contact. Figure 10.20 describes the critical points inside the braided fabric.

The first critical gap is situated along the braid axis on a plane that cuts the BYs between the MEYs. This gap depends on the width of the BY situated at mid-diameter (a_{BYP}), the pitch, the number of BY, and the braiding angle. This gap is calculated by the following equation

$$\text{Gap}_{BYP} = \frac{p}{N_{BY}} - \frac{a_{BYP}}{\sin\theta} \tag{10.29}$$

The second critical pitch separates the BYs at the surface of the braid and depends on the BY width at surface (a_{BYS}), the braid angle, and the pitch divided by half of

the amount of BYs. This gap is calculated by Eq. (10.30).

$$\mathrm{Gap}_{\mathrm{BYS}} = \frac{2p}{N_{\mathrm{BY}}} - \frac{a_{\mathrm{BYS}}}{\sin\theta} \tag{10.30}$$

The third gap describes the separation between the BYs and MEYs at the braid diameter. This gap depends on the BYs crimped section projected on the cylindrical surface having a diameter equal to the braid mid-diameter. This BY section has a width equal to the BY width at pitch, but the perpendicular direction is the BY thickness at pitch (b_{BYP}) projected on the crimp angle. This gap is the difference between the circumference of the braid divided by half the number of BYs, the width of the MEY, and the distance between two parallel lines enclosing the crimped section of the BYs ($a_{\mathrm{BYP}//}$ in Figure 10.20). The following equation (10.31) is used to calculate the parallel gap ($\mathrm{Gap}_{\mathrm{BY}//}$).

$$\mathrm{Gap}_{\mathrm{BYP}//} = \frac{2\pi D_{\mathrm{B}}}{N_{\mathrm{BY}}} - a_{\mathrm{MEY}} - \frac{2}{\sqrt{\frac{1}{\left(\frac{a_{\mathrm{BYP}}}{2}\right)^2 \cos^2\theta + \left(\frac{b_{\mathrm{BYP}}}{2\cos\alpha}\right)^2 (1-\cos^2\theta)}}} \tag{10.31}$$

These three gaps can be used to calculate yarn cross-section dimensions using calculation software. The necessary initial data are the braid diameter and the pitch and the maximum yarn widths and minimum thickness for both the BYs and the MEYs. The algorithm converges on yarns dimensions at the surface and along the pitch direction using the three gaps as limitations. If one of the calculated gaps has a negative value, the dimensions of the yarns involved in the calculation of that particular gap are modified, and all the braid geometry is recalculated using the new values. This loop is repeated until the yarn dimension does not significantly change from one calculation step to another.

As the cross-sectional area of the BYs on the plane perpendicular to the braid axis changes depending on the projection plan position, the cross-sectional area will be taken as the volume of material in one pitch length normalized by the pitch length, as calculated by Eq. (10.32).

$$A_{\mathrm{B}} = \sum_{i=1}^{n} \left(\frac{N_{\mathrm{BY},i} A_{\mathrm{BY},i} R_{\mathrm{c},i}}{\cos\theta} + N_{\mathrm{MEY},i} A_{\mathrm{MEY},i} + N_{\mathrm{CY},i} A_{\mathrm{CY},i} \right) \quad \text{for } n \text{ layers} \tag{10.32}$$

The factors influencing the area of material inside the braided preform are the total cross-sectional area ($A_{\mathrm{BY}}, A_{\mathrm{MEY}}, A_{\mathrm{CY}}$) of the yarn filaments, the number of yarns in each layer (N_{BY}, N_{MEY}, N_{CY}), the braid angle (θ), and the crimp ratio (R_{C}), for the n layers. The yarn filament total cross-sectional area is calculated using the fineness (G, in tex or grams per kilometer) divided by the density (ρ) of each of the constituents of the yarns.

$$A_{\mathrm{Y}} = A_{\mathrm{f}} + A_{\mathrm{m}} = \frac{G_{\mathrm{f}}}{\rho_{\mathrm{f}}} + \frac{G_{\mathrm{m}}}{\rho_{\mathrm{m}}} \tag{10.33}$$

When compressed inside the pultrusion die, the thickness of the braid, and so the amplitude of the BY cosine path, will reduce. However, the pitch length and

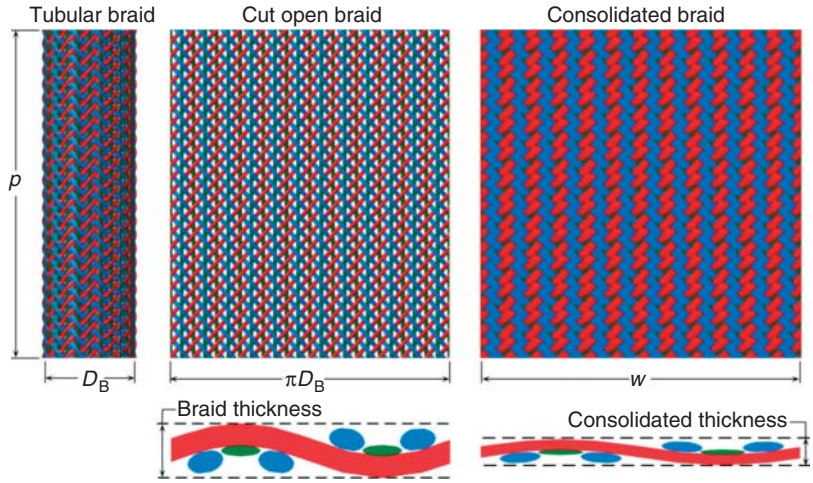

Figure 10.21 Expansion of the circumference of the consolidated braid over the braid perimeter value upon consolidation in the pultrusion die.

the BY length will usually stay the same. This causes the braid to spread along its circumferential direction inside the die. This expansion phenomenon of the braid circumference is shown in Figure 10.21.

Calculation software is again needed to find this consolidated braid circumference (w). The BY and MEY thicknesses are first found by multiplying the yarn thicknesses in the braid by the compression ratio, that is, the consolidated braid divided by the braid thickness. Then, the BY consolidated length is calculated for a given consolidated beam angle. This length is compared to the BY length in the braid. If the error is significant, the consolidation circumference (w) is modified, which will change the consolidated braid angle. These calculations are repeated until the BY consolidated length in the plate is equal to the BY length in the braid.

The fiber volume content calculation of the pultruded product is obtained by a development similar to Eq. (10.32), that is, the total material volume normalizes the reinforcement volume for one pitch length and is adjusted with the fill ratio R_F. The fill ratio is the ratio of the area of the braid (Eq. (10.32)) over the die exit area. Note that the angle θ is the consolidated BY angle.

$$V_f = \sum_{i=1}^{n} \left(\frac{N_{BY,i} A_{f,\ BY,i} R_{C,i}}{\cos\ \theta} + N_{MEY,i} A_{f,MEY,i} + N_{CY,i} A_{f,\ CY,i} \right) \frac{R_F}{A_B} \quad \text{for } n \text{ layers} \tag{10.34}$$

10.2.3.2 Experiments

10.2.3.2.1 Yarns

Jute fiber tows were mixed with PLA fibers in a parallel hybrid yarn configuration. The jute fiber tow ($\rho_j = 1.44$ g cm^{-3}, Bangladesh Janata Jute Mills Ltd) is a

discontinuous filament spun yarn having a fineness of ~400 tex. The PLA fibers ($\rho_{PLA} = 1.59$ g cm^{-3}, 84T-26-LA10, Toray) were continuous fibers originally in a tow configuration. The first type of parallel hybrid yarn was obtained by mixing two jute fiber tows together with a 1120 tex PLA tow to obtain a jute weight ratio of ~42%. The second type of parallel hybrid yarns was obtained by mixing only one jute fiber tow together with a 602 tex PLA tow to obtain a jute weight ratio of ~40%. Finally, a glass fiber yarn ($\rho_G = 2.5$, DWR1150F-165, Nippon Electric Glass Co. Ltd) having a fineness of 1150 tex was also used. Five yarns of each of the material types were sandwiched between two 1 mm thick microscope glass slides to measure their average thickness and width in a compressed state. Strong pressure was applied with hands on the top slide and the sandwich thickness was locked with transparent tape. The width of the yarns was measured from top-view photographs of the sandwiched yarns by image analysis software (ImageJ). The thickness was measured with a caliper.

10.2.3.2.2 Braiding

All braids were done using 48 braiding yarns (BY) and 24 MEYs in a regular braid arrangement with a 48-carrier circular braiding machine. The braids were done using a 40 mm braiding ring without using a mandrel. The braider rotation speed was 1.74 rpm and the pulling speed was adjusted to obtain an outside diameter of around 35 mm. Table 10.3 lists the four different preforms braided with different material configurations. The two first preforms (No. 1 and 2) were braided using only jute/PLA yarns. The two last preforms were braided with glass fiber MEY. The four preforms had different arrangement of layers. Preform no. 1 and 3 used two

Table 10.3 Braiding conditions for the four pultruded preforms.

Numbers	Braiding yarns	Middle-yarns	Core yarns	Layer quality	Layer configuration	Pitch	Outside diameter
	Quantity, materials, and fiber/matrix fineness			—		(mm)	(mm)
1	48 Jute/PLA yarns 800 tex/1120 tex	24 Jute/PLA 800 800 tex/1120 tex	None	2	Superposed Bottom Top	 223 223	 35 ± 2 31 ± 1
2	48 Jute/PLA 400 tex/600 tex	24 Jute/PLA 800 tex/1120 tex	35 Jute/PLA 800 tex/1120 tex	1	—	112	38 ± 1
3	48 Jute/Pla yarns 800 tex/1120 tex	24 Glass 1150 tex	None	2	Superposed Bottom Top	 223 223	 33 ± 1 33 ± 1
4	48 Jute/Pla yarns 800 tex/1120 tex	24 Glass 1150 tex	None	2	Concentric Inside Outside	 278 223	 23 ± 2 40 ± 1

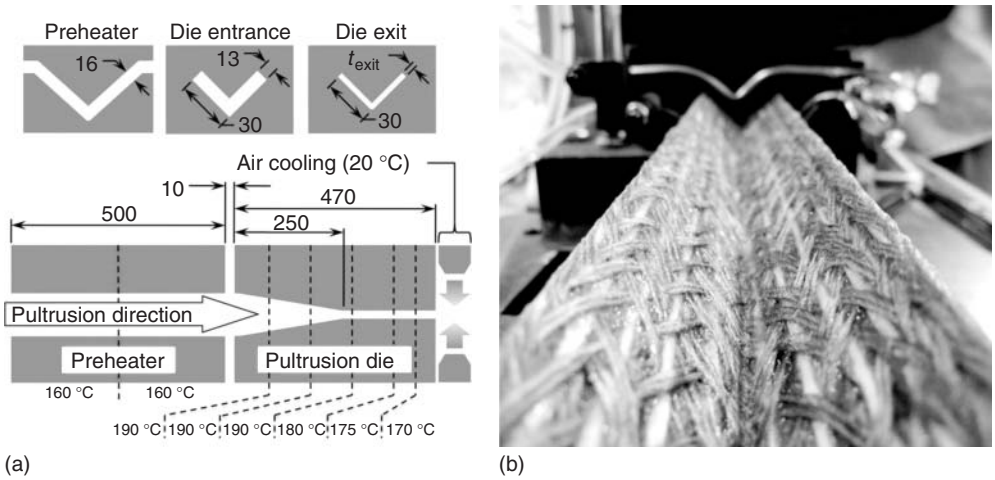

Figure 10.22 (a) Pultrusion die system. Dimensions are in millimeters. (b) Pultruded beam at die exit.

braids braided separately that were flattened and placed on top of each other. The preform no. 2 used only one layer with 35 CYs placed inside the braid. The preform no. 4 used two layers braided one over the other. The braids' outside diameter was calculated from the external circumference, which was measured by smoothly wrapping a tape over the braided preform right after the braiding operation. The braiding pitch was measured as the distance along the braid axis for one fiber to make a complete revolution.

10.2.3.2.3 Pultrusion

Figure 10.22 shows the schematic of the pultrusion die assembly, consisting of the preheater, the pultrusion die, and an air blower placed at the die exit. Before the pultrusion step, the preforms were dried overnight at 40 °C in a convection oven. The circular braided preforms were flattened and pulled through the forming assembly by a pulling machine at a speed of ~30 mm min^{-1}.

The die "*L*" thickness was large at the consolidation die entrance and gradually reduced in the 250 mm taper region until a constant thickness of 3 mm was reached in fully closed configuration. However, all the pultrusion experiments were started with a die exit "*L*" thickness opening of ~6.7 mm and gradually reduced every 25 mm of pultruded beam. The whole system had eight separate heating zones. The preheating temperature was set to be slightly under the melting point of the PLA (165 °C). The entrance region was set to the processing temperature of 190 °C. Toward the end of the pultrusion die, the set temperature was decreased to 170 °C. An air-cooling system was used to quench the pultruded material surface immediately after exit from the die.

After pultrusion, the pitch was measured on the beams as having the length of 24 surface yarns along the beam axis direction. Rectangular coupons of 20 mm × 60 mm were cut from each pultruded beam for three-point bending

Table 10.4 Yarn characterization results.

Materials	Fiber/matrix fineness (tex)	Width at maximum ratio (mm)	Thickness at maximum ratio (mm)	Compressed aspect ratio (mm^2)
Jute/PLA	800/1120	4.7 ± 4	1.12 ± 0.05	4.2
Jute/PLA	400/602	3.2 ± 0.6	0.8 ± 0.1	4.0
Glass	1150/0	4.4 ± 0.3	0.15 ± 0.03	29.3

testing (55R4206, Instron) with a span of 48 mm according to ASTM D790 standard. The constant speed of testing was set to 1 mm min^{-1}. The cross-section images of all the pultruded beams were acquired with a microscope (PME3, Olympus) equipped with a digital camera (Powershot A540, Canon).

10.2.3.3 Results and Discussion

The measurements done on the compressed yarns are presented in Table 10.4. The glass fiber is easily deformed under compression to reach a high aspect ratio.

The pultrusion of preform no. 1 was early interrupted owing to jute/PLA MEY breakage inside the pultrusion die when the "*L*" thickness was reduced from 6.7 to 6.1 mm. The pultrusion of preform no. 2 also interrupted for the same reason when the "*L*" thickness at exit was reduced to 4.0 mm

The pultrusion no. 3 and 4 were performed without problems with a final "*L*" thickness of 3.2 mm. In both experiments, the closing of the dies was stopped because of apparent jute/PLA braiding yarn breakage that was observed on the beams after the die exit. Table 10.5 shows all the measurements of the beams after pultrusion.

In an attempt to understand the breakage of the preform no. 1 and 2, useful braid and beam dimensions can be calculated from the braid model presented here and are presented in Table 10.6. The braid angle and braid thickness are

Table 10.5 Pultrusion results.

Numbers	Die exit "L" thickness (mm)	Die exit area (mm^2)	Pitch of surface fibers (mm)	Thickness (mm)	Bending modulus (GPa)	Bending strength (MPa)	Note
1	6.1	328	n/a	n/a	n/a	n/a	Interrupted because of MEY breakage
2	4.0	223	n/a	n/a	n/a	n/a	Interrupted because of MEY breakage
3	3.2	181	239 ± 5	3.6 ± 0.2	5.7 ± 0.5	143 ± 20	Successful
4	3.2	181	201 ± 5	4.02 ± 0.08	5.9 ± 0.1	155 ± 17	Successful

Table 10.6 Calculation of braid and consolidated beam properties.

Numbers	Layer position	Braid angle (°)	Braid thickness (mm)	Consol. braid thickness (mm)	Composite ratio	Available width in die (mm)	Layer consolidated width (mm)	Die exit fill ratio	Fiber volume content
1	Bottom	24	2.75	1.53	1.80	113.88	110.60	0.60	0.26
	Top	21	3.00	1.52	1.80	113.92	102.09		
2	Only one	45	1.9	1.26	1.60	114.96	116.67	0.54	0.23
3	Bottom	23	2.18	0.80	2.75	116.8	103.15	0.86	0.45
	Top	23	2.18	0.80	2.75	116.8	103.15		
4	In	26	2.08	0.75	2.77	111.05	111.75	0.93	0.49
	Out	28	1.98	0.75	2.64	116.98	123.3		

first shown for different layers of the preforms. The second calculated value is the consolidation braid thickness – that is, the final thickness that each braided layer occupies in the beam when the beam exits the die. The compression ratio is the braid thickness divided by the consolidated braid thickness. The available width in the die is the perimeter of the consolidated cross-section midline for a certain layer. The consolidation width is the circumference of the braid when compressed to the consolidated braid thickness, for a constant pitch (see w in Figure 10.21). The die exit fill ratio and the fiber volume content are the ratio of the area of material and the area of fibers on the die exit area, respectively.

The consolidated braid thickness and the compression ratio gives information on the space available for the BY and MEY in the thickness of the beam. Pultrusions no. 1 and 2 had much larger space for the braiding yarns in the beam than no. 3 and 4. The scissoring action of fiber-to-fiber contact was then higher in pultrusions no. 3 and 4. The width available calculated for layer deformation along the braid circumference was enough for all the preforms except for the outer layer of pultrusion no. 4. According to the model, only the outer layer of preform no. 4 would fill all the available space. This means that the friction between the outer fibers and the die surface was the highest for pultrusion no. 4, due to higher contact area. The fill ratio also indicates the amount of friction that the outer fibers will endure during pultrusion. The highest fill ratios were calculated for pultrusions no. 3 and 4, leading to the inference that the friction was also the highest in these pultrusions. Finally, the calculated fiber volume content is also an indication of the amount of fiber contact with the die surface. The highest fiber volume content was also calculated for pultrusions no. 3 and 4, meaning that more fibers were resisting the pultrusion action by their friction with the die wall in these experiments. Even if the friction forces were most probably higher in pultrusions no. 3 and 4, it was still possible to pultrude the material

with minimal yarn breakage. This is attributed to the role of the strong glass fiber MEY that resisted the pulling force and held the braid structure in position during its passage inside the hot pultrusion die. The comparable pitch before and after pultrusion for pultrusions no. 3 and 4 provides further evidence for this observation.

In a previous publication, the bending strength and modulus for a unidirectional jute/PLA composite having a fiber volume content of 40% was measured to be ~17 MPa and 9.5 GPa [7]. It is difficult to compare the mechanical properties measured here to those results because of the different fiber orientation and the presence of glass fibers. However, these previously published results show that there is room for improvement of the mechanical properties of beams manufactured by braid-trusion. The bad impregnation quality is attributed to the fill ratio under 100% for all the experiments. The braid compression when entering the die was most likely taken by the fiber bed and probably almost no pressure was applied to the resin to enhance impregnation flow.

10.2.4 Conclusion

By combining the textile technique for making intermediate materials and textile reinforcements, textile biocomposites were realized. This concept was applied into the manufacturing of textile biocomposite beams using jute fibers and PLA resin by the braid-trusion manufacturing method. A geometrical model was presented that helps understand the deformation of the braid inside the pultrusion die. Pultrusions using only jute fibers for reinforcement were not successful because of jute middle-end-yarn breakage. Successful braid-trusions were realized using glass fibers for middle-end-yarn in the braid architecture. For further studies, stronger natural fiber yarns will be selected to achieve an all biocomposite braid-trusion. The braid-trusion of biocomposites demonstrated in this study is an important step toward the economically viable production of high performance all-natural composite products.

References

1. Hearle, J.W.S., Grosberg, P., and Backer, S. (1969) *Structural Mechanics of Fibers, Yarns and Fabrics*, Vol. I, John Wiley & Sons, Inc., New York.
2. Nakamura, R., Nomura, H., Goda, K., Noda, J., and Ohgi, J. (2009) *J. Soc. Mater. Sci.*, **58**, 382–388 (in Japanese).
3. Gegauff, C. (1907) *Bull. Soc. Ind. Mulhouse*, **77**, 153.
4. Madhavan, V. and Naik, N.K. (1999) Elastic behavior of twisted impregnated yarns. AIAA/ASME/ASCE/ASC Structures, Structural Dynamics and Materials Conference, Vol. 2, 1999, pp. 936–944.
5. Rao, Y. and Farris, R.J. (2000) *J. Appl. Polym. Sci.*, **77**, 1938–1949.
6. Nakamura, R., Goda, K., Noda, J., and Netravali, A.N. (2010) *J. Solid Mech. Mater. Eng.*, **4**, 1605–1614.
7. Shikamoto, N., Wongsriraksa, P., Ohtani, A., Leong, Y.W., and Nakai, A. (2008) Processing and mechanical properties of jute reinforced PLA

composite. Proceedings of the 52nd International SAMPE Symposium: Material and Process Innovations: Changing our World (SAMPE'08), Long Beach, California, May 2008.
8. Michaeli, W. and Juerss, D. (1996) Thermoplastic pull-braiding: pultrusion of profiles with braided fibre lay-up and thermoplastic matrix system (PP). *Composites Part A*, **27** (1), 3–7.
9. Rosselli, F., Santare, M.H., and Guceri, S.I. (1997) Effects of processing on loser assisted thermoplastic tape condition. *Composites Part A*, **28A**, 1023–1033.
10. Mohanty, A.K., Misra, M., and Hinrichsen, G. (2000) *Macromol. Mater. Eng.*, **276/277**, 1–24.
11. Taki, T. and Amaoka, T. (1998) Low-cost moldingIII of aviation ACM-investigation and recommendation of thermoplastic composites with low-cost molding techniques. *J. Jpn. Soc. Compos. Mater.*, **24** (2), 41–48.
12. Carlsson, L.A. (1991) in *Thermoplastic Composite Materials*, Composite Materials Series, Vol. 7 (ed. R.B. Pipes), Elsevier Science, New York, p. 389.
13. Iyer, S.R. and Drzal, L.T. (1990) Manufacture of powder-impregnated thermoplastic composites. *J. Thermoplast. Compos. Mater.*, **3** (10), 325–355.
14. Rijisdijils, A., Contant, M., and Peijis, A.A.J.M. (1993) Continuos glass-fiber-reinforced polypropylene composites: I. Influence of maleic-anhydride-modified polypropylene on mechanical properties. *Compos. Sci. Technol.*, **48**, 161–172.
15. Youjiang Wang, A.R. and Muzzy, J. (1996) Braided thermoplastic composites from powder-coated towpregs. Part I: towpreg characterization. *Polym. Compos.*, **17**, 497–504.
16. Ramasamy, A. and Wang, Y. (1996) Braided thermoplastic composites from powder-coated towpregs. Part II: braiding characteristics of towpregs. *Polym. Compos.*, **17**, 505–514.
17. Hamada, H., Maekawa, Z., Ikegawa, N., Matuo, T., and Yamane, M. (1993) Influence of the impregnating properties on mechanical properties of commingled yarn composites. *Polym. Compos.*, **14**, 308–313.
18. Ye, L., Friedrich, K., Kastel, J., and Mai, Y.-W. (1995) Consolidation of unidirectional CF/PEEK composites from commingled yarn prepreg. *Compos. Sci. Technol.*, **54**, 349–358.
19. Beehag, A. and Ye, L. (1996) Role cooling pressure on interlaminar fracture properties of commingled CF/PEEK composites. *Composites Part A*, **27A**, 175–182.
20. Diao, X., Ye, L., and Mai, Y.-W. (1997) Fatigue behavior of CF/PEEK composite laminates mode from commingled prepreg. Part I: experimental studies. *Composites Part A*, **28A**, 739–747.
21. Diao, X., Ye, L., and Mai, Y.-W. (1997) Fatigue behavior of CF/PEEK composite laminates mode from commingled prepreg. Part II: statistical simulations. *Composites Part A*, **28A**, 749–755.
22. Bernet, N., Wakeman, M.D., Bourban, P.-E., and Manson, J.-A.E. (2002) An integrated cost and consolidation model for commingled yarn based composites. *Composites Part A*, **A 33**, 495–506.
23. Thanomsilp, C. and Hogg, P.J. (2003) Penetration impact resistance of hybrid composites based on commingled yarn fabrics. *Compos. Sci. Technol.*, 467–482.
24. Ye, L. and Friedrich, K. (1997) Processing of CF/PEEK thermoplastic composites from flexible preforms. *Adv. Compos. Mater.*, **6** (2), 83–97.
25. Ye, L. and Friedrich, K. (1993) Mode I interlaminar fracture of co-mingled yarn based glass/polypropylene composites. *Compos. Sci. Technol.*, 187–198.
26. Lauke, B., Bunzel, U., and Schneider, K. (1998) Effect of hybrid yarn structure on the delamination behaviour of thermoplastic composites. *Composites Part A*, **A29**, 1397–1409.
27. Sakaguti, M., Nakai, A., Hamada, H., and Takeda, N. (2000) The mechanical properties of unidirectional thermoplastic composites manufactured by a micro-braiding technique. *Compos. Sci. Technol.*, **60**, 717–722.
28. Khondker, O.A., Ishiaku, U.S., Nakai, A., and Hamada, H. (2006) A novel technique for thermoplastics manufacturing of unidirectional composites reinforced with jute yarns. *Composites Part A*, **37**, 2274–2284.

29. Fujihara, K., Hung, Z.-M., Ramakrishna, S., and Hamada, H. (2004) Influence of processing conditions on bending property of continuous carbon fiber reinforced PEEK composites. *Compos. Sci. Technol.*, **64**, 2525–2534.
30. Brunnschweiler, D. (1953) Braids and braiding. *Tex. Inst. J.*, **44** (9), 666–686.
31. Peirce, F.T. (1937) The geometry of cloth structure. *J. Text. Inst.*, **28** (3), T45–T96.
32. Pastore, C.M., Birger, A.B., and Clyburn, E. (1995) Geometrical modelling of textile reinforcements. Mechanics of Textile Composites Conference, Hampton, Virginia.
33. Lomov, S.V., Parnas, R.S., Ghosh, S.B., Verpoest, I., and Nakai, A. (2002) Experimental and theoretical characterization of the geometry of two-dimensional braided fabrics. *Text. Res. J.*, **72** (8), 706–712.

11
Bionanocomposites

Eliton S. Medeiros, Amélia S.F. Santos, Alain Dufresne, William J. Orts, and Luiz H.C. Mattoso

11.1
Introduction

Commonly used polymeric materials, many of which are derived from petroleum, pose problems after their intended life-span. The fast-paced consumption of petroleum (roughly 100 000 times faster than nature can replenish) and the general disposal possibilities, incineration and land filling contribute to the unsustainability of the current situation [1] and imply future problems in supplying advanced materials. This fact has created the urgent need for replacing petroleum-based polymers by renewable and biodegradable ones. As a result, there has been a growing effort to develop new biodegradable materials from environment-friendly, biodegradable, and renewable resources whose feasibility in suiting their properties to a particular application can result in easily tailored materials such as *bionanocomposites*.

The term *bionanocomposites* has been defined as those nanocomposites involving biopolymers in combination with nanosized reinforcements to produce composites with improved properties by varying stiffness, permeability, crystallinity, thermal stability, biodegradability, and biocompatibility. In bionanocomposites, biology, chemistry, materials science, engineering, and nanotechnology are combined to produce materials that can be used to replace many conventional materials in applications such as regenerative medicine, drug vectorization, and food packaging [1–8]. Moreover, the utilization of bionanocomposites is considered a viable approach to develop ''green'' materials from renewable resources with a more favorable carbon footprint than petroleum-derived feedstock.

From wood to blood vessels [8–10], nature ''uses'' composites to create nanocomposite structures such as wood (essentially cellulose-reinforced fibrils bound together by lignin and hemicellulose matrix), and bones (this basic structure of all vertebrates is made of collagen fibrils embedded in an inorganic apatite matrix) [11–13]. All that scientists need to do is to try to mimic nature or to exploit these natural biocomposites in order to develop novel materials that can be suitable to our needs without being harmful to the environment.

Polymer Composite: Volume 3, First Edition.
Edited by Sabu Thomas, Kuruvilla Joseph, S. K. Malhotra, Koichi Goda and M. S. Sreekala.

Bionanocomposites have benefited from the advances in nanocomposites that have been studied since the early 1990s when researchers created composites using nanostructured clay reinforcements (i.e., nanoscale clay particles imbedded in polymer matrices) that provided significant improvements in dimensional stability, stiffness, and heat distortion temperature relative to the nascent polymer [14–17]. Since then, many other pioneering works along with further achievements in characterization techniques and synthesis of new nanomaterials have opened up many research avenues, leading to a vast number of biopolymer matrices and nanostructured reinforcements that can be used to produce bionanocomposites.

11.2 Bionanocomposites

The advent of nanotechnology principles and characterization techniques means that materials that have been used for many decades are being revisited in search of new properties and applications. Among the new discoveries, bionanocomposites not only exhibit enhancement in mechanical properties (tensile strength (TS), elastic modulus, etc.) and physical properties (better barrier properties, reduced flammability), but also show improved optical transparency, biodegradability, and biocompatibility when compared to traditional composites [17–22].

The biggest factor in determining the mechanical and physical properties of bionanocomposites is the nature and effectiveness of interactions at the interfacial region between the nanostructured reinforcement and the matrix [11, 12, 23]. This means that both the interfacial region and particle dispersion in nanocomposites play an even more important role. Nanoreinforcements have tremendously high surface areas, usually between 250 and 1000 $m^2\ g^{-1}$, when compared to materials such as glass and natural fibers with surface areas less than 10 $m^2\ g^{-1}$ [23–29]. A strong interface is required to assure that any applied load is easily transferred from the matrix to reinforcements, thus avoiding premature failure. A poor interface is also a drawback in situations other than external mechanical loading; for example, because of differential thermal expansions of reinforcement and matrix, premature failure can occur at a weak interface when the composite is subjected to thermal stress [11, 23]. Controlling interface properties is of major importance in bionanocomposites as the reinforcement/matrix interfacial area can be very large compared to conventional fiber-reinforced composites.

11.2.1 Bionanocomposite Classification

There are several methods for classification of bionanocomposites according to criteria which include types of matrix used; their application; and the origin, shape, and size of the reinforcements [11–13]. For example, nanocomposites

classified according to the shape of the particle reinforcements can be classified into particulate, elongated particle, and layered structures.

11.2.1.1 Particulate Bionanocomposites

Particulate bionanocomposites generally use isodimensional particles as reinforcements. Owing to the low aspect ratio, the reinforcing effect is moderate and the general purpose of using these reinforcements is to enhance composites' resistance to flammability, decrease permeability, or costs.

11.2.1.2 Elongated Particle Bionanocomposites

Elongated particle bionanocomposites use elongated particles such as cellulose nanofibrils and carbon nanotubes as reinforcement. This category yields nanocomposites with much better mechanical properties because of the higher aspect ratio of the reinforcement. Cellulose nanofibrils have been one of the most studied organic reinforcements because of their remarkable mechanical properties. The affinity between hydrophilic matrices and cellulose [30] can be exploited, not only to enhance the mechanical properties of composites, but, depending on the matrix used, also to produce totally biodegradable materials [31, 32].

There are four significant differences between clay-reinforced and cellulose nanofibril-reinforced nanocomposites: (i) typical cellulose nanofibrils are long crystalline ''needles'' ranging in size from 10 to 20 nm in width and an average aspect ratio of 20–100 (this is in contrast to the lamellar structure of most clays); (ii) cellulose surfaces provide a greater potential for surface modification using well-established carbohydrate chemistry; and (iii) sources of cellulose microfibrils, including wood, straw, bagasse, bacteria, and sea animals (tunicates), are widely diverse, providing a wide range of potential nanoparticle properties [17]. Moreover, cellulose nanofibrils are known to align in magnetic and electric fields [33–35]; therefore, opening up the possibility of controlling the degree of orientation during processing, for example, in extrusion blow molding of packaging films an electric or magnetic device could be placed at the die exit, conferring some orientation to the film as it is formed and cooled down.

11.2.1.3 Layered Particle-Reinforced Bionanocomposites

A layered particle-reinforced bionanocomposite, also known as a *layered polymer nanocomposite* (*LPN*), can be classified into three subcategories depending on how the particles are dispersed in the matrix. *Intercalated nanocomposites* are produced when polymer chains are intercalated between sheets of the layered nanoparticles, whereas *exfoliated nanocomposites* are obtained when there is separation of individual layers, and *flocculated* or *phase-separated nanocomposites* are produced when there is no separation between the layers due to particle–particle interactions. This last class of composites is often named microcomposites as the individual laminas do not separate, thus acting as microparticles dispersed in the polymeric matrix. Their mechanical and physical properties are poorer than exfoliated and intercalated nanocomposites [17, 20, 21, 36, 37]. Figure 11.1 shows a schematic drawing of the structure of layered nanocomposites.

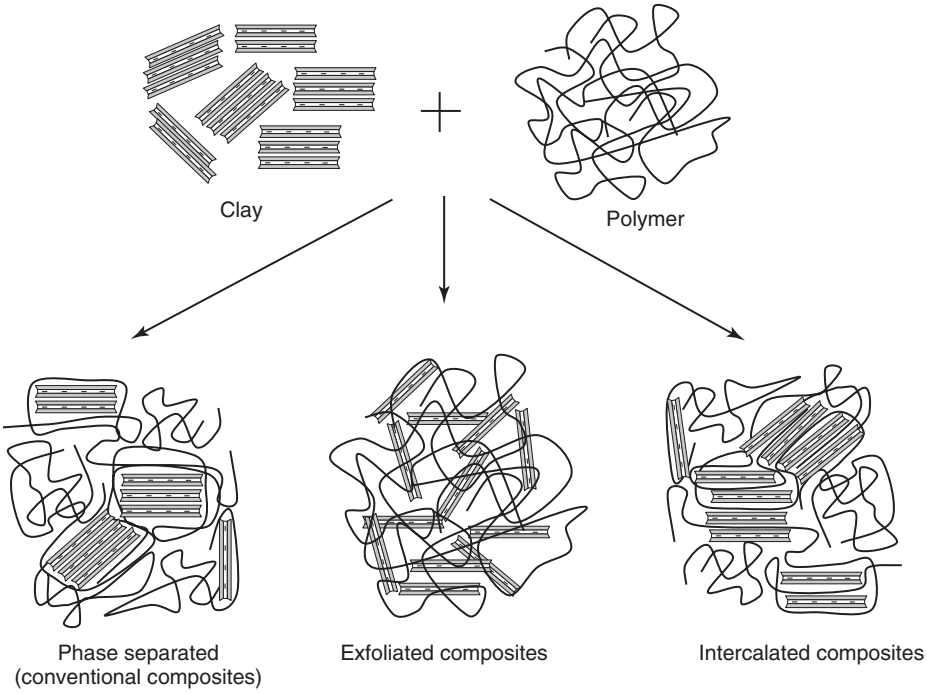

Figure 11.1 Different types of nanocomposites from polymers and clays. Conventional clay composites are also known as *microcomposites*.

11.2.2
Reinforcements Used in Bionanocomposites

Reinforcements can generally be defined as organic or inorganic particulate material (spheres, plates, flakes, sheets, fibers, fibrils, and whiskers) used in composites to improve composite properties. They often modify a specific mechanical and/or physical property such as processability, flammability, conductivity, shrinkage, weight, and visual appearance [10, 11, 20, 37–41]. Reinforcements are normally classified into three major categories according to their particle size and shape. When the aspect ratio is usually close to unity ($L/D \approx 1$), which means that the dimensions of the particles have the same size in all directions, they are named *isodimensional* or *zero-dimensional particles*; examples include spherical silica, nanoclusters, metallic nanoparticles, carbon black, and fullerenes. The second category of particles is *elongated particles* or *fibrils* with diameter between 1 and 100 nm and length of several hundreds of nanometers, represented mainly by cellulose nanofibrils, also known as *microfibrillated cellulose*, *cellulose nanocrystals*, or *nanowhiskers*. The third category is comprised of particles whose shape is a lamina or sheet with width and thickness ranging from few angstroms to several hundreds of nanometers and length of thousands of nanometers named *layered particles*. These particles are composed by stacks of laminas and are commonly

found in nature, although they can also be produced synthetically [20, 21, 36, 42, 43]. Nanomaterials from the last two categories are most typically used in nanocomposites, because their high aspect ratio confers greater enhancement of the mechanical properties of the nanocomposites.

The most common fillers used in polymer nanocomposites are carbon nanotubes, carbon black, fumed silica clays (inorganic fillers), and cellulose nanofibrils (organic filers). Carbon nanotubes are molecular-scale tubes formed by rolled-up graphene sheets, which result in outstanding mechanical and electrical properties. They are among the stiffest and strongest nanoreinforcements known [23, 44], although their costs may be prohibitive.

11.2.2.1 **Nanoclays**

Clays are constituted by colloidal fragments of primary silicates, also known as *clay minerals*. The structure of clay minerals is made up of tetrahedral and octahedral sheets of small cations, such as aluminum or magnesium coordinated by oxygen atoms. Clays are classified based on the way that tetrahedral (*n*) and octahedral (*m*) sheets are packaged into layers as *n*:*m* clays. For example, 1 : 1 clays are formed by one tetrahedral and one octahedral group in each layer. Figure 11.2 shows the tetrahedral/octahedral structure of some of the clay minerals used in nanocomposites. One important feature of clays is that the space between layers has hydrated cations such as Na^+ or K^+ that can undergo exchange reaction with organic as well as inorganic cations [42, 43]. Cation exchange reactions in clay are very important to impart functionality and compatibility with polymers as shown schematically in Figure 11.3 [36, 37, 45].

11.2.2.2 **Cellulose**

Cellulose is the most abundant organic polymer in nature with an estimated annual production of 1.5×10^{12} ton [46–48]. Cellulose can be found in an almost pure form in cotton, but is generally found in combination with other materials such as lignin and hemicelluloses in wood, leaves, and stalks. It can also be found in pure form in marine animals such as tunicin and is produced by some form of bacteria, algae, and fungi [49]. Chemically, cellulose is a linear polymer made up of several hundred to over ten thousand repeating units of $\beta(1 \rightarrow 4)$ linked D-glucose (see Figure 11.4) [30, 49–52].

Physically, cellulose is found in the form of microfibrils constituted by amorphous and crystalline domains in combination with other substances like lignin, hemicelluloses, and proteins constituting the basic structural unit of plant cell walls [53, 54]. Crystalline cellulose can be isolated from animals and other sources of cellulose such as cotton, sisal, and wood by treatment with strong acids such as hydrochloric and sulfuric acid (acid hydrolysis) in order to remove the amorphous domains, yielding mostly crystalline fibrils with diameters in the range of 5–20 nm and aspect ratio of about 1–100 times [49–53]. As a result of the acid treatment used in a typical isolation process, cellulose nanofibrils often have electronegative surface charges on their surface (usually sulfate and polar hydroxyl groups) that are capable of hydrogen bonding. Particle–particle or particle–solvent–particle

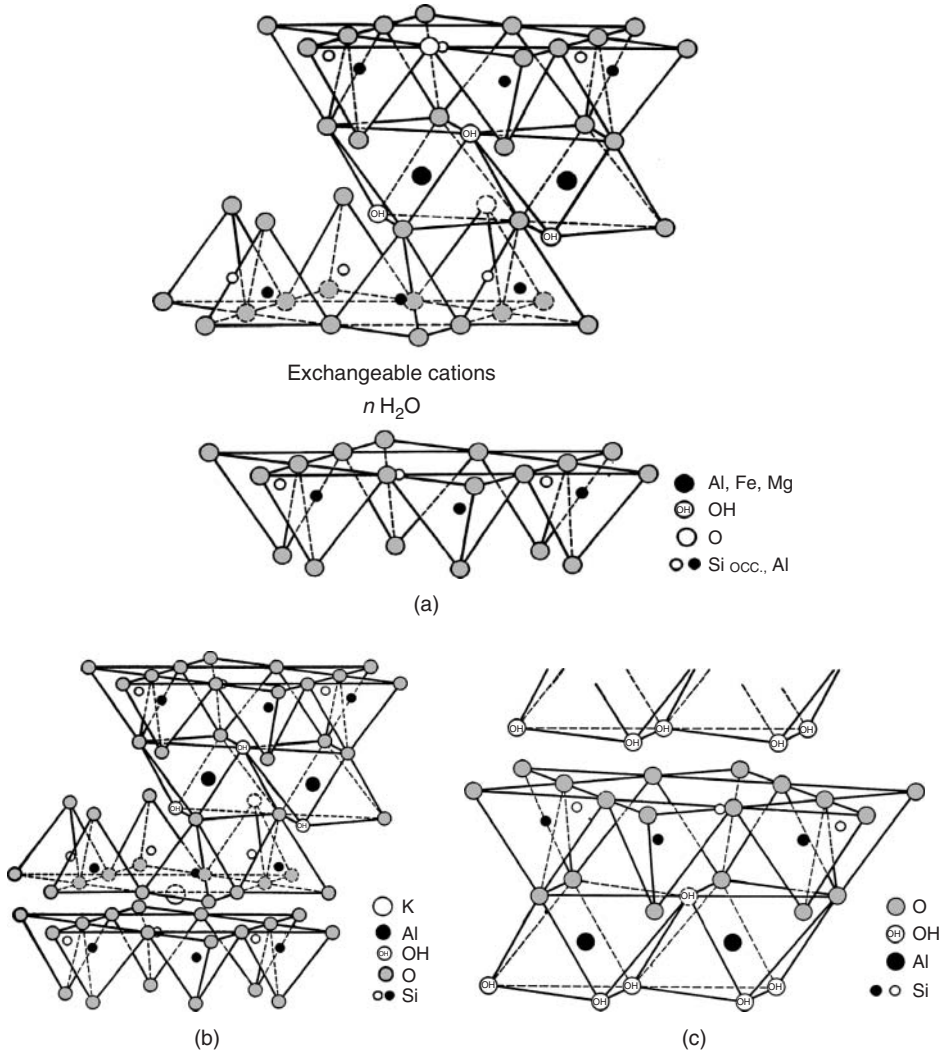

Figure 11.2 Structure of some of the clay minerals used as fillers in nanocomposites: (a) montmorillonite (MMT), (b) muscovite, and (c) kaolinite. Note the layered structure composed by tetrahedrons and octahedrons with atoms positioned at both interstitial and corner positions [42].

interactions form three-dimensional networks giving rise to a rheological behavior typical of clay nanocomposite behavior [50–52, 55–57]. However, acid hydrolysis also decreases thermal stability of nanofibrils, whose thermal degradation lies in the range of processing temperatures for most thermoplastics [58–60]. Thermal stability can be recovered to a certain extent either by modifying the extraction process, such as by the use of low acid concentrations, low acid-to-cellulose ratio, and short reaction times [55], or in a postextraction process, such as restabilization

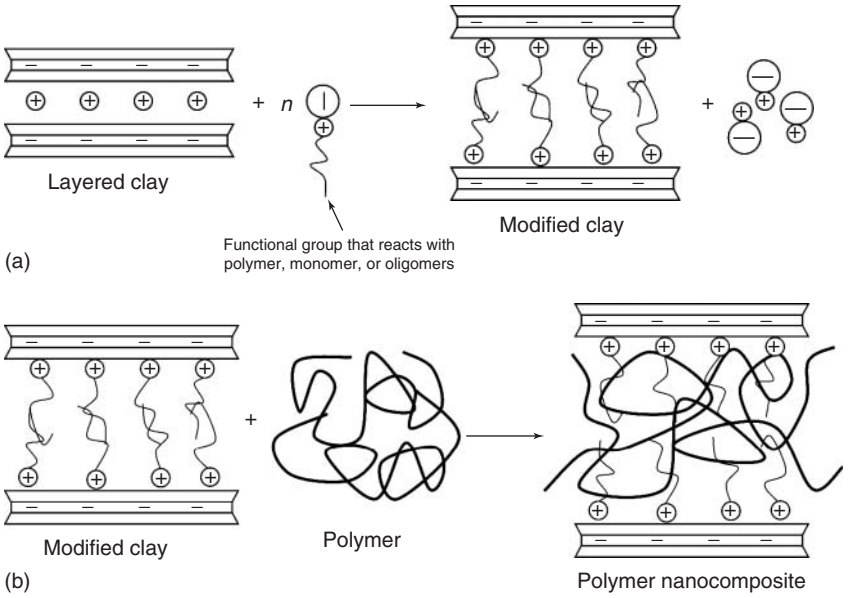

Figure 11.3 (a) Cation exchange reaction to produce organically modified clays and (b) compounding with a polymer matrix to make nanocomposites.

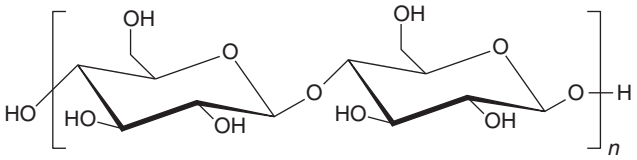

Figure 11.4 Chemical structure of cellulose.

by partly neutralizing the sulfuric acid groups with strong bases such as sodium hydroxide [56].

Although cellulose nanofibrils have been studied and industrially used since the 1960s [50–52], these nanostructures have gained more scientific attention only recently owing to the search for nanomaterials from renewable resources. These nanofibrils possess several advantages as an engineering material, such as low cost and density, renewability, biodegradability, nontoxicity, formation of stable aqueous suspension, and remarkable mechanical properties; with the capability of improving the mechanical performance of polymers at very low fiber concentrations [17, 61]. In simple terms, purely crystalline cellulose has a modulus rivaling steel, therefore representing an appropriate material for nanocomposites. With the above-mentioned benefits, cellulose-based bionanocomposites are organic alternatives to clay-based particulates, with the added advantage of applying well-understood cellulose chemistry. Moreover, owing to cellulose polyfunctionality,

chemical reactions can be carried out on the surface of the nanofibrils, enhancing their interaction with a vast number of polymeric matrices [62].

Cellulose nanowhiskers (CNWs) have been obtained from a variety of matrices such as cotton [63], sisal [64], and coconut husk fibers [65]. Other alternative sources of cellulose nanofibrils includes naturally colored cotton, curaua (*Ananas erectifolius*), and sugarcane bagasse have been successfully used to prepare nanowhiskers [66–69].

11.2.2.3 **Chitin and Chitosan**

Chitin is one of the main components in the cell walls of fungi, the exoskeleton of shellfish, insects and other arthropods, and in some other animals. It is the second most important natural polymer in the world and was first identified in 1884. Zooplankton cuticles (in particular small shrimps constituting krill) are the most significant source of chitin. However, fishing of these tiny organisms (a few millimeters in length) is too difficult to consider for any industrial use. Despite the widespread occurrence of chitin, shellfish canning industry waste (shrimp or crab shells) in which the chitin content ranges between 8% and 33% constitutes the main source of this biopolymer. In industrial processing, chitin is extracted from crustaceans by acid treatment to dissolve calcium carbonate followed by alkaline extraction to solubilize proteins. In addition, a decolorization step is often carried out to remove leftover pigments and obtain a colorless product. These treatments must be adapted to each chitin source, owing to differences in the ultra-structure of the initial materials. The resulting extracted material needs to be graded in terms of purity and color as residual protein and pigment can cause problems for further utilization, especially for biomedical applications.

Chitin is a polysaccharide, made out of units of acetylglucosamine (more completely, N-acetyl-D-glucose-2-amine) (Figure 11.5). These are linked together in β-1,4 fashion, the same as the glucose units that make up cellulose. So chitin may be thought of as cellulose, with one hydroxyl group on each monomer replaced by an acetylamino group. This allows for increased hydrogen bonding between adjacent polymer chains, giving the material increased strength.

Native chitin is highly crystalline and, depending on its origin, it occurs in three forms identified as α-, β-, and γ-chitin, which can be differentiated by infrared and solid-state NMR spectroscopy together with X-ray diffraction (XRD). From a detailed analysis, it seems that the latter is just a variant of the α form [70]. In both

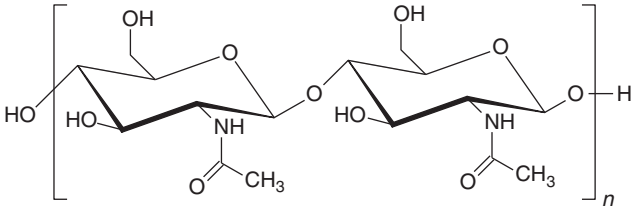

Figure 11.5 Chemical structure of chitin.

α and β forms, the chitin chains are organized in sheets where they are tightly held by a number of intra-sheet hydrogen bonds. In α-chitin, all chains are arranged in an antiparallel fashion whereas the β form consists of a parallel arrangement. As it constitutes arthropod cuticles and mushroom cellular walls, α-chitin is the most abundant and stable form. It occurs in fungal and yeast cell walls, krill, lobster and crab tendons and shells, shrimp shells, and insect cuticles. In addition to the native chitin, α-chitin systematically results from recrystallization from solution [71–73], *in vitro* biosynthesis [73], or enzymatic polymerization [74]. The rarer β-chitin is found in association with proteins in squid pens [75], tubes synthesized by pogonophoran and vestimentiferan worms [76, 77], *Aphrodite chaetae* [78], and *Lorica* built by some seaweeds or protozoa [79, 80].

Chitin has been known to form microfibrillar arrangements embedded in a protein matrix, and these microfibrils have diameters ranging from 2.5 to 2.8 nm [81]. Crustacean cuticles possess chitin microfibrils with diameters as large as 25 nm [82, 83]. Although it has never been specifically measured, the stiffness of chitin nanocrystals thought to be at least 150 GPa, based on the observation that cellulose is about 130 GPa and the extra bonding in chitin crystallites is going to stiffen it further [84].

Chitosan is a partly deacetylated chitin resulting from alkali treatment or enzymatic degradation of chitin (Scheme 11.1), which is insoluble in its native form. Chitosan is preferred over chitin in many biopolymer applications because of its relative solubility and/or better film-forming properties. Both chitin and chitosan are biocompatible material and have antimicrobial activities as well as the ability to absorb heavy metal ions [85].

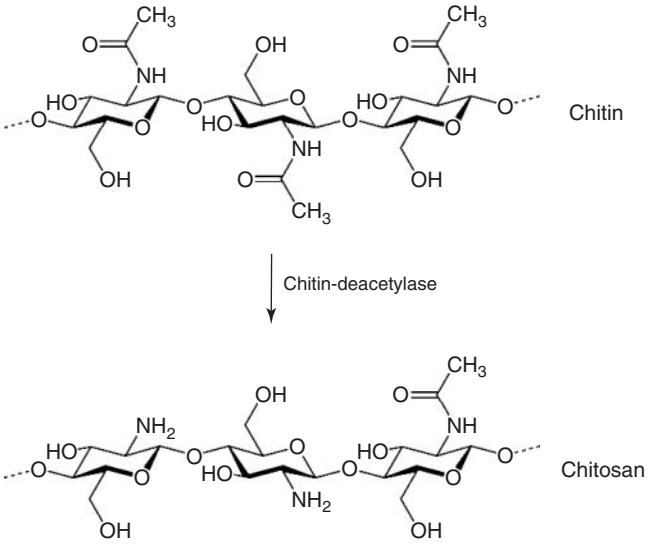

Scheme 11.1 Schematic representation of the deacetylation reaction of chitin to produce chitosan.

11.2.3 Matrices for Bionanocomposites

Similar to conventional composites, the role of the matrix is to support and protect their nanoreinforcements, which are the stronger and stiffer components held together by the matrix. The matrix then transmits and distributes applied load to the nanoreinforcements [11, 12, 18, 19]. Because the range of particle sizes is in the nanoscale, the surface area of the reinforcement is much higher, so the role of the particle/matrix interfacial region is even more important.

Matrix molecules can be anchored to the reinforcement surface by chemical reactions or adsorption, which determines the strength of interfacial adhesion. In certain cases, the interface may be composed of an additional constituent such as a bonding agent or an interlayer between the two components of the composite. The choice of a matrix depends on several factors like application, compatibility between the components, technique of processing, and costs.

Several biopolymers have been used as matrices for bionanocomposites, including starch; poly(lactic acid), PLA; poly(ε-caprolactones), PCLs; polyhydroxyalkanoates, PHAs, that include polyhydroxybutyrate, PHB and poly(3-hydroxybutyrate-*co*-3-hydroxyvalerate), PHBV, and poly(butylene succinate), PBS [10, 36–58, 86]. These matrices can be chemically synthesized or biosynthesized by some organisms [8, 87]. Biopolymers can be classified into four different groups depending on their synthesis (Figure 11.6) [87–89]:

1) polymers from biomass such as polymers from agricultural resources such as starch and cellulose;
2) polymers from microbial production such as PHAs;
3) polymers chemically synthesized using monomers obtained from agroresources, for example, PLA; and
4) polymers whose monomers and polymers are both obtained by chemical synthesis from fossil resources. This category is therefore obtained from nonrenewable sources.

Here, we will only give a brief description of some of the most important biopolymers. A detailed description can be found elsewhere [3, 89–95] as this has been the object of several reviews and books.

11.2.3.1 Polysaccharides

Polysaccharides form part of the group of molecules known as *carbohydrates* and have been proposed as the first biopolymers to have formed on Earth [96]. This term was applied originally to compounds with the general formula $C_x(H_2O)_y$, but now it is also used to describe a variety of derivatives including nitrogen- and sulfur-containing compounds. They are classified on the basis of their main monosaccharide components and the sequences and linkages between them, as well as the anomeric configuration of linkages, the ring size (furanose or pyranose), the absolute configuration (D- or L-), and any other constituents present.

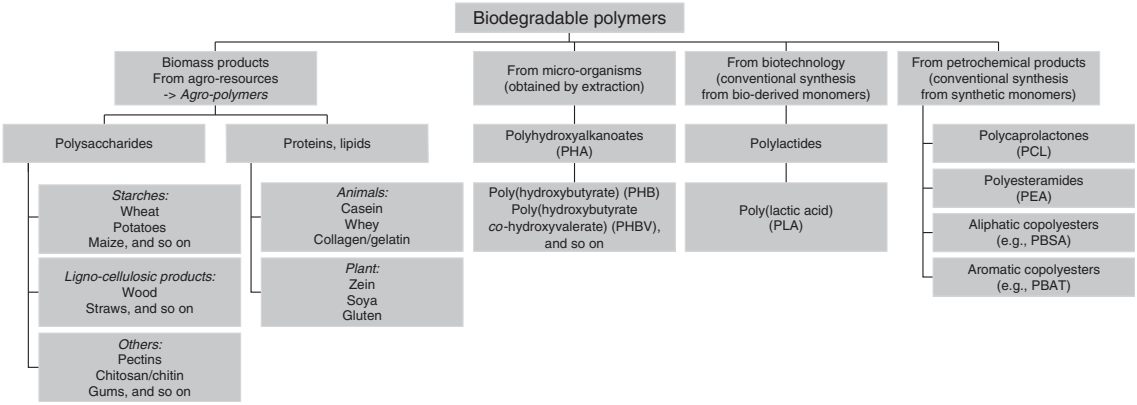

Figure 11.6 Classification of biodegradable polymers used in bionanocomposites [87, 88].

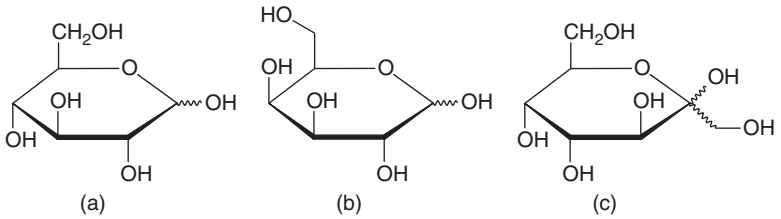

Figure 11.7 Chemical structure of the three common "single" sugars or monosaccharides. (a) Glucose, (b) galactose, and (c) fructose.

Three common monosaccharides, that is, glucose, galactose, and fructose, share the same molecular formula $C_6H_{12}O_6$; and, because of their six carbon atoms, each is a hexose (Figure 11.7). Although all three share the same molecular formula, the arrangement of atoms differs in each case; substances which have different structural formulas are known as *structural isomers*.

Two monosaccharides can be linked together to form disaccharides such as sucrose (common table sugar, consisting of glucose + fructose), lactose (major sugar in milk, consisting of glucose + maltose), and maltose (product of starch digestion, consisting of glucose + glucose). Although the process of linking of two monomers is rather complex, the end result in each case is the loss of a hydrogen atom from one of the monosaccharides and a hydroxyl group from the other. The resulting linkage between the sugars is called a *glycosidic bond*. All sugars are very soluble in water because of their many hydroxyl groups and although not as concentrated a fuel as fats, they are the most important source of energy for many cells. Further linkages of disaccharides lead to polysaccharides. Starch, cellulose, pectin, chitin, and chitosan are among the most known polysaccharides used as matrices for bionanocomposites.

11.2.3.1.1 Starch

For many years, starch has been considered a natural polymer with high potential for applications in biodegradable plastics because of its renewability, biodegradability, low cost, availability (it is the second most abundant biomass material in nature), and mechanical properties [4–7, 97, 98]. It can be found in plant roots, stalks, and crop seeds, and is the prime ingredient of most of the world's staple crops – rice, corn, wheat, cassava, tapioca, and potato, to name a few [99–101]. Chemically, starch consists of a mixture of amylose and amylopectin in an amylose/amylopectin proportion which, depending on its origin, naturally ranges from 20/80% to 30/70%, with some specialty hybrids high in amylose (85/15) or vice-versa (10/90). Amylose is a linear or slightly branched high molecular weight polymer consisting of long chains with an average of hundreds to thousands of glucose units linked together by α-D-(1,4)-glycoside bonds, while amylopectin is a highly branched polymer consisting of relatively short segments or branches of D-glucopyranose residues linked by α-D-(1,4)-bonds that are connected by α-D-(1,6)-glucosidic linkages approximately every 25 glucose units (Figure 11.8) [98, 102–104].

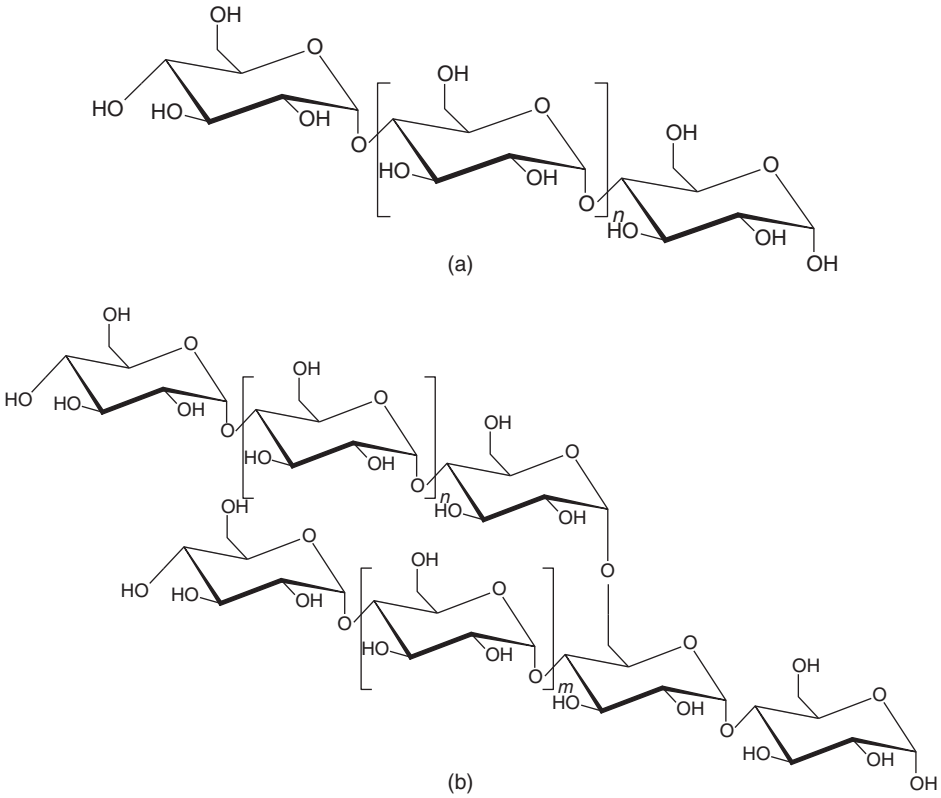

Figure 11.8 Chemical structure of (a) amylose and (b) amylopectin.

Starch crystallizes into a double helix structure that includes significant hydrogen bonding between chains, which is partially responsible for its brittle behavior in the natural state [105]. By destructurization, a process in which the granular structure is broken down by heat, shear, and time, starch can behave like thermoplastic materials especially in the presence of plasticizers such as water, glycerol, and sorbitol. Destructurization enables starch processing by injection, extrusion, and blow molding, similarly to most conventional synthetic thermoplastic polymers, thus making starch an excellent matrix for biodegradable composites. However, starch suffers from several major drawbacks generally related to aging; moisture sensitivity and postprocessing crystallization and can cause a decrease in mechanical properties with time [7, 98, 102, 105, 106].

11.2.3.1.2 Proteins

Proteins are polymers formed by the polycondensation of amino acids where the carboxyl group of one amino acid joins with the amino acid group of another amino acid, eliminating water and forming an amide linkage called a *peptide bond*. Each protein is made up of a sequence of amino acids. Proteins such as

wool, silk, and collagen could be potential candidates for matrices to be used in bionanocomposites if they were soluble or fusible without degradation, which has proven difficult. As a consequence, most proteins used in bionanocomposites are gelatin and plant proteins such as chickpea and soy protein isolates (SPIs). However, these proteins suffer from moisture sensitivity and low strength which limits their range of application in bionanocomposites [90–92].

Proteins can be classified according to their origin in animal and plant proteins. Short proteins can also be synthesized chemically by a family of methods known as *peptide synthesis*, which rely on organic synthesis techniques such as chemical ligation to produce peptides in high yield [93]. Plant proteins such as zein, soy protein, and wheat gluten have also found in many industrial applications and can also be used in composites and bionanocomposites.

Collagen is the most abundant protein found in mammals and typically constitutes 30% of total protein. It is an insoluble fibrous protein found in many animal connective tissues and it is present in skins, hides blood vessels, tendons, and ligaments. Each polypeptide chain of collagen consists of a repeating tripeptide sequence containing the common residue glycine as in gly-X-Y, where X is often the common residue proline and Y is often the common residue hydroxyproline. In collagen, long chains of the polypeptide form triply stranded helices that arrange in groups to form fibrils approximately 300 nm long and 1.5 nm in diameter (Figure 11.9), which give strength to bones and allow them to flex under stress [91, 92].

Gelatin is a denatured collagen in which the triple helices of collagen are disrupted and partially hydrolyzed, leaving polymer chains that are largely disordered and unorganized. This protein consists of amino acids joined by peptide linkages

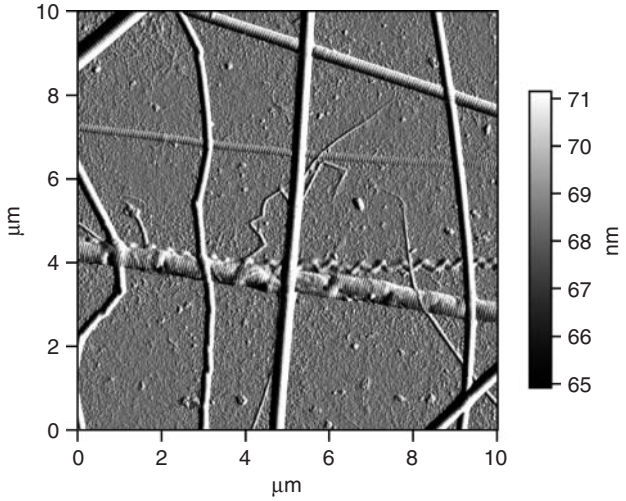

Figure 11.9 Atomic force microscopy (AFM) image of collagen showing their fibrous structure [107].

and can be hydrolyzed by a variety of the proteolytic enzymes to yield its constituent amino acids or peptide components. This nonspecificity is a desirable factor in intentional biodegradation. Gelatin is a water soluble, biodegradable polymer with extensive industrial, pharmaceutical, and biomedical uses, which has been employed for coatings and microencapsulating various drugs, as well as in bionanocomposites as shall be seen in further sections [3, 90–92].

11.2.3.2 Biodegradable Polymers from Microorganisms and Biotechnology

11.2.3.2.1 Polyhydroxyalkanoates

PHAs are a family of renewable biopolymers first identified in 1925 by Maurice Lemoigne, a French microbiologist. These polymers are produced in the form of intracellular particles which accumulate as a carbon and energy sink when grown under nutrient stress in the presence of carbon. Under controlled fermentation conditions, some microorganisms use renewable sources such as glucose to produce up to 90% of their dry mass of biopolymer [90, 91, 108]. The fact that PHAs can be produced from renewable resources allied with their good processability, make PHAs suitable for applications in several areas as a partial substitute for nonbiodegradable synthetic polymers and in the bionanocomposite field.

PHA polymers comprise mainly homopolymers such as polyhydroxybutyrate (PHB) and polyhydroxyhexanoate (PHH), and different copolyesters, polyhydroxybutyrate-*co*-hydroxyalkanoates such as poly(hydroxybutyrate-*co*-hydroxyvalerates) (PHBV) and poly(hydroxybutyrate-*co*-hydroxyoctanoate) (PHBO) (see Figure 11.10) [91, 108].

PHB can be obtained by solvent extraction after fermentation to yield a highly crystalline (80%) polyester with a high melting point, $T_m = 173–180\,^{\circ}C$, and a glass transition temperature (T_g) of about $5\,^{\circ}C$, higher than other biodegradable polyesters. PHB homopolymer has a narrow processing window that can be altered

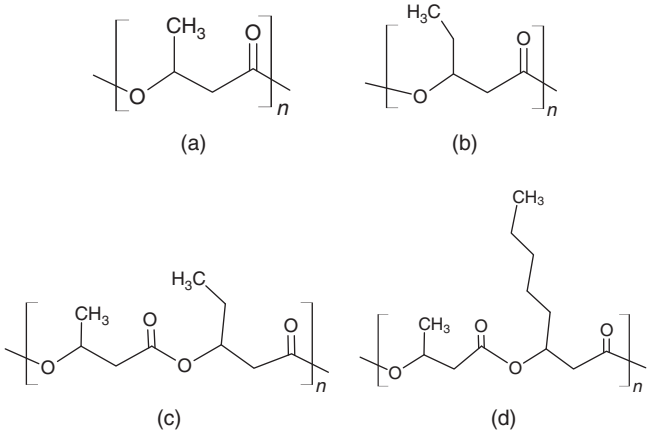

Figure 11.10 Chemical structure of some of the PHA polymers and copolymers: (a) PHB, (b) PHV, (c) PHBV, and (d) PHBO.

by adding plasticizers such as citrate ester, but the corresponding copolymer (PHBV) is more adapted for the process [109].

Poly(hydroxybutyrate-*co*-hydroxyvalerate) (PHBV), a random copolymer comprised of 3-hydroxybutyrate (HB) and hydroxyvalerate (HV) units, can be obtained by a fermentation medium [85, 90, 110] using bacteria such as *Alcaligenes eutrophus*. According to their feedstock during synthesis, different structures are obtained, many of which are isotactic and others with random stereo sequences [111–114].

11.2.3.2.2 Polylactides

Polylactides are linear polymers obtained from lactic acid, $CH_3CHOHCOOH$, commonly known as *poly*(*lactic acid*) or *polylactide*. Lactic acid occurs naturally in animals and microorganisms and is found in many natural foods especially in fermented foods such as yogurt, buttermilk, sourdough breads, and sauerkraut [90, 91]. Besides being biodegradable, bioresorbable, and biocompatible, PLAs can be easily conformed by conventional thermoplastic melt processing, which makes this class of biodegradable polymers very suitable for uses in bionanocomposites.

The presence of an asymmetric chiral carbon atom in PLA leads to the existence of stereoisomers (Figure 11.11). Therefore, levorotatory (L), dextrorotatory (D), or racemic (DL) forms of PLA can be obtained. Stereoregular PLAs result from polymerization of optically pure lactides. Optically pure PLAs – poly(L-lactide), PLLA, and poly(D-lactide), PDLA – are therefore usually semicrystalline, while if there is an LL/DD motif distribution in PLA chains, then PLAs are stereo-irregular and can be regarded as copolymers whose crystallization ability decreases with optical purity [114, 115].

Polymers and copolymers of lactic acid are best prepared by a condensation reaction at elevated temperature, via ring-opening polymerization of the corresponding lactide as can be seen in Scheme 11.2.

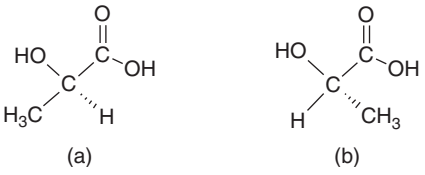

Figure 11.11 Stereoisomers of lactic acid: (a) D(−) lactic acid (DLA) and (b) L(+) lactic acid (LLA).

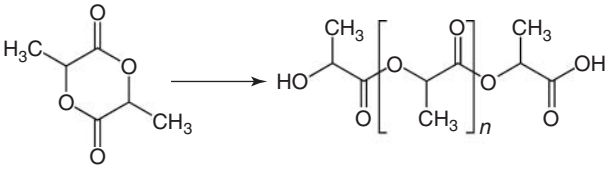

Scheme 11.2 Ring-opening polymerization reaction of lactide to produce polylactide.

As a consequence of the D, L, and DL forms of lactic acid, mechanical properties as well as erosion rates depend on the lactic acid configuration and proportion in the polymer. Moreover, because glycolic and L-lactic acid are natural metabolites which are eliminated from the body, these polymers are nontoxic and can be used in many applications such as bioerodible sutures, drug delivery systems, and bionanocomposites. Compared to other biodegradable polyesters, PLA is one of the biopolymers that presently have high potential in bionanocomposites because of its availability, low price, and relatively good properties [109, 114, 115]. PLA can be copolymerized with other monomers such as glycolic acid to produce a copolymer, poly(lactic-*co*-glycolic acid) (PLGA) which would also vary bionanocomposite properties.

11.2.3.3 **Biodegradable Polymers from Petrochemical Products**

Synthetic biodegradable polymers are generally made by polycondensation methods from petroleum-based feedstocks. However, different from other petrochemical-based resins that may take centuries to degrade, these synthetic polyesters decompose rapidly into carbon dioxide, water, and humus under appropriate conditions where they are exposed to the combined attack of water and microorganisms [109, 116, 117]. Petroleum-based biodegradable polymers that have been used in bionanocomposites are PCL, polyesteramides (PEAs), PBS, aliphatic polyesters (APES), and poly(vinyl alcohol) (PVA) [116].

11.2.3.3.1 **Poly(ε-Caprolactone)**

PCL is a biodegradable polyester prepared by ring-opening polymerization of ε-caprolactone using catalysts such as stannous octanoate and aluminum isopropoxide (Scheme 11.3). Although not produced from renewable materials, PCL is fully biodegradable.

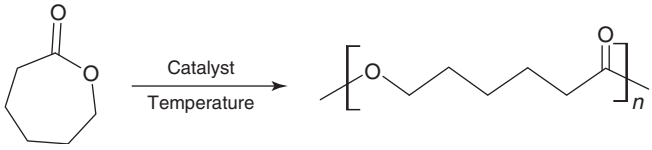

Scheme 11.3 Ring-opening polymerization reaction of ε-caprolactone to produce poly(ε-caprolactone).

Owing to its low melting point of about 60 °C and a glass transition temperature of about −60 °C, PCL is generally blended or modified in order to be used in many applications. For example, PCL/starch blends can be produced with lower cost and increased biodegradability. The degradation of PCL takes place by hydrolysis of ester linkages in physiological conditions, such as in the human body. One of the advantages of PCL over polymers such as PLA is the rate at which hydrolysis takes place. As a consequence, PCL can be used in many long-term biological applications such as in controlled release of drugs, soft compostable packaging, implantable devices, dentistry, and scaffolds for tissue repair. Another advantage of PCL polymers is that its slow rate of bioerosion can be substantially accelerated

by copolymerization with other monomers, such as lactic acid or by controlling its molecular weight. For example, the rate of hydrolysis of PCL–PLA copolymers is directly proportional to PLA content [109, 115]. Much research is currently focused on the use of PCL biocomposites and bionanocomposites with both natural and synthetic polymers [118].

11.2.3.3.2 Polyesteramides

APES are biodegradable but often lack good mechanical and physical properties, whereas aliphatic polyamides have good mechanical properties but are not biodegradable. Achieving a successful combination of both favorable properties has been the reason for the development of PEAs [119].

PEAs can be synthesized by statistical condensation copolymerization of polyamide monomers (PA 6 or PA 6.6), adipic acid, and 1,4-butanediol (Scheme 11.4). A variety of amino acids and aliphatic diols, poly(ethylene glycol), or cyclic diols like dianhydrosorbitol or dianhydromannitol have also been used to prepare PEAs [109, 119, 120].

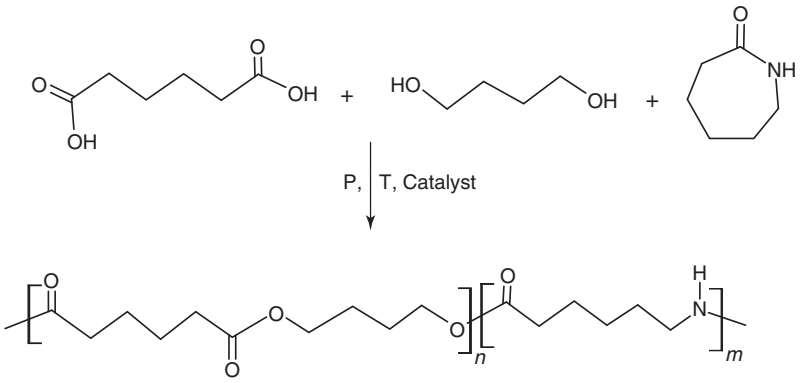

Scheme 11.4 A polyesteramide produced by polymerization of adipic acid, 1,4-butanediol, and ε-caprolactam.

In PEA polymers, monomers are linked via ester and amide bonds providing a good susceptibility to bacterial degradation in which these monomers are converted to carbon dioxide, water, and biomass. The degradation is also influenced by different mass fractions of ester and amide groups and the proportions of the monomers. As it is the polyester that presents the highest polar component, PEAs with different degradation rates can be synthesized by adjusting ester ratio. Moreover, because of the presence of hydroxyl groups that give rise to their hydrophilic character, PEAs can have good compatibility with other polar products such as starch compounds.

PEAs have found many industrial applications and can be processed like conventional plastics. However, the market share is relatively low because of their high production cost.

11.2.3.3.3 Aliphatic and Aromatic Polyesters and Their Copolymers

Several aliphatic and some aromatic (co)polyesters based on petroleum resources are biodegradable. APES can be produced by polymerization of diols such as 1,2-ethanediol, 1,3-propanediol, and 1,4-butanediol, with dicarboxylic acids such as adipic, sebacic, and succinic acids [3, 87, 109]. The biodegradability of these polymers depends on their structure, that is, on the monomers and their degradation by-products can enter the metabolic cycles of organisms [121]. Similar to other biopolymers derived from petrochemical products, most polyesters of this class can be blended with starch to yield blends with improved and/or tailored rate of degradation. Biodegradability can also be improved by increasing polymer hydrophilicity, which can be achieved by properly choosing the combination of monomers such as short-chain esters [1, 3, 88, 109, 112, 122, 123]. Examples include PBS, poly(butylene succinate-*co*-adipate) (PBSA), poly(butylene adipate-*co*-terephthalate) (PBAT), adipic acid aliphatic/aromatic copolyesters (AACs), and poly(hydroxybutyrate-*co*-valerate) (PHBV).

Aromatic polyesters are formed by the polycondensation of aliphatic diols and aromatic dicarboxylic acids. The aromatic ring gives the polymer an excellent resistance to hydrolysis and to chemical agents [8, 122, 124, 125]. They are difficult to hydrolyze and therefore not biodegradable. For example, PET (polyethylene terephthalate) and PBT (polybutylene terephthalate) are well-known polyesters obtained by polycondensation of aliphatic glycols and terephthalic acid. They can be modified by the addition of hydrolysis sensitive monomers (ether, amide, or aliphatic groups) giving a family of biodegradable polyesters such as polybutylene adipate/terephthalate (PBAT) and polymethylene adipate/terephthalate (PTMAT), known as *modified PET* [124–127].

Figure 11.12 shows a schematic depiction of the biodegradable aromatic and APES used in bionanocomposites, some of which have already been described in previous sections. The use of these polymers in bionanocomposites will be further discussed in this chapter.

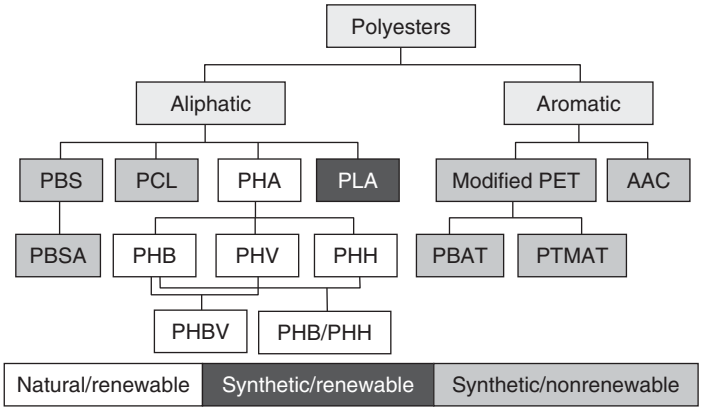

Figure 11.12 Schematic depiction of the aromatic and aliphatic polyesters natural and synthetically derived from renewable and nonrenewable resources [128].

11.2.3.3.4 Other Biodegradable Polymers of Interest in Bionanocomposites

Several biodegradable polymers such as PVA, poly(vinyl acetate) (PVAc), and poly(glycolic acid) (PGA) can be used in bionanocomposites. A detailed description of these polymers can be found in the specialized literature [2, 10, 88, 108–116, 129].

PVA is a water soluble polymer used in applications such as packaging films where water solubility is desired. PVA is the most readily biodegradable of vinyl polymers, which makes it a potentially useful material in biomedical, agricultural, and water treatment areas, for example, as a flocculant, metal-ion remover, and excipient for controlled release systems. It is readily degraded by microbes and enzymes from soil bacteria of the Pseudomonas strain [3].

PVA can be readily obtained from PVAc by replacing the acetate groups with hydroxyl groups via hydrolysis (or alcoholysis), which can be achieved using alkali such as sodium hydroxide as catalyst [3, 125]. Because PVA is obtained from the alcoholysis of PVAc, which can be controlled easily in terms of the extent of alcoholysis and the sequence of PVAc and PVA, a controlled alcoholysis of PVA followed by controlled oxidation provides degradable materials having a wide range of properties and degradation rate.

PGA is a rigid thermoplastic material with high crystallinity (between 46% and 50%) produced by ring opening of glycolide, a diester of glycolic acid. PGA is not soluble in most organic solvents but has a high sensitivity to hydrolysis. It can be processed by extrusion, injection, and compression molding similarly to other thermoplastics; however PGA is especially attractive in medical applications because its degradation product (glycolic acid) is a natural metabolite [125]. Figure 11.13 shows the chemical structures of PVA, PVAc, and PGA.

11.2.4
Mixing, Processing, and Characterization of Bionanocomposites

11.2.4.1 Mixing

One of the most important steps in the preparation of polymer nanocomposites is the mixing process. In order for the properties of a compatible nanostructured reinforcement to be fully exploited, it has to be well distributed and well dispersed.

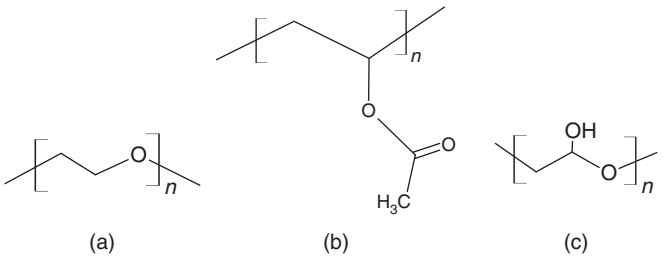

Figure 11.13 Chemical structure of some biodegradable synthetic polymers: (a) poly(vinyl alcohol), (b) poly(vinyl acetate), and (c) poly(glycolic acid).

This is of paramount importance because reinforcement content in bionanocomposites is low and also because high surface area nanoparticles have a natural tendency to agglomerate rather than disperse in the matrix [37, 45, 58, 59, 130]. Bionanocomposites can be prepared mostly by solution and melt dispersion, and *in situ* polymerization [20, 36, 37, 131–134].

Solution dispersion is a process where the nanostructured reinforcement is first dispersed in an organic solvent to allow it to swell while the polymer is dissolved in the same solvent for further mixing. Both the mixing intensity and duration is critical to ensure a good distribution and dispersion of the nanoparticles. This process has major limitations; first, the polymer needs to be soluble in the same solvent used to disperse and swell the nanostructured reinforcement, and, second, solvent removal is an additional step which limits the utility of this process in large-scale industrial applications.

Melt dispersion is generally the most practical method of bionanocomposite preparation as traditional methods of composite mixing such as twin- and single-screw extruders, rheometers, and mixers can be used, provided they have a good mixing efficiency [58, 59]. Melt dispersion consists of mixing the nanostructured reinforcement with a polymer melt to assure a good dispersion, which is caused by high shear and temperature. Shear prevents the nanostructured reinforcement particles from aggregation and heat favors polymer chain diffusion between unaggregated particles. The thermodynamic driving forces for mixing to occur depend on polarity of the nanostructured reinforcements, chemical similarity with the polymeric matrix, mixing temperature, polymer molecular weight, and so on [18, 19].

In situ polymerization is a method of bionanocomposite preparation whereby the nanostructured reinforcement, usually layered clays, is dispersed in a liquid monomer or a monomer dissolved in a suitable solvent for a certain amount of time, allowing monomer molecules to diffuse between the layers. Upon further addition of initiator or exposure of appropriate source of light or heat, the polymerization takes place *in situ* forming the nanocomposite.

11.2.4.2 **Processing**

Processing is the second most important step toward a finished product. Although it can be carried out separately, mixing and processing generally take place at the same time for reduction of costs and processing time. The quality of finished products depends strongly on this step, as it can impart defects, inefficient dispersion, and undesired orientation of the reinforcement, all of which would contribute to premature failure and other environmental stress cracking processes [11–13, 58, 59].

In bionanocomposites, the reinforcement content is very low, so they can be processed by the same methods used for the pure polymers. These methods are mainly limited by the fusibility of the polymer, nature of the reinforcements, and their thermal resistance (if melt processing methods are used). The most common methods are extrusion, injection molding, casting, and compression molding, with reactive extrusion a potential option [22, 59, 123, 130]. More information

on polymer processing operations can be found in the specialized literature [58, 59, 135–138].

Another method that has been used to produce bionanocomposites is electrospinning. This technique has been extensively explored as a simple and versatile technique to produce micro and nanofibers of polymers and biopolymers. A typical electrospinning setup is comprised of a reservoir for polymer solution, pump, capillary spinneret, grounded collector, and high voltage power supply. The electrospinning process consists of applying a strong electrostatic field supplied by the high voltage source to polymer solution as it exits its reservoir through a spinneret. Under the influence of the electrostatic field, a pendant droplet of the polymer solution at the capillary tip is deformed into a conical shape. When the surface tension is overcome by the electrostatic forces generated by the electric potential, a fine charged jet is ejected and moves toward the grounded collector, meanwhile the solvent rapidly evaporates, and polymer fibers accumulate on the collector. Control of process parameters, such as rate of polymer injection, distance between the capillary and collector, polymer–solvent combination, and polymer concentration, allows the production of fibers with controllable properties and diameters ranging from tens of microns down to a few tens of nanometers. Electrospun bionanocomposites have been successfully produced in the form of uniform fibrous mats that can be used in drug release systems, wound dressing, and tissue engineering [139–141].

11.2.4.3 **Characterization**

Choosing the optimal characterization technique for nanocomposites is not easy, in part because of the large number of techniques, the vast technical literature available on this matter [142], and no clear agreement on one ''best'' method. Characterization depends strongly on the materials, its end applications, and on equipment availability/timeliness.

Although a certain degree of dispersion of the nanostructured reinforcements in a matrix is essential, ideal dispersion does not necessarily imply improved properties unless there is a strong reinforcement/matrix interaction. In cases where the nanostructured reinforcement is used as reinforcement, its aspect ratio needs to be above a minimum value that assures efficient load transference from the matrix. Particle size, distribution and dispersion, degree of interaction, and the nanostructured reinforcement/matrix interface can be studied by direct or indirect methods; direct methods include scanning electron microscopy (SEM), transmission electron microscopy (TEM), scanning probe microscopy (SPM), and XRD. Methods of indirect investigation, such as rheology, differential scanning calorimetry (DSC), differential thermal analysis (DTA), thermogravimetry (TG), tensile, and flexural tests have been used to characterize bionanocomposites in order to access their rheological, thermal, thermomechanical, and mechanical properties. The use of the above-mentioned techniques to characterize nanocomposites has been published elsewhere [29].

11.2.5 Polysaccharide Bionanocomposites

Replacements of conventional plastics by degradable polymers, particularly for short-lived applications such as packaging, catering, surgery, or hygiene, is of major interest to an array of the different parties in the socioeconomic chain, from the plastics industry to the citizen, and to the waste management industry. The potential of biodegradable polymers and more specifically of polymers derived from agro-resources such as polysaccharides, has long been recognized. However, to date, these agro-polymers largely used in some applications (e.g., in the food industry) have not found extensive application in nonfood industries, although they could be an interesting way to overcome the limitation of petrochemical resources in the future. Material validation implies some limitations linked to difficulties in achieving accurate and economically viable outlets. Polysaccharides present some well-known advantages, namely low cost, lightweight, renewable character, high specific strength and modulus, availability in a variety of forms throughout the world, reactive surface and the possibility to generate energy, without residue, after burning at the end of their life cycle. The main drawback is their inherent high water permeability and low water resistance at high relatively humid conditions.

11.2.5.1 Starch Bionanocomposites

Starch is one of the most studied natural polymers in biopolymer research for creation of, for example, biodegradable food wraps, single use trays and plates, food utensils, and nonfood packaging because of its availability, biodegradability, renewable nature, and low cost. However, the major drawbacks associated with the use of starch-based materials in packaging applications are its hydrophilic nature, and poor processability and brittleness, especially if it is not well-plasticized to prevent moisture affects and postprocessing crystallization [143]. Starch-based packages generally absorb moisture and undergo environmental stress cracking, causing significant problems with shelf life storage. Any improvement in these negative characteristics is of fundamental importance to assure durability of both packages and stored products.

Several attempts to improve starch-based materials via traditional composite formulation resulted in materials with moderately improved properties but with the additional drawback of having limited processability due to high viscosity. Recently, however, starch-based nanocomposites, with the addition of low quantities of nanostructured reinforcements, give rise to large-scale improvement in physical, mechanical, and barrier properties without high viscosity during processing [63, 144–147]. This section is divided into two such examples, starch nanocomposites reinforced with inorganic clays and/or carbon nanotubes and organic (cellulosic) nanostructured reinforcements.

Bionanocomposites based on starch reinforced with inorganic and organic nanostructured reinforcements such as carbon nanotubes, clays, and cellulose whiskers have been reported in the literature [147–164]. Cao *et al.* [147] studied the utilization of multiwalled carbon nanotubes (MWCNTs) as nanostructured

reinforcement to improve the performance of plasticized starch (TPS, thermoplastic starch), prepared by solution casting. Addition of MWCNT content up to 3.0 wt% increased TS by 66% from 2.85 to 4.73 MPa, and Young's modulus by 89% from 20.74 to 39.18 MPa without decreasing elongation at break, which was even higher than that of TPS, reaching a maximum at 1 wt% MWCNT. The incorporation of MWCNT into the TPS matrix also led to a decrease in water uptake of up to 14%, which was attributed to strong hydrogen bond formation between carbon nanotubes and TPS molecules.

Addition of kaolinite in bionanocomposites with glycerol-plasticized cornstarch increased tensile properties, while strain at break was found to decrease by about 50% of its initial value with addition of clay. Similar to MWCNT, this clay also led to a reduction in water uptake of the bionanocomposites as reported by Carvalho *et al*. [149].

Addition of several types of clays as well as modified (organophilized clays) were found to improve mechanical properties and decrease water uptake of starch-based bionanocomposites; viz., natural sodium montmorillonite (MMT) [155], MMT, hectorite, hectorite modified with 2-methyl, 2-hydrogenated tallow quaternary ammonium chloride and kaolinite [150], natural sodium montmorillonite (Na^+MMT, Cloisite Na^+), and organically modified montmorillonite (OMMT) with methyl tallow bis-2-hydroxyethyl ammonium cations located in the silicate gallery (Cloisite 30B) [151], MMT (hydrophilic Cloisite Na^+ clay and hydrophobic Cloisite 30B, 10A, and 15A) [152, 153].

The addition of plasticizers such as glycerol and urea has also been studied [153, 156, 157]. Addition of glycerol to some bionanocomposites not only affected their mechanical properties but also the type of composite (exfoliated, intercalated) produced [153]. For example, addition of 5 wt% glycerol produced mostly exfoliated clay, whereas 10 or 15 wt% glycerol produced intercalated clay. This behavior was attributed to an increase in starch–glycerol interactions in samples containing higher glycerol concentrations which competed with interactions between starch, glycerol, and clay surface.

Chen *et al*. [156] produced nanocomposite foams by melt processing TPS using urea as plasticizer and ammonium-treated montmorillonite (NH_4MMT). They noticed that the use of urea also enhanced the dispersion of NH_4MMT in the TPS, making exfoliated TPS–clay nanocomposites possible. Synergistic effects of the urea plasticizer with ammonium treatment of the clay enhanced clay dispersion and foaming due to ammonia production.

Modified starch matrices have also been reported [151, 154]. Qiao *et al*. [154] prepared nanocomposites with MMT, OMMT, and thermoplastic acetylated starch (TPAS) plasticized with glycerol. They found that the TS and storage modulus of the TPAS nanocomposites were remarkably enhanced because of the interaction of layered silicates with the TPAS matrix. Moreover, the reinforcing effect of OMMT was greater than that of MMT because of the reduced hydrophilic nature of acetylated starch, which improved the dispersion of OMMT in TPAS more than unmodified MMT. These results are, therefore, in accordance with those

obtained by Park *et al*. [151], in which unmodified MMT had better interaction with unmodified starch because of their similar hydrophilic nature.

Anglès and Dufresne [158, 159] studied bionanocomposites from glycerol-plasticized waxy maize starch and cellulose whiskers extracted from tunicate. Although a very low reinforcing effect was observed on the addition of tunicin whiskers as a consequence of plasticizer accumulation at the interfacial zone, other bionanocomposites were successfully prepared. For example, bionanocomposites from potato pulp cellulose microfibrils gelatinized with potato starch [160] had reduced water sensitivity and a strong increase in thermomechanical stability. Additionally, Dufresne *et al*. [161] found that the mechanical properties of this system, similar to bionanocomposites from glycerol-plasticized waxy maize starch and cellulose whiskers [158, 159], depended on plasticizer content and relative humidity. The reinforcing effect was more significant in plasticized starch due to the decrease in glass transition temperature of the matrix down to temperatures lower than room temperature. The strongest, most flexible filaments were obtained with nonplasticized starch matrix in a dry atmosphere. Mechanical properties of highly plasticized materials were found to depend strongly on relative humidity. Moreover, it was found that these composites had reduced water uptake with the addition of nanofibrils.

However, the previous works on glycerol-plasticized nanocomposites resulted in an accumulation of glycerol on the surface of the cellulose whiskers giving rise to antiplasticization effects [158, 159, 161] and thus poor mechanical properties. Mathew and Dufresne [162] overcame this drawback by utilizing nanocomposites from waxy maize starch, plasticized with sorbitol, and with tunicin whiskers as reinforcement. Contrary to the previous works, they found that the sorbitol-plasticized system exhibited a single glass transition without any evidence of preferential migration of plasticizers toward the cellulose and no transcrystallization of amylopectin on cellulose surface. It was also found that the glass transition temperature of the plasticized amylopectin matrix first increases up to a whisker content of ~10–15 wt% and then decreases. A significant increase in crystallinity was also observed in the composites by increasing either moisture content or whisker content, while water uptake of the composites remained roughly constant on whisker addition. These studies suggest that the reinforcing effect of cellulose nanofibrils in plasticized starch matrices is very complex depending on moisture, amount, and type of plasticizer and reinforcement.

Orts *et al*. [17] investigated composites of wheat or potato starch blended with pectin and reinforced with cellulose nanofibrils extracted from cotton, softwood, or bacterial cellulose. Mechanical and thermal properties of composites produced by casting and extrusion (extruded under a ''low'' and ''high'' shear mode) were evaluated. The addition of cellulose microfibrils to starch had a significant effect on mechanical properties at low concentrations. For example, Young's modulus of wheat starch nanocomposites reinforced with cotton nanofibrils increased by five times with the addition of only 2.1 wt% of nanofibrils (see Table 11.1).

The authors also found out that the source of cellulose nanofibrils influenced mechanical properties of the composites. Whereas mechanical properties

Table 11.1 Young's modulus (E) and elongation at maximum load (ε_m) of composites of wheat starch and cellulose nanofibrils extracted from cotton as a function of fiber content [17].

Nanofibrils (%)	E (GPa)	ε_m (%)
0.0	1.39 (0%)[a]	2.7 (0%)
2.1	5.09 (266%)	3.9 (44%)
5.0	9.34 (572%)	8.4 (210%)
10.3	12.45 (796%)	8.8 (226%)

[a] Percent increase with addition of cellulose nanofibrils in relation to pure starch.

for composites reinforced with cotton and wood-derived microfibrils were indistinguishable, both Young's modulus and elongation at maximum load were significantly lower for composites reinforced with bacterial cellulose. On the other hand, the addition of 5 wt% of cellulose nanofibrils to a 50/50 wt% starch/pectin blend resulted in a decrease in mechanical properties. These results therefore corroborate previous works on starch-based nanocomposites [158, 159, 161] where the addition of a third component can give rise to complex interactions between the components, often resulting in poorer mechanical properties. Further studies on starch-based bionanocomposites reinforced with CNWs [163, 164] also displayed improved mechanical properties and water uptake with the addition of these nanowhiskers.

Blends of starch with natural and synthetic polymers have also been extensively studied in order to overcome aging effects (i.e., recrystallization after processing), to impart better mechanical properties, and to reduce the hydrophilic character of starch [3, 86, 129]. The addition of natural biodegradable polymers, nevertheless, has gained more attention with the intent of producing fully biodegradable blends [7, 98, 99].

McGlashan and Halley [165] prepared nanocomposite blends of starch and polyester reinforced with MMT. Their results showed that the addition of MMT significantly improved both the processing and tensile properties over the original starch blend and the type of nanocomposite produced (intercalated or exfoliated) depended on the amount of clay added and the ratio of starch to polyester, which also influenced mechanical and thermal properties. Biodegradable blends of starch and polyester with significantly improved tensile properties were produced with small amounts of MMT. For example, the TS, strain at break, and Young's modulus of a 30/70 starch/polyester nanocomposite blend were improved by about 38%, 38%, and 240%, respectively, with values of deformation at break improved by 1500%. However, further increasing the amount of starch decreased the mechanical properties of the blends. It was also observed that these nanocomposite blends were easier to process than the base blends using a film blowing tower.

In a similar study, Kalambur and Rizvi [166, 167] employed reactive extrusion to develop biodegradable starch–polyester (PCL) nanocomposite blends with higher

starch content and enhanced properties. They used a Fenton's reagent to oxidize starch and initiate cross-linking between oxidized starch and PCL in order to improve interfacial adhesion between starch and PCL. Their biodegradable nanocomposite blends contained up to 40% starch, resulting in tough materials with elongational properties comparable to that of 100% polyester.

Nanocomposite blends with enhanced properties were also produced using polyethylene-octene elastomer, starch, and MMT [168], commercial starch/PCL blend, and MMT (Cloisite Na^+, Cloisite 30B, and Cloisite 10A) [169], starch, PVA, and MMT [170], starch, PLA, and MMT (Cloisite 10A, Cloisite 25A, Cloisite 93A, and Cloisite 15A) [171].

As observed previously, starch has been largely utilized in blends and nanocomposites with a variety of reinforcements. Less known is the ability to use starch nanocrystals (StNs) as reinforcement in polymer matrices. StNs with dimensions of a few nanometers are formed from acid hydrolysis of starch granules. These starch crystals are mainly formed of crystalline amylose, as acid hydrolysis removes the amorphous domains comprised mostly of amylopectin [172, 173]. Such StN-reinforced nanocomposites were prepared with poly(β-hydroxyoctanoate) (PHO) [174], natural rubber [175–177], poly(styrene-*co*-butyl acrylate) [178], waxy maize starch [179, 180], sorbitol-plasticized pullulan [181], and PVA [182]. Moreover, the possibility of surface modification by grafting can lead to reinforcements compatible with hydrophilic and hydrophobic matrices [183, 184]. Using a glycerol-plasticized starch matrix, a temperature increase was reported for the main relaxation process associated with the glass-rubber transition of amylopectin-rich domains when increasing the StNs content [179]. The reduction in the molecular mobility of matrix amylopectin chains for filled materials was explained by the establishment of hydrogen bonding between both components. This increase of T_g led to a considerable slowing down of the retrogradation of the matrix, perhaps corresponding to a reduction in chain mobility. This is a very interesting result considering that retrogradation and crystallization of TPS during aging lead to undesired changes in thermomechanical properties, the main drawback for application of starch-based plastics. For this system, an increase in the degree of crystallinity of the TPS matrix was also reported [179]. It was suggested that crystallization of the matrix occurred at the interface between the nanostructured reinforcement and the matrix, owing to the similar chemical structure of both components.

11.2.5.2 **Chitin Bionanocomposites**

Although chitin can be processed in the form of films, it has been largely used as reinforcement to bionanocomposites. Chitin nanowhiskers have been used to prepare a variety of bionanocomposites with matrices such as natural rubber, PLA, PCL, PVA, silk fibroin, and chitosan [185–194], as will be discussed throughout the text below.

For example, Lu *et al*. [195] developed environmentally friendly thermoplastic nanocomposites using a colloidal suspension of chitin whiskers as a filler to reinforce SPI plastics. Chitin whiskers prepared from commercial chitin by acid hydrolysis were added to SPI. The authors reported that SPI/chitin whisker

nanocomposites at 43% relative humidity improved both TS and Young's modulus. Moreover, they also reported that incorporation of chitin whiskers into the SPI matrix resulted in an improvement in water resistance for the nanocomposites.

11.2.5.3 **Chitosan Bionanocomposites**

Chitosan has also been used as a matrix for bionanocomposites with a variety of nanoreinforcements such as chitin, clays, and cellulose nanofibrils [189, 196–200].

Mathew *et al.* [196] developed cross-linked bionanocomposites using chitosan reinforced with chitin nanocrystals and gluteraldehyde as the cross-linker. These composites were characterized by FTIR, XRD, and atomic force microscopy (AFM). The authors found that cross-linking and chitin whiskers content were both found to impact the water uptake mechanism. Cross-linking provided dimensional stability in acidic medium and significantly decreased the equilibrium water uptake. Moreover, incorporation of chitin nanocrystals provided increased permeation selectivity to chitosan in neutral and acidic medium.

In a similar study, Sriupayo *et al.* [189] developed bionanocomposites via solution-casting films of chitosan reinforced with chitin whiskers. The addition of chitin whiskers did not significantly affect the thermal stability and the apparent degree of crystallinity of the chitosan matrix. The TS of chitosan films reinforced with chitin whiskers increased from that of the pure chitosan film, with initial increase in the whisker content, to reach a maximum at the whisker content of 2.96 wt%. TS then decreased gradually with further increase in the whisker content. The elongation at break (percentage change) decreased from that of the pure chitosan with initial increase in the whisker content and leveled off when the whisker content was greater than or equal to 2.96 wt%. Both the addition of chitin whiskers and heat treatment helped improve water resistance, leading to nanocomposite films with decreased percentage of weight loss and percentage degree of swelling.

Chitosan-based bionanocomposites with improved properties, namely barrier and mechanical properties, were also prepared by Moura *et al.* [200] who added chitosan/tripolyphosphate (CS–TPP) nanoparticles to hydroxypropyl methylcellulose (HPMC) edible films (Figure 11.14). Samples were characterized by FTIR, TEM, SEM, mechanical properties, water vapor permeability (WVP), and thermal stability. The authors reported that the incorporation of chitosan nanoparticles into the films improved their mechanical and film barrier properties significantly. This behavior was attributed to the chitosan nanoparticles that tend to occupy the empty spaces in the pores of the HPMC matrix, increasing the collapse of the pores and thereby improving film tensile properties and WVP.

Bionanocomposites using chitosan reinforced with different concentrations of cellulose nanofibers (CNFs) and glycerol as the plasticizer were developed by Azeredo *et al.* [197]. The effect of reinforcement on tensile properties, WVP, and glass transition temperature was studied. The authors showed that CNFs improved the mechanical and water vapor barrier properties of chitosan films. The bionanocomposite with 15% CNF, plasticized with 18% glycerol, was found to be comparable to some synthetic polymers in terms of strength and stiffness. However, their films had relatively poor flexibility and water vapor barrier.

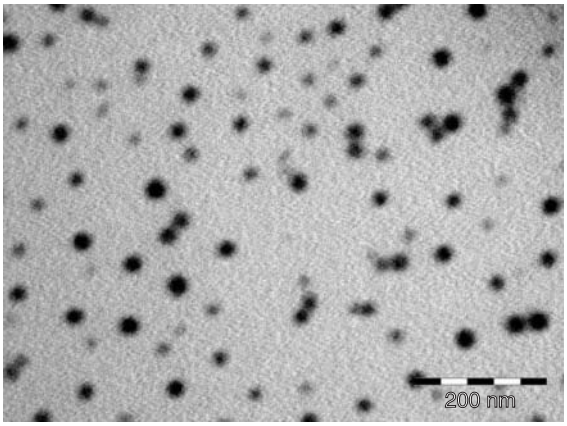

Figure 11.14 TEM microphotography of chitosan/tripolyphosphate (CS-TPP) nanoparticles used in the hydroxypropyl methylcellulose (HPMC) bionanocomposites [200].

Rhim *et al*. [198] also developed chitosan-based bionanocomposite films with antimicrobial activity. Four different types of chitosan-based nanocomposite films were prepared by solvent-casting method followed by incorporation of unmodified montmorillonite (Na-MMT), OMMT (Cloisite 30B), nano-silver, and Ag-zeolite (Ag-Ion). The authors reported that XRD patterns of the nanocomposite films indicated that a certain degree of intercalation was formed in the nanocomposite films, with the highest intercalation in the Na-MMT-incorporated films followed by films with Cloisite 30B and Ag-Ion. Scanning electron micrographs showed that in all of the nanocomposite films except for the one incorporating silver, nanoparticles were dispersed homogeneously throughout the chitosan polymer matrix. Consequently, mechanical and barrier properties of chitosan films were affected through intercalation of nanoparticles; that is, TS increased by 7–16%, whereas WVP decreased by 25–30% depending on the nanoparticle material tested. In addition, chitosan-based nanocomposite films, especially silver-containing ones, showed a promising range of antimicrobial activity.

Chitosan/vermiculite (VMT) bionanocomposites were studied by Zhang *et al*. [199] who prepared their composites by solution mixing of chitosan with three different modified VMTs, viz., hydrochloride (HVMT), sodium (NVMT), and cetyl trimethyl ammonium bromide (OVMT) treated VMT. Wide-angle X-ray diffraction (WAXD), TEM, and TGA were employed in composite characterization. The authors reported that both WAXD and TEM characterization indicated that the silicate layers were dispersed into the chitosan matrix in a disordered array. It was also found that the thermal stability of the bionanocomposites was dependent on the clay modification process. The chitosan/HVMT nanocomposites had the best thermal performance, compared to that of neat chitosan, which was attributed to the good dispersion of acid-modified VMT and better interaction between HVMT and chitosan in the bionanocomposites.

Bionanocomposites based on chitosan with clays or carbon nanotubes have also been developed to be used in sensor applications such as detection of ionic species and heavy metals in contaminated waters and immunosensors [201–203]. For example, Darder *et al.* [202] developed bionanocomposites of chitosan reinforced with Na^+-MMT for applications in sensors. CHN chemical analysis, XRD, Fourier transform infrared spectroscopy, scanning transmission electron microscopy, energy-dispersion X-ray analysis, and thermal analysis were employed to characterize their nanocomposites. The adsorption in mono- or bilayers of chitosan chains (Figure 11.15) were confirmed depending on the relative amount of chitosan with respect to the cationic exchange capacity of the clay. The first chitosan layer was adsorbed through a cationic exchange procedure, while the second layer was adsorbed in the acetate salt form. Because the deintercalation of the biopolymer was very difficult, the NH_3^+(acetate salt)$^-$ species belonging to the chitosan second layer acted as anionic exchange sites and, in this way, such nanocomposites became suitable systems for the detection of anions. According to the authors, these materials were successfully used in the development of bulk-modified electrodes exhibiting numerous advantages as easy surface renewal, ruggedness, and long-time stability.

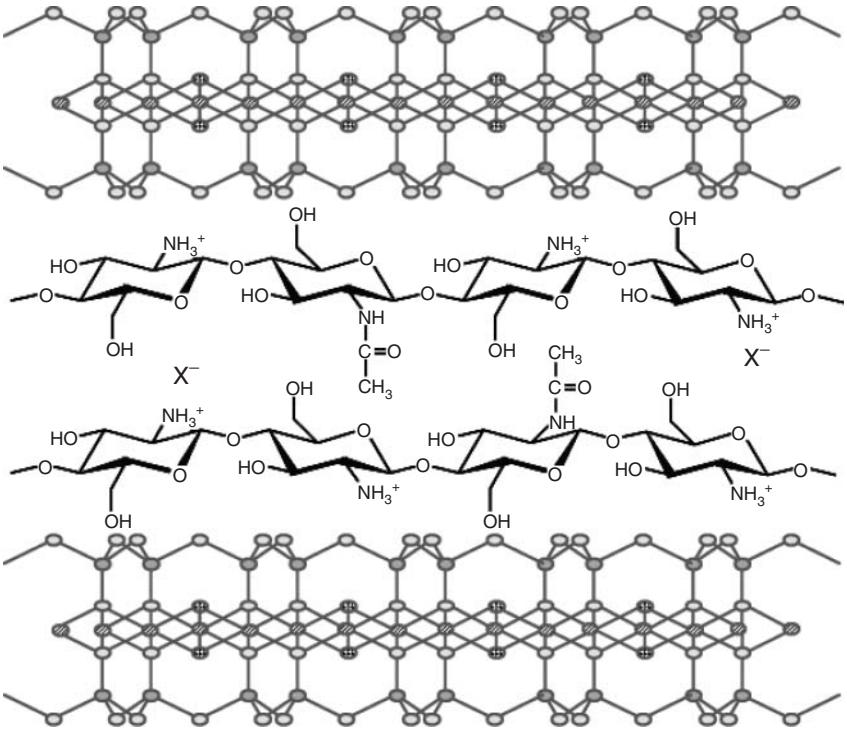

Figure 11.15 Schematic representation of chitosan intercalated in the clay substrate as a bilayer used in bionanocomposite-based sensors [202].

Chitosan has also been used as reinforcement in nanocomposites. Chitosan nanoparticles were used by Kampeerapappun *et al.* [204] to produce bionanocomposites with cassava starch and MMT nanocomposites. The authors reported that the addition of chitosan, due to its hydrophilicity and ability to attach to the clay surface, played a role in compatibilizing the interface between starch matrix and MMT. As a result, the starch/MMT composite film at low MMT content exhibited an improvement in tensile properties due to a reinforcement effect. It was also found that the surface hydrophobicity of the composite film increased with an increase in chitosan content. In association with film hydrophobicity, the water vapor transmission rate and moisture absorption were found to decrease with an increase in chitosan content.

The use of chitosan bionanocomposites with hydroxyapatite has also been reported in the literature as potential biomaterials. Chitosan (CS)/hydroxyapatite (HA) bionanocomposites prepared by *in situ* hybridization, according to Hu *et al.* [205] can be potentially applied in internal fixation of bone fractures. Also, Zhang *et al.* [206] developed biomimetic nanocomposite nanofibers of hydroxyapatite/chitosan (HA/CS) prepared by combining an *in situ* coprecipitation synthesis approach with an electrospinning process. A model HA/CS nanocomposite with the HA mass ratio of 30 wt% was synthesized through a coprecipitation method so as to attain homogeneous dispersion of the spindle-shaped HA nanoparticles (about 100 nm × 30 nm) within the chitosan matrix. By using a small amount (10 wt%) of ultra-high molecular weight poly(ethylene oxide) (UHMWPEO) as a fiber-forming facilitating additive, continuous HA/CS nanofibers with a diameter of 214 ± 25 nm were produced successfully and the HA nanoparticles with some aggregations were incorporated into the electrospun nanofibers. Biological *in vitro* cell culture with human fetal osteoblast (hFOB) cells maintained for up to 15 days demonstrated that the incorporation of HA nanoparticles into chitosan nanofibrous scaffolds led to significant bone formation compared to that of the pure electrospun CS scaffolds.

11.2.6
Protein Bionanocomposites

Proteins are amphoteric molecules that can migrate spontaneously to an air–water interface or an oil–water interface. Once at the interface, proteins have the ability to interact with neighboring molecules and form strong cohesive, viscoelastic films that can withstand thermal and mechanical motions. Traditionally, proteins are used in adhesives and edible films/coatings [31]. However, their main drawback in these applications is their inherent high water permeability and low water resistance at relatively high humid conditions. Some studies in the literature [207] show that these drawbacks can be overcome by adding nanoreinforcements such as clays and CNWs. Different protein-based bionanocomposites have been prepared using collagen, gelatin, zein, gluten, milk protein, and silk fibroin as their matrices [31, 207].

11.2.6.1 Soy Protein Isolate

Lu *et al.* [195] studied bionanocomposites of SPI thermoplastics reinforced with chitin whiskers using a colloidal suspension of chitin whiskers prepared from commercial chitin by acid hydrolysis. The dependence of morphology and properties on the chitin whiskers content, ranging from 0 to 30 wt% for the glycerol-plasticized SPI nanocomposites, was investigated by dynamic mechanical analysis (DMA), SEM, swelling tests, and tensile testing. The authors concluded that the strong interactions between fillers and SPI matrix played an important role in reinforcing the composites without interfering with their biodegradability. The SPI/chitin whisker nanocomposites at 43% relative humidity increased both TS and Young's modulus from 3.3 MPa for the SPI sheet to 8.4 MPa (250%), and from 26 MPa for the SPI sheet to 158 MPa (600%), respectively. Incorporation of chitin whiskers into the SPI matrix also lead to an improvement in water resistance for the SPI-based nanocomposites.

Chen and Zhang [208] studied the interaction and properties of highly exfoliated SPI/MMT bionanocomposites by XRD, TEM, DSC, TGA, and tensile testing. The interactions between the soy protein macromolecules and MMT in aqueous media were analyzed with ζ-potential measurements, FTIR, and electrostatic surface potential calculations. The results revealed soy globulins, which bear net negative charges, were able to anchor into the negatively charged MMT galleries because of the heterogeneous distribution of surface positive charges providing positive-charge-rich domains. Electrostatic attraction and hydrogen bonding interactions on the interfaces of the soy protein and MMT led to the good dispersion of the phyllosilicate layers in the protein matrix (Figure 11.16). The highly exfoliated MMT layers with a dimension of 1–2 nm in thickness were randomly dispersed in the protein matrix containing MMT lower than 12 wt%, whereas the intercalated structure was predominant when the MMT content was higher than 12 wt%. Consequently, the fine dispersion of the MMT layers and the strong interactions between SPI and MMT created the significant improvement of the mechanical strength and thermo-stability of the SPI/MMT plastics.

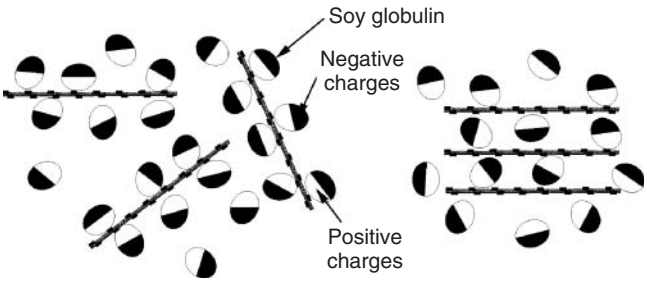

Figure 11.16 Scheme of the interaction between soy protein isolate (SPI) and montmorillonite (MMT) in the bionanocomposites: (a) highly exfoliated state and (b) intercalated state. Positively charged domains are colored in white, and negatively charged domains are in black [208].

The effect of type and content of modified MMT on the structure and properties of bionanocomposite based on SPI and MMT was studied by Kumar *et al*. [209, 210]. Bionanocomposite of SPI and two types of modified MMT were prepared by melt extrusion. The effect of clay modification (Cloisite 20A and Cloisite 30B) and content (0–15%) on the structure (degree of intercalation and exfoliation) and properties (color, mechanical, dynamic mechanical, thermal stability, and WVP) of SPI-MMT bionanocomposites were investigated. They concluded that extrusion of SPI and modified MMT resulted in bionanocomposites with exfoliated structures at lower MMT content (5%), whereas at higher MMT content (15%), the structure of bionanocomposites ranged from intercalated for Cloisite 20A to disordered intercalated for Cloisite 30B (Figure 11.17). At an MMT content of 5%, bionanocomposites based on modified MMTs (Cloisite 20A and Cloisite 30B) had better mechanical (TS and elongation at break), dynamic mechanical (glass transition temperature and storage modulus), and water barrier properties as compared to those based on natural MMT (Cloisite Na^+). The authors concluded

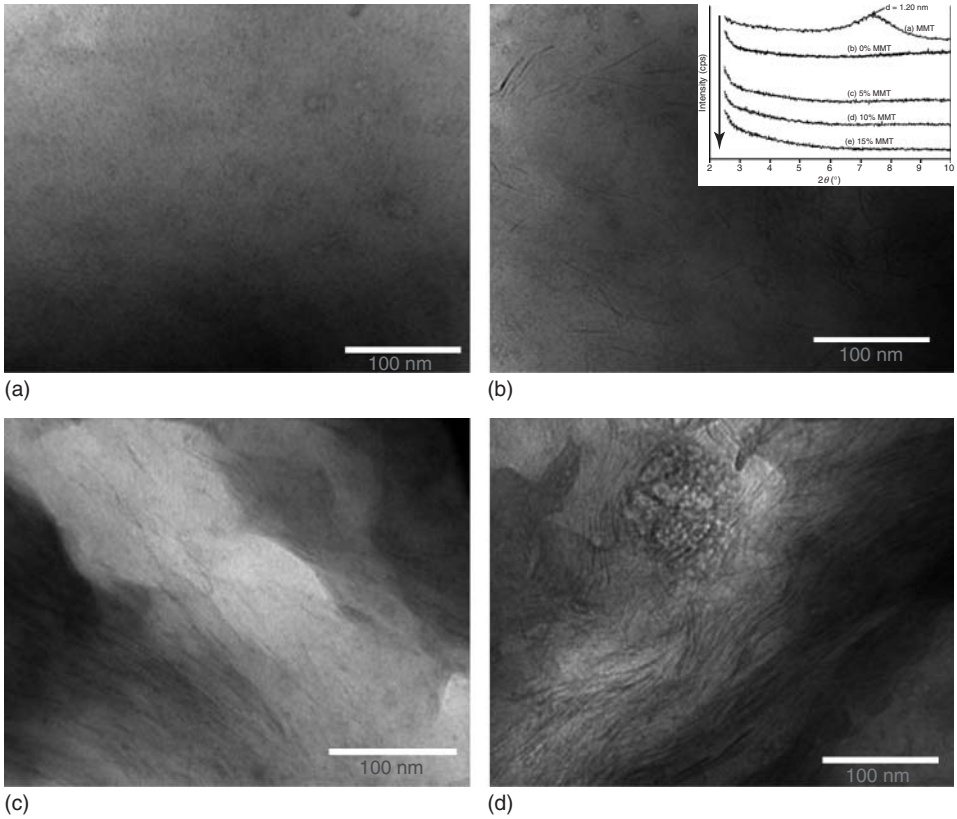

Figure 11.17 TEM images of SPI–MMT bionanocomposites with (a) 0%, (b) 5%, (c) 10%, and (d) 15% MMT contents [210]. Scale bar = 100 nm. Inset: XRD patterns with increasing MMT content.

that bionanocomposites based on 10% Cloisite 30B had mechanical properties comparable to those of some of the plastics that are currently used in food packaging applications. However, according to the authors, high values of WVP for these films, as compared to those of existing plastics, might limit the application of these bionanocomposites to packaging of high moisture foods such as fresh fruits and vegetables.

Zheng *et al*. [211] used pea StNs to prepare bionanocomposites with a SPI matrix that was plasticized with glycerol and then molded by compression molding in order to produce fully biodegradable nanocomposites. According to the authors, the StN with low loading level (2 wt%) showed a predominant reinforcing function, resulting in an enhancement in strength and Young's modulus by about 50% and 200%, respectively (Figure 11.18). This behavior was attributed to uniform dispersion of StN in the amorphous region of the SPI matrix and to the interfacial interaction between the active StN surface and the SPI matrix. With increasing content, number, and size, of StN, its domains increased because of a strong self-aggregation tendency of StN. The increased filler level also destroyed the ordered structure of the soy protein matrix, causing a gradual decrease in strength and Young's modulus. The introduction of relatively hydrophilic StN did not cause an obvious decrease of water resistance for any of the nanocomposites. The water uptake behavior of all the nanocomposites, similar to that of neat SPI material, was

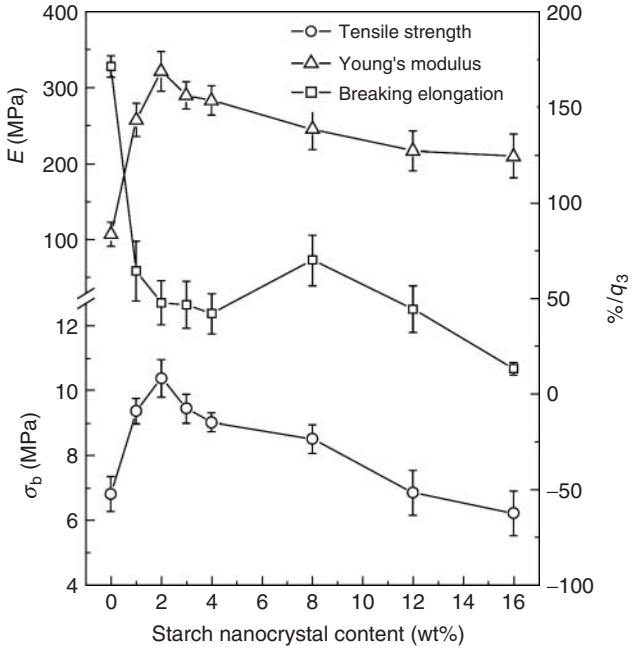

Figure 11.18 Effect of starch nanocrystal content on mechanical performance of SPI/StN bionanocomposites [211].

attributed mainly to the strong interfacial interaction between the StN filler and the SPI matrix.

Bionanocomposites based on SPI reinforced with bentonite, talc powder, zeolite, and rectorite have also been reported in the literature [212–214]. In most cases, they had improved mechanical and barrier properties as compared to unfilled matrices.

11.2.6.2 **Gelatin**

Gelatin is prepared by the thermal denaturation of collagen, isolated from animal and fish skin and bones, with very dilute acid. Gelatin has also been successfully and largely used as a matrix to produce bionanocomposites which are reinforced with nanoreinforcements such as clays and hydroxyapatite to be used in applications ranging from packaging materials to artificial bones.

Zheng *et al.* [215, 216] prepared gelatin/MMT hybrid bionanocomposites with unmodified MMT and gelatin aqueous solution. They showed that intercalated or partially exfoliated nanocomposites with significantly improved properties could be obtained by the addition of MMT to gelatin. The intercalation with MMT greatly improved mechanical properties of the bionanocomposites. For example, a composite with 5 wt% MMT had a TS of 78.9 MPa and a Young's modulus of 1.6 GPa which were, respectively, 1.6 and 1.8 times higher than those of neat gelatin. When MMT content reached 17 wt%, TS and Young's modulus raised to 89.1 MPa and 2.0 GPa, respectively. This enhancement was attributed to the uniform dispersion of MMT layers in gelatin matrix and the strong interaction between gelatin and MMT, which resulted in the increased TS and Young's modulus. As the MMT content increased over 17 wt%, the TS and Young's modulus began to decrease because of MMT aggregation. According to the authors, these nanocomposites also exhibited remarkable barrier properties.

The same group [217, 218] also studied the *in vitro* biodegradation and biocompatibility of gelatin (Gel)/MMT–chitosan (CS) intercalated bionanocomposites that were prepared via solution intercalation. *In vitro* degradation tests showed that the bionanocomposites had a lower degradation rate than Gel–CS composite, with a controllable degradation rate when changing the MMT content. Cell attachment, as well as spread and proliferation on the Gel/MMT–CS membranes, were investigated by SEM and mitochondrial activity assay. The results provided evidence of good adhesion, proliferation, and morphology of rat stromal stem cells on Gel/MMT–CS membranes compared to the tissue culture plates (TCPs), making the Gel/MMT–CS nanocomposite a promising candidate toward tissue engineering.

Martucci *et al.* [219] also developed gelatin/MMT bionanocomposites with different clay concentrations in order to evaluate the influence of bionanocomposite morphology on their thermal stability. Morphologies changed from partially exfoliated to exfoliated/intercalated and eventually agglomerated with increasing clay loading, as observed by AFM. Formulations containing 3–10 wt% MMT resulted in bionanocomposites with enhanced thermal stability due to stabilizing interactions between components, such as strong hydrogen-type bonds, in agreement with the partially exfoliated/intercalated morphologies. Higher clay concentrations showed

lower stabilizing effect in agreement with the agglomerated structures developed and the less effective interactions between the components.

Rao [220] reported that bionanocomposites of gelatin and MMT made through solution processing also exhibited enhanced physical performance. The Young's modulus of the composite film was 8.3 GPa, almost three times that of gelatin alone, by dispersing only 10 wt% of one type of MMT clay into the nanosized phase in the gelatin. With the addition of the clay nanoparticles, the crystallinity of gelatin decreased and the melting point increased slightly. XRD and TEM revealed that clay nanoplatelets were well exfoliated and dispersed, and are parallel to the plane of film in the bionanocomposite. The property enhancements of gelatin were affected by particle dispersion (i.e., intercalation and exfoliation), properties (i.e., aspect ratio), and particle–matrix interaction.

For several years, hydroxyapatite/gelatin bionanocomposite using biomimetic coprecipitation has been pursued as a biological bone substitute because of its biocompatibility, biodegradability and its usage as a scaffold site for regeneration of new bones [221–226].

Chang *et al*. [225] developed bionanocomposites of gelatin and hydroxyapatite (HA). The chemical bonding between calcium ions of HA and carboxyl ions of gelatin molecules was studied by FTIR. TEM images and electron diffraction patterns for the nanocomposite strongly indicate the self-organization of HA nanocrystals along gelatin fibrils. Electron diffraction for the nanocomposites showed a strong preferred orientation of the (002) plane in HA nanocrystals. It was also found that the development of HA nanocrystals in aqueous gelatin solutions was highly influenced by the concentration ratio of gelatin related to HA. A higher concentration of gelatin induced the formation of tiny crystallites (4 nm × 9 nm), while a lower one contributed to the development of larger crystallites (30 nm × 70 nm).

Chang and Douglas [226] also developed hydroxyapatite (HA)/gelatin bionanocomposites via coprecipitation. The HA/gelatin nanocomposite slurries were cross-linked by imide-based cross-linking agent such as N-(3-dimethylaminopropyl)-N′-ethylcarbodiimide (EDC) and N-hydroxysuccinimide (NHS). The chemical bond formation and microstructure in HA/Gel nanocomposite was investigated as a function of cross-linking agents and temperature. The single addition of EDC to the composite slurries resulted in a tougher microstructure in both samples prepared at 37 and 48 °C. However, in the case of the simultaneous addition of EDC and NHS, the sample prepared at 48 °C showed a coarse microstructure. These results were consistent with the fact that the chemical reactivity of NHS was degraded at 48 °C whereas the reactivity of EDC increased up to 80 °C. In general, these hydroxyapatite/polymer bionanocomposites show good biocompatibility and biodegradability that might render them useful as components in tissue replacement material [227].

11.2.6.3 **Collagen**

Collagen/hydroxyapatite (HA) bionanocomposites have also been extensively studied as bone grafts due to their composition and structural similarity with natural

bone and their unique functional properties such as larger surface area and superior mechanical strength than their single phase constituents. These results indicate that HA-based bionanocomposites are probably the most suitable systems for bone replacement or regenerative therapy [228–230].

Kikuchi *et al.* [231] produced bionanocomposites of bioactive glass nanofiber (BGNF) and collagen for bone regenerative medicine. The authors used a sol–gel derived glass with a bioactive composition ($58SiO_2 \cdot 38CaO \cdot 4P_2O_5$) which was electrospun to a nanoscale fiber and subsequently hybridized with type I collagen, the main organic constituent of bone matrix. The bionanocomposite matrices induced rapid formation of bonelike apatite minerals on their surfaces when incubated in a simulated body fluid, exhibiting excellent bioactivity *in vitro*. Osteoblasts showed favorable growth on the BGNF–collagen bionanocomposite. In particular, the alkaline phosphatase activity of the cells on the nanocomposite was significantly higher than that on the collagen. This nanocomposite is believed to have significant potential in bone regeneration and tissue engineering applications.

Chang *et al.* [221] prepared porous bionanocomposites based on hydroxyapatite (HA) and collagen using glutaraldehyde as a cross-linking agent. Because of the cross-linked collagen network formation, three-dimensional columnar pore channels were developed. During natural drying, collagen bundles underwent self-alignment that was intensified by the appropriate amount of glutaraldehyde. The polymerization was induced by the existence of the self-organized HA nanocrystals.

Biocompatibile hydroxyapatite/collagen bionanocomposites were also studied by Santos *et al.* [232] using osteoblast cell culture assay. Their results showed that, after 72 h, their bionanocomposites did adversely affect cell morphology, and had similar cell viability and alkaline phosphatase activity related to the control. This demonstrated that these bionanocomposites can potentially be used in bone tissue replacement applications.

Pek *et al.* [233] also developed hydroxyapatite/collagen bionanocomposite bone scaffold that chemically, structurally, and mechanically matched natural bone. The foamlike scaffold has a similar microstructure as trabecular bone, with nanometer-sized and micron-sized pores. The apatitic phase of the scaffold also exhibited similar chemical composition, crystalline phase, and grain size, thus exhibiting excellent bioactivity for promoting cell attachment and proliferation. These bionanocomposites were osteoconductive in that they successfully healed a nonunion fracture in rat femur, as well as a critical-sized defect in pig tibia, therefore showing their potential in bone reconstitution.

Silica has also been used in collagen to produce bionanocomposites for biomedical applications. Desimone *et al.* [234] prepared silica–collagen bionanocomposites as three-dimensional scaffolds for fibroblast immobilization by addition of silica nanoparticles to a protein suspension followed by neutralization (Figure 11.19). Electron microscopy studies indicated that larger silica nanoparticles (80 nm) did not interact strongly with collagen, whereas smaller ones (12 nm) formed beaded ''rosaries'' along the protein fibers. However, the composite network structurally evolved with time because of the contraction of the cells and the dissolution of the

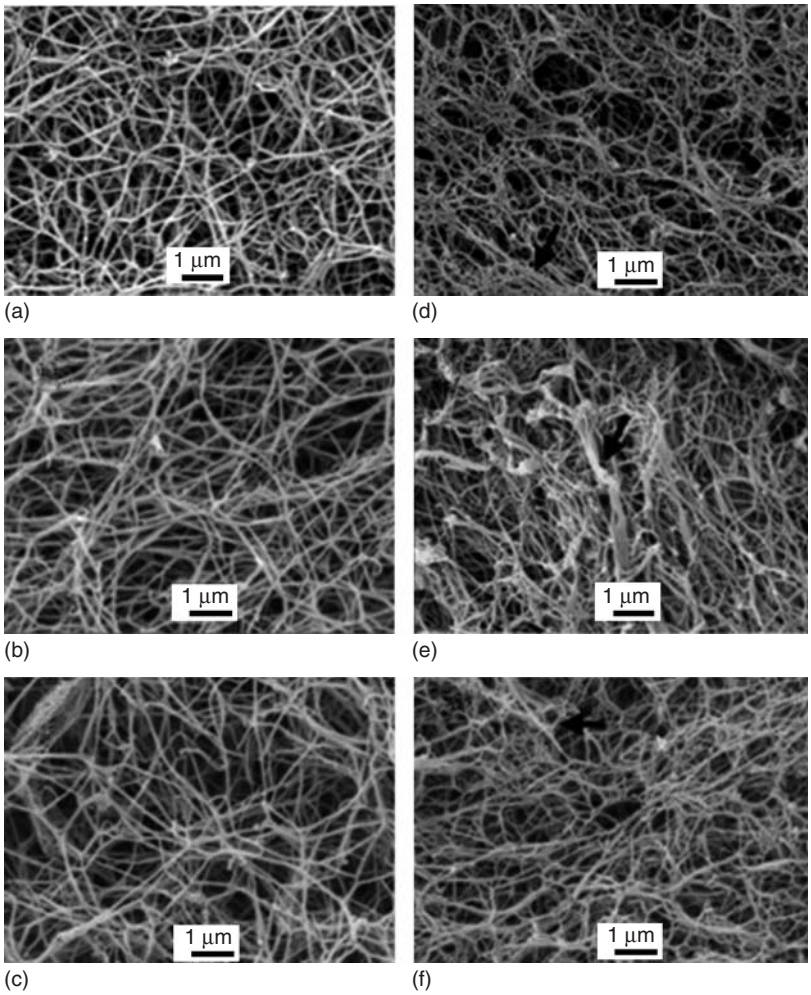

Figure 11.19 Representative SEM images of collagen (a,d), Si (12 nm)/collagen (b,e), and Si (80 nm)/collagen (c,f) bionanocomposites after incubation for 1 day (a–c) and 21 days (d–f) [234].

silica nanoparticles. These bionanocomposite matrices constitute a suitable environment for fibroblast adhesion, proliferation, and biological activity and therefore constitute an original three-dimensional environment for *in vitro* cell culture and *in vivo* applications, especially as biological dressings.

11.2.6.4 **Other Protein-Based Bionanocomposites**

Other proteins such as zein, gluten, and silk fibroin have also been used to produce bionanocomposites. Film-forming proteins, such as casein, whey protein, keratin, and fish myofibrillar protein, can also be used to prepare bionanocomposites

[143]. Below are some examples of how nanoreinforcements can be added to biodegradable matrices based on proteins to create nanocomposites with improved properties.

Luecha *et al.* [235] studied the properties of corn zein/MMT bionanocomposites produced by solvent casting and blow-molding extrusion. The two methods resulted in partially exfoliated nanocomposite structures that were studied by XRD and TEM. The thermal resistance of the zein nanocomposite films fabricated from both methods improved as the MMT content increased. However, mechanical and barrier properties showed nonlinear relationships with increasing MMT content (0, 1, 3, 5, and 10 wt%). The impact of MMT on properties of zein films strongly depended on the preparation techniques. Zein reinforced with organically modified and unmodified mica, kaolinite, MMT, and zeolite has also been developed using electrospinning in order to produce bionanocomposites with potential uses in packaging, active packaging, high surface area biomedical films, and pharmaceutical applications [236].

Silk fibroin-reinforced chitin whiskers were used to produce highly porous bionanocomposites [192]. The presence of chitin whiskers embedded into silk fibroin sponge not only improved its dimensional stability but also enhanced its compression strength. Regardless of the chitin whisker content, SEM micrographs showed that all samples possessed an interconnected pore network with an average pore size of 150 μm. To investigate the feasibility of the nanocomposites for tissue engineering applications, active (L929) cells were seeded onto their surfaces. Their results indicated that silk fibroin sponges both with and without chitin whiskers were cytocompatible. Moreover, when compared to the neat silk fibroin sponge, the incorporation of chitin whiskers into the silk fibroin matrix was found to promote cell spreading.

Olabarrieta *et al.* [237] studied wheat gluten-based bionanocomposites containing up to 4.5 wt% natural montmorillonite or those surface-modified with quaternary ammonium salt. These bionanocomposites a good barrier to water vapor as compared to the pristine polymer.

11.2.7
Bionanocomposites Using Biodegradable Polymers from Microorganisms and Biotechnology

11.2.7.1 Polyhydroxyalkanoates

PHAs are a family of linear polyesters of 3, 4, 5, and 6-hydroxyacids, synthesized by a wide variety of bacteria through the fermentation of sugars, lipids, alkanes, alkenes, and alkanoic acids. They are recyclable, natural materials, and can be easily degraded to carbon dioxide and water. This makes them as excellent replacements for petroleum-derived plastics in terms of processability, physical characteristics, and biodegradability. In addition, these polymers are biocompatible and hence have several medical applications [238], leading to vast interest in PHAs in bionanocomposites as well. The main polymers studied are poly(3-hydroxybutyrate), PHB and poly(hydroxybutyrate-*co*-hydroxyvalerate),

PHBV: although, as they become more commercially available, PHO and poly(hydroxybutyrate-*co*-hydroxyhexanoate), PHB-*co*-PHH, have also been employed in bionanocomposites.

Hajiali *et al*. [239, 240] prepared bionanocomposite scaffolds based on PHB and bioglass nanoparticles for bone tissue engineering. They added 10% bioglass nanoparticles to PHB by a salt leaching technique and showed that it was possible to produce scaffolds with uniform porosities of about 250–300 μm that are interconnected to resemble bone structures. Furthermore, higher magnification SEM images showed that the scaffold possessed less agglomeration yet had rough surfaces that may improve cell attachment for potential application in bone tissue engineering.

Hablot *et al*. [241] studied the influence of fermentation residues and quaternary ammonium salts on the thermal and thermomechanical degradation of a biodegradable bacterial poly(3-hydroxybutyrate), PHB. Results obtained from DSC, SEC, and TG analyses performed on mixtures revealed that ammonium cations greatly enhanced the degradation, leading to a dramatic decrease in PHB molecular weight and a subsequent adverse affect on thermomechanical behavior. However, the presence of fermentation residues did not affect PHB thermal stability in contrast to the ammonium cations that effectively had a catalytic effect on the PHB degradation. (Ammonium cations can be found in ammonium surfactants commonly used in commercial nanoclays for bionanocomposite production.) The same group [242] found a similar effect on thermal degradation of poly(hydroxybutyrate-*co*-hydroxyvalerate), PHBV.

Zhang *et al*. [243] prepared bionanocomposites based on poly(3-hydroxybutyrate-*co*-3-hydroxyhexanoate) (PHBHx), PHB-*co*-PHH, with OMMTs (clay 20A and clay 25A), mica, and talc by solution mixing. Wide-angle X-ray scattering results and TEM images confirmed that these two clays were intercalated and finely distributed in the PHB-*co*-PHH matrix. It was also found that the layered clays led to remarkable improvements in mechanical properties even at very low loadings; however, in some cases, the layered fillers slightly decreased the thermal stability of the bionanocomposites.

Hsu *et al*. [244] studied the nonisothermal crystallization behavior and crystalline structure of bionanocomposites derived from poly(3-hydroxybutyrate)/phosphonates (PEOPAs) modified with layered double hydroxide (PMLDH) by XRD and DSC. Effects of cooling rates and PMLDH contents on the nonisothermal crystallization behavior of PHB were explored. The addition of 2 wt% PMLDH to PHB caused heterogeneous nucleation, increasing the crystallization rate and reducing the activation energy. The addition of PMLDH to the PHB resulted in a decrease in crystallity of the latter, thus increasing the activation energy.

The isothermal degradation and kinetics of PHB-based bionanocomposites were studied by Erceg *et al*. [245]. Their bionanocomposites consisted of OMMT Cloisite 30B (30B) and PHB prepared by solution casting and isothermally degraded at 230, 235, 240, and 245 °C. They found that the addition of 30B increased the thermal stability of PHB with the most pronounced effect being the addition of 1 wt% 30B.

Maiti *et al.* [246] prepared new biodegradable polyhydroxybutyrate/layered silicate bionanocomposites via melt extrusion. Characterization by WAXD and TEM indicated that intercalated hybrids were obtained, and that the extent of intercalation depended on the amount of silicate and the nature of organic modifier present in the layered silicate. The nanohybrids showed significant improvement in thermal and mechanical properties of the matrix as compared to the neat polymer. They also found that silicate particles acted as a strong nucleating agent for PHB. The biodegradability of pure PHB and its nanocomposites was studied at two different temperatures under controlled conditions in compost media. It was found that the rate of biodegradation of PHB was enhanced dramatically in the bionanocomposites (Figure 11.20).

Silver sulfide (Ag_2S) has also been used with poly(3-hydroxybutyrate) to produce bionanocomposites. Yeo *et al.* [247] investigated the thermal behavior of these PHB/Ag_2S bionanocomposites using TG. They found that Ag_2S caused the degradation of PHB at a lower temperature as opposed to that of neat PHB. Moreover, an increase in Ag_2S loading in the PHB decreased the onset temperature of thermal degradation. Interestingly, this onset temperature increased at higher heating rates, which was attributed to the catalytic activity of Ag_2S nanoparticles facilitating the thermal degradation of PHB.

Polyhydroxybutyrate copolymers with polyhydroxyvalerate have also been extensively employed in bionanocomposites. Jiang *et al.* [248] developed bionanocomposites of poly(3-hydroxybutyrate-*co*-3-hydroxyvalerate) reinforced with CNWs by solution casting and melt processing. Homogeneous dispersion of the whiskers was achieved during solution casting, and the composites exhibited improved TS and modulus, as well as increased glass transition temperature. However, melt processed (extrusion and injection molding) PHBV/CNW composites had low dispersion of CNW, even when using polyethylene glycol (PEG) as a compatibilizer. As a result, the melt processed PHBV/CNW composites exhibited decreased strength and constant glass transition temperature, a typical trend of microparticles acting as ''fillers'' rather than as reinforcements.

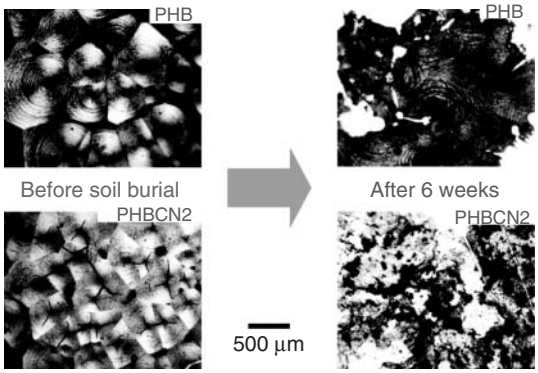

Figure 11.20 Effect of the addition of clay on the biodegradability of PHB/clay bionanocomposites as evidenced by a break down of their spherulitic crystalline structure [246].

Bruzaud and Bourmaud [249] studied the thermal degradation and (nano)mechanical behavior of bionanocomposites based on poly(3-hydroxybutyrate-*co*-3-hydroxyvalerate) reinforced with different amounts of organophilic MMT by process of solution intercalation. They concluded that thermal stability and tensile properties were greatly enhanced with the addition of only a few percent of organoclay. The effect of various loading levels of nanoclay reinforcement on the nanomechanical material properties was also investigated by nanoindentation technique, which confirmed that a significant increase of mechanical properties had been realized, in line with tensile tests.

Chen *et al*. [250] studied the crystallization kinetics of poly(3-hydroxybutyrate-*co*-3-hydroxyvalerate)/clay nanocomposites and found that, during the crystallization process, the addition of organophilic clay led to an increase in crystallization temperature (T_c) of PHBV compared with that for neat PHBV. This caused a corresponding increase in the overall crystallization rate of PHBV, but did not influence either the mechanism of nucleation, or growth of the PHBV crystals. They also concluded that the increase in T_c caused by adding a small quantity of clay is more effective than exceeding that small percentage. Also, the TS of hybrid, with the incorporation of 3 wt% clay, increased to 35.6 MPa, which is about 32% higher than that of the original PHBV. Tensile modulus was also increased.

Choi *et al*. [251] applied melt intercalation to prepare bionanocomposites of poly(hydroxybutyrate-*co*-hydroxyvalerate) reinforced with organoclay, Cloisite 30B, a monotallow bis-hydroxyethyl ammonium-modified MMT clay. XRD and TEM analyses confirmed that an intercalated microstructure was formed and finely distributed in the PHBV copolymer. Good dispersion was attributed to strong hydrogen bond interaction of PHBV with the hydroxyl group in the organic modifier of Cloisite 30B. They also found that the organoclays acted as nucleating agents, increasing the temperature and rate of crystallization of PHBV. Moreover, thermal stability and tensile properties in these organoclay-based nanocomposites were enhanced.

Carbon nanotubes have also been used to prepare bionanocomposites with PHBV. The addition of carbon nanotubes may improve the thermal stability and act as nucleating agents to PHBV [252, 253].

Bionanocomposites of PHBV reinforced with hydroxyapatite nanoparticles have been studied and compared to nanoclays-reinforced PHBV [254–257]. Maiti and Yadav [254] prepared bionanocomposites based on PHBV reinforced with layered silicate and hydroxyapatite by melt extrusion. The nanostructure, as observed from WAXS and TEM, indicated intercalated hybrids for layered silicates and uniformly distributed hydroxyapatite nanoparticles which conferred improvement in thermal and mechanical properties as compared to the neat copolymer. The layered silicate nanocomposites exhibited superior mechanical properties as compared to hydroxyapatite bionanocomposites. It was also found that the rate of biodegradation of the copolymer was enhanced dramatically with both nanoreinforcements, and the hydroxyapatite bionanocomposite showed the highest rate of biodegradation.

Addition of hydroxyapatite modified with a silane coupling agent was introduced into PHBV by Tang *et al.* [255] in an effort to understand the influence of the bioceramic phase on water absorption, solubility, and biodegradation. They concluded that, compared to neat PHBV, diffusion coefficients for the bionanocomposites decreased, whereas the sorption coefficients and the solubility show an opposite tendency. In another work [256], the dynamic mechanical properties, thermal properties, and bioactivity of these bionanocomposite were examined, indicating that better mechanical properties and improved bioactivity were achieved with the introduction of hydroxyapatite. Moreover, thermal analysis revealed that when incorporating hydroxyapatite nanoparticles, the decomposition of PHBV was accelerated at the initial stage but retarded thereafter.

With the ultimate goal to design bionanocomposites with optimal mechanical properties, Bordes *et al.* [257] developed bionanocomposites based on PHBHx, reinforced with two types of silica nanoparticles, spheres, and fibers. Simultaneous improvement of both stiffness and toughness was observed at 1 wt% loading. The highly aggregated SiO_2 fibers had a greater toughening effect than SiO_2 spheres. Compared to the unfilled polymer matrix, a 30% increase in Young's modulus and 34% increase in toughness were obtained for the 1 wt% SiO_2 fiber/PHBHx nanocomposite. When the loading was 3 wt% and above, Young's modulus continued to increase, but the strain at break and toughness decreased, and the ultimate strength did not change compared with the unfilled polymer. Zhang *et al.* [258] produced bionanocomposites by using silane-modified kaolinite/silica core–shell nanoparticles (SMKS) into PHBHx. These reinforcements were found to significantly improve the mechanical properties of the composites.

PHB has also been used together with other polymer matrices to produce bionanocomposite blends. For example, Sanchez-Garcia *et al.* [259] added PCL, to PHB which was reinforced with organomodified kaolinite and MMT clays. It was found that the addition of PCL reduced oxygen permeability. The addition of highly swollen organomodified MMT clays, with their intergalleries opened, to the PHB/PCL blend led to a high dispersion of the filler, but simultaneously increased melt instability of the biopolymer. It was also found that the organomodified kaolinite clay resulted in enhanced barrier properties to oxygen, D-limonene, and water.

PHO has also been used to prepare bionanocomposites. Dubief *et al.* [174] used PHO with hydrolyzed starch or cellulose whiskers to prepare bionanocomposites. They found that high-performance materials were obtained from these systems, preserving the natural character of PHO. The resulting properties were strongly related to the aspect ratio L/d (L being the length and d the diameter) of the filler and to the geometric and mechanical percolation effects. Also considered were specific polymer–filler interactions and geometrical constraints due to the particle size of the latex relative to the polymer free space. Addition of single wall carbon nanotubes (SWCNTs), investigated by Yun *et al.* [260] to PHO produced bionanocomposites with increased hardness (H) and Young's modulus (E), with increasing SWCNT concentration.

11.2.7.2 **Polylactides**

Like PHAs, polylactides have attracted the attention of the scientific community as matrices for bionanocomposites due to their increased commercial availability and interesting properties such as biodegradability, high strength, flexibility, and the relative ease in processing. Although some work has been published on PLAs reinforced with CNWs [261, 262] and carbon nanotubes [263, 264], most work is dedicated to layered silicates, specifically unmodified or OMMT [87].

Ray *et al*. [265] developed bionanocomposites based on PLA with OMMT by simple melt extrusion and found that intercalated nanocomposites exhibited remarkable improvement of materials properties as compared to PLA without clay. They also [266] used synthetic fluorine mica modified with N-(coco alkyl)-N,N-[bis(2-hydroxyethyl)-N-methylammonium cation for bionanocomposite preparation and found that all nanocomposites exhibited remarkable improvement of various materials properties with simultaneous improvement in biodegradability compared to neat PLA. The addition of MMT modified with trimethyl octadecylammonium cation to PLA, which was intercalated and well distributed in the matrix, was reported by Ray *et al*. [267] to produce PLA bionanocomposites with improved properties, especially their biodegradability in a compost environment (Figure 11.21).

Ray *et al*. [268] also found that the biodegradability of polylactides in bionanocomposites depends completely on both the nature of pristine layered silicates and surfactants used for the modification of layered silicate. Based on this behavior, they reported that composite biodegradability can be controlled by a judicious choice of the organically modified layered silicate (OMLS).

Maiti *et al*. [269] used organically modified smectite, MMT, and mica to prepare bionanocomposites with PLA. With a modifier of the same chain length, the gallery spacing of the organoclay was largest for mica and smallest for smectite because of the higher ion-exchange capacity of mica. Also, with its larger size, mica is more likely to restrict polymer chain mobility because of the restricted conformation at the core of the clay. The increase in modulus for a smectite nanocomposite, compared to that of PLA, was higher than for MMT or for mica nanocomposite due

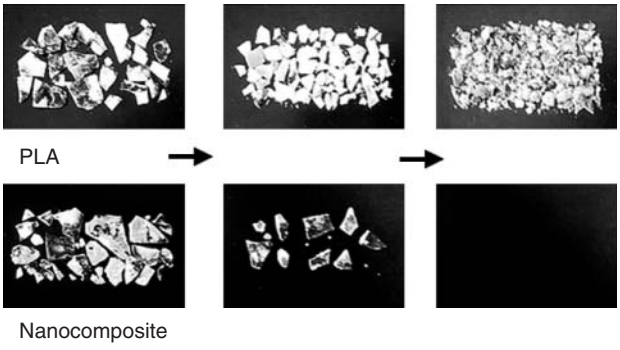

Figure 11.21 Comparison of the degradation behavior between neat PLA and PLA bionanocomposite with montmorillonite after 32, 50, and 60 days (from left to right) [267].

to better dispersion in the smectite system, at the same clay loading. Apart from being a well-dispersed system, smectite nanocomposites had the best gas barrier properties among the three, despite the fact that the MMT or mica systems are larger in size; however, they are stacked in their nanocomposites.

MMT modified with functionalized ammonium salts [270–277] and layered titanate modified with N-(cocoalkyl)-N,N-[bis(2-hydroxyethyl)]-N-methylammonium cation [278] were added to PLA in order to produce bionanocomposites with improved mechanical and thermal properties, reduced oxygen permeability, and good biodegradability. Addition of nanoclays was also found to reduce the flammability of the PLA-based bionanocomposites [279].

Gorrasi *et al*. [280] improved water vapor barrier properties by creating bionanocomposites of PLA and MMT modified with a functionalized ammonium. Both intercalated and exfoliated composites were obtained. They concluded that nanocomposite formation yielded better barrier properties specifically when exfoliated morphology was obtained.

Plasticized PLA has also been the subject of significant investigation in bionanocomposites [281–284]. Bionanocomposites of PLA plasticized with 20 wt% poly(ethylene glycol) and different amounts of MMT (modified organically or not) were studied by Paul *et al*. [282]. At constant filler level, OMMT produced bionanocomposites with the best thermal stability. Increasing the amount of clay delayed the onset of thermal degradation of this plasticized polymer matrix, with a reported competition between PEG and PLA for intercalation into the interlayer spacing of the clay.

Compatibilizers to increase dispersion of nanoclays have also been used in PLA, with a noticeably enhanced degree of exfoliation of the organoclay [285]. Addition of PCL, as a compatibilizer to PLA was also found to improve processability and mechanical properties of the bionanocomposites [286].

The permeability – water vapor, oxygen, and carbon dioxide – of polylactide nanocomposites reinforced with MMT, was affected using two types of MMT (Cloisite 30B and Nanofil 2), with the addition of two organic modifiers (poly(methyl methacrylate) and ethylene/vinyl alcohol copolymer) and two compatibilizers (PCL and poly(ethylene glycol)). Żenkiewicz and Richert [287] found that Cloisite 30B decreased the film permeability much more than Nanofil 2 and that all the modifiers and compatibilizers reduced the carbon dioxide transmission rate, while only the modifiers reduced the transmission rates of water vapor and oxygen.

Bionanocomposites based on PLA and organically modified VMT by *in situ* intercalative polymerization were prepared by Zhang *et al*. [288]. They concluded that exfoliated composites were obtained and that the bionanocomposites had improved storage and loss modulus, as well as increased glass transition temperature. Tensile tests also showed that the exfoliated nanocomposites are reinforced and toughened by the addition of nanometer-size VMT layers.

CNWs separated from commercially available microcrystalline cellulose (MCC) were added to PLA by compounding extrusion [261]. The MCC was treated with N,N-dimethylacetamide (DMAc) containing lithium chloride (LiCl) in order to swell the MCC and partly separate the cellulose whiskers. The suspension of whiskers was

pumped into the polymer melt during the extrusion process. Their results showed that DMAc/LiCl can be used as a swelling/separation agent for MCC but caused degradation of the composites at high processing temperature. When poly(ethylene glycol) was used as a processing aid, the structure of composites was made up of partly separated nanowhiskers, resulting in improved mechanical properties as compared to reference material; for example, for one material combination, the elongation to break was increased to about 800%.

In another study, applying extrusion, Bondeson and Oksman [262] prepared biodegradable nanocomposites based with 5% CNWs and PLA in which an anionic surfactant (5, 10, and 20 wt%) was used to improve the dispersion of the CNW in the PLA matrix. Increased surfactant content resulted in improved dispersion, but at the same time degraded the PLA matrix. A maximum modulus for the composite was observed at 5 wt% surfactant; and, as the surfactant content increased, the CNW dispersion, TS, and elongation at break were improved compared to its unreinforced counterpart.

PLA nanocomposites with TiO_2 nanoparticles [288], nanoclays [289], hydroxyapatite [290–293], and glass nanofibers [294] have also been produced and their promising application in pharmacology and biomedical engineering areas pointed out.

11.2.8
Bionanocomposites Using Biodegradable Polymers from Petrochemical Products

PCL, PEAs, aliphatic, or aromatic copolyesters have been largely employed to produce bionanocomposites. Here, we will show some of these bionanocomposites from preparation to application.

11.2.8.1 Poly(ε-Caprolactone)

PCL, is an important APES with many potential applications in biomedical and environmental fields [144]. This polymer was the first one to be studied in bionanocomposite when in the early 1990s, Giannelis group from Cornell University (Ithaca, NY, USA) started to work on the elaboration of PCL-based nanocomposites by intercalative polymerization [295]. Since then, a vast number of bionanocomposites have been prepared [87]. Several groups used intercalation, master batches, and *in situ* polymerization of PCL with clays to produce a variety of nanocomposites as can be seen in Table 11.2. Not only clays, but also various types of nanoreinforcements such as cellulose [296] and StNs [297, 298], chitin [299] nanowhiskers, carbon nanotubes [300, 301], and silica nanoparticles [302] have been used to prepare bionanocomposites with PCL.

Messersmith and Giannelis [303] developed bionanocomposites of PCL and MMT organically modified with a protonated amino acid to promote delamination/dispersion of the host layers and initiate ring-opening polymerization of ε-caprolactone monomer. This resulted in PCL chains that were ionically bound to the silicate layers (Figure 11.22). Films with a significant reduction

Table 11.2 Details of the processing method, type of clay, and structure obtained for PCL–clay bionanocomposites [87].

Process	System	Structure
Solvent intercalation	MMT-$N^+(Me)_2(C_{18})_2$/chloroform	Slightly intercalated
Melt intercalation	MMT-$N^+(Me)_2(C_{18})_2$	Intercalated
	MMT-$N^+(Me)_2(C_8)$(tallow)	Intercalated
	MMT-$NH_3^+(C_{11}COOH)$	Microcomposite
	MMT-$N^+(Me)(EtOH)_2$(tallow)	Intercalated/exfoliated Exfoliated
	Smectite-$P^+(But)_3(C_8)$/o-PCL	Intercalated
	Smectite-$P^+(But)_3(C_{12})$-/o-PCL	Intercalated
	Smectite-$P^+(But)_3(C_{16})$/o-PCL	Intercalated
	Smectite-$P^+(Me)(\phi)_3$/o-PCL	Intercalated
	SFM-$P^+(But)_3(C_{16})$/o-PCL	Intercalated
	Hectorite-$P^+(But)_3(C_{16})$/o-PCL	Intercalated, almost exfoliated
Masterbatch	MMT-Na-g-PCL + PCL	Intercalated
	MMT-$N^+(Me)_2(C_8)$(tallow)-g-PCL + PCL	Intercalated
	MMT-$N^+(Me)(EtOH)_2$(tallow)-g-PCL + PCL	Intercalated
	MMT/dibutylamine terminated o-CL + PCL	Intercalated (low o-CL chain length) Intercalated/exfoliated (high o-CL chain length)
In situ intercalation	Fluorohectorite-Cr^{3+}	Intercalated
	MMT-$NH_3^+(C_{18})$	Intercalated
	MMT-$NH_3^+(C_{11}COOH)$	Exfoliated Intercalated
	MMT-$N^+(Me)_2(C_{18})_2$	Microcomposite
	MMT-$N^+(Me)_3(C_{16})$	Intercalated
	MMT-$N^+(Me)_2(C_8)$(tallow)	Microcomposite
	MMT-$N^+(Me)(EtOH)_2$(tallow)	Exfoliated
	MMT/water	Slightly intercalated
	MMT-Na/tin octoate	Intercalated
	MMT-Na/dibutyltin dimethoxide	Intercalated
	MMT-$NH_3^+(C_{18})$/tin octoate or dibutyltin dimethoxide	Intercalated
	MMT-$NH_3^+(C_{11}COOH)$/tin octoate or dibutyltin dimethoxide	Intercalated
	MMT-$N^+(Me)_2(C_{18})_2$/tin octoate or dibutyltin dimethoxide	Intercalated
	MMT-$N^+(Et)_2(CH_2CHOHCH_3)(C_{18})$/tin octoate	Exfoliated or intercalated/exfoliated

(*continued overleaf*)

Table 11.2 (*Continued*)

Process	System	Structure
	MMT-$N^+(Me)_2(C_8)$(tallow)/tin octoate	Intercalated
	MMT-$N^+(Me)_2(C_8)$(tallow)/dibutyltin dimethoxide	Intercalated
	MMT-$N^+(Me)(EtOH)_2$(tallow)/tin octoate	Exfoliated
	MMT-$N^+(Me)(EtOH)_2$(tallow)/dibutyltin dimethoxide	Exfoliated
	MMT-$[N^+(Me)_2(EtOH)(C_{16})]_x[N^+(Me)_3(C_{16})]_y$/Tin(II) or Tin(IV) or Al(III) alkoxide	Exfoliated or intercalated/exfoliated
	MMT-$[N^+(Me)_2(EtOH)(C_{16})]_x[N^+(Me)_3(C_{16})]_y$/triethylaluminium/toluene	Exfoliated
	SAP-$N^+(Me)_3(C_{16})$/dibutyltin dimethoxide	Intercalated
	SAP-$N^+(Me)_2(EtOH)(C_{16})$/dibutyltin dimethoxide	
	SAP-$N^+(Me)(EtOH)_2(C_{16})$/dibutyltin dimethoxide	
	SAP-$P^+(Me)_3(C_{16})$/dibutyltin dimethoxide	
	LAP-$N^+(Me)_3(C_{16})$/dibutyltin dimethoxide	
	LAP-$N^+(Me)_2(EtOH)(C_{16})$/dibutyltin dimethoxide	
	LAP-$N^+(Me)(EtOH)_2(C_{16})$/dibutyltin dimethoxide	
	LAP-$P^+(Me)_3(C_{16})$/dibutyltin dimethoxide	
	SAP-$P^+(Me)_3(C_{14})$/dibutyltin dimethoxide	Intercalated
	SAP-$P^+(Me)_3(C_{12})$/dibutyltin dimethoxide	

SAP, saponite; MMT, montmorillonite; LAP, laponite.

in WVP were produced. For example, the addition of 4.8 vol% of clay caused a reduction by nearly an order of magnitude in permeability compared to pure PCL

Di *et al*. [304] investigated the barrier and mechanical properties of PCL bionanocomposites prepared with MMT, Cloisite 30B (30B), and Cloisite 93A (93A), by melt mixing. Barrier performance of PCL/30B nanocomposite film to air permeation was much more improved than that of pure PCL and PCL/93A microcomposites at low organoclay concentration. With the increase of organoclay content, the permeability coefficient was also increased, which they attributed to the extra tortuous pathway for gas permeation caused by organoclay exfoliation. The mechanical properties were also enhanced with the addition of nanoclay. An increase in tensile modulus by 50% at 8 wt% clay addition and in elongation at break by 165–550% for additions of up to 10 wt% clay was observed by Chen and Evans [305].

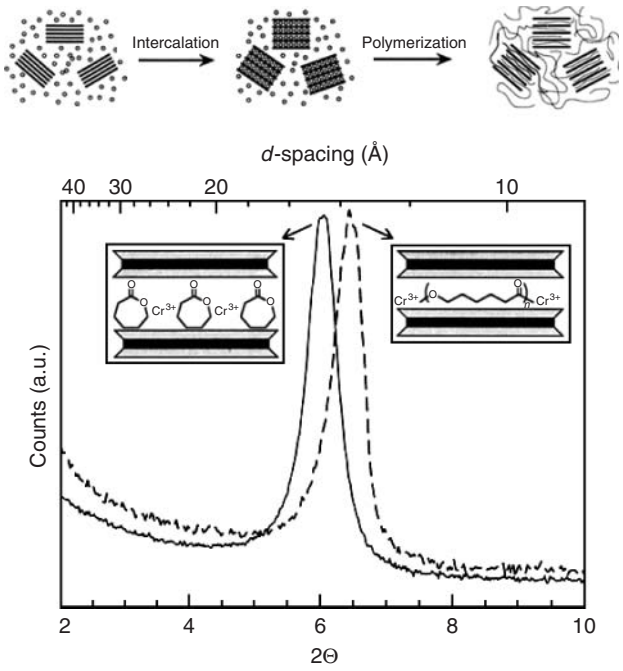

Figure 11.22 X-ray diffraction patterns of the composite before (solid line) and after (dashed line) polymerization. Insets are schematic illustrations corresponding to the intercalated monomer (left) and intercalated polymer (right). The upper figure is a scheme of the preparation procedure used [295].

Pantoustier *et al.* [306] prepared bionanocomposites based on PCL and MMT, prepared either by melt interaction with PCL or by *in situ* ring-opening polymerization of ε-caprolactone. Studies of both nonmodified clays (Na+-MMT) and silicates modified by various alkylammonium cations showed that even at a filler content as low as 3 wt% of inorganic layered silicate, the PCL-layered silicate nanocomposites exhibited improved mechanical properties (higher Young's modulus) and increased thermal stability. Also important was its enhanced flame retardancy as a result of a charring effect. The formation of PCL-based nanocomposites depended not only on the nature of the ammonium cation and related functionality but also on the selected synthetic route, melt intercalation versus *in situ* intercalative polymerization. Interestingly enough, when the intercalative polymerization of ε-caprolactone was carried out in the presence of MMT organomodified with ammonium cations bearing hydroxyl functions, nanocomposites with much improved mechanical properties were recovered. Those hybrid polyester layered silicate nanocomposites were characterized by a covalent bonding between the polyester chains and the clay organo-surface as a result of the polymerization mechanism, which was actually initiated from the surface hydroxyl functions adequately activated by selected tin (II) or tin (IV) catalysts.

In other studies [307, 308], this same group produced bionanocomposites by melt intercalation of PCL and MMT modified by various alkylammonium cations. Depending on whether the ammonium cations contain nonfunctional alkyl chains or chains terminated by carboxylic acid or hydroxyl functions, microcomposites or nanocomposites were produced. The layered silicate PCL nanocomposites exhibited some improvement in mechanical properties and increased thermal stability as well as enhanced flame retardancy. The authors concluded that formation of PCL-based nanocomposites, not only depended on the nature of the ammonium cation and its functionality, but also on the selected synthetic route, that is, melt intercalation versus *in situ* intercalative polymerization.

Fukushima *et al*. [309] used OMMTs and one sepiolite to produce PCL nanocomposites by melt blending. All clays showed a good dispersion level with both polymeric matrices, while the highest thermomechanical improvements were reached depending on the type of clay. These improvements were considerably higher in the case of PLA-based nanocomposites probably because of the higher polymer/filler compatibility.

Chrissafis *et al*. [302] compared four different nanoparticles to produce nanobiocomposites based on PLA: two layered silicates (Cloisite Na^+ and Cloisite 20A MMTs), spherical nanoparticles (fumed silica SiO_2) and MWCNTs. All nanoparticles induced a substantial enhancement of Young's modulus and TS compared to neat PCL. From TGA analysis it was also observed that modified MMT and fumed silica accelerate the decomposition of PCL owing to respective aminolysis and hydrolytic reactions. On the other hand, carbon nanotubes and unmodified MMT slowed the thermal degradation of PCL due to a shielding effect.

Carbon nanotubes have also been used to prepare conductive bionanocomposites with PCL to improve, among other characteristics, their electromagnetic, electrical, and thermomechanical properties [310, 311]. Conductive films can be used in electrostatic charge dissipation, a critical factor in the electronics industry, and in many other applications ranging from sensors and biosensors to packaging [312, 313]. A key factor to improve properties and produce bionanocomposites with uniform properties is to reach a good dispersion. According to Dubois and Alexandre [300] this can be achieved by several ways such as *in situ* polymerization/grafting on the nanofiller surface, also known as the *polymerization-filling technique* (*PFT*). They reported that such surface-coated carbon nanotubes were further added as ''masterbatch'' in commercial polymeric matrices by twin-screw extrusion and, as a result of the predestructurization of the nanofillers by PFT, the resulting polymer nanocomposites displayed much improved thermomechanical properties even at nanofiller loading as low as 1 wt%. Addition of a zwitterionic surfactant by Mitchell and Krishnamoorti [314] was reported to improve carbon nanotube dispersion and geometrical and electrical percolation for PCL-based nanocomposites with 0.08 wt% nanotubes.

StNs and chitin nanowhiskers have also been reported to produce PCL bionanocomposites with improved properties [296, 298, 315]. For example, Habibi and Dufresne [316] prepared cellulose and StNs obtained from the acid hydrolysis of ramie fibers and waxy maize starch granules, respectively, which were subjected to

isocyanate-mediated reaction to graft PCL chains with various molecular weights on their surface. The authors observed that the nanoparticles kept their initial morphological integrity and native crystallinity. Moreover, nanocomposite films processed from both unmodified and PCL-grafted nanoparticles and PCL as matrix using a casting/evaporation technique displayed mechanical properties which were notably different. Compared to unmodified nanoparticles, the grafting of PCL chains on the surface resulted in lower modulus values but significantly higher strain at break. This unusual behavior clearly reflected the originality of the reinforcing phenomenon of polysaccharide nanocrystals resulting from the formation of a percolating network, thanks to chain entanglements and cocrystallization. The grafting onto approach was also used to graft PCL on cellulose ramie whiskers [317].

11.2.8.2 **Polyesteramides**

PEAs can be synthesized by statistical condensation copolymerization of polyamide monomers (PA 6 or PA 6.6), adipic acid, and 1,4-butanediol. One of the main drawbacks for this class of polymers is their inherently high water permeability, which makes the use of nanofillers necessary to improve hydrophobicity, particularly if such materials are used in packaging [87].

Krook *et al*. [318, 319] prepared bionanocomposites of PEA reinforced with octadecylamine (ODA)-treated MMT clay (5 and 13 wt%) by melt mixing and studied their barrier (oxygen and water) and mechanical properties. They noticed an increase in the periodic distance from 23.7 Å for pure filler to 32–36 Å for the processed composites, suggesting that the collapsed stacks of clay particle became intercalated on extrusion. A decrease in the intensity with increasing rotation speed was observed, which suggested that higher shear rates promoted delamination, especially in composites with higher filler content. TEM indicated that a sizable portion of the clay stacks were delaminated into smaller aggregates, containing generally one to three clay sheets. The presence of voids limited the improvement in barrier properties with increasing filler content. However, the very large improvement in stiffness and strength with filler content indicated that these properties were unaffected by these voids.

Nanoscale fillers, specifically nano-$CaCO_3$ and nano-SiO_2 were added to PEA by Liu *et al*. [320] who found that improved mechanical properties were obtained around a critical filler concentration, specifically the concentration at the onset of percolation. Moreover, when the composites underwent hydrolysis, the inert filler played a role as a mechanical obstacle in the matrix and retarded the hydrolysis; on the other hand, the interfacial area between the filler particle and the matrix resin increased with the filler, which would accelerate the hydrolysis. As a result of these two inverse effects, a minimum and a maximum value appeared in the plot of the degradation rate-filler content graph.

Bionanocomposites based on PEA and OMMT (Cloisite C25A), prepared by twin-screw corotating extrusion revealed three degradation steps instead of the two decomposition processes detected in the pristine sample [321]. The onset mass loss temperature decreased in the nanocomposite as a result of the presence of

the organomodifier compound, but the presence of the silicate layers significantly decreased the degradation rate at the last stages of decomposition. Their results clearly indicated that the presence of the organically modified clay modified the mechanisms of degradation.

Deng *et al.* [322] prepared bionanocomposites of aliphatic PEA reinforced with hydrothermally synthesized nano-hydroxyapatite (n-HA) which was added to PEA at concentrations ranging from 10% to −30%. It was found that the shape and size of the n-HA crystals were similar to those of the apatite crystals in natural bone and that bionanocomposites with enhanced mechanical property and bioactivity were produced, indicating that the PEA/n-HA bionanocomposites may serve as potential candidate scaffold for tissue engineering.

Morales *et al.* [323] prepared bionanocomposites of PEA (derived from glycolic acid and 6-aminohexanoic acid by *in situ* polymerization) reinforced with OMMTs. The most dispersed structure was obtained by addition of C25A organoclay. Evaluation of thermal stability and crystallization behavior of these samples showed significant differences between the neat polymer and its nanocomposite with C25A. Isothermal and nonisothermal calorimetric analyses of the polymerization reaction revealed that the kinetics was highly influenced by the presence of the silicate particles. Crystallization of the polymer was observed to occur when the process was isothermally conducted at temperatures lower than 145 °C. In this case, dynamic FTIR spectra and WAXD profiles obtained with synchrotron radiation were essential to study the polymerization kinetics. Clay particles seemed to reduce chain mobility and the Arrhenius preexponential factor.

Most of the discussions have revolved around linear polymers. In contrast, Wen *et al.* [324] prepared bionanocomposites using a hyperbranched polyesteramide (HBP) and PLA reinforced with SiO_2 nanoparticles. The ternary composites displayed dramatically improved mechanical properties including excellent toughness and fairly high stiffness. TEM images revealed that an encapsulation structure was formed by HBP surrounding SiO_2 nanoparticles, and their surfaces became flocculent due to the migration process of silica. The linear viscoelastic behavior of the nanocomposites measured by parallel plate rheometry indicated that strong interface adhesion existed between PLA matrix and silica nanofiller after incorporating of HBP. The compatibilization effect of HBP and the enhanced mobility of nanoparticles contributed to the improved mechanical properties.

11.2.8.3 **Aliphatic and Aromatic Polyesters and Their Copolymers**

Among the aliphatic and aromatic polyesters and their copolymers, PBS, PBSA, poly(butylene adipate-*co*-terephthalate) (PBAT), polybutylene adipate/terephthalate (PBAT), and PTMAT are the most known polymers. Some of these polymers such as PBS have been largely used as a matrix to bionanocomposites with a variety of reinforcements [87]. For example, Table 11.3 lists some of the modified clays used to prepare PBS-based bionanocomposites via solvent and melt intercalation and master batch formation [87].

Table 11.3 Details of the processing method, type of clay, and structure obtained for PBS-clay bionanocomposites [87].

Process	System	Structure
Solvent intercalation	MMT-($C_5H_5N^+$)(C_{16})	Intercalated
	MMT-$N^+(Me)_3(C_{16})$	Intercalated
Melt intercalation	MMT-$NH_3^+(C_{18})$	Intercalated and flocculated
		Highly intercalated and homogeneous dispersion
	MMT-$NH_3^+(C_{18})$/high molecular weight PBS (HMWPBS)	Intercalated and flocculated
	MMT-$NH_3^+(C_{12})$	Highly intercalated and homogeneous dispersion
	MMT-$NH_3^+(C_{11}COOH)$	Microcomposite
	MMT-$NH^+(EtOH)_2(C_{12})$	Highly intercalated and homogeneous dispersion
	MMT-$NH^+(EtOH)_2(CH_2CHOHCH_3)$	Microcomposite
	MMT-$N^+(Me)_2(C_8)$(tallow)	Intercalated
	GPS-g-MMT-$N^+(Me)_2(C_8)$(tallow)	Intercalated/exfoliated
	MMT-$N^+(Me)(EtOH)_2$(tallow)	Intercalated and flocculated
	MMT-$N^+(Me)(EtOH)_2$(tallow)/dibutyltin dilaurate	Intercalated/exfoliated
	Or titanium butoxide	Intercalated
	Or antimony oxide	Intercalated
	SAP-$P^+(But)_3(C_{16})$/HMWPBS	Stacked intercalated and delaminated
Masterbatch	MMT-$NH_3^+(C_{18})$/HMWPBS + HMWPBS	Intercalated and flocculated
	MMT-$N^+(Me)_3(C_{18})$/HMWPBS + HMWPBS	Intercalated and flocculated
	MMT-$N^+(Me)(EtOH)_2$(tallow)-g-PCL/dibutyltin dilaurate or titanium butoxide or antimony oxide + PBS	Intercalated
	SAP-$P^+(But)_3(C_{16})$/HMWPBS + HMWPBS	Stacked intercalated and delaminated

GPS, (glycidoxypropyl)trimethoxy silane; SAP, saponite; MMT, montmorillonite; HMWPBS, high molecular weight PBS.

PBS, is an APES with good biodegradability, melt processability, and thermal and chemical resistance. It is generally synthesized by polycondensation of 1,4-butanediol with succinic acid. Thanks to the successful incorporation of nanoparticles into other polyesters resulting in remarkable improvements of properties, this technique also has been introduced into PBS systems [144]. Ray *et al.* [325, 326] studied the structure and properties of PBS based with OMMT with a

substantial increase in the storage modulus of the nanocomposites over the entire temperature range investigated with addition of nanoparticles. The tensile property measurements showed a relative increase in the stiffness with a simultaneous decrease in the yield strength in comparison with that of neat PBS, while the oxygen gas barrier property was also improved. This same group in a different study of PBS/clay bionanocomposites [327] also concluded that the intercalated nanocomposites exhibited remarkable improvement of mechanical properties in both solid and melt states; melt processing is an important consideration for commercial application of these materials. As such, this work was extended to a series of PBS/layered silicate nanocomposites by simple melt extrusion of PBS and OMLSs [328]. Three different types of OMLS were applied for the preparation of nanocomposites: two functionalized ammonium salts modified MMT and a phosphonium salt modified saponite (SPT) whereby all additives conferred improvements of material properties when compared with pure PBS. A similar behavior was found by Shih *et al.* [329].

Chen *et al.* [330] developed bionanocomposites of PBS and a commercially available organoclay, Cloisite 25A (C25A), and Cloisite 25A (C25A) modified, by the addition of epoxy groups to the clay. Epoxy groups were grafted to C25A by treating with (glycidoxypropyl)trimethoxy silane to produce twice functionalized organoclay (TFC). They found a higher degree of exfoliation of the silicate layers in PBS/TFC and the improved mechanical properties, in comparison with those of PBS/C25A. This behavior was attributed to the increased interfacial interaction between PBS and TFC.

Chen *et al.* [331, 332] also studied bionanocomposite blends by adding PLLA to PBS and reinforcing with TFC. They found that not only the tensile modulus and TS but also elongation at break of PLLA/PBS was greatly enhanced as a result of melt compounding with TFC. The larger amount of exfoliation of the silicate layers in PLLA/PBS/TFC as compared with that in PLLA/PBS/C25A was attributed to the increased interfacial interaction between the polyesters and the clay through chemical reaction. Thermogravimetric analysis revealed that both $T_{5\%}$, which was the temperature corresponding to 5% weight loss, and activation energy of thermal decomposition of PLLA/PBS/TFC were far superior to those of PLLA/PBS/C25A as well as to those of PLLA/PBS, indicating that the composites with exfoliated silicate layers were more thermally stable than those with intercalated silicate layers.

Someya *et al.* [333] studied the thermal and mechanical properties of PBS bionanocomposites with various OMMTs. They used the following protonated ammonium cations: dodecylamine (DA-M), ODA-M, 12-aminolauric acid (ALA-M), N-lauryldiethanolamine (LEA-M), and 1-[N,N-bis(2-hydroxyethyl)amino]-2-propanol (HEA-M). It was found that DA-M, ODA-M, and LEA-M were homogeneously dispersed, whereas some clusters or agglomerated particles were observed for ALA-M, HEA-M, and pure MMT. They also showed that the enlargement of the difference in the interlayer spacing between the clay and PBS/clay composite, as measured by XRD, had a good correlation with the improvement of the clay dispersion and with the increase in the tensile modulus and the decrease in the TS of the PBS

composites with an inorganic concentration of 3 wt%. Dynamic viscoelastic measurements of the PBS/LEA-M nanocomposite revealed that the storage modulus and glass transition temperature increased with the inorganic concentration from 3 to 10 wt%.

In situ polymerization of PBS with nanosized silica was used to create bionanocomposites in which silanol-bonded carbonyl groups were established within PBS/silica nanocomposite materials, as evidenced by solid-state ^{29}Si NMR and FTIR analyses [334]. As a result, bionanocomposites of 3.5 wt% silica exhibited greatly improved mechanical properties; for example, the TS and elongation at break were about 38.6 MPa and 515%, while those of the parent PBS were 26.3 MPa and 96%, respectively. PBS reinforced with carbon nanotubes have also been reported in the literature [335–337]. These works reported that improved mechanical and thermal properties were obtained with the addition of carbon nanotubes. Moreover, some of these composites exhibited high antistatic efficiency, which would be potentially useful in electronic packaging materials [336, 337].

Copolymers of PBS and butylene adipate, PBSA, have been largely used to prepare bionanocomposites [338–343]. Ray and Bousmina [338] prepared PBSA/layered silicate nanocomposites by melt extrusion of PBSA and commercially available OMMT. They showed that increasing the level of interactions (miscibility) between the organic modifier and PBSA matrix, increased the tendency of the silicate layers to delaminate and distribute nicely within the PBSA matrix. Thermal analysis revealed that the extent of crystallinity of PBSA matrix was directly related to the extent of exfoliation of silicate layers in the nanocomposites and DMA and tensile property measurements showed concurrent improvement in mechanical properties when compared to the neat PBSA and the extent of improvement is directly related to the extent of delamination of silicate layers in the PBSA matrix. DMA also revealed remarkable increase in flexural storage modulus when compared with that of neat PBSA. Tensile properties were also improved with nanoclay addition [339], therefore in agreement with other studies reported in the literature for similar systems [344–347].

Addition of organically modified synthetic fluorine mica (OSFM) [341] to PBSA was also found to cause substantial enhancement in the mechanical properties of PBSA. For example, at room temperature, storage flexural modulus increased from 0.5 GPa for pure PBSA to 1.2 GPa for the nanocomposite, an increase of about 120% in the value of the elastic modulus. It was also observed that the stability of PBSA was increased moderately in the presence of OSFM.

Bionanocomposites of copolymers of butylene adipate and butylene terephthalate, poly(butylene adipate-*co*-terephthalate), PBAT, have been reported in the literature [348–350]. For example, Someya *et al.* [348] prepared bionanocomposites based on poly(butylene adipate-*co*-terephthalate) and MMT. They used unmodified MMT and OMMT by protonated ammonium cations. They concluded that both morphology and increase in mechanical properties were found to depend on nanoclay loading and organic modifier used. Addition of nanoclays to bionanocomposite blends of PBSA with starch and PLA have also been reported to improve mechanical and thermal properties and biodegradability [349, 350].

As described in Section 11.2.3.3.3, APES can be biodegradable depending on their chemical formulation. Park *et al.* [351] prepared bionanocomposites of a biodegradable APES prepared by polycondensation of aliphatic glycols (ethylene glycol and 1,4-butanediol) and aliphatic dicarboxylic acids (succinic and adipic acids), TPS, and MMT (Cloisite 30B) via melt intercalation. They found that adding APES to the TPS/Cloisite 30B hybrids led to higher TS and improved barrier properties.

Shi *et al.* [352] reported that bionanocomposites of poly(propylene fumarate) reinforced with SWCNTs with improved properties were produced by the addition of SWCNT and suggested that these bionanocomposites hold significant implications for the fabrication of bone tissue engineering scaffolds.

11.2.9
Other Biodegradable Polymers

Biodegradable polymers such as PVA, PVAc, and PGA have been used in bionanocomposites, but to a less extent compared to polymers such as PCL, PLA, and PHB. Nonetheless, these polymers, among other factors, can be used as model to prepare bionanocomposites with hydrophilic material such as clays and CNWs. Moreover, nanobiocomposites based on these polymers can be potentially used as bioscaffolds for cell growth among other applications.

11.2.9.1 Poly(Vinyl Alcohol)

As already mentioned, PVA is a water soluble polymer used in applications such as packaging films where water solubility is desired. It is the most readily biodegradable of the vinyl polymers, which makes it a potentially useful material in biomedical, agricultural, and water treatment areas, for example, as a flocculant, or scavenger of metal ions. Moreover, due to its water solubility, PVA can also be used as a model for particle dispersion in aqueous suspensions, especially those from CNWs and some clays. As a consequence, PVA has been largely used to produce nanocomposites with clays, cellulose, and chitin whiskers, silver nanoparticles, graphite oxide, and carbon nanotubes.

Strawhecker and Manias [353] prepared bionanocomposites of PVA and Na^{+}MMT of various compositions by casting from a polymer/silicate water suspension, revealing the coexistence of exfoliated and intercalated MMT layers, especially for low and moderate silicate loadings. The inorganic layers promoted a new crystalline phase different from neat PVA, characterized by a higher melting temperature and a different crystal structure. This new crystal phase corresponded to changes in properties, namely, the hybrid polymer/silicate systems have mechanical, thermal, and water vapor transmission properties that are superior to that of the neat polymer. For example, a 5 wt% MMT exfoliated composite exhibited a softening temperature increase by 25 °C and a tripling of the Young's modulus with a decrease of only 20% in toughness. Furthermore, water permeability was reduced to 60% and, because of the nanoscale dispersion of filler, the nanocomposites retained their optical clarity.

Chang *et al*. [354] prepared bionanocomposites of PVA with different clays: Na ion-exchanged clays [Na^+-SPT and Na^+-MMT] and alkyl ammonium ion-exchanged clays (C_{12}-MMT and C_{12}OOH-MMT). From morphological studies, they found that Na ion-exchanged clay was more easily dispersed in a PVA matrix than the alkyl ammonium ion-exchanged clay. It was also found that the addition of only a small amount of clay was sufficient to improve thermal and tensile properties. Both the ultimate TS and the initial modulus for the nanocomposites increased gradually with clay loading up to 8 wt%. In C_{12}OOH-MMT, the maximum enhancement of the ultimate TS and the initial modulus for the nanocomposites was observed for composites containing 6 wt% organoclay. Na ion-exchanged clays had higher TS than those of organic alkyl-exchanged clays in PVA nanocomposites films. On the other hand, organic alkyl-exchanged clays had initial moduli that were better than those of Na ion-exchanged clays. Overall, the content of clay particles in the polymer matrix affected both the thermal stability and the tensile properties of the polymer/clay nanocomposites and had little or no significant effect on thermal stability of the bionanocomposites.

Yeun *et al*. [355] prepared PVA bionanocomposites reinforced with saponite via solution intercalation method. It was found that clay particles were highly dispersed in the PVA matrix without any agglomeration of particles for up to 5 wt% clay and that the thermal stability increased linearly with increasing amount of clay up to 10 wt%. Oxygen permeability values monotonically decreased with increases in the clay loading in the range (0–10 wt%) studied. The addition of α-chitin whiskers to PVA improves thermal stability, TS, and water resistance, leading to decreased percentage degree of swelling of PVA-based bionanocomposite [356]. A similar effect in mechanical properties was also found when cellulose fibrils were added to PVA [357, 358]. PVA–PVAc copolymers reinforced with cotton whiskers were also investigated [357]. All the results showed that stronger filler/matrix interactions occur for fully hydrolyzed PVA compared to partially hydrolyzed samples. Other nanoreinforcements such as VMT [359], attapulgite [360], SWCNTs [361], silver nanoparticles [362], graphite oxide [363], $CoFe_2O_4$ magnetic nanoparticles [364], and Ag_2S and CuS nanoparticles [365] have also been used to produce PVA-based bionanocomposites with improved mechanical, optical, and magnetic properties.

11.2.9.2 **Poly(Vinyl Acetate)**

PVAc is biodegradable under certain conditions. PVAc is a relatively polar polymer that may interact strongly with hydroxyl-rich surface of cellulose whiskers and clays, as a result, hydrogen bonds are expected to strengthen the interface significantly with a positive impact on the mechanical properties of the composite material. Rodriguez *et al*. [64] used sisal nanowhiskers to obtain nanocomposites with PVAc. It was found that whisker addition stabilized the nanocomposites up to the percolation threshold. Beyond this limit, the water uptake remained constant, and the T_g did not vary with whisker content at a given relative humidity. Below the whisker percolation concentration, stabilization was only noticed at low relative humidity, whereas high humidity resulted in disruption of whisker–PVAc

interactions. Their work showed the potential use of CNWs to stabilize polar polymers even at high humidity conditions with minimal reinforcement addition.

In a novel application of supercritical CO_2, Charpentier *et al.* [366] prepared bionanocomposites of PVAc and SiO_2 nanoparticles using a one-pot synthesis in supercritical CO_2 wherein all raw chemicals, tetraethoxysilane (TEOS)/tetramethoxysilane (TMOS), vinyltrimethoxysilane (VTMO), vinyl acetate, initiator, and hydrolysis agent were introduced into one autoclave. They found that PVAc nanocomposites with well-dispersed SiO_2 nanoparticles of 10–50 nm were formed opening new opportunities such as the production of metal-oxide-polymer nanocomposites from liquid precursors.

Choi *et al.* [367] investigated the electrical and rheological characteristics of PVAc/MWCNT nanocomposites and found that a small amount of MWNT remarkably decreased the electrical resistivity of the nanocomposites. Moreover, an increase in storage and loss moduli was observed with addition of MWCNT.

Other nanoreinforcements such as hydroxyapatite [368] and silver [369] have been employed to prepare bionanocomposites with PVAc. The use of two matrices to produce bionanocomposites that combine properties of both matrices such as PVA/PVAc reinforced with clays have also been reported [370, 371].

11.2.9.3 **Poly(Glycolic Acid)**

PGA, is another biodegradable polymer with applicability in bionanocomposites [372]; and, like PVA and PVAc, PGA is readily soluble in water and can be processed by extrusion, injection, and compression molding similarly to other thermoplastics. Murugan *et al.* [373] produced bionanocomposites of PGA and clay by polymerizing glycolic acid under vacuum in the presence and absence of nanoclay which act as a catalyst to the condensation polymerization of PGA. They found that addition of clay improved flame retardancy.

Copolymers of PGA and PLA, PLGA, have attracted increasing attention as scaffold materials in bone tissue engineering because their degradation products can be removed by natural metabolic pathways. However, one main concern with the use of these specific polymers is that their degradation products reduce local pH, which in turn induces an inflammatory reaction and damages bone cell health at the implant site [374].

Liu *et al.* [374] studied the *in vitro* degradation behavior of PLGA bionanocomposites reinforced with titania nanoparticles. They observed that the increased dispersion of titania in PLGA decreased the harmful change in pH normal for PLGA degradation. Moreover, these bionanocomposites significantly improved osteoblast (bone-forming cell) functions (such as adhesion, collagen synthesis, alkaline phosphatase activity, and calcium-containing minerals deposition), indicating that bionanocomposites based on titania nanoparticles and PLGA can be promising scaffold materials for effective orthopedic tissue engineering applications.

Hong *et al.* [375] reported the production of bionanocomposites of PLGA reinforced with hydroxyapatite nanoparticles (30–40 nm in diameter and 100–200 nm in length). They found that the addition of these nanoparticles improved bionanocomposites' mechanical properties and facilitated the adhesion

and proliferation of osteoblasts on the bionanocomposite film. Bionanocomposites based on poly(lactide-*co*-glycolide) and hydroxyapatite (HA) were also studied by Cui *et al*. [376] indicating that their bionanocomposites, especially those with 10 and 10 wt% HA are optimal for bone repair.

These are some examples, although limited, of how bionanocomposites have been employed in a vast number of applications and how their properties can be tailored by modification with nanoreinforcements and blending with other biopolymers in order to produce bionanocomposite blends with the main goal of improving electrical, mechanical, thermal, and magnetic properties as well as barrier and biodegradability.

11.3 Final Remarks

There has been tremendous progress in bionanocomposites in recent years. The work reviewed here shows how biodegradable materials from environmentally friendly, biodegradable, and renewable resources can be exploited to produce bionanocomposites with tailored properties. They show a growing effort to produce bionanocomposites with improved properties and imply that the next important step is to scale up their production to commercial applicability, thus expanding applications that range from packaging of food to biosensors, to scaffolds for cell growth.

Owing the high surface area of nanoparticles, a much greater effort is needed to reach a good dispersion, a key factor in producing bionanocomposites with improved properties and fully exploiting these properties in industrial and practical applications. Great challenges still remain. Reaching a high level of nanoparticle dispersion in the selected polymer matrix and fine tuning industrial processing parameters in order to obtain further enhancement of composite properties remain as commercial challenges.

Organic fillers such as cellulose whiskers still suffer from poor thermal stability, which inhibit their use in many thermoplastics whose processing temperatures are close or above their degradation temperature. These whiskers are still produced in aqueous dispersions, so even by applying solvent exchange and lyophilization, the volume of nanowhiskers produced is well below commercial viability. Optimized separation methods must be developed and scaled up.

Bionanocomposites help the environment by not only creating materials with tailored properties such as improved mechanical properties and reduced permeability, but also by creating new hybrid materials with controlled degradation. These new biopolymers can be degraded in much shorter times when compared to traditional petroleum-based polymers which may take up to several centuries to be fully absorbed by the environment. Degradation paths are also well understood, with resulting degradation products generally safe for the environment. As a consequence, the rational use of biopolymers and bionanocomposites is an improvement over traditional plastics.

References

1. Netravali, A.N. and Chabba, S. (2003) *Mater. Today*, **6**, 22.
2. Scott, G. and Gilead, D. (1995) *Degradable Polymers: Principles and Applications*, Chapman & Hall, London.
3. Chandra, R. and Rustgi, R. (1988) *Prog. Polym. Sci.*, **23**, 273.
4. Röper, H. and Koch, V. (1990) *Starch/Stärke*, **42**, 123.
5. Wiedmann, W. and Strobel, E. (1991) *Starch/Stärke*, **43**, 138.
6. Shogren, R.L., Fanta, G., and Doane, W.M. (1993) *Starch/Stärke*, **45**, 276.
7. Corradini, E., Medeiros, E.S., Carvalho, A.J.F., Curvelo, A.A.S., and Mattoso, L.H.C. (2004) Book of Abstracts of the 5th International Symposium on Natural Polymers and Composites (5th ISNAPol), Sao Pedro, Brazil, September 12–15, 2004, p. 346.
8. Darder, M., Aranda, P., and Ruiz-Hitzky, E. (2007) *Adv. Mater.*, **19**, 1309.
9. Busel, J.P. and Lockwood, J.D. (2000) *Revolutionary Materials: Technology and Economics, 32nd International SAMPE Technical Conference*, Engineering FRP in Civil Engineering, Vol. 32, CRC Press, p. 15, November 5–9, 2000.
10. Shalaby, S.W. and Latour, R.A. (1997) in *Handbook of Composites*, 2nd edn (ed. S.T. Peters) Chapter 44, Springer, p. 957.
11. Chawla, K.K. (1998) *Composite Materials, Science and Engineering*, 2nd edn, Springer, New York.
12. Callister, W.D. Jr., (2006) *Materials Science and Engineering: An Introduction*, 7th edn, Wiley-InterScience, New York.
13. Shackelford, J.F. (1999) *Introduction to Materials Science for Engineers*, 5th edn, Prentice Hall.
14. Okada, A., Kawasumi, M., Usuki, A., Kojima, Y., Kurauchi, T., and Kamigaito, O. (1990) *Mater. Res. Symp. Proc.*, **171**, 45.
15. Kawasumi, M., Hasegawa, N., Kato, M., Usuki, A., and Okada, A. (1997) *Macromolecules*, **30**, 6333.
16. Gao, F. (2004) *Mater. Today*, **7**, 50.
17. Orts, W.J., Shey, J., Imam, S.H., Glenn, G.M., Guttman, M.E., and Revol, J.-F. (2005) *J. Polym. Environ.*, **13**, 301.
18. LeBaron, P.C., Wang, Z., and Pinnavaia, T.J. (1999) *Appl. Clay Sci.*, **15**, 11.
19. Giannellis, E.P. (1996) *Adv. Mater.*, **8**, 29.
20. Ajayan, P.M., Schadler, L.S., and Braun, P.V. (eds) (2003) *Nanocomposite Science and Technology*, Wiley-VCH Verlag GmbH, Weinheim.
21. Gacitua, W., Ballerini, A., and Jinwen, Z. (2005) *Maderas Cienc. Tecnol.*, **7**, 159.
22. Orts, W.J., Chiou, B.-S., Baker, D.-A., Shey, J., Imam S.H., G.M. Glenn, and L.H.C. Mattoso (2006) Nanocomposites from agricultural based materials. Macro 2006–41st International Symposium on Macromolecules Proceedings.
23. Medeiros, E.S., Mattoso, L.H.C., Sreekumar, P.A., and Joseph, K. (2009) *Role of Interface in Lignocellulosic Fiber Reinforced Polymer Composites*, Old House Publishing, Philadelphia, PA.
24. Balaposzhinimaev, B.S. (2003) Glass fiber based catalysts for environment protection, science and technology, 2003. Proceedings KORUS 2003. The 7th Korea-Russia International Symposium, 2003, Vol. 4, p. 115.
25. J. Simonsen, Bio-Based Nanocomposites: Challenges and Opportunities, *http://www.swst.org/meetings/AM05/simonsen.pdf* (accessed 8 April 2013)
26. Bismarck, A., Mishra, S., and Lampke, T. (2005) in *Natural Fibers, Biopolymers and their Biocomposites* (eds A.K. Mohanty, M. Misra, and L.T. Drzal), CRC Press, Boca Raton, FL, p. 37.
27. Yang, C.M., Kim, D.Y., and Lee, Y.H. (2005) *J. Nanosci. Nanotechnol.*, **5**, 970.
28. Dresselhaus, M.S., Dresselhaus, G., and Avouris, P. (eds) (2001) *Carbon Nanotubes: Synthesis, Structure, Properties, and Applications*, Springer, Munich.
29. Medeiros, E.S., Dufresne, A., and Orts, W.J. (2009) in *Starch: Characterization,*

Properties and Applications (ed. A.C. Bertolini) Chapter 9, Taylor & Francis, Boca Raton, FL, p. 205.
30. Klemm, D., Heublein, B., Fink, H.-P., and Boh, A. (2005) *Angew. Chem. Int. Ed.*, **44**, 3358.
31. Zhao, R., Torley, P., and Halley, P.J. (2008) *J. Mater. Sci.*, **43**, 3058.
32. Avérous, L. (2004) *J. Macromol. Sci., Polym. Rev.*, **C44**, 231.
33. Sugiyama, J., Chanzy, J.H., and Maret, G. (1992) *Macromolecules*, **25**, 4232.
34. Ebeling, T., Paillet, M., Borsali, R., Diat, O., Dufresne, A., Cavaille, J.-Y., and Chanzy, H. (1999) *Langmuir*, **15**, 6123.
35. Yoshiharu, N., Shigenori, K., Masahisa, W., and Takeshi, O. (1997) Cellulose microcrystal film of high uniaxial orientation. *Macromolecules*, **30**, 6395.
36. Alexandre, M. and Dubois, P. (2000) *Mater. Sci. Eng.*, **28**, 1.
37. Ray, S.S. and Okamoto, M. (2003) *Prog. Polym. Sci.*, **28**, 1539.
38. Medeiros, E.S., Agnelli, J.A.M., Joseph, K., Carvalho, L.H., and Mattoso, L.H.C. (2005) *Polym. Compos.*, **6**, 1.
39. Bledzki, A.K. and Gassan, J. (1999) *Prog. Polym. Sci.*, **24**, 221.
40. Medeiros, E.S., Tocchetto, R.S., Carvalho, L.H., Conceição, M.M., and Souza, A.G. (2002) *J. Therm. Anal. Calorim.*, **67**, 279.
41. Medeiros, E.S., Tocchetto, R.S., Carvalho, L.H., Santos, I.M.G., and Souza, A.G. (2001) *J. Therm. Anal. Calorim.*, **66**, 523.
42. Grim, R.E. (1962) Clay mineralogy. *Science*, **135**, 890.
43. Grim, R.E. (1988) *Clays Clay Miner.*, **26**, 97.
44. Popov, V.N. (2004) *Mater. Sci. Eng., R*, **43**, 61.
45. Fischer, H. (2003) *Mater. Sci. Eng., C*, **23**, 763.
46. Deguchi, S., Tsujii, K., and Horikoshi, K. (2006) *Chem. Commun.*, 3293.
47. Crawford, R.L. (1981) *Lignin Biodegradation and Transformation*, John Wiley & Sons, Inc., New York.
48. Kim, I.S., Kim, J.P., Kwak, S.Y., Ko, Y.S., and Kwon, Y.K. (2006) *Polymer*, **47**, 1333.
49. ACS *http://membership.acs.org/C/CELL/apayen.htm* (accessed 3 April 2011).
50. Battista, O.A. and Smith, P.A. (1962) *Ind. Eng. Chem.*, **54**, 20.
51. Battista, O.A., Erdi, N.Z., Ferraro, C.F., and Karasinski, F.J. (1967) *J. Appl. Polym. Sci.*, **11**, 481.
52. Battista, O.A. (1975) *Microcrystalline Polymer Science*, McGraw-Hill, New York, p. 39.
53. Wikipedia File:Plant Cell Wall Diagram.svg *http://en.wikipedia.org/wiki/Image:Plant_cell_wall_diagram.svg* (accessed 3 April 2011).
54. Lima, M.M.S. and Borsali, R. (2004) *Macromol. Rapid Commun.*, **25**, 771.
55. Roman, M. and Winter, W.T. (2004) *Biomacromolecules*, **5**, 1671.
56. Wang, N., Ding, E., and Cheng, R. (2007) *Polymer*, **48**, 3486.
57. Araki, J., Wada, M., Kuga, S., and Okano, T. (1998) *Colloids Surf., A*, **142**, 75.
58. Morton-Jones, D.H. (1989) *Polymer Processing*, Chapman & Hall, London.
59. Tadmor, Z. and Gogos, C.G. (1979) *Principles of Polymer Processing*, John Wiley & Sons, Inc., New York.
60. Glasser, W.G., Taib, R., Jain, R.K., and Kander, R. (1999) *J. Appl. Polym. Sci.*, **73**, 1329.
61. Marcovich, N.E., Auad, M.L., Bellesi, N.E., Nutt, S.R., and Aranguren, M.I. (2006) *J. Mater. Res.*, **21**, 870.
62. Orts, W.J., Baker, D.A., Shey, J., Chiou, B.-S., Imam, S.H., Glenn, G.M., and Mattoso, L.H.C. (2007) in *Biopolymers and Technology* (ed. A.C. Bertolini), Cultura Academica Editora, São Paulo, p. 85.
63. Samir, M.A.S.A., Alloin, F., and Dufresne, A. (2005) *Biomacromolecules*, **6**, 612.
64. Rodriguez, N.L.G., Thielemans, W., and Dufresne, A. (2006) *Cellulose*, **13**, 261.
65. Rosa, M.F., Medeiros, E.S., Malmonge, J.A., Gregorski, K.S., Wood, D.F., Mattoso, L.H.C., Glenn, G., Orts, W.J.,

and Imam, S.H. (2010) *Carbohydr. Polym.*, **81**, 83.
66. Teixeira, E.M., Corrêa, A.C., Manzoli, A., Leite, F.L., Oliveira, C.R., and Mattoso, L.H.C. (2010) *Cellulose*, **17**, 595.
67. Corrêa, A.C., Teixeira, E.M., Pessan, L.A., and Mattoso, L.H.C. (2010) *Cellulose*, **17**, 1183.
68. Teixeira, E.M., Bondânica, T.J., Teodoro, K.B.R., Corrêa, A.C., Marconcini, J.M., and Mattoso, L.H.C. (2011) *Ind. Crops Prod.*, **33**, 63.
69. Teixeira, E.M., Corrêa, A.C., Teodoro, J K.B.R., Marconcini, J.M., and Mattoso, L.H.C. (2011) Thermoplastic corn starch reinforced with cotton cellulose nanofibers. *J. Appl. Polym. Sci.*, **120**, 2428–2433 (accepted to publication).
70. Atkins, E.D.T. (1985) *Biosci. J.*, **8**, 375.
71. Persson, J.E., Domard, A., and Chanzy, H. (1990) *Int. J. Biol. Macromol.*, **13**, 221.
72. Helbert, W. and Sugiyama, J. (1998) *Cellulose*, **5**, 113.
73. Bartnicki-Garcia, S., Persson, J., and Chanzy, H. (1994) *Arch. Biochem. Biophys.*, **310**, 6.
74. Sakamoto, J., Sugiyama, J., Kimura, S., Imai, T., Itoh, T., Watanabe, T., and Kobayashi, S. (2000) *Macromolecules*, **33**, 4155.
75. Rudall, K.M. and Kenchington, W. (1973) *Biol. Rev.*, **40**, 597.
76. Blackwell, J., Parker, K.D., and Rudall, K.M. (1965) *J. Mar. Biol. Assoc. U. K.*, **45**, 659.
77. Gaill, F., Persson, J., Sugiyama, J., Vuong, R., and Chanzy, H. (1992) *J. Struct. Biol.*, **109**, 116.
78. Lotmar, W. and Picken, L.E.R. (1950) *Experientia*, **6**, 58.
79. Herth, W., Kuppel, A., and Schnepf, E. (1977) *J. Cell Biol.*, **73**, 311.
80. Herth, W., Mulisch, M., and Zugenmaier, P. (1986) in *Nature and Technology* (eds R. Muzzarelli, C. Jeuniaux, and G.W. Gooday), Plenum, New York, p. 107.
81. Revol, J.F. and Marchessault, R.H. (1993) *Int. J. Biol. Macromol.*, **15**, 329.
82. Muzzarelli, R.A.A. (1977) *Chitin*, Pergamon Press, New York, p. 51.
83. Brine, C.J. and Austin, P.R. (1975) in *Marine Chemistry in the Coastal Environment*, ACS Symposium Series, Vol. 18 (ed. T.D. Church), ACS, Washington, DC, p. 505.
84. Vincent, J.F.V. and Wegst, U.G.K. (2004) *Arthropod Struct. Dev.*, **33**, 187.
85. Arvanitoyannis, I.S. (2008) in *Environmentally Compatible Food Packaging* (ed. E. Chiellini) Chapter 1, Woodhead Publishing Ltd, Cambridge, p. 137.
86. Pandey, J.K., Reddy, K.R., Kumar, A.P., and Singh, R.P. (2005) *Polym. Degrad. Stab.*, **88**, 234.
87. Bordes, P., Pollet, E., and Avérous, L. (2009) *Prog. Polym. Sci.*, **34**, 125.
88. Averous, L. and Boquillon, N. (2004) *Carbohydr. Polym.*, **56**, 111.
89. Pavlidou, S. and Papaspyrides, C.D. (2008) *Prog. Polym. Sci.*, **33**, 1119.
90. Robertson, G. (2008) in *Environmentally Compatible Food Packaging* (ed. E. Chiellini) Chapter 1, Woodhead Publishing Ltd, Cambridge, p. 3.
91. Stevens, E.S. (2002) *Green Plastics*, Princeton University Press, Princeton, NJ.
92. Walton, A.G. and Blackwell, J. (1973) *Biopolymers*, Academic Press, New York.
93. Bruckdorfer, T., Marder, O., and Albericio, F. (2004) *Curr. Pharm. Biotechnol.*, **5**, 29.
94. Mallapragada, S. and Narasimhan, B. (2005) *Handbook of Biodegradable Polymeric Materials and their Applications*, American Scientific Publishers.
95. Domb, A.J., Kost, J., and Wiseman, D.M. (eds) (1997) *Handbook of Biodegradable Polymers*, CRC Press, Boca Raton, FL.
96. Tolstoguzov, V. (2004) *Food Hydrocolloids*, **18**, 873.
97. Avérous, L., Fringant, C., and Moroa, L. (2001) *Starch/Stärke*, **53**, 368.
98. Corradini, E., Medeiros, E.S., Carvalho, A.J.F., Curvelo, A.A.S., and Mattoso, L.H.C. (2006) *J. Appl. Polym. Sci.*, **101**, 4133.
99. Corradini, E., Lotti, C., Medeiros, E.S., Carvalho, A.J.F., Curvelo, A.A.S., and Mattoso, L.H.C. (2005) *Polímeros:*

Ciência e Tecnologia, **15**, 268. (In Portuguese).
100. Whistler, R.L. and Paschall, E.F. (1965) *Starch: Chemistry and Technology*, Vol. 1, Academic Press, New York.
101. Whistler, R.L. and Paschall, E.F. (1967) *Starch: Chemistry and Technology*, Vol. 2, Academic Press, New York.
102. Herrero-Martínez, J.M., Schoenmakers, P.J., and Kok, W.T. (2004) *J. Chromatogr. A*, **1053**, 227.
103. McMurry, J. (1996) *Organic Chemistry*, 4th edn, Brooks, Pacific Grove, CA.
104. Sajilata, M.G., Singhal, R.S., and Kulkarni, P.R. (2006) *Compr. Rev. Food Sci. Food Saf.*, **5**, 1.
105. Alexander, R.J. and Zobel, H.F. (eds) (1992) *Development in Carbohydrate Chemistry*, The American Association of Cereal Chemists Inc., Saint Paul.
106. Aichholzer, W. and Fritz, H.-G. (1998) *Starch/Stärke*, **50**, 77.
107. *http://mntl.illinois.edu/*.
108. Steinbuchel, A. and Doi, Y. (2002) *Biopolymers*, Wiley-VCH Verlag GmbH, Weinheim.
109. Averous, L. Bioplastics: Biodegradable Polyesters (PLA, PHA, PCL ...) *http://www.biodeg.net/bioplastic.html* (accessed 13 September 2010).
110. Sudesh, K. and Doi, Y. (2005) in *Handbook of Biodegradable Polymers* (ed. C. Bastionli) Chapter 7, Rapra Technology, Shawbury, p. 219.
111. Holmes, P.A. (1988) in *Developments in Crystalline Polymers*, Vol. 2 (ed. C.D. Basset), Elsevier, New York, p. 1.
112. Bastioli, C. (1998) *Polym. Degrad. Stab.*, **59**, 263.
113. Averous, L. *http://www.biodeg.net/bioplastic.html#biodegradable* (accessed 12 September 2010).
114. Sarasua, J.R., Arraiza, A.L., Balerdi, P., and Maiza, I. (2005) *Polym. Eng. Sci.*, **45**, 745.
115. Perrin, D.E. and English, J.P. (1997) Polyglycolide and polylactide, in *Handbook of Biodegradable Polymers* (eds A.J. Domb, J. Kost, and D.M. Wiseman), CRC Press, Boca Raton, FL.
116. Ray, S.S. and Bousmina, M. (2005) *Prog. Mater. Sci.*, **50**, 962.
117. Albertsson, A.-C. and Karlsson, S. (1995) *Acta Polym.*, **46**, 114.
118. Williams, J.M., Adewunmi, A., Schek, R.L.M., Flanagan, C.L., Krebsbach, P.H., Feinberg, S.E., Hollister, S.J., and Das, S. (2005) *Biomaterials*, **26**, 4817.
119. Lips, P.A.M. and Dijkstra, P.J. (2005) in *Biodegradable Polymers for Industrial Applications* (ed. R. Smith) Chapter 5, CRC Press, Boca Raton, FL, p. 107.
120. Grigat, E., Koch, R., and Timmermann, R. (1998) *Polym. Degrad. Stab.*, **59**, 223.
121. Jovanovic, D., Nikolic, M.S., and Djonlagic, J. (2004) *J. Serb. Chem. Soc.*, **69**, 1013.
122. Roman, I.V. and Tighzert, L. (2009) *Materials*, **2**, 307.
123. Beyer, G. (2002) *Plast. Addit. Compd.*, **4**, 22.
124. Seal, B.L., Otero, T.C., and Panitch, A. (2001) *Mater. Sci. Eng.*, **R34**, 147.
125. Clarinval, A.M. and Halleux, J. (2005) in *Biodegradable Polymers for Industrial Applications* (ed. R. Smith) Chapter 1, CRC Press, Boca Raton, FL, p. 3.
126. Jérôme, R. and Lecomte, P. (2005) in *Biodegradable Polymers for Industrial Applications* (ed. R. Smith) Chapter 4, CRC Press, Boca Raton, FL, p. 77.
127. Chen, Y., Tan, L., Chen, L., Yang, Y., and Wang, X. (2008) *Braz. J. Chem. Eng.*, **25**, 321.
128. Environment Australia (2002) *Report on Biodegradable Plastics–Developments and Environmental Impacts*, NOLAN-ITU Pty Ltd, And ExcelPlas.
129. Okamoto, M. (2005) in *Handbook of Biodegradable Polymeric Materials and their Applications*, Vol. 1 (eds S. Mallapragada and B. Narasimhan) Chapter 8, American Scientific Publishers, Stevenson Ranch, CA, p. 1.
130. Vaia, R.A. and Wagner, H.D. (2004) *Mater. Today*, 32.
131. Gill, I. (2001) *Chem. Mater.*, **13**, 3404.
132. Decher, G. and Schlenoff, J.B. (eds) (2002) *Multilayer Thin Films*, Wiley-VCH Verlag GmbH, Weinheim.
133. Medeiros, E.S., Paterno, L.G., and Mattoso, L.H.C. (2006) in *Encyclopedia of Sensors*, Vol. 10 (eds C.A. Grimes, E.C. Dickey, and M.V. Pishko), American Scientific Publishers, Stevenson Ranch, CA, p. 1.

134. Kamel, S. (2007) *Express Polym. Lett.*, **1**, 546.
135. Begishev, V.P. and Malkin, A.Y. (1999) *Reactive Processing of Polymers*, Chern-Tec Publishing, Toronto.
136. Brydson, J.A. (1999) *Plastics Materials*, 7th edn, Butterworth-Heinemann, Orford.
137. Rosato, D.V. (1997) *Plastics Processing Data Handbook*, 2nd edn, Chapman & Hall, London.
138. Crawford, R.J. (1999) *Plastics Engineering*, 3rd edn, Butterworth-Heinemann, Orford.
139. Kaplan, D.L. (1998) *Biopolymers from Renewable Resources*, Springer-Verlag, Heidelberg.
140. Ramakrishna, S., Fujihara, K., Teo, W.E., Lim, T.C., and Ma, Z. (2005) *An Introduction to Electrospinning and Nanofibers*, World Scientific Publishing, Singapore.
141. Medeiros, E.S., Mattoso, L.H.C., Ito, E.N., Gregorski, K.S., Robertson, G.H., Offeman, R.D., Wood, D.F., Orts, W.J., and Imam, S.H. (2008) *J. Biobased Mater. Bioenergy*, **2**, 231.
142. Brundle, C.R., Evans, C.A. Jr.,, and Wilson, S. (1992) *Encyclopedia of Materials Characterization, Surfaces, Interfaces, Thin Films*, Butterworth-Heinemann, Boston, MA.
143. Rhim, J.-W. and Ng, P.K.W. (2007) *Crit. Rev. Food Sci. Nutr.*, **47**, 411.
144. Yang, K.K., Wang, X.L., and Wang, Y.Z. (2007) *J. Ind. Eng. Chem.*, **13**, 485.
145. Ruiz-Hitzky, E., Darder, M., and Aranda, P. (2005) *J. Mater. Chem.*, **15**, 3650.
146. Sorrentino, A., Gorrasi, G., and Vittoria, V. (2007) *Trends Food Sci. Technol.*, **18**, 84.
147. Cao, X., Chen, Y., Chang, P.R., and Huneault, M.A. (2007) *J. Appl. Polym. Sci.*, **106**, 1431.
148. Ma, X., Yu, J., and Wang, N. (2008) *Compos. Sci. Technol.*, **68**, 268.
149. Carvalho, A.J.F., Curvelo, A.A.S., and Agnelli, J.A.M. (2001) *Carbohydr. Polym.*, **45**, 189.
150. Chen, B. and Evans, J.R.G. (2005) *Carbohydr. Polym.*, **61**, 455.
151. Park, H.M., Lee, W.K., Park, C.Y., Cho, W.J., and Ha, C.S. (2003) *J. Mater. Sci.*, **38**, 909.
152. Chiou, B.-S., Yee, E., Glenn, G.M., and Orts, W.J. (2005) *Carbohydr. Polym.*, **59**, 467.
153. Chiou, B.-S., Wood, D., Yee, E., Imam, S.H., Glenn, G.M., and Orts, W.J. (2007) *Polym. Eng. Sci.*, **47**, 1898.
154. Qiao, X., Jiang, W., and Sun, K. (2005) *Starch/Stärke*, **57**, 581.
155. Pandey, J.K. and Singh, R.P. (2005) *Starch/Stärke*, **57**, 8.
156. Chen, M., Chen, B., and Evans, J.R.G. (2005) *Nanotechnology*, **16**, 2334.
157. Cyras, V.P., Manfredi, L.B., Ton-That, M.T., and Vázquez, A. (2008) *Carbohydr. Polym.*, **73**, 55.
158. Anglès, M.N. and Dufresne, A. (2000) *Macromolecules*, **33**, 8344.
159. Anglès, M.N. and Dufresne, A. (2001) *Macromolecules*, **34**, 2921.
160. Dufresne, A. and Vignon, M.R. (1998) *Macromolecules*, **31**, 2693.
161. Dufresne, A., Dupeyre, D., and Vignon, M.R. (2000) *J. Appl. Polym. Sci.*, **76**, 2080.
162. Mathew, A.P. and Dufresne, A. (2002) *Biomacromolecules*, **3**, 609.
163. Lu, Y., Weng, L., and Cao, X. (2006) *Carbohydr. Polym.*, **63**, 198.
164. Kvien, I., Sugiyama, J., Votrubec, M., and Oksman, K. (2007) *J. Mater. Sci.*, **42**, 8163.
165. McGlashan, S.A. and Halley, P.J. (2003) *Polym. Int.*, **52**, 1767.
166. Kalambur, S. and Rizvi, S.S.H. (2005) *J. Appl. Polym. Sci.*, **96**, 1072.
167. Kalambur, S. and Rizvi, S.S.H. (2006) *Polym. Eng. Sci.*, **46**, 650.
168. Liao, H.T. and Wu, C.S. (2005) *J. Appl. Polym. Sci.*, **97**, 397.
169. Pérez, C.J., Alvarez, V.A., Mondragón, I., and Vázquez, A. (2007) *Polym. Int.*, **56**, 686.
170. Dean, K.M., Do, M.D., Petinakis, E., and Yu, L. (2008) *Compos. Sci. Technol.*, **68**, 1453.
171. Lee, S.Y., Chen, H., and Hanna, M.A. (2008) *Ind. Crops Prod.*, **28**, 95.
172. Dufresne, A., Cavaillé, J.-Y., and Helbert, W. (1996) *Macromolecules*, **29**, 7624.

173. Dufresne, A. and Cavaillé, J.-Y. (1998) *J. Polym. Sci., Part B: Polym. Phys.*, **36**, 2211.

174. Dubief, D., Samain, E., and Dufresne, A. (1999) *Macromolecules*, **32**, 5765.

175. Angellier, H., Molina-Boisseau, S., and Dufresne, A. (2005) *Macromolecules*, **38**, 9161.

176. Angellier, H., Molina-Boisseau, S., Lebrun, L., and Dufresne, A. (2005) *Macromolecules*, **38**, 3783.

177. Angellier, H., Molina-Boisseau, S., and Dufresne, A. (2006) *Macromol. Symp.*, **233**, 132.

178. Angellier, H., Putaux, J.L., Molina-Boisseau, S., Dupeyre, D., and Dufresne, A. (2005) *Macromol. Symp.*, **221**, 95.

179. Angellier, H., Molina-Boisseau, S., Dole, P., and Dufresne, A. (2006) *Biomacromolecules*, **7**, 531.

180. Viguié, J., Molina-Boisseau, S., and Dufresne, A. (2007) *Macromol. Biosci.*, **7**, 1206.

181. Kristo, E. and Biliaderis, C.G. (2007) *Carbohydr. Polym.*, **68**, 146.

182. Chen, Y., Cao, X., Chang, P.R., and Huneault, M.A. (2008) *Carbohydr. Polym.*, **73**, 8.

183. Thielemans, W., Belgacem, M.N., and Dufresne, A. (2006) *Langmuir*, **22**, 4804.

184. Labet, M., Thielemans, W., and Dufresne, A. (2007) *Biomacromolecules*, **8**, 2916.

185. Nair, K.G. and Dufresne, A. (2003) *Biomacromolecules*, **4**, 657.

186. Nair, K.G. and Dufresne, A. (2003) *Biomacromolecules*, **4**, 666.

187. Nair, K.G., Dufresne, A., Gandini, A., and Belgacem, M.N. (2003) *Biomacromolecules*, **4**, 1835.

188. Laborie, M.P.G. and Oksman, K. (2009) *Biomacromolecules*, **10**, 1627.

189. Sriupayo, J., Supaphol, P., Blackwell, J., and Rujiravanit, R. (2005) *Carbohydr. Polym.*, **62**, 130.

190. Junkasem, J., Rujiravanit, R., and Supaphol, P. (2006) *Nanotechnology*, **17**, 4519.

191. Darder, M., Colilla, M., and Ruiz-Hitzky, E. (2003) *Chem. Mater.*, **15**, 3774.

192. Wongpanit, P., Sanchavanakit, N., Pavasant, P., Bunaprasert, T., Tabat, Y., and Rujiravanit, R. (2007) *Eur. Polym. J.*, **43**, 4123.

193. Wang, S.F., Shen, L., Tong, Y.J., Chen, L., Phang, I.Y., Lim, P.Q., and Liu, T.X. (2005) *Polym. Degrad. Stab.*, **90**, 123.

194. Feng, L., Zhou, Z., Dufresne, A., Huang, J., and Wei, M. (2009) *J. Appl. Polym. Sci.*, **112**, 2830.

195. Lu, Y., Weng, L., and Zhang, L. (2004) *Biomacromolecules*, **5**, 1046.

196. Mathew, A.P., Laborie, M.-P.G., and Oksman, K. (2009) *Biomacromolecules*, **10**, 1627.

197. Azeredo, H.M.C., Mattoso, L.H.C., Avena-Bustillos, R.J., Ceotto-Filho, G., Munford, M.L., Wood, D., and McHugh, T.H. (2010) *J. Food Sci.*, **75**, 1.

198. Rhim, J.-W., Hong, S.-I., Park, H.-M., and Ng, P.K.W. (2006) *J. Agric. Food Chem.*, **54**, 5814.

199. Zhang, K., Xu, J., Wang, K.Y., Cheng, L., Wang, J., and Liu, B. (2009) *Polym. Degrad. Stab.*, **94**, 2121.

200. Moura, M.R., Aouada, F.A., Avena-Bustillos, R.J., McHugh, T.H., Krochta, J.M., and Mattoso, L.H.C. (2009) *J. Food Eng.*, **92**, 448.

201. Kaushik, A., Solanki, P.R., Pandey, M.K., Kaneto, K., Ahmad, S., and Malhotra, B.D. (2010) *Thin Solid Films*, **519**. doi: 10.1016/j.tsf.2010.08.062

202. Darder, M., Colilla, M., and Ruiz-Hitzky, E. (2005) *Appl. Clay Sci.*, **28**, 199.

203. Liu, X., Hu, Q., Fang, Z., Zhang, X., and Zhang, B. (2009) *Langmuir*, **25**, 3.

204. Kampeerapappun, P., Aht-ong, D., Pentrakoon, D., and Srikulkit, K. (2007) *Carbohydr. Polym.*, **67**, 155.

205. Hu, Q., Li, B., Wang, M., and Shen, J. (2004) *Biomaterials*, **25**, 779.

206. Zhang, Y., Venugopal, J.R., El-Turkic, A., Ramakrishna, S., Su, B., and Lim, C.T. (2008) *Biomaterials*, **29**, 4314.

207. Lagarón, J.M. and Fendler, A. (2009) *J. Plast. Film Sheeting*, **25**, 47.

208. Chen, P. and Zhang, L. (2006) *Biomacromolecules*, **7**, 1700.

209. Kumar, P., Sandeep, K.P., Alavi, S., Truong, V.D., and Gorga, R.E. (2010) *J. Food Sci.*, **75**, N46.

210. Kumar, P., Sandeep, K.P., Alavi, S., Truong, V.D., and Gorga, R.E. (2010) *J. Food Eng.*, **100**, 480.

211. Zheng, H., Ai, F., Chang, P.R., Huang, J., and Dufresne, A. (2009) *Polym. Compos.*, **30**, 474.

212. Yu, J., Cui, G., Wei, M., Huang, J., Yu, J., Cui, G., Wei, M., and Huang, J. (2007) *J. Appl. Polym. Sci.*, **104**, 3367.

213. Rhim, J.W., Lee, J.H., and Kwak, H.S. (2005) *Food Sci. Biotechnol.*, **14**, 112.

214. Smith, R. (ed.) (2005) *Biodegradable Polymers for Industrial Application*, CRC Press, Boca Raton, FL, p. 289.

215. Zheng, J.P., Li, P., Ma, Y.L., and Yao, K.D. (2002) *J. Appl. Polym. Sci.*, **86**, 1189.

216. Zheng, J.P., Li, P., and Yao, K.D. (2002) *J. Mater. Sci. Lett.*, **21**, 779.

217. Zhuang, H., Zheng, J.P., Gao, H., and Yao, K.D. (2007) *J. Mater. Sci. -Mater. Med.*, **18**, 951.

218. Zheng, J.P., Wang, C.Z., Wang, X.X., Wang, H.Y., Zhuang, H., and De Yao, K. (2007) *React. Funct. Polym.*, **67**, 780.

219. Martucci, J.F., Vázquez, A., and Ruseckaite, R.A. (2007) *J. Therm. Anal. Calorim.*, **89**, 117.

220. Rao, Y.Q. (2007) *Polymer*, **48**, 5369.

221. Chang, M.C., Ikoma, T., Kikuchi, M., and Tanaka, J. (2001) *J. Mater. Sci. Lett.*, **20**, 1199.

222. Chang, M.C., Ko, C.-C., and Douglas, W.H. (2003) *Biomaterials*, **24**, 3087.

223. Chang, M.C., Ko, C.-C., and Douglas, W.H. (2005) *J. Mater. Sci. Lett.*, **40**, 505.

224. Mann, S. and Ozin, G.A. (1996) *Nature*, **365**, 499.

225. Chang, M.C., Ko, C.-C., and Douglas, W.H. (2003) *Biomaterials*, **24**, 2853.

226. Chang, M.C. and Douglas, W.H. (2007) *J. Mater. Sci. -Mater. Med.*, **18**, 2045.

227. Li, J., Yin, Y., Yao, F., Zhang, L., and Yao, K. (2008) *Mater. Lett.*, **62**, 3220.

228. Murugan, R. and Ramakrishna, S. (2005) *Compos. Sci. Technol.*, **65**, 2385.

229. Li, X. and Chang, J. (2008) *J. Biomed. Mater. Res. Part A*, **85**, 293.

230. Thomas, V., Dean, D.R., Jose, M.V., Mathew, B., Chowdhury, S., and Vohra, Y.K. (2007) *Biomacromolecules*, **8**, 631.

231. Kikuchi, M., Matsumoto, H.N., Yamada, T., Koyama, Y., Takakuda, K., and Tanaka, J. (2004) *Biomaterials*, **25**, 63.

232. Santos, M.H., Valerio, P., Goes, A.M., Leite, M.F., Heneine, L.G.D., and Mansur, S. (2007) *Biomed. Mater.*, **2**, 135.

233. Pek, Y.S., Gao, S., Arshad, M.S.M., Leck, K.J., and Ying, J.Y. (2008) *Biomaterials*, **29**, 4300.

234. Desimone, M.F., Hélary, C., Rietveld, I.B., Bataille, I., Mossera, G., Giraud-Guille, M.-M., Livage, J., and Coradin, T. (2010) *Acta Biomater.*, **6**, 3998.

235. Luecha, J., Sozer, N., and Kokini, J.L. (2010) *J. Mater. Sci.*, **45**, 529.

236. Torres-Giner, S. and Lagaron, J.M. (2010) *J. Appl. Polym. Sci.*, **118**, 778.

237. Olabarrieta, I., Gällstedt, M., Ispizua, I., Sarasua, J.-R., and Hedenqvist, M.S. (2006) *J. Agric. Food Chem.*, **54**, 1283.

238. Philip, S., Keshavarz, T., and Roy, I. (2007) *J. Chem. Technol. Biotechnol.*, **82**, 233.

239. Hajiali, H., Karbasi, S., Hosseinalipour, M., and Rezaie, H.R. (2010) *J. Mater. Sci. -Mater. Med.*, **21**, 2125.

240. Hajiali, H., Hosseinalipour, M., Karbasi, S., and Rezaie, H.R. (2010) *IFMBE Proc.*, **31**, 1238.

241. Hablot, E., Bordes, P., Pollet, E., and Avérous, L. (2008) *Polym. Degrad. Stab.*, **93**, 413.

242. Bordes, P., Hablot, E., Pollet, E., and Avérous, L. (2009) *Polym. Degrad. Stab.*, **94**, 789.

243. Zhang, X., Lin, G., Abou-Hussein, R., Hassan, M.K., Nodac, I., and Mark, J.E. (2007) *Eur. Polym. J.*, **43**, 3128.

244. Hsu, S.-F., Wu, T.-M., and Liao, C.-S. (2007) *J. Polym. Sci., Part B: Polym. Phys.*, **45**, 995.

245. Erceg, M., Kovačića, T., and Klarića, I. (2009) *Thermochim. Acta*, **485**, 26.

246. Maiti, P., Batt, C.A., and Giannelis, E.P. (2007) *Biomacromolecules*, **11**, 3393.

247. Yeo, S.Y., Tan, W.L., Abu Bakar, M., and Ismail, J. (2010) *Polym. Degrad. Stab.*, **95**, 1299.

248. Jiang, L., Morelius, E., Zhang, J., Wolcott, M., and Holbery, J. (2008) *J. Compos. Mater.*, **42**, 2629.

249. Bruzaud, S. and Bourmaud, A. (2007) *Polym. Test.*, **26**, 652.

250. Chen, G.X., Hao, G.J., Guo, T.Y., Song, M.D., and Zhang, B.H. (2004) *J. Appl. Polym. Sci.*, **93**, 655.

251. Choi, W.M., Kim, T.W., Park, O.O., Chang, Y.K., and Lee, J.W. (2003) *J. Appl. Polym. Sci.*, **90**, 525.

252. Lemes, A.P., Marcato, P.D., Ferreira, O.P., Alves, O.L., and Durn, N. (2008) Book of Abstracts of the Nanotechnology and Applications (NANA 2008), Crete, Greece, September 29–October 1, 2008.

253. Lai, M., Li, J., Yang, J., Liu, J., Tong, X., and Cheng, H. (2004) *Polym. Int.*, **53**, 1479.

254. Maiti, P. and Yadav, J.P. (2008) *J. Nanosci. Nanotechnol.*, **8**, 1858.

255. Tang, C.Y., Chen, D.Z., Yue, T.M., Chan, K.C., Tsui, C.P., and Yu, P.H.F. (2008) *Compos. Sci. Technol.*, **68**, 1927.

256. Chen, D.Z., Tang, C.Y., Chan, K.C., Tsui, C.P., Yu, P.H.F., Leungc, M.C.P., and Uskokovic, P.S. (2007) *Compos. Sci. Technol.*, **67**, 1617.

257. Bordes, P., Pollet, E., Bourbigot, S., and Avérous, L. (2008) *Macromol. Chem. Phys.*, **209**, 1473.

258. Zhang, Q., Liu, Q., Mark, J.E., and Noda, I. (2009) *Appl. Clay Sci.*, **46**, 51.

259. Sanchez-Garcia, M.D., Gimenez, E., and Lagaron, J.M. (2008) *J. Appl. Polym. Sci.*, **108**, 2787.

260. Yun, S.I., Gadd, G.E., Latella, B.A., Lo, V., Russell, R.A., and Holden, P.J. (2008) *Polym. Bull.*, **61**, 267.

261. Oksman, K., Mathewa, A.P., Bondesona, D., and Kviena, I. (2006) *Compos. Sci. Technol.*, **66**, 2776.

262. Bondeson, D. and Oksman, K. (2007) *Compos. Interfaces*, **14**, 617.

263. Krul, L.P., Volozhyn, A.I., Belov, D.A., Poloiko, N.A., Artushkevich, A.S., Zhdanok, S.A., Solntsev, A.P., Krauklis, A.V., and Zhukova, I.A. (2007) *Biomol. Eng.*, **24**, 93.

264. Moon, S.-I., Jin, F., Lee, C.-J., Tsutsumi, S., and Hyon, S.-H. (2005) *Macromol. Symp.*, **224**, 287.

265. Ray, S.S., Maiti, P., Okamoto, M., Yamada, K., and Ueda, K. (2002) *Macromolecules*, **35**, 3104.

266. Ray, S.S., Yamada, K., Okamoto, M., Ogami, A., and Ueda, K. (2003) *Chem. Mater.*, **15**, 1456.

267. Ray, S.S., Yamada, K., Okamoto, M., and Ueda, K. (2002) *Nano Lett.*, **2**, 1093.

268. Sinha Ray, S., Yamada, K., Okamoto, M., and Ueda, K. (2003) *Macromol. Mater. Eng.*, **288**, 203.

269. Maiti, P., Yamada, K., Okamoto, M., Ueda, K., and Okamoto, K. (2002) *Chem. Mater.*, **14**, 4654.

270. Ray, S.S., Yamada, K., Okamoto, M., and Ueda, K. (2003) *J. Nanosci. Nanotechnol.*, **3**, 503.

271. Ray, S.S., Yamada, K., Okamoto, M., and Ueda, K. (2003) *Polymer*, **44**, 857.

272. Ray, S.S., Yamada, K., Okamoto, M., Fujimoto, Y., Ogami, A., and Ueda, K. (2003) *Polymer*, **44**, 6633.

273. Krikorian, V. and Pochan, D.J. (2003) *Chem. Mater.*, **15**, 4317.

274. Wu, T.-M. and Wu, C.-Y. (2006) *Polym. Degrad. Stab.*, **91**, 2198.

275. Ray, S.S., Yamada, K., Okamoto, M., Ogami, A., and Ueda, K. (2003) *Compos. Interfaces*, **10**, 435.

276. Lewitus, D., McCarthy, S., Ophir, A., and Kenig, S. (2006) *J. Polym. Environ.*, **14**, 171.

277. Chang, J.-H., An, Y.U., and Sur, G.S. (2003) *J. Polym. Sci., Part B: Polym. Phys.*, **41**, 94.

278. Hiroi, R., Ray, S.S., Okamoto, M., and Shiroi, T. (2004) *Macromol. Rapid Commun.*, **25**, 1359.

279. Pluta, M., Galeski, A., Alexandre, M., Paul, M.-A., and Dubois, P. (2002) *J. Appl. Polym. Sci.*, **86**, 1497.

280. Gorrasi, G., Tammaro, L., Vittoria, V., Paul, M.-A., Alexandre, M., and Dubois, P. (2005) *J. Macromol. Sci.*, **B43**, 565.

281. Paul, M.-A., Alexandre, M., Degée, P., Henrist, C., Rulmont, A., and Dubois, P. (2003) *Polymer*, **44**, 443.

282. Pluta, M., Paul, M.-A., Alexandre, M., and Dubois, P. (2006) *J. Polym. Sci., Part B: Polym. Phys.*, **44**, 299.

283. Pluta, M. (2004) *Polymer*, **45**, 8239.

284. Pluta, M., Paul, M.-A., Alexandre, M., and Dubois, P. (2006) *J. Polym. Sci., Part B: Polym. Phys.*, **44**, 312.

285. Pluta, M., Jeszka, J.K., and Boiteux, G. (2007) *Eur. Polym. J.*, **43**, 2819.

286. Gu, S.-Y., Ren, J., and Dong, B. (2009) *Biomaterials*, **30**, 58.

287. Żenkiewicz, M. and Richert, J. (2008) *Polym. Test.*, **27**, 835.

288. Zhang, J.H., Zhuang, W., Zhang, Q., Liu, B., Wang, W., Hu, B.X., and Shen, J. (2007) *Polym. Compos.*, **28**, 545.

289. Zhou, H., Kim, K.-W., Giannelis, E., and Joo, Y.L. (2006) in *Polymeric Nanofibers*, ACS Symposium Series, Vol. 918 (eds D.H. Reneker and H. Fong) Chapter 16, American Chemical Society, Washington, DC, p. 217.

290. Kim, H.W., Lee, H.-H., and Knowles, J.C. (2006) *J. Biomed. Mater. Res.*, **79A**, 643.

291. Zhou, S., Zheng, X., Yu, X., Wang, J., Weng, J., Li, X., Feng, B., and Yin, M. (2007) *Chem. Mater.*, **19**, 247.

292. Cai, X., Tong, H., Shen, X., Chen, W., Yan, J., and Hu, J. (2009) *Acta Biomater.*, **5**, 2693.

293. Deng, X., Hao, J., and Wang, C. (2001) *Biomaterials*, **22**, 2867.

294. Kim, H.W., Lee, H.H., and Chun, G.-S. (2008) *J. Biomed. Mater. Res.*, **85A**, 651.

295. Messersmith, P.B. and Giannelis, E.P. (1993) *Chem. Mater.*, **5**, 1064.

296. Siqueira, G., Bras, J., and Dufresne, A. (2009) *Biomacromolecules*, **10**, 425.

297. Habibi, Y. and Dufresne, A. (2008) *Biomacromolecules*, **9**, 1974.

298. Chen, G., Dufresne, A., Huang, J., and Chang, P.R. (2009) *Macromol. Mater. Eng.*, **294**, 59.

299. Castillo, V., Matos, M., and Muller, A.J. (2003) *Rev. Latinoam. Metal. Mater.*, **23**, 12.

300. Dubois, P. and Alexandre, M. (2006) *Adv. Eng. Mater.*, **8**, 147.

301. Saeed, K. and Park, S.Y. (1957) *J. Appl. Polym. Sci.*, **104** (207).

302. Chrissafis, K., Antoniadis, G., Paraskevopoulos, K.M., Vassiliou, A., and Bikiaris, D.N. (2007) *Compos. Sci. Technol.*, **67**, 2165.

303. Messersmith, P.B. and Giannelis, E.P. (1995) *J. Polym. Sci., Part A: Polym. Chem.*, **33**, 1047.

304. Di, Y., Iannac, S., Sanguigno, L., and Nicolais, L. (2005) *Macromol. Symp.*, **228**, 115.

305. Chen, B. and Evans, J.R.G. (2006) *Macromolecules*, **39**, 747.

306. Pantoustier, N., Lepoittevin, B., Alexandre, M., Dubois, P., Kubies, D., Calberg, C., and Jérôme, R. (2002) *Polym. Eng. Sci.*, **42**, 1928.

307. Pantoustier, N., Alexandre, M., Degée, P., Calberg, C., Jérôme, R., Henrist, C., Cloots, R., Rulmont, A., and Dubois, P. (2001) *e-Polymers*, **9**, 1.

308. Lepoittevin, B., Pantoustier, N., Devalckenaere, M., Alexandre, M., Kubies, D., Calberg, C., Jérôme, R., and Dubois, P. (2002) *Macromolecules*, **35**, 8385.

309. Fukushima, K., Tabuani, D., and Camino, G. (2009) *Mater. Sci. Eng.*, **C29**, 1433.

310. Sepahvand, R., Adeli, M., Astinchap, B., and Kabiri, R. (2008) *J. Nanopart. Res.*, **10**, 1309.

311. Thomassin, J.-M., Lou, X., Pagnoulle, C., Saib, A., Bednarz, L., Huynen, I., Jérôme, R., and Detrembleur, C. (2007) *J. Phys. Chem.*, **C111**, 11186.

312. Marras, S.I., Kladi, K.P., Tsivintzelis, I., Zuburtikudis, I., and Panayiotou, C. (2008) *Acta Biomater.*, **4**, 756.

313. Saeed, K., Park, S.-Y., Lee, H.-J., Baek, J.-B., and Huh, W.-S. (2006) *Polymer*, **47**, 8019.

314. Mitchell, C.A. and Krishnamoorti, R. (2007) *Macromolecules*, **40**, 1538.

315. Morin, A. and Dufresne, A. (2002) *Macromolecules*, **35**, 2190.

316. Habibi, Y. and Dufresne, A. (2008) *Biomacromolecules*, **9**, 1974.

317. Habibi, Y., Goffin, A.L., Schiltz, N., Duquesne, E., Dubois, P., and Dufresne, A. (2008) *J. Mater. Chem.*, **18**, 5002.

318. Krook, M., Albertsson, A.-C., Gedde, U.W., and Hedenqvist, M.S. (2002) *Polym. Eng. Sci.*, **42**, 1238.

319. Krook, M., Morgan, G., and Hedenqvist, M.S. (2005) *Polym. Eng. Sci.*, **45**, 135.

320. Liu, X., Zou, Y., Cao, G., and Luo, D. (2007) *Mater. Lett.*, **61**, 4216.

321. Morales-Gámez, L., Franco, L., and Puiggalí, J. (2010) *Thermochim. Acta*, **51**, 5788–5798. doi: 10.1016/j.tca.2010.09.017

322. Deng, X., Chen, Z., Qian, Z., Liu, C., and Li, H. (2008) *J. Biomed. Eng.*, **25**, 378.

323. Morales, L., Franco, L., Casas, M.T., and Puiggalí, J. (2009) *J. Polym. Sci., Part A: Polym. Chem.*, **47**, 3616.

324. Wen, X., Lin, Y., Han, C., Han, L., Li, Y., and Dong, L. (2010) *Macromol. Mater. Eng.*, **295**, 415.

325. Ray, S.S., Okamoto, K., and Okamoto, M. (2006) *J. Appl. Polym. Sci.*, **102**, 777.

326. Ray, S.S., Okamoto, K., and Okamoto, M. (2003) *Macromolecules*, **36**, 2355.

327. Ray, S.S., Okamoto, K., Maiti1, P., and Okamoto, M. (2002) *J. Nanosci. Nanotechnol.*, **2**, 171.

328. Okamoto, K., Ray, S.S., and Okamoto, M. (2003) *J. Polym. Sci., Part B: Polym. Phys.*, **41**, 3.

329. Shih, Y.F., Wang, T.Y., Jeng, R.J., Wu, J.Y., and Teng, C.C. (2007) *J. Polym. Environ.*, **15**, 151.

330. Chen, G.-X., Kim, E.-S., and Yoon, J.-S. (2005) *J. Appl. Polym. Sci.*, **98**, 1727.

331. Chen, G.-X. and Yoon, J.-S. (2005) *Polym. Degrad. Stab.*, **88**, 206.

332. Chen, G.-X., Kim, H.-S., Kim, E.-S., and Yoon, J.-S. (2005) *Polymer*, **46**, 11829.

333. Someya, Y., Nakazato, T., Teramoto, N., and Shibata, M. (2004) *J. Appl. Polym. Sci.*, **91**, 1463.

334. Han, S.-I., Lim, J.S., Kim, D.K., Kim, M.N., and Im, S.S. (2008) *Polym. Degrad. Stab.*, **93**, 889.

335. Song, L. and Qiu, Z. (2009) *Polym. Degrad. Stab.*, **94**, 632.

336. Shih, Y.F., Chen, L.S., and Jeng, R.J. (2008) *Polymer*, **49**, 4602.

337. Ray, S.S., Vaudreuil, S., Maazouz, A., and Bousmina, M. (2006) *J. Nanosci. Nanotechnol.*, **6**, 2191.

338. Ray, S.S. and Bousmina, M. (2005) *Polymer*, **46**, 12430.

339. Ray, S.S., Bousmina, M., and Okamoto, K. (2005) *Macromol. Mater. Eng.*, **290**, 759.

340. Ray, S.S., Bandyopadhyay, J., and Bousmina, M. (2008) *Eur. Polym. J.*, **44**, 3133.

341. Ray, S.S., Bandyopadhyay, J., and Bousmina, M. (2007) *Polym. Degrad. Stab.*, **92**, 802.

342. Ray, S.S., Bandyopadhyay, J., and Bousmina, M. (2007) *Macromol. Materi. Eng.*, **292**, 729.

343. Ray, S.S. and Bousmina, M. (2006) *Macromol. Chem. Phys.*, **207** (14), 1207–1219.

344. Steeves, D.M., Farrell, R., and Ratto, J.A. (2007) *J. Biobased Mater. Bioenergy*, **1**, 94.

345. Dean1, K.M., Pas, S.J., Yu, L., Ammala, A., Hill, A.J., and Wu, D.Y. (2009) *J. Appl. Polym. Sci.*, **113**, 3716.

346. Chen, G. and Yoon, J.-S. (2005) *Polym. Int.*, **54**, 939.

347. Chen, G. and Yoon, J.-S. (2005) *J. Polym. Sci., Part B: Polym. Phys.*, **43**, 478.

348. Someya, Y., Sugahara, Y., and Shibata, M. (2005) *J. Appl. Polym. Sci.*, **95**, 386.

349. Mohanty, S. and Nayak, S.K. (2010) *Int. J. Plast. Technol.*, **13**, 163.

350. Jiang, L., Liu, B., and Zhang, J. (2009) *Ind. Eng. Chem. Res.*, **48**, 7594.

351. Park, H.-M., Kim, G.-H., and Ha, C.-S. (2007) *Compos. Interfaces*, **14**, 427.

352. Shi, X., Hudson, J.L., Spicer, P.P., Tour, J.M., Krishnamoorti, R., and Mikos, A.G. (2006) *Biomacromolecules*, **7**, 2237.

353. Strawhecker, K.E. and Manias, E. (2000) *Chem. Mater.*, **12**, 2943.

354. Chang, J.-H., Jang, T.-G., Ihn, K.J., Lee, W.-K., and Sur, G.S. (2003) *J. Appl. Polym. Sci.*, **90**, 3208.

355. Yeun, J.-H., Bang, G.-S., Park, B.J., Ham, S.K., and Chang, J.-H. (2006) *J. Appl. Polym. Sci.*, **101**, 591.

356. Sriupayo, J., Supaphol, P., Blackwell, J., and Rujiravanit, R. (2005) *Polymer*, **46**, 5637.

357. Roohani, M., Habibi, Y., Belgacem, N.M., Ebrahim, G., Karimi, A.N., and Dufresne, A. (2008) *Eur. Polym. J.*, **44**, 2489.

358. Cheng, Q., Wang, S., and Rialsa, T.G. (2009) *Composites Part A*, **40**, 218.

359. Xu, J., Meng, Y.Z., Li, R.K.Y., Xu, Y., and Rajulu, A.V. (2003) *J. Polym. Sci., Part B: Polym. Phys.*, **41**, 749.

360. Peng, Z. and Chen, D. (2006) *J. Polym. Sci., Part B: Polym. Phys.*, **44**, 534.

361. Liu, L., Barber, A. .H., Nuriel, S., and Wagner, H. .D. (2005) *Adv. Funct. Mater.*, **15**, 975.

362. Mbhele, Z.H., Salemane, M.G., van Sittert, C.G.C.E., Nedeljković, J.M., Djoković, V., and Luyt, A.S. (2003) *Chem. Mater.*, **15**, 5019.

363. Xu, J., Hu, Y., Lei, S., Wnag, Q., Fan, W., and Chen, Z. (2002) *Carbon*, **40**, 445.

364. López, D., Cendoya, I., Torres, F., Tejada, J., and Mijangos, C. (2001) *J. Appl. Polym. Sci.*, **82**, 3215.

365. Kumar, R.V., Palchik, O., Koltypin, Y., Diamant, Y., and Gedanken, A. (2002) *Ultrason. Sonochem.*, **9**, 65.

366. Charpentier, P.A., Xu, W.Z., and Li, X. (2007) *Green Chem.*, **9**, 768.

367. Choi, C.S., Park, B.J., and Choi, H.J. (2007) *Diamond Relat. Mater.*, **16**, 1170.

368. Kalfus, J. and Jancar, J. (2007) *Polym. Compos.*, **28**, 743.

369. Yeum, J.H., Sun, Q., and Deng, Y. (2005) *Macromol. Mater. Eng.*, **290**, 78.

370. Yu, Y.-H., Lin, C.-Y., Yeh, J.-M., and Lin, W.-H. (2003) *Polymer*, **44**, 3553.

371. Jung, H.M., Lee, E.M., Ji, B.C., Deng, Y., Yun, J.D., and Yeum, J.H. (2007) *Colloid Polym. Sci.*, **285**, 705.

372. Hule, R.A. and Pochan, D.J. (2007) *MRS Bull.*, **32**, 354.

373. Murugan, D., Radhika, S., Baskaran, I., and Anbarasan, R. (2008) *Chin. J. Polym. Sci.*, **26**, 393.

374. Liu, H., Slamovich, E.B., and Webster, T.J. (2006) *Int. J. Nanomed.*, **1**, 541.

375. Hong, Z., Zhang, P., Liu, A., Chen, L., Chen, X., and Jing, X. (2007) *J. Biomed. Mater. Res. Part A*, **81**, 515.

376. Cui, Y., Liu, Y., Cui, Y., Jing, X., Zhang, P., and Chen, X. (2009) *Acta Biomater.*, **5**, 2680.

12
Fully Biodegradable "Green" Composites

Rie Nakamura and Anil N. Netravali

12.1
Introduction

In the past few decades, high strength advanced composites that combine high strength fibers such as carbon, Kevlar®, and glass fibers and synthetic polymers such as epoxies have been widely used in many applications, particularly in replacing metals. Advanced composites based on petroleum have been critical in the production of aircraft parts, propeller blades for windmills, sporting goods, and automobiles because they provide excellent performance including lightweight, high specific mechanical properties, and chemical durability. One significant advantage of the composites is that they can be engineered for the desired performance by using the right combination of fibers and resins as well as the composite structure.

While these composites have excellent properties, it is difficult to separate fibers and resins once they are bonded together. As a result, they cannot be reused or recycled easily [1, 2]. This is particularly true for composites that use thermoset resins. Although recycling of composites is being studied, practical solutions that could be used on a commercial scale have yet to be found. In addition, most petroleum-based composites do not degrade in a normal environment for several decades [3, 4]. While a small fraction of the composites is crushed into fine powder and used as filler or incinerated to obtain energy, over 90% of the composites are landfilled. The number of landfills has decreased all over the world in the past decade making landfilling expensive [5]. In the United States alone, the number of landfills has dropped from 8000 to 2314 between 1988 and 1998 and it continues to decrease [5]. As composites do not degrade for several decades or even centuries under the anaerobic conditions that exist in landfills, the land is rendered useless for any other application. When disposed of improperly, these composites may cause land and water pollution. As the use of plastics is still rising, it continues to generate more waste as well. Chris Jordan, a creative artist has used various types of plastic wastes to create novel pictures and send messages all over the world in an effort to protect the earth [6, 7].

Polymer Composite: Volume 3, First Edition.
Edited by Sabu Thomas, Kuruvilla Joseph, S. K. Malhotra, Koichi Goda and M. S. Sreekala.

It is commonly understood that petroleum is not sustainable and at the current rate of consumption, it will last for the next 50–60 years only [8]. By some calculations, we are consuming petroleum at the rate of about 100 000 times the rate the earth can produce [8, 9]. Further, the rate of consumption has only gone up in the last decade as countries with large populations such as China and India have significantly improved their economies and living standards. Approximately 6–7% of the petroleum production today is used for making plastics, chemicals, fibers, and composites. While there is significant concern about the current situation, there are many efforts in the scientific world to tackle the situation and develop alternative materials that are fully sustainable and pollution-free. More and more of the next generation of advanced materials, products, and processes are expected to be based on the sustainable raw materials and environment-friendly green processes. Petroleum products produce CO_2 through product manufacturing as well as disposal processes, increasing the carbon footprint. One of the most pressing environmental problems at present is the global warming. The idea of making carbon-neutral products and processes is important to reduce the CO_2 level in the atmosphere. The Kyoto protocol adopted in 1997 has been signed by 187 countries. When followed, the Kyoto protocol expects a reduction in the rate of CO_2 for each country. Therefore, it is critical to adopt a holistic view in designing products for their entire life as well as their end-of-life disposal. In fact, the cradle-to-cradle design dictates that a product at the end of its life becomes raw material for the next product, fully eliminating the waste [10].

The only sustainable source for materials on earth is the plants, many of which grow every year. Plants have been cultivated in every corner of the world and relate to our life from ancient times. Natural plant fibers such as ramie, flax, hemp, sisal, jute, kenaf, bamboo, and regenerated fibers that are made from cotton linters and/or purified wood pulp such as viscose rayon or cellulose acetate have been studied for use as reinforcement of composites in place of synthetic fibers [11–13]. Fibers from plants are not only sustainable but are also carbon neutral and have lower cost than synthetic fibers. One way in which the effect of environment can be compared between natural materials and synthetic materials is by the life cycle assessment (LCA). Detailed information about LCA and its application can be found in Chapter XV of this book. Although it is stated that cellulose crystals within the plant-based fibers have high elastic modulus of about 138 GPa, this is not reflected in the fibers, and, as a result, plant-based fibers are generally not as strong as synthetic fibers [14]. This is due to the short and discontinuous nature of the crystals and the microfibrils, which are made up of cellulose molecules. Further, these crystals and microfibrils are not aligned with the fiber axis but make an angle. In addition, the noncrystalline material, that is, lignin and hemicelluloses, which are part of the fiber, are not strong. Table 12.1 presents mechanical properties of typical plant-based fibers [14]. One of the disadvantages of the plant-based fibers compared to synthetic fibers is their inherent and large variation in terms of their diameters and cross-sectional shape. Fiber diameters and their cross-sections, which, quite often, are not circular, are often difficult to characterize and/or quantify experimentally. This often results in a significant error in their

Table 12.1 Mechanical properties of typical plant-based fibers.

	Density (g cm^{-3})	Diameter (mm)	Young's modulus (GPa)	Tensile strength (MPa)	Tensile strain (%)
Bamboo	—	0.186	18.0–55.0	465	—
Cotton	1.5–1.6	—	5.5–12.6	287–597	3.0–10.0
Flax	1.4–1.5	—	27.6–80	345–1500	1.2–3.2
Hemp	1.48	—	70	550–900	1.6
Jute	1.3–1.46	0.01	10–30	393–800	1.5–1.8
Kenaf	—	0.078	24.6	448	
Ramie	1.5	0.034	44–128	220–938	2.0–3.8
Sisal	1.33–1.5	—	9.0–38.0	400–700	2.0–14

tensile strength and Young's modulus values [15, 16]. Terasaki *et al*. [17] have suggested a new method of evaluating correctly the fiber cross-sectional area. They investigated a distribution of natural fiber diameters through measurements made in several directions at the same position, which reduced the measurement error significantly. With significant research in the past few years, several biodegradable resins have been developed and used as resin to fabricate fully biodegradable green composites. Although their costs may be high at present, they are expected to go down in the future once they are mass produced. There are four commonly used resins including those based on plant proteins [18] and starches [19, 20] as well as polylactic acid (PLA) [21] and poly(hydroxyalkanoates) (PHAs) and their copolymers such as poly(hydroxy butyrate-*co*-valerate), (PHBV) [13, 22]. Of these, PLA and PHBV are thermoplastic, whereas protein and starch-based resins could be thermoplastic or thermosets depending on their modification and processing. PLA is obtained through fermentation of starch by lactic acid bacteria. PHBV is also a fermentation product and is obtained through microorganisms. The mechanical and physical properties of some of these resins are presented in Table 12.2.

A fully biodegradable composite consisting of both biodegradable fibers and soy-based resin was developed in 1999 [22]. Luo and Netravali called fully biodegradable and sustainable composites made from natural fibers and biodegradable resins, truly "*green*" composites. In recent years, green composites have been fabricated

Table 12.2 Mechanical properties of biodegradable resins.

	Young's modulus (GPa)	Tensile strength (MPa)	Fracture strain (%)	Melting point (°C)
Protein resin (SPI) [18]	0.099	6.0	206.0	—
Starch-based resin [20]	0.53	10.6	6.5	57
PLA [20]	3.76	28.4	2.0	58
PHBV [22]	1.1	25.0	10.0	—

and studied in many research groups all over the world [23–27]. However, applications of green composites using commercially available natural fibers have been limited because of their higher costs and lower properties. Many ideas have been tried to obtain better properties of the green composites. Firstly, several combinations of natural fibers and biodegradable resins have been tried to obtain higher performance of the composites [28]. Secondly, fiber orientation and fiber/resin interface are often manipulated to optimize composite stiffness and strength [20, 29]. Finally, various modifications of natural fibers and biodegradable resins have been studied to further improve their mechanical and interfacial properties [30, 31]. In addition, faster and inexpensive fabrication processes such as injection molding have also been used [32].

This chapter focuses on soy protein and starch-based green composites and discusses the effects of biodegradable resin modifications and fiber treatment on mechanical and chemical properties. In addition, biodegradation of green composites has been briefly described.

12.2 Soy Protein-Based Green Composites

12.2.1 Introduction

One of the least expensive green resins is based on soy protein. Soybeans are grown commercially all over the world, mainly to obtain oil. Soy protein, a by-product of the soy oil extraction process, is commercially available in three different compositions: defatted soy flour (SF), which contains about 53% protein and 32% carbohydrates (sugars); soy protein concentrate (SPC), which contains about 72% protein and 18% sugars; and soy protein isolate (SPI), which contains over 90% protein and almost no sugars [33]. Higher protein contents are obtained by removing the sugars by dissolving and filtering. Mechanical, physical, and thermal properties of soy proteins are shown to depend on the protein contents [34]. The mechanical properties of SPC and SPI resins are usually expected to be higher than those of SF. This is because of the plasticization of SF by the low molecular weight sugars in SF. Soy protein contains 18 different amino acids that have polar functional groups such as hydroxyl, amine, and carboxyl groups [34]. These functional groups have the potential to react or hydrogen bond to natural cellulose fibers, which contain plenty of hydroxyl groups. As a result, a high fiber/resin interfacial interaction can be expected.

Soy protein resins, however, have three major disadvantages. First, soy protein contains many polar amino acids, which indicate its highly hydrophilic nature that allows large amount of moisture to be absorbed. Second, soy protein resins show brittle behavior when they are in dry conditions. In other words, soy protein properties are water sensitive. Third, soy protein resin shows low tensile strength. These disadvantages have limited their applications. Plasticizers and cross-linkers

have been commonly used to overcome these disadvantages. In Section 12.2.2, interfacial properties between natural fiber and soy protein resin and various attempts to improve mechanical properties have been discussed.

12.2.2
Fiber/Soy Protein Interfacial Properties

Fiber/resin interfacial property plays an important role in determining the mechanical properties of composites. While composite mechanical properties are mainly a function of the fibers, some important properties including fracture stress, toughness, and so on, are controlled by the fiber/resin interfacial shear stress (IFSS). A strong fiber/resin bond makes the composites strong but brittle and a weak fiber/resin bond makes composites tough as it provides significant opportunity to absorb energy through interfacial cracks. It is commonly known that while fibers support load in fiber-reinforced composites, the resin transfers loads to the fibers through shear in the resin. If a fiber in the composite breaks when stress is applied, the resin transfers the load to intact fibers around the fracture location through the interface. In order to investigate fiber/resin interfacial property, several mechanical tests have been developed [35–37]. One of them, the microbond test, has been found to be most suitable test for soy-based resin [38]. In this technique, a resin microbead is formed around a single fiber, cured as the resin would be under normal conditions and then the fiber is pulled out from the microbead. The failure occurs at the interface as the microbead is sheared. A schematic of the microbond test is shown in Figure 12.1 [38].

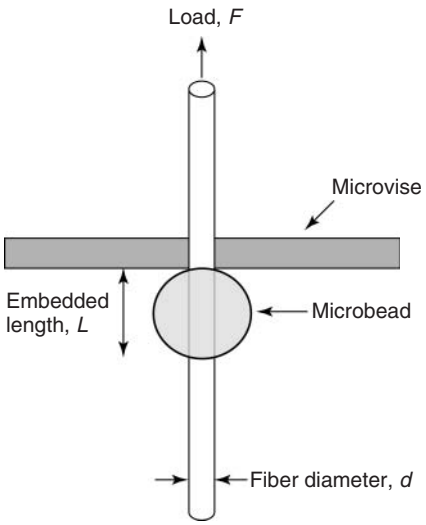

Figure 12.1 Schematic of the microbond test [38].

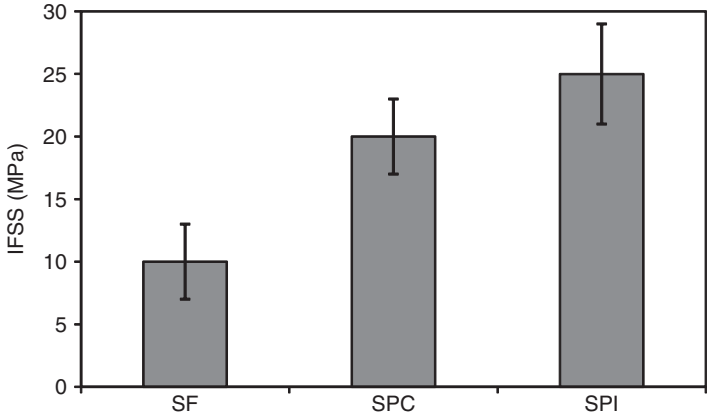

Figure 12.2 IFSS between ramie fiber and three types of soy protein resins [34].

The IFSS, τ, is calculated from these experimental results using a simple formula:

$$\text{IFSS}(\tau) = \frac{F}{\pi d L} \tag{12.1}$$

where F is the debonding force, d is the fiber diameter, and L is the embedment length [36]. The fiber diameter and embedment length are measured using an optical microscope. Figure 12.2 shows the comparison of IFSS values obtained for ramie single fiber with the three soy protein-based resins without any plasticizer. The IFSS values were found to be 9.5 MPa for SF resin (53% protein), 20.7 MPa for SPC (72% protein), and 25.7 MPa for SPI resin (90% protein) [34]. The IFSS tends to increase with the protein content. Sugars in SF and fiber can form strong hydrogen bonds as both contain hydroxyl groups. However, sugars being small molecules, this bonding does not help the overall fiber/resin bonding as the sugars prevent fiber/protein bonding. In addition, sugars tend to plasticize the soy resin, further reducing the IFSS.

Many researchers have studied the interfacial adhesion between natural fibers and thermoplastic resins to develop natural fiber-reinforced composites [22, 38, 39, 40]. Luo and Netravali [22] reported that the IFSS values for PHBV resin with pineapple and henequen fibers were 8.23 and 6.97 MPa, respectively. These are low compared to the SPC and SPI resins. In this case, the PHBV resin is nonpolar and the IFSS values obtained were attributed mainly to mechanical bonding. Plant-based natural fibers mainly consist of cellulose, hemicelluloses, and lignin, and a small fraction of pectin. While cellulose, hemicellulose, and pectin are carbohydrates, lignin is largely a complex hydrocarbon and hence nonpolar compared to the other three. As a result, lignin can increase bonding of fibers with nonpolar resins. On the other hand, soy proteins contain many polar amino acids such as glutamic acid, aspartic acid, lysine, arginine, serine, threonine, cysteine, proline, and others. These polar amino acids contain polar groups such as hydroxyl, amine, and carboxyl groups that allow strong chemical interactions, such as hydrogen bonding, with natural fibers.

As a result, higher interfacial adhesion between natural fibers and soy protein resins can be expected. Previous studies by Lodha and Netravali [40] and Nam and Netravali [38] found that interfacial strengths of multifibrillar ramie fibers with SPC and SPI resins having no plasticizer were 22.8 and 29.8 MPa, respectively by the microbond test. These values are about 10–15% higher than the results obtained by Kim and Netravali [34]. This is because multifibrillar fibers have a rougher surface than a single fiber. These results confirm that the surface roughness of the fiber increased the interfacial adhesion by increased mechanical interlocking as well as by increasing the interfacial area with the soy protein resins.

12.2.3
Effect of Soy Protein Modification on the Properties of Resins and Composites

12.2.3.1 Effect of Phytagel® Addition

Several modifications of soy protein have been tried to improve their mechanical, physical, and thermal properties. These modifications also have profound impact on the fiber/resin IFSS. SPI and Phytagel® were blended to form an interpenetrating networklike cross-linked complex [33]. Phytagel® is commonly used as a gelling agent for electrophoresis to determine the molecular weights and also in detection of microbial contamination. Phytagel® is produced by bacterial fermentation and is composed of glucuronic acid, rhamnose, and glucose. Glucuronic acid contains the carboxyl groups, which are the main reactive functional groups in Phytagel®. This compound has been known to form gels through ionic cross-links at its glucuronic acid sites, using the divalent cations naturally present in most plant tissue culture media [33]. In the absence of divalent cations, a higher concentration of Phytagel® is also known to form strong gels through hydrogen bonding. The carboxyl groups are also capable of reacting with the amine, hydroxyl, and carboxyl groups present in the SPI to form amide, ester, and anhydride linkages, respectively, provided right conditions are present. The hydroxyl groups and glucose molecules can also react with carboxyl groups in SPI, when mixed, to form ester bonds as well as interact with SPI via weak hydrogen bonds. In this section, modified SPI resins are characterized and compared to unmodified SPI.

Table 12.3 shows the effect of Phytagel® content on the tensile and moisture properties of SPI resin containing 30% glycerol [33]. As the Phytagel® content was increased from 0% to 40%, the Young's modulus increased from 98.7 to 388.7 MPa, tensile strength increased from 6.2 to 31.8 MPa and fracture strain decreased from 206.4% to 20.4%. From their chemistry, it is clear that the hydroxyl groups from rhamnose and glucose molecules and carboxyl group from the glucuronic acid can also hydrogen bond with the polar groups in the soy protein molecules, further increasing the intermolecular interactions between Phytagel® molecules and SPI chains. Owing to the formation of this cross-linking, Phytagel®-modified SPI resin having interpenetrating polymer network (IPN)-like structure was significantly stronger than the pure SPI resin [33].

The ATR-FTIR spectra of resins are presented in Figure 12.3. The spectra of pure Phytagel® powder and Phytagel® resin did not show any significant difference as

Table 12.3 Effect of Phytagel® content on the tensile and moisture properties of modified SPI resin containing 30% glycerol [33].

Phytagel® (%)	Young's modulus (MPa)	Fracture stress (MPa)	Fracture strain (%)	Moisture contents (%)
0	98.7 (10.3)	6.0 (0.4)	206.4 (30.6)	19.2
10	146.3 (10.1)	14.9 (0.5)	42.4 (3.2)	18.2
20	225.8 (31.8)	22.4 (1.5)	35.5 (6.1)	17.2
30	277.0 (15.1)	29.7 (2.6)	33.9 (5.5)	16.2
40	388.7 (23.9)	31.8 (2.3)	20.4 (2.9)	17.2
50	337.2 (26.5)	28.9 (2.6)	20.0 (2.2)	17.2

Numbers in parentheses are standard deviation.

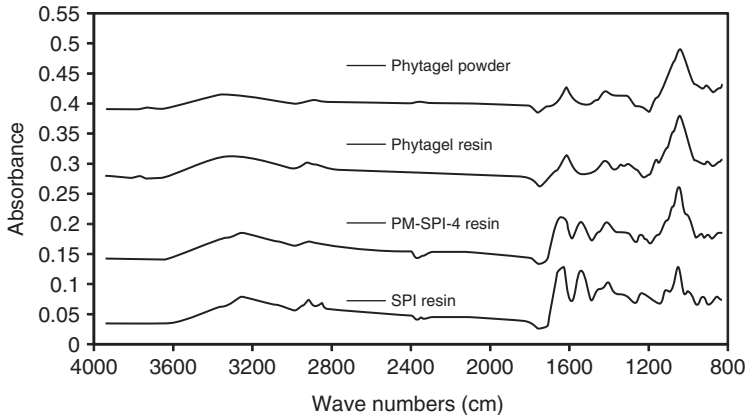

Figure 12.3 ATR-FTIR spectra of Phytagel®, SPI resin, and PM-SPI-4 resin [33].

can be expected. The ATR-FTIR spectra of PM-SPI-4 resin (SPI resin with 40% Phytagel® and 12.5% glycerol) showed absorption peaks for both SPI resin and Phytagel®. Since a large number of amide (peptide) linkages are also present in the SPI backbone, it was difficult to see if additional amide linkages were formed through the ATR-FTIR spectrum.

Tensile properties such as Young's modulus, fracture stress, and fracture strain of flax yarn/SPI with or without Phytagel® composites in the axial direction are presented in Table 12.4. The 20% Phytagel®-containing composite showed significantly higher Young's modulus and fracture stress values as compared to the 40% Phytagel® composite. This might be related with interfacial property because 20% Phytagel® composite showed shorter pullout length than 40% Phytagel® composite, indicating better fiber/resin interaction.

Table 12.4 Effect of Phytagel® on the tensile properties of flax yarn/SPI composites containing 12.5% glycerol [33].

Phytagel® (%)	Young's modulus (GPa)	Fracture stress (MPa)	Fracture strain (%)
0	2.41 (0.25)	197.2 (14.6)	11.2 (1.1)
20	4.11 (0.16)	220.2 (28.5)	7.5 (0.7)
40	3.10 (0.38)	174.0 (20.1)	8.8 (1.0)

Numbers in parentheses are standard deviation.

12.2.3.2 Effect of Stearic Acid Modification

As mentioned earlier, pure SPI resin is extremely brittle when it is dried, making it difficult to process into flat sheets or use as resin. The low fracture strain also makes it very weak. In order to solve this problem, there are two techniques [30, 41–43]. External plasticizers such as glycerol and sorbitol have been commonly used. However, an internal plasticizer such as stearic acid has also been found to be effective. Alkaline pH and heat treatment have been shown to denature the soy protein molecules and expose the functional groups trapped inside to improve the protein functionality [42, 43]. It is known that the stearic acid can react with the hydroxyl groups to form ester bonds and with the amine side and end groups to form amide linkages, resulting in internal plasticization of the SPI resin [42]. In the following paragraphs, the effect of stearic acid on the tensile properties of the SPI resin is discussed.

Table 12.5 shows the effect of stearic acid on the tensile properties and moisture content of the SPI resin containing 30% glycerol as plasticizer [42]. The Young's modulus of the resin increased when the stearic acid content was increased, while the tensile strength remained unchanged and the fracture strain reduced significantly. Stearic acid was shown to improve the Young's modulus of the SPI resin by three mechanisms. First, stearic acid being inherently hydrophobic in nature because of to its 18-carbon-atom long hydrocarbon chain, it is effective

Table 12.5 Effect of stearic acid content on the tensile properties of the modified SPI resin containing 30% glycerol [42].

Stearic acid (%)	Young's modulus (MPa)	Fracture stress (MPa)	Fracture strain (%)	Moisture content (%)
0	125 (8.1)	6.1 (0.5)	154.1 (18.9)	16.3
20	181 (12.1)	6.1 (0.5)	64.5 (18.1)	14.0
30	212 (21.9)	6.8 (0.6)	31.4 (17.5)	13.9
50	278 (27.5)	6.6 (0.5)	10.6 (3.6)	12.6
75	307 (14.0)	6.2 (1.0)	3.4 (0.8)	12.8

Numbers in parentheses are standard deviation.

in reducing the moisture absorption by SPI. Since water acts as a plasticizer, reduction in moisture absorption leads to improved Young's modulus [38]. Second, being hydrophobic, unreacted stearic acid can phase separate, at least partially, and crystallize into tiny crystals. This modified soy protein isolate (MSPI) system containing stearic acid crystals behaves similar to nanocomposites, increasing the tortuosity of the polymer chains and restricting the mobility of soy molecules when loaded, hence increasing its modulus [42, 43]. Third, the carboxylic acid group of stearic acid molecule can react with SPI protein chains at hydroxyl, imine, and amine side groups present in various amino acids [43]. Once grafted, the stearic acid can act as an internal plasticizer with no concerns of it leaching out. However, as it reacts with the protein molecule at different locations along the chain, it also increases the average molecular weight and enhances the possibility of further entanglement with neighboring protein molecules. This further leads to increased Young's modulus of the SPI resin. All three mechanisms combine to make the SPI resin stiffer.

The ATR-FTIR spectra of pure stearic acid, SPI, and MSPI resins are shown in Figure 12.4 [43]. Pure glycerol compound is known to show five absorption peaks in the fingerprint region from 800 to 1150 cm^{-1} wavenumbers as reported by the National Institute of Standards and Technology (NIST). In Figure 12.4, the ATR-FTIR spectrum of SPI resin containing 30% glycerol shows five peaks at 850, 900, 925, 1045, and 1117 cm^{-1} wavenumbers. This indicates that some glycerol is present in free form in the SPI. On the other hand, the spectrum of pure stearic acid shows a sharp absorption at 1700 cm^{-1} wavenumber for carbonyl. The spectrum of the MSPI resin, however, did not show absorption at 1700 cm^{-1}. This means that the surface of the MSPI resin did not have any stearic acid in its pure form. Under neutral pH conditions, stearic acid can be expected to react with the hydroxyl groups from serine, threonine, and tyrosine, and/or with amine groups from lysine and arginine, or imine groups from arginine, histidine, proline, and tryptophan to

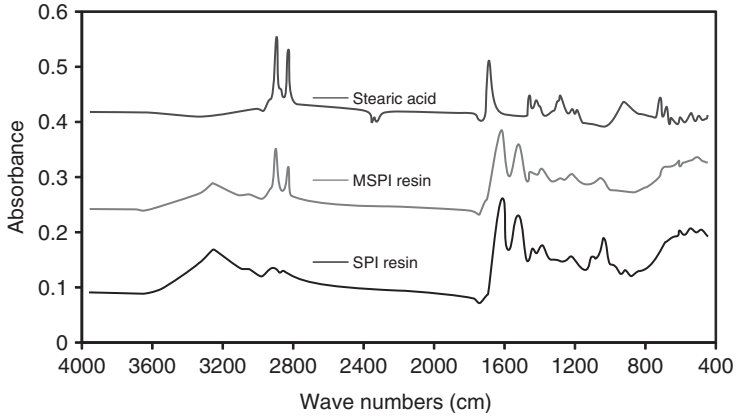

Figure 12.4 ATR-FTIR spectra of pure stearic acid, SPI, and modified SPI (MSPI) resins [43].

Table 12.6 Effect of stearic acid content on the tensile properties of the Ramie fiber/SPI resin composite [42].

Load direction	Stearic acid (%)	Young's modulus (MPa)	Fracture stress (MPa)	Fracture strain (%)
Longitudinal	0	3.42 (0.44)	180.2 (33.7)	9.02 (1.7)
	20	5.82 (0.51)	267.5 (66.5)	8.42 (1.6)
Transverse	0	0.25 (0.05)	6.6 (1.1)	8.7 (2.4)
	20	1.26 (0.26)	9.6 (2.2)	4.3 (1.5)

Numbers in parentheses are standard deviation.

form ester or amide linkages, respectively. The MSPI resin also shows a small peak at 1730 cm^{-1}, corresponding to the stretching vibration of ester linkages expected between 1725 and 1750 cm^{-1} [43]. However, the new amide linkages were not observed in the spectra because of the large number of amide linkages already present in the backbone of the soy protein molecule. Another point to note in the ATR-FTIR spectra presented is that pure stearic acid does not absorb any moisture (the broad peak at 3290 cm^{-1}). Similarly, the reduction in moisture content of the MSPI resin, compared to the SPI resin, is also seen in the spectra.

Tensile properties such as fracture stress and strain and Young's modulus of unidirectional ramie fiber/SPI and ramie fiber/MSPI composites tested in the longitudinal and transverse directions are presented in Table 12.6. As the data indicate, composites with stearic acid-modified resin showed significantly higher Young's modulus and fracture stress values as compared to the composites without stearic acid. These trends were similar to the results obtained for pure resins. In the case of composites, the fracture stress in the transverse direction also increased. Tensile properties of the unidirectional composites in the transverse direction are known to be a function of the resin and/or the interface properties. It is clear that interfacial property increased because tensile properties improve after stearic acid modification as indicated from data presented in Table 12.6.

12.3 Starch-Based Green Composites

12.3.1 Introduction

There are several steps that need to be followed in developing green composites using starch-based resins. First, fabrication methods and variables such as pressure and temperature need to be optimized because the material is quite new and unknown. The second step is to improve the composite properties through treatment and new techniques. Once the problems are clearly defined, it is easier to set up

mechanisms to improve the mechanical properties. Also, natural fibers have their own problems. For example, as discussed earlier, their diameters are irregular and cannot be determined accurately and slivers made using natural fibers also tend to be wavy or irregular. These variations result in lower mechanical properties. As mentioned earlier, once these problems are recognized, mechanisms can be set up to resolve them. Similar approach may be applied to starch-based nanocomposites as well.

In the following sections, various composite studies carried out using starch-based resins are discussed. First, the effect of alkali treatment of natural fibers on the mechanical properties of fibers and green composites is explained. Next, the potentials and problems of cellulose nanofiber composites are discussed. Finally, fiber orientation angle and mechanical properties are discussed and a way to predict the Young's modulus has been suggested.

12.3.2 Fiber Treatments

12.3.2.1 Studies on Fiber Treatment

Alkali (NaOH) treatment (mercerization) of natural cellulosic fibers is commonly used for surface modification and pretreatment for dyes in textile applications. It has also been adopted as one of the inexpensive chemical treatments to improve mechanical properties of cellulosic fibers. Bledzki *et al*. [44] reported that the Young's modulus of hemp fibers increased after alkali treatment although the fracture strain decreased. Gañan *et al*. [45], Kim and Netravali [29], and Ishikawa *et al*. [46] also found an increase in tensile strength of sisal and ramie fibers after treating them with alkali. On the other hand, Sao *et al*. [47] and Zhou *et al*. [48] observed a decrease in tensile strength of a ramie fiber. The studies obtained different results because of different treatment conditions used in their studies. Although several studies have been reported, such different results indicate that the effect of alkali treatment on mechanical properties of plant-based natural fibers has not been fully understood. The properties are dependent on many factors including the NaOH concentration, treatment time and temperature, as well as the applied stress. Treatments with and without applying weight (or stress) also provide different results. The fiber bundle, slightly stretched or kept under stress during the alkali treatment to minimize the shrinkage of the fibers, has shown to improve the fracture strength and Young's modulus and reduce fracture strain [49]. Most often, the improvement is dependent upon the stress.

In this section, first, the relationship between NaOH concentration and mechanical properties of plant fibers is discussed using X-ray analysis. Further, the effect of alkali treatment on the mechanical properties of ramie fiber-reinforced composites is explained.

12.3.2.2 Relationship between NaOH Concentration and Cellulose

It is known that the diffraction peaks for cellulose I (CI) occur at around 14.6°, 16.1°, and 22.5° and the diffraction peaks for cellulose II (CII) occur around

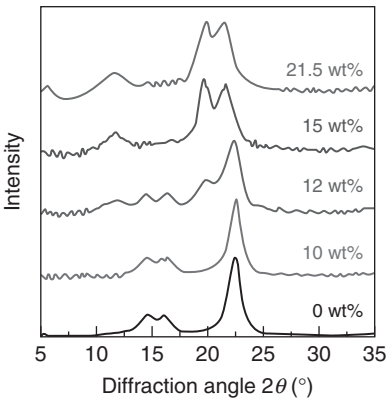

Figure 12.5 X-ray diffraction diagrams of NaOH-treated ramie fibers [53].

12.1°, 19.8°, and 21.8° inform the X-ray analysis for natural fiber [50–52]. Crystal structure is found easily as the differences between CI and CII are clear. CI is a crystal structure found in natural fibers, while CII is obtained from CI through high concentration alkali treatment. Figure 12.5 shows X-ray diffraction diagrams of NaOH-treated ramie fibers under different loads (wt%) [53]. As can be seen in Figure 12.5, diffraction diagrams for 0 wt% (no load) and 10 wt% load (10% of fracture load) show same peaks indicating no change in the CI structure. However, the diffraction diagram for 12 wt% load, shows peaks of both CI and CII, and the diffraction diagrams for 15 wt% load and 21.5 wt% load show only CII peaks. In other words, the crystal structure begins to change from CI to CII at around 12 wt% load and changes completely to CII at 15 wt% load.

In this study, the crystalline transition rate α_{tr} was additionally calculated from the obtained X-ray diffraction patterns using a peak method to be given as

$$\alpha_{tr} = \frac{I_{12.1}}{I_{12.1} + 0.5(I_{14.6} + I_{16.5})} \tag{12.2}$$

where $I_{12.1}$, $I_{14.6}$, and $I_{16.5}$ are diffraction intensities at 12.1°, 14.6°, and 16.5°, respectively. Figure 12.6 shows the relation between α_{tr} and NaOH concentration. It is observed that α_{tr} remained almost unchanged until about 10% NaOH concentration. However, it showed a steep increase at 12% and achieved the maximum at 21.5% NaOH concentration. This means that the crystalline transition of CI to CII starts at NaOH concentration from around 12%. Zhou *et al.* [48] also reported that the crystalline transition to CII started at 12% and was already completed before 16% NaOH concentration. It can be concluded from the X-ray diffraction diagrams in Figure 12.6 and crystalline transition rates that ramie fibers are locally mercerized at NaOH concentration of 12%, and almost completely mercerized at concentrations above 16%. Crystallinity indexes of untreated and alkali-treated ramie fibers were calculated through the integration method. Table 12.7 shows tensile properties of the ramie yarns used. Fracture load was normalized by dividing by the fineness (tex). The data clearly indicate that the tensile strength decreased and fracture strain increased with NaOH concentration. These results seem to relate with the crystallinity values. Composite properties directly depend

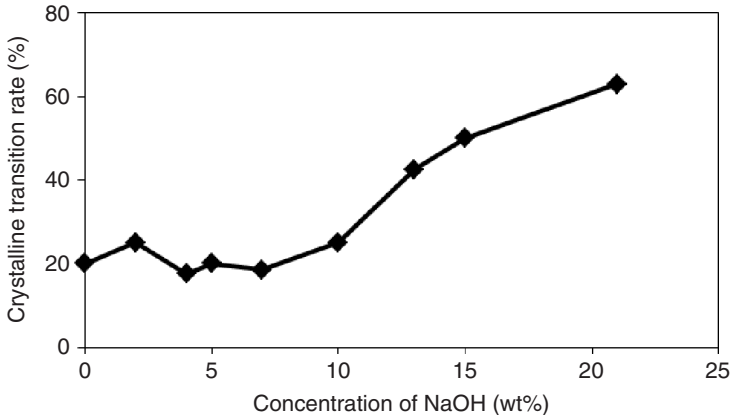

Figure 12.6 Relation between crystalline transition rate α_{tr} and NaOH concentration [53].

Table 12.7 Effect of alkali concentration on the tensile properties of ramie yarns [53].

Concentration of NaOH (%)	Tex (g km^{-1})	Fracture load (N)	Tensile strength (N tex^{-1})	Fracture strain (%)
0	533	192	0.361	4.46
5	527	152	0.288	5.54
10	568	187	0.329	8.91
12	667	187	0.280	17.6
21.5	830	182	0.219	29.9

on the reinforcement properties, yarn, in this case. As a result, the changes in yarn properties with the NaOH treatment discussed in this section should have significant effect on the composite properties. In the next section, effects of alkali treatment on composites are discussed.

12.3.2.3 Effect of NaOH Treatment of Ramie Yarns on the Tensile Properties of Starch-Based Green Composites

Haraguchi *et al.* [53] fabricated unidirectional composites using alkali-treated ramie yarns and CP-300, a modified cornstarch-based resin. Yarns were wound on a metal plate under slight tension and soaked into the resin to infiltrate it. The resin containing yarns were and dried to obtain prepregs. The composite fabrication was done by hot pressing the ramie yarn prepregs [53]. Table 12.8 shows that the effect of NaOH concentration (on ramie yarns) on the tensile properties of green composites. The data indicate that the Young's modulus and tensile strength remain unchanged up to 10 wt% concentration of NaOH. After that, both tensile strength and Young's modulus decreased, while the fracture strain increased. Generally, hemicelluloses and lignin are removed from fiber surface when treated

Table 12.8 Effect of NaOH concentration on the tensile properties of ramie fiber green composites [53].

Concentration of NaOH (%)	Volume fraction (%)	Tensile strength (MPa)	Fracture strain (%)	Young's modulus (GPa)
0	63	275	1.94	25.1
5	59	280	2.21	23.5
10	57	262	2.64	21.3
12	71	253	3.00	17.1
21.5	63	239	4.21	15.4

with NaOH. It may be possible that the yarn/resin interfacial interaction increases as a result of the NaOH treatment until the NaOH concentration reaches 10%. However, any higher concentration damages the yarn. This was also seen from the tensile data for the ramie yarn in Table 12.7. The fracture strain of the composites increased as a function of the NaOH concentration. One advantage of this might be improved impact property of the composites.

Suizu *et al.* [54] used alkali-treated and untreated ramie yarns as reinforcement to fabricate three types of composites: untreated unidirectional laminated composites ($0^\circ/90^\circ/0^\circ$), denoted as *UT composite*; alkali-treated unidirectional laminated composites ($0^\circ/90^\circ/0^\circ$), denoted as *AT composite*; and alkali-treated textile composites, denoted as *AT fabric composite*. The fabric was woven using alkali-treated ramie yarns. These composites were characterized for their impact properties using the drop-weight impact test according to ASTM D7136. Table 12.9 shows maximum loads and impact energies obtained for each type of composite [54]. Impact response for each composite was noted. As the data in Table 12.9 indicate, impact energy increased from 5.71 to 12.7 J after alkali treatment. In the case of AT composites, the projectile rebounded after hitting the composite because the alkali-treated composites provide ductility, that is, higher fracture strain as seen in Table 12.9. In the case where the projectile penetrated the composite, the impact energy was 12.7 J, that is, more than 100% improvement in composite toughness was observed when the ramie yarns were alkali treated, in the case of unidirectional

Table 12.9 Impact properties of laminated composites reinforced with UT and AT yarns.

	Thickness (mm)	Fiber volume fraction (%)	Maximum load (kN)	Impact response	Impact energy (J)
UT composite	2.24	42.7	0.699	Penetration	5.71
AT composite	2.33	55.9	1.90	Rebound	—
	2.21	57.1	1.95	Penetration	12.7
AT fabric composite	1.89	45	24.5	Penetration	13.9
GFRP	1.34	62	24.5	Penetration	9.04

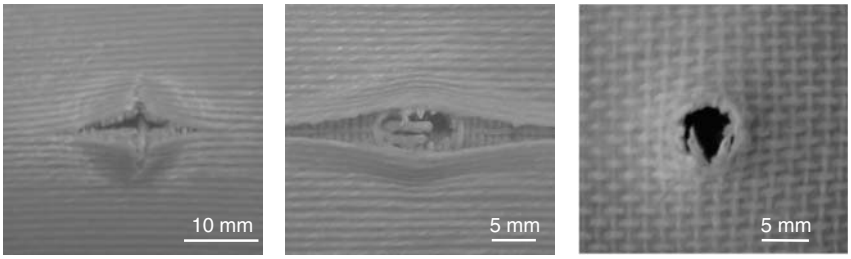

Figure 12.7 Typical surfaces showing damage incurred for (a) UT, (b) AT, and (c) AT fabric composites [54].

composites. Usually fabric composites show high impact energy because of their ductility, resulting from the yarn crimp. The AT fabric composites indicate similar impact energy and higher maximum load compared to AT composites. For comparison, glass fiber roving cross-mat-reinforced unsaturated polyester composites (GFRP, glass fiber-reinforced polyester) were fabricated by hand lay-up method. These composites were also impact tested in a similar fashion. As indicated in Table 12.9, the GFRP composites showed higher energy absorption (9 J) compared to that of UT composites but lower than that of both AT composites and AT fabric composites.

Typical UT, AT, and AT fabric composite specimen surfaces after the impact test are shown in Figure 12.7a–c, respectively. The UT composite shows damage with yarn breaks to the transverse direction as shown in Figure 12.7a, which means that the yarn cannot be deformed greatly. In contrast, the AT composite, shown in Figure 12.7b, is damaged with an interfacial crack or delamination of about 60 mm length between yarn layers without much breakage of the yarns. This signifies that the delamination absorbs significant impact energy along with the ramie yarns, which have become significantly tougher. The AT fabric composites, shown in Figure 12.7c, also exhibited higher impact property because of the plain woven structure as well as the mercerization effect. Because the fabric is woven, the interlacing of the yarns does not give them the flexibility to move. As a result, both warp and weft yarns were broken in these specimens. In conclusion, it is clear that mercerization significantly improves the fiber properties. These improvements result in significant improvements in toughness of the composites made using alkali-treated fibers and yarns.

12.3.3
Cellulose Nanofiber-Reinforced "Green" Composites

"Nanotechnology" and "nanomaterial" have become buzzwords in recent years. Although these words refer specifically to advanced technologies and materials, all cellulosic fibers obtained from plants provide nanostructural elements that are called *cellulose nanofibrils*. Natural fibers show significantly lower Young's modulus and tensile strength compared to high strength synthetic fibers because

natural fibers contain lignin and hemicellulose along with cellulose. The Young's modulus values of common natural fibers are commonly found between 2 and 60 GPa and their tensile strength is between 100 and 800 MPa. On the other hand, the Young's modulus of cellulose microfibril or nanofibril, which is the basic fibrous element of all plants, is 140 GPa and the tensile strength is over 1.7 GPa [55]. Therefore, cellulose microfibril-based composites have potential for having excellent mechanical properties. Takagi and Asano [56] have developed green nanocomposites using cellulose nanofibrils and cornstarch-based resin (CP-300). Uniform dispersion of the cellulose microfibrils in the resin was obtained by mechanical stirring. The flexural strength and flexural modulus of such green nanocomposites and pure resin were approximately 62 and 38 MPa and 5.6 and 2.8 GPa, respectively, showing significant improvement. The stirring was seen to keep the nanofibrils straight with less bowing, thus aiding the improvement in the properties. However, they found it difficult to characterize fiber orientation. If the fiber orientation can be manipulated, it could significantly improve the composite properties as it is directly related to mechanical properties.

12.3.4
Evaluation of Mechanical Properties of Green Composites

Fiber-reinforced green composites may be fabricated using fibers in the form of slivers. Slivers are readily produced by the carding machine in the textile industry. The slivers provide fibers in more or less unidirectional orientation. However, the morphology of slivers may be wavy and significant fluctuation in the fiber orientation may be observed. According to Gomes *et al*. [28], the stiffness and strength of composites can be improved by reducing the variation (fluctuation) in fiber orientation. Their study showed a relationship between such fluctuation and the composite mechanical properties. In this section, the effect of fiber orientation angle on the Young's modulus of green composites is reported. In addition, the Young's modulus has been analyzed on the basis of the classical lamination theory and theoretical and experimental results have been compared.

Green composites consisting of cornstarch-based resin (CP-300) and curaua fibers (sliver) were prepared for this study [28]. Two fabrication methods, a prepreg sheet method (PS) and a direct method (DM) were used to characterize the fiber orientation angle and investigate its effect. In the PS method, curaua fibers in sliver form were wound and stretched around a metal plate. The corn starch-based resin was then applied using a paintbrush and dried to make PSs. Finally, these PSs were put into molds to form composites. In the DM method, curaua sliver fibers were directly placed into the mold and the resin was poured directly in to the mold. Tensile test results of PS and DM composites are shown in Table 12.10. As can be seen, the Young's modulus and tensile strength of PS composites are higher than for DM composites. While the DM method is faster and more appropriate for mass production than the PS method, as there is no control on the fiber orientation in DM composites, large fluctuation in fiber orientation can be seen. It is widely known that fiber orientation angle strongly affects tensile properties

Table 12.10 Comparison of tensile properties of curaua fiber green composite fabricated using DM and PS methods [28].

Fabrication method	Young's modulus (MPa)	Fracture stress (MPa)	Fracture strain (%)
DM	13	216	1.53
PS	36	327	1.16

Volume fraction was about 69%.

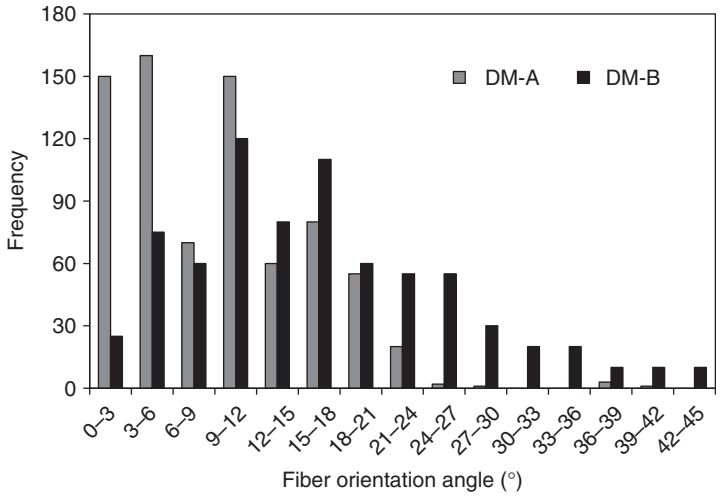

Figure 12.8 Histogram showing the distribution of the measured fiber orientation angles of DM-A and DM-B surfaces [57].

in unidirectional composites. Fibers oriented in the direction of the stress (0° angle) can contribute to the strength and Young's modulus, while others can only partially contribute, depending on the angle of orientation. The orientation angle in DM composites was measured for each segment on both sides (A and B) of the specimen by optical micrograph and were designated as A (DM-A) and B (DM-B). The segment size for optical measurements was set as 1 mm × 1 mm. The frequency of representative angle distributions is shown in Figure 12.8 in the form of a histogram. The angles were valid from 7.5° to 19.8° for side A and from 11° to 21.5° for side B. Specimen DM-A showed a smaller angle and DM-B showed a larger angle. This means that different orientations were obtained on each surface (bottom and top) because fibers were just placed in the mold directly.

Figure 12.9a,b show the contour maps of angle distributions for DM-A and DM-B surfaces. The values obtained from the optical measurements were used to generate the contour maps. It is clear from Figure 12.9a that lighter spectra (lower contrast) are seen for DM-A as it has a smaller angle than DM-B.

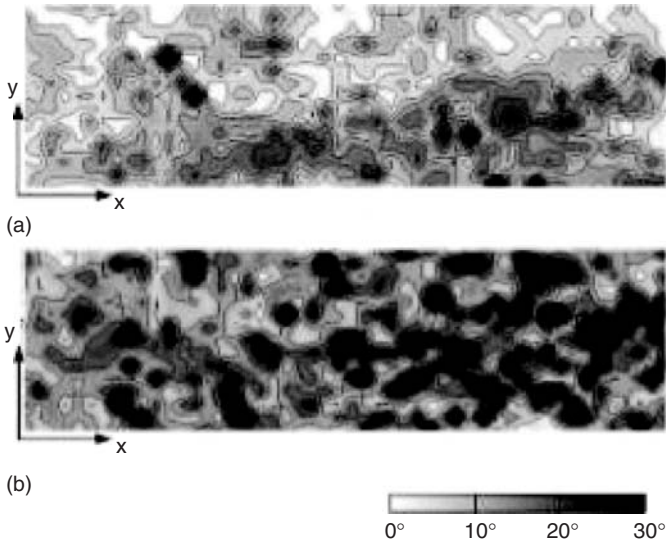

Figure 12.9 Contour maps of angle distributions for (a) DM-A and (b) DM-B surfaces [57].

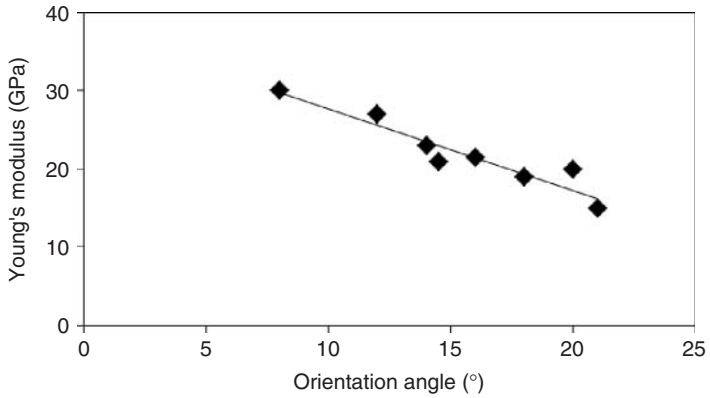

Figure 12.10 Dependence of Young's modulus on fiber orientation angle [57].

The Young's modulus and tensile strength of the DM composites were respectively 37% and 31% lower than those of the PS composites. As mentioned earlier, fiber orientation angles are closely related to the mechanical properties of the unidirectional composites; the lower the angle, the higher the Young's modulus, and fracture strength. Figure 12.10 shows the dependence of the Young's modulus on orientation angles [57]. As one can see, the Young's modulus decreases when orientation angles increase.

Estimation of the Young's modulus was proposed using laminate theory owing to its relation with the orientation angle. An orthotropic theory was applied, given as [58]

$$\frac{1}{E_\theta} = \frac{\cos^4\theta}{E_1} + \frac{\sin^4\theta}{E_2} + \left(\frac{1}{G_{12}} - \frac{2\nu_{12}}{E_1}\right)\cos^2\theta\sin^2\theta \tag{12.3}$$

where E_θ is the Young's modulus of an orthotropic body with angle θ, the Young's modulus of each segment varies depending on angle θ, of the distribution, which was measured for each specimen. $E_1 = 36.0\,\text{GPa}$, $E_2 = 3.57\,\text{GPa}$, $G_{12} = 1.78\,\text{GPa}$, $\nu_{12} = 0.40$ are used for calculation. E_1 is the Young's modulus in the longitudinal direction and E_2 is the Young's modulus in the transverse direction, G_{12} is the shear stiffness, and ν_{12} is the Poisson's ratio. As expected, the Young's modulus E might be defined as shown below.

$$\overline{E} = \int E_\theta f(\theta)\mathrm{d}\theta = \sum E_\theta f_i \tag{12.4}$$

where $f(\theta)$ is the fiber angle distribution function for each composites specimen and f_i is the relative frequency measured at every 3° angle interval.

Figure 12.11 presents a comparison between the theoretical values calculated from Eqs. (12.2) and (12.3) and the experimental values. Each plot shows the average of both the sides A and B. The solid line represents the value calculated from a simple orthotropic theory for comparison (Eq. (12.2)). Theoretical and experimental values show good agreement and similar trend. However, the value calculated using simple orthotropic theory for information provides consistently lower value. It can be concluded that the proposed statistical estimation method using Eq. (12.3) is useful for prediction of the Young's modulus of sliver-based green composites.

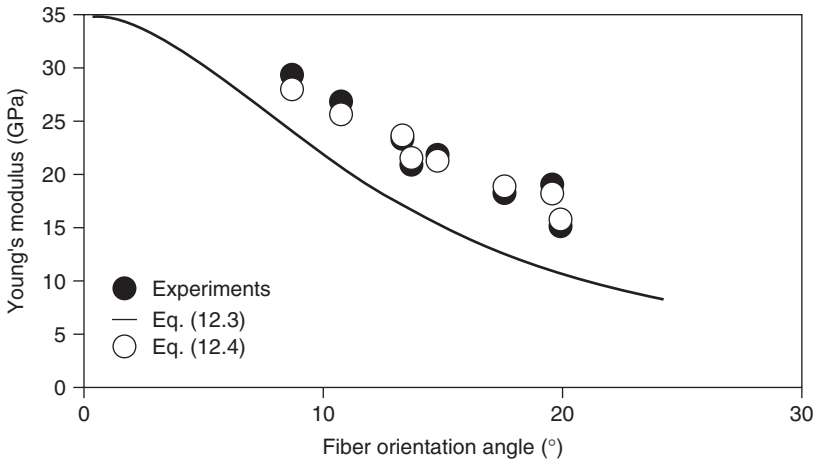

Figure 12.11 Comparison between theoretical and experimental Young's modulus values [57].

12.4
Biodegradation of "Green" Composites

The main concept behind green composites, besides their being sustainable and nonpetroleum-based materials, is that they are fully biodegradable and do not have any adverse effect on the environment. As many modifications to natural materials (starch, protein, etc.) are made, it is important to know how these modifications affect their biodegradation. In this section, degradation of PHBV, modified soy protein resin, and starch-based resin have been briefly discussed. Many techniques including weight loss measurement, mechanical property measurement, FTIR spectroscopy, scanning electron microscopy (SEM), and many others have been used for such characterization.

12.4.1
Biodegradation of PHBV

PHAs represent a family of biodegradable polymers synthesized by microorganisms [22, 39]. Poly(hydroxybutyrate) (PHB) and copolymers are the most prominent polymers in this group. The physical and mechanical properties of copolymers of PHB, including PHBV, are controlled by the fermentation conditions and the carbon source used. PHBV is commercially available and has physical and mechanical properties comparable to that of conventional thermoplastics such as polyethylene and polypropylene. The most exciting characteristic of PHAs is their ability to degrade. The degradation of PHAs depends on several factors including their chemical composition, physical state (i.e., granule suspension, solvent or melt-cast films, and single crystals), crystallinity and crystal size, temperature, and so on. As a result, the evaluation of degradation characteristics of PHAs is very complex.

Luo and Netravali [59] have reported the changes occurring in the mechanical, physical, and surface properties of PHBV films as a function of degradation under typical composting conditions. The composting medium was prepared by blending together chicken manure and wood chip dust 50 : 50 (w/w) with a C/N ratio of 50/50. In the laboratory-controlled experiment, the compost mix was placed in a 20 gallon plastic container and water was added, initially and periodically, to reach and maintain 50% moisture content during the composting. PHBV film specimens were completely dried in a vacuum oven and weighed using a Cahn 29 automatic electrobalance before being placed at the center of the composting medium. During the 50 days of composting, seven specimens were taken out for the analysis, every 10 days. Figure 12.12 shows the PHBV specimen weight as a function of composting time and provides direct evidence of PHBV film degradation during the composting. It can be seen in this figure that the PHBV specimens lost about 80% of their original weight after 50 days. The degradation at the end of 50 days was so severe that the PHBV specimens broke up into pieces.

Figure 12.13 presents the SEM images of the specimen before and after different composting times. It can be seen that the control specimen surface is smooth except

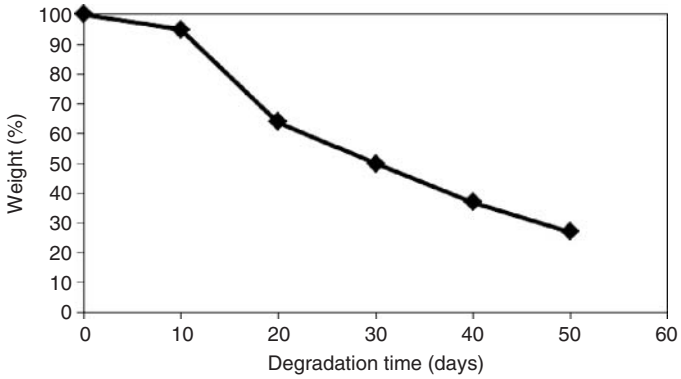

Figure 12.12 PHBV specimen weight as a function of composting time [59].

for a few scratches before composting. However, after composting, the surfaces of the specimens as shown Figure 12.13 became rougher as a result of the active microbial colonies present at different locations. Figure 12.14 illustrates the weight-average molecular weight of PHBV as a function of composting time. It is clear that the molecular weight of the bulk PHBV did not change during composting. This result indicates that the polymer chain cleavage occurred only at the specimen surface where the microbial colonies were active and, as a result, the polymer erosion (weight loss) occurred at the surface. Koyama and Doi [60] also found that the molecular weight of PHBV did not change during the enzymatic degradation by PHB depolymerases, while it decreased during the hydrolytic degradation at 55 °C in pH 7.4. On the basis of their observations, the composting of PHBV may be viewed as mostly enzymatic degradation.

Figure 12.15 shows typical FTIR-ATR spectra between 700 and 1500 cm^{-1} wavenumbers for quenched PHBV films annealed at room temperature for different periods of time. The shapes and intensities of some IR absorption bands are sensitive to the degree of crystallinity. In these spectra, the relative intensity of the absorption band at 1182 cm^{-1} displays the largest difference between the crystalline and amorphous states. The band decreases with increase in the degree of crystallinity.

Table 12.11 shows the relative surface crystallinity index (SCI) values obtained from these spectra. It can be seen that the SCI increased with the annealing time, indicating an increase in the crystallinity of the surface of PHBV films. The results of Koyama and Doi [60] indicated that the rate of enzymatic degradation for the PHB chains in the amorphous region was approximately 20 times higher than the rate for the chains in the crystalline region. After the initial 10-day period, the enzyme seemed to degrade and remove the polymer chains from both the crystalline and the amorphous regions.

Table 12.12 provides the tensile properties of control and composted PHBV specimens as a function of composting time. It can be seen from these data that tensile strength and fracture strain decreased significantly as a function of composting time. However, the Young's modulus did not show much change with

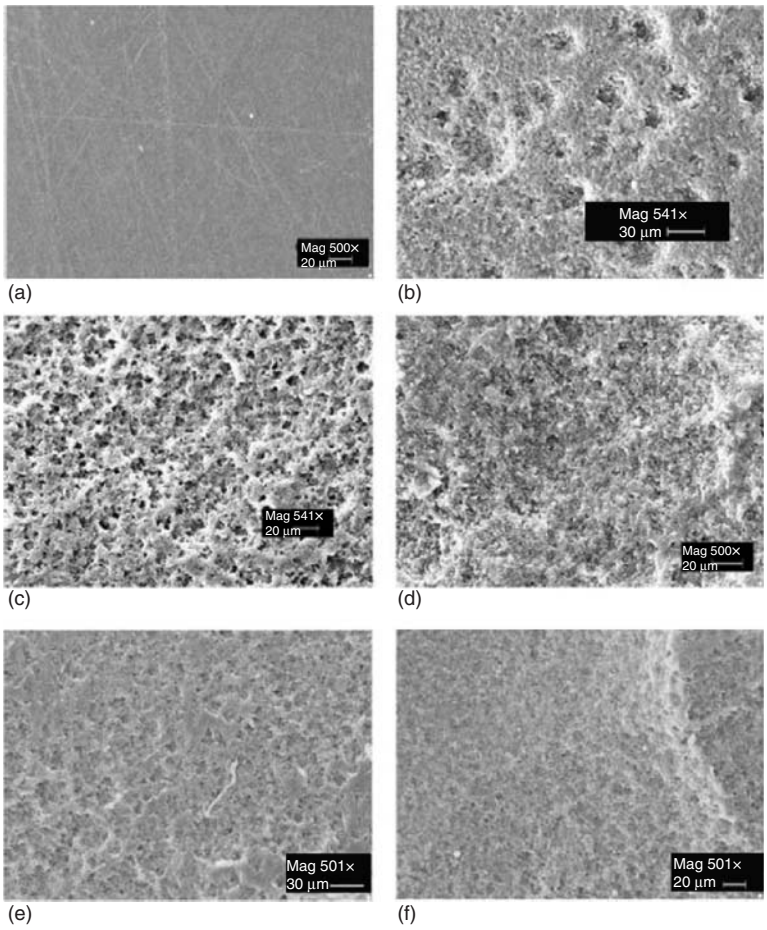

Figure 12.13 SEM images of PHBV surfaces after different composting times [59]. (a) 0, (b) 10, (c) 20, (d) 30, (e) 40, and (f) 50 days.

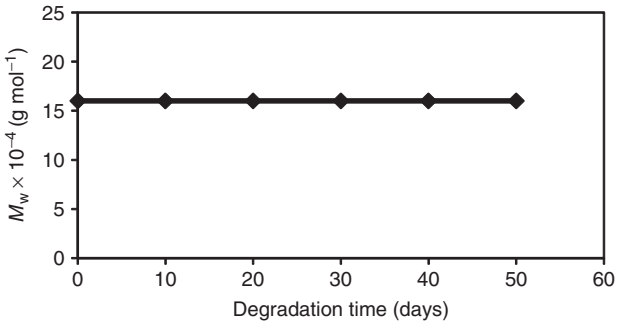

Figure 12.14 Weight-average molecular weight (M_w) of PHBV as a function of composting time [59].

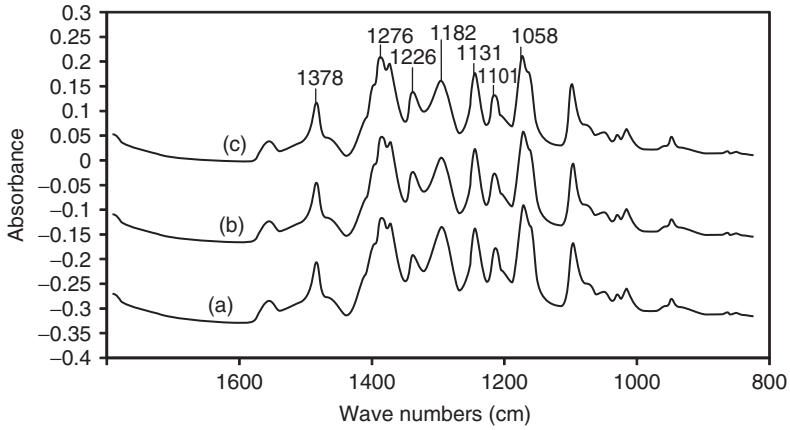

Figure 12.15 FTIR-ATR spectra of PHBV quenched for different periods of time (a) 0, (b) 9, and (c) 24 h [59].

Table 12.11 Effect of the annealing time on the SCI index of PHBV [59].

Annealing time (h)	0	9	24
SCI (%)	69	76	83

Table 12.12 Tensile properties of PHBV specimens composted for different periods of time [59].

Composting time (days)	Young's modulus (MPa)	Fracture stress (MPa)	Fracture strain (%)
0	1315 (5.9)	31.3 (0.5)	5.2 (4.3)
10	1272 (4.0)	28.3 (2.5)	4.4 (4.1)
20	1198 (6.6)	18.2 (21.5)	2.2 (25.0)
30	1260 (3.6)	16.8 (14.8)	1.9 (17.8)
40	1276 (6.7)	8.4 (7.7)	1.1 (38.2)
50	1242 (7.4)	0.9 (59.8)	1.0 (61.0)

Numbers in parentheses are coefficient of variation (%).

composting time. It is well understood that the modulus, an inherent property of the polymer, is a function of bulk morphology, while fracture strain and tensile strength are affected by the surface and/or internal defects in the specimen. As the film composted, the surface became rougher and thus more defects were created. This is the reason for the decrease in tensile strength and fracture strain. Since the degradation occurred at the specimen surface only and the bulk morphology did not change significantly, the modulus remained mostly unchanged.

12.4.2
Effect of Soy Protein Modification on Its Biodegradation

As a mentioned earlier, Phytagel and stearic acid modifications of SPI-based ''green'' resins improves their mechanical and chemical properties. This section presents the effect of Phytagel and stearic acid modifications of SPI-based ''green'' resins on their biodegradation in a composting environment [19]. The composting medium composition and preparation has been described in Section 12.4.1. The effect of composting time on the weight loss of the SPI, stearic acid-modified soy protein isolate (SAM-SPI) resin, and Phytagel-modified soy protein isolate (PM-SPI) resin is presented in Figure 12.16 [19]. After 37 days of composting, both SPI and SAM-SPI resins were broken to small pieces. The data indicated that the rate of weight loss for SAM-SPI resin was lower than for the SPI resin. The presence of stearic acid containing the long hydrocarbon chain reduced the moisture content of SPI resin from 19.2% to 9.2%. The reduction in moisture uptake affects the growing conditions for the microorganisms and reduces hydrolysis. This effect leads to a reduction in the rate of weight loss. The PM-SPI, however, showed the slowest rate of degradation among the three types of resins characterized. The higher cross-linking in the PM-SPI resin was supposed to be a major factor in reducing its rate of degradation.

The photographs of SPI, SAM-SPI, and PM-SPI resin specimens at various composting times are shown in Figure 12.17, Figure 12.18, and Figure 12.19. The change in the color of the specimens as well as their breaking up into small pieces is clearly visible for both SPI and SAM-SPI resins. However, PM-SPI resin did not break down into small pieces after composting. Even after 60 days, the PM-SPI resin sheet was still intact.

The effect of composting time on the SAM-SPI resin through the ATR-FTIR analysis is presented in Figure 12.20. The absorption peaks corresponding to $-CH_2$ of the stearic acid main chain, between 2800 and 3010 cm^{-1} wavenumbers,

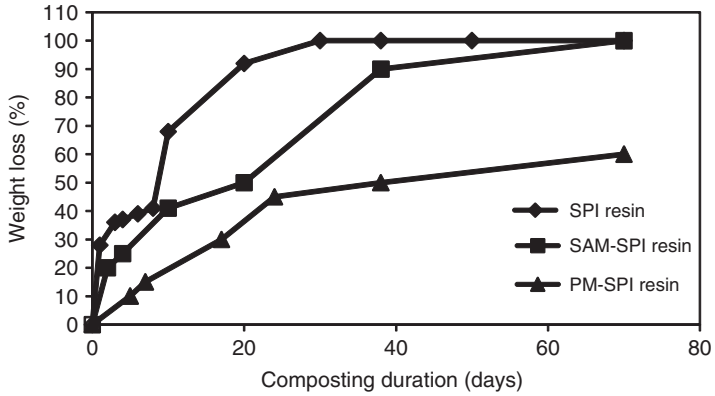

Figure 12.16 Effect of composting time on the weight loss of the SPI, SAM-SPI, and PM-SPI resins [19].

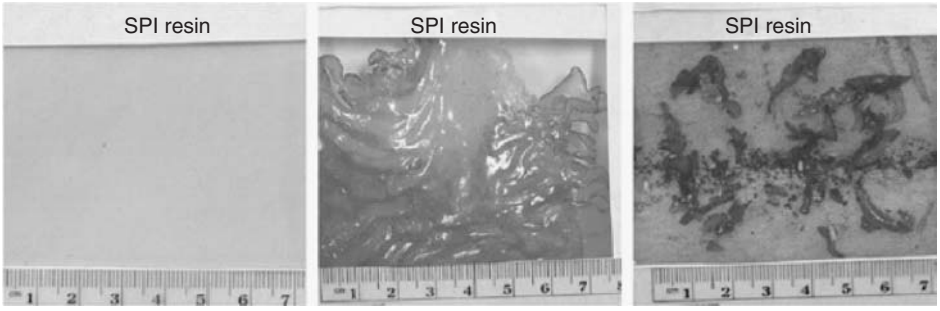

Figure 12.17 Photographs of SPI resin after different composting times [19]. (a) 0 days, (b) 5 days, and (c) 11 days.

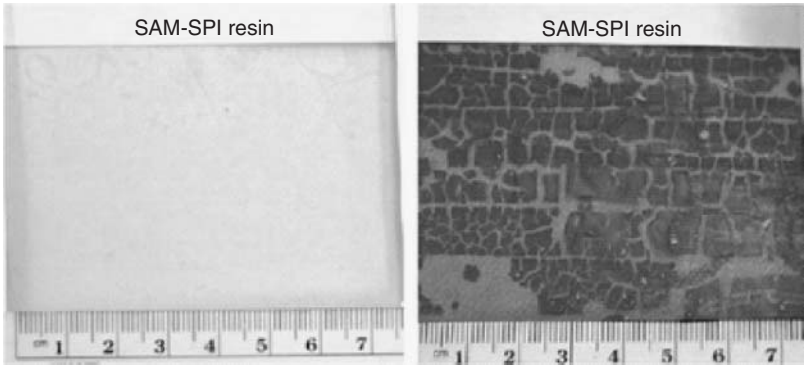

Figure 12.18 Photographs of SAM-SPI resin after different composting times [19]. (a) 0 days and (b) 11 days.

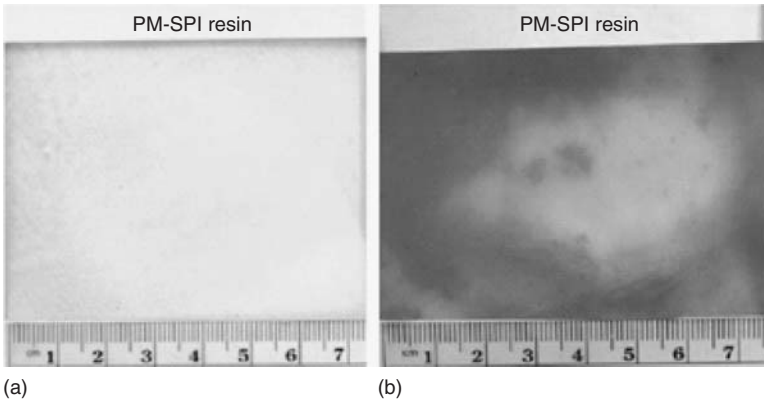

Figure 12.19 Photographs of PM-SPI resin after different composting times [19]. (a) 0 days and (b) 15 days.

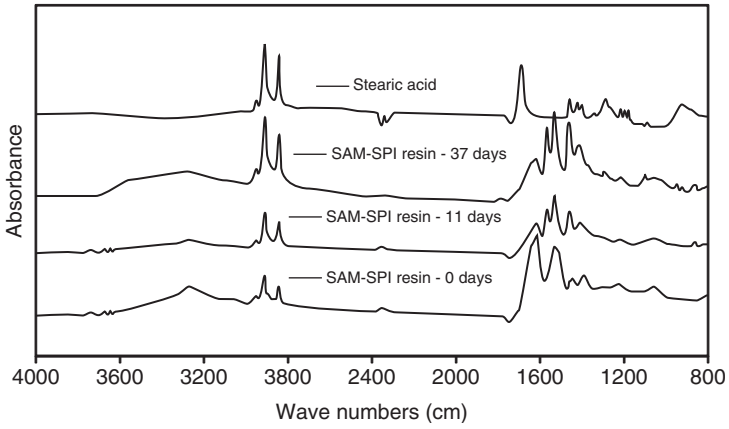

Figure 12.20 ATR-FTIR spectra showing the effect of composting time on the SAM-SPI resin and stearic acid [19].

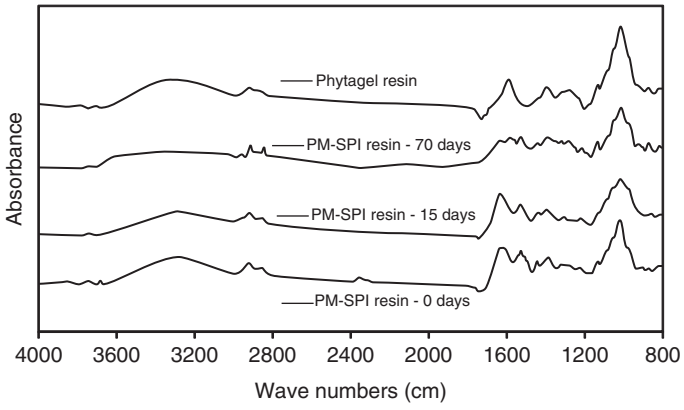

Figure 12.21 ATR-FTIR spectra showing the effect of composting time on the PM-SPI resin and pure Phytagel® [19].

increased steadily with the increase in composting time. Stearic acid is insoluble in water and is less degradable compared to SPI. For the same reason, stearic acid crystals are not affected by composting. This indicates that while SPI degraded in the composting medium, the stearic acid did not.

Figure 12.21 shows the ATR-FTIR spectra of PM-SPI resin composted for different times. Phytagel was responsible for four peaks between 1190 and 965 cm^{-1}. These four peaks were found to remain intact even after 70 days of composting. This indicates that the rhamnose component in the PM-SPI resin did not degrade in the compost mixture. However, the carbonyl peaks corresponding to the soy protein component in the PM-SPI resin reduced significantly in intensity as a function of composting time. This study also suggested that the service life of the SPI-based resin can be controlled by the addition of stearic acid and Phytagel.

12.4.3 Biodegradation of Starch-Based Green Composites

The research was characterized to examine biodegradation of green composites using manila hemp fiber and starch-based biodegradable resin by Ochi and Takagi [61]. A garbage disposal (Hitachi Ltd, BGD-150) system was used in this study and temperature was maintained between 35 and 40 °C during composting. Biodegradation was evaluated using change in weight, mechanical properties, and surface characterization, using SEM. In addition, the degree of degradation $D_d(\%)$ was calculated using the following equation:

$$D_d(\%) = \frac{m_{(0)} - m_{(t)}}{m_{(0)}} \times 100 \tag{12.5}$$

where $m_{(0)}$ and $m_{(t)}$ are the specimen mass before and after composting, respectively.

Figure 12.22 shows the relationship between tensile strength and composting time for green composites and manila hemp fibers. As seen from this figure, the tensile strength of the green composites decreased exponentially after 2 days and up to 15 days, after which the degradation rate slowed down. In the case of manila hemp fibers, the tensile strength of fiber drastically decreased after 2 days but the rate of strength reduction reduced after 5 days of composting.

After 20 days of composting, the manila hemp fibers broke into small pieces and it was difficult to carry out the tensile tests. In the case of the green composites, the tensile strength reduction rate was larger as the resin degraded first. In addition, the fiber/resin interface is also affected during composting. SEM images of manila hemp fiber fracture surfaces before and after composting are shown in Figure 12.23a,b. It can be clearly seen that the resin is still bonded to the fiber before composting, that is, for control specimens (Figure 12.23a). However, for specimens that were composted, there is no resin attached to the surface of the fiber. Also, many fiber pullouts were observed following a tensile test for composted

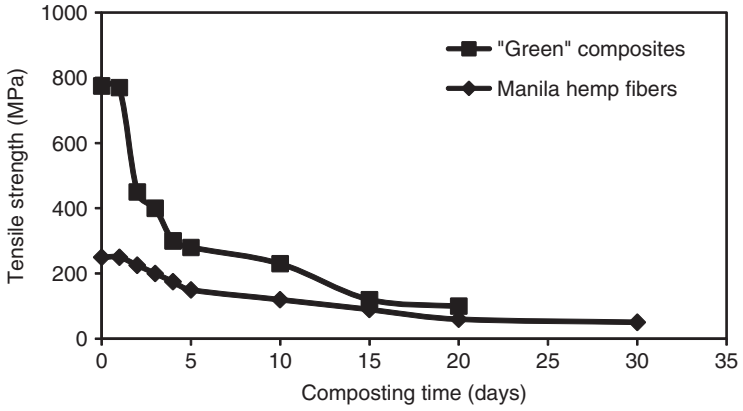

Figure 12.22 Relationship between tensile strength and composting time for manila hemp/starch green composites and manila hemp fibers [61].

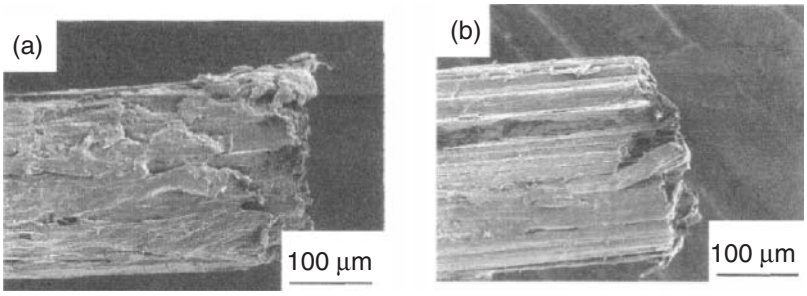

Figure 12.23 SEM images of fracture surfaces of manila hemp fibers in green composites; (a) before composting and (b) after composting [61].

specimens. This confirms that the fiber/resin bond deteriorated after composting. The main reason for this was that the manila hemp fibers absorbed water, resulting in swelling. It needs to be stated again that the composite properties are a function of not only the fiber properties but also the fiber/resin interface. Composite properties are a function of all these factors.

Figure 12.24a–d shows SEM surface images of green composites composted for 0, 5, 10, and 20 days, respectively. It can be seen in Figure 12.24a that the control (0 days) specimen surface is smooth. However, after composting resin erosion can be observed as the fibers get exposed. As a result, the specimen surface becomes

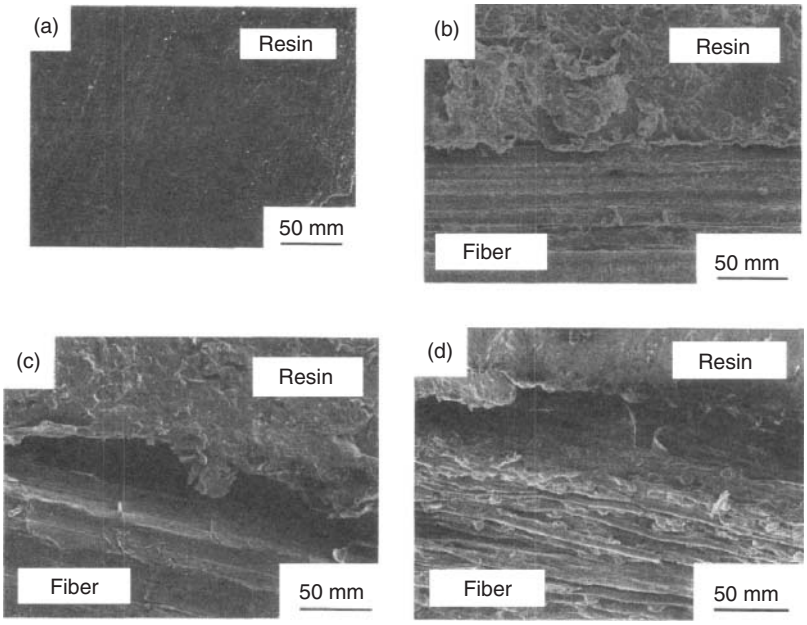

Figure 12.24 SEM images of green composites surfaces; (a) before composting, (b) after 5 days, (c) 10 days, and (d) 20 days of composting [61].

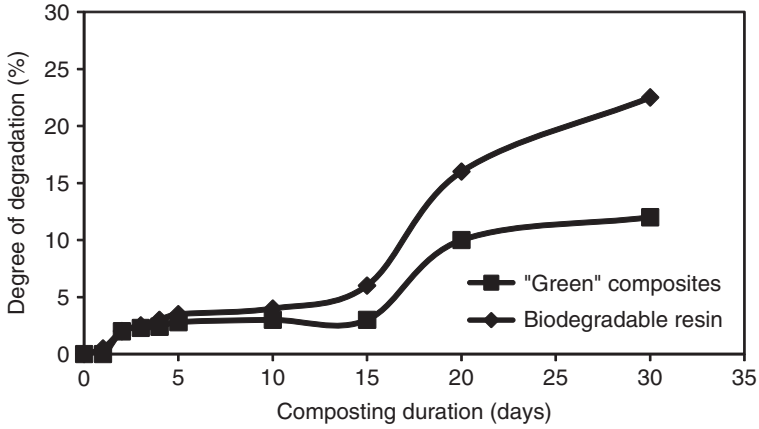

Figure 12.25 Degree of degradation (%) in after different composting times [61].

rougher. This roughness increases with the composting. In Figure 12.24c, after 10 days of composting, space can be observed between the resin and the fiber. With further increase in composting, splitting of the fibers is observed.

Figure 12.25 shows degree of degradations (D_d) as a function of composting time for both the resin and the composite. For up to 10 days of composting, both green composites and biodegradable resin degrade at approximately the same rate. After 10 days, the D_d of green composites increases dramatically because of the fiber/resin debonding.

From the results described earlier, the degradation process, in general, can be described to occur in three steps. In the first step, composite surfaces start biodegrading. In the second step, the fiber/resin interface fails as the fiber absorbs the water, and swells. Finally, the third step involves degradation of both fibers and the resin. The fiber and the resin may degrade at different rates depending on their chemistry and morphology.

References

1. Pickering, S.J. (2006) Recycling technologies for thermoset composite materials–current status. *Composites Part A*, **37** (8), 1206–1215.
2. Conroy, A. and Halliwell, S. (2006) Composite recycling in the construction industry. *Composites Part A*, **37** (8), 1216–1222.
3. Mohanty, A.K. and Misra, M. (2002) Sustainable bio-composites from renewable resources: opportunities and challenges in the green materials world. *J. Polym. Environ.*, **10** (1), 19–26.
4. Matsui, J. (2001) Aim at environment friendly composites, IV: how to judge the property of composite materials recycling. *Zairyo*, **50** (11), 1288–1293.
5. Stevens, E.S. (2002) *Green Plastics–An Introduction to the New Science of Biodegradable Plastics*, Princeton University Press, Princeton, NJ.
6. *http://www.chrisjordan.com/gallery/rtn/#unsinkable*.
7. *http://www.theglobalintelligencer.com/december07/chrisjordan.php*.

8. Stevens, E.S. (2002) *Green Plastics*, Princeton University Press, Princeton, NJ.
9. Johnson, H.R., Crawford, P.M., and Bunger, J.W. (2004) *Strategic Significance of America's Oil Shale Resource*, Assessment of Strategic Issues, Vol. I. Office of Naval Petroleum and Oil Shale Reserves U.S. Department of Energy, Washington, DC, *http://www.fossil.energy.gov/programs/reserves/npr/publications/npr_strategic_significancev1.pdf* (accessed 30 March 2013).
10. Wambua, P. and Ivens, J. (2003) Natural fibres: can they replace glass in fibre reinforced plastics? *Compos. Sci. Technol.*, **63** (9), 1259–1264.
11. Mohanty, A.K. and Wibowo, A. (2004) Effect of process engineering on the performance of natural fiber reinforced cellulose acetate biocomposites. *Composites Part A*, **35** (3), 363–370.
12. Fowler, P.A. and Hughes, J.M. (2006) Biocomposites: technology, environmental credentials and market forces. *J. Sci. Food Agric.*, **86** (12), 1781–1789.
13. Bledzki, A.K. and Jaszkiewicz, A. (2010) Mechanical performance of biocomposites based on PLA and PHBV reinforced with natural fibres–a comparative study to PP. *Compos. Sci. Technol.*, **70** (12), 1687–1696.
14. Li, X., Tabil, L., and Panigrahi, S. (2007) Chemical treatments of natural fiber for use in natural fiber-reinforced composites: a review. *J. Polym. Environ.*, **15** (1), 25–33.
15. Tanabe, K., Matsuo, T., Gomes, A., Goda, K., and Ohgi, J. (2008) Strength evaluation of curaua fibers with variation in cross-sectional area. *Zairyo*, **57** (5), 454–460.
16. Suzuki, K., Kimpara, I., Saito, H., and Funami, K. (2005) Cross-section area measurement and monofilament strength test of kenaf bast fibers. *Zairyo*, **54**, 887–894.
17. Terasaki, Y., Noda, J., and Goda, K. (2009) Strength evaluation of green composite with variation in cross-sectional area of plant-based natural fiber. *Adv. Mater. Res.*, **79** (82), 235–238.
18. Oksman, K. and Skrifvars, M. (2003) Natural fibres as reinforcement in polylactic acid (PLA) composites. *Compos. Sci. Technol.*, **63** (9), 1317–1324.
19. Lodha, P. and Netravali, A.N. (2005) Effect of soy protein isolate resin modifications on their biodegradation in a compost medium. *Polym. Degrad. Stab.*, **87** (3), 465–477.
20. Gomes, A., Goda, K., and Ohgi, J. (2004) Effects of alkali treatment to reinforcement on tensile properties of curaua fiber green composites. *JSME Int. J., Ser. A*, **47** (4), 541–546 Special Issue on Green Composites).
21. Nakamura, R., Goda, K., Noda, J., and Netravali, A.N. (2010) Elastic properties of green composites reinforced with ramie twisted yarn. *J. Solid Mech. Mater. Eng.*, **4**, 1605–1614.
22. Luo, S. and Netravali, A.N. (1999) Interfacial and mechanical properties of environment-friendly "green" composites made from pineapple fibers and poly(hydroxybutyrate-co-valerate) resin. *J. Mater. Sci.*, **34** (15), 3709–3719.
23. Zhang, M.Q., Lu, X., Rong, M.Z., Shi, G., Yang, G.C., and Zeng, H.M. (1999) Natural vegetable fibre/plasticised natural vegetable fibre–a candidate for low cost and fully biodegradable composite. *Adv. Compos. Lett.*, **8** (5), 231–236.
24. Netravali, A.N. and Chabba, S. (2003) Composites get greener. *Mater. Today*, **6** (4), 22–29.
25. Nishino, T. and Hirao, K. (2003) Kenaf reinforced biodegradable composite. *Compos. Sci. Technol.*, **63** (9), 1281–1286.
26. Okubo, K., Fujii, T., and Yamamoto, Y. (2004) Development of bamboo-based polymer composites and their mechanical properties. *Composites Part A*, **35**, 377–383.
27. Nakamura, R., Goda, K., Noda, J., and Ohgi, J. (2009) High temperature tensile properties and deep drawing of fully green composites. *Express Polym. Lett.*, **3**, 19–24.
28. Gomes, A., Matsuo, T., Goda, K., and Ohgi, J. (2007) Development and effect of alkali treatment on tensile properties of curaua fiber green composites. *Composites Part A*, **38** (8), 1811–1820.

29. Kim, J.T. and Netravali, A.N. (2010) Mercerization of sisal fibers: effect of tension on mechanical properties of sisal fiber and fiber-reinforced composites. *Composites Part A*, **41** (9), 1245–1252.
30. Kim, J.T. and Netravali, A.N. (2010) Mechanical, thermal, and interfacial properties of green composites with ramie fiber and soy resins. *J. Agric. Food Chem.*, **58** (9), 5400–5407.
31. Chabba, S., Matthews, G.F., and Netravali, A.N. (2005) 'Green' composites using cross-linked soy flour and flax yarns. *Green Chem.*, **7** (8), 576–581.
32. Mohanty, A.K., Tummala, P., Liu, W., Misra, M., Mulukutla, P.V., and Drzal, L.T. (2005) Injection molded biocomposites from soy protein based bioplastic and short industrial hemp fiber. *J. Polym. Environ.*, **13** (3), 279–285.
33. Lodha, P. and Netravali, A.N. (2005) Characterization of Phytagel® modified soy protein isolate resin and unidirectional flax yarn reinforced "green" composites. *Polym. Compos.*, **26** (5), 647–659.
34. Kim, J.T. and Netravali, A.N. (2010) Effect of protein content in soy protein resins on their interfacial shear strength with ramie fibers. *J. Adhes. Sci. Technol.*, **24**, 203–215.
35. Herrera Franco, P.J. and Drzal, L.T. (1992) Comparison of methods for the measurement of fibre/matrix adhesion in composites. *Composites*, **23** (1), 2–27.
36. Fu, S.Y. and Lauke, B. (2000) Comparison of the stress transfer in single- and multi-fiber composite pull-out tests. *J. Adhes. Sci. Technol.*, **14**, 437–452.
37. Netravali, A.N., Henstenburg, R.B., Phoenix, S.L., and Schwartz, P. (1989) Interfacial shear strength studies using the single-filament-composite test. I: experiments on graphite fibers in epoxy. *Polym. Compos.*, **10** (4), 226–241.
38. Nam, S. and Netravali, A.N. (2004) Characterization of ramie fiber/soy protein concentrate (SPC) resin interface. *J. Adhes. Sci. Technol.*, **18**, 1063–1076.
39. Luo, S. and Netravali, N.A. (2001) Characterization of henequen fibers and the henequen fiber/poly(hydroxybutyrate-co-hydroxyvalerate) interface. *J. Adhes. Sci. Technol.*, **15**, 423–437.
40. Lodha, P. and Netravali, A.N. (2002) Characterization of interfacial and mechanical properties of "green" composites with soy protein isolate and ramie fiber. *J Mater. Sci.*, **37** (17), 3657–3665.
41. Chabba, S. and Netravali, A. (2005) 'Green' composites Part 1: characterization of flax fabric and glutaraldehyde modified soy protein concentrate composites. *J. Mater. Sci.*, **40** (23), 6263–6273.
42. Lodha, P. and Netravali, A.N. (2005) Thermal and mechanical properties of environment-friendly 'green' plastics from stearic acid modified-soy protein isolate. *Ind. Crops Prod.*, **21** (1), 49–64.
43. Lodha, P. and Netravali, A.N. (2005) Characterization of stearic acid modified soy protein isolate resin and ramie fiber reinforced 'green' composites. *Compos. Sci. Technol.*, **65** (7-8), 1211–1225.
44. Bledzki, A.K., Fink, H.P., and Specht, K. (2004) Unidirectional hemp and flax EP- and PP-composites: influence of defined fiber treatments. *J. Appl. Polym. Sci.*, **93** (5), 2150–2156.
45. Gañan, P., Garbizu, S., Llano, P.R., and Mondragon, I. (2005) Surface modification of sisal fibers: effects on the mechanical and thermal properties of their epoxy composites. *Polym. Compos.*, **26** (2), 121–127.
46. Ishikawa, A., Okano, T., and Sugiyama, J. (1997) Fine structure and tensile properties of ramie fibres in the crystalline form of cellulose I, II, IIII and IVI. *Polymer*, **38** (2), 463–468.
47. Sao, K.P., Samantaray, B.K., and Bhattacherjee, S. (1994) X-ray study of crystallinity and disorder in ramie fiber. *J. Appl. Polym. Sci.*, **52** (12), 1687–1694.
48. Zhou, L.M., Yeung, K.W., Yuen, C.W.M., and Zhou, X. (2004) Characterization of ramie yarn treated with sodium hydroxide and crosslinked by 1,2,3,4-butanetetracarboxylic acid. *J. Appl. Polym. Sci.*, **91** (3), 1857–1864.
49. Goda, K., Sreekala, M.S., Gomes, A., Kaji, T., and Ohgi, J. (2006) Improvement of plant based natural fibers for

toughening green composites–effect of load application during mercerization of ramie fibers. *Composites Part A*, **37** (12), 2213–2220.

50. Mansikkamäki, P. and Lahtinen, M. (2007) The conversion from cellulose I to cellulose II in NaOH mercerization performed in alcohol-water systems: an X-ray powder diffraction study. *Carbohydr. Polym.*, **68** (1), 35–43.

51. Oh, S.Y. and Yoo, D.I. (2005) Crystalline structure analysis of cellulose treated with sodium hydroxide and carbon dioxide by means of X-ray diffraction and FTIR spectroscopy. *Carbohydr. Res.*, **340** (15), 2376–2391.

52. Sugiura, K., Jeong, D.S., Lee, M., Nakajima, T., Nishi, K., Tokuyama, T., Wakida, T., and Okada, S. (2007) Analysis of fine structure of subtropical plant fibers treated with sodium hydroxide or liquid ammonia by microscope observation and X-ray diffraction measurement. *J. Text. Eng.*, **53**, 95–100.

53. Haraguchi, K., Suizu, N., Uno, T., Goda, K., Noda, J., and Ohgi, J. (2009) Effect of alkali treatment on tensile and impact properties of ramie plied yarn-reinforced green composites. *J. Soc. Mater. Sci. Jpn.*, **58** (5), 374–381.

54. Suizu, N., Uno, T., Goda, K., and Ohgi, J. (2009) Tensile and impact properties of fully green composites reinforced with mercerized ramie fibers. *J. Mater. Sci.*, **44** (10), 2477–2482.

55. Goda, K. (2006) Environmentally friendly FRP using natural fibers. *J. Jpn. Reinf. Plast. Soc.*, **52** (4), 171–174.

56. Takagi, H. and Asano, A. (2008) Effects of processing conditions on flexural properties of cellulose nanofiber reinforced ''green'' composites. *Composites Part A*, **39** (4), 685–689.

57. Ren, B. and Noda, J. (2010) Effect of fiber orientation angle and fluctuation on the stiffness and strength of sliver-based green composites. *J. Soc. Mater. Sci. Jpn.*, **59** (7), 567–574.

58. Hull, D. (1981) *An Introduction to Composite Materials*, Cambridge University Press, Cambridge, pp. 89–91.

59. Luo, S. and Netravali, A.N. (2003) A study of physical and mechanical properties of poly(hydroxybutyrate-co-hydroxyvalerate) during composting. *Polym. Degrad. Stab.*, **80** (1), 59–66.

60. Koyama, N. and Doi, Y. (1997) Miscibility of binary blends of poly[(R)-3-hydroxybutyric acid] and poly[(S)-lactic acid]. *Polymer*, **38** (7), 1589–1593.

61. Ochi, S. and Takagi, H. (2004) Biodegradation behavior of unidirectional fiber reinforced ''green'' composites. *Zairyo*, **53** (4), 454–458.

13
Applications and Future Scope of "Green" Composites

Hyun-Joong Kim, Hyun-Ji Lee, Taek-Jun Chung, Hyeok-Jin Kwon, Donghwan Cho, and William Tai Yin Tze

13.1
Introduction

A line of "green" composites (also called *biocomposites*), defined here as *composites of biomass* and either *biodegradable* or *biobased polymers*, has been investigated for various applications. These application areas range from automotive parts, construction, and insulation materials to specialty textiles (nonwoven textiles) [1]. For construction applications, hurricane-resistant structural biocomposites have been developed, for instance, from lignocellulosic fibers and soy-oil-based resin. Other identified uses for these plant-oil-based fiber composites include bathtubs, archery bows, golf clubs, and boat hulls [2–4]. A summary of some biodegradable composite products investigated by various researchers is shown in Figure 13.1.

Although many "all-green" composites have been explored, only limited amounts of these have been commercialized to date. This is because a product designer should satisfy a variety of challenging requirements even though eco-friendly composites offer new alternatives. Nevertheless, with technical innovations, identification of new applications, persistent political and environmental pressures, and investments from governments [2, 3, 5], the market and commercialization of biocomposites are anticipated to expand in the future.

Among the biocomposite products developed, automotive and structural materials for indoor applications are gaining commercial importance. In Europe, where natural fiber composites are largely used for automotive applications [6], the sales of natural fibers for composites were 20 000 tons in the year of 2010, with a projected increase to 40 000-50 000 tons by 2015 [7]. Parallel to this scenario, the estimated global market of wood plastics and natural fiber composites is about 900 000 metric tons [8]. In view of their importance, application to automotive and structural materials is the focus of this chapter.

Polymer Composite: Volume 3, First Edition.
Edited by Sabu Thomas, Kuruvilla Joseph, S. K. Malhotra, Koichi Goda and M. S. Sreekala.

Figure 13.1 Current and potential applications of biocomposites with natural fibers [52].

13.1.1 Biodegradable Plastics versus Traditional Plastics

In recent years, biodegradable polymer materials have been one of the important solutions to problems related to waste disposal of conventional petroleum plastics. The total consumption of packaging plastics, for example, was 29% in 1996, making it the second in terms of sector importance behind paper and board [9]. Biodegradable polymers are designed to address the dwindling landfill availability and the growing environmental awareness of the public [10]. They are a category of polymers that degrade through microorganisms and yet can be replaced by traditional nonbiodegradable polymers when recycling is unpractical or not economical. Most biodegradable polymers are intended to be used in packaging industries, farming, automotive applications, and also in specialized biomedical applications.

Many research efforts in laboratories and companies have been invested on blending biodegradable polymers in order to substitute nonbiodegradable polymers.

Prices of biodegradables can be reduced only on mass-scale production, which, in turn, will be feasible through constant R&D efforts in performance improvement. In any case, the potential of biodegradable materials is significant, even if they only manage to capture a small segment of the commodity plastics market.

In fact, the main goal of PLA (polylactic acid) manufacturers is to reduce the selling price of PLA achieved by the stable and increased production capacity. Cargil Dow has aimed at suggesting a competitive price with commodity thermoplastics as soon as possible and is now trying to provide PLA with \$0.90–1.0 per pound by 2030. Another producer, Hycail, anticipated that PLA production of 200 000–300 000 tons per annum will open up the possibility of the price of PLA in the range of \$0.73–0.78 per pound being achievable soon [11].

13.2
Applications of Biocomposites (Products/Applications/Market)

13.2.1
Survey of Technical Applications of Natural Fiber Composites

Cellulose fibers in the form of papers and cotton had been used in combination with phenol–formaldehyde polymer as one of the earliest fiber–polymer composites [12]. Glass fibers later came on the scene and contributed to the commercialization of fiber-reinforced plastics [13]. The technical applications of fiber-reinforced plastic composites are shown in Figure 13.2. At least 50% of the fiber-reinforced plastics is used for automotive and construction applications.

More recently, there has been renewed interest in the use of natural fibers as reinforcing agents in the automotive and construction industries. Local renewable fibers such as flax and hemp are added to plastics used in European cars (e.g., car

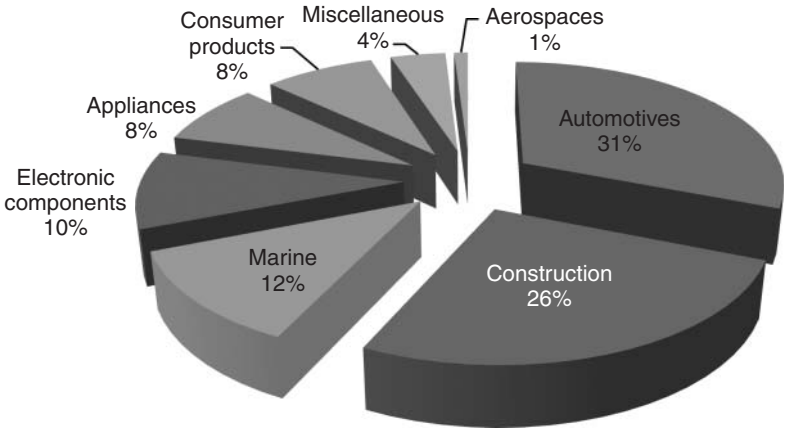

Figure 13.2 Fiber-reinforced plastic composites used in 2002 [13].

roofs). One such example is the K-car series of Mercedes, in which ''K'' represents ''kraut'' or ''compost.'' In construction applications, jute fibers, for example, are used to reinforce polyester polymers in buildings and grain elevators in India. A survey regarding possible applications of natural fibers in automobiles was published elsewhere [14].

13.2.1.1 The International Trend in Biocomposites

The use of biodegradable products has been growing rapidly due partly to government policies that instigate the utilization of biodegradable polymers for compostable packaging. The growing demand for biodegradable materials is reflected in the increasing trend of production capacities. The global production capacity of biodegradable plastics (including fossil-based) has grown from 174 000 metric tons in 2008 to 428 000 metric tons in 2010, and is projected to attain 1.7 million metric tons in 2015 [15].

Wood and nonwood natural fibers have been increasingly favored over glass fibers for reinforcing polymers. Research shows that the specific tensile strength and modulus of flax fiber/poly-L-(lactic) acid (PLLA) composites are quite comparable to those of structural glass fiber/polyester composites [16]. In addition, a variety of real-life complex profiles such as tubes, sandwich plates, and car door interior paneling can be fabricated from biocomposites [17]. An early achievement in ''greening'' automotive products is the replacement of glass fibers using coconut fibers in Mercedes Benz's components [18]. In a different example, flax fibers have been used to replace asbestos fibers in car disk brakes [18]. The increasing use of plant-based composites is reflected by the product market growth. The global market for wood- and nonwood natural fiber–plastic composites was $1.1 billion in 2004, $2.2 billion in 2010, and is projected to be $3.8 billion in 2016 [19].

Building and construction are the major markets for wood–plastic composites (WPCs), for which the largest producer is North America. Eighty percent of the total value of WPC in the North American market is for decking and railing, capturing an increasing market share of 24% in 2007 [20] compared to 2, 8, and 15% in 1997, 2000, and 2004. Although the commonly used matrix polymers (polyethylene, polypropylene, and polyvinyl chloride (PVC)) in WPC are currently nonbiobased and nonbiodegradable, its favorable market share suggests opportunities of incorporating durable but ultimately biodegradable polymers.

Nonwood natural fiber–plastic composites are mostly produced in Europe, and their primary applications are in the interior automotive body. The European Union End of Life Vehicles (ELV) Directive (2000/53/EC) specifies that by 2015 vehicles must be made of 95% recyclable materials – 85% recoverable through reuse or mechanical recycling and 10% recoverable through energy recovery or thermal recycling [21]. This policy will stimulate more uses of biocomposite materials. Indeed, the demand for natural fiber composites is reported to grow 17%/year in the European automotive sector, with a projected capacity of 800 000 metric tons by 2016 [22].

Table 13.1 Example of interior and exterior automotive parts produced from natural materials [54, 55].

Vehicle part	Material used
Interior	Wood/cotton fibers
Glove box	Molded, flax/sisal
Door panels	Flax/sisal with thermoset resin
Seat coverings	Leather/wool backing
Seat surface/backrest	Coconut fiber/natural
Trunk panel	Rubber
Trunk floor	Cotton fiber
Insulation	Cotton with PP/PET Fibers
Exterior	Cotton fiber
Floor panel	Flax mat with polypropylene

13.2.2 Automotive Applications

13.2.2.1 Materials

Natural fibers have been proved a viable reinforcement agent in many automotive parts. For example, flax, sisal, and hemp are applied in door cladding, seatback linings, and floor panels. Coconut fibers are used in seat bottoms, back cushions, and head restraints, while cotton fibers are used in vehicle parts that require effective sound proofing. In addition, wood fibers and acaba fibers are used in seatback cushions and floor body panels (Table 13.1).

The ratio at which petrochemical-based materials are replaced by biocomposites is increasing. Typical amounts of plant fibers used for different components in automobiles (except trucks and buses) are shown here [23]:

- Front door linens: 1.2–1.8 kg
- Rear door linens: 0.8–1.5 kg
- Boot linens: 1.5–2.5 kg
- Parcel shelves: up to 2.0 kg
- Seat backs: 1.6–2.0 kg
- Sunroof sliders: up to 0.4 kg
- Headliners: 2.5 kg in average

The light vehicle production in Western Europe accounted for 33% of the world's 59 million unit light vehicle production [24]. This market share represents about 19.4 million vehicles per year for potential applications of plant fibers. On the basis of the uses of plant fibers listed earlier (up to 12.7 kg/vehicle), the potential (European) automotive consumption of plant fibers would be up to 250 000 ton per year [24]. Statistics wise, the use of plant fibers did see an increasing trend. The fiber usage (in tons) for German automobiles, for example, rose from 9600

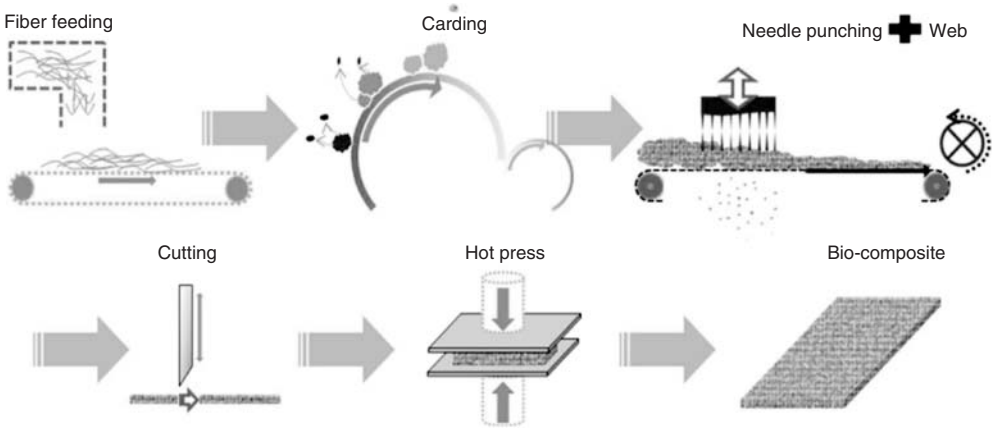

Figure 13.3 Carding process for manufacturing biocomposites [27].

(in 1999) to 17 200 (in 2002) to 19 000 (in 2005) [25]. In summary, plant fibers used as reinforcements are currently the fastest growing fillers for polymers to render the products more environmentally benign [26].

In terms of material processing, natural fibers used for biocomposites can be preformed into nonwoven mats through a carding process before incorporating polymer and compression molding. Carding is a mechanical process that breaks up fiber clumps and aligns fibers to be relatively parallel to one another. This process is usually followed by a needle punching step to entangle fibers in the direction across the thickness of the carded web. The carding process can also be used to comingle natural fibers and matrix polymer in the form of discontinuous fibers. The comingled blend of fibers will then undergo compression molding during which the polymer portion of the web is melted to bind the natural fibers. The overall carding process for manufacturing biocomposites is shown in Figure 13.3 [27].

13.2.2.2 **Requirements**

The automotive industry requires that materials and substrates used in car components must pass a wide range of performance tests, many of which are quite specialized and expensive. It is probably this reason that testing centers equipped with a full range of testing equipment are widely spread – some facilities are available at the OEM, some at Tier One, but few are owned by nonwoven producers. In the United Kingdom, independent laboratories capable of carrying out most of the required tests include MIRA at Nuneaton, LTC at Leyland, and Laboratory 2000 at Automotive Insulations at Rugby.

Recently, fabrication of environmentally friendly automotive headliners (interior ceiling) and package trays was reported [27]. The materials used were biocomposites made of kenaf, PLA, and so on. The headliners and package trays were subjected to the qualifying tests necessary for the respective applications using standard test methods of the Korea Institute of Industrial Technology.

13.2.2.3 Market and Products

On the basis of 50 000 tons/year of natural fibers (estimated from ref [28]) to be consumed for automotive parts by 2015, the corresponding annual market for natural fiber–plastic composites for automotive applications in Europe would be 125 000 tons (based on a mass fraction of 40% fibers in the composite).

There is a broad range of biocomposite parts in the production of automobiles. Honda used wood-fiber materials in the floor areas of its *Pilot* sport utility vehicle (SUV) [29]. General Motors uses a mixture of kenaf and flax in the package trays and door panel inserts for its Saturn L300s and European-market Opel *Vectras*. It also uses wood fibers in the seatbacks of its Cadillac *DeVille* and in the cargo area floor of its GMC *Envoy* and Chevrolet *TrailBlazer*. Ford incorporates wood fibers in the sliding door of its *Freestar*. Toyota blends kenaf into the package shelves of its *Lexus* and into the body structure of its *i-foot* and *i-unit* concept vehicle. Mack Trucks employ headliners comprising a mixture of hemp, flax, kenaf, and sisal (Figure 13.4).

Biobased polymers are also being used to produce automotive parts. For example, soy–resin body panels are used to replace steel doors in John Deere tractors (Figure 13.4). Tires infused with corn are produced by Goodyear and used in Ford *Fiestas* in Europe [29]. These tires are found to have a lower rolling resistance, which means a higher fuel mileage.

Apart from legislative requirements, using plant fibers for automobile components is justified from the engineering perspective. Bast fibers (e.g., kenaf and hemp) are mostly used in automotive applications because, being long compared to their width, the fibers induce greater mechanical performance than wood fibers. Recent research has also shown that biocomposites made of hemp and thermoplastics are promising candidates in automotive applications that require high specific stiffness [30]. The rationale for using natural fibers includes cost reduction and weight, thus saving fuel. Figure 13.5 shows automobile parts made from natural-fiber-reinforced composites.

Prototype automotive interior parts based on PLA and kenaf were recently reported. An interior headliner prototype is shown in Figure 13.6.

(a) (b)

Figure 13.4 On its (a) HarvesterWorks combines, John Deere has replaced steel gull-wing doors with (b) soy–resin body panels [29].

(a)

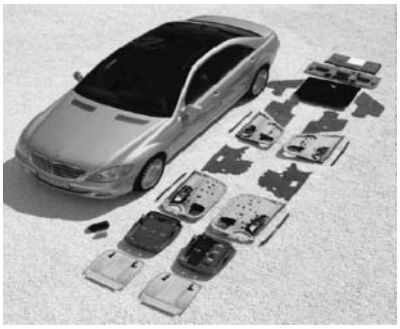

(b)

Figure 13.5 (a) Under floor protection trim of Mercedes A class made from banana-fiber-reinforced composites. (b) Newest Mercedes S class automotive components made from different biofiber-reinforced composites [53].

(a)

(b)

Figure 13.6 Prototypical automotive headliner made from a 50/50 PLA/kenaf fiber biocomposite: (a) back side and (b) front side [27].

13.2.3 Structural Applications

Currently, polymeric composites based on WPCs have been used in various building components, for instance, decks, flooring, docks, window frames, and molded panel products [31]. Many recent research efforts have been made to explore the use of fully biobased composite materials in order to alleviate stress

to the environment. Therefore, applications of these structural biocomposites are discussed in this section.

13.2.3.1 Materials for Structural Applications of Green Composites

Plant-based fibers have been employed to add biobased contents and reinforce traditional building materials. In Australia, wood pulp fibers are used to substitute asbestos in fiber cement products [32]. These fibers, being cheap and readily available, afford a relatively low processing energy. Pulp from residues of eucalyptus wood, sisal, and coir fibers has also been used to replace asbestos in roofing components [33]. In a less processed form, agrofibers such as chopped barley straw are added as a reinforcement agent in making composite soil [34].

To produce green composites, plant-based fibers in various forms are blended with biobased or biodegradable polymers to examine potentials in construction applications. Paper sheets from recycled car boxes are blended with soy-oil-based resin to fabricate roof structures using a vacuum-assisted resin transfer molding process [35]. The one-third-scale structure showed the satisfactory strength and stiffness required for roof structure. Mats of flax fibers were also used to fabricate sandwich structures by infusion with PLLA biopolymer in the presence of balsa wood core using a high-temperature vacuum-bagging process [36]. The resulted structures exhibited promising mechanical properties, although they are slightly inferior to the sandwich made of glass-fiber/polyester skin and balsa core. Another hybrid assembly comprised hemp fiber-unsaturated polyester composites in the core, and jute fiber mats on top and bottom (as flanges) were also produced for load-bearing cellular plates [37]. The test data for this product are detailed in a subsequent section.

13.2.3.2 Requirements

13.2.3.2.1 Mechanical Performance

The mechanical performance required of biocomposites is dependent on specific structural applications. Crude inferences can be made by comparing properties of materials that these biocomposites are intended to substitute. Mechanical data and/or allowable design values of wood and engineered wood products were used to evaluate potential applications of hemp fabric/cellulose acetate composites and hemp fabric/poly(hydroxybutyrate) composites (Table 13.2). From the comparisons, it can be inferred that these biocomposites, despite not passing the design values of wood structural material, can potentially substitute engineered wood products (of the same size) such as plywood and oriented strand boards to partially capture existing markets as crates, pallets, and formwork [38].

The disadvantageous low stiffness of biocomposites could be remedied by manipulating their structural shape. This manipulation is possible because (i) biocomposites are moldable and (ii) the actual deformation of a structure is dependent on the moment of inertia in addition to modulus of elasticity. Manipulation of shapes and profiles is also important from the perspective of reducing product

Table 13.2 Comparisons of biocomposites with wood-based construction materials [38].

	Flexural modulus of rupture (MPa)	Flexural modulus of elasticity (GPa)	Shear strength (MPa)	Density (g/cm^3)
Clear wood properties	35	6.9	4.8	0.45
Allowable properties for wood	0.7–16	5.9–7.3	2.3	—
Plywood (B-B Class 1)	27	10.3	1	0.40–0.81
Oriented strand board	21	5.3	1.2	0.49–0.81
Glulam	26–72	10.6	—	0.32–0.72
Hemp/cellulose acetate composites	95	6.6	12	1.30–1.37
Hemp/poly(hydroxybutyrate) composites	65	5.1	9.9	1.27–1.30

Note: Ponderosa pine is used as sample wood; allowable properties are after taking into account strength ratio, quality factors, and adjustment factors in accordance with ASTM D245.

Table 13.3 Dimensions of bioplate for structural applications.

System	Allowable defection limit	Section dimensions needed to be within deflection limit	
		Biocomposites	Typical
Highway bridge deck	$\Delta_{allow} = l/300$	$d = 305$ mm $t_{flange} = 13$ mm	$d = 180$–230 mm
Commercial building slab	$\Delta_{allow} = l/360$	$d = 229$ mm $t_{flange} = 13$ mm	$d = 152$ mm (concrete slab)
Residential floor	$\Delta_{allow} = l/360$	$d = 51$ mm $t_{flange} = 6$ mm	$d = 25.4$–76.2 mm

Note: "l" stands for length, "d" for section depth, "t_{flange}" for thickness of the top or bottom flange.

weight as the biocomposites (Table 13.4) are much denser than wood products. One approach, proved successful in commercial WPCs, is fabricating hollow profiles.

When strength is not a limiting factor, stiffness requirements could be met by adjusting the dimensions or shape of biocomposites. Table 13.3 shows adjusted section depth of a biobased cellular plate discussed earlier (core: hemp-fiber-reinforced unsaturated polyester; flange: jute fiber mats; [37]). On the basis of adjusted dimensions, it was concluded that the depth required of the bioplate would be too thick for practical applications such as highway bridge decks and commercial building slabs. The bioplate, however, is a potential for residential flooring systems.

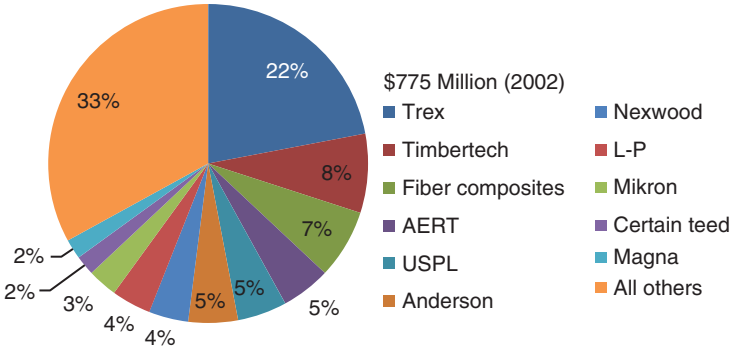

Figure 13.7 Top 10 suppliers of wood and agro-fiber composites in North America and Europe, 2002 [28].

13.2.3.2.2 Flame Retardancy

Apart from satisfactory mechanical properties, additional features are often required in product applications. One important requirement for construction applications is flame retardancy. Biocomposites are, however, flammable because they are composed of organic materials. To improve flame retardancy, addition of inorganic materials would be needed. Various flame retardants composing of halogens (Cl, Br), heavy and transition metals (Zn, V, Pb, Sb), or phosphorus organic compounds may reduce the risk of combustion [39].

13.2.3.2.3 Markets and Products

In North America and Europe, the top 10 suppliers of wood and agro-fiber polymer composites accounted for about 70% of the total industry sales (Figure 13.7). About 15 companies are in Europe and more than 60 companies are in North America. It indicates that the demand for using plant fibers to produce biocomposites is higher in North America than Europe.

The major use of WPCs is in building and construction. The largest application of WPC in the North American market in terms of product value is decking and railing (over 80%), followed by windows and door parts (~12%). For Asia, pallets constitute the majority of the total Chinese WPC market. While WPC in the North American market is favored over wood materials for its durability, it has been reported that Japanese and Korean WPC markets value its wood-like appearance compared to nonwood materials [40]. It follows that value adding of WPC in the latter region is focused on surface treatments such as embossing to produce patterns resembling solid wood appearance.

WPCs have increasingly replaced solid wood as clads. Solid wood such as clear ponderosa pine for cladding is limited in supply and high priced. In addition, fabrication of claddings using solid wood for windows and doors requires edge gluing, board cutting, and finger jointing to obtain clear surfaces. Therefore, manufacturers use wood fiber plastic composites as an alternative to solid wood in

Table 13.4 Selected commercial WPC products in the US market [28].

Company	Plastic type	Plastic source	Wood source
Trex	PE mix	Recycled	Pallets and furniture waste
Fiber composites	HDPE, LDPE, PVC	Recycled and virgin	Oak and pine from millwork
AERT	PE	Recycled and virgin	Reclaimed cedar wood chips, oak from millwork
USPL	HDPE	Recycled	Wood and natural fiber
Anderson	PVC	Recycled and virgin	Waste from pine wood
Nexwood	HDPE	Recycled	Rice hull flour
LP Specialty Products	PE	Recycled	Sawmill wastes
Mikron	HDPE, LDPE	Virgin	Hardwood and softwood flour

clad components in order to reduce cost and wastes. Andersen Windows Company, for example, adopts WPC in its products [41].

There are a variety of WPC products in the market. These commercial products could originate from virgin or recycled polymers and virgin or reclaimed wood. For instance, Andersen Windows Company utilizes waste PVC from their manufacturing plant in producing WPC window components. Certain Teed Company uses recycled fibers in their Boardwalk plastic composites. Some examples of WPC products and their major components are listed in Table 13.4, with a focus on the United States, which has the biggest WPC market for building applications.

Finally, it is worthwhile recognizing that the commonly used matrix polymers (polyethylene, polypropylene, and polyvinyl chloride) in WPC are currently nonbiobased and nonbiodegradable in nature. The positive aspect of this scenario, however, is the opportunity of incorporating durable but ultimately biodegradable polymers into the composites, which are increasing in market share.

13.3 Future Scope

So far, we have taken a look at applications to automotive and construction sectors, which are the main markets for biocomposites. Although green composites are gaining in interest these days, the challenge still remains in replacing conventional plastics with those that exhibit comparable structural and functional stability during storage, use, and environmental degradation on disposal. Therefore, with further developments and improvements in performance, new opportunities and applications will likely arise. For example, biocomposites designed for a structural purpose should meet regulations regarding the management of huge volumes of waste. Also, new generations of composites are expected to be used in a wide range

of applications in mass-produced consumer products for short-term uses, as well as for long-term indoor applications [42, 43]. Meanwhile, many researchers have been conducting research on the addition of lignocellulosic fibers to bioplastics for improvement of the chemical, physical, and mechanical properties.

Natural-fiber-based composites are gaining in market demand as strict environmental regulations increasingly arise and consumers start to engage in using a variety of eco-friendly products. New environmental regulations, depletion, and uncertainty of petroleum sources have revived the interest of scientists in deriving a new generation of composite materials from plant-based plastics and natural fibers. However, some reasons that are elaborated in the subsequent text complicate the realization of this concept.

It is reported that one of the major hurdles for commercialization of lignocellulosic fiber composites until recently is the nonrecognition of research and development in developing countries in which these kinds of fibers are abundantly available. This hurdle has been overcome by many industrialized countries, particularly in Europe, which are now taking the lead in this area [44]. However, materials scientists are supposed to deal with challenges regarding the acceptance criteria for these composites, that is, performance and cost, even though the renewability and recyclability of the matrix and reinforcements are attractive. Furthermore, there is a need for product standards to support the performance of the products.

13.3.1
Choice of Materials and Processing Methods

Introduction of new types of fibers, processing, and additives may result in expanded applications and opportunities for the existing biocomposites while improving mechanical performance at the same time. Natural fibers are an emerging alternative especially for automotive companies seeking materials to reduce automotive weight for fuel efficiency. It is estimated that up to 75% of a vehicle's energy consumption is directly related to factors associated with the weight of the vehicle; thus, there is a critical need to produce safe and cost-effective light-weight vehicles. Accordingly, natural fibers have better energy management characteristics than glass fibers in addition to the excellent sound absorption efficiency [45].

Besides product performance, the energy use, substitution with new materials, and reuse/recycling should also be considered. First, to ensure an efficient resource use, less material or energy to achieve the same function should be emphasized. Substitution with a less harmful material or process for comparable achievements is also preferred. Reuse or/and recycling including adding values to materials to avoid primary production and manufacturing are also essential [46].

Even though the adoption of new technology or materials may open up new possibilities and applications, more attention should be paid to scrutinize the processing and resulted products. In adopting nanoscience and nanofiller materials in biodegradable composites, safety issues should be considered carefully despite the many possibilities that the product cost may be reduced through a more efficient

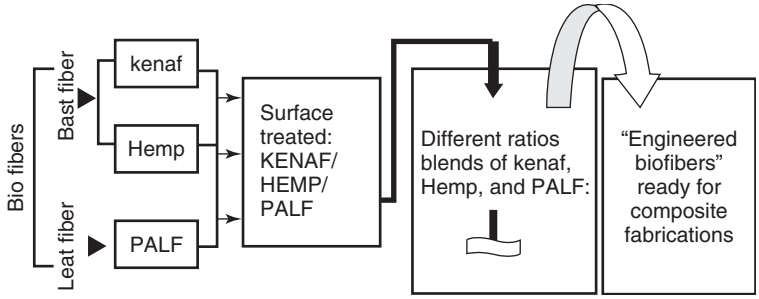

Figure 13.8 Concept on design of engineered natural/biofiber [42].

production. Especially when using these products in food packaging, many legal and ethical aspects have not been deliberated upon.

The choice of materials should also take into account the end-of-life options of the products and their associated environmental cost. Related to this, degradation models should be developed for biocomposites to understand and predict environmental influence and determine the appropriate disposal means. An example of the degradation model is that of a woven composite system reported in Reference [47]. Understanding and modeling the aging of composites allows the prediction of their lifetime as was recently done for glass fibers [48]. This area is intriguing to enhance the utilization potential of biocomposites in a variety of applications.

Blending different biofibers could result in biocomposites with balanced properties. Engineered biofibers, defined as the suitable blend of surface-treated bast and leaf fibers as shown in Figure 13.8, have been studied and reported. By manipulating the blend ratio of biofibers, an optimum balance in mechanical properties of the resulted biocomposites could be attained. For example, kenaf- and/or hemp-based composites exhibit excellent tensile and flexural properties, while leaf fiber (PALF) composites have high impact properties. The combination of bast and leaf fibers is expected to achieve a balance of flexural and impact properties of the targeted biocomposites [49].

A proper processing technique would directly affect the structure and properties of composites [50]. Temperature is important in ensuring minimum degradation of the matrix polymer while keeping it in a molten state to impart flow properties and facilitate molding. Further, the selection of a suitable processing technique for blending of fibers and matrix is also important despite the availability of various batch and continuous compounding equipments [51].

13.4 Conclusion

In this chapter, green composites were reviewed with emphasis on the products used for automotive and structural/indoor applications. The use of plant fibers in the composites is promising and they have been incorporated in many commercial

products nowadays. Efforts in employing bioplastics and biodegradable plastics for the matrix polymer are beginning to embark, although there are many challenges such as price issues that need to be addressed. The market and commercialization of biocomposites are anticipated to expand in the future owing to political pressures, social and environmental awareness among consumers and producers, development of efficient processing technology, and identification of new applications.

References

1. FAO Corporate Document Repository (2001) Common Fund for Commodities – Alternative Applications for Sisal and Henequen, *http://www.fao.org/DOCREP/004/Y1873E/y1873e0b.htm* (accessed 12 December 2011).
2. O'donnell, A., Dweib, M., and Wool, R. (2004) Natural fiber composites with plant oil-based resin. *Compos. Sci. Technol.*, **64** (9), 1135–1145.
3. Dweib, M., Hu, B., O'donnell, A., Shenton, H., and Wool, R. (2004) All natural composite sandwich beams for structural applications. *Compos. Struct.*, **63** (2), 147–157.
4. George, J., Sreekala, M.S., and Thomas, S. (2001) A review on interface modification and characterization of natural fiber reinforced plastic composites. *Polym. Eng. Sci.*, **41** (9), 1471–1485.
5. Clemons, C.M. and Caulfield, D.F. (2005) *Functional Fillers for Plastics*, 1st edn, Wiley-VCH Verlag GmbH, Weinheim.
6. Lucintel (2011) Opportunities in Natural Fiber Composites, *http://www.lucintel.com/LucintelBrief/PotentialofNaturalfiber-composites-Final.pdf* (accessed 5 November 2011).
7. Textile Intelligence press release on 28 July 2011, Sales of Natural Fibers for Use in Composites Set to Double by 2015, *http://www.textilesintelligence.com/til/press.cfm?prid=431* (accessed 9 July 2013).
8. Markarian, J. (2008) Outdoor living space drives growth in wood-plastic composites. *Plast. Addit. Compd.*, **10** (4), 20–25.
9. Gonsalves, K.E. and Mungara, P.M. (1996) Synthesis and properties of degradable polyamides and related polymers. *Trends Polym. Sci.*, **4** (1), 25–31.
10. Simon, J., Müller, H., Koch, R., and Müller, V. (1998) Thermoplastic and biodegradable polymers of cellulose. *Polym. Degrad. Stab.*, **59** (1-3), 107–115.
11. Wolf, O. (2005) Techno-Economic Feasibility of Large-Scale Production of Bio-Based Polymers in Europe. Technical Report EUR 22103 EN, European Commission.
12. Bledzki, A.K. and Gassan, J. (1999) Composites reinforced with cellulose based fibres. *Prog. Polym. Sci.*, **24** (2), 221–274.
13. John, M.J. and Thomas, S. (2008) Biofibres and biocomposites. *Carbohydr. Polym.*, **71** (3), 343–364.
14. Pal, P. (1984) Jute reinforced plastics: a low cost composite material. *Plast. Rubber Process. Appl.*, **4** (3), 215–219.
15. European Biop Astics Bioplastics to pass the one million tonne mark in 2011, Press Release, *http://www.en.european-bioplastics.org/wp-content/uploads/2011/press/pressreleases/PR_market_study_bioplastics_ENG.pdf* (accessed 5 November 2011).
16. Bodros, E., Pillin, I., Montrelay, N., and Baley, C. (2007) Could biopolymers reinforced by randomly scattered flax fibre be used in structural applications? *Compos. Sci. Technol.*, **67** (3-4), 462–470.
17. Herrmann, A.S., Nickel, J., and Riedel, U. (1998) Construction materials based upon biologically renewable resources – from components to finished

parts. *Polym. Degrad. Stab.*, **59** (1-3), 251–261.
18. Suddell, B. and Evans, W. (2005) *Natural Fibers, Biopolymers, and Biocomposites*, CRC Press.
19. Lucintel (2011) Opportunities in Natural Fiber Composites, *http://www.lucintel.com/LucintelBrief/PotentialofNaturalfibercomposites-Final.pdf* (accessed 5 November 2011).
20. Crespell P. and Vidal, M. (2008) Market and technology trends and challenges for wood plastic composites in North America. Proceedings of International Convention of Society of Wood Science and Technology, Concepción, Chile, November 10–12, 2008.
21. Peijs, T. (2003) Composites for recyclability. *Mater. Today*, **6** (4), 30–35.
22. Crain Communication, Inc. *http://plasticsnews.com/china/english/consumerproducts/headlines2.html?id=1319425566* (accessed 30 November 2011).
23. Ellison, G., McNaught, R., and Eddleston, E. (2000) The Use of Natural Fibres in Nonwoven Structures for Applications as Automotive Component Substrates, Ministry of Agriculture Fisheries and Food Agri-Industrial Materials.
24. Holmes, A. (2004) Interactive European Network for Industrial Crops and their Applications (IENICA) IENICA Summary Report for the European Union 2000-2005, Brussels.
25. Karus, M., Ortmann, S., and Vogt, D. (2004) Use of Natural Fibres in Composites in the German Automotive Production 1996 till 2003, Nova-Institute, September 2004.
26. Bismarck, A., Baltazar-Y-Jimenez, A., and Sarikakis, K. (2006) Green composites as panacea? Socio-economic aspects of green materials. *Environ. Dev. Sustainability*, **8** (3), 445–463.
27. Lee, B.H., Kim, H.S., Lee, S., Kim, H.J., and Dorgan, J.R. (2009) Bio-composites of kenaf fibers in polylactide: role of improved interfacial adhesion in the carding process. *Compos. Sci. Technol.*, **69** (15-16), 2573–2579.
28. Suddell, B.C. and Evans, W.J. (2003) The increasing use and application of natural fibre composite materials within the automotive industry. Proceedings of the 7th International Conference on Woodfiber-Plastic Composites, Madison, Wisconsin.
29. Holbery, J. and Houston, D. (2006) Natural-fiber-reinforced polymer composites in automotive applications. *JOM*, **58** (11), 80–86.
30. Pervaiz, M. and Sain, M.M. (2003) Sheet molded polyolefin natural fiber composites for automotive applications. *Macromol. Mater. Eng.*, **288** (7), 553–557.
31. Li, Q. and Matuana, L.M. (2003) Surface of cellulosic materials modified with functionalized polyethylene coupling agents. *J. Appl. Polym. Sci.*, **88** (2), 278–286.
32. Soroushian, P., Marikunte, S., and Won, J.P. (1994) Wood fiber-reinforced cement composites under wetting-drying and freezing-thawing cycles. *J. Mater. Civ. Eng.*, **6** (4), 595–611.
33. Tonoli, G.H.D., Savastano, H., Fuente, E., Negro, C., Blanco, A., and Lahr, F.A.R. (2010) Eucalyptus pulp fibres as alternative reinforcement to engineered cement-based composites. *Ind. Crops Prod.*, **31** (2), 225–232.
34. Swan, A.J., Rteil, A., and Lovegrove, G. (2011) Sustainable earthen and straw bale construction in north american buildings: codes and practice. *J. Mater. Civ. Eng.*, **23** (6), 866–872.
35. Njuguna, J., Wambua, P., Pielichowski, K., and Kayvantash, K. (2011) Natural fiber-reinforced polymer composites and nanocomposites for automotive applications, in *Cellulose Fibers: Bio-and Nano-Polymer Composites*, Springer.
36. Le Duigou, A., Deux, J.M., Davies, P., and Baley, C. (2011) PLLA/flax mat/balsa bio-sandwich manufacture and mechanical properties. *Appl. Compos. Mater.*, **18** (5), 421–438.
37. Burgueno, R., Quagliata, M.J., Mohanty, A.K., Mehta, G., Drzal, L.T., and Misra, M. (2005) Hybrid biofiber-based composites for structural cellular plates. *Composites Part A*, **36** (5), 581–593.
38. Christian, S.J. and Billington, S.L. (2011) Mechanical response of PHB- and cellulose acetate natural fiber-reinforced

composites for construction applications. *Composites Part B*, **42** (7), 1920–1928.
39. Zaikov, G.E. and Lomakin, S.M. (1997) New aspects of ecologically friendly polymer flame retardant systems. *Polym. Plast. Technol. Eng.*, **36** (4), 647–668.
40. Gardner, D.J., Han, Y., and Song, W. (2008) Wood plastic composites technology trends. Proceedings of International Convention of Society of Wood Science and Technology, Concepción, Chile, November 10–12, 2008.
41. English, B. (1996) *The Use of Recycled Wood and Paper in Building Applications*, USDA Forest Service and The Forest Products Society, Madison, WI, pp. 79–81.
42. Mohanty, A., Misra, M., and Drzal, L. (2002) Sustainable bio-composites from renewable resources: opportunities and challenges in the green materials world. *J. Polym. Environ.*, **10** (1-2), 19–26.
43. Netravali, A.N. and Chabba, S. (2003) Composites get greener. *Mater. Today*, **6** (4), 22–29.
44. Evans, W., Isaac, D., Suddell, B., and Crosky, A. (2002) Natural fibres and their composites: a global perspective. Proceedings of the 23rd Riso International Symposium on Materials Science, Roskilde, Denmark.
45. Mohanty, A.K., Misra, M., and Drzal, L.T. (2001) Surface modifications of natural fibers and performance of the resulting biocomposites: an overview. *Compos. Interfaces*, **8** (5), 313–343.
46. Pease, W.S. (1996) Pesticide Use in California: Strategies for Reducing Environmental Health Impacts. CPS Report (USA), California Policy Seminar, University of California.
47. Bahei-El-Din, Y., Rajendran, A., and Zikry, M. (2004) A micromechanical model for damage progression in woven composite systems. *Int. J. Solids Struct.*, **41** (9-10), 2307–2330.
48. Julien, M., Anthony, B., Philippe, C., and Jacques, R. (2008) Characterization and modeling of aging of composites. *Composites Part A*, **39**, 428–438.
49. Mohanty, A.K., Drzal, L.T., and Misra, M. (2002) Engineered natural fiber reinforced polypropylene composites: influence of surface modifications and novel powder impregnation processing. *J. Adhes. Sci. Technol.*, **16** (8), 999–1015.
50. Tucker, N. and Johnson, M. (2004) *Low Environmental Impact Polymers*, Rapra Technology, Shawbury.
51. Czarnecki, L. and White, J.L. (1980) Shear flow rheological properties, fiber damage, and mastication characteristics of aramid, glass, and cellulose fiber reinforced polystyrene melts. *J. Appl. Polym. Sci.*, **25** (6), 1217–1244.
52. Cho, D. and Kim, H.J. (2009) Naturally cyclable biocomposites. *Elast. Compos.*, **44** (1), 13–21.
53. Kalia, S. and Kaur, I. (2011) *Cellulose Fibers: Bio-and Nano-Polymer Composites: Green Chemistry and Technology*, Springer-Verlag, Berlin and Heidelberg.
54. Singh, B., Verma, A., and Gupta, M. (1998) Studies on adsorptive interaction between natural fiber and coupling agents. *J. Appl. Polym. Sci.*, **70** (9), 1847–1858.
55. Winandy, J.E., Stark, N.M., and Clemons, C.M. (2004) Considerations in recycling of wood-plastic composites. Proceedings of Global Wood and Natural Fibre Composites Symposium, Kassel, Germany, April 27–28, 2004.

14
Biomedical Polymer Composites and Applications

Dionysis E. Mouzakis

14.1
Introduction

A definition for Biomaterials as proposed by Black in 1992 is as follows [1]: ''Natural or synthetic materials that are used to direct, supplement, or replace the functions of living tissues of the human body.'' The use of Biomaterials has a very long history and dates back to ancient times. To date, a huge variety of biomaterials has been made available to medical doctors and surgeons of all specialties thanks to immense effort provided in this field of research by scientists internationally. Historical steps in the creation of suitable biomaterials are, for example, the invention of total hip replacement by Sir John Charnley in 1962 [2] using ultra high molecular weight polyethylene (UHMWPE); poly(methyl methacrylate) (PMMA) was used in the 1940s in plastic reconstructive craniofacial surgery [3] and ever since as bone cement in total hip replacements and knee surgery; silicones (polysiloxane) were used in 1946 for bile duct repair [4] and artificial urethra transplants in 1948. Hydroxyapatite (HAp) from coral or tricalcium phosphate ceramic has been proposed [5] as bone regenerative material though brittle for low stress applications [6] and is today widely used as osteoinductive sizing in many dental and orthopedic implant surfaces. John Robert Dugan of Shelbyville invented the coronary stent in the mid 1980s and in 1986, Puel and Sigwart implanted the first coronary stent in a human patient. In 1988, the first urethral stent followed [7]. In 1978, the first commercial titanium dental implant was issued by Bofors AB though the first one was experimentally used in patients back in 1965 by Dr Med Per Brånemark. Nowadays, they are also made of zirconia ceramics [8] in spite of the problems surrounding this material. In 1988, Skinner issued the idea of isoelastic (stiffness equals that of natural bone) composite materials for total hip arthroplasty [9].

As can be concluded from the above facts, biomaterials have been used for more than seven decades now to replace damaged tissues and improve body functions in the human body. Advances in technology and the arrival of innovative products have enhanced the performance and widened the field of applications of biomaterials. While metals and ceramics currently have the lion's share in the biomaterials market, polymers, and composites based on polymer matrices are

Polymer Composite: Volume 3, First Edition.
Edited by Sabu Thomas, Kuruvilla Joseph, S. K. Malhotra, Koichi Goda and M. S. Sreekala.

expected to provide impetus to the next wave of market demand for biomaterials. A comprehensive report on biomaterial types, properties, and applications can be found in [10] and also in [11] for applications of polymer composites covered until 2001.

This work aims to focus on the important advances made in the last decade in the field of biomaterials based on polymer matrix composites. But first let us take a look at the pure economic facts and discover the reason behind the intense interest on the research on biomaterials, of course, those apart from the humanitarian aspects it includes.

The global biomaterial market is currently worth more than $25 billion and is expected to grow twofold Compound Annual Growth Rate (CAGR) in the next few years according to Marketsandmarkets (Dallas, TX). According to this source [12], the total global biomaterials market is expected to rise to US$ 58.1 billion by 2014, growing at a CAGR of 15.0% from 2009 to 2014. The US market is expected to account for nearly 42% of the total sales. The biomaterials market in 2010 was worth more than $28 billion.

The biomaterials market is still in a flourishing phase, with about 100 000 heart valves, 200 000 pacemakers and 1 million orthopedic devices implanted worldwide every year. Increase in applications has increased the demand for new biomaterials from 8% to 15%. Improved patient life and faster recovery are the most important factors stimulating market growth for biomaterials. The other market drivers are increase in mortality rate, increasing health awareness, shorter product approval time, and larger application areas as the field is growing wider and wider.

While the orthopedic biomaterials market was the biggest segment in 2008 with $9.8 billion, the cardiovascular biomaterial market is estimated to be the dominating segment in 2014 with an estimated $20.7 billion. The cardiovascular biomaterial market is expected to grow with a CAGR of 14.5% from 2009 to 2014 mainly due to increasing stress levels and bad nutritional habits that have in turn increased the incidence of cardiac arrest. Moreover, the improvement of life standards and liberalization of many economies such as in China and India, are also important factors to the increasing numbers of cardiovascular episodes.

The US market is the largest geographical segment for biomaterials nowadays; and is expected to be worth $22.8 billion by 2014 with a CAGR of 13.6% from 2009 to 2014. Europe is the second largest segment and is expected to reach $17.7 billion by 2014 with a CAGR of 14.6% and the Asian market size is estimated to increase at the highest CAGR of 18.2% from the year 2009–2014.

Although more expensive than traditional metals and ceramics, polymer composites such as carbon- and glass fiber-reinforced epoxy resins are widely accepted nowadays in orthopedic surgery and dental restoration applications. This work aims at a deeper insight in the progress made in the last 10 years in this family of materials. Polymer nanocomposites are also in focus since the past decade when they have been used as engineering materials and consequently have been investigated and adopted in several biomedical applications. Extensive research nowadays invests heavily on expanding the applications of nanocomposites in the biomaterials regime and also in developing newer types that has attracted huge

investment. Before discussing the progress made in the last decade, issues regarding biocompatibility are addressed.

14.2 Biocompatibility Issues

The most important factors when choosing a material to be used in the manufacturing of a medical implant is shown in Table 14.1 [11]. Also mentioned in Table 14.1 are the key-functions of biomaterials: biofunctionality (nonthrombogenic cell adhesion), bioinertness (nontoxic, nonirritant, noncarcinogenic, etc.), bioactive (to induce beneficial cell differentiation, e.g., osteoblast), biostability (resistant to corrosion, hydrolysis, oxidation), and biodegradation (dissolution and absorption from the body). All these functions can be summarized as the constituents of biocompatibility, the outmost quality a biomaterial must exhibit before application. Indeed many articles in the literature deal with these qualities and attempts have been made either to confirm them or not for many types of common or new biomaterials. A radical article on the ''Organic Polymer Biocompatibility and Toxicology'' (exact title) was already published back in 1972 [13], by F. Bischoff who wrote, ''Human solid-state carcinogenesis constitutes a calculated risk with polymer implants. In rodents, all solid polymers tested produced cancer; chemical carcinogenesis was induced by a polyvinyl chloride copolymer, vinyl chloride, polycaprolactam, liquid silicone, and some brands of polytetrafluoroethylene'', all of the aforementioned are common biomaterials in our days. Being prophetic the same wrote: ''It is hoped that proper allocation of research funds for the study of polymer biocompatibility will be stimulated. Perhaps too much money is spent on the artificial heart and not enough on testing the safety of polymers used in food packaging and cooking.''

In our decade, many new fillers/reinforcements were used for the improvement of polymer biomaterial properties: of which two of the newest ones are carbon nanotubes (CNs) or nanotubes [14] and the Nobel-awarded invention of Graphene [15]. The discussion on their short- or long-term impact on the human organism is far from concluded yet. Despite a plethora of research works and applications into potential medical devices, biosensors, and biomaterials, only recently important valid information on toxicity and biocompatibility of single and multiwall carbon nanotubes has been reviewed and published [16]. On the basis of the work reviewed in [16] it is concluded that the scientific community should remain cautious and restrained with the use and handling of single walled nanotubes (SWNTs) and multiwalled nanotubes (MWNTs) until lung toxicity studies, dermal cell impact, and macrophage inflammatory response are fully determined. Rare transition metal catalysts present in them as production residues have also been proven to cause some degree of toxicity, when using CNs. As far as graphene is concerned, it was recently shown that bovine protein can be well attached covalently to graphene oxide layers via diimide-activated amidation procedure [17]. Of course, although protein attachment to biomaterials is considered to be of paramount importance the fact that such a quality could also

Table 14.1 Important factors in material selection [11].

Factors	Description		
First level material properties	Chemical/biological characteristics	Physical characteristics	Mechanical/structural characteristics
	Chemical composition (bulk and surface)	Density	Elastic modulus
			Poisson's ratio
			Yield strength
			Tensile strength
			Compressive strength
Second level material properties	Adhesion	Surface topology (texture and roughness)	Hardness
			Shear modulus
			Shear strength
			Flexural modulus
			Flexural strength
Specific functional requirements (based on application)	Biofunctionality (nonthrombogenic, cell adhesion, etc.)	Form (solid, porous, coating, film, fiber, mesh, and powder)	Stiffness or rigidity
			Fracture toughness
	Bioinert (nontoxic, nonirritant, nonallergic, noncarcinogenic, etc.)	Geometry	Fatigue strength
		Coefficient of thermal expansion	Creep resistance
		Electrical conductivity	Friction and wear resistance
	Bioactive	Color, aesthetics	Adhesion strength
	Biostability (resistant to corrosion, hydrolysis, oxidation, etc.)	Refractive index	Impact strength
		Opacity or translucency	Proof stress
	Biodegradation		Abrasion resistance
Processing and fabrication	Reproducibility, quality, sterilizability, packaging, and secondary processability		

Characteristics of host: tissue, organ, species, age, sex, race, health condition, activity, and systemic response.
Medical/surgical procedure, period of application/usage.
Cost.

attract the attachment of a microbial biofilm onto an implant itself cannot be overlooked. This brings into discussion the issue of biofilm creation on biomaterials. ''Biofilms are communities of micro-organisms anchored to a surface (substratum) and each other by EPS (extra-cellular polymeric substance) [18]. Cellular adherence and formation of biofilms to synthetic surfaces such as polymer and polymer composite biomaterials is extensively studied. Such biofilms may have undesirable consequences. The colonization and bacterial adherence to biomedical implants and devices are prone to cause infections in the area of the implant. In most occasions, the formation of biofilms, acts as a protective shield for the encapsulated microorganisms from antibiotics and defense mechanisms of the body. Biofilms can be accounted as responsible for the complexities in treating external infections and their infamous persistent durability [18]. Owing to the extensive use of biomaterials in various functions of the body, the treated areas can be considered as potential nuclei for microbial colonization and consequent infection. Microbial contamination of implants is due to several factors. After implanting is finished, local antimicrobial immune reaction is eminent. The result can be a multiplication of microbial colonies.

The mechanism behind biofilm formation can be distinguished in three separate phase processes according to Francolini *et al.* [19]. Phase 1 is characterized by the initial and irreversible cellular attachment to the polymer surface. Phase 2 involves the growth and maturation of the biofilm scaffold. In Phase 3, individual cells or cellular colonies from the biofilm detach and travel to colonize other areas. Immediately after surgical application of an implant, the human body reacts by coating the implant with a protein layer. The composition of this layer includes albumin, laminin, fibrin, and fibronectin. It is already well established by numerous workers that polymer implants in endourological applications such as the various types of catheters suffer from inorganic salt encrustations [20, 21]. These encrustations or also the kidney stones, according to [22], might be the actual nesting sites for pathogens, and are usually covered by a type of biofilm.

Several methodologies were proposed to prevent the formation of this protein layer, or biofilm expansion, on biomedical devices. One especially refers to polymers that have been chemically modified so as to block the initial microbial colonization (Phase 1) and further are able to release antimicrobial agents to prevent biofilm surface growth [19]. Another technique proposes to change the electrical surface charge of the polymer. Considering that most bacteria are negatively charged, a negatively charged polymer deters bacteria in a more efficient way than an uncharged polymer after Jansen *et al.* [20]. A more aggressive but efficient way to counteract microbial growth, adhesion, and consequent colonization of the implant, is the application of silver coatings. Silver and silver salts are well known for their antimicrobial properties. Silver ions bind to microbial DNA and sulfydryl groups, restrict bacterial replication, and deactivate metabolic enzymes [18, 19].

To sum up, it is of paramount importance that not only biocompatibility but also biofilm prevention qualities should be taken into account when designing a polymer or polymer-based composite biomaterial or implant in order to avoid phenomena as microbial colonization.

14.3
Natural Matrix Based Polymer Composites

Biocomposites based on natural polymers exploit mainly the wide range of physicochemical properties and processing techniques available from conventional polymer technology. These advantages are augmented by the outstanding biocompatibility of natural polymers and the diverse biological interactions between cells and the natural composite substrate. Several types of natural polymers are available as matrices for biocomposites and fibers such as silk, chitin, and chitosan (CTS), collagen, hyaluronic acid, and starch. These can be made available in matrices in pure or cross-linked form. Synthetic polymers exhibit a much more limited biocompatibility and biodegradability than those of natural polymers and therefore the study of natural polymer matrices is nowadays one of the preferred subjects in the field of biomaterials science and engineering. It has also been proposed that the combination of gene therapy and tissue engineering exploits the power of genetic cell engineering to provide the biochemical signals influencing proliferation or differentiation of cells growing on suitable scaffolds (see Section 14.3.4 below and references therein). Natural polymers with their ability to serve as gene carriers and tissue engineering scaffolds are predicted to play a key role in the field of regenerative medicine in the coming years.

14.3.1
Silk Biocomposites

Silk is a natural biological fiber composed of fibrous proteins with astonishing mechanical properties in addition to environmental stability, biocompatibility, controlled proteolytic biodegradability, morphologic flexibility, and the ability for amino acid side change modification to immobilize growth factors (GFs) [24]. Silk is naturally produced in fiber form by Lepidoptera worms, silkworm, and many kinds of orb-weaver spiders (*Nephila clavipes*). Physicians have used sutures for at least 4000 years. Silk fibers for medical suturing have been used for many centuries [25]. Silk sericin is a natural macromolecular protein produced by from silkworm (*Bombyx mori*) [26].

Sericin is recovered during the various stages of producing raw silk. Sericin is oxidation-, bacterial-, and UV-resistant, and it absorbs and releases moisture rapidly. Sericin can be cross-linked, copolymerized, and blended with other macromolecular materials, especially artificial polymers. The materials modified with sericin and sericin composites are useful as degradable biomaterials, biomedical materials, polymers, functional membranes, fibers, and fabrics [26].

Progress made in electrospinning in the past decade has allowed for the production of fibers in nanoscale diameters from various polymers. Tissue engineering has benefited a lot from this process and quite often silk protein is used to produce nanofiber scaffolds for cell cultures. Human bone marrow stromal cells were found to proliferate *in vitro* very well on mats made from poly(ethylene oxide) (PEO) and *B. mori* silk aqueous solution electrospun nanofibers [27]. A very interesting work by

Table 14.2 Cell and tissue applications of silk fibroin scaffolds [24].

Application	Morphologic form
Wound dressings	Film
	Sponge
Bone tissue engineering	Sponge
	Film
	Hydrogel
	Nonwoven
Cartilage tissue engineering	Porous sponge
	Hydrogel
Ligament tissue engineering	Fiber
Tendon tissue engineering	Fibers
Hepatic tissue engineering	Films
Connective tissue	Nonwoven mats
Endothelial and blood vessel	Nonwoven mats
Antithrombogenesis	Films

Kaplan *et al*. [28], combined bone morphogenetic proteins and HAp nanoparticles in the mixtures for electrospinning composite silk nanofibers. They have shown that this combination resulted in the highest calcium deposition in nanofibrous electrospun scaffolds for mesenchymal stem cell cultures.

Silk biomaterials are biocompatible both in *in vitro* and *in vivo* conditions. Silk solutions mixed with other polymers, were used as precursor materials to produce a variety of biomaterials, such as gels, sponges and films [24]. Owing to their structure, silks can be chemically modified with relative ease by amino acid side chains thus altering surface properties or practically immobilizing cellular GFs. Molecular engineering of silk sequences has resulted in the modification of silks with tailored features, such as cell recognition or mineralization. The degradability/bioresorbability of silk biomaterials can be altered by the art of processing and the resulting content of b-sheet crystallinity [24]. Several primary cells and cell lines have been successfully grown on different silk biomaterials to demonstrate a range of biological outcomes.

Properly engineered silk scaffolds have been successfully applied in wound healing and in tissue engineering/regeneration of bone, cartilage, tendon, and ligament tissues as shown in Table 14.2 [24].

14.3.2
Chitin and Chitosan as Matrices

Chitin, is a naturally abundant mucopolysaccharide, derivative of glucose, and has been reported as the keystone material of invertebrates' radula (molluscs), exoskeletons (insects, crustaceans), and the beaks of cephalopods. It consists of a homopolymer of β-(1 → 4) linked 2-acetamido-2-deoxy-D-glucopyranose

residue [29]. Its immunogenicity is exceptionally low, in spite of the presence of nitrogen. Chitin is highly insoluble and resembles cellulose in its solubility and chemical reactivity due to close chemical structure. CTS is the deacetylated derivative of chitin [29]. Recently, it was concluded in a review study that sulfated chitin and CTS can be very valuable biomaterials. Sulfonation leads to structures similar to heparin and therefore sulfonated chitin and CTS has anticoagulant, antisclerotic, and antiviral properties [29]. Therefore, composites employing these matrices should inherit these benefits too.

Nanostructures of CTS, such as nanoparticles and nanofibers, attracted attention and were studied because of their expected good biomechanical performance. Back in 2002 it was proposed that HAp/CTS nanocomposites could compose a proper biomaterial system [30] without *in vivo* testing though. Electrospun CTS-based nanofibers (Ø 38–62 nm) with a content in PEO 9 to 1 respectively, were found to compose a very promising scaffold in both chondrocytes and osteoblasts *in vivo* cultures [31]. Blends of CTS with other synthetic and natural biodegradable polymers were also attracting attention as potential biomaterials. Poly(ε-caprolactone) (PCL) and CTS blends were used to fabricate porous scaffolds by lyophilization which were tested for their biocompatibility showed positive results. At a 50 : 50 ratio PCL/CTS porous 2D scaffolds showed improved mechanical properties and mouse fibroblast cellular support [32]. Collagen/CTS blends were prepared and tested for hepatocytes compatibility (rat samples) and showed very promising results [33] and complex core shell CTS/hyaluronan particles were proposed for pharmaceutical purposes, for example, drug delivery [34]. CTS has been also used as a matrix controlling the mineralization of HAp in CTS/HAp nanocomposites [35] with a hierarchical nearly biomimicking structure.

14.3.3
Mammal Protein-Based Biocomposites

Protein-based polymers derived from mammals (such as elastin, collagen, and gelatin) have the advantage of mimicking many features of extracellular matrix (ECM) and thus have the potential to direct the migration, growth, and organization of cells during tissue regeneration and wound healing, and for stabilization of encapsulated and transplanted cells [36].

Collagen is one of the most extensively used materials for scaffold production in soft tissue repair and reconstruction, as artificial skin grafting, although it is difficult to control its exact form in a reproducible manner [37]. Collagen matrices are often chemically cross-linked (e.g., using glutaraldehyde) to improve biological stability, ease of handling and inherently low mechanical properties [36]. In Table 14.1 some of its most characteristic applications are summarized following the review by Malafaya *et al*. [36].

Many researchers try to exploit polymer composites' manufacturing techniques in order to tailor/improve the performance of collagen as biomaterial. In 2001, Kikuchi *et al*., have succeeded in manufacturing implants of HAp/collagen with a self-organized nanostructure and composition similar to bone. These implants

showed good resorption by phagocytosis but had only one quarter of the mechanical strength of bone [38]. PCL/collagen composites prepared by solution impregnation of freeze-dried collagen mats were investigated against human osteoblast (HOB) adhesion and proliferation. It was found that preferably, HOB cells attach and migrate better on the PCL/collagen composites rather than the pure PCL films [39]. A similar composite based on the PCL/collagen was also studied as substrate for skin tissue engineering. The results revealed that composite films of collagen/PCL composites are favorable substrates for the growth of fibroblasts and keratinocytes and provide adequate system for skin repair [40]. Multilayered polyelectrolyte films synthesized from hyaluronic acid, collagen, and poly(ethyleneimine), were investigated for their *in vitro* response as chondrosarcoma cells proliferation with interestingly tunable antitumor properties [41] (Table 14.3).

Electrospinning has also been utilized as in the case of silk, in order to produce nanofibers from pure composite collagen systems. Random mats of collagen nanospun fibers (Ø 100–1200 nm) cross-linked after electrospinning, were found to produce a positive effect for wound healing or ceratinocyte spreading [42]. Such a system can be valuable for skin tissue repair in cases of extensive burns, tumors, and so on. Composite PCL/gelatin electrospun nanofibrous scaffolds (PCL/gelatin 70 : 30 nanofiber) was found to exhibit the most balanced properties to meet all the required specifications for nerve tissue and was used for *in vitro* culture of nerve stem cells. Results showed that the biocomposite of PCL/gelatin 70 : 30 nanofibrous scaffolds enhanced the nerve differentiation and proliferation compared to PCL nanofibrous scaffolds [43]. Other proteins of mammalian origin can be also used to electrospin fibers for the fabrication of tissue engineering scaffolds. Alpha-elastin (bovine) and tropoelastin (human, recombined) were dissolved for electrospinning, in 1,1,1,3,3,3-hexafluoro-2-propanol and the electrospun-resulting scaffolds were cross-linked with 1,6-diisocyanatohexane [44]. It was stated that electrospun fibrous scaffolds based on tropoelastin–elastin behaved equally well as those from collagen/gelatin, thus paving the way for the tissue engineering of functional cardiac, cardiovascular, and pulmonary tissue cultures. Human tropoelastin has also been proven to build self-organized massive complex assemblies such as tubes and sponges, suitable for cell transplanting and three-dimensional scaffolds [45] in elastic tissue repairing applications. A very recent study proposed the use of electrospun PCL/collagen I, for the manufacturing of a composite vascular scaffold that withstands physiological vascular pressure conditions [45].

14.3.4
Hyaluronic Acid Composites

Recently, the use of alginic acid/HAp composites as scaffolds in tissue engineering applications has received considerable interest due to the unique properties they possess, such as high biocompatibility and biodegradability [46, 47]. Alginate or alginic acid is a natural biopolymer (anionic polysaccharide) extracted from brown algae. It is composed of linear chains of α-L-gluronic acid (G) and β-D-mannuronic acid (M). Alginates form hydrogels in the presence of divalent cations through

Table 14.3 Collagen-based matrices/scaffolds for drug, cell and gene delivery used in different tissue engineering applications [36] and references therein.

Polymer(s)/carrier/ scaffold structure	TE application	Active biomolecule	Encapsulated/seeded cell type (source)	Animal model
Collagen/ hydroxylapatite	Bone	NGF	—	Calvaria defects
Collagen sponge	Cartilage	bFGF	Chondrocytes	Nude mice subcutaneous implantation
Collagen gel	Bone/cartilage	BMP-2 gene	Bone marrow stromal cells	Mouse femoral muscle
Collagen gel	Skin	PDGF-A gene	—	Rabbit dermal ulcer
	—	PDGF-B gene	—	Swine dermal would
Collagen gel	Vascularization	VEGF	—	Chorioallantoic membrane
Collagen/heparan sulfate matrix	Vascularization	bFGF	—	Rat
Collagen gel with gelatin microspheres	Adipose	FGF-2	—	Mouse groin
Collagen–agarose beads	Not defined	—	Adults mesenchymal stem cells	—
Collagen sponge	Bone	—	Alveolar osteoblasts gingival fibroblasts	Critical-size defect in mouse skull
Collagen electrospun nanofibers	Bone	—	Bone marrow-derived mesenchymal stem cells (adult)	—
Collagen sponge and hydrogel	Intervertebral disc	—	Human intervertebral disc cells	—
Collagen sponge	Tooth	—	Porcine third molar cells	Omentum of immunocompromised rats
Collagen sponge	Cartilage	—	Chondrocytes (autologous)	Sheep chondral defects
Collagen membrane	Cartilage	—	Chondrocytes	Medial femoral condyle of New Zealand rabbits
Collagen sponge	Adipose	—	Preadipocytes (human)	Nude mice subcutaneous implantation
Collagen–GAG scaffold	Cardiovascular	—	Bone marrow-derived mesenchymal stem cells	Rat myocardial infarction
Collagen scaffold (fleece)	Genito-urinary tract	—	Smooth muscle cells (human)	Nude mice subcutaneous implantation
Collagen vitrigel	Renal glomerular tissue	—	Glomerular mesangial cells, epithelial cells	—

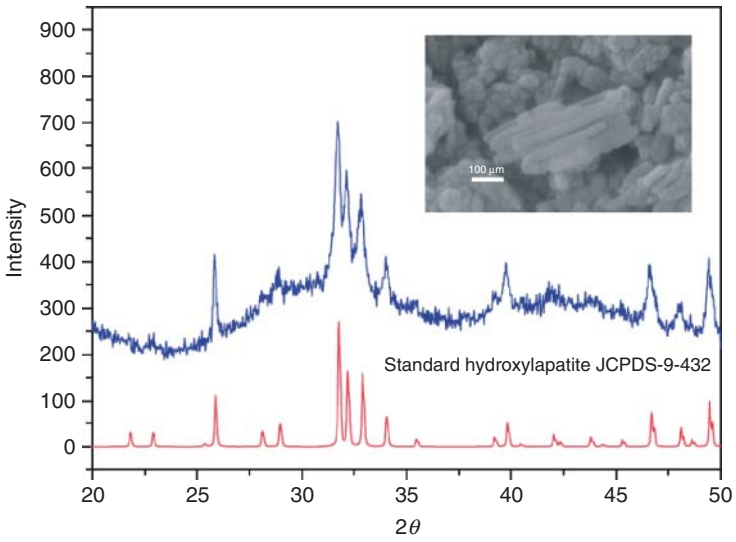

Figure 14.1 XRD spectra of synthetic and standard hydroxyapatite (JCPDS file number 9-0432). The insert SEM picture shows a typical morphology of the synthetic HAp nanocrystals in needle shape [52]. Courtesy of the authors.

interactions between carboxylic groups of G units and the divalent ion. Their power lies in their similarity of chemical structure and nature with hyaluronan or hyaluronic acid; that is, their counterpart found in the animal kingdom abundant in the articulate cartilage, synovial fluid, and ECM [48, 49]. Lin *et al.* prepared porous alginate/HAp scaffolds and showed that the above composite is a promising material for tissue engineering applications [50]. Hosoya *et al.* prepared a HAp–alginate hybrid by modification of alginate with silanol groups and subsequent soaking in calcium solution and simulated body fluid [51]. Applications of calcium alginate hydrogels, in the reinforced or pure state in tissue engineering are influenced directly by their mechanical properties [52]. Nanocomposites based on nanoscale needle-form HAp in alginate matrix showed excellent viscoelastic mechanical behavior for small weight fractions of HAp < 0.5 wt% [52] (Figure 14.1). Hybrid triphasic systems such as gelatin/chondoitin-6-sulfate/hyaluronan tri-copolymer mimicking natural cartilage matrix were manufactured for use as a scaffold for cartilage tissue engineering [53, 54]. *In vitro* testing in spinner flasks, showed that chondrocyte cultures were evenly distributed in the hybrid scaffold, secreted new ECM, retained their phenotype, and also secreted type II collagen [54].

14.3.5
Other Natural Polymer Matrices

Quite a few alternative polymer matrices originating directly from nature have been proposed as potential matrices for composite biomaterials. Examples are starch, corn protein, and bacterial synthesized cellulose, and polysaccharides. Starch is

a very attractive matrix due to its abundance in cereals and eases of extraction and of course its high biodegradability. Starch can even be expanded into foam with open cell architecture, a material widely known as *pop-corn*. Starch is a polysaccharide produced by higher plants as energy storage [55] and is composed of two polymers of D-glucose: amylose and amylopectin. It has been proposed as matrix mixed with gelatin and bacterial polysaccharide for the manufacturing of 3D porous scaffolds by rapid prototyping with interesting mechanical properties [56]. Other latest approaches utilize composite systems with starch/cellulose acetate (50/50 wt%), ethylene vinyl alcohol (50/50 wt%), and polycaprolactone (30/70 wt%) also reinforced with 10% HAp and surface-modified with plasma. These systems were impregnated with bovine serum albumin, fibronectin, and vitronectin as bone cell modulating proteins [57].

Another useful natural polymer is Zein [58]. The ability of Zein and resulting polymers to form tough, glossy, and hydrophobic greaseproof coatings with considerable resistance to microbial attack raised commercial interest [58]. Zein has been applied in the production of pharmaceutical microspheres to delay drugs release until they reach the intestine, to protect the drugs from stomach acid, and to provide a mechanism for the controlled release of drugs in the stream [59]. Zein has also been used as a base to produce biodegradable films and plastics [60]. Zein films have been also prepared and tested as potential material for tissue engineering of liver cells with promising results [61].

It is worthy to mention polymers produced by microorganisms such as bacteria. Earlier, the case of bacterial polysaccharides was mentioned [56]. This is a natural polymer available commercially as Dextran. It is used medicinally as an antithrombotic (antiplatelet) to reduce blood viscosity, as a volume expander in anemia, and also as lubricant in eye drops. Further, cellulose can also be produced from bacteria (*Gluconacetobacter hansenii*). This type of cellulose patented as XCell® and approved by the FDA, is currently available in the market (Xylos Corporation: Langhorne, PA, USA) [62]. XCell is a high performance wound dressing which maintains the moisture balance in the wound, speeds up healing, and epithelialization [62]. Bacterial cellulose composites *in situ* reinforced with in-matrix precipitated calcium-deficient HAp to mimic biomineralization, was found to resemble the natural bone apatitic structure [63]. Further, bacteria are known to synthesize biodegradable polyesters; the most known since the 1920s is poly(3-hydroxybutyrate) (PHB), which was discovered in 1920 as produced by the bacteria ''Bacillus megaterium'' and also by other strains of bacteria [64].

14.4 Synthetic Polymer Matrix Biomedical Composites

Needless to mention, many types of the usual synthetic polymer composites are in use for decades now as matrices for several kinds of biomedical composite materials. Before the authors elaborate the progress made in the last decade with the ''conventional'' composites, for example, fiber-reinforced implants, they would

like to discuss the types of synthetic polymer matrices that are characterized by biodegradability and bioresorption. As reported earlier, this is a major characteristic of the natural polymer matrices, but also some synthetic ones possess the same advantage. Some of the most known synthetic polymer matrices or medical grade plastics are

- CELCON®, TECAFORM™ AH, MT (Acetal Copolymer with antimicrobial fillers)
- RADEL® R (Polyphenylsulfone)
- UDEL® Polysulfone
- ULTEM (Polyetherimide)
- Lot controlled UHMWPEs
- IMPLANTABLE GRADE LENNITE UHME-PE
- TECANAT PC (USP Class VI Polycarbonate Rod)
- ZELUX® GS (Gamma Stabilized Polycarbonate)
- ACRYLIC (Medical Grade Cast Acrylics)
- TECAPRO™ MT (Polypropylene Heat Stabilized)
- TECAPEEK™ MT (Limited contact, 24 h, USP Class VI compliant PEEK®)
- TECAPEEK CLASSIX™ (Prolonged to 30 days implantable Invibio® PEEK-CLASSIX™ Product)
- TECANYL™ Polyphenylene Oxide (or Noryl®)
- TYGON® Flexible Tubing, Sanitary Silicone
- IMPLANTABLE GRADE MediPEEK-IM™ PEEK (EVONIK PEEK Resin)
- PVDF (Meets USP Class VI), polyvinylidene fluoride
- PROPYLUX®, polypropylene resin
- Medical Grade PMMA (Acrylic)
- ANTIMICROBIAL filled plastics, that is, TIVAR®
- TEXOLON™ Medical Grade PTFE (USP Class VI, FDA 21CFR177.1550).

14.4.1
Biodegradable Polymer Matrices

In a very thorough 2003 review article, Gunatillake and Adhikari [65] studied in detail and presented an extensive analysis of the most known synthetic polymers (mostly from works published in the 1990s) for biomedical applications. They categorized this class of polymers into the following main families: polyesters, poly(glycolic acid), poly(lactic acid) and their copolymers, polylactones, poly(propylene fumarates), poly(anhydrides), Tyrosine-derived polycarbonates, polyorthoesters, polyurethanes (PUs), and polyphosphazenes. Their results are summarized in Table 14.4 [65]. It is noteworthy that in their study they included many references with respect to the actual biocompatibility issues accompanying each synthetic polymer. Indeed, the issue of biocompatibility is not new with these materials. As reported it is not only an issue of the material degradation and resorption mechanism by the organism.

This mechanism usually includes enzymatic reactions or hydrolysis of the polymer backbone chain or some functional groups (e.g., -ester) [64]. In a more detailed review in 2007, Nair and Laurencin included [64] poly(trimethylene carbonate) in

Table 14.4 Basic properties of biodegradable polymers [65].

Polymer	Thermal and mechanical properties						
	Melting point (°C)	Glass transition (°C)	Approximate strength	Processing method	Approximate degradation time (months)	Degradation products	Biocompatibility and biodegradation (References)
				Polyesters			
Poly(glycolic acid)	225–230	35–40	7.0 GPa (modulus)	E, IM, CM, and SC	6–12	Glycolic acid	Many studies have shown that polyglycolides, polylactides, and their copolymers to have acceptable biocompatibility. Some studies have shown systemic or local reactions due to acidic degradation products. Biodegradation of these polymers takes place by random hydrolysis resulting in decrease in molecular weight followed first, by a reduction in mechanical properties and mass loss. Natural pathways (metabolism, excretion) harmlessly eliminate the final degradation product (Middleton and Tipton, 2000)
Poly(L-lactic acid)	173–178	60–65	2.7 GPa (modulus)	E, IM. CM, and SC	>24	L-Lactic acid	
Poly(D,L-lactic acid)	Amorphous	55–60	1.9 GPa (modulus)	E, IM, CM, and SC	12–16	D,L-Lactic acid	
Poly(D,L-lactic-*co*-glycolic acid) (85/15)	Amorphous	50–55	2.0 GPa (modulus)	E, IM, CM, and SC	4–5	D,L-Lactic acid and glycolic acid	
Poly(D,L-lactic-*co*-glycolic acid) (85/15)	Amorphous	45–50	20 GPa (modulus)	E, IM, CM, and SC	3–4	D,L-Lactic acid and glycolic acid	
Poly(D,L-lactic-*co*-glycolic acid) (85/15)	Amorphous	45–50	2.0 GPa (modulus)	E, IM, CM, and SC	1–2	D,L-Lactic acid and glycolic acid	—
Poly (caprolactone)	58–63	−65 to 60	0.4 GPs (modulus)	E, IM, CM, and SC	>24	Caproic acid	Generally considered as a nontoxic and tissue compatible polymer (Holland and Tighe, 1992; Hayashi, 1994)
Poly(propylene fumarate)	—	—	2–30 MPa (compressive strength)	Injectable prepolymer cross-linked via free radical initiation	Depends on the formulation, several months based on (*in vitro*) data	Fumaric acid, propylene glycol, and poly(acrylic acid-*co*-fumaric acid)	Initial mild inflammatory response and no deleterious long-term response based on rat implant studies (Kharas *et al.* 1997; Peter *et al.* 1998; Temenoff and Mikos, 2000)

Polyanhydrides, polycarbonates, polyurethanes, and polyphosphazenes							
Poly[1,6-bis (carboxy-phenoxy) hexane]	—	—	1.3 MPa (Youngs modulus)	Thermoplastic	12 (*in vitro*)	Dicarboxylic acids	Polyanhydrides are biocompatible and have well defined degradation characteristics. Degrades by hydrolysis of the anhydride linkage (surface degradation) (Leong *et al.* 1985; Uhrich *et al.* 1997)
Tyrosine-derived polycarbonate	—	—	Sufficient mechanical strength for load bearing bond fixation	Thermoplastic	Very slow degradation (*in vitro*)	Tyrosine, carbondioxide and alcohols	Biocompatible and promotes bone growth (*in vivo* studies) (Pulapura and Kohn, 1992; Muggli *et al.*, 1998)
Polyurethane based on LDI and poly(glycolide-*co*-γ-caprolactone)	—	—	8–40 MPa tensile strength	Castable thermoset	1–2	Lysine, glycolic, and caproic acids	No adverse tissue reaction (guinea pigs) (Bruin *et al.* 1988)
Ethylglycinate polyphosp-hazene	—	—	—	Thermally processable	>1 (*in vitro*)	Phosphates and ammonia from backbone and other products depending on side chain structure	Biocompatible and support osteogenic cell growth (*in vitro*) (Qui and Zhu, 2000)

E, extrusion; IM, injection molding; CM, compression molding; SC, solvent casting.

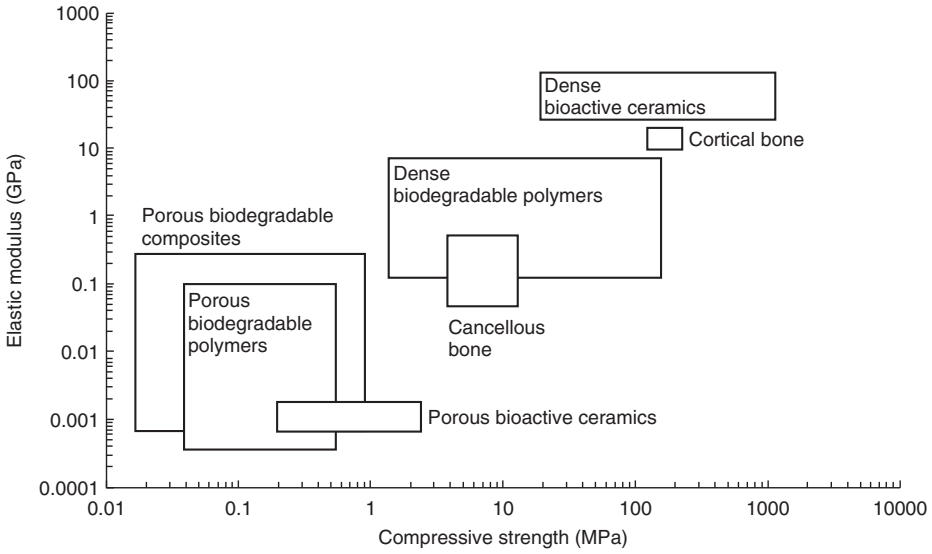

Figure 14.2 Elastic modulus versus compressive strength of biodegradable polymers, bioactive ceramics, and composites after [78]. Porosities of the porous scaffolds are >75% and mostly interconnected. (under permission)

the biomedical polyester family characterized by high *in vivo* biodegradability, a material usually used in sutures and orthopedic screws. They also reported results from synthetic bacterial-origin polyesters such as the PHB, currently being produced synthetically (Biopol™, Metabolix) with similar properties. The *in vivo* degradation of these polymers is reported to be slow, although not many degradation studies have been concluded as yet. Typically, they are thought to be prime-time matrices for the fabrication of long-term implants. Another wonderful property they possess is their piezoelectric nature, which is much desired in orthopedic applications [64].

In their 2006 review, Boccaccini *et al.* [78] elaborated on the study of combinations of many biodegradable polymer matrices reinforced with inorganic ceramics, bioactive glasses and glass-ceramics, and calcium phosphates as scaffolds for bone tissue engineering applications.

Their review results with respect to the comparison of the mechanical properties of such systems with those of human bone are summarized in Figure 14.2. They concluded that up to date, the mechanical integrity of man-made composite scaffolds is still at least one order of magnitude lower than that of cancellous or cortical bone. Achieving the mechanical properties of bone might also allow replacing bigger parts of damaged bone tissue than what is possible today. The other challenge of the near future, according to the same authors, is to incorporate biomolecules such as growth proteins and also seed three-dimensional scaffolds with tailored porosity. This will provide the surgeons with living ''scaffolds of choice'' suitable for highly targeted orthopedic applications [78].

14.4.2 Synthetic Polymer Composites

In their 2001 review on biomedical applications of polymer composites, Ramakrishna *et al*. [11] concluded that up to that date, medical doctors and surgeons were reluctant to use polymer composite materials in biomedical applications because of lack of long-term scientific data, as compared with the data available for monolithic materials such as metals and ceramics. Now, almost 10 years later, many applications have met the needs of the medical field and a plentiful of scientific data has been made available to the open literature. Time and again, reviews are written with respect to the efficiency of polymer composites in the biomedical field. The applications mostly vary from the orthopedic to the dental area of use.

14.4.2.1 Orthopedic Applications

The most widely accepted and commercially available polymer biomedical composite matrix is poly(ether ether ketone) (PEEK), which belongs to the family of polyaryl ether ketones (also called *PAEK*s or *polyaromatic ether ketone*s) known for their high chemical and temperature resistance, high molecular weight, and strong mechanical properties. Another known biomedical polymer of this family is PEKK characterized by its radiolucence, density, and stiffness similar to bone, excellent abrasion resistance, minimal stress shielding, and compatibility with all sterilization methods. The latter polymer also features 100% higher compressive strength than that of PEEK™ according to its manufacturer (Oxford Performance Materials Inc.).

Being chemically inert and nonabsorbable, polymer PEEK composites have a 15-year history of products available in the market and then suddenly abandoned by the marketing companies [11]. Though its most popular orthopedic applications are osteosynthetic plaques and screws and also spinal implants, fiber-reinforced composites with PEEK matrix have been proposed for more demanding applications such as hip and knee arthroplasty [79]. In fact, until 2001, the combination of PEEK and zirconia ceramics in hip arthroplasty was considered as the optimum one. However, several hundred reported cases of zirconia ceramic implant femoral head failure due to phase transformation [80, 81] and consequent fatigue failure [82] have resulted in the retraction of this ceramic from the orthopedics market. One has to say that PEEK blended by a variety of techniques with HAp, results in a bone inductive polymer matrix, at the cost of matrix toughness and strength [11, 83]. These properties can be enhanced by fiber reinforcement in parallel. The carbon or even glass fibers may be used in continuous form (unidirectional laminated systems) [84], chopped [85], or knitted [86] or in braided fabrics [87]. Further, more modern studies advise the use of HAp precursors as osteoinductive materials and not crystalline HAp itself because of its exceptionally high thermodynamic stability, causing its low absorbance rate by the organism [87]. Still, many researchers strongly support the use of crystalline HAp particles as fillers, for orthopedic implants [88], but these cannot be suggested for high load bearing applications. Maybe, in the

future, PEEK implants enriched or sputtered with Hap particles exactly as their metal counterparts made from steel, Ti, Ta, and so on, will be available.

A rather famous HAp reinforced system was made commercially available in the end of 1990s under the name HAPEX™. It is composed of high density polyethylene (HDPE) and HAp particles [89]. However, its low mechanical properties limit its applications in nonload bearing regimes such as the craniofacial repair, as bone grafts. This usually provides a better alternative to PMMA-based bioactive composite cements [90, 91]. Further orthopedic applications of synthetic polymer composites include internal and external fixation devices and screws used in bone fracture. The excess rigidity and small weight of carbon fiber-reinforced polymer composites makes them ideal for fixation systems such as those for wrist and tibia [92] fracture, for example, the hybrid frames of Gexfix S.A. (Carouge, CH). It is expected that in the forthcoming years many "traditional" metal implants will be substituted successfully by composite implants such as the Cambridge epiphyseal cup [93] made from HAp plasma coated carbon fiber-reinforced polybutylene terephthalate which is currently under clinical evaluations. Moreover, polymer composite biomaterials with hybrid reinforcements such as E-glass fibers and bioactive glass particles based on PMMA and PS matrices have been reported as efficient load bearing orthopedic implants [94].

14.4.2.2 **Dental Applications**

Favorable attention has been drawn to polymer composites in the field of dental restorative materials because of their tailored load bearing capability characteristics. An increasing number of applications varying from dental restoration posts to maxillofacial implants and dental fixtures are reported for what an experienced scientist would call *traditional fiber-reinforced composites*. This is just a measure of the advancement of the composite technology nowadays.

It took merely a decade for dentists to be convinced from *in vitro* and *in vivo* studies that fiber-reinforced root canal posts possess high advantages over their metal alloy cast and ceramic adversaries. The reason is that experimental, clinical, and arithmetic analysis (finite elements) data on teeth restored with composite posts, have shown, beyond any doubt that the root stresses are much lower [95, 96] and thus the restoration longevity is ensured. This is because the composite posts and especially those reinforced with glass fibers match the stiffness of the dentine and the elastic mismatch causing stress concentrations in the root area vanishes. Only silica–zirconium fibers have been reported to exhibit even better results than glass fiber-reinforced ones, under flexural loading though [97]. Apart from uses in endodontical treatment, the new era of metal-free dentistry features quite a few other technologies based on fiber-reinforced polymer composites. Partial dentures [98, 99] and related clasps [100] based on fibrous polymer composites were proven to be as functional as cast metal resin-bonded ones. Strong cusp composite restorations [101], even esthetic composite archwires and brackets for orthodontics made from pultruded glass fiber-reinforced polymers [102] are a wonderful alternative to their corresponding metal ones. Dental composite resins were also investigated for their mechanical response after reinforcement with polymer (UHMWPE) or

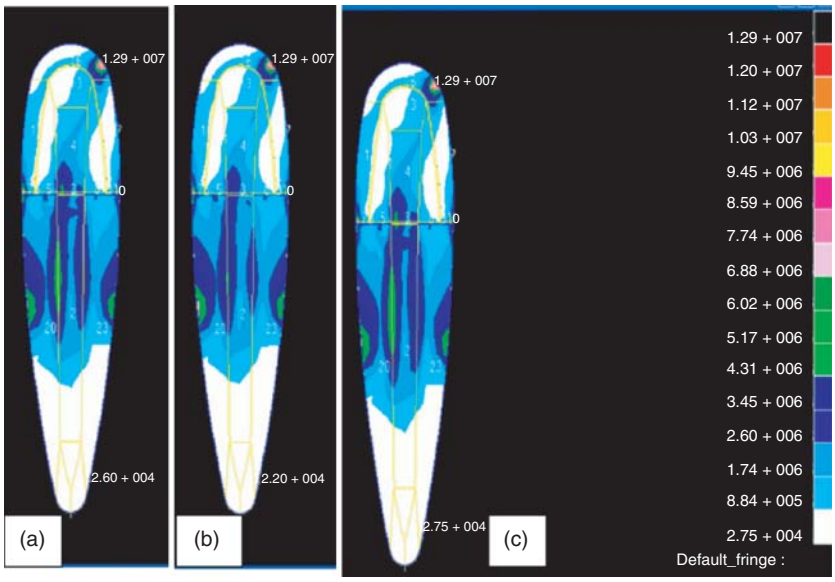

Figure 14.3 FEM analysis of Internal stress build-up in teeth restored with composite posts. (a) Titanium, (b) glass fiber-reinforced, and (c) carbon fiber-reinforced. Courtesy of the authors [96].

glass fiber systems with interesting results [103]. Further, the addition of bidirectional or random continuous fibers has proven not to affect the bond strength compared to control of particulate filler polymer dental composites [104]. On the other hand, the compressive and flexural strength data were significantly improved in interpenetrating network restorative resins when reinforced with short glass fibers [105]. Biomimetic mineralization has also been observed on the surface of a glass fiber-reinforced composite with a partially resorbable biopolymer matrix. E-glass fibers were preimpregnated with a novel biopolymer of poly(hydroxyproline) amide, and further impregnated in the monomer system of bis-phenyl glycidyl dimethacrylate (Bis-GMA)–triethylene glycol dimethacrylate (TEGDMA). The two polymers formed interpenetrating polymer networks (IPNs) and the resultant glass fiber composite showed remarkable biomineralization characteristics, opening the path for partially resorbable bioactive composite restorative resins [106].

Finally, maxillofacial composite implants are gaining acceptance in clinical cases nowadays [107]. A glass fiber-reinforced composite (FRC) substructure was shaped into a framework and embedded into the silicone elastomer of a large facial prosthesis. Such types of composite prostheses are designed to overcome the disadvantages associated with traditionally fabricated prostheses; namely, delamination of the acrylic base silicone, poor marginal adaptation over time, and poor simulation of facial expressions [107]. We will refer to further usage of composites technology with respect to maxillofacial prosthetics in the section on nanocomposites below (Figure 14.3).

14.4.2.3 Other Tissue Engineering Applications

Tissue engineering could not be excluded from the area in which synthetic composite applications are foreseen. Coronary artery and peripheral vascular disease are the largest causes of mortality in the western world, requiring surgical interventions including small-diameter bypass grafting with autologous veins or arteries. These autografts however suffer from compliance mismatch between veins and arteries causing hyperplasia in sites where vascular anastomosis has been applied. Composite fiber PCL–PU vascular scaffolds have been prepared for this reason. It was shown that such systems can support the growth and proliferation of human umbilical vein cells [108]. Another approach used sacrificial fibers selectively removed to improve cell infiltration. The application involved PEO/PCL simultaneously electrospinned fibers, tested for cultures of mesenchymal stem cells. The PEO fibers being water soluble, where selectively diluted in water, provided tunable porosity and enhanced the proliferation of the tested cells [109]. One of the latest developments include the creation of a composite scaffold made of a poly(ether)urethane–polydimethylsiloxane (PEtU–PDMS) semi-interpenetrating polymeric network (semi-IPN) and fibrin loaded GFs, such as vascular endothelial growth factor (VEGF) and basic fibroblast growth factor (bFGF), was manufactured using spray, phase-inversion technique. This multiphase, growth enhanced, and proangiogenic GFs delivery system has proven to possess therapeutic potential for the local treatment of ischemic tissue and wound healing [110].

14.5 Smart Polymers and Biocomposites

The past 10 years have been characterized by an explosion in the field of materials science. It cannot be denied that scientists all over the world excited by the development of smart polymers, composites, and systems invest effort in studying them in potential biomedical applications. The term *Smart* defines a material or system having the ability of adapting itself to external stimulus by a number of ways, for example, shape shifting. The most known nonpolymer biomaterial is the shape memory alloys, such as NiTinol, with many dental applications [111]. Smart polymers are still under development [112, 113], some are already commercially available as in the case of smart polyurethanes (DiAPLEX™) by Mitsui Polymers. Recently, a cardiology product has been released in the market featuring smart characteristics. The discussion is about a cardiology stent dilated with the help of a balloon made from smart shape memory polyurethane as described in a 2002 US patent, and placed inside the blocked arteries of a patient [114].

Many other applications of smart polymer biomaterials and systems have been proposed, and the outcome is presented in some review articles and the open literature. It is the personal belief of the author that intensive biomaterials research on these systems should be conducted along with the novel ones that are being prepared even at a time this article is being written. The demand of the biomaterials market in the coming years, will be for effective adaptive materials for implants,

with self-adjusting material properties, acting as anticoagulants, antimicrobial, antiinflammatory, responsive to mechanical shocks, antiaging, antioxidative, self-cleaning, anti, or promineralizing, pH sensitive, and so on. In other words, materials and systems constantly adapt to the demanding human organism. Shape memory polymers (SMPs) and composites which are responsive to infrared light, water, UV-light, electric current, and so on are available nowadays [115]. Moreover, many more types of shape memory composite biomaterials can be tailored to respond to magnetic fields (e.g., Ni–Zn ferrite nanocomposites) electric or electromagnetic fields [116].

In a recent review on smart polymers for biomedical applications, the authors indicate some examples of commercially available pharmaceutical products based on sol–gel reversible hydrogels used as pulsed drug delivery systems (DDS) [113, 117]. In fact, smart hydrogels have drawn much attention to themselves, due to several features and applications projected in their immediate future. Research in the area of thermoresponsive polymers for drug and gene delivery as well as for tissue adhesion prevention and wound covering has been well established in the past years as reported by Klouda and Mikos [117]. Hydrogels exhibiting a thermosensitive sol–gel behavior have been also studied as cell carriers for tissue engineering purposes [106]. Poly(N-isopropylacrylamide) (pNiPAAm) and its copolymers with other synthetic or natural polymers is one of the most investigated thermoresponsive systems. By controlling the copolymerization process, inherent drawbacks of pNiPAAm like its nonbiodegradability and low mechanical response were improved [107]. Moreover, researchers have achieved to resolve the instability problems of another popular thermoresponsive hydrogel system, Pluronic® [107]. Cases of pH-, glucose-, antigen-, and other biomolecules-sensitive systems are extensively reported [106, 107].

It is generally proposed that tissue engineering will be benefited from advances made with smart polymers and composites. It is expected that the new generation of smart biomaterials will actively promote new functional tissue regeneration or cause self-assembly of supramolecular architectures in cellular levels [107]. As an example, it has been suggested that cartilage can be repaired and regenerated by the use of composites from gelatin, hyaluronic acid, and chondroitin-6-sulfate, mixed with fibrin glue or poly(lactide-*co*-glycolide)alcohol (PLGA), and combined with CTS and/or HAp for mechanical property improvement, combined with cell growth and differentiation factors [108]. Recently, Barrere *et al*. [109] claimed that not only smart biomaterials need to be developed, but also ''smart'' designs of biomaterials systems which incorporate smart and instructive strategies for tissue regeneration. In such a manner, multifunctional smart biocomposites can be designed with tailored properties such as shape memory-biodegradable, osteoconductive composites for bone regeneration based on poly(D,L-lactide) (PDLLA)/HAp biomaterials can be prepared [110]. SMP foams are also a last decade-developed biomaterial aspiring system. The concept of ''cold hibernated elastic memory'' or CHEM is attributed to by Sokolowski *et al*. [111] as novel, simple, ultralight, and self-deployable smart structure. CHEM technology utilizes polyurethane-based SMP in open cellular (foam) structures or sandwich structures made of SMP foam cores and

polymeric composite skins [112]. The CHEM foam technology takes advantage of the polymer's heat activated shape memory in addition to the foam's elastic recovery to deploy a compacted structure. T_g is tailored to deploy and, if needed, rigidize the structure in fully deployed configuration [111]. These smart foams in pure form or as composite structures have been singled out as very useful systems for the endovascular treatment of aneurysms [113].

14.6 Polymer-Nanosystems and Nanocomposites in Medicine

If one would raise the question on how and why the scientists got inspired and went on to pursue nanotechnology applications in the biomedical area, the answer would be profound: ''We just tried to mimic the hierarchical nano-structures of the nature. Some keywords on this: bio-mineralization, hydroxyapatite, collagen, biomimetic structures [114]''.

In the past years, processing techniques such as self-assembly, phase separation, and electrospinning have evolved to allow the fabrication of nanofibers for biomedical scaffolds. These scaffolds are considered as nanostructured systems but can also be enhanced with other types of nanofibers such as SWNTs and MWNTs, a true invention of the new century. With these advances, the long-awaited and much anticipated construction of a truly ''biomimetism'' or ''ideal'' tissue engineered environment, or scaffold, for a variety of tissues is closing nearer. The issue is the creation of highly available nanomaterials for tissue engineering scaffolds that are capable of mimicking native tissue. In a recent review, the most prominent nanofiber-manufacturing techniques for tissue engineering scaffolds were thoroughly examined. It was concluded that nanotechnology will be a key component in the development of the next generation of scaffolds, particularly with respect to the fabrication component [115]. However, still in its infancy, and have already been recognized as strong factors influencing initial cell response, nanomaterials brought in highly specialized high-resolution imaging and analysis techniques and tools that are being developed in parallel with nanotechnology [116].

Almost all types of natural, synthetic, or biodegradable polymers can be electrogel- or melt-spun into nanofibrous composite scaffolds reinforced with nanoparticles such as HAp, collagen, and bioglass particles. Especially PGA/collagen nanosystems are very conducive to research because of the dominant role of collagen in the ECM, bone, cartilage, tendon, and skin, and muscle structural integrity [117]. Complex composite nanofibers made from collagen–CTS were recently proposed as adequate fiber system for tissue engineering [118]. Poly(3-caprolactone)/collagen nanofiber meshes supported well skeletal muscle myotubes, which were self-aligned on the related scaffold. These systems could possibly provide a solution for patients with large muscle defects [119]. HAp being the inorganic part of the human skeleton has been investigated by many in nanoscaled form of particles on needles as the ideal filler for biomedical polymer nanofibers. Candidate soft tissue graft material was prepared by coating chemically grafted silk fibroin

fibers with sintered HAp nanoparticles of about 200 nm [120]. Biodegradable and biocompatible poly(3-hydroxybutyrate-*co*-3-hydroxyvalerate) (PHBV), a copolymer of microbial polyester, was fabricated as a nanofibrous film by electrospinning and composited with HAp by soaking in simulated body fluid and tested for COS-7 cell proliferation with satisfactory results [121]. Alginate hydrogels reinforced with synthetic HAp nanoneedles [52] were studied with respect to their dynamic stiffness with encouraging properties. Very recently, a novel hybrid biomimetic nanocomposite nanofiber of HAp/CTS, with the HAp mass ratio of 30 wt%, prepared by combining an *in situ* coprecipitation synthesis approach with an electrospinning process after the incorporation of about 10 wt% ultrahigh molecular weight poly(ethylene oxide) (UHMWPEO) as a fiber-forming facilitating additive was produced. The hybrid scaffold studied exhibited high bone forming ability, cell proliferation, and mineral deposition as reported by the authors [122]. Hybrid nanofiber membranes based on PLGA and CTS/poly(vinyl alcohol) (PVA) were simultaneously electrospun and cross-linked by glutaraldehyde. Cell culture suggested that electrospun PLGA–chitosan/PVA membrane appears to promote fibroblast attachment and proliferation; it can therefore be assumed that nanofibrous composite membrane of electrospun PLGA–chitosan/PVA could be potentially used for skin reconstruction [123]. We have reported that PCL is quite a useful polymer for tissue engineering purposes, which is slowly resorbed. Hybrid grafting of polymer nanofibers has been also reported to be an efficient way to improve the bioactivity of corresponding engineered scaffolds. Poly(ethylene terephthalate) (PET) fibers were electrospun and treated with methacrylic acid and gelatin to increase their endothelial cell colonization and proliferation properties [124]. Nanofibers of PCL can be easily electrospun from appropriate solutions to produce tissue engineering scaffolds [125]. Moreover, composite nanofibers can also be manufactured by the same technique: for example, calcium carbonate reinforced PCL nanofibers can be formed into membranes for guided bone regeneration [126].

Nanoparticle polymer composites have also been the object of investigation. Zinc oxide nanoparticles were incorporated in an room temperature vulcanizing (RTV) silicone for maxillofacial prosthetics to improve its physical aging characteristics with success [127]. Further, polymer/bioactive glass nanocomposite systems are also under investigation due to the osteoinductive and osteoconductive properties of bioglasses [128]. The combination of bioactive glass nanoparticles or nanofibers with synthetic, natural, or biodegradable polymer systems facilitates the production of nanocomposites with increased potential to be used in orthopedic applications, including scaffolds for tissue engineering and regenerative medicine.

Amidst discussions whether CNs are toxic or nontoxic for the organism, as reported in the introduction of this work and the debut of the graphite monolayers (graphenes), many researchers still hold the debate on their influence on cell differentiation and proliferation [16, 17]. Back in 2003, Gao *et al.* [129] have shown that MWNT can be incorporated into solution-cast UHMWPE films increasing the tensile mechanical properties. This fact can provide a new ultrastrong modified UHMWPE for orthopedic applications. The same authors returned in 2006 with gel-spun UHMWPE/MWNT ultrastrong fibers showing that a mere 5 wt% in

MWNT can significantly increase the fiber performance [130]. As far as the cell attachment and proliferation on CN polymer composite implants is concerned, results are somewhat controversial. Webster *et al*. [131] have shown that CNs in a polycarbonate–polyurethane (PCU) matrix promoted osteoblast adhesion whereas smooth muscle cell, fibroblast, and chondrocyte adhesion decreased with an increase in either carbon nanofiber (CNF) surface energy or simultaneous change in CNF chemistry. The greater weight percentages of high surface energy CNFs in the PCU/CNF composite the more osteoblast adhesion increased while at the same time fibroblast adhesion decreased [131]. The same authors in a 2004 review study insisted that PU/MWNT nanocomposites provide good support for neural cell function, decreased astrocyte adhesion density [132] and can be easily tailored with respect to their electrical properties. These conditions, together, represent acceptable parameters for further investigation of CNs as a neural probes. Similarly, the increased adhesion of osteoblasts, accompanied by the decreased adhesion of fibroblasts, and tunable mechanical properties of PU composites containing CNs provide strong candidateship for these materials in bone tissue engineering applications [133]. Graphene, in few-layered leafs, has been used to reinforce chitosan films produced by solution casting method. The mechanical properties of these nanocomposite films were tested by nanoindentation. The addition of small amounts of graphene (0.1–0.3 wt%), resulted in an increase of elastic modulus over ~200%. The biocompatibility of graphene/chitosan composite films was checked by tetrazolium-based colorimetric assays *in vitro*. The cell adhesion experiments showed that L929 cells adhere well and flourish on the graphene/chitosan composite films indicating that graphene/chitosan composites show good biocompatibility [134].

14.7 Conclusions

The past decade has brought about many changes in our views of polymers and polymer composites applications in the biomedical field. There were two main reasons for investing huge amount of money for research work in this field: Firstly, the boom in tissue engineering which facilitated the use of multiple cell cultures in the screening of new categories of polymer composite biomaterials. The second reason was the availability of many types of nanophase fillers, fibers, particles, or the techniques for their synthesis for the manufacturing of the corresponding candidate polymer biomedical nanocomposites. It is evident in many studies that numerous systems of polymer composites and nanocomposites are nowadays strong potential candidates for usage in tissue engineering and biomaterial applications as implants. There are however several drawbacks which still have not been overcome. In the field of orthopedics for instance, no candidate composite polymer biomaterial has the ability to match the mechanical properties of the bone and cannot be therefore used for load bearing applications. Commercially available PEEK/CF implant systems are quite well studied, but real long-term results from implants

have not been made available as yet. In the field of neural axis scaffolds, it is difficult to alter the growth of neural axis lengths above a critical defect size in any system. Cartilage and ligament tissue engineering still struggle to make polymer composite materials work for the reconstruction of damaged tissue and regeneration of new ones. Polymers and composites cannot survive long periods of time inside the urinary system when used as stents owing to aging and stone formations. On the other hand, substantial progress can be foreseen in the field of tissue engineering especially for composite implants and scaffolds impregnated with targeted cell growth factors (i.e., bone growth factors (BGF) and nerve growth factors (NGF)). Further, smart polymer composite systems slowly emerge in cardiology and other applications [147]. Much hope is placed in nanomechanics and nanomaterials engineering that, in combination with smart polymer technology, will probably provide the next generation biomaterials.

14.8 Outlook

The dawn of the twenty-first century has provided science with new methods, paths, and technologies for the manufacture of the new generations of biomaterials. Nanomaterials and nanoengineering are still in their infancy and soon applications from that regime will emerge in the biomedical sector. Smart bioresorbable composite scaffolds impregnated with bioactive molecules and proteins, reinforced with fibers in the macro or in the nano scale with tunable load bearing capabilities were needed, and if possible seeded with the appropriate cell types will provide solutions in restoration of scarred tissue or in smaller or larger hard or soft tissue defects. The actual challenge for scientists from all different fields active in biomaterials science and engineering is to harness and combine all the above characteristics in practical systems to provide increased functionality to medical surgeons and at rational costs.

References

1. Park, J.B. (1984) *Biomaterials Science and Engineering*, Plenum Publishing Co., New York.
2. J. Charnley. (1974) *The Closed Treatment of Common Fractures*, 3rd edn, Churchill Livingstone Edinburgh and London, ISBN: 0-443-00119-7.
3. Gage, E., Langevin, C.-J., and Papay, F. (2010) . *Plast. Reconstr. Surg.: Springer Specialist Surg. Ser.* Pt. 2, 125–135. doi: 10.1007/978-1-84882-513-0_11
4. Colas, A. and Curtis, J. (2004) Silicone biomaterials: history and chemistry and medical applications of silicones, in *Biomaterials Science*, 2nd edn, Elsevier, New York.
5. Wahl, D.A. and Czernuszka, J.T. (2006) Collagen-hydroxyapatite composites for hard tissue repair. *J. Eur. Cells Mater.*, **11**, 43–56.
6. Vallet-Regı´, M. and Gonza´lez-Calbet, J.M. (2004) Calcium phosphates as substitution of bone tissues. *Prog. Solid State Chem.*, **32**, 1–31.
7. Goel, R., Aron, M., Kesarwani, P.K., and Gupta, N.P. (2003) An unusual complication of urethral stent. *Int. Urol. Nephrol.*, **35**, 197–198.

8. Chevalier, J. (2006) What future for zirconia as a biomaterial? *Biomaterials*, **27** (4), 535–543.
9. Skinner, H.B. (1988) Composite technology for total hip arthroplasty. *Clin. Orthop. Relat. Res.*, **235**, 224–36.
10. Buddy, D. Ratner, Michael, L. and Myrna, Darland *Biomaterials Science*, 3rd edn, An Introduction to Materials in Medicine,Academic Press-Elsevier ISBN: 9780123746269.
11. Ramakrishna, S., Mayer, J., Wintermantel, E., and Leong, K.W. (2001) Biomedical applications of polymer-composite materials: a review. *J. Compos. Sci. Technol.*, **61** (9), 1189–1224.
12. MarketsandMarkets Global Biomaterials Market (2009–2014) *http://www.marketsandmarkets.com/PressReleases/global-biomaterials-market-worth-US58.1-Billion-by-2014.asp* (accessed 1 April 2013).
13. Bischoff, F. (1972) Organic polymer biocompatibility and toxicology. *J. Clin. Chem.*, **18** (9), 869.
14. M. Endo, S. Iijima, M.S. Dresselhaus (eds) *Carbon Nanotubes*, Carbon, Vol. 33 Pergamon Press, New York, (1996) ISBN: 0080426824 (reprinted).
15. Novoselov, K.S., Geim, A.K., Morozov, S.V., Jiang, D., Zhang, Y., Dubonos, S.V., Grigorieva, I.V., and Firsov, A.A. (2004) Electric field effect in atomically thin carbon films. *Science*, **306**, 666.
16. Smart, S.K., Cassady, A.I., Lu, G.Q., and Martin, D.J. (2006) The biocompatibility of carbon nanotubes. *Carbon*, **44**, 1034–1047.
17. Shen, J., Shi, M., Yan, B., Ma, H., Li, N., Hu, Y., and Ye, M. (2010) Covalent attaching protein to graphene oxide via diimide-activated amidation. *Colloids Surf., B*, **81**, 434–438.
18. Christopher, M.B. (2009) Biocompatibility of polymer implants for medical applications. MSc thesis. University of Akron, August 2009.
19. Francolini, I., Donelli, G., and Stoodley, P. (2004) Polymer designs to control biofilm growth on medical devices. *J. Environ. Sci. Biotechnol.*, **2**, 307–319.
20. Jansen, B. and Kohnen, W. (1995) Prevention of biofilm formation by polymer modification. *J. Ind. Microbiol.*, **15**, 391–396.
21. Bithelis, G., Bouropoulos, N., Latinos, E., Perimenis, P., Koutsoukos, P., and Barbalias, G. (2004) Assessment of encrustations in polyurethane ureteral stents. *J. Endourol.*, **18**, 550.
22. Mouzakis, D.E., Bouropoulos, N., Bithelis, G., Liatsikos, E., and Barbalias, G. (2006) Ageing assessment by dynamic mechanical analysis of in-vivo encrusted polymeric urinary stents. *J. Endourol.*, **20**, 64.
23. Bouropoulos, N., Mouzakis, D.E., Bithelis, G., Liatsikos, E., and Barbalias, G. (2006) Vickers hardness studies of calcium oxalate monohydrate and brushite urinary stones. *J. Endourol.*, **20**, 59.
24. Veparia, C. and Kaplan, D.L. (2007) Silk as a biomaterial. *J. Prog. Polym. Sci.*, **32**, 991–1007.
25. Moy, R.L., Lee, A., and Zalka, A. (1991) Commonly used suture materials in skin surgery. *J. Am. Fam. Phys.*, **44** (6), 2123–2128.
26. Zhang, Y.-Q. (2002) Applications of natural silk protein sericin in biomaterials. *Biotechnol. Adv.*, **20**, 91–100.
27. Jin, H.-J., Chen, J., Karageorgiou, V., Altman, G.H., and Kaplan, D.L. (2004) Human bone marrow stromal cell responses on electrospun silk fibroin mats. *J. Biomater.*, **25**, 1039–1047.
28. Li, C., Vepari, C., Jin, H.-J., Kim, H.J., and Kaplan, D.L. (2006) Electrospun silk-BMP-2 scaffolds for bone tissue engineering. *J. Biomater.*, **27**, 3115–3124.
29. Jayakumar, R., Nwe, N., Tokura, S., and Tamura, H. (2007) Sulfated chitin and chitosan as novel biomaterials. *Int. J. Biol. Macromol.*, **40**, 175–181.
30. Chen, F., Wang, Z.-C., and Lin, C.-J. (2002) Preparation and characterization of nano-sized hydroxyapatite particles and hydroxyapatite/chitosan nano-composite for use in biomedical materials. *J. Mater. Lett.*, **57**, 858–861.
31. Bhattarai, N., Edmondson, D., Veiseh, O., Matsen, F.A., and Zhang, M. (2005) Electrospun

chitosan-based nanofibers and their cellular compatibility. *J. Biomater.*, **26**, 6176–6184.
32. Sarasam, A. and Madihally, S.V. (2005) Characterization of chitosan–polycaprolactone blends for tissue engineering applications. *J. Biomater.*, **26**, 5500–5508.
33. Wang, X.H., Li, D.P., Wang, W.J., Feng, Q.L., Cui, F.Z., Xu, Y.X., Song, X.H., and van der Werf, M. (2003) Crosslinked collagen/chitosan matrix for artificial livers. *J. Biomater.*, **24**, 3213–3220.
34. Vasiliu, S., Popa, M., and Rinaudo, M. (2005) Polyelectrolyte capsules made of two biocompatible natural polymers. *Eur. Polym. J.*, **41**, 923–932.
35. Rusu, V.M., Ng, C.-H., Wilke, M., Tiersch, B., Fratzl, P., and Peter, M.G. (2005) Size-controlled hydroxyapatite nanoparticles as self-organized organic–inorganic composite materials. *J. Biomater.*, **26**, 5414–5426.
36. Malafaya, P.B., Silva, G.A., and Reis, R.L. (2007) Natural–origin polymers as carriers and scaffolds for biomolecules and cell delivery in tissue engineering applications. *Adv. Drug Delivery Rev.*, **59**, 207–233.
37. Sikorski, Z.E. (2001). *Chemical and Functional Properties of Food Proteins.* Boca Raton, FL: CRC Press, p. 242, ISBN: 1566769604.
38. Kikuchi, M., Itoh, S., Ichinose, S., Shinomiya, K., and Tanaka, J. (2001) Self-organization mechanism in a bone-like hydroxyapatite/collagen nanocomposite synthesized in vitro and its biological reaction in vivo. *J. Biomater.*, **22**, 1705–1711.
39. Coombes, A.G.A., Verderio, E., Shaw, B., Lib, X., Griffin, M., and Downes, S. (2002) Biocomposites of non-crosslinked natural and synthetic polymers. *J. Biomater.*, **23**, 2113–2118.
40. Dai, N.-T., Williamson, M.R., Khammo, N., Adams, E.F., and Coombes, A.G.A. (2004) Composite cell support membranes based on collagen and polycaprolactone for tissue engineering of skin. *J. Biomater.*, **25**, 4263–4271.
41. Zhang, J., Senger, B., Vautier, D., Picart, C., Schaaf, P., Voegel, J.-C., and Lavalle, P. (2005) Natural polyelectrolyte films based on layer-by layer deposition of collagen and hyaluronic acid. *J. Biomater.*, **26**, 3353–3361.
42. Rho, K.S., Jeong, L., Lee, G., Seo, B.-M., Park, Y.J., Hong, S.-D., Roh, S., Cho, J.J., Park, W.H., and Min, B.-M. (2006) Electrospinning of collagen nanofibers: effects on the behavior of normal human keratinocytes and early-stage wound healing. *J. Biomater.*, **27**, 1452–1461.
43. Ghasemi-Mobarakeh, L., Prabhakaran, M.P., Morshed, M., Nasr-Esfahani, M.-H., and Ramakrishna, S. (2008) Electrospun poly(3-caprolactone)/gelatin nanofibrous scaffolds for nerve tissue engineering. *J. Biomater.*, **29**, 4532–4539.
44. Li, M., Mondrinos, M.J., Gandhi, M.R., Ko, F.K., Weiss, A.S., and Lelkes, P.I. (2005) Electrospun protein fibers as matrices for tissue engineering. *J. Biomater.*, **26**, 5999–6008.
45. Mithieux, S.M., Raskob, J.E.J., and Weiss, A.S. (2004) Synthetic elastin hydrogels derived from massive elastic assemblies of self-organized human protein monomers. *J. Biomater.*, **25**, 4921–4927.
46. Kuo, C.K. and Ma, P.X. (2001) Ionically crosslinked alginate hydrogels as scaffolds for tissue engineering: part 1. Structure, gelation and mechanical properties. *J. Biomater.*, **22** (6), 511–521.
47. Griffith, L.G. (2000) Polymeric biomaterials. *Acta Mater.*, **48**, 263–277.
48. Solchaga, L.A., Goldberg, V.M., and Caplan, A.I. (2001) Cartilage regeneration using principles of tissue engineering. *Clin. Orthopaedics*, **391S**, S161.
49. Hoffman, A. (2002) Hydrogels for biomedical applications. *Adv. Drug Delivery Rev.*, **54** (1), 3–12.
50. Lin, H.R. and Yeh, Y.J. (2004) *J. Biomed. Mater. Res. Part B*, **71**, 52.
51. Hosoya, K., Ohtsuki, C., Kawai, T., Kamitakahara, M., Ogata, S., Miyazaki, T., and Tanihara, M. (2004) A novel covalently crosslinked

gel of alginate and silane with the ability to form bone-like apatite. *J. Biomed. Mater. Res.*, **71A**, 596–601. doi: 10.1002/jbm.a.30189

52. Bouropoulos, N., Stampolakis, A., and Mouzakis, D.E. (2010) Dynamic mechanical properties of calcium alginate-hydroxyapatite nanocomposite hydrogels. *Sci. Adv. Mater.*, **2**, 1–4.
53. Dang, J.M. and Leong, K.W. (2006) Natural polymers for gene delivery and tissue engineering. *Adv. Drug Delivery Rev.*, **58**, 487–499.
54. Chang, C.-H., Liu, H.-C., Lin, C.-C., Chou, C.-H., and Lin, F.-H. (2003) Gelatin–chondroitin–hyaluronan tri-copolymer scaffold for cartilage tissue engineering. *J. Biomater.*, **24**, 4853–4858.
55. Paturau, J.M. (1989) *By-Products of the Cane Sugar Industry*, Sugar Series, Vol. 11, Elsevier, New York.
56. Lam, C.X.F., Mo, X.M., Teoh, S.H., and Hutmacher, D.W. (2002) Scaffold development using 3D printing with a starch-based polymer. *Mater. Sci. Eng., C*, **20**, 49–56.
57. Alves, C.M., Yang, Y., Carnes, D.L., Ong, J.L., Sylvia, V.L., Dean, D.D., Agrawal, C.M., and Reis, R.L. (2007) Modulating bone cells response onto starch-based biomaterials by surface plasma treatment and protein adsorption. *J. Biomater.*, **28** (2), 307–315.
58. Shukla, R. and Munir, C. (2001) Zein: the industrial protein from corn. *Ind. Crops Prod.*, **13**, 171–92.
59. Mathiowitz, E., Bernstein, H., Morrel, E., and Schwaller, K. (1991) Method for producing protein microspheres. WO Patent 91/06286.
60. Lai, H.M. and Padua, G.W. (1997) Properties and macrostructure of zein sheets plasticized with palmitic and stearic acids. *Cereal Chem.*, **74** (77), 1–5.
61. Dong, J., Sun, Q., and Wang, J.-Y. (2004) Basic study of corn protein, zein, as a biomaterial in tissue engineering, surface morphology and biocompatibility. *J. Biomater.*, **25**, 4691–4697.
62. Frankel, V.H., Serafica, G.C., and Damien, C.J. (2004) Development and testing of a novel biosynthesized XCell for treating chronic wounds. *Surg Technol Int.*, **12**, 27–33.
63. Hutchens, S.A., Benson, R.S., Evans, B.R., O'Neill, H.M., and Rawn, C.J. (2006) Biomimetic synthesis of calcium-deficient hydroxyapatite in a natural hydrogel. *J. Biomater.*, **27**, 4661–4670.
64. Nair, L.S. and Laurencin, C.T. (2007) Biodegradable polymers as biomaterials. *Prog. Polym. Sci.*, **32**, 762–798.
65. Gunatillake, P.A. and Adhikari, R. (2003) Biodegradable synthetic polymers for tissue engineering. *Eur. Cells Cultures*, **5**, 1–16.
66. John C, Middleton and Arthur J, Tipton (2000) Biodegradable synthetic polymers for tissue engineering. *Biomaterials*, **21** (23), 2335–2346.
67. Holland, S.J., and Tighe, B.J. (2007) in *Biodegradable polymers*, in Advances in Pharmaceutical Science, Vol. 6 pp. 101–164.
68. Hayashi, T. (1994) Biodegradable polymers for biomedical uses. *Prog. in Polym. Sci. (Oxford)*, **19**, (4) 663–702.
69. Kharas, G.B., Kamenetsky, M, Simantirakis, J., Beinlich, K.C. Rizzo, A.T., Caywood, G.A. and Watson, K. (1997) Synthesis and characterization of fumarate-based polyester for use in bioresorbable bone cement composites. *J. Appl. Polym. Sci.*, **66**, 1123–1137.
70. Peter, S.J., Miller, S.T., Zhu, G., Yasko, A.W., and Mikos, A.G. (1998) *In vivo* degradation of a poly(propylene fumarate)/í-tricalcium phosphate injectable composite scaffold. *J. Biomed. Mater. Res.*, **41**, 1–7.
71. Temenoff, J.S., and Mikos, A.G. (2000) Injectable biodegradable materials for orthopedic tissue engineering. *Biomaterials*, **21** (23), 2405–2412.
72. Leong, K.W., Brott, B.C., and Langer, R. (1985) Bioerodible polyanhydrides as drug-carrier matrices. I: Characterization, degradation, and release characteristics. *J. Biomed. Mater. Res.*, **19**, 941–955.
73. Uhrich, K.E., Thomas, T.T., Laurencin, C.T., and Langer, R. (1997) *In vitro*

degradation characteristics of poly(anhydride-imide) containing trimellitylimidoglycine. *J. Appl. Polym. Sci.*, **63**, 1401–1411.

74. Pulapura, S., and Kohn, J. (1992) Tyrosine-derived polycarbonates: Backbone-modified ''pseudo''-poly(amino acids) designed for biomedical applications. *Biopolymers*, **32**, 411–471 doi: 10.1002/bip.360320418

75. Muggli, D.S., Burkoth, A.K., Keyser, S.A., Lee, H.R., and Anseth, K.S. (1998) Reaction behaviour of biodegradable, photo cross-linkable polyanhydrides. *Macromolecules*, **31**, 4120–4125.

76. Bruin, P., Venstra, G.J., Nijenhuis, A.J., and Pennings, A.J. (1988) Design and synthesis of biodegradable poly(esterurethane) elastomer networks composed of non-toxic building blocks. *Makromol. Chem. Rapid Commun.*, **9**, 589–594.

77. Qui, L.Y. and Zhu, K.J. (2000) Novel biodegrable polyphosphazenes containing glycine ethyl ester and benzyl ester of amino acethydroxamic acid as cosubsituents: synthesis, characterization and degradation properties. *J. Appl. Polym. Sci.*, **77**, 2987–2955.

78. Rezwan, K., Chen, Q.Z., Blaker, J.J., and Boccaccini, A.R. (2006) Biodegradable and bioactive porous polymer/inorganic composite scaffolds for bone tissue engineering. *J. Biomater.*, **27**, 3413–3431.

79. Kurtz, S.M. and Devine, J.N. (2007) PEEK biomaterials in trauma, orthopedic, and spinal implants. *J. Biomater.*, **28**, 4845–4869.

80. Chowdhury, S., Vohra, Y.K., Lemons, J.E., Ueno, M., and Ikeda, J. (2006) Accelerating aging of zirconia femoral head implants: change of surface structure and mechanical properties. *J. Biomed. Mater. Res. Part B*, **81B** (2007), 486–492.

81. Haraguchi, K., Sugano, N., Nishii, T., Miki, H., Oka, K., and Yoshikawa, H. (2001) Phase transformation of a zirconia ceramic head after total hip arthroplasty. *J. Bone Joint Surg. Br.*, **83-B**, 996–1000.

82. Panagiotopoulos, E.C., Kallivokas, A.G., Koulioumpas, I., and Mouzakis, D.E. (2007) Early failure of a zirconia femoral head prosthesis: fracture or fatigue? *Clin. Biomech.*, **22** (7), 856–60.

83. Abu Bakar, M.S., Cheng, M.H.W., Tang, S.M., Yuc, S.C., Liao, K., Tan, C.T., Khor, K.A., and Cheang, P. (2003) Tensile properties, tension–tension fatigue and biological response of polyetheretherketone–hydroxyapatite composites for load-bearing orthopedic implants. *J. Biomater.*, **24**, 2245–2250.

84. Kim, J.K., Wo, D.Z., Zhou, L.M., Huang, H.T., Lau, K.T., and Wang, M. (2007) Study on a stiffness design method of femoral prosthesis stem using fiber reinforced composites. *Key Eng. Mater.*, **334–335**, 1257–1260.

85. Biermann, P.J., Roberts, J.C., and Corvelli, A.A. (2003) Polymeric composite orthopedic implant. US Patent 6,602,293, Aug. 5, 2003.

86. Fujihara, K., Huang, Z.-M., Ramakrishna, S., Satknanantham, K., and Hamada, H. (2004) Feasibility of knitted carbon/PEEK composites for orthopedic bone plates. *J. Biomater.*, **25**, 3877–3885.

87. Fujihara, K., Huang, Z.-M., Ramakrishna, S., Satknanantham, K., and Hamada, H. (2003) Performance study of braided carbon/PEEK composite compression bone plates. *J. Biomater.*, **24**, 2661–2667.

88. Zhao, J.-L., Fu, T., Han, Y., and Xu, K.-W. (2003) Reinforcing hydroxyapatite/thermosetting epoxy composite with 3-D carbon fiber fabric through RTM processing. *Mater. Lett.*, **58**, 163–168.

89. Bonfield, W., Wang, M., and Tanner, K.E. (1998) Interfaces in analogue biomaterials. *Acta Mater.*, **46**, 2509–2518.

90. Salernitano, E. and Migliaresi, C. (2003) Composite materials for biomedical applications: a review. *J. Appl. Biomater. Biomech.*, **1**, 3–18.

91. Ohtsuki, C., Miyazaki, T., Kyomoto, M., Tanihara, M., and Osaka, A. (2001) Development of bioactive PMMA-based cement by modification with alkoxysilane and calcium salt. *J. Mater. Sci. - Mater. Med.*, **12** (10–12), 895–899.

92. Mouzakis, D.E., Dimogianopoulos, D., and Giannikas, D. (2009) Contact-free

magnetoelastic smart microsensors with stochastic noise filtering for diagnosing orthopedic implant failures. *IEEE Trans. Ind. Electron.*, **56** (4), 1092–1100.

93. Brooks, R.A., Jones, E., Storer, A., and Rushton, N. (2004) Biological evaluation of carbon-fibre-reinforced polybutyleneterephthalate (CFRPBT) employed in a novel acetabular cup. *J. Biomater.*, **25**, 3429–3438.

94. Aho, A.J., Hautamäki, M., Mattila, R., Alander, P., Strandberg, N., Rekola, J., Gunn, J., Lassila, L.V.J., and Vallittu, P.K. (2004) Surface porous fibre-reinforced composite bulk bone substitute. *Cell Tissue Banking*, **5**, 213–221.

95. Pegoretti, A., Fambri, L., Zappini, G., and Bianchetti, M. (2002) Finite element analysis of a glass fibre reinforced composite endodontic post. *J. Biomater.*, **23**, 2667–2682.

96. Papadopoulos, T., Papadogiannis, D., Mouzakis, D.E., Giannadakis, K., and Papanicolaou, G. (2010) Experimental and numerical determination of the mechanical response of teeth with reinforced posts. *Biomed. Mater.*, **5**. doi: 10.1088/1748-6041/5/3/035009

97. Lassila, L.V.J., Tanner, J., Le Bell, A.-M., Narva, K., and Vallittu, P.K. (2004) Flexural properties of fiber reinforced root canal posts. *Dent. Mater.*, **20**, 29–36.

98. Xie, Q., Lassila, L.V.J., and Vallittu, P.K. (2007) Comparison of load-bearing capacity of direct resin-bonded fiber-reinforced composite FPDs with four framework designs. *J. Dent.*, **35**, 578–582.

99. Vallittu, P.K. (2004) Survival rates of resin-bonded, glass fiber–reinforced composite fixed partial dentures with a mean follow-up of 42 months: a pilot study. *J. Prosthet. Dent.*, **91**, 241–6.

100. Narva, K.K., Lassila, L.V.J., and Vallittu, P.K. (2004) Fatigue resistance and stiffness of glass fiber-reinforced urethane dimethacrylate composite. *J. Prosthet. Dent.*, **91** (2), 158–163.

101. Fennis, W.M.M., Tezvergil, A., Kuijs, R.H., Lassila, L.V.J., Kreulen, C.M., Creugers, N.H.J., and Vallittu, P.K. (2005) In vitro fracture resistance of fiber reinforced cusp-replacing composite restorations. *Dent. Mater.*, **21**, 565–572.

102. Fujihara, K., Teo, K., Gopal, R., Loh, P.L., Ganesh, V.K., Ramakrishna, S., Foong, K.W.C., and Chew, C.L. (2004) Fibrous composite materials in dentistry and orthopaedics: review and applications. *Compos. Sci. Technol.*, **64**, 775–788.

103. Dyer, S.R., Lassila, L.V.J., Jokinen, M., and Vallittu, P.K. (2004) Effect of fiber position and orientation on fracture load of fiber-reinforced composite. *Dent. Mater.*, **20**, 947–955.

104. Tezvergil, A., Lassila, L.V.J., and Vallittu, P.K. (2005) The shear bond strength of bidirectional and random-oriented fibre-reinforced composite to tooth structure. *J. Dent.*, **33**, 509–516.

105. Garoushi, S., Vallittu, P.K., and Lassila, L.V.J. (2007) Short glass fiber reinforced restorative composite resin with semi-inter penetrating polymer network matrix. *Dent. Mater.*, **23**, 1356–1362.

106. Väkiparta, M., Forsback, A.-P., Lassila, L.V., Jokinen, M., Yli-Urpo, A.U.O., and Vallittu, P.K. (2005) Biomimetic mineralization of partially bioresorbable glass fiber reinforced composite. *J. Mater. Sci. - Mater. Med.*, **16**, 873–879.

107. Kurunmäki, H., Kantola, R., Hatamleh, M.M., Watts, D.C., and Vallittu, P.K. (2008) A fiber-reinforced composite prosthesis restoring a lateral midfacial defect: a clinical report. *J. Prosthet. Dent.*, **100**, 348–352.

108. Williamson, M.R., Black, R., and Kielty, C. (2006) PCL–PU composite vascular scaffold production for vascular tissue engineering: attachment, proliferation and bioactivity of human vascular endothelial cells. *J. Biomater.*, **27**, 3608–3616.

109. Baker, B.M., Gee, A.O., Metter, R.B., Nathan, A.S., Marklein, R.A., Burdick, J.A., and Mauck, R.L. (2008) The potential to improve cell infiltration in composite fiber-aligned electrospun scaffolds by the selective removal of sacrificial fibers. *J. Biomater.*, **29**, 2348–2358.

110. Losi, P., Briganti, E., Magera, A., Spiller, D., Ristori, C., Battolla, B., Balderi, M., Kull, S., Balbarini, A., Di Stefano, R., and Soldani, G. (2010) Tissue response to poly(ether)urethane-polydimethylsiloxane-fibrin composite scaffolds for controlled delivery of pro-angiogenic growth factors. *J. Biomater.*, **31** (20), 5336–5344.

111. Gautam, P. and Valiathan, A. (2008) Bio-smart dentistry: stepping into the future!. *Trends Biomater. Artif. Organs*, **21** (2), 94–97.

112. Yakacki, C.M. and Gall, K. (2010) Shape-memory polymers for biomedical applications in: shape-memory polymers. *Adv. Polym. Sci.*, **226**, 147–175. doi: 10.1007/978-3-642-12359-7_23

113. Aguilar, M.R., Elvira, C., Gallardo, A., Vázquez, B., and Román, J.S. (2007) in *Smart Polymers and Their Applications as Biomaterials*, Topics in Tissue Engineering, Vol. 3 (eds N. Ashammakhi, R. Reis, and E. Chiellini). e-book, University of Oulu, Finland http://www.oulu.fi/spareparts/ebook_topics_in_t_e_vol3/index.html.

114. Chrisnan, M. (2002) Polyurethane elastomer article with ''shape memory'' and medical devices therefrom. US Patent 2002/0065373 A1, May 30.

115. Behl, M. and Lendlein, A. (2007) Shape-memory polymers. *Mater. Today*, **10** (4), 20–28.

116. Ratna, D. and Karger-Kocsis, J. (2008) Recent advances in shape memory polymers and composites: a review. *J. Mater. Sci.*, **43**, 254–269.

117. Klouda, L. and Mikos, A.G. (2008) Thermoresponsive hydrogels in biomedical applications. *Eur. J. Pharm. Biopharm.*, **68**, 34–45.

118. Kopecek, J. (2007) Hydrogel biomaterials: a smart future? *J. Biomater.*, **28**, 5185–5192.

119. Chaterji, S., Kwon, K. II,, and Park, K. (2007) Smart polymeric gels: redefining the limits of biomedical devices. *Prog. Polym. Sci.*, **32**, 1083–1122.

120. Stoop, R. (2008) Smart biomaterials for tissue engineering of cartilage. Injury. *Int. J. Care Inj.*, **39S1**, S77–S87.

121. Barrere, F., Mahmood, T.A., de Groot, K., and van Blitterswijk, C.A. (2008) Advanced biomaterials for skeletal tissue regeneration: instructive and smart functions. *Mater. Sci. Eng. R*, **59**, 38–71.

122. Zheng, X., Zhou, S., Li, X., and Weng, J. (2006) Shape memory properties of poly(D,L-lactide)/hydroxyapatite composites. *J. Biomater.*, **27**, 4288–4295.

123. Sokolowski, W., Metcalfe, A., Hayashi, S., Yahia, L., and Raymond, J. (2007) Medical applications of shape memory polymers. *Biomed. Mater.*, **2**, S23–S27.

124. Sokolowski, W. (2004) Cold hibernated elastic memory self-deployable and rigidizable structure and method therefore. US Patent 6,702,976 B2, Mar. 9, 2004.

125. Metcalfe, A., Desfaits, A.C., Salazkin, I., Yahia, L., Sokolowski, W.M., and Raymond, J. (2003) Cold hibernated elastic memory foams for endovascular interventions. *J. Biomater.*, **24**, 491–497.

126. G.M. Luz, J.F. Mano. Mineralized structures in nature: examples and inspirations for the design of new composite materials and biomaterials. *Compos. Sci. Technol.* (2010) **70** (13), 1777–1788 doi: 10.1016/j.compscitech.2010.05.013

127. Barnes, C.P., Sell, S.A., Boland, E.D., Simpson, D.G., and Bowlin, G.L. (2007) Nanofiber technology: designing the next generation of tissue engineering scaffolds. *Adv. Drug Delivery Rev.*, **59**, 1413–1433.

128. Liu, H. and Webster, T.J. (2007) Nanomedicine for implants: a review of studies and necessary experimental tools. *J. Biomater.*, **28**, 354–369.

129. Cen, L., Liu, W., Cui, L., Zhang, W., and Cao, Y. (2008) Collagen tissue engineering: development of novel biomaterials and applications. *Pediatric Res.*, **63** (5), 492–496.

130. Chen, Z., Mo, X., and Qing, F. (2007) Electrospinning of collagen–chitosan complex. *Mater. Lett.*, **61**, 3490–3494.

131. Choi, J.S., Lee, S.J., Christ, G.J., Atala, A., and Yoo, J.J. (2008) The

influence of electrospun aligned poly(3-caprolactone)/collagen nanofiber meshes on the formation of self-aligned skeletal muscle myotubes. *J. Biomater.*, **29**, 2899–2906.

132. Furuzono, T., Kishida, A., and Tanaka, J. (2004) Nano-scaled hydroxyapatite/polymer composite I. Coating of sintered hydroxyapatite particles on poly(γ-methacrylopropyl trimethoxysilane)-grafted silk fibroin fibers through chemical bonding. *J. Mater. Sci. - Mater. Med.*, **15**, 19–23.

133. Ito, Y., Hasuda, H., Kamitakahara, M., Ohtsuki, C., Tanihara, M., Kang, I.-K., and Kwon, O.H. (2005) A composite of hydroxyapatite with electrospun biodegradable nanofibers as a tissue engineering material. *J. Biosci. Bioeng.*, **100** (1), 43–49. doi: 10.1263/jbb.100.43

134. Zhang, Y., Venugopal, J.R., El-Turki, A., Su, S.R.B., and Lim, C.T. (2008) Electrospun biomimetic nanocomposite nanofibers of hydroxyapatite/chitosan for bone tissue engineering. *J. Biomater.*, **29**, 4314–4322.

135. Duan, B., Yuan, X., Zhu, Y., Zhang, Y., Li, X., Zhang, Y., and Yao, K. (2006) A nanofibrous composite membrane of PLGA–chitosan/PVA prepared by electrospinning. *Eur. Polym. J.*, **42**, 2013–2022.

136. Ma, Z., Kotaki, M., Yong, T., Heb, W., and Ramakrishna, S. (2005) Surface engineering of electrospun polyethylene terephthalate (PET) nanofibers towards development of a new material for blood vessel engineering. *J. Biomater.*, **26**, 2527–2536.

137. Xie, J., Willerth, S.M., Li, X., Macewan, M.R., Rader, A., Sakiyama-Elbert, S.E., and Xia, Y. (2009) The differentiation of embryonic stem cells seeded on electrospun nanofibers into neural lineages. *J. Biomater.*, **30**, 354–362.

138. Fujihara, K., Kotaki, M., and Ramakrishna, S. (2005) Guided bone regeneration membrane made of polycaprolactone/calcium carbonate composite nano-fibers. *J. Biomater.*, **26**, 4139–4147.

139. Mouzakis, D.E., Papadopoulos, T.D., Polyzois, G.L., and Griniari, P.G. (2010) Dynamic mechanical properties of a maxillofacial silicone elastomer incorporating a ZnO additive: the effect of artificial aging. *J. Craniofac. Surg.*, **21** (6), 1867–1871.

140. Boccaccini, A.R., Erol, M., Stark, W.J., Mohn, D., Hong, Z., and Mano, J.F. (2010) Polymer/bioactive glass nanocomposites for biomedical applications: a review. *Compos. Sci. Technol.*, **70**, 1764–1776.

141. Ruan, S.L., Gao, P., Yang, X.G., and Yu, T.X. (2003) Toughening high performance ultrahigh molecular weight polyethylene using multiwalled carbon nanotubes. *J. Polym.*, **44**, 5643–5654.

142. Ruan, S., Gao, P., and Yu, T.X. (2006) Ultra-strong gel-spun UHMWPE fibers reinforced using multiwalled carbon nanotubes. *J. Polym.*, **47**, 1604–1611.

143. Price, R.L., Waid, M.C., Haberstroh, K.M., and Webster, T.J. (2003) Selective bone cell adhesion on formulations containing carbon nanofibers. *Biomaterials*, **24**, 1877–1887.

144. McKenzie, J.L., Waid, M.C., Shi, R., and Webster, T.J. (2004) Decreased functions of astrocytes on carbon nanofiber materials. *J. Biomater.*, **25**, 1309–1317.

145. Webster, T.J., Waid, M.C., McKenzie, J.L., Price, R.L., and Ejiofor, J.U. (2004) Nano-biotechnology: carbon nanofibres as improved neural and orthopaedic implants. *Nanotechnology*, **15**, 48–54.

146. Fan, H., Wang, L., Zhao, K., Li, N., Shi, Z., Ge, Z., and Jin, Z. (2010) Fabrication, mechanical properties, and biocompatibility of graphene-reinforced chitosan composites. *J. Biomacromol.*, **11**, 2345–2351.

147. Furth, M.E., Atala, A., and Van Dyke, M.E. (2007) Smart biomaterials design for tissue engineering and regenerative medicine. *J. Biomater.*, **28**, 5068–5073.

15
Environmental Effects, Biodegradation, and Life Cycle Analysis of Fully Biodegradable "Green" Composites

Ajalesh Balachandran Nair, Palanisamy Sivasubramanian, Preetha Balakrishnan, Kurungattu Arjunan Nair Ajith Kumar, and Meyyarappallil Sadasivan Sreekala

15.1
Introduction

Research efforts are progressing toward developing a new class of fully biodegradable green composites by combining fibers with biodegradable resins. The major attractions about green composites are that they are eco-friendly, fully degradable, and sustainable, that is, they are truly green in every way. Green composites may be used effectively in many applications such as mass-produced consumer products with short life cycles or products intended for one time or short time use before disposal. The important biodegradable matrices are polyamides, polyvinyl alcohol (PVA), polyvinyl acetate, polyglycolic acid, and polylactic acid (PLA), which are synthetic as well as polysaccharides, starch, chitin, cellulose, proteins, collagens/gelatin, lignin, and so on, which are natural [1]. Bio-based composites with their constituents developed from renewable resources are being developed and their application has extended to almost all fields. Natural fiber composites can be used as a substitute for timber and for a number of other applications. It can be molded into sheets, boards, gratings, pallets, frames, structural sections, and many other shapes. They can be used as a substitute for wood, metal, or masonry for partitions, false ceiling, facades, barricades, fences, railings, flooring, roofing, wall tiles, and so on [2]. It can also be used for prefabricated housing, cubicles, kiosks, awnings, and sheds/shelters.

Fully green composites [3] receive great attention nowadays because of their environment-friendly qualities. Generally, glass fiber-reinforced plastics (GFRPs) have enhanced thermal and mechanical properties, and because of such properties it is not easy to dispose GFRP products after use. Natural fiber-reinforced composites, which are easily disposable, have recently been developed, in which plant-based high strength natural fibers are used in place of glass fibers [4, 5]. Although the natural fiber strength is inferior to glass fiber strength, mechanical properties of natural fibers can be improved through mechanical and/or chemical treatments [6, 7]. Especially, it is expected that, through such treatments, the fibers will exhibit the high toughness necessary for structural components.

Polymer Composite: Volume 3, First Edition.
Edited by Sabu Thomas, Kuruvilla Joseph, S. K. Malhotra, Koichi Goda and M. S. Sreekala.

At the end of biodegradable ''green'' composites' life, they can be easily disposed or composed without harming the environment. Another important biocomposite category is based on agro polymers matrices, mainly focused on starchy materials. Plasticized starch, the so-called ''thermoplastic starch'' (TPS) is obtained after disruption and plasticization of native starch, with water and plasticizer by applying thermo mechanical energy is a continuous extrusion process. Unfortunately, TPS shows some drawbacks such as a strong hydrophilic character (water sensitive), rather poor mechanical properties compared to conventional polymers and an important postprocessing variation of the properties. To improve these material weaknesses, TPS is usually associated with other compounds. Green composites may be used for indoor applications with useful life of several years.

The energy issue has been taken care of by using the sun and the wind to replace petroleum in terms of electricity. However, the issue of materials must be fixed as well. In order to contribute to materials that are not reliant on the use of petroleum, research on ''green'' composites has been conducted.

''Truly green'' composites are fully degradable; they come directly from the earth (through plants) and when they are disposed after being used they can go directly back into the earth and composted in organic soil with no waste whatsoever. These composites have the desired properties that are necessary in everyday composites, but do not cause the problems that are faced with petroleum. There is no scarcity with plants; they can be continuously grown and regrown all over the world. This will prevent countries from being reliant on the organizations that control petroleum, which will make the composites much more affordable. Additionally, there is no waste produced by ''green'' composites. These composites can be composted and therefore will never be left to take up space in a landfill. Lastly, ''green'' composites will not pollute any other limited resource. Unlike petroleum-based composites, there are no harsh chemicals used, which not only benefits freshwater and other resources, but also presents a much safer environment for the workers producing the composites.

''Green'' composites are not hindered by their environmentally friendly properties; they can be used for a wide range of applications because of their mechanical properties and can be engineered to required specifications. These applications include, but are not limited to furniture (i.e., desks, cubicles, and tables), sports equipment (i.e., tennis racquets and skateboards), transportation panels (i.e., car parts and airplanes), packaging applications, and housing panels (i.e., walls and floors).

The use of traditional composites made by glass, aramid, or carbon fiber-reinforced plastics has recently been discussed critically because of increasing environmental consciousness [8]. Thus, the recent research and development (R&D) efforts have led to new products based on natural resources. Some of these are biodegradable polymers like PLA, cellulose esters, polyhydroxyalkanotes (PHAs), and starch polymers. Furthermore, natural fiber-reinforced plastics made of natural fibers like flax, hemp, kenaf, jute, and cotton fibers are important R&D achievements. Composites made of natural fibers and biopolymers

are completely biodegradable and are called *green composites* because of their environmentally beneficial properties [9]. Lower manufacturing costs as well as better performance of polymers based on natural resources when compared with the traditional, petrochemical plastics are the outcome of the R&D efforts of several decades, whereas only recently, scientists have been trying to improvise biopolymers so that they can become cheaper and more competitive [8]. Natural fibers as reinforcement for petrochemical polymers like polypropylene (PP) have already been established in the automotive industry [10]. Natural fibers themselves are fiber-reinforced structures in which the cellulose content and the angle of microfibrils influence their mechanical properties [11]. Natural fibers are light and renewable; they are a low cost and high-specific strength resource. For these reasons, natural fiber composites have already been applied for fabricating some products such as furniture and architectural components. Recently, they have gained widespread use in the automobile industry. In their application, synthetic resins, such as PP and polyethylene (PE), are commonly used as a matrix for natural fiber composites. However, these composites often display problems of fiber–matrix compatibility which results in a decrease of mechanical properties. Therefore, in order to improve the interaction between fiber and matrix, surface treatments are necessary for modifying the fiber morphology. Treatments using alkaline solutions have been applied by several researches [12–15] to improve mechanical properties and fiber–matrix adhesion of natural fiber-reinforced plastics. The fiber undergoes physical changes as a result of bleaching during alkali treatment, which removes waxy materials and impurities. This action often leads to improvement of the interfacial bonding between fiber and matrix.

The main obstacles in the use of natural fibers in plastics have been the poor compatibility between the fibers and the matrix, and the inherent high moisture absorption, which could result in dimensional changes of the fibers that may lead to microcracking of the composite and poor mechanical properties. Various chemical treatments have been used by many researchers in the past to improve the mechanical performance of natural fibers, including jute and hemp [16–18]. Not much literature on the adhesion between the matrix and the fibers in ''green composites'' has been published, although it influences their mechanical properties significantly. Most of the publications are based on the interaction between fibers and polyolefins. It is known that natural fibers have poor adhesion to hydrophobic matrices like PP because of their hydrophobic nature [19]. Heinemann and Fritx [20] observed a better interaction between PLA and natural fibers than between PP and natural fibers. Oksman *et al.* [21] reported on long fiber pull-outs and clean fiber surfaces in the fracture surface of the PLA/flax fiber composites, which indicates poor adhesion between the fibers and the matrix. This investigation [21] focuses on the development of completely biodegradable composites by using natural fibers of woven flax as reinforcement and a cobiopolyester as a matrix material.

15.2 Environmental Aspects

Growing environmental awareness has led to new trend in materials development, which is a great motivating factor for material scientists [22]. Composite materials, which are prepared using natural or synthetic matrix and reinforcement materials, come under this category. Developments of commercially viable biodegradable composites based on natural sources for a wide range of applications are developing day by day [23]. Composite is a material having two or more chemically distinct phases, which at the microscopic scale are separated by a distinct interface. From the structural point of view, composites are anisotropic in nature. Mechanical properties of composites are different in different directions and composite is a commodity having superior properties than the individual constituent. Some of the basic properties of composite such as light in weight, high strength to weight ratio, and stiffness make them a suitable product for the replacement of conventional materials like wood [24].

Composite materials play an important role in various industrial sectors. These materials generally lack in mechanical strength, which can be enhanced using synthetic or natural fibers as a reinforcing material. On the other hand agro-based materials can also be used as filler in composite materials to reduce the final cost and improve their environmental degradability [25] Most of the living tissues like bone, collagen, dentine, and cartilage are essentially composites [26–29]. Biocomposites (biodegradable composites) consist of biodegradable polymers as the matrix material and biodegradable fillers, usually biofibers (e.g., lignocelluloses fibers). As both components are biodegradable, the composite as the integral part is also expected to be biodegradable [30].

Composite materials have gone through significant developments in terms of use of different raw materials, processes and even applications [31–37]. Huang and Netravali [38] reported in their research, that fully environment-friendly, sustainable, and biodegradable ''green'' composites were fabricated using modified soy protein concentrate (SPC) resins and flax yarns and fabrics. Kim *et al*. [39] reported aromatic polyester nanocomposites based on poly(ethylene 2,6-naphthalate) (PEN) and carbon nanotube (CNT) were prepared by melt blending using a twin-screw extruder. Modification of CNT to introduce carboxylic acid groups on the surface was performed to enhance intermolecular interactions between CNT and the PEN matrix through hydrogen bonding formation. Gojny *et al*. [40] reported nanocomposites consisting of double-walled carbon nanotubes (DWCNTs) and an epoxy matrix were produced by a standard calendaring technique. Gatani *et al*. [41] studied the peanut husks as raw material for cementitious covering panels. Pads of peanut husks in cementitious-based composites, produced by dewatering molding followed by pressing, resulted in a material with attractive esthetical properties, due to their superficial texture on one of the surfaces. Gaspar *et al*. [42] reported the mechanical strength, water absorption, and enzymatic degradation of composite by the addition of natural polymer cellulose, hemicellulose, zein (protein), and polycaprolactone (PCL).

Taking into consideration the concerns of the society in terms of energy crisis and ecological problems, reduction in the usage of materials made from fossil oil becomes more and more pertinent. In the field of composite materials, for example, a series of works have been done to replace the conventional synthetic fiber composites by means of natural vegetable fiber composites [43, 44]. So far, two main technical routes have been developed. One deals with the compounding of natural fiber with traditional petroleum-based polymers, like thermosetting polymers (unsaturated polyester [45], epoxy [12], phenol formaldehyde resin [46], etc.), or low processing temperature thermoplastic polymers (PP [47], PE [48], etc.). The other mixes plant fibers with biodegradable polymers including PLA [49], starch plastics [50], soybean plastics [51], and cellulosic plastics [52]. Comparatively, the composites prepared in the former way cannot be regarded as fully biodegradable materials because of the nonbiodegradability of the matrix polymers. However, many biodegradable polymers are not cost-effective enough at present. Their potential application as the matrices of structural composites has to be confined to some specific area with high value-added. For manufacturing affordable and fully biodegradable composites, matrix polymers derived from annually renewable resources except food and feed coupled with low cost processing techniques are critical. In this context, the authors proposed the concept of all-plant fiber composites, in which plasticized plant fiber serves as matrix while discontinuous or continuous plant fiber plays the role of reinforcement [53, 54]. As most components of plant fibers can be kept when they are converted into thermally formable materials through simple substitution reactions on the side chains of cellulose in association with partial removal of lignin, the resultant thermoplastics differ from commercially available cellulosic plastics and are characterized by environment-friendly and economically viable nature. The results indicated that sisal/cyano ethylated wood sawdust and sisal/benzylated wood sawdust composites prepared according to these idea exhibit mechanical properties similar to those of glass fiber-reinforced composites while possessing the biodegradability of the feedstock [55]. Besides the above stated advantages, physical heterogeneity in the so-called all-plant fiber composites instead of chemical heterogeneity of conventional composites is also favorable for interfacial interaction as well. Recently, another type of all-plant fiber composites was developed, which has the advantages of gradient plasticization along the radial direction of sisal fibers [56, 57]. That is, through slight benzylation treatment, skin layers of sisal fibers were converted into thermoplastic material while the core of the fiber cells remained unchanged. Then self-reinforced composites of sisal can be prepared using hot pressing, in which the plasticized parts of sisal serve as matrix and the unplasticized cores of the fibers as reinforcement. The inherent interfacial compatibility guarantees efficient stress transfer between the components.

Figure 15.1 summarizes the development possibilities of the all-plant fiber composites. It is worth noting that although etherification or esterification that provides lignocellulosic substances with certain thermoplasticity has been investigated in detail [58, 59]; biodegradabilities of the resultants are not systematically documented to the author's knowledge. As the above chemical reaction takes

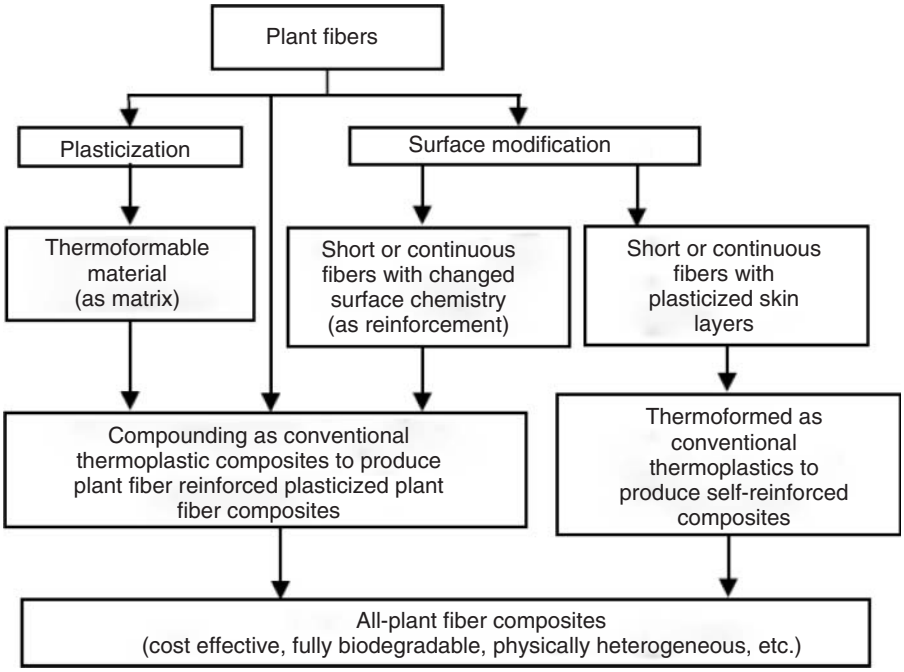

Figure 15.1 Concept of all-plant fiber composites.

place mostly at the side chains of cellulose of plant fibers, the backbone structure of cellulose might not be affected in principle so that the plasticized products can still be biodegraded like the unmodified versions. Earlier studies of sisal-reinforced benzylated wood composites [55] and phenolated wood-based molding materials [60] evidenced the consideration. Unlike other all-plant fiber composites analyzed previously, these self-reinforced composites are made from unitary raw material–sisal. The complexity of the composite system is reduced accordingly. With respect to the assessment of materials biodegradability, structure analysis as well as characterization of the variations in polymerization degree, weight, and mechanical properties of the deteriorated products is common by all means [61].

15.3 Environmental Impacts of Green Composite Materials

The three categories that would be taken into account are global warming, acidification, and abiotic depletion. The method that has been used to analyze the impacts is Center for environmental science (CML) 2 baseline 2000. This method is an update from the CML 1992 method. This version is based on the spread sheet

version 2.7 (April 2004) as published on the CML web site. This method shows an overall picture of the specific impacts. It takes into account global warming, acidification, and abiotic depletion.

15.4 Choice of Impact Categories

As mentioned earlier, the impact categories that will be taken into account are global warming, acidification, and abiotic depletion as they all play an important role in the life cycle of green composites. These are some of the areas where green composites are interested in reducing the environmental impacts.

15.4.1 Global Warming

Over the year's emissions from industries, cars, fuel combustion, deforestation has led to the phenomena called as the *global warming*. This is caused by the greenhouse effect. Gases as carbon dioxide (CO_2), nitrogen oxides (NO_x), sulfur oxides (SO_x), and methane (CH_4) cause the heat to be trapped within the earth and stop it from moving into space. This has led to increase in the temperature of the earth which again has led to climate changes. In this life cycle assessment (LCA) we will discuss the impact of the superstructure on these phenomena, as we believe that it will consume a lot of fuel especially in the operation phase where it is being used resulting in various emissions into air. Therefore it is necessary to study this impact. The lighter the structure, the faster the vessels move resulting in more fuel efficiency and therefore it would be interesting to know how the weight and material of the structure could help in reducing global warming.

15.4.2 Acidification

Acidification is another process where, SO_X, ammonia, and NO_X produced because of combustion of fuel may result in acid rain on reaction with water vapors (fog, snow). This results in acidification of water, which is a threat to fresh water organisms and marine life. It also has negative impacts on rivers, lakes, and forests.

15.4.3 Abiotic Depletion

Abiotic depletion is another term used for resource depletion. Abiotic depletion should be studied in the context of identifying problems within clear system boundaries of economy and environment.

15.5 Environmental Impact of Polylactide

Low cost, efficient technology, eco-friendly treatments capable of reducing and even eliminating plastics, are developed by the researchers. Among biological agents, microbial enzymes are one of the most powerful tools for the biodegradation of plastics. Activity of biodegradation of most enzymes is higher in fungi than in bacteria. Various individual groups of enzymes such as laccase, cutinase, hydrolase, esterase, protease, and urease, were produced by the microbial species like streptococcus, bacillus, pseudomonas, staphylococcus, and the fungal species like aspergillus, penicillium, phaenarochete, pestalotiopsis, and so on. In plastics surface aspects, significant changes indicate its biodegradation. Some polymers are being used for the manufacture of biodegradable plastics like polyhydroxybutyrate (PHB) and copolymers containing other hydoxyalkanoates. These polymers are consumed by various microorganisms as carbon and energy sources and various enzymes, that is, PHA depolymerases secreted by them help in the degradation of these types of plastics [62]. Bioplastics are the biodegradable plastics. It means these types of plastics are either produced from fossil materials or can be synthesized from biomass or renewable resources. Some petroleum-based plastics are PCL and poly(butylene succinate) (PBS) but they can be degraded by microorganisms. The plastics that are produced from biomass or renewable resources are PHB, PLA, and starch blends [63].

Plastics are made biodegradable by improving the hydrophilic level or reducing the polymer chain length by oxidation and to be accessible by microbial growth [64]. Biodegradability of these polymers can be assessed by measuring changes macroscopically or by observing the microbial growth after exposure to biological or enzymatic environment, but mostly by CO_2 evolution [65–68]. PLA plastics are sensitive to moisture and heat. The carboxylic acid end groups of low molecular weight PLA self-catalyzed the polymers hydrolysis in submerged environments. With most applications of PLA plastics, there is a need to investigate the stability and degradation of PLA plastics in environments with different temperatures and relative humidities (RHs). The enzymes catalyze the hydrolysis of PLA, which is the plastic obtained from renewable resources and the hydrolysate can be recycled as material for polymers. Lipase from *Rhizopus delemar* and polyurethane esterase from *Comamonas acidovorans* have been investigated for the degradation of low molecular weight PLA and high molecular weight PLA have been found to be degraded with the strains of Amycolatopsis sp. [69]. PLA is commercially available linear, semicrystalline, aliphatic, biodegradable polyester that can be produced from lactic acid by the fermentation of renewable sources such as whey, corn, potato, or molasses [70]. The resulting polymer can be processed similarly as polyolefins and other thermoplastics. Properties of PLA can be modified through the use of lignocellulosic fibers that reduce the cost of the material without restricting their biodegradability [71].

15.6
Environmental Effect of Polyvinyl Alcohol (PVA)

Today environmental pollution is a major concern of our society. They include pollution of atmosphere, water bodies, and soil. Environment pollution is a phenomenon where human discharge materials or energy in excess of its self cleaning capacity to environment directly or indirectly, which reduces the quality of the environment and has a negative effect on human survival and development, and the ecological system and property. The research on PVA film is a focus these days because it has many outstanding qualities such as water solubility and degradability.

Water-soluble PVA film belongs to green eco-friendly packaging materials. On packing, it has some features as follows:

1) Environmental protection and safety, thorough degradation, and eliminating the problem of disposal of packaging wastes by producing carbon dioxide and water as the final degradative products.
2) It is safe and convenient for application, and it can prevent the packed products from contacting the users directly during application. In addition, we can measure exactly and guard against wasting if it is used. In addition it is nontoxic and pollution free.
3) The water-soluble PVA film has comparatively higher mechanical performance and heat seal strength as well as outstanding gas barrier property and maintains fragrance.
4) Excellent oil, organic solvent, and fat resistance.
5) Has a good quality of static electricity resistance, and will not absorb powder or dust when packing powdery substance.

Environment-friendly package bags of water-soluble PVA have some advantages as follows:

1) The dissolving speed of water-soluble PVA film can be controlled and can be dissolved in cold water.
2) It can greatly reduce the adverse impact of agricultural chemicals and industrial chemicals on humans and on the environment.
3) It reduces the costs of production and transportation, and resolves the problems of enclosing and recycling.
4) It avoids production loss due to overusing or insufficiently employing agricultural chemicals.

The medical package bags made of environment-friendly material of water-soluble PVA film have ideal antifriction and is environment-friendly. They have some advantages as follows:

1) PVA films hardly invoke electrostatic effect and can reduce dust pollution.
2) The bags can be dissolved completely in water. The whole dissolution process results in no residues and the water will not be polluted.

3) They have a unique quality of remaining separate. As soon as products are packaged, they will stay away from the outside environment when they are circulated. It can keep the fragrance of packaged products and avoid the effect of outside smell. As material used to package food, it is nonpoisonous and will not pollute food. More over it can prolong the period of validity of packaged food.

We realize that the worth of PVA film lies in its features of low contamination, dissolution, and biological degradation. These prove that it has little influence on the environment. It is approved by developed countries such as America and Japan. It further illustrates that protecting environment is feasible and PVA film should be widely popularized in market. All in all, we can draw a conclusion that PVA film is nontoxic and it will protect the environment. At present, the main methods of disposing plastic wastes are by landfill, burning, and recycling. But none of them is ideal. In common, plastic needs decades or hundreds of years to degrade and become pieces which cause no pollution to the environment or turn into carbon dioxide and water that can return to natural circulation. As for degradation mechanism, PVA films have two kinds of degradation characteristics: water degradation and biological degradation.

From a macroscopic perspective, almost all the water-soluble films are hydrophilic materials. There is a large number of hydrophilic polar group in the molecular structure. The dissolution mechanism of water-soluble PVA film can be explained as follows: PVA absorbs large amounts of water molecules and in order to make the molecules expand and resolve, the temperature is raised with continued heating. Then the numerous molecules which are made of carbon, oxygen, and hydrogen, are resolved into CO_2 and H_2O. And CO_2 ultimately evaporates into air. It explains the fact that hydrolysis products of PVA do not harm the environment and they are environment-friendly materials.

Since the 1930s, PVA is considered to be a special kind of polymer which can be broken down by living things. During resolving substrate, the growth of a microorganism will be influenced by temperature, pH value, the content, and kinds of sustenance and the characters of sustenance. So, the resolving properties of water-soluble PVA film are closely related to other factors, such as the degree of polymerization and alcoholysis, the distribution of hydroxyl groups, and crystallinity. Now there are two main orientations to research PVA degradation by living things. One is to change the properties of PVA to make it to be resolved by living things. The other is to choose a high efficiency flora for degrading PVA by means of filtering and domestication from environment. The two orientations solve the same problem in different ways. Both of them are to make PVA degradation more easy.

When disused PVA film is resolved by microorganism and produces positive influence on environment as follows:

1) It will largely reduce the loss of soil moisture content. Moreover it will promote the formation of soil aggregated structure and increase the vapor permeability and moisturization. So it is beneficial to the growth of plants.

2) It can improve the pH value of alkaline soil and the pH value increases as the concentration is increases. In addition, the proper alkaline environment has contributed to the growth of flora for degrading and improving the degradation rate.
3) Water-soluble PVA film has low toxicity to living organisms and it is hardly absorbed by the gastrointestinal tract. Furthermore, PVA cannot be accumulated in one's body.

From all the above discussions, we can see that the abandoned and decomposed PVA film by the microbes in environment is absolutely nonpoisonous and nonharmful. It will be able to change the construction of soil. PVA is compatible with its surroundings. Biodegradable polymers could be composted with organic garbage. Recently, they have drawn a lot of interest for reducing the load on landfills and incinerators. Degradation of PVA by microorganisms takes place very slowly, and when biodegradable plastics containing PVA are composted with organic garbage, most of the PVA residue remains behind after the composting [72, 73]. Therefore, soil fertilized with the compost could contain accumulating amount of PVA residues.

The morphology of red pepper 65 days after the sowing is exhibited in Figure 15.2. Red pepper in the control experiment had a very strong stem with 30 large, deep green leaves (Figure 15.2a). In contrast, 0.25% PVA made red pepper bear 15, much smaller leaves with a lighter green color compared to the control experiment (Figure 15.2b). Red pepper affected by 5% PVA had 8, even smaller yellow leaves with pale veins (Figure 15.2d).

PVA and PE were blended with a soil for cultivation, and their effects were investigated on the growth behavior of red pepper and tomato by examining the stems, the leaves, and the roots. PVA retarded the growth of red pepper significantly even at a concentration as low as 0.05%. The roots were depauperated more than the stems and the leaves. Tomato was also affected by PVA but to a lesser extent than red pepper. In contrast, the presence of both round pieces (10 mm diameter) of PE film and powdery PE influenced negligibly the growth of red pepper as well as that of tomato up to 35 wt% in soil [74].

Figure 15.2 Effect of PVA concentration on the growth of red pepper 65 days after sowing; (a) control, (b) 0.25% PVA, (c) 2% PVA, and (d) 5% PVA.

15.7 Potential Positive Environmental Impacts

Full LCA studies of biodegradable plastics in comparison to conventional petroleum-based plastics are required. However, environmental benefits that may be derived from the use of biodegradable plastics compared to conventional materials are outlined below.

15.7.1 Composting

Compost derived from biodegradable plastics along with other organic products increases soil organic carbon, water and nutrient retention, while reducing fertilizer inputs and suppressing plant disease. The composting of biodegradable plastics also cycles matter rather than ''locking'' it up in persistent materials, particularly when the nondegradable plastics are destined for landfill.

15.7.2 Landfill Degradation

The use of biodegradable shopping and waste bags may have the potential to increase the rate of food degradation in landfills, and therefore has the potential to enhance methane harvesting potential where infrastructure is in place and decrease landfill space usage. The use of biodegradable plastic film as daily landfill covers has the potential to considerably extend landfill life, as they could replace traditional soil cover material which uses approximately 25% of landfill space.

15.7.3 Energy Use

The energy required to synthesize and manufacture biodegradable plastics is shown in Table 15.1, along with values for high density polyethylene (HDPE) and low density polyethylene (LDPE). PHA biopolymers presently consume similar energy inputs to PEs. New feed stocks for PHA should lower the energy required for their production.

15.8 Potential Negative Environmental Impacts

There is an increasing movement of scientists and engineers who are dedicated to minimizing the environmental impact of polymer composite production. LCA is of paramount importance at every stage of a product's life, from initial synthesis through to final disposal and a sustainable society needs environmentally safe materials and processing methods. With an internationally recognized team

Table 15.1 Energy for production of biodegradable plastics polymer energy (MJ kg^{-1}).

Polymer	Energy (MJ kg^{-1})
LDPE	81
PHA-fermentation process	80
HDPE	80
PCL	77
PVOH	58
PLA	57
TPS + 60% PCL	52
TPS + 52.5% PCL	48
TPS	25
TPS + 15% PVOH	25

PVOH, poly(vinyl alcohol).

of contributors, green composites examines fiber-reinforced polymer composite production and explains how environmental footprints can be diminished at every stage of the life cycle.

15.8.1 Pollution of Aquatic Environments

Aquatic pollution occurs when harmful, or potentially harmful effects, can result from the entry into the ocean of chemicals, particles, industrial, agricultural, and residential waste, noise, or the spread of invasive organisms. Most sources of marine pollution are land based. The pollution often comes from nonpoint sources such as agricultural runoff and windblown debris and dust.

Many potentially toxic chemicals adhere to tiny particles which are then taken up by plankton and benthos animals, most of which are either deposit or filter feeders. In this way, the toxins are concentrated upward within ocean food chains. Many particles combine chemically in a manner highly depletive of oxygen, causing estuaries to become anoxic.

15.8.1.1 Increased Aquatic BOD

Pollution from high nutrient levels in waterways, determined by high biological oxygen demand (BOD) and chemical oxygen demand (COD), lead to the degradation of aquatic ecosystems and algal blooms. The breakdown of starch-based biodegradable plastic materials can result in increased BOD if the plastics make their way into water ways.

15.8.1.2 Water Transportable Degradation Products

Plastic degradation by-products, such as dyes, plasticizers, or catalyst residues, in landfills or compost can potentially migrate to groundwater and surface water bodies

via runoff and leachate. Organisms inhabiting these water bodies could thereby be exposed to degradation products, some of which may be toxic. Groundwater contamination from pigments, catalyst residues, and isocyanate coupling agents may also occur. Liberated plastic additives and polymer degradation products in landfills or compost heaps can potentially migrate to nearby bodies of water through liquids percolating in the ground (leaching) or via rainfall runoff. If current metal-based pigments continue to be used in biodegradable plastics, then the potential for release and accumulation in soil and water is high.

15.8.1.3 Risk to Marine Species

Plastic pollution in marine environments can result in the death of marine species that ingest it in the belief that it is a jellyfish, squid or other translucent, amorphous organism. In the animal's gut, biodegradable plastics will not degrade rapidly and injury to the animal is likely to remain an outcome. Turtles can die of starvation as plastic bags block the alimentary canal.

15.8.2 Litter

The visual impact of littering is unlikely to decrease with the use of biodegradable plastics as windblown plastic litter and plastic films/bags snagged on branches and bushes will not be exposed to sufficient level of microbes for proper biodegradation to take place. Consequently biodegradation of such litter may take many years. This problem may potentially be combined with the possibility that conspicuous littering of plastics may actually increase because of the misconceived notion of consumers that biodegradable plastics will disappear quickly in the environment.

15.8.2.1 Determination of Appropriate Disposal Environments

Extensive consultation with the product supply chain and potential disposal chain, including sorting, reprocessing, and composting bodies, will be necessary before the widespread introduction of biodegradable products that may impact on existing recycling and composting systems.

Composting as a planned disposal route, particularly for film and sheet, should only occur once a system is in place to identify these materials as distinct from non-degradable products. One possible solution is to introduce a unique standard color (i.e., bright lime green) so they can be easily differentiated from nonbiodegradable plastics in a composting environment. In this way, nonbiodegradable plastics can still be manually removed while the biodegradable plastics can be left *in situ*.

Unique color-based identification of biodegradable plastics would also assist plastic recyclers in identifying those plastics that are not compatible with mechanical recycling processes. A parallel identification system involving a logo such as the ''Compost OK'' mark would allow consumers to identify these products. There does not appear to be any significant impediment, however, to the introduction of biodegradable products destined for landfill disposal, such as garbage bags, landfill

covers, and nonrecycled shopping bags, provided that they meet the appropriate testing standards.

15.8.2.2 Role of the Built Environment

Environmentally harmful activities differ from one industry to another, but it is well-known that the biggest contributor to green house gas (GHG) emissions is the built environment, accounting for up to 50% of global carbon dioxide emissions [75]. In addition, the embodied environmental impacts generated by the building during its whole life cycle, can be of the same order of magnitude as those generated during the utilization stage [76]. The building construction industry consumes 40% of the materials entering the global economy and generates 40–50% of the global output of GHG emissions and the agents of acid rain [77].

The construction sector is responsible for a high percentage of the environmental impacts produced by the developed countries. In the European Union, the construction and building sector is responsible for roughly 40% of the overall environmental burden [78]. Homes in the United Kingdom (their construction and occupation) are responsible for the consumption of 40% of primary energy in the country [79]. If the other 30% of the building stock (nonresidential) is considered, the impact of buildings is greater. The construction industry is a highly active sector all over the world [78], and it is the largest industrial employer, accounting for 7% of total employment, and 28% of industrial employment. It is responsible for a high rate of energy consumption, environmental impact, and resource depletion.

15.9 Biodegradation

Biodegradation is the chemical dissolution of materials by bacteria or other biological means. Although often conflated, biodegradable is distinct in meaning from compostable. While biodegradable simply means to be consumed by microorganisms and return to compounds found in nature, ''compostable'' makes the specific demand that the object break down in a compost pile. The term is often used in relation to ecology, waste management, biomedicine, and the natural environment (bioremediation) and is now commonly associated with environmentally friendly products that are capable of decomposing back into natural elements. Organic material can be degraded aerobically with oxygen, or anaerobically, without oxygen. Biosurfactant, an extracellular surfactant secreted by microorganisms, enhances the biodegradation process.

Petroleum hydrocarbons will degrade with relative ease as a result of biological metabolism. Although virtually all petroleum hydrocarbons are biodegradable, biodegradability is highly variable and dependent somewhat on the type of hydrocarbon. In general, biodegradability increases with increasing solubility; solubility is inversely proportional to molecular weight.

15.9.1 Biodegradability Test

Tests for biodegradation are used to predict how quickly and completely hydrocarbons will break down in the environment. However, these tests can underestimate a chemical's ability to biodegrade if they do not examine real-world factors, such as the effects of waste water treatment or microorganism acclimation. Because biodegradability is widely recognized as an indicator of environmental safety, it is critical that realistic test conditions be used to determine biodegradability.

15.9.1.1 Natural Soil Burial Test and Simulated Municipal Solid Waste (MSW) Aerobic Compost Test

Natural soil burial test and simulated municipal solid waste (MSW) aerobic compost test were determined according to ASTM D 6003-96 (ASTM, American society for testing materials). The natural soil test of the PBS and biocomposites was conducted for 80 days. The compost test method is used to determine the degree and rate of aerobic biodegradation of plastic materials exposed to a controlled composting environment. The test is designed to be applicable to all plastic materials that are not inhibitory to the bacteria and fungi present in the simulated MSW (municipal solid waste). The test was conducted with PBS and capable of maintaining a temperature of $30 \pm 2\,^{\circ}C$ and reactor. The pH of the compost soil was maintained at 7 and the water content at 50–60%. The specimens underwent testing for tensile strength and Izod impact strength. HDPE was used as the negative reference material. After each natural and compost test of 10, 30, 40, 60, and 80 days duration, the buried specimens were dug out, removed from the soil and washed in distilled water. Finally, the specimens were dried in an air dried oven at $60 \pm 2\,^{\circ}C$ for 24 h. Table 15.2 shows the constituents of the simulated MSW aerobic compost.

15.9.1.2 Mechanical Property and Weight Loss Tests after Biodegradability

After the biodegradability tests of PBS, HDPE, and biocomposites at 10, 30, 40, 60, and 80 days, the tensile strength was obtained using a Universal Testing Machine. Notched Izod impact strength before and after the biodegradability test was measured using an Impact Tester at room temperature. The percentage weight

Table 15.2 Constituents of simulated municipal solid waste (MSW) aerobic compost soil.

Category	Wet weight (%)	Wet weight of specific component (%)
Food waste	16.6	Solid wastes (16.6)
Garden waste	13.9	Leaves (6.9), grass (7)
Paper	58.5	Bleached (19.5), brown (19.5), cardboard (19.5)
Plastics	7.7	HDPE from milk bottles
Textiles	0.8	Cotton
Wood	2.5	Twigs

loss was determined by Eq. (15.1):

$$\text{Weight loss}(\%) = \left[\frac{M_0 - M_d}{M_0}\right] \times 100 \tag{15.1}$$

where M_0 is the initial mass and M_d is the degradation mass at each designated day. The percentage weight loss was taken from the average of five samples.

15.9.1.3 Microbial Counts in Natural and Compost Soil

The number of microorganisms in natural soil and compost soil was determined by a count of the growth colonies on Nutrient Agar (NA) and Anaerobe Isolation Agar (AIA) plates. The NA medium consisted of 3 g bacto beef extract, 5 g bacto peptone, and 15 g bacto agar/l of distilled water and was adjusted to pH 6.8. The AIA medium consisted of 2 g bacto casitone, 0.1 g asparagine, 4 g sodium propionate, 0.5 g KH_2PO_4, 0.1 g $MgSO_4 \cdot 7H_2O$, 0.001 g $FeSO_4 \cdot 7H_2O$, and 15 g bacto agar per liter of distilled water and was adjusted to pH 6.5. Three samples of NA and AIA plates were prepared for measuring microbial count in natural soil and compost soil. Each of the three NA and AIA plates were sterilized in an autoclave for 15 min at 121 °C, allowed to cool to 60 °C, and poured into Petri dishes. Natural and compost soil samples, each 1 g soil, were dissolved in 9 ml sterile water using a vortex mixer. They were each then diluted to 10 by adding 1 ml of the soil suspensions to 9 ml sterile water. From each of the 10 diluted solution samples, 100 ml was removed and spread onto NA and AIA plates, after which they were incubated at 30 °C for 24 and 48 h, respectively. After the incubation of each plate (NA and AIA), the number of colonies was measured by a colony counter. Three measurements were conducted and an average of the three samples was calculated.

15.9.1.4 Molecular Weight after Biodegradability

After the natural and compost soil burial tests of the PBS, each PBS specimen was eluted using 1,2,4-trichlorobenzene (TCB) at 140 °C and filtered through a 0.2 mm polytetrafluoroethylene (PTFE) syringe filter. Molecular weights were measured by gel permeation chromatography (GPC) at 145 °C equipped with refractive index (RI) detectors and a gel 10 mm column (two mixed-B). TCB was used as an eluent solvent at a flow rate of 1 ml min^{-1}. The number-average (M_n) and weight-average (M_w) molecular weights were calculated using a calibration curve from polystyrene standards.

15.9.1.5 Differential Scanning Calorimetry (DSC) Analysis

Differential scanning calorimetry (DSC) analysis was carried out using a TA Instrument DSC Q1000 with 5–8 mg of PBS samples at the designated time points. Each sample was scanned as the temperature was raised from 80 to 200 °C at a heating rate of 10 °C min^{-1} and then cooled at the same rate under a nitrogen atmosphere. Glass transition temperature (T_g), melting temperature (T_m), and crystallization temperature (T_c) were determined from the second scan. T_m was taken as the maximum of the endothermic melting peak from the heating scans and T_c was obtained from the temperature at the top of the peak on the crystallization

peak from the cooling scans. T_g was considered to be a deflection of the base line from the cooling scan. Heat of fusion (ΔH_f) and heat of crystallization (ΔH_c) were obtained from the areas of melting peaks and crystallization peaks, respectively.

15.9.1.6 FTIR-ATR Analysis

The infrared spectra in the FTIR–ATR (FTIR, Fourier transform infrared; ATR, Attenuated total reflectance) spectra of the compost soil burial tested PBS and biocomposite buried for 60 days were obtained using a FTIR spectrophotometer. A diamond was used as an ATR crystal. The specimens after the compost burial test were analyzed over 525–4000 cm^{-1} range and the resolution of the spectrum was 4 cm^{-1}. All spectra were averaged over 32 scans. This analysis was performed at point-to-point contact with a pressure device when analyzing the solid specimens.

15.9.1.7 Morphological Test

Scanning electron microscope (SEM) was used to study the morphology of the surface degradation of PBS and biocomposites. Electron micrographs were obtained using a SEM microscope before and after the biodegradability tested specimens in natural and compost soil. Prior to the measurement, the specimens were coated with gold (purity, 99.99%) in order to prevent electrical discharge.

15.10 Advantages of Green Composites over Traditional Composites

The advantages of green composites over traditional composites are as follows: less expensive, reduced weight, increased flexibility, renewable resource, sound insulation, thermal recycling is possible where glass poses problems and friendly processing and no skin irritation.

15.11 Disadvantages of Green Composites

The major disadvantages of green composites are lower strength properties (especially impact strength), good moisture absorption causing swelling of fibers, lower durability, poor fire resistance, and irregular fiber lengths. However, recent fiber treatments have improved these properties.

15.12 Application and End-Uses

Green composites are applied to various components with moderate and high strength such as cars and mobile phones. Various problems associated with green composites include effects of moisture and humidity, strength reliability, enhancement in fire resistance, and so on. Moreover, there are some concerns over

natural fiber quality and consistency, fogging and odor emission, and processing temperature limits (200 °C).

Some of the other areas in which the green composites are used are as follows: false ceilings, partition purposes, doors, furniture, boxes for agriculture purposes, and so on. Other miscellaneous applications are rims, mobile panels, toys, aircraft, ships, and so on.

15.12.1 Automobiles

The automotive market is becoming increasingly competitive; the latest European legislation limits the emission of CO_2 and requires car designers to take into account pedestrian safety in case of impact. These influences are forcing the automotive industry to change the habits and to ''Think composites'' more and more, although composites will only be employed more extensively if those materials and technologies are competitive.

Composites made of natural fibers are attractive because of ecological concerns and also because they allow a decrease in the weight of parts and have good mechanical properties. Green composites are used in door panels, headliners, package trays, dashboards, and trunk liners, based on natural fiber composites with thermoplastic or thermo set matrix, challenging the glass fiber-reinforced composites. With natural fiber composites, car weight reduction up to 35% is possible. This can be translated into lower fuel consumption and the lower environmental impact. Natural fiber-based composites also offer good mechanical performance, good formability, high sound absorption, and cost savings due to low material costs. Moreover their ''Green look'' as well as ecological and logistical benefits of the natural fiber-based technologies looks more attractive. In 2000, more than 23 000 tons of natural fibers have been used in the automotive sector alone. Natural fibers in automotive should experience a sustainable growth as EU regulations regarding recycling and ''end-of-life vehicle'' directives set car recycling targets to 95% by 2015.

15.12.2 Aircrafts and Ships

The green composites are used in aircrafts and ships because of less weight and eco-friendly character which is also biodegradable. It is known that the fuel consumption will come down certainly if the weight of the vehicle is decreased. These types of green composites are also used in trains for the above reason.

15.12.3 Mobile Phones

Green composites are used in mobile phones. For example, kenaf and PLA composites are applied to mobile phone parts in Japan to reduce the amount

of CO_2 emissions during fabrications. Nippon Telegraph and Telephone (NTT) Docomo is one of the models of mobile phones in Japan in which green composites are used for such purposes.

15.12.4 Decorative Purposes

Green composites are used for indoor structural applications in housing. The composite used for the interior decorations are banana, jute, hemp, kenaf, sisal fiber, and its composites. Also the walls can be covered with the boards, which will be attractive and will decrease the cost of construction.

15.12.5 Uses

In addition, these green composites may be easily composted after their life, completing nature's carbon cycle. Biocomposites can supplement and eventually replace petroleum-based composite materials in many applications, offering new agricultural, environmental, manufacturing, and consumer benefits. Eco-friendly biocomposites from plant-derived fiber (natural/biofiber) and crop-derived plastics (bioplastic) are novel materials of the twenty-first century and would be of great importance to the materials world, not only as a solution to growing environmental threat but also as a solution to the uncertainty of petroleum supply.

The use of materials from renewing resources is gaining increased importance, and the world's leading industries and manufacturers prefer to stock the store place with composites derived from natural fibers and biopolymers as against the dwindling resources of petrochemical-based feedstock.

15.13 Biodegradation of Polyvinyl Alcohol (PVA) under Different Environmental Conditions

PVA can be completely mineralized in the presence of selected microbial strains and under suitable incubation conditions [80]. Many studies were aimed at investigating the biodegradability of pure PVA, whereas PVA items dispersed in the environment are based on blown films. These films contain thermally induced modifications, and may contain process additives up to a maximum of 20% by weight. Recently, a study was undertaken under various environmental conditions in order to ascertain the degradation behavior of PVA-based blown films obtained by thermal processing as compared to unprocessed pure PVA samples. Different test conditions were selected, including simulated aerobic composting, soil burial, and in aqueous media containing sewage sludge from different sources and PVA-acclimated microorganisms [81]. The rate and extent of mineralization of the film samples was monitored by respirometric measurements. The amount of evolved CO_2 was then converted to calculate the extent of degradation.

15.13.1
Biodegradation of Polyvinyl Alcohol under Composting Conditions

Test materials were confined in a mature compost matrix and their relevant biodegradation measured as a percentage of the polymer carbon content converted to CO_2 during the test period. A temperature profile of consecutive mesophylic (e.g., 28–37 °C), thermophilic (e.g., 55–60 °C), and further mesophilic phases was applied to the test containers in order to mimic the thermal conditions occurring in open-field composting processes. Stabilized compost from urban solid waste was utilized as a microbial-active incubation media. Biodegradation of PVA-based plastic films did not exceed 7% in 48 days; this figure was only reached in the presence of film samples based on PVA with a hydrolytic degradation (HD) of 88% [81]. Very moderate PVA biodegradation was also detected when using compost extract as a microbial source [82]. Under the adopted conditions, PVA underwent very limited biodegradation, reaching a plateau in the mineralization profile corresponding to approximately 12% of cumulative CO_2 conversion after 30 days of incubation. A starch sample used as reference was extensively mineralized (75%) by compost microorganisms under the same conditions [83].

15.13.2
Biodegradation of Polyvinyl Alcohol in Soil Environment

Simulated soil burial tests providing information regarding the soil biodegradation tendency of PVA-based blown films [81] were performed according to a procedure aimed at reducing the experimental error in the presence of polymeric materials that can be mineralized at moderate or slow rates [84]. The very limited tendency of fully hydrolyzed PVA to biodegradation in soil environments was repeatedly observed [85–88]. Other possibilities must be taken into account when attempting to explain PVA's low tendency toward biodegradation by soil-associated microflora. In particular, the almost irreversible adsorption of PVA on soil's mineral and organic components can play an essential role [89]. Indeed, the development of strong interactions with solid substrates was one reason presented for the limited biodegradability of microbial polysaccharides and proteins observed in soil [90, 91]. The reported results seem to indicate that PVA adsorption on inorganic substrates effectively inhibits biodegradation processes, at least under the adopted incubation conditions [92]. The above reported data suggest that the comparable, very low extent of PVA biodegradation recorded under composting and soil burial test conditions may be ascribed to the adsorption of the synthetic polymer by inorganic and organic components present in soil. Accordingly, the small increase of PVA adsorption with the degree of saponification (DS), indicating the active role held by polymer hydroxyl groups in the adsorption process, may also account for the slightly larger mineralization observed for the PVA sample having 88% DS with respect to the 99% DS sample.

15.13.3
Anaerobic Biodegradation of Polyvinyl Alcohol in Aqueous Environments

A detailed investigation of the anaerobic biodegradability of PVA was carried out by Matsumura *et al*. [93], using anaerobically preincubated microorganisms deriving from both river sediments and activated sludge from municipal sewage plants. In the presence of anaerobic microorganisms from river water sediments, the overall CO_2 production promoted by cultures fed with low molecular weight PVA was similar to that recorded in the presence of D-glucose, used as a reference compound. Both rate and extent of CO_2 evolution were affected by PVA molecular weight, with lower values being observed for the higher molecular weight sample [93]. The anaerobic biodegradation of PVA was investigated by monitoring the biogas evolution and Total organic carbon (TOC) decrease in anaerobic respirometric tests performed in the presence of a microbial inoculum consisting of river sediment [94].

In recent years, environmentally degradable plastics (EDPs) have attracted growing attention because of their potential use in the replacement of traditional nondegradable plastic items deriving from fossil fuel feed stocks. In this connection, PVA has been widely utilized in specific mereological segments for the preparation of blends and composites with several natural, renewable polymers.

15.14
Biodegradation of Polylactic Acid

Among these biodegradable polymers, PLA has received the most attention because its raw material, L-lactic acid, can be efficiently produced by fermentation from renewable resources such as starchy materials and sugars. Moreover, it has good properties such as high melting point (175 °C), high degree of transparency, and ease of fabrication. PLA can be synthesized either by condensation polymerization of lactic acid or by ring opening polymerization of lactide (the cyclic dimer of lactic acid). This polymer exists in three stereoforms: poly(L-lactide) (L-PLA), poly(D-lactide) (D-PLA), and poly(DL-lactide) (DL-PLA). L-PLA and D-PLA are semicrystalline and exhibit high tensile strength and low elongation. On the other hand, DL-PLA is more amorphous exhibiting a random distribution of both isomeric forms of lactic acid depending on the amount of D or L.

The mechanical properties of PLA, which are comparable to polystyrene and PE, have also stimulated interest in its application as packaging materials. Hence, it would be of interest to study the biodegradation mechanisms and biological treatment of PLA. The degradation of PLA has been studied several years ago, but understanding on this subject is still inadequate. This is clearly evidenced by lack of information on the mechanisms involved and the microorganisms associated with the degradation. Majority of reports concluded that PLA degradation occurred strictly through hydrolysis with no enzymatic involvement. Other reports suggest that enzymes have a significant role in the degradation of PLA [95–97]. Recently, several microorganisms that are capable of degrading PLA have been discovered [98–100].

15.15
Biodegradation of Polylactic Acid and Its Composites

Biodegradable polymers have recently attracted great interest in the scientific community because environmental pollution by plastics has assumed significant proportions. Among the various possible routes to eliminate plastics wastes, biodegradation and biorecycling are regarded as attractive solutions, and it has become a rather widely adopted opinion that biodegradable polymers have a well-grounded role in solving the waste problem [101, 102]. In the family of biodegradable synthetic polymers, PLA appears to be one of the most attractive for film applications in agriculture and as a packaging material [103], because of its facile availability, good biodegradability, and good mechanical properties. PLA (from L-lactic acid, D-lactic acid, or mixes of both) can be obtained by means of a fermentation process using glucose from corn. The proportion of the L- and D-isomeric forms will determine the properties of the polymer, that is, if the material is amorphous or semicrystalline [104, 105].

The main limitations of PLA toward its wider industrial application are its poor thermal and mechanical resistance and limited gas barrier properties which prevent its complete access to industrial sectors such as packaging [106]. Nevertheless, it has been found [107–112] that the above drawbacks can be overcome by the addition of nanoparticles. As far as biodegradability of PLA-based nanocomposites is concerned, Lee *et al*. [110] and Paul *et al*. [113] have observed higher rates of PLA biodegradation in compost by the addition of nanoclays, which was attributed to the high relative hydrophilicity of the clays, allowing an easier permeability of water into the polymer matrix and activating the HD process. Fukushima *et al*. [114] studied the degradation mechanism of PLA and its nanocomposites prepared with two organically modified montmorillonites at 5% w/w loading, in laboratory controlled composting as well as by isolated microorganisms belonging to the compost in order to gain insights into the process of biodegradation of these materials.

The preliminary phase of this study was to determine by visual observation the degradation of the samples after contact with compost. Figure 15.3 shows the materials before and after different times in compost. All samples exhibit a considerable surface deformation and whitening, this being more evident for the nanocomposites after only 3 weeks of degradation. It has been reported [115], that the surface whitening could be a signal that the process of HD of the polymer matrix has started, thus inducing a change in the refraction index of the sample as a consequence of water absorption and/or presence of products formed by the hydrolytic process.

The compost degradation of PLA is reported to occur by two processes: during the initial phases of the degradation, the high molecular weight PLA chains are hydrolyzed to form lower molecular weight chains [116]. This reaction can be accelerated by acids or bases and it is also affected by both temperature and moisture [117]. During this step, some microorganisms in the compost are able to catalyze the degradation, probably by hydrolytic scission of ester groups into an

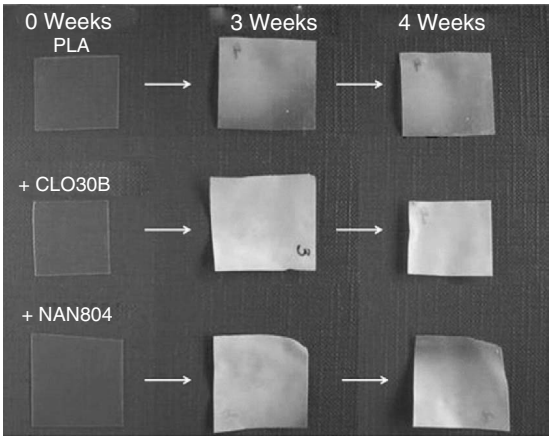

Figure 15.3 PLA and nanocomposites based on montmorillonites (CLOISITE 30B and NANOFIL 804) before degradation (0 weeks) and after 3 and 4 weeks of degradation in compost at 40 °C.

acid and an alcohol, finally converting the lower molecular chains to CO_2, water, and humus.

Therefore, any factor which increases the hydrolysis tendency of PLA matrix can in principle accelerate the degradation of PLA in compost.

The faster appearance of visual signs of degradation in nanocomposites as compared to PLA in Figure 15.3 is likely to be due to the presence of hydroxyl groups belonging to the silicate layers of the clays, which being finely dispersed in the PLA, may play a catalytic role on hydrolysis of the ester groups of the PLA matrix as suggested in Ref. [118]. Despite the visual degradation observed for all samples, they do not show weight decreases within experimental error (±5%) up to 39 weeks. As surface degradation usually leads to loss of degradation products, such as lactic acid for PLA in soil or compost [116], these results suggest either that these products at this stage are adherent to the material surface and/or that the microorganisms belonging to the compost are not able to considerably assimilate them. It is also possible that the degradation mainly proceeds, at least in this period of time; from the interior of the samples and that the diffusion rate of degradation products is relatively slow. Indeed, Hakkarainen [119] reported that the HD of PLA in aqueous media proceeds faster in the center of the sample than at the surface, suggesting that the hydrolysis products formed near the surface are dissolved in the degradation medium, while in the inner part there is a high concentration of carboxylic end groups able to catalyze ester hydrolysis. In biodegradation studies, we screened and isolated from compost microorganisms potentially responsible for PLA degradation; among the isolates no yeasts and actinomycetes were found whereas one bacterium showed a high capacity to degrade the PLA.

15.16
Biodegradation of Cellulose

Biodegradation of cellulose wastes by fungal or bacterial enzymatic activities represents a large area of research experiments concerning the influence of different physical and biochemical factors, which interfere in cellular dynamics of such biotechnological processes [120]. The survey of these important factors could give much useful information about the optimal parameters of biodegradation in continuous-culture systems in order to maximize the efficiency of these biotechnological procedures and to achieve increasing rates of biocomposting and bioconversion into useful products, using immobilized bacteria and fungi [121].

There are many well-known methods to immobilize bacterial and fungal spores by entrapment inside various polymeric matrices prepared by chemical polymerization. The main disadvantage of these procedures is their inability to be used as immobilization technique for whole viable microorganism cells, by which it could be, generated a new potential efficiency for many biotechnological continuous processes [122].

Basically, the cellulose is the most widely distributed skeletal polysaccharide and represents about 50% of the cell wall material of plants. Beside hemicellulose and lignin, cellulose is a major component of agricultural wastes and municipal residues [123–125]. The cellulose and hemicellulose comprise the major part of all green plants and this is the main reason for using such terms as *cellulosic wastes* or simply *cellulosic's* for those materials which are produced especially as agricultural crop residues, fruit and vegetable wastes from industrial processing, and other solid wastes from canned food and drinks industries [125, 126].

Many fungi from Asco- and Basidiomycetes can produce extracellular enzymes that enable them to break down polysaccharides such as celluloses and convert these polymeric compounds into sugars, and otherwise, there are several Gram-positive bacteria, such as those from Bacillus genus, which have the enzymatic potential to cut down proteins into amino-acids that can be assimilated easily by other organisms during the specific food chains existing in any ecosystems [127, 128]. In this respect, there will be shown some short morphophysiological characteristics of such microorganisms, which were used as biocatalysts in the experiments concerning cellulose biodegradation by immobilized viable cells [128].

15.17
Cellulose Fiber-Reinforced Starch Biocomposites

In recent years, natural fibers have attracted much attention as reinforcements for both thermoplastic and thermosetting polymer composites. It should be pointed out that a lot of previous work focused on developing partially biodegradable composite materials including natural fibers-reinforced nonbiodegradable matrices

[129] or nonbiodegradable fillers such as CNTs-reinforced biodegradable matrices [130]. Currently, more and more researchers are developing fully biodegradable composites, the so-called ''green'' composites, ecocomposites, or biocomposites which are composed of natural fibers and natural matrices [131] or synthetic biodegradable matrices such as PLA [132]. To date, numerous natural fibers such as cotton, hemp, sisal, jute, flax, ramie, coir, and cellulose have been explored [43] and a lot of ''green'' matrices such as starch and cellulose have been employed [133]. Cellulose, the most abundant natural homopolymer, is considered to be one of the most promising renewable resources and an environmentally friendly alternative to products derived from the petrochemical industry. Besides cellulose from plants, cellulose is also secreted extracellularly as synthesized cellulose fibers by some bacterial species, which is called *bacterial cellulose* (*BC*) or *microbial cellulose* (*MC*). Though identical in chemical composition, the mechanical properties and structure of BC differ from those of plant cellulose. It has high mechanical properties like tensile strength and modulus. Compared with cellulose from plants, BC possesses higher water holding capacity, higher crystallinity, and a finer weblike network. BC has been widely used in foods, in acoustic diaphragms for audio speakers or headphones, for making unusually strong paper, and has medical applications as wound dressings and artificial skins, artificial blood vessels, and tissue engineering scaffolds [134]. However, there is little literature regarding the combination of BC and starch [135]. So far no information on mechanical properties, moisture absorption, and environmental biodegradability of the BC/starch composites has been reported. To this end, biocomposites based on starch and BC fibers were developed by a solution impregnation method by Wan *et al*. [136]. Like plant cellulose, BC molecules have two regions: one of which, called *crystalline cellulose* is composed of highly oriented molecules, and the other one, called *amorphous cellulose*, comprises less-oriented molecules. The ability of cellulolytic microorganisms to degrade cellulose varies greatly with the physicochemical characteristics of the substrate, such as the degree of crystallinity and polymerization of cellulose [137–139], of which the crystallinity degree of cellulose is the most important structural parameters [139]. It is reported that crystalline regions are more difficult to degrade [140]. Compared to plant cellulose, BC shows much higher crystallinity, which renders it a relatively higher resistance to microorganism attacks than starch. The BC nanofiber–starch biocomposites have been manufactured by solution impregnation method. The difference in resistance to microorganism attacks between BC and starch suggest that in the BC/starch composites, microorganism attacks start with starch. As the microorganisms consume the surrounding starch, the composites lose their structural integrity. This process can lead to the deterioration of the mechanical properties, thus allowing the attack of the BC by microorganisms. Undoubtedly, the results obtained here reveal that the BC/starch composites will not cause any deleterious ecological impact. In other words, the BC/starch biocomposites are fully biodegradable. The BC/starch biocomposites possess much higher tensile strength and modulus than the unreinforced starch, but show lower elongation at break. The higher resistance to water absorption for the biocomposites than the unreinforced

matrix is believed to be attributable to the higher resistance of BC fibers and the strong hydrogen bonding formed at the fiber–matrix interfaces. The BC/starch biocomposites consisting of biodegradable BC and starch are fully biodegradable, which renders them advantageous in terms of environmental protection.

15.18
Life Cycle Assessment (LCA)

Sustainable or green products are increasing in popularity, as evidenced by the growth in green labeling initiatives, eco-marketing, and bio-based materials. Unfortunately there is no universally recognized standard system for evaluating the sustainability of a product or process. Instead, sustainable design is guided by principles such as the ''12 Principles of Green Chemistry,'' the ''12 Additional Principles of Green Chemistry,'' and the ''12 Principles of Green Engineering'' [141–143], as well as by similar concepts of sustainable design, such as ''Cradle to Cradle,'' ''Design for the Environment,'' ''Industrial Ecology,'' and ''Pollution Prevention'' [144–146]. These principles increased in status over the past two decades with the creation of the United States Environmental Protection Agency (EPA) ''Green Chemistry Program'' in 1993, the adoption of similar government programs in Italy and the United Kingdom, and the inaugural publication of the journal *Green Chemistry* by the Royal Society of Chemistry in 1999 [147]. The application and efficacy of green chemistry and other green design principles are documented for many case studies, including biodegradable polymers, and the production of polymers from biomaterials [141, 147–150]. LCA is a tool that quantifies the environmental impacts resulting from the production, use, and disposal of a product or process. LCA has many benefits for making informed environmental decisions [141]: products are compared in defined environmental impact categories, which can be conceptualized by real environmental detriment [142]; unintended environmental trade-offs can be identified between impact categories [143]; and a standardized methodology allows LCAs from separate studies to be used to compare product choices [151]. Previous publications have outlined the effects of green chemistry on various aspects of a product's life cycle [149]. Lankey and Anastas [150] points out the benefit of using LCA within green chemistry to assess the trade-offs in switching between supply chemicals or processes. However, no published study quantitatively assesses what effect adherence to green design principles will have on the life cycle environmental impacts of similar products. This study empirically compares adherence to green design principles in currently available plastics to the life cycle environmental impacts of each plastic's production. Twelve polymers are assessed in this study. Seven polymers are generated from petroleum or other fossil fuel feedstocks: poly(ethylene terephthalate) (PET), HDPE, LDPE, PP, polycarbonate (PC), poly(vinyl chloride) (PVC), and general purpose polystyrene (GPPS). Two biopolymers are accessed via different production processes: polylactic acid made via a general process (PLA-G) and a process reported by Nature Works Limited liability company (LLC) (PLA-NW) as defined

in the ecoinvent database, and polyhydroxyalkanoate was assessed separately as derived from corn grain (PHA-G, polyhydroxyalkanoate derived from corn grain) and from corn stover (PHA-S, polyhydroxyalkanoate derived from corn stover). Lastly, one hybrid bio/petroleum polymer is assessed biopoly(ethylene terephthalate) (B-PET) which is made from one fossil fuel feedstock and one biological feedstock.

15.18.1 Methods

LCAs were completed for each polymer using the ecoinvent v1.2 database, the EPA Tool for the Reduction and Assessment of Chemical and other Environmental Impacts (TRACI 2 v.3.01) [152], and data from peer reviewed literature. Green design principles found in literature were reduced to quantifiable green design metrics. Each polymer's adherence to green design principles was assessed via these metrics. A decision matrix was used to normalize the results of both assessments and rank each polymer for preference in either assessment. Single value metrics generated by the decision matrix were also used to compare the adherence to green design principles and the life cycle environmental impacts in a two-dimensional chart.

LCAs were determined in accordance with the ISO 14040-14043 series [151]. The functional unit of comparison was 1 l of polymer contained in pellets (before product molding). Previous material assessments compared impacts based on mass [153–155]; however, varying physical properties for each plastic (e.g., density and modulus) cause vastly different masses to be required for the same plastic product, for example, see Pietrini *et al*. [156]. Volume was chosen as a functional unit for this study because of the approximately standard size of many plastic products (e.g., gift cards, bottles, and cups). The scope of each LCA was ''cradle-to-gate,'' including only the impacts resulting from the production of each plastic and not the use or disposal. The use phase is excluded because each polymer can be used in multiple products that are consumed at different rates. The disposal phase is excluded because the environmental impacts of biopolymer disposal are yet to be studied and adequate data on the emissions and energy use of degradation are unavailable. A qualitative discussion on the effects of product disposal methods is included in the discussion. Life cycle inventories in the ecoinvent v1.2 were used for all petroleum-based polymers (PET, HDPE, LDPE, PP, PC, PVC, GPPS) and both PLA scenarios (PLA-G and PLA-NW). The B-PET life cycle inventory was completed specifically for this study. No inventory was available for PHA; instead, data from the impact assessment stage was obtained using a literature review of published LCAs [156–162]. A life cycle inventory for B-PET was created for this study. The chemical composition of B-PET is identical to traditional PET and the production methods for both polymers are similar. In the B-PET production method, one monomer, ethylene glycol, is generated from sugar cane ethanol instead of natural gas. Ecoinvent inventory data on ethanol fuel and PET as well as literature sources were used to complete this inventory. The life cycle impact assessment (LCIA) was completed using the TRACI [152].

Ten different impact categories were assessed: acidification, carcinogenic human health hazards, noncarcinogenic human health hazards, ecotoxicity, eutrophication, global warming potential (GWP), ozone depletion, respiratory effects, smog, and nonrenewable energy use (NREU). No life cycle inventory data were available for PHA within the ecoinvent v1.2 database. Impact assessment data were obtained from previously published LCAs [156–162]. All studies contain assessments of NREU and GHG emissions; one study also includes eutrophication potential, smog formation, and acidification potential. To maintain complete assessments for use in the decision matrix, the average impact from the PLA scenarios is used as substitutes for PHA's impacts on human health, respiratory effects, ozone depletion, and ecotoxicity.

15.18.2 Green Design Metrics

Table 15.3 summarizes previously published green design principles used in this study. Principles were reduced into "themes" that are quantitatively or qualitatively evaluated by metrics. Table 15.4 lists each theme, each associated metric and specific principles associated with each theme/metric. The metrics from Table 15.4 were evaluated for each polymer in order to measure adherence to each design principle.

Waste Prevention: Waste reduction is measured through atom economy, defined in Eq. (15.2) where M_{input} is the mass of chemicals input to all reactions and M_{product} is the mass of the final chemical product. Atom economy is evaluated for the entire synthesis of each polymer using the theme defined by Blowers *et al*. [163]. The scope of each atom economy calculation begins with chemicals refined from petroleum or fructose in the case of plant sugars and ends with the final chemical structure of the polymer.

$$\text{Atom economy} = \frac{M_{\text{product}}}{M_{\text{input}}} \tag{15.2}$$

Material Efficiency: The ability of a material to promote efficient use is measured through its density, which is reflected in the volumetric functional unit used for all assessments. Less dense materials are able to serve many purposes with less mass, thus a lower density plastic is more preferable.

Avoidance of Hazardous Materials and Pollution: The avoidance of hazardous materials and pollution is measured via an average of the normalized life cycle impacts in TRACI categories of respiratory effects, human health cancer, human health noncancerous, and ecotoxicity [152].

Maximization of Energy Efficiency: Overall energy efficiency was measured by the cumulative life cycle energy use found by the cumulative energy demand (CED) LCIA method. This energy demand includes all energy use in the production of the product, as well as any embedded energy in input materials

Table 15.3 Previously published green design principles.

12 Principles of green chemistry	
GC 1	Prevention overall
GC 2	Atom economy
GC 3	Less hazardous chemical synthesis
GC 4	Designing safer chemicals
GC 5	Safer solvents and auxiliaries
GC 6	Design for energy efficiency
GC 7	Use of renewable feedstocks
GC 8	Reduce derivatives
GC 9	Catalysis
GC 10	Design for degradation
GC 11	Real time analysis of pollution prevention
GC 12	Inherently safer chemistry for accident prevention
12 Additional principles of green chemistry	
A 1	Identify by-products: quantify if possible
A 2	Report conversions, selectivities, and productivities
A 3	Establish a full mass balance for the process
A 4	Quantify catalyst and solvent losses
A 5	Investigate basic thermochemistry to identify
A 6	Anticipate other potential mass and energy transfer
A 7	Consult a chemical or process engineer
A 8	Consider the effect of overall process on
A 9	Help develop and apply sustainable measures
A 10	Minimize use of utilities and other inputs
A 11	Identify safety and waste minimization are incompatible
A 12	Monitor, report, and minimize wastes
12 Principles of green engineering	
GE 1	Inherent rather than circumstantial
GE 2	Prevention instead of treatment
GE 3	Design for separation
GE 4	Maximize mass, energy, space, and time
GE 5	Out-pulled verses input-pushed
GE 6	Conserve complexity
GE 7	Durability rather than immortality
GE 8	Meet need. Minimize excess
GE 9	Minimize material diversity
GE 10	Integrate local material and energy flows
GE 11	Design for commercial afterlife
GE 12	Renewable rather than depleting

such as oil, natural gas, or biomass, calculated using the higher heating value (HHV) as explained by Huijbregts *et al*. [164].

Use of Renewable Sources: The use of renewable sources is measured by the percent of material from biological sources in the final product, by mass.

Table 15.4 Matrices for green design principles.

Theme	Metric	Principles referenced
Avoid waste	Atom economy	GC 2, A1, A3
Material efficiency	Density	GE 8, GE 4
Avoid hazardous materials/pollution	TRACI health and ecotoxicity impacts	GC 3–5, 11, GE 2
Maximize energy efficiency	Total energy demand	GC 6, A 10, GE 3, 4, 10
Use of renewable resources	Percent from renewable resources	GC 7, GE 12
Use of local sources	Feed stock distance	GE 10
Design products for recycle	Percent recycled	GE 3, 6, 9, and 11
Design to degrade	Biodegradability	GC 10
Cost efficiency	Price	GE 9

Design Products for Recycle: Adherence to these principles is measured by the recovery percentage of a material in the U.S. municipal recycle stream [165].

Design Biodegradable Products: The biodegradability of a product is measured through categorical classifications: nonbiodegradable, biodegradable in an industrial facility, or biodegradable in typical backyard conditions. For quantitative purposes, these categories are assigned values of 1, 2, and 3, respectively.

Use Local Sources: The categorical distance of the furthest feedstock location is assessed as a metric. Petroleum sources are categorized as international, often routed to the U.S. through Canada or from the Middle East. Renewable sources may be either local or not. Bioethylene for use in B-PET is only produced in India, and is assumed to be an international source for the U.S. PLA and PHA are often produced from regional corn crops. For quantitative purposes, categorical distances of international, national, and regional (roughly 600 mile radius) are assigned values of 1, 2, and 3, respectively.

Cost Efficiency: Sustainable products that are competitively priced will more effectively integrate into markets. The cost effectiveness of each polymer was measured via a median price per liter of the polymer [166].

15.18.3 Decision Matrix

A decision matrix was used to create two single value metrics for each polymer, one evaluating each polymer for life cycle environmental impacts and the other evaluating each polymer for adherence to green design principles. Results from both assessments were normalized to the average across all polymers, shown in Eq. (15.3), where N_{ij} is the normalized value for polymer i in metric/impact j, V_{ij} is the

value for polymer i in metric/impact j, n is the total number of polymers studied, and j is a multiplication factor which is 1 for metrics/impacts in which higher values are more preferable and −1 for metrics/impacts in which lower values are more preferable. The resulting normalized values in each category all average to either 1 or −1 depending on the value of ij. An alternate normalization method employs the maximum value in place of the average value and was also completed for comparison.

$$N_{ij} = \left[\frac{\left(V_{ij*n}\right)}{\sum(V_{ij})}\right] * \Psi_j \tag{15.3}$$

Single value metrics were created in order to rank polymers with respect to adherence to green design principles or life cycle environmental impacts. The single value metrics are the sum of the normalized impacts for each polymer in either the LCA or the green design assessment of each impact category or green design metric is equally weighted in the single value metric system. While equal weighting is arguably nonideal, it reduces bias toward specific metrics and maintains clear transparency.

15.19 Life Cycle Assessment Results

The cradle-to-gate environmental impacts resulting from the production of each packaging polymer are shown in Table 15.5. The resulting life cycle impacts are normalized to the largest impact found in this study. Table 15.5 shows biopolymer production resulting in the highest impact in 5 of the 10 categories: ozone depletion, acidification, eutrophication, carcinogens, and ecotoxicity. PLA-G results in the greatest eutrophication potential, most likely as a result of fertilizer use [167]. B-PET results in the greatest impact on ecotoxicity and human health categories, and this impact is largely attributed to sugar cane farming and ethanol production which accounts for anywhere from 13% to 21% of impacts in each category. It should be noted that the high eutrophication impact of B-PET is not solely attributable to agriculture/ethanol production; traditional PET production produces the second highest impact in this category. PHA-G results in the greatest acidification impact. The production of polyolefin polymers (HDPE, LDPE, and PP) does not result in the maximum impact in any category. This result is likely due to the limited chemical processing required for polyolefin polymers. Monomers for polyolefin polymers are the direct products of oil refining. The more complex petro-polymers (PET, PC, and PS) require additional synthetic steps between the oil refinery and polymerization. Additional processing requires additional transportation and chemical process emissions, thus increasing the likelihood of emissions and environmental impact.

Table 15.5 Evaluation of polymers using green design matrices.

Material	Overall atom economy (%)	Carcinogens (kg benzene, equiv l^{-1})	Noncarcinogens (kg toluene, equiv l^{-1})	Respiratory effects (kg PM2.5, equiv l^{-1})	Ecotoxicity (kg benzene, equiv l^{-1})	Cumulative energy demand (MJ, equiv l^{-1})	% Renewable material	Distance of feed stocks	% Recovery	Biodegradable	Price (USD l^{-1})
PET	80	1.1×10^{-2}	62.9	4.9×10^{-3}	5.72	123.8	0	Intern.	**18**	N/A	4.13
B-PET	62	1.3×10^{-2}	72.7	5.7×10^{-3}	6.98	146.2	15	Intern.	**18**	N/A	4.13
PVC	55	1.1×10^{-2}	**31.7**	7.3×10^{-3}	**0.40**	**82.9**	0	Intern.	0	N/A	4.02
PLA-NW	80	6.1×10^{-2}	**22.5**	$\mathbf{1.2 \times 10^{-3}}$	1.21	**79.4**	**100**	**Region**	0	Indus.	4.66
PLA-G	80	8.4×10^{-3}	**37.5**	$\mathbf{3.1 \times 10^{-3}}$	4.31	98.3	**100**	**Region**	0	Indus.	4.66
PHA-G	48	7.2×10^{-3}	**30.0**	$\mathbf{3.1 \times 10^{-3}}$	2.76	**91.5**	**100**	**Region**	0	**Backyard**	6.20
PHA-S	48	1.1×10^{-2}	**30.0**	$\mathbf{2.1 \times 10^{-3}}$	2.76	**91.5**	**100**	**Region**	0	**Backyard**	6.20
HDPE	**100**	$\mathbf{6.5 \times 10^{-4}}$	**18.7**	$\mathbf{1.3 \times 10^{-3}}$	**0.65**	**73.4**	0	Intern.	10	N/A	**1.52**
LDPE	**100**	$\mathbf{6.9 \times 10^{-4}}$	**19.6**	$\mathbf{1.5 \times 10^{-3}}$	**0.82**	**72.3**	0	Intern.	5	N/A	**1.58**
GPPS	**98**	$\mathbf{3.2 \times 10^{-3}}$	92.7	$\mathbf{2.5 \times 10^{-3}}$	1.79	**92.2**	0	Intern.	1	N/A	**2.35**
PC	59	$\mathbf{3.0 \times 10^{-3}}$	85.6	9.5×10^{-3}	3.13	128.9	0	Intern.	0	N/A	5.25
PP	**100**	$\mathbf{5.8 \times 10^{-4}}$	**16.8**	$\mathbf{1.2 \times 10^{-3}}$	**0.54**	**67.6**	0	Intern.	0	N/A	**1.78**

Bolder cells symbolize more preferable values [167].
Indus– biodegradable in an industrial facility and Intern– the categorical distance of the feed stock is international.

15.20
Green Principles Assessment Results

Table 15.6 shows the results of the green principles assessment for each of the 12 polymers studied. The biopolymers adhere well to several green design principles: the use of renewable and regional resources, low emissions of carcinogens, and low emissions of particulates. Polyolefin polymers exhibit the highest atom economy, the lowest price, and low pollutant emissions

15.21
Comparison

Rankings generated by the decision matrices are shown in Table 15.6. The two ranking systems represent design choices based on either the green design principles or the LCA results. Biodegradable polymers are on top of the green design rankings, owing mostly to their low energy demand, use of renewable materials, and biodegradability. Comparing the green design rankings to the LCA rankings, the biopolymers, which ranked 1, 2, 3, and 4, in the green design system, are 6, 4, 8, and 9 respectively in the LCA rankings (as shown in Table 15.6). Polyolefins (PP, LDPE, and HDPE) rank 1, 2, and 3 in the LCA rankings. Complex polymers, such as PET, PVC, and PC are placed at the bottom of both ranking systems. Specifically, B-PET ranked eighth in the green design ranking is placed last in the LCA ranking. The production of B-PET requires agriculture, fermentation, and multiple chemical processing steps, resulting in a low atom economy and a large potential for emissions and environmental impact. To further study the relationship between green design metrics and environmental impacts, the single value metrics used to rank each polymer are presented in Figure 15.3, where the

Table 15.6 Rankings for each of the polymers based the normalized green design assessment results and the normalized life cycle assessment results.

Material	Green design rank	LCA rank
PLA (nature works)	1	6
PHA (utilizing stover)	2	4
PHA (general)	2	8
PLA (general)	4	9
High density polyethylene	5	2
Poly(ethylene terephthalate)	6	10
Low density polyethylene	7	3
Biopoly(ethylene terephthalate)	8	12
Polypropylene	9	1
General purpose polystyrene	10	5
Poly(vinyl chloride)	11	7
Polycarbonate	12	11

x-axis represents adherence to green design principles and the *y*-axis represents life cycle environmental impacts. The close relationship between many of the polymers in the green design principles dimension shows the relatively small differentiation between rankings 1–5, as well as rankings 6–8. In contrast, single values in the life cycle environmental impacts dimension are relatively continuous, exhibiting tight differentiation only between the polyolefin polymers, ranking 1–3. The relationship between green design principles and lifecycle environmental impacts shows a distinct difference between biopolymers and petroleum polymers. With the exception of PET, petroleum polymers exhibit lower lifecycle environmental impacts when they adhere more strictly to green design principles. Biopolymers exhibit a range of life cycle environmental impacts; however, their rank based on green design principles does not vary widely, with the exception of B-PET. Adhering to green design principles reduces environmental impact in either the petroleum or biological polymer categories. Switching from petroleum feedstock's to biofeedstock does not necessarily reduce environmental impacts. The use of maximum values instead of average values for normalization does not alter the LCA rankings; however, this does alter the green design rankings. Regardless of normalization, the overall disparity between biological and petroleum polymers remains. Results for the maximum normalization method are shown in Figure 15.4 [168].

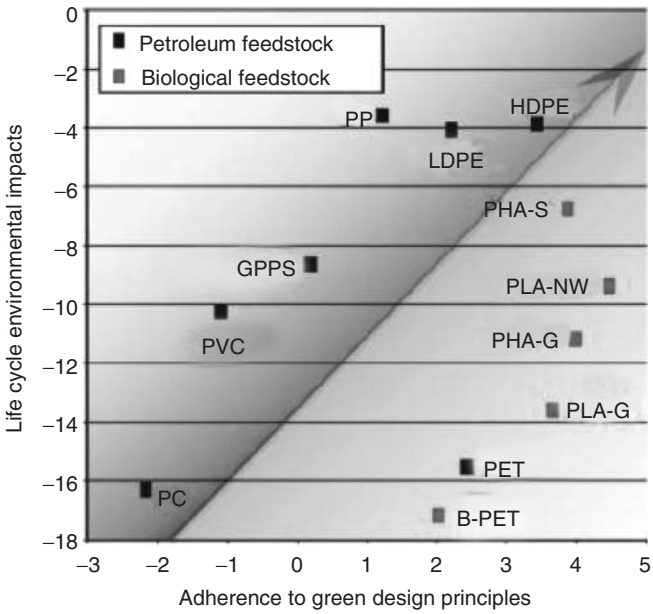

Figure 15.4 Polymer assessments displayed in two dimensions, with "adherence to green design principles" on the *x*-axis and "life cycle environmental impacts" in the *y*-axis. In this system, greater values are more preferable, meaning greater adherence to principles, or normalized environmental impacts.

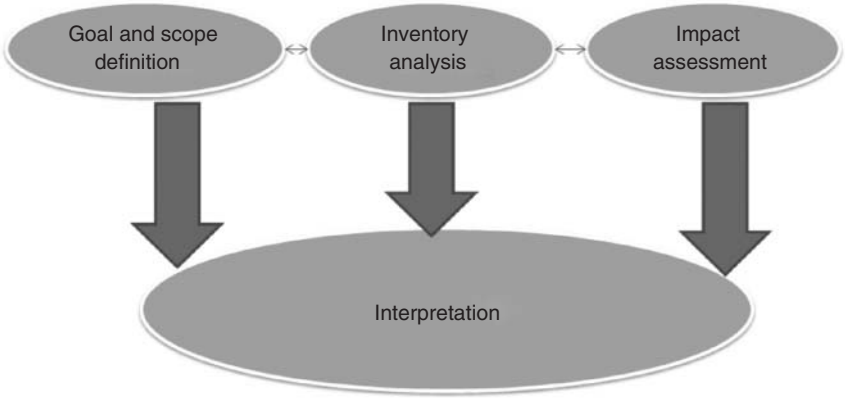

Figure 15.5 Important LCA requirements [169].

A LCA consists of four independent elements that is, (i) the definition of goal and scope, (ii) the life cycle inventory analysis, (iii) the LCIA, and (iv) the life cycle interpretation. The definition of the goal and scope (i) includes a decision about the functional unit that forms the basis of comparison, the product system to be studied, system boundaries, allocation procedures, assumptions made, and limitations.

The life cycle inventory analysis (ii) involves data collection and calculation procedures to quantify the total system's inputs and outputs that are relevant from an environmental point of view, that is, mainly resource use, atmospheric emissions, aqueous emissions, solid waste, and land use. The LCIA (iii) aims at evaluating the significance of potential environmental impacts using the results of the life cycle inventory analysis. The life cycle interpretation (iv) is the final step of the LCA where conclusions are drawn from both the life cycle inventory analysis and the LCIA or, in the case of life cycle inventory studies, from the inventory analysis only. The important LCA requirements are given in Figure 15.5 [150].

The methodology for impact assessment is widely accepted and ISO standards have been established to compare and quantify the various weighing factors. The assessment consists of weighing the classes to integrate the environmental profiles such as effects on GHG emission, ozone depletion, acidification, or eutrophication. It is however unrealistic to desire unification into one environmental impact number for widely diverse ecological and economical effects.

LCA is a tool that quantifies the environmental impacts resulting from the production, use, and disposal of a product or process. LCA has many benefits for making informed environmental decisions: (i) products are compared in defined environmental impact categories, which can be conceptualized by real environmental detriment, (ii) unintended environmental trade-offs can be identified between impact categories, and (iii), a standardized methodology allows LCAs from separate studies to be used to compare product choices [150]. Lankey *et al.* points out the

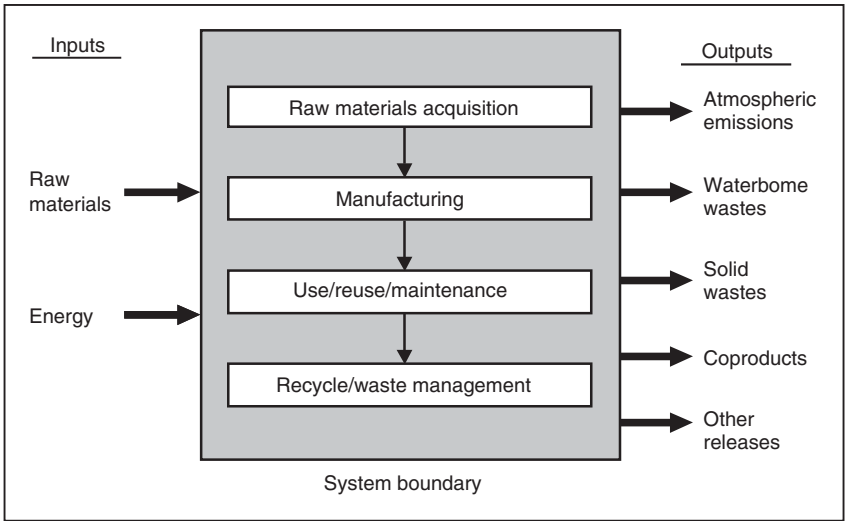

Figure 15.6 Life cycle stages [170].

benefit of using LCA within green chemistry to assess the trade-offs in switching between supply chemicals or processes [151].

The term *life cycle* refers to the major activities in the course of the product's life-span from its manufacture, use, and maintenance, to its final disposal, including the raw material acquisition required to manufacture the product. Figure 15.6 [151] illustrates the possible life cycle stages that can be considered in an LCA and the typical inputs/outputs measured.

15.22 Life Cycle Inventory Analysis of Green Composites

15.22.1 Fiber Composites

The concept of fiber composites is very old as it dates back to 800 BC when Israelites and Egyptian pharaohs in third millennium BC used straw in bricks manufacturing as a reinforcement. Later on the Chinese used to do this as well. The papyrus is another such example where papyrus reed was placed parallel to each other and stacked on perpendicular layers and pressure was exerted on it in order to form papyrus paper. In 108 AD, the Chinese invented the paper, as we know it in the similar manner [171]. In the 1930s, a more advanced version of fiber composites came into being in the United States where they used short glass fiber reinforcement in cement and fiber-enforced composites were developed in 1940. Composites were also used in World War II when glass fiber and polyester resin composites were used to make boat hulls and radomes (radar cover) In the 1950s, for

the first time, composites were used in cars because of their desirable properties. Researches conducted on studying different characteristics and improving the manufacturing process have increased over a period of time. Composites began to be used more and more in everyday commodities like bath tubs, railings, electrical goods, sports equipment, cars, and so on. Aerospace and ship industry also started using composites initially for some of the parts and later on for the whole structure. For the first time in the field of construction, composites were used to build a dome structure in Benghazi in 1968. Now their application in construction has enhanced fourfold [172].

15.22.2
Natural Fibers

Natural fibers have come into use after centuries. They have been around for a decade and natural fibers have really come to stay once again. Now they are being highly recommended because they are naturally derived from plants and are far lesser in weight as compared to glass. These reinforcements are reusable, good insulator of heat and sound, degradable, and cost-effective. They also have their own share of disadvantages: they are more prone to catching fire, their quality cannot be maintained equally, moisture causes swelling of fibers and their price may fluctuate according to the yield of the crop, and so on. It is being used widely for building purposes, manufacture of cars, and so on. The natural fibers used for composites are jute, hemp, flax, china grass, and so on.

15.22.3
Life Cycle Analysis of Polylactide (PLA)

PLA (Figure 15.7) is a biodegradable polymer derived from lactic acid. It is a highly versatile material and is made from 100% renewable resources like corn, sugar beets, wheat, and other starch-rich products.

Cargill Dow's PLA is a versatile new compostable polymer that is made from 100% renewable resources like corn, sugar beets, or rice. Figure 15.8 [173] illustrates the various steps involved in the production of PLA starting with corn growing and ending with the production of PLA granules.

PLA exhibits many properties that are equivalent to or better than many petroleum-based plastics, which makes it suitable for a variety of applications. It is pertinent to note that PLA competes well with other popular plastics already used for packaging. It is clear and naturally glossy like the polystyrene used in

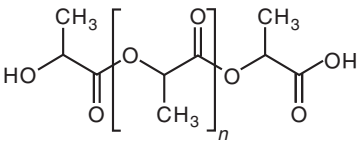

Figure 15.7 Chemical structure of polylactide.

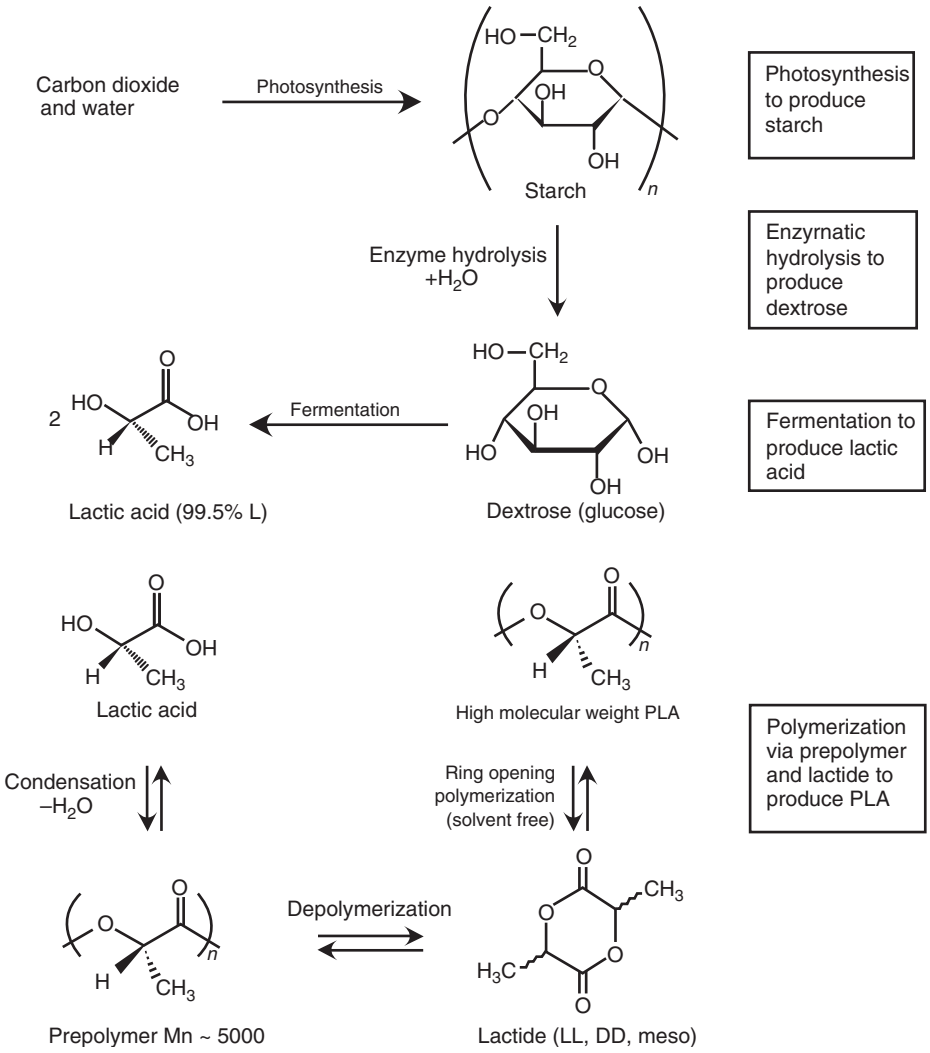

Figure 15.8 PLA manufacturing overview.

''lister packs'' for products such as batteries, toys, and many others. PLA is resistant to moisture and grease. It has flavor and odor resistant characteristics similar to the popular plastic PET used for soft drinks and many other food products.

LCA is a method to account for the environmental impacts associated with a product or service. The term *life cycle* indicates that all stages in a product's life, from resource extraction to ultimate disposal, are taken into account.

Nowadays, the most important tool to evaluate the environmental impact of a bioplastic and/or of a petroleum-based plastic (conventional plastic) is the LCA that determines the overall impact of a plastic on the environment by defining

and analyzing several impact indices directly related to production, utilization, and disposal of the considered plastics. The starting material for PLA is starch from a renewable resource such as corn. Corn is milled, which separates starch from the raw material. Unrefined dextrose is then processed from the starch. Dextrose is turned into lactic acid using fermentation, similar to that used by beer and wine producers. Turning the lactic acid into a polymer plastic takes some specialized chemistry. Through a chemical process called *condensation*, two lactic acid molecules are converted into one cyclic molecule called a *lactide*. This lactide is purified through vacuum distillation. A solvent-free melt process causes the ring-shaped lactide polymers to open and join end-to-end to form long chain polymers. A wide range of products that vary in molecular weight and crystallinity can be produced, allowing the PLA to be modified for a variety of applications. PLA is a versatile polymer that has many potential uses, including many applications in the textile and medical industries as well as the packaging industry.

PLA polymers are fully compostable in commercial composting facilities. With proper equipment, PLA can be converted back to monomer, which then can be converted back into polymers. Alternatively, PLA can be biodegraded into water, carbon dioxide, and organic material. At the end of a PLA-based product's life cycle, a product made from PLA can be broken down into its simplest parts so that no sign of the original product remains.

One major criticism of the polymer occurs during its biological breakdown phase. PLA releases carbon dioxide and methane during this process. These are generally recognized as two heat-trapping GHGs that are being targeted for reduced emissions standards by international committees. Another criticism is that fossil fuels are still needed to produce PLA. Although fossil fuels are not used in the polymer itself, they are needed to power the processes involved in plant harvests and chemical production. Skeptics also warn that biodegradable plastics degrade too slowly to make a substantial difference to waste streams. In response to these concerns, PLA supporters acknowledge that fossil fuels are being used to produce the plastic, but state that this process requires between 20% and 50% less fossil resources than making plastics from petroleum. Also, while petroleum is the primary resource for conventional plastic production, coal and natural gas are mainly used in the plastic-from-plant making process. Since plant-based methods involve switching from a less abundant resource (oil) to a more abundant one (coal), it is argued that this is a step toward sustainability.

In response to the argument about release of GHGs, PLA and plant-based plastic supporters argue that plants process carbon dioxide as they are growing and living so the carbon dioxide that they release into the atmosphere as they are degrading is reused by new plants, leading to no net increase in carbon dioxide gases in the atmosphere (Figure 15.9) [174].

LCA is a technique that could help to assess the benefits and drawbacks of PLA. According to The Society of Environmental Toxicology and Chemistry (SETAC), LCA is an objective process to evaluate the environmental burdens associated with a product, process, or activity by identifying and quantifying energy and materials used and wastes released to the environment, and to evaluate, and consequently

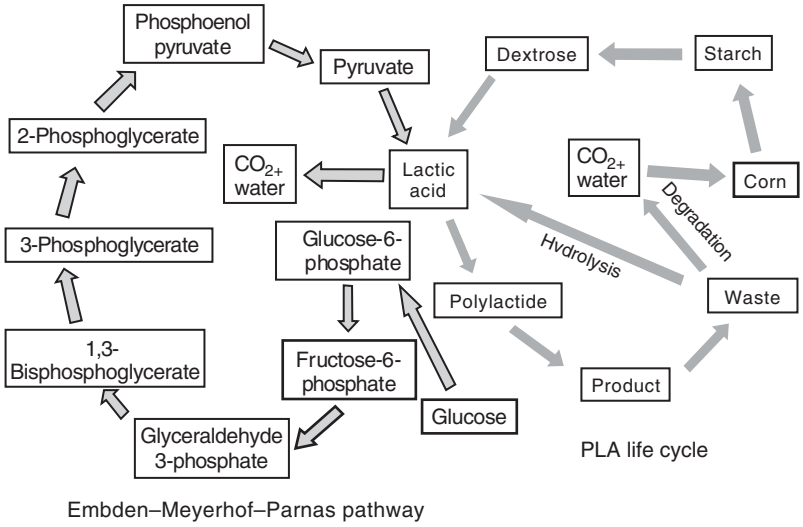

Figure 15.9 Biocompatibility of PLA.

enhance the commercial value of the product through ''cradle-to-grave'' analysis. During the impact assessment, potential contribution of each of these exchanges to important environmental effects (i.e., global warming, photochemical smog, fossil fuel depletion) is estimated. Results are then interpreted and recommendations are made. Using LCA will help companies and governments decide whether PLA is an appropriate material for a particular product (Figure 15.10) [174].

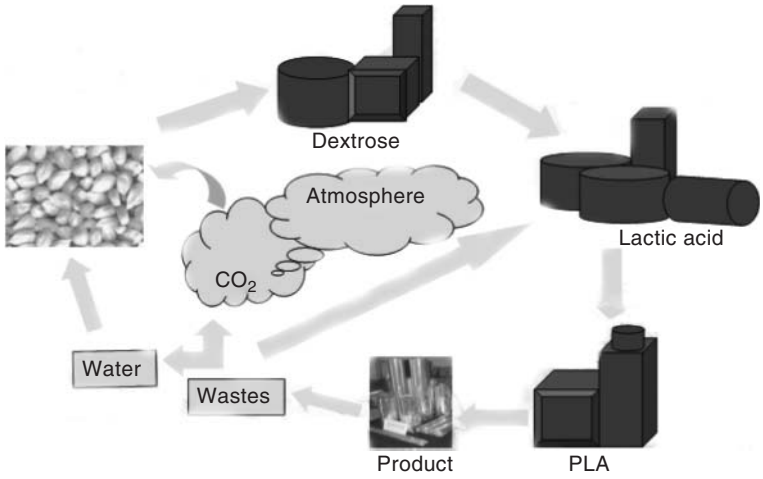

Figure 15.10 PLA life cycle.

15.23
Life Cycle Analysis of Poly(hydroxybutyrate)

More recently, because of the availability of potential natural resources for the manufacture of improved environment-friendly materials, and reduced dependency on petroleum resources, bio-based biodegradable plastics have garnered attention from researchers, industries, and governments as possible substitutes for conventional plastics. PHAs are one such class of biopolymers. The LCA applied to a potential pathway for PHB production, from the cellulosic fraction of organic residuals, normally disposed of by landfill (Figure 15.11) [175], shows GHG emissions lower than a PHB produced from a dedicated agricultural feedstock.

15.24
Life Cycle Analysis of Cellulose Fibers

Shen and Patel [176] studied the life cycle analysis of cellulose fibers (Figure 15.12). The production of textile materials has undergone dramatic changes in the last century. Man-made cellulose fibers have played an important role for more than 70 years. Today, the man-made cellulose fiber industry is the world's second largest biorefinery (next to the paper industry). In the last few years, the interest in man-made cellulose fibers has grown as a consequence of increased environmental awareness and the depletion of fossil fuels. However, an environmental assessment of modern man-made cellulose fibers has not been conducted so far. This study will assess the environmental impact of man-made cellulose fibers [177]. Five staple fiber products, that is, (i) Lenzing Viscose Asia, (ii) Lenzing Viscose Austria, (iii) Lenzing Modal, (iv) Tencel Austria, and (v) Tencel Austria 2012, are analyzed by means of LCA. The system boundary is cradle to factory gate (Figure 15.13). Shen and Patel [176] compared the results with conventional cotton, novel bio-based fibers (PLA fibers), and fossil fuel-based fibers (PET and PP). The inventory data for the production of man-made cellulose fibers were provided by Lenzing AG. The inventory data for cotton, PET, PP, and PLA were obtained from literature sources. The environmental indicators analyzed include resources and the impact categories covered by CML 2000 baseline method. The indicators for resources include NREU, renewable energy use (REU), CED, water use, and land use. The environmental impact indicators covered by the CML method are GWP 100a, abiotic depletion, ozone layer depletion, human toxicity, fresh water aquatic ecotoxicity, terrestrial ecotoxicity, photochemical oxidation, acidification, and eutrophication. In addition, the system boundary of cradle to factory gate plus end-of-life waste management was analyzed for NREU and GWP. Furthermore, sensitivity analyses have been carried out to understand the influence of various assumptions and allocation methods. The LCA results show that Lenzing Viscose Austria and Lenzing Modal offer environmental benefits in all categories (except for land use and water use) compared to Lenzing Viscose Asia. Tencel Austria 2012, Lenzing Viscose Austria, Lenzing Modal, and Tencel Austria are the most favorable choices from

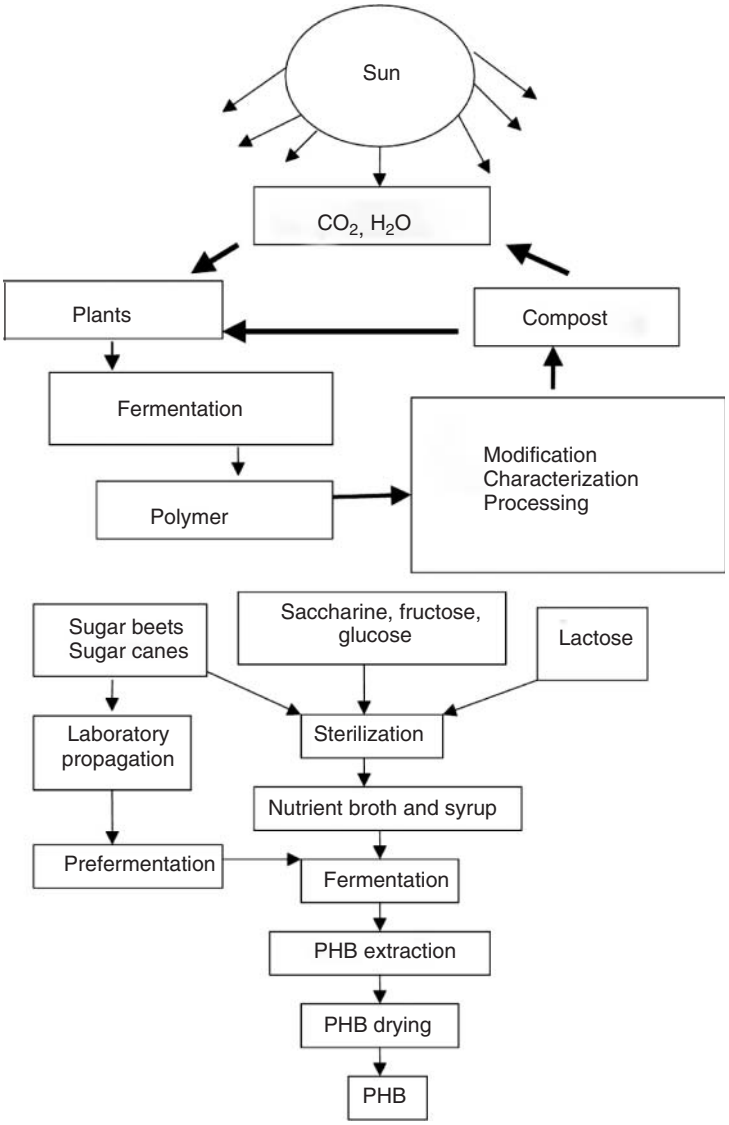

Figure 15.11 The life cycle of PHB is a cycle process.

an environmental point of view among all the fibers studied. These four man-made cellulose fibers offer important benefits for reducing NREU, GWP, toxicity impacts, water use, and land use. Lenzing Viscose Asia has higher impacts than the other man-made cellulose fibers with regard to NREU, GWP, abiotic depletion, photochemical oxidation, and acidification. Cotton is identified as the least preferred choice because of its high ecotoxicity impacts, eutrophication, water use, land use, and relatively low land use efficiencies. Cellulose is the most abundant renewable

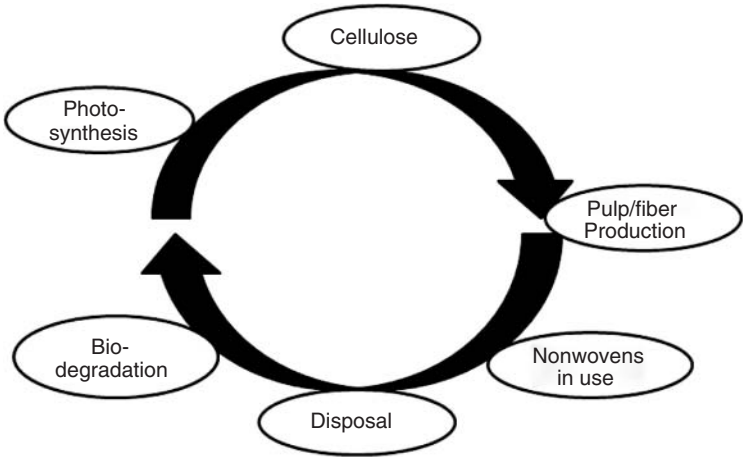

Figure 15.12 Natures life cycle.

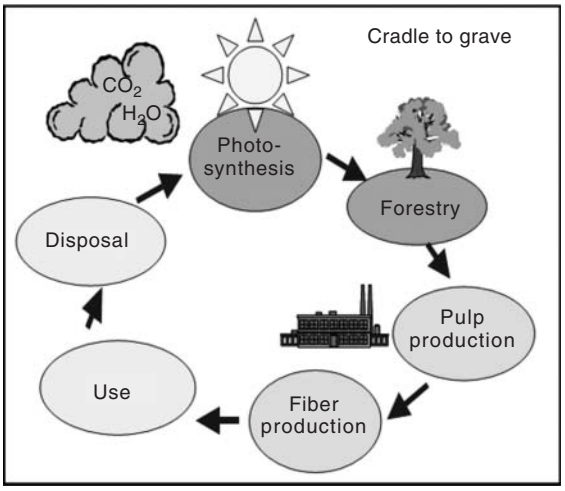

Figure 15.13 Life cycle of man-made cellulosic fibers.

polymer on the planet. It is generated by photosynthesis. Available from most plant structures and is fully biodegradable [177].

15.25 Conclusions

Green materials are the wave of the future. There is an immense opportunity in developing new bio-based products, but the real challenge is to design sustainable bio-based products. New environmental regulations and societal concern have

triggered the search for new products and processes that are compatible with the environment. The major limitations of present biodegradable polymers are their high cost. Biocomposites are emerging as a realistic alternative to glass-reinforced composites. Because biocomposites are derived from renewable resources, material costs can be markedly reduced with their large-scale usage. Natural fibers are biodegradable, but renewable resource-based bioplastics can be designed to be either biodegradable or not according to the specific demands of a given application. Their unique balance of properties would open up new market development opportunities for biocomposites in the twenty-first century green materials world.

It can be concluded that green composites is an essential guide for agricultural crop producers, government agricultural departments, automotive companies, composite producers, and material scientists, all dedicated to the promotion and practice of eco-friendly materials and production methods. The natural fiber composites or green composites can be effectively used as a material for structural, automotive, medical, and electronic applications. Natural/biofiber composites (green composites) are emerging as a viable alternative to glass fiber-reinforced composites especially in automotive and building product applications.

Abbreviations

GFRP	glass fiber-reinforced plastics
TPS	thermoplastic starch
PLA	polylactic acid
R&D	research and development
PP	polypropylene
SPC	soy protein concentrate
PEN	poly(ethylene 2,6-naphthalate)
CNT	carbon nanotube
DWCNTs	double-wall carbon nanotubes
CO_2	carbon dioxide
NO_x	nitrogen oxides
SO_x	sulfur oxides
PHB	polyhydroxybutyrate
PCL	polycaprolactone
PBS	poly(butylene succinate)
RHs	relative humidities
H_2O	water
PE	polyethylene
PVA	poly(vinyl alcohol)
BOD	biological oxygen demand
COD	chemical oxygen demand
COAG	Council of Australian Governments
GHG	green house gas
UK	United Kingdom

EPBD	European Community's energy performance directive for buildings
ASTM	American Society for Testing Materials
MSW	municipal solid waste
HDPE	high density polyethylene
M_0	initial mass
M_d	degradation mass
AIA	Anaerobe Isolation Agar
g	gram
TCB	1,2,4-trichlorobenzene
PTFE	polytetrafluoroethylene
GPC	gel permeation chromatography
RI	refractive index
M_n	number-average molecular weights
M_w	weight-average molecular weights
DSC	differential scanning calorimetry analysis
T_g	glass transition temperature
T_m	melting temperature
T_c	crystallization temperature
FTIR	Fourier transform infrared
ATR	attenuated total reflectance
cm^{-1}	centimeter inverse one
SEM	scanning electron microscopy
EDPs	environmentally degradable plastics
L-PLA	poly(L-lactide)
D-PLA	poly(D-lactide)
DL-PLA	poly(DL-lactide)
L	laevorotatory
D	dextrorotatory
BC	bacterial cellulose
MC	microbial cellulose
LCA	life cycle assessment
EPA	Environmental Protection Agency
PET	poly(ethylene terephthalate)
LDPE	low density polyethylene
PC	polycarbonate
PVC	poly(vinyl chloride)
GPPS	general purpose polystyrene
PLA-G	polylactic acid made via a general process
PHA-G	polyhydroxyalkanoate derived from corn grain
PHA-S	polyhydroxyalkanoate derived from corn stover
B-PET	biopoly(ethylene terephthalate)
SI	Supporting Information
TRACI	Tool for the Reduction and Assessment of Chemical and Environmental Impacts
NREU	nonrenewable energy use

LCIA	life cycle impact assessment
HHV	higher heating value
SETAC	Society of Environmental Toxicology and Chemistry
PHAs	polyhydroxyalkanoates
REU	renewable energy use
CED	cumulative energy demand
GWP	global warming potential

References

1. Jayanarayanan, K., Jose, T., Thomas, T., and Joseph, K. (2009) *Eur. Polym. J.*, **45**, 1738–1747.
2. Paul, S.A., Joseph, K., Mathew, J.D.G., Pothen, L.A., and Thomas, S. (2010) *Part A*, **41**, 1380–1387.
3. Netravali, A.N. and Chabba, S. (2003) *Mater. Today*, **6**, 22.
4. Wambua, P., Ivens, J., and Verpoest, I. (2003) *Compos. Sci. Technol.*, **63**, 1259.
5. Joshi, S.V., Drzal, L.T., Mohanty, A.K., and Arora, S. (2004) *Composites Part A*, **35**, 371.
6. Goda, K., Sreekala, M.S., Gomes, A., Kaji, T., and Ohgi, J. (2006) *Composites Part A*, **37**, 2213.
7. Doi, T., Itoh, M., Kaji, T., Nakamura, R., Goda, K., and Ohgi, J. (2009) *J. Jpn. Soc. Compos. Mater.*, **35** 56–63 (in Japanese).
8. Mohanty, A.K., Misra, M., and Hinrichsen, G. (2000) *Macromol. Mater. Eng.*, **276–277**, 1–24.
9. Mohanty, A.K., Misra, M., Drzal, L.T., Selke, S.E., Hart, B.R., and Hinrichsen, G. (2005) Natural fibers, biopolymers and biocomposites: an introduction, in *Natural Fibers, Biopolymers and Biocomposites* (eds A.K. Mohanty, M. Mistra, and L.T. Drzal), CRC Press, Boca Raton, FL.
10. Karus, M., Ortmann, S., and Vogt, D. (2005) All natural on the inside? Natural fibers in automotive interiors. *Kunstst. Plast. Eur.*, **7**, 1–3.
11. Sanadi, A.R., Prasad, S.V., and Rohatgi, P.K. (1986) *J. Mater. Sci.*, **21**, 4299–4300.
12. Rong, M.Z., Zhang, M.Q., Liu, Y., Yang, G.C., and Zeng, H.M. (2001) The effect of fiber treatment on the mechanical properties of unidirectional sisal-reinforced epoxy composites. *Compos. Sci. Technol.*, **61**, 1437–1447.
13. Bledzki, A.K., Fink, H.-P., and Specht, K. (2004) *J. Appl. Polym. Sci.*, **93**, 2150–2156.
14. Van de Weyenberg, I., Truong Chi, T., Vangrimde, B., and Verpoest, I. (2006) *Composites Part A*, **37** (9), 1368–1376.
15. Aziz, S.H., Ansell, M.P., Clarke, S.J., and Panteny, S.R. (2005) *Compos. Sci. Technol.*, **65**, 525–535.
16. Albuquerque, A.C., Joseph, K., and Carvalho, L.H. (1999) *Compos. Sci. Technol.*, **60**, 833–844.
17. Aziz, S.H. and Ansell, M.P. (2003) *Compos. Sci. Technol.*, **65**, 535–535.
18. Karnani, R., Krisnan, M., and Narayan, R. (1997) *Polym. Eng. Sci.*, **37** (2), 476–483.
19. Herrera Franco, P.J. and Valadez-GonzaleZ, A. (2005) Fiber-matrix adhesion in natural fiber composites, in *Natural Fibers, Biopolymers and Biocomposties* (eds A.K. Mohanty, M. Misra, and L.T. Drzal), CRC Press, Boca Raton, FL.
20. Heinemann, M. and Fritz, H.-G. (2005) Polylactid-Struktur, Eigenschaften und Anwendungen. 19. Stuttgater Kunststoff-Kolloquium.
21. Oksman, K., Skrifvars, M., and Selin, J.F. (2003) *Compos. Sci. Technol.*, **63**, 1324–1327.
22. Mohanty, A.K., Misra, M., and Drzal, L.T. (2002) *Polym. Environ.*, **10**, 19.
23. Satyanarayana, K.G. (2007) International Conference on Advanced Materials and Composites (ICAMC-2007), October 24.

24. Averousa, L. and Boquillonb, N. (2004) *Carbohydr. Polym.*, **56**, 111.
25. Moszner, N. and Salz, U. (2001) *Prog. Polym. Sci.*, **26**, 535.
26. Marques, A.P., Reis, R.L., and Hunt, J.A. (2002) *Biomaterials*, **23**, 1471.
27. Azevedo, H.S., Gama, F.M., and Reis, R.L. (2003) *Biomacromolecules*, **4**, 1703.
28. Boesel, L.F., Mano, J.F., and Reis, R.L.J. (2004) *Mater. Sci.*, **15**, 73.
29. Gomes, M.E., Sikavitsas, V.I., Behravesh, E., Reis, R.L., and Mikos, A.G. (2003) *J. Biomed. Mater. Res. Part A*, **67**, 87.
30. Dai, N.T. and Kung, Y.M. (2000) *Biochem. Biophys. Res. Commun.*, **329**, 905.
31. Khan, M.A., Kopp, C., and Hinrichsen, G. (2001) *J. Reinf. Plast. Compos.*, **20**, 1414.
32. Curvelo, A.A.S., Carvalho, A.J.F., and Agnelli, J.A.M. (2001) *Carbohydr. Polym.*, **45**, 183.
33. Van de Velde, K. and Kiekens, P. (2002) *Polym. Test.*, **21**, 433.
34. Kumar, M.N.S. and Siddaramaiah (2007) *Autex Res. J.*, **7**, 111–118.
35. Keller, A. (2003) *Compos. Sci. Technol.*, **63**, 1307.
36. Placket, D., Andersen, T.L., Pedersen, W.B., and Nielsen, L. (2003) *Compos. Sci. Technol.*, **63**, 1287.
37. Godbole, S., Gote, S., Latkar, M., and Chakrabarti, T. (2003) *Bioresour. Technol.*, **86**, 33.
38. Huang, X. and Netravali, A. (2007) *Compos. Sci. Technol.*, **67**, 2005.
39. Kim, J.Y., Han, S., and Hong, S. (2008) *Polymer*, **49**, 3335.
40. Gojny, F.H., Wichman, M.H.G., Klopke, U., Fiedle, B., and Schulte, K. (2004) *Compos. Sci. Technol.*, **64**, 2363.
41. Gatani1, M.P., Tonoli, G.H.D., Freitas, Z.D., Battisti, M., and Savastano, H. (2009) Peanut husks as raw material for cementitious covering panels, 11th International Conference on Non-Conventional Materials and Technologies (NOCMAT 2009), September 6.
42. Gaspar, M., Benko, Z., Dogossy, G., Reczey, K., and Czigany, T. (2005) *Polym. Degrad. Stab.*, **90**, 563.
43. Bledzki, A.K. and Gassan, J. (1999) Composites reinforced with cellulose based fibre. *Prog. Polym. Sci.*, **24**, 221–274.
44. Mohanty, A.K., Misra, M., and Drzal, L.T. (2002) Sustainable bio-composites from renewable resources: opportunities and challenges in the green materials world. *J. Polym. Environ.*, **10**, 19–26.
45. Semsarzadeh, M.A. (1986) Fiber matrix interaction in jute reinforced polyester resin. *Polym. Compos.*, **7**, 23–25.
46. Sreekala, M.S., Kumaran, M.G., Joseph, S., Jacob, M., and Thomas, S. (2000) Oil palm fibre reinforced phenol formaldehyde composites: influence of fibre surface modifications on the mechanical performance. *Appl. Compos. Mater.*, **7**, 295–329.
47. Collier, J.R., Lu, M., Fahrurrozi, M., and Collier, B.J. (1996) Cellulosic reinforcement in reactive composite systems. *J. Appl. Polym. Sci.*, **61**, 1423–1430.
48. Joseph, K., Thomas, S., Pavithran, C., and Brahmakumar, M. (1993) Tensile properties of short sisal fiber-reinforced polyethylene composites. *J. Appl. Polym. Sci.*, **47**, 1731–1739.
49. Avella, M., Martuscelli, E., Pascucci, B., Raimo, M., Focher, B., and Marzetti, A. (1993) A new class of biodegradable materials: poly-3-hydroxybutyrate/steam exploded straw fiber composites. I. Thermal and impact behavior. *J. Appl. Polym. Sci.*, **49**, 2091–2103.
50. Cyras, V.P., Martucci, J.F., Iannace, S., and Vazquez, A. (2002) Influence of the fiber content and the processing conditions on the flexural creep behavior of sisal-PCL-starch composites. *J. Thermoplast. Compos. Mater.*, **15**, 253–265.
51. Liu, Z.S., Erhan, S.Z., Xu, J., and Calvert, P.D. (2002) Development of soybean oil-based composites by solid freeform fabrication method: epoxidized soybean oil with bis or polyalkyleneamine curing agents system. *J. Appl. Polym. Sci.*, **85**, 2100–2107.

52. Lundquist, L., Marque, B., Hagstrand, P.-O., Leterrier, Y., and Månson, J.-A.E. (2003) Novel pulp fibre reinforced thermoplastic composites. *Compos. Sci. Technol.*, **63**, 137–152.
53. Lu, X., Zhang, M.Q., Rong, M.Z., Shi, G., Yang, G.C., and Zeng, H.M. (1999) Natural vegetable fibre/plasticised natural vegetable fibre–a candidate for low cost and fully biodegradable composite. *Adv. Compos. Lett.*, **8**, 231–236.
54. Lu, X., Zhang, M.Q., Rong, M.Z., Shi, G., and Yang, G.C. (2002) All-plant fiber composites I. Unidirectional sisal fiber reinforced benzylated wood. *Polym. Compos.*, **23**, 624–633.
55. Lu, X., Zhang, M.Q., Rong, M.Z., Shi, G., and Yang, G.C. (2003) All-plant fiber composites II. Water absorption behavior and biodegradability of unidirectional sisal fiber reinforced benzylated wood. *Polym. Compos.*, **24**, 367–379.
56. Lu, X., Zhang, M.Q., Rong, M.Z., Shi, G., and Yang, G.C. (2001) All-plant fibre composites: self reinforced composites based on sisal. *Adv. Compos. Lett.*, **10**, 73–79.
57. Lu, X., Zhang, M.Q., Rong, M.Z., Shi, G., and Yang, G.C. (2003) Self-reinforced melt processable composites of sisal. *Compos. Sci. Technol.*, **63**, 177–186.
58. Morita, M. and Sakata, I. (1986) Chemical conversion of wood to thermoplastic materials. *J. Appl. Polym. Sci.*, **31**, 832–840.
59. Hon, D.N.S. (1992) Chemical modification of lignocellulosic materials: old chemistry, new approaches. *Polym. News*, **17**, 102–107.
60. Alma, M.H., Diğrak, M., and Bektaş, I. (2000) Deterioration of wood wastes-based molding materials by using several fungi. *J. Mater. Sci. Lett.*, **19**, 1267–1269.
61. Arvanitoyannis, I.S. (1999) Totally and partially biodegradable polymer blends based on natural and synthetic macromolecules: preparation, physical properties, and potential as food packaging materials. *J. Macromol. Sci.*, **39**, 205–258.
62. Shimao, M. (2001) Biodegradation of plastics. *Curr. Opin. Biotechnol.*, **12**, 242–247.
63. Tokiwa, Y. and Calabia, B.P. (2009) Biodegradability of plastics. *Int. J. Mol. Sci.*, **10**, 3722–3742.
64. Bikiaris, D., Aburto, J., Alric, I., Borredon, E., Botev, M., and Betchev, C. (1999) Mechanical properties and biodegradability of LDPE blends with fatty-acid esters of amylase and starch. *J. Appl. Polym. Sci.*, **71**, 1089–1100.
65. Glass, J.E. and Swift, G. (1989) *Agricultural and Synthetic Polymers, Biodegradation and Utilization*, ACS Symposium Series, Vol. 433, American Chemical Society, Washington, DC, pp. 9–64.
66. Gu, J.D. (2003) Microbiological deterioration and degradation of synthetic polymeric materials: recent research advances. *Int. Biodeterior. Biodegrad.*, **52**, 69–91.
67. Imam, S.H., Gould, J.M., Gordon, S.H., Kinney, M.P., Ramsey, A.M., and Tosteson, T.R. (1992) Fate of starch-containing plastic 61 ms exposed in aquatic habitats. *Curr. Microbiol.*, **25**, 1–8.
68. Lee, B., Pometto, A.L., Fratzke, A., and Bailey, T.B. (1991) Biodegradation of degradable plastic polyethylene by phanerochaete and streptomyces species. *Appl. Environ. Microbiol.*, **57**, 678–685.
69. Masaki, K., Kamini, N.R., and Ikeda, H. (2005) Cutinase-like enzyme from the yeast Cryptococcus sp. strain S-2 hydrolyzes polylactic acid and other biodegradable plastics. *Appl. Environ. Microbiol.*, **71**, 7548–7550.
70. Shanks, R.A., Hodzic, A., and Ridderhof, D. (2006) *J. Appl. Polym. Sci.*, **99**, 2305.
71. Iannace, S., Nocilla, G., and Nicolais, L. (1999) *J. Appl. Polym. Sci.*, **73**, 583.
72. Abdul Khalil, H.P.S.A. and Ismail, H. (2000) *Polym. Test.*, **20**, 65–75.
73. Sharma, N., Changs, L.P., and Mohd Ishak, Z.A. (2001) *Polym. Degrad. Stab.*, **71**, 381–393.

74. Lee, J.-A. and Kim, M.-N. (2001) Effect of poly(vinyl alcohol) and polyethylene on the growth of red pepper and tomato. *J. Polym. Environ.*, **9** (2), 91–95.
75. Raynsford, N. (1999) The UK's approach to sustainable development in construction. *Build Res. Inf.*, **27**, 419–423.
76. Citherlet, S. (2001) Towards the Holistic Assessment of Building Performance Based on an Integrated Simulation Approach, Swiss Federal Institute of Technology EPFL, Lausanne.
77. California Integrated Waste Management Board (2000) Designing With Vision: A Technical Manual for Material Choices in Sustainable Construction, California Environmental Protection Agency, California, CA.
78. United Nations Environment Programme UNEP (2003) Sustainable Building and Construction, Division of Technology, Industry and Economics, Paris.
79. Department for Environment Food and Rural Affairs Defra Notes on Scenarios of Environmental Impacts Associated with Construction and Occupation of Homes. Defra Economics and Statistics, (2008) *http://www.statistics.defra.gov.uk/esg/reports/housing/appendh.pdf* (accessed 15 December 2008).
80. Solaro, R., Corti, A., and Chiellini, E. (2000) Biodegradation of poly(vinyl alcohol) with different molecular weights and degree of hydrolysis. *Polym. Adv. Technol.*, **11**, 873–878.
81. Chiellini, E., Corti, A., and Solaro, R. (1999) Biodegradation of poly(vinyl alcohol) based blown films under different environmental conditions. *Polym. Degrad. Stab.*, **64**, 305–312.
82. David, C., De Kesel, C., Lefebvre, F., and Weiland, M. (1994) The biodegradation of polymers: recent results. *Angew. Makromol. Chem.*, **216**, 21–35.
83. Bloembergen, S., David, J., Geyer, D., Gustafson, A., Snook, J., and Narayan, R. (1994) in *Biodegradable Plastics and Polymers* (eds Y. Doi and K. Fukuda), Elsevier, Amsterdam, pp. 601–609.
84. Solaro, R., Corti, A., and Chiellini, E. (1998) A new respirometric test simulating soil burial conditions for the evaluation of polymer biodegradation. *J. Environ. Polym. Degrad.*, **6**, 203–208.
85. Chen, L., Imam, S.H., Gordon, S.H., and Greene, R.V. (1997) Starch-polyvinyl alcohol crosslinked film–performance and biodegradation. *J. Environ. Polym. Degrad.*, **5**, 111–117.
86. Krupp, L.R. and Jewell, W.J. (1992) Biodegradability of modified plastic films in controlled biological environments. *Environ. Sci. Technol.*, **26**, 193–198.
87. Sawada, H. (1994) in *Biodegradable Plastics and Polymers* (eds Y. Doi and K. Fukuda), Elsevier, Amsterdam, pp. 298–310.
88. Kimura, M., Toyota, K., Iwatsuki, M., and Sawada, H. (1994) in *Biodegradable Plastics and Polymers* (eds Y. Doi and K. Fukuda), Elsevier, Amsterdam, pp. 92–106.
89. Corti, A. (1998) Studi sulla biodegradazione di materiali plastici e loro analoghi strutturali a basso peso molecolare. PhD thesis. University of Pisa, p. 166.
90. Allison, F.E. (1968) Soil aggregation. Some facts and fallacies as seen by a microbiologyst. *Soil Sci.*, **106**, 136–143.
91. Pinck, L.A., Dyal, R.S., and Allison, F.E. (1954) Protein-montmorillonite complexes, their preparation and the effects of soil microorganisms on their decomposition. *Soil Sci.*, **78**, 109–118.
92. Chiellini, E., Corti, A., Politi, B., and Solaro, R. (2000) Adsorption/desorption of poly(vinyl alcohol) on solid substrates and relevant biodegradation. *J. Polym. Environ.*, **8**, 67–79.
93. Matsumura, S., Kurita, H., and Shimokobe, H. (1993) Anaerobic biodegradability of polyvinyl alcohol. *Biotechnol. Lett.*, **15**, 749–754.
94. Matsumura, S. and Tanaka, T. (1994) Novel malonate-type copolymers containing vinyl alcohol blocks as biodegradable segments and their builder performance in detergent formulations. *J. Environ. Polym. Degrad.*, **2**, 89–97.

95. Williams, D.F. (1981) Enzymatic hydrolysis of polylactic acid. *Eng. Med.*, **10**, 5–7.
96. Pranamuda, H., Tsuchii, A., and Tokiwa, Y. (2001) Poly(L-lactide)-degrading enzyme produced by Amycolatopsis sp. *Macromol. Biosci.*, **1**, 25–29.
97. Nakamura, K., Tomita, T., Abe, N., and Kamio, Y. (2001) Purification and characterization of an extracellular poly(L-lactic acid) depolymerase from a soil isolate, Amycolatopsis sp. strain K104-1. *Appl. Environ. Microbiol.*, **67**, 345–353.
98. Pranamuda, H., Tokiwa, Y., and Tanaka, H. (1997) Polylactide degradation by an Amycolatopsis sp. *Appl. Environ. Microbiol.*, **63**, 1637–1640.
99. Pranamuda, H. and Tokiwa, Y. (1999) Degradation of poly(L-lactide) by strains belonging to genus Amycolatopsis. *Biotechnol. Lett.*, **21**, 901–905.
100. Tokiwa, Y., Konno, M., and Nishida, H. (1999) Isolation of silk degrading microorganisms and its poly(L-lactide) degradability. *Chem. Lett.*, **28**, 355–356.
101. Sun Yang, H., San Yoon, J., and Nam, K.M. (2005) Dependence of biodegradability of plastics in compost on the shape of specimens. *Polym. Degrad. Stab.*, **87** (1), 131–135.
102. Hoshino, A., Tsuji, M., Ito, M., Momochi, M., Mizutani, A., Takakuwa, K. *et al.* (2003) in *Study of the Aerobic Biodegradability of Plastics Materials under Controlled Compost* (eds E. Chiellini and R. Solaro) Chapter 21, Plenum Press, New York, p. 47.
103. Liu, L., Li, S., Garreau, H., and Vert, M. (2000) Selective enzymatic degradations of poly(L-lactide) and poly(3-caprolactone) blend films. *Biomacromolecules*, **1** (3), 350–359.
104. Li, S., Girard, A., Garreau, H., and Vert, M. (2001) Enzymatic degradation of polylactide stereocopolymers with predominant D-lactyl contents. *Polym. Degrad. Stab.*, **71** (1), 61–67.
105. Cabedo, L., Feijoo, J.L., Villanueva, M.P., Lagaron, J.M., Saura, J.J., and Jimenez, L. (2005) Comparacion entre nanocompuestos biodegradables de poli(acido lactico) (PLA) amorfo con arcillas de distinta naturaleza. *Rev. Plast. Mod.*, **89** (584), 177–183.
106. Sinha, R.P., Pandey, J.K., Rutot, D., Degee, P., and Dubois, P. (2003) Biodegradation of poly(3-caprolactone)/starch blends and composites in composting and culture environments: the effect of compatibilization on the inherent biodegradability of the host polymer. *Carbohydr. Res.*, **338** (17), 1759–1769.
107. Pollet, E., Paul, M.A., and Dubois, P. (2003) in *Biodegradable Polymers and Plastics. New Aliphatic Polyester Layered–Silicate Nanocomposites* (ed. E. Chiellini) Chapter 21, Plenum Press, New York, p. 535.
108. Shimao, M. (2001) Biodegradation of plastics. *Biotechnology*, **12** (3), 242–247.
109. Kiersnowski, A., Dabrowski, P., Budde, H., Kressler, J., and Pig1owski, J. (2004) Synthesis and structure of poly(3-caprolactone)/synthetic montmorillonite nano-intercalates. *Eur. Polym. J.*, **40** (11), 2591–2598.
110. Lee, S.R., Park, H.M., Lim, H., Kang, T., Li, X., Cho, W.J. *et al.* (2002) Microstructure, tensile properties, and biodegradability of aliphatic polyester/clay nanocomposites. *Polymer*, **43** (8), 2495–2500.
111. Sinha Ray, S. and Bousmina, M. (2005) Biodegradable polymers and their layered silicate nanocomposites: in greening the 21st century materials world. *Prog. Mater. Sci.*, **50** (8), 962–1079.
112. Bandyopadhyay, S., Chen, R., and Giannelis, E.P. (1999) Biodegradable organic–inorganic hybrids based on poly(L-lactide). *Polym. Mater. Sci. Eng.*, **81**, 159–160.
113. Paul, A., Delcourt, C., Alexandre, M., Degee, P., Monteverde, F., and Dubois, P. (2005) Polylactide/montmorillonite nanocomposites: study of the hydrolytic degradation. *Polym. Degrad. Stab.*, **87** (3), 535–542.
114. Fukushima, K., Abbate, C., Tabuani, D., Gennari, M., and Camino, G. (2009) Biodegradation of poly(lactic acid) and its nanocomposites. *Polym. Degrad. Stab.*, **94**, 1646–1655.

115. Li, S. and McCarthy, S. (1999) Further investigations on the hydrolytic degradation of poly(DL-lactide). *Biomaterials*, **20** (1), 35–44.

116. Ho, K.L.G., Pometto, A.L., Gadea, A., Briceno, J.A., and Rojas, A. (1999) Degradation of polylactic acid (PLA) plastic in Costa Rican soil and Iowa state university compost rows. *J. Environ. Polym. Degrad.*, **7** (4), 173–177.

117. Sinha Ray, S., Yamada, K., and Okamoto, M. (2003) New polylactide/layered silicate nanocomposites. 3. High-performance biodegradable materials. *Chem. Mater.*, **15** (7), 1456–1465.

118. Fukushima, K., Abbate, C., Tabuani, D., Gennari, M., and Camino, G. (2009) Biodegradation of poly(lactic acid) and its nanocomposites. *Polym. Degrad. Stab.*, **94**, 1646–1655.

119. Hakkarainen, M. (2002) Aliphatic polyesters: abiotic and biotic degradation and degradation products. *Adv. Polym. Sci.*, **157**, 113–138.

120. Verstraete, W. and Top, E. (1992) *Holistic Environmental Biotechnology*, Cambridge University Press, Cambridge, pp. 1–18.

121. Alexander, M. (1996) in *Biodegradation and Bioremediation* (ed. M. Alexander), Academic Press, London, pp. 248–270.

122. Zarnea, G. (1994) *Treatise of Microbiology*, Vol. 5, Romanian Academy Publishing House, Bucharest, pp. 154–163.

123. Eggins, H.O.W. and Allsopp, D. (1975) in *The Filamentous Fungi*, Vol. 1 (eds J.E. Smith, D.R. Berry, and B. Kristiansen), Edward Arnold, London, pp. 151–173.

124. Mandels, M. (1981) *Cellul. Annu. Rep. Ferment Processes*, **5**, 35–78.

125. Wood, T.M. (1992) Fungal cellulases. *Biochem. Soc. Trans.*, **20**, 46–52.

126. Ryu, D. and Mandels, M. (1980) Cellulase: biosynthesis and applications. *Enzyme Microb. Technol.*, **2**, 90–103.

127. Rosevear, A. (1984) Immobilized biocatalysts: a critical review. *J. Chem. Technol. Biotechnol.*, **34B**, 127–150.

128. Akin, C. (1987) Biocatalysis with immobilized cells. *Biotechnol. Genet. Eng. Rev.*, **5**, 319–367.

129. Lu, J., Askeland, P., and Drzal, L.T. (2008) Surface modification of microfibrillated cellulose for epoxy composite applications. *Polymer*, **49**, 1285–1296.

130. Fugetsu, B., Sano, E., Sunada, M., Sambongi, Y., Shibuya, T., Wang, X.S. *et al.* (2008) Electrical conductivity and electromagnetic interference shielding efficiency of carbon nanotube/cellulose composite paper. *Carbon*, **46**, 1256–1258.

131. Sreekala, M.S., Goda, K., and Devi, P.V. (2008) Sorption characteristics of water, oil and diesel in cellulose nanofiber reinforced corn starch resin/ramie fabric composites. *Compos. Interfaces*, **15**, 281–299.

132. Takatani, M., Ikeda, K., Sakamoto, K., and Okamoto, T. (2008) Cellulose esters as compatibilizers in wood/poly (lactic acid) composite. *J. Wood Sci.*, **54**, 54–61.

133. Darder, M., Aranda, P., and Ruiz-Hitzky, E. (2007) Bionanocomposites: a new concept of ecological, bioinspired, and functional hybrid materials. *Adv. Mater.*, **19**, 1309–1319.

134. Czaja, W.K., Young, D.J., Kawecki, M., and Brown, R.M. (2007) The future prospects of microbial cellulose in biomedical applications. *Biomacromolecules*, **8**, 1–12.

135. Grande, C.J., Torres, F.G., Gomez, C.M., Troncoso, O.P., Canet-Ferrer, J., and Martinez-Pastor, J. (2008) Morphological characterisation of bacterial cellulose–starch nanocomposites. *Polym. Polym. Compos.*, **16**, 181–185.

136. Wan, Y.Z., Luo, H., He, F., Liang, H., Huang, Y., and Li, X.L. (2009) Mechanical, moisture absorption, and biodegradation behaviours of bacterial cellulose fibre-reinforced starch biocomposites. *Compos. Sci. Technol.*, **69**, 1212–1217.

137. Amano, Y., Nozaki, K., Araki, T., Shibasaki, H., Kuga, S., and Kanda, T. (2001) Reactivities of cellulases from fungi towards ribbon-type bacterial cellulose and band-shaped bacterial cellulose. *Cellulose*, **8**, 267–274.

138. Beltrame, P.L., Carnitti, P., and Focher, B. (1984) Enzymatic hydrolysis of cellulosic materials: a kinetic study. *Biotechnol. Bioeng.*, **31**, 160–167.

139. Fan, L.T., Lee, Y.H., and Beadmore, D.H. (1980) Mechanism of the enzymatic hydrolysis of cellulose: effects of major structural features of cellulose on enzymatic hydrolysis. *Biotechnol. Bioeng.*, **22**, 177–199.

140. Alvarez, V.A., Ruseckaite, R.A., and Vazquez, A. (2006) Degradation of sisal fibre/mater Bi-Y biocomposites buried in soil. *Polym. Degrad. Stab.*, **91**, 3156–3162.

141. Anastas, P. and Warner, J. (2000) *Green Chemistry: Theory and Practice*, Oxford University Press, New York.

142. Anastas, P.T. and Zimmerman, J.B. (2003) Design through the 12 principles of green engineering. *Environ. Sci. Technol.*, **37** (5), 94A–101A.

143. Gonzalez, M.A. and Smith, R.L. (2003) A methodology to evaluate process sustainability. *Environ. Prog.*, **22** (4), 269–276.

144. McDonough, W. and Braungart, M. (2002) *Cradle to Cradle: Remaking the Way We Make Things*, North Point Press, New York.

145. Graedel, T. and Allenby, B. (1996) *Design for Environment*, Prentice Hall, Englewood Cliffs, NJ.

146. Graedel, T. and Allenby, B. (1995) *Industrial Ecology*, Prentice Hall, Englewood Cliffs, NJ.

147. Anastas, P.T. and Kirchhoff, M.M. (2002) Origins, current status, and future challenges of green chemistry. *Acc. Chem. Res.*, **35** (9), 686–694.

148. Lankey, R. and Anastas, P. (2002) *Advancing Sustainability Through Green Chemistry and Engineering*, American Chemical Society, Washington, DC.

149. Anastas, P. and Lankey, R. (2000) Life cycle assessment and green chemistry the yin and yang of industrial ecology. *Green Chem.*, **2** (6), 289–295.

150. Lankey, R.L. and Anastas, P.T. (2002) Life-cycle approaches for assessing green chemistry technologies. *Ind. Eng. Chem. Res.*, **41** (18), 4498–4502.

151. Guinée, J. (2002) Handbook onlife cycle assessment operational guide to the ISO standards. *Int. J. Life Cycle Assess.*, **7** (5), 311–313.

152. Bare, J., Norris, G., Pennington, D., and McKone, T. (2002) The tool for the reduction and assessment of chemical and other environmental impacts. *J. Ind. Ecol.*, **6** (3–4), 49–78.

153. Erwin, T.H., Vink, K.R.R., Glassner, D.A., Springs, B., O'Connor, R.P., Kolstad, J., and Gruber, P.R. (2004) The sustainability of NatureWorks^{TM} polylactide polymers and Ingeo^{TM} polylactide fibers: an update of the future. *Macromol. Biosci.*, **4** (6), 551–564.

154. Vink, E., Rabago, K., Glassner, D., and Gruber, P. (2003) Applications of life cycle assessment to NatureWorks^{TM} polylactide (PLA) production. *Polym. Degrad. Stab.*, **80** (3), 403–419.

155. Shen, L. and Patel, M. (2008) Life cycle assessment of polysaccharide materials: a review. *J. Polym. Environ.*, **16** (2), 154–167.

156. Pietrini, M., Roes, L., Patel, M., and Chiellini, E. (2007) Comparative life cycle studies on poly (3-hydroxybutyrate)-based composites as potential replacement for conventional petrochemical plastics. *Biomacromolecules*, **8** (7), 2210–2218.

157. Heyde, M. (1998) Ecological considerations on the use and production of biosynthetic and synthetic biodegradable polymers. *Polym. Degrad. Stab.*, **59** (1–3), 3–6.

158. Kim, S. and Dale, B. (2005) Life cycle assessment study of biopolymers (polyhydroxyalkanoates) derived from no-tilled corn. *Int. J. Life Cycle Assess.*, **10** (3), 200–209.

159. Kim, S. and Dale, B. (2008) Energy and greenhouse gas profiles of polyhydroxybutyrates derived from corn grain: a life cycle perspective. *Environ. Sci. Technol.*, **42** (20), 7690–7695.

160. Yu, J. and Chen, L. (2008) The greenhouse gas emissions and fossil energy requirement of bioplastics from cradle to gate of a biomass refinery. *Environ. Sci. Technol.*, **42** (18), 6961–6966.

161. Akiyama, M., Tsuge, T., and Doi, Y. (2003) Environmental life cycle comparison of polyhydroxyalkanoates produced from renewable carbon resources by

bacterial fermentation. *Polym. Degrad. Stab.*, **80** (1), 183–194.

162. Kurdikar, D., Fournet, L., Slater, S., Paster, M., Gruys, K., Gerngross, T., and Coulon, R. (2000) Greenhouse gas profile of a plastic material derived from a genetically modified plant. *J. Ind. Ecol.*, **4** (3), 107–122.

163. Blowers, P., Zhao, H., Case, P., and Swan, J. (2004) Atom economy, expanding boundaries to incorporate upstream reactions. Proceedings of the 2004 AIChE Annual Meeting, Austin, Texas, November 7–12, 2004.

164. Huijbregts, M.A.J., Rombouts, L.J.A., Hellweg, S., Frischknecht, R., Hendriks, A.J., van de Meent, D., Ragas, A.M.J., Reijnders, L., and Struijs, J. (2005) Is cumulative fossil energy demand a useful indicator for the environmental performance of products? *Environ. Sci. Technol.*, **40** (3), 641–648.

165. U.S. EPA, Office of Solid Waste (2008) *Municipal Solid Waste in the United States: 2007 Facts and Figures*, U.S. Environmental Protection Agency, Washington, DC.

166. ICIS Indicative Chemical Prices, *http://www.icis.com/ StaticPages/A-E.htm* (accessed 14 January 2010).

167. Landis, A., Miller, S., and Theis, T. (2007) Life cycle of the corn-soybean agroecosystem for biobased production. *Environ. Sci. Technol.*, **41** (4), 1457–1464.

168. Tabone, M.D., Cregg, J.J., Beckman, E.J., and Landis, A.E. (2010) Sustainability metrics: life cycle assessment and green design in polymers. *Environ. Sci. Technol.*, **44** (21), 8264–8269.

169. International Standards Organization (2006) ISO 14040:2006. *Environmental Management-Life Cycle Assessment-Principals and Framework*. Revises ISO 14040:1997, Developed by TC 207 Environmental Management, Geneva. June 30, 2006.

170. Environmental Protection Agency (1993) Life Cycle Assessment: Inventory Guidelines and Principles. EPA/600/R-92/245, Office of Research and Development, Cincinnati, OH.

171. Tang, B. (1997) Fiber Reinforced Polymer Composites Application in USA *http://www.fhwa.dot.gov/BRIDGE/frp/frp197.htm* (accessed 23 July 2006).

172. Åstrom, B.T. (1997) *Manufacturing of Polymer Composites*, 1st edn, Chapmann & Hall, London.

173. Kawashima N, Ogawa S, Obuchi S, Matsuo M, Yagi T. in *Polyesters III Applications and Commercial Products*, Biopolymers in 10 Volumes, Vol. 4, (eds Doi Y, Steinbuchel A), Weinheim, Wiley-VCH Verlag GmbH; (2002) pp. 251–274, ISBN: a3-52730225-5.

174. *http://www.docstoc.com/docs/43044638/%20Life-Cycle-Assessment-of-Polylactide*.

175. Manufacturing and Properties of PHB, *http://sundoc.bibliothek.uni-halle.de/diss-online/02/02H017/t2.pdf* (accessed 4 April 2013).

176. Shen, L. and Patel, M.K. (2010) Life cycle assessment of man-made cellulose fibres. *Lenzinger Berichte*, **88**, 1–59.

177. Lenzing Fibers Cellulose–Nature's Polymer, *http://www.lenzing.com/fileadmin/template/pdf/nonwoven_fibers/presseinformationen/Vorschau_LCA.pdf* (accessed 4 April 2013).

Index

Polymer Composite: Volume 3, First Edition.
Edited by Sabu Thomas, Kuruvilla Joseph, S. K. Malhotra, Koichi Goda and M. S. Sreekala.

h